ANL/PHY--81-1

DE82 007875

SYMPOSIUM ON ACCELERATOR MASS SPECTROMETRY

Argonne National Laboratory

Argonne, Illinois 60439

11 - 13 May 1981

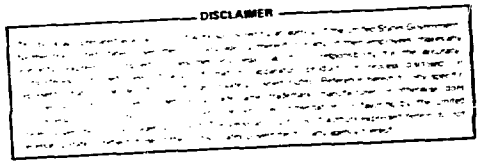

A limited number of copies
of this report are available
for general distribution.
For further copies contact
W. Kutschera, Physics Division,
Building 203,
Argonne National Laboratory,
Argonne, Illinois 60439.

DISTRIBUTION OF THIS DOCUMENT IS UNLIMITED

INTRODUCTION

The area of accelerator mass spectrometry has expanded considerably over the past few years and, in our opinion, indeed established itself as an independent and interdisciplinary research field. Three years have passed since the first meeting was held at Rochester, and we felt it timely to gather and discuss the recent developments and present status of the field. A Symposium on Accelerator Mass Spectrometry was held at Argonne on May 11-13, 1981. In attendance were 96 scientists of which 26 were from outside the United States. The present proceedings document the program and excitement of the field. Papers are arranged according to the original program. A few papers not presented at the meeting have been added to complete the information on the status of accelerator mass spectrometry.

Much of the success of the program was due to the advice from our program committee: H. R. Andrews (Chalk River), H. E. Gove (Rochester), E. T. Hall (Oxford), A. E. Litherland (Toronto), R. Middleton (Philadelphia), R. A. Muller (Berkeley), K. H. Purser (General Ionex Corporation), G. Raisbeck (Orsay), and J. P. Schiffer (Argonne). We should like to thank the members of the program committee and all participants of the meeting for contributing to its success.

Walter Henning
Walter Kutschera
Robert K. Smither
Jan L. Yntema
(The Organizing Committee)

TABLE OF CONTENTS

Table of Contents (cont'd)

Table of Contents (cont'd)

THE EARLY DAYS OF ACCELERATOR MASS SPECTROMETRY

Luis W. Alvarez
Lawrence Berkeley Laboratory
University of California
Berkeley, CA 94720

Before 1978, there were just three papers that had reported work in high energy mass spectrometry—two in 1938, by me and my student Robert Cornog, and one in 1977, a preprint by another of my students, Richard Muller, and me. But a year later, Rich Muller published his classic paper on accelerator dating, and used a cyclotron to determine the age of a water sample from its Tritium content. This paper clearly outlined the techniques of ^{14}C dating by accelerator, and it was published before anyone else started to work on this now important field. Although he mentioned the usefulness of linear accelerators, he did not refer explicitly to the tandem accelerator, which is now the most widely used instrument. The fact that several tandem machines are now being dedicated to accelerator dating gives me an excuse to tell you of my involvement in the origin of charge exchange acceleration, an interesting story that is not part of the general lore of physics.

I have an intense dislike of pictures of the white-haired Albert Einsten because he was then no longer the wonderfully creative physicist who gave us special and general relativity. I have a picture of the real Einstein on my desk—a very young patent examiner who did marvelous things in his spare time. And although I am exceedingly interested in the history of physics, I have recently declined invitations to two conferences on the subject. That is because I would rather remember my friends who did pioneering work in nuclear physics as the vigorous young men they were, four and half decades ago, instead of the white-haired old men I would meet at such conferences and see in my shaving mirror. Emilio Segre brought this problem into focus for me at a talk he gave a few years ago on the life of Enrico Fermi. He told of Fermi's first visit to Gottingen, "where he met the boys who made quantum mechanics."

So I'll be telling you about what a couple of boys did in 1939, what a young man did in 1951, and what another young man and a now older man did in 1977, all of which was a prologue to this meeting. I should apologize for talking so much about my own work, even though that is what I was asked to do. In case you think I seem carried away by its importance, I'll ask you to remember that in 1977 I had stored away in various parts of my brain all the facts that Rich Muller put together to come up with the concept of

accelerator dating. If I can get you to ask the appropriate question, "How could anyone know all that Alvarez knew about the techniques, the dating problem, and its importance, and not arrive at the solution?", I will perhaps help you to put my remarks today in their proper perspective.

I'll make one more comment on my reasons for accepting this speaking assignment. I have always been unhappy about scientific history because, in my view, it so often skirts what I think is the most important element in a new observation or theory—how did this person happen to be doing this thing or thinking along these new lines? So, in a sense, I'm giving this talk to take you behind the scenes, to help you understand how I happened to be mixed up in three unusual projects.

I arrived in Berkeley, in May of 1936, with a brand new Ph.D. and essentially no knowledge at all of nuclear physics; I had worked with Arthur Compton in the field of cosmic rays. Very fortunately for me, the first of Hans Bethe's three monumental articles on nuclear physics appeared in the April 1936 issue of the Reviews of Modern Physics. I studied "Bethe's Bible" with great diligence, and very quickly I was "up to speed" in that I knew all kinds of important things about nuclear physics that even my new and experienced colleagues hadn't known the week before. Hans Bethe was making his transition from spectroscopist to nuclear physicist, and, in his characteristically thorough manner, he learned everything that had been done in his new field, added a lot of new ideas and calculations, and, most importantly for the rest of us, put it all down in very clear prose.

In addition to learning almost everything I knew about nuclear physics from those wonderful articles, I was most fascinated by several things that Hans said couldn't be done with the then present state of the art; and I worked on several of them. (Some of them became possible when reactors were built.) My most successful venture was discovering nuclear K-electron capture, a mode of decay I learned about from his article, which he said couldn't be directly observed because nothing was emitted except a neutrino. I corrected a minor error in one of his papers when I showed that internal conversion of gamma rays occurred in ^{67}Ga; he had said that such an effect could only be seen in the heavy "natural" radioactivities. The next of his "unobservables" that I tried to observe was the beta-decay of the free neutron, which I wouldn't have known about except for his article. He said, "The lifetime is too long to allow observation of the beta-decay of neutrons." The last pre-World War II experiment to be set up at the Berkeley 37-inch cyclotron was a search for that decay; my graduate student collaborator was Cornelius Tobias, and the experiment was terminated when the

cyclotron was reconfigured as a mass spectrometer to separate the uranium isotopes. Robert F. Mozley and I tried a different technique, using our Van de Graaff generator as a source, to observe the neutron decay after the war; but before it was successful, Art Snell of Oak Ridge and John Robson of Chalk River both did such good jobs using reactor neutrons that we were effectively "wiped out." (An interesting aspect of our unpublished work was the first observation that charged particles—electrons, in our case—could be stored in a "magnetic bottle" for long periods of time; this clue may help some of you to reinvent our experiment.) My last challenge of this kind involved Bethe's statement that "the probability of the disintegration of nuclei by neutrinos is so unobservably small—." Shortly after the war when all papers on nuclear physics were born "classified," Bruno Pontecorvo and I independently suggested that neutrino interactions could be observed in CCL_4, and if the Majorana theory was correct, anti-neutrinos from reactors could also be so observed. (My very long paper, which discussed the many sources of background counts, was declassified about ten years later.) As you all know, Ray Davis has spent about twenty years looking for solar neutrinos by this technique, and showing very importantly that the sun produces only about one third as many neutrinos as theory says it should.

One of the problems to which Bethe devoted a lot of attention involved Helium 3 and Hydrogen 3. He didn't question the universal belief that ^3He was heavier than the stable ^3H, and he quoted experimental results, from the D-D reaction energetics, to indicate that ^3He was about 0.2 Mev heavier than ^3H and should capture an electron to become ^3H with a "lifetime of about 5,000 years." ^3He and ^3H had of course been observed for the first time, as high speed reaction products from D+D collisions, by Oliphant, Harteck, and Rutherford in 1934. It was as though the alpha particle had been discovered but the Helium atom had not yet been seen—neither of the nuclei of mass three had been observed after they had come to rest, although several mass spectroscopists had incorrectly reported that they had seen stable ^3H in enriched water samples. The best way I know to show that everyone (and I don't even need to put quotation marks around that word) believed ^3H to be stable is to tell you of the very last paper Lord Rutherford published. It appeared in Nature, just 414 pages before the announcement of his death, and was entitled "Search for the Isotopes of Hydrogen and Helium of Mass 3." Rutherford made arrangements with the Norwegians to process nearly 50 kg. of 99.2% heavy water by further electrolysis down to a volume of 11 cubic centimeters. The overall reduction in water volume was about a factor of 10^9. Aston used his mass spectrometer to examine this sample, and reported that he could find "no trace of ^3H"; Rutherford was "very disappointed after the time and labor spent in

Norway in preparing this material." In the last three sentences he wrote during his fabulously successful life as an experimental physicist, he said,

> "A number of experiments have been made to detect the Helium isotope of mass 3 in ordinary Helium by direct spectroscopic methods, but with entirely negative results. This, however, is not surprising when we consider that terrestrial Helium is probably derived from alpha particles of mass 4 expelled from radioactive substances present on our earth. It is a striking fact that while in transmutation experiments using counter methods the D_3-D reaction is on a marked scale, giving rise to very large numbers of ^3H and ^3He particles, yet it does not seem feasible at the moment to obtain sufficient quantities of these two interesting isotopes to study their properties by ordinary physical chemical methods."

I'm terribly sorry that Lord Rutherford didn't live another two years, so that he could have learned how I showed in a very simple way that all three of the last sentences he wrote in his distinguished career suddenly were in need of revamping. I am confident that had he lived, one of my most prized possessions would be a letter from the grand old man himself, complimenting me on my work with Hydrogen and Helium of mass 3, which I shall describe.

But first let me relate an interesting incident that should convice anyone that Lord Rutherford never for an instant suspected that ^3H was radioactive. Bill Libby (the inventor of ^{14}C dating) told me that shortly after World War II, he was at the Cavendish Laboratory and asked the curator of the laboratory's museum if he could locate Lord Rutherford's old enriched water sample. When the sample was produced, Bill Libby had already found a portable Geiger counter, and he immediately put the water sample close to the detector tube. The result was a loud and rapid clicking of the loudspeaker, as the bremsstrahlung from the radioactivity of Tritium was detected by the Geiger counter. The fact that Lord Rutherford, with the great resources of the Cavendish Laboratory at his disposal, never made this simple test is what made me start this section with the observation that everybody at this time thought that Tritium was not radioactive, but rather a stable form of Hydrogen. And, as Hans Bethe had shown in his "Bible," that meant that ^3He was radioactive.

One night at home, almost two years after Lord Rutherford's article appeared in Nature, I was contemplating the ^3H-^3He problem, and I quickly calculated how much of both isotopes could be produced at the 37-inch cyclotron by a bombardment of Deuterium with deuterons. I was immediately impressed by the magnitude of the numbers, just as Rutherford had been, independently, two years earlier. My numbers showed that if I bombarded Deuterium in the 37-inch cyclotron for only an hour, introduced it into the ion source of the 60-inch cyclotron, and "tuned" the magnetic field so that the cyclotron

could accelerate ^{3}He ions, there should be a large enough beam current for the individual ^{3}He ions to be detected easily with my "thin ionization chamber." Since the 60-inch cyclotron had just been turned on, and since I had a thin ionization chamber plus pulse amplifier that I had used in many experiments, I decided to look for the radioacitvity of ^{3}He. I thought that if I tuned the 60-inch cyclotron for ^{3}He and fed it with bombarded Deuterium, I would certainly see the accelerated ^{3}He ions; and if I was lucky and the half-life of ^{3}He was not more than a year, I would be able to see the beam current slowly decay with its radioactive half-life, as I did the experiment on various occasions spaced out over the next few years. The only uncertain element in the experiment was a possible background of accelerated "junk ions," that might be produced in the cyclotron when it was tuned to accelerate the ^{3}He ions. As far as I knew, no one had ever put an ionization chamber able to detect individual accelerated ions in front of the beam window when the cyclotron was tuned through the range of magnetic fields where one would expect to see ^{3}He ions. If for some unsuspected reason there was a large background of ions in this region, then I couldn't do the experiment that I have just outlined. It was obvious to me that I should take a look myself to see if there were any background ions that would mask the effect that I would otherwise certainly see.

I therefore talked to one of the laboratory's uncommitted graduate students, Bob Cornog, and asked him if he would like to work with me on a search for the fate of the ^{3}H and ^{3}He ions that were produced in the D-D reaction. Bob was a friendly and energetic young man who hadn't yet done an experiment at the laboratory. He agreed with me that the first thing we had to do was check the background at the 60-inch cyclotron with the magnetic field set at three quarters of its normal value. Bob helped me push my amplifier cabinet from the old wooden 37-inch cyclotron laboratory to the new 60-inch laboratory just across the alleyway. I set the ionization chamber in front of the cyclotron's thin window and got the equipment running. Bob said that he had to throw the hammer in a track meet that afternoon, but he'd be back to work with me in the evening. But things started to work well in the middle of the afternoon, and I made arrangements with the cyclotron crew to operate the machine with its normal field—where I could observe both the deuterons and the ^{4}He ions being accelerated through the thin window and into my ionization chamber. Huge bursts of these ions paralyzed the amplifier, but it recovered quickly as soon as the oscillator was turned off. I then asked the crew to lower the magnetic field to three-quarters of its normal value, where ^{3}He, rather than ^{4}He, would be accelerated according to the cyclotron equation. They must have spent about half an hour adjusting the magnetic field to various values in this general range, while my eyes were glued to the cathode ray oscilloscope looking for

pulses. We had no intercom between the recently finished cyclotron target area and the control room, so most communications were by shouts. On occasion I would go into the control room to talk with my old friend Bill Farley about new search procedures. But it seemed pretty clear now that there were no "junk ions" being accelerated at any magnetic field values where the ^{3}He ions Bob and I were about to make with the 37-inch cyclotron should appear. This was naturally good news to me, since it meant that the "real experiment" could soon be undertaken, with almost a guarantee of success.

In my last conversation in the control room with Bill Farley and the other operators, I said that I was now convinced that there was no background in the ^{3}He range, but that I would like them to take the magnetic field once again up to full value so that I could make sure that my ionization chamber and amplifier were still working by watching the scope screen become paralyzed with enormous numbers of beam particles. I thought this simple act would terminate the exploratory experiment, but as we will now see, it led to one of the most important observations I ever made. If anyone were writing a scenario for this experiment, he would have ordered two things that fortunately didn't happen. In the first place, the operators should have turned off the radiofrequency oscillator that powered the "D's"—the cyclotron's accelerating electrodes. In keeping with good cyclotron practice, only after cutting the oscillator power would the operator have then turned off the magnetic field. But probably because the operators had been running the magnetic field up and down for the past half hour, always with the oscillator on, they cut the magnet power while the oscillator was left on. That was the first fortunate accident. And the second thing that would have been written into the scenario was that I would have walked away from my apparatus, knowing that the experiment was over. But for some reason I kept watching the oscilloscope screen after I had shouted "Cut." I was startled to see a burst of pulses on the oscilloscope that quickly appeared and then disappeared, as the magnetic field dropped through the "Helium three region." (The time constant of the magnet was many seconds because it wasn't constructed of laminated iron as a transformer is. So by Lens' law, eddy currents in the iron kept the magnetic field from dropping rapidly to zero strength.) Soon thereafter there was a huge burst of pulses as the magnetic field went through one-half its normal value, where protons were accelerated. After I'd seen the protons, I ran to the control room and said, "Let's try that again." I probably also told them what had happened, so we repeated the experiment several times, and every time the magnetic field dropped rapidly throughout the Helium three region, I saw the pulses suddenly appear and then disappear. It was quickly obvious to me what was making them appear during the rapidly decreasing field although they hadn't shown up when the magnetic field had the same constant value. My

knowledge of the way eddy currents would behave, of the long "time constants for decay" of the cyclotron, and of the principles of the magnetic "shimming process" (the tailoring of the field shape to give proper vertical focusing) all combined quickly to tell me that the cyclotron was being fortuitously reshimmed by eddy currents in the pole pieces of the magnet caused by the rapid rate of change of the magnetic field downward. The long apprenticeship I had spent in the early design of the 60-inch cyclotron was now paying good dividends, as I quickly diagnosed the situation. (But that same apprenticeship had failed me earlier in the afternoon when I hadn't realized that the non-linear characteristics of the iron poletips of the magnet had destroyed the vertical focusing characteristics of the magnetic field when it was operating "far below saturation." So my observation that there was no "interfering background" at the ^{3}He magnet setting was now demonstrably wrong.)

The pulse height of the new particles was equal to that of the ^{4}He ions seen at full magnetic field. Since the ions had the same velocity, this meant that the new ones had a charge of 2. I now dashed over to my radioactivity laboratory where I had a box of carefully calibrated aluminum foils of various thicknesses that I had long used as absorbers of beta rays. I quickly calculated the range of ^{3}He particles in air, after such particles had been accelerated in the 60-inch cyclotron. (It was of course just 3/4 of the range of the ^{4}He ions.) I could therefore pick out just the proper amount of aluminum to keep these ^{3}He particles from entering my ionization chamber. After perhaps a score of "quick passages," with various thicknesses of aluminum foil interposed between cyclotron and ion chamber, I had confirmed the fact that the particles I was seeing on the oscilloscope were truly ^{3}He ions that had come from the Helium bottles that fed the cyclotron ion source. The Helium had in turn come from deep wells in Oklahoma where it had rested undisturbed for about one hundred million years. So ^{3}He wasn't radioactive, as everyone had so long believed—it was stable against beta decay; it was a natural constituent of ordinary gas-well Helium.

When Bob Cornog returned, after he had won the hammer throw, I had an exciting experience telling him everything that had happened that afternoon. It was obvious that the first thing we should do was shim the cyclotron with a set of circular pieces of iron, so that it would produce a steady beam of ^{3}He ions. Nothing further could be gained by observing isolated bursts of ^{3}He ions while the cyclotron was shimming itself through eddy currents. That seemed to be too much like Charles Lamb's famous story of the Chinese gentleman who accidentally discovered the joys of roast pork, and then had to burn down a house every time he wanted to experience again that delicious taste.

The importance of high energy mass spectrometry was demonstrated that afternoon for the first time. Instead of measuring a current of ions to a collector plate in a vacuum chamber, as the men who had incorrectly reported observing ^3He had done (when they were probably observing the molecular ion HD^+), I made the ions traverse an aluminum window which would split a molecular ion apart. I could then measure the true charge of the ions by pulse height and the true kinetic energy from the range. I also measured e/M from the cyclotron equation and velocity from the frequency and final orbit circumference, and all these numbers agreed among themselves to give both e and M. You are all familiar with these advantages of the accelerator technique, but I stumbled on them accidentally that Saturday afternoon. I had used a cyclotron in my experiment, not because of these advantages, but because it was the only mass spectrometer to which I had access!

In the next few days, and after a lot of trial and error, Bob Cornog put together a set of circular iron shims that would permit the 60-inch cyclotron to yield a constant beam of ^3He ions. Because of the work of Bob Wilson, the art of shimming had been replaced by a science of shimming, and this was of great assistance to Bob Cornog in his adjustment of the 60-inch cyclotron. So now we were ready to do some experiments with our newly discovered stable ^3He ions.

We did three principal experiments—a rough measurement of the relative abundance of ^3He and ^4He in a normal tank of gas-well Helium, and a fairly accurate measurement of the relative amounts of ^3He in gas-well Helium and in Helium derived from the atmosphere. And finally we used ^3He as a new kind of bombarding projectile to excite the reaction $^{28}Si(^3He,p)^{30}P$. We observed the famous 2.5 minute period of Phosphorous 30—the first artificially radioactive isotope ever made, which had the seen the light of day five years earlier in the laboratory of Fredrick Joliot and Irene Curie.

Bob Cornog and I wrote two very short Letters to the Editor of The Physical Review in the summer of '39. (Taken together, they occupied less than one page of the journal.) The first, dated July 31, was entitled "^3He in Helium" and it described the observations I made with the rapidly varying magnetic field. The second was dated August 29, and was entitled "Helium and Hydrogen of Mass 3." In this letter we described our experiments that were done after Bob had shimmed the cyclotron to produce the steady ^3He beam. We correctly observed the unexpected effect that ^3He was 10 times more abundant in atmospherically derived Helium than in gas-well Helium—we now know that the extra ^3He is produced by cosmic rays, just as ^{14}C is produced by cosmic rays in the atmosphere. We were off by a factor of 10 in our absolute abundance

of ^{3}He, but that was not an unreasonable error to make when the cyclotron was adjusted so differently to accelerate ^{3}He ions and ^{4}He ions. (We quoted 10^{-8} and 10^{-7} as the abundance of ^{3}He in gas-well and atmospheric Helium, whereas the present values are 10^{-7} and 10^{-6}.) Although we didn't mention it in our letter, we also obtained samples of Helium, from Professor Giauque's laboratory, which had been liquefied and evaporated many times. I thought that we might see the effect of fractional distillation, but there was no such effect. And we did report seeing ^{30}P.

In the second paragraph of our second letter we reported the first observations of the radioactivity of ^{3}He. I'm embarrassed to recall that it took me more than a week after the first observation of ^{3}He to realize that this meant that ^{3}H must be radioactive, and that we should search for that radioactivity. As soon as I told Bob Cornog what I had concluded about the radioactivity of ^{3}H, or Tritium as it is now universally called, he took charge of this part of the experiment and worked like a Trojan to build the equipment and make the observations. He bombarded a sample of Deuterium gas at the 37-inch cyclotron and showed that it was very radioactive with a lot of contamination activities. He then passed the gas through activated charcoal at liquid air temperature, which removed most of the contaminants, and then finally let the gas diffuse through hot Palladium. Hydrogen is the only gas known to diffuse through Palladium, so the gas which came out of the other side, and was used to fill an ionization chamber, was all heavy Hydrogen with no trace of impurities. We introduced this gas into a large ionization chamber with a volume of about one liter and observed its radioactivity on a vacuum tube electrometer. In our second letter we said:

> "The gas showed a definite activity of long half-life. The radiation emitted by this Hydrogen is of very short range as was shown by the almost linear form of the intensity vs. pressure curve when the gas was pumped out of the chamber. Once sufficient time has elapsed for us to make some statement regarding the half-life of this activity, we will submit the details of the work to this journal for publication."

The beta rays from Tritium were so low in energy, and of such a short range, that we could not get them through the thinnest aluminum foils into a more conventional radiation detector. Since we were unable to make a normal range measurement on the beta rays, I thought up the idea of looking at the activity vs. pressure curve. (For ordinary beta rays, the ionization would vary as the square of the pressure; if the pressure were cut in half, half the radioactive atoms would be lost, and each beta ray would make only half as many ion pairs in the lower density gas.) I doubt if anyone every used this technique, either before or since, but it showed very well that the beta ray

energy was small indeed. (We now know that the beta rays have a maximum energy of 18.6 keV—about 1% of the typical beta ray energy one meets in nuclear physics.)

As far as I know, these were the last uses of an accelerator as a mass spectrometer until 1975 when I proposed a quark search to Rich Muller. I'll now describe how the tandem accelerator came into being.

In the Spring of 1975 I was eating breakfast before teaching an eight o'clock class in nuclear physics and reviewing what I would say about accelerators. I was prepared to tell my students that whenever they saw a singly charged particle beam produced in an acclerator that had an energy in electron volts that was greater, numerically, than the highest voltage seen in the machine, they would know that there was a changing magnetic field somewhere inside the box. I couldn't think of an exception to this general principle until I had finished my coffee and started to drive to the campus. But during the ten minute drive I realized that, if I made the accelerated ion change its charge from -1 to +1 inside an electrode, I could violate my newly postulated "law."

I published a one page article in the Review of Scientific Instruments in September 1951 entitled "Energy Doubling in dc Accelerators." This paper started with these sentences:

> "It is generally believed that charged particles cannot be accelerated from ground potential to ground potential unless they pass through a system which has associated with it a time varying magnetic field. Dc electric fields must satisfy the equation $\oint$ Eds = 0, while the time varying fields used in radiofrequency accelerators and betatrons are freed from this restriction of scalar potential theory."

As soon as the paper appeared, I had a call from an old friend from wartime days, Dennis Robinson, who was then President of the High Voltage Engineering Corporation. He asked if he could visit with me the next week to talk about my recent invention, which he said he'd like to build and sell with a license from the Atomic Energy Commission (which I had thanked for supporting my work). I was of course pleased, and when he came to Berkeley we did talk about it for several days. One thing that concerned us was an unusual discharge mode that might be seen in a "straight through" charge exchange accelerator, where electrons could oscillate back and forth through the high voltage electrode. I thought for a while about converting my own 4 Mev Van de Graaff generator into a charge exchange accelerator, with a magnet in the high voltage terminal, but I ended up deciding to leave the whole business to Dennis Robinson. He invited me to be a consultant to his company, but I was actively consulting with Ernest

Lawrence's color television company at the time, and regretfully told Dennis that I couldn't spare the time. You are all familiar with the success his company has had in building and selling tandem accelerators, the possibility of which he first learned from my article.

I'll now transport you back thirty years to show that "everyone" at that time accepted the fact that the tandem was a brand new idea, which I had invented. This time, I'll have to put quotes around "everyone," because it turned out that there was a U.S. patent on such accelerators, but the accelerator fraternity didn't know of its existence. You have all heard of an identical situation, where the idea of strong focusing was first published in 1952 by Courant, Livingston, and Snyder, but then Nick Christophilos was found to have patented the idea two years earlier quite unbeknownst to the accelerator fraternity. The fact that Courant, Livingston, and Snyder are almost always credited with the discovery of strong focusing is probably somewhat due to to the fact that Christophilos wasn't "a member of the club"—he was an engineer who designed elevators in Athens and invented accelerators as a hobby. Contributing reasons may also be that strong focusing was the first major scientific accomplishment of the relatively new Brookhaven National Laboratory, but most importantly, in my view, was the fact that the independent Brookhaven discovery led immediately to the building of many strong focused accelerators, whereas Christopholos' work was buried in the patent literature, and had no influence on the development of accelerator technology.

The parallels between the tandem and strong focusing inventions are extraordinarily close, with one exception. The second inventors of the focusing scheme have received almost all the credit, whereas the man whose name is always associated with the tandem—Robert Van de Graaff—was not another independent inventor, but rather an excellent developmental engineer and Chief Scientist at the High Voltage Engineering Co. Neither Willard H. Bennett, who applied for a patent on the tandem in 1937, nor I, who first published it in 1951, are remembered as having anything to do with the matter. I really can't complain, since the accelerator fraternity has treated me well; for years they have used my name as an adjective to describe resonant cavity ionic linear accelerators. My personal satisfaction in the tandem matter is best illustrated by the following story that concerns the infinitely more important, and hotly contested, invention of medical anesthesia. Medical men almost universally credit that to W.T.G. Morton, who demonstrated it at the Massachusetts General Hospital in 1846. Later it was found that Crawford Long, a Georgian doctor, had performed operations under ether in 1842, but had then given up that practice without publishing his work. Long's statue is

in the U.S. Capitol's Statuary Hall as the "father of anesthesia." I remember reading a poignant statement by Morton's widow who defended her husband's claim as a public benefactor by saying something to the effect that although others may have been first, her husband's demonstration was followed immediately, worldwide, by the universal use of anesthesia. In an aside she wondered how those who claimed the credit could live with the knowledge that, because of their neglect to publish their work, countless people had suffered terrible tortures from which they could have been saved by a knowledge of anesthesia.

Compared to the invention of anesthesia, one of mankind's greatest boons, the tandem affair is of negligible importance. For that reason, I have never mentioned it either in print or in a talk in the past 30 years. But now that the occasion seems ripe for such a mention, I'll say that my satisfaction comes from two considerations: Number one is that I did it independently, and number two is that my publication led immediately to the worldwide use of a valuable technique that until then had been buried for more than a dozen years in the patent literature. I'll add in passing that, although everyone knows that all major accelerator improvements such as the cyclotron, betatron, and linear accelerator have been patented, the accelerator literature doesn't contain references to such patents, but only to articles in the open literature.

I'll conclude this vignette with an observation I once made when reading Livingston and Blewett's classic book on accelerators. In their brief section on charge exchange acceleration, they say that this idea was "proposed by W.H. Bennett[42] and L.W. Alvarez[43]." I expected the Bennett reference to be to his U.S. patent, because I was sure that he hadn't mentioned it in the open literature. But instead, I found three separate references to the 1936 Physical Review—one article and two abstracts. I immediately looked them up, and there was not a single word about charge exchange in any of them; they were all simply on the generation of negative hydrogen ions!

The experiment that revived Accelerator Mass Spectrometry was published in 1977, and came about in the following way. As a particle physicist I had been in conversations about quarks from the earliest days—in fact my bubble chamber group had published a good deal of the data that had led Murray Gell-Mann and, independently, George Zweig to propose the quark theory in 1964. Their quarks had electrical charges that were +2/3 and -1/3 times e, and many searches for such fractionally charged particles were soon underway. A year after the original quark papers appeared, Han and Nambu proposed a theory of integrally charged quarks. It was not taken very seriously at the time, because it required that there be nine kinds of such quarks, rather than the simpler original

theory that needed only three kinds of fractionally charged quarks. But as the years went by, it became apparent that the original three-quark theory needed to be modified by the addition of "color," and the number of quarks was therefore raised to nine. As more and more quark searches failed, I became interested in looking for integrally charged quarks because the two theories now seemed equally simple. I spoke to John Reynolds about the possibility of looking for Hydrogen ions of anomalous mass with one of his mass spectrometers. In fact, I suggested that we use two such devices in tandem, so scattering from slits, etc. could be eliminated as a source of incorrect mass measurements; and I further suggested that we use time of flight techniques as an additional verification of the mass of the Hydrogen-like quarks. John was anxious to collaborate, but we weren't able to fund the apparatus development, and we lost interest in the matter.

Several years later, when I was reading the performance specifications of our Laboratory's 88-inch cyclotron, I realized that it was ideally suited to look for positive singly charged stable quarks. It had been designed to give good magnetic focusing over a wide range of magnetic fields, and its frequency could also be changed quite easily. I explained to Rich Muller that if we looked for Hydrogen ions in the mass range from 0.3 AMU to 8 or 9, which was a practical limit for the 88-inch cyclotron, we would either find the quarks or set quite fantastic limits on their abundances in water. Not long after we started our search, I read a paper by Okun and Zeldovich in which they not only discussed the production of such quarks by cosmic ray bombardment—the mechanism I had calculated—but also suggested that such quarks could also be remnants of the big bang.

I once heard Rich Muller talk about his work in accelerator mass spectrometry, some of which greatly extended the work we did together on the quark search. He said, "Since the ideas all came from Luie, I felt that the only way I could earn the right to have my name on the paper was to do <u>all</u> the work." And he did do all the work except for running the cyclotron, which was done by Bill Holley and Ed Stevenson, whose names also appear on our paper. He borrowed all the solid state ionization detectors, counting equipment, etc., and I had the pleasure of sitting in the cyclotron control room, night after night, watching Rich make all the adjustments and request all the changes in operating conditions that I had personally made, by shouting, forty years earlier. It was Rich's first encounter with a cyclotron and he obviously enjoyed it.

Our paper gave limits on +1 charged quarks relative to protons as less than 2×10^{-19}, from mass 3 to mass 8.5 and about 10^{-14}, below mass 2. From mass 2 to 3, the limit varied from 10^{-18} to 2×10^{-19}. We said,

> "The advantage of the cyclotron over an ordinary mass spectrometer does not come from its high resolution—but from the high energy of the emerging beam: several Mev per nucleon. This high energy allowed us to send the beam into the particle identification detectors, and to get useful information on a particle-by-particle basis."

As far as I know, this statement in 1977 is the first overt mention of those features of acclerator mass spectrometry which you all appreciate. I had known them for some time, but they hadn't ever been stated so clearly until then.

That wraps up the early history of accelerator mass spectrometry; but I might say a few words about its application to "accelerator dating," a field in which I've had no direct involvement, even though I did contribute to its evolution in three ways. The first came from some conversations I had several years ago with Rich Muller when he was spending the summer trying to help our navy find Soviet submarines. He was studying the "wake radioactivity" left in the water behind any nuclear submarine whose reactor is not perfectly shielded. Seawater is the cheapest material with which to shield such a reactor and the question is then what is the easiest radioactive material to detect. Sodium 24 will certainly be made in quantity, and it emits two very high energy gamma rays in coincidence—a most unusual signature. But one's first guess is seldom the best, and I can't remember what Rich looked at next, but it had a higher production rate, and an uncomfortably long half-life, and therefore a smaller counting rate. I told Rich that some years earlier, I had seen a research proposal in which someone from SRI had suggested improving the accuracy of ^{14}C dating, by counting the atoms in a mass spectrometer, rather than waiting for them to decay, with their very long half life. I remembered that he had proposed using negative ions as a way of eliminating background. Rich and I agreed that the method probably hadn't worked, or we would have heard about it, but the idea of counting atoms rather than decays did appeal to him, and he tried to make use of it in the submarine detection business but with no success.

Then after we had made our quark search on the cyclotron, Rich put all the parts together and proposed to do accelerator dating, using ^{14}C, ^{10}Be, and ^{3}H, among other materials. So I soon found myself in my old role as spectator in the control room at the 88-inch cyclotron, as Rich performed the first accelerator dating experiment ever done—the measurement of the age of a water sample from its ^{3}H content. The sample was 24 years old and had been collected before the Tritium content had been raised by the thermonuclear bomb testing in the 1950's. Rich measured its age as 33 years.

So my first two contributions to accelerator dating, if they could be dignified by that description, were to introduce Rich Muller to the concept of accelerator mass spectrometry and to the fact that someone, unknown to me, had suggested that ^{14}C dating might be done by counting atoms, rather than decays. I did make one concrete suggestion to reduce background, after Rich had first proposed accelerator dating, but I'm sure he would have arrived at the same solution without my help. That was to separate isobars, for example ^{14}C from ^{14}N, by the "range method.

I've been pleased to see the rapid strides that have been made in a field that I apparently kicked off, quite unknowingly, and I've also enjoyed the opportunity to meet so many of the people who have contributed to the technology—people who were familiar to me by name, but not by face. And thank you for the opportunity to reminisce about events of long ago.

ULTRASENSITIVE MASS SPECTROMETRY WITH A TANDEM VAN DE GRAAFF ACCELERATOR

H. E. Gove
Nuclear Structure Research Laboratory,†
University of Rochester
Rochester, New York 14627

For the past four years a mass spectrometry program has been underway at the University of Rochester employing the Nuclear Structure Research Laboratory's MP tandem Van de Graaff accelerator. The work has been a collaboration between scientists at General Ionex Corporation,[1] The University of Toronto,[2] and the University of Rochester.[3]

Figure 1 shows a schematic of the system presently being employed for the ultrasensitive mass spectrometry work at Rochester. It has been described in recent publications[4,5] with the exception that a different sputter ion source is presently in use.[6,7,8] This new ion source which was designed for the dedicated systems presently under construction[6] gives a much more uniform output current than the one previously used and, as a consequence, produces much more reproducible results.[6,7]

The earliest experiment carried out at Rochester was to determine whether $^{14}N^-$ ions were stable.[9] The various focussing and deflecting elements in the accelerator were adjusted to accept $^{12}CH_2^-$ ions and to detect $^{12}C^{6+}$ at the high energy end. These ions perfectly mimic $^{14}N^-$ with $^{14}N^{7+}$ being detected at the high energy end. No evidence for $^{14}N^-$ was found.

After some measurements of ^{14}C in contemporary wood charcoal and graphite[9,10] measurements of ^{14}C were made[11] in a number of charcoal samples previously dated by the U.S. Geological Survey.[12] The results are shown in Table 1. The agreement between the two sets of measurements is reasonable but in the Rochester measurements only milligrams of carbon were required as compared to the gram quantities needed for the conventional decay counting technique. A small ^{14}C background is observed when graphite (a petroleum based form of carbon) is used in the ion source. The background changes from run to run and, translating it into an "age" for the graphite, varies between 50,000 and 65,000 years. The source of this background is presently unknown. Other groups using existing tandem Van de Graaff accelerators report similar background, again of unknown origin.

TABLE 1. Comparison of ages - USGS and Rochester

Sample	Age in Years - Rochester	Age in Years - USGS
Mount Hood	220±300	220±150
Mount Shasta	5700±400	4590±250
Lake Agassiz	8800±600	9150±300
Hillsdale	41000±1000	39400±1000
Graphite	48000±1300	

^{14}C has not been measured at Rochester during the past year pending the installation of the new ion source system.[6,7,8] The latest results are shown in Table 2, and were reported at the Tenth International Radiocarbon Conference.[5] The method used to clean and convert the bull mummy cloth to carbon is the same as would be used to date any other linen artifact.[13]

TABLE 2. Recent ^{14}C results from Rochester

Sample	Rochester Age (years B.P.)[1]	Expected Age
Mount Shasta	4580±90	4590±250[2]
Bull Mummy Cloth Dahshur, Egypt	2200±150	2050±200[2]
Baby Wooly Mammoth (U.S.S.R.)	27000±1000	Available sample size too small to date by conventional methods
Australian Sucrose	1.47±0.03[3]	1.45 - 1.51[4]

1. B.P. = years before 1950. ^{14}C half-life assumed to be 5568 years.
2. As measured by the U.S.G.S.
3. This is the ratio of $^{14}C/^{12}C$ in the proposed sucrose standard to the $^{14}C/^{12}C$ ratio in 1950 wood.
4. Measurements of this ratio from other laboratories fall in this range.

Table 3 lists the radionuclides which have been measured at Rochester along with their half lives, the stable isotopes and interfering stable

isobars, the chemical form used in the ion source, the charge state and energy of the accelerated beam of the radioisotope and the presently achieved limit of detection. The latter refers to the minimum value of the ratio of the particular radionuclide to its stable isotope or isotopes that has been measured to date at Rochester. It is worth emphasizing that, in the case of ^{14}C and ^{36}Cl, this present limit of sensitivity approaches one part in 10^{16}. A comparison between conventional mass spectrometry and the new accelerator based mass spectrometry which analyses the reasons why the new technique is able to achieve these extraordinarily low limits of detection will be published shortly.[14]

TABLE 3. Radionuclides studied at Rochester

Radio-Nuclide	Half-life (yr)	Stable isotopes	Stable isobars	Chemical form	Charge state	Energy (MeV)	Limit of Detection
^{10}Be	1.6×10^{6}	^{9}Be	^{10}B	BeO	3^{+}	33**	7×10^{-15}
^{14}C	5730	$^{12,13}C$	^{14}N*	C	4^{+}	40	0.3×10^{-15}
^{26}Al	7.2×10^{5}	^{27}Al	^{26}Mg*	Al	5^{+}	48	10×10^{-15}
^{32}Si	108	$^{28,29,30}Si$	^{32}S	SiO_2	5^{+}	55	7×10^{-12}
^{36}Cl	3.0×10^{5}	$^{35,37}Cl$	^{36}Ar*, ^{36}S	AgCl	7^{+}	80	0.2×10^{-15}
^{129}I	15.9×10^{6}	^{127}I	^{129}Xe*	AgI	5^{+}	30	0.3×10^{-12}

*does not form negative ions

**BeO^{-} from source

^{10}Be has been measured at Rochester only in samples of spectroscopically pure ^{9}Be irradiated in a known thermal neutron flux of a reactor.[15] It has been measured in natural samples by several other groups using both cyclotrons[16] and tandem Van de Graaff accelerators.[17,18,19,20]

The ^{14}C measurements at Rochester have been discussed above. They mainly involved natural samples although measurements on artificially prepared samples have also been made. Several other groups have also measured ^{14}C both in artificial and natural samples.[19,21,22] No group has yet been able to routinely measure $^{14}C/^{12}C$ ratios with a reproducibility of 1% or better which is a desirable goal for most samples 10,000 years old or younger but the prognosis for doing so looks encouraging.[6,7]

So far ^{26}Al has only been measured by three groups one at the René Bernas Laboratory,[23] one at the Univeristy of Rochester[24] and the other at the Argonne National Laboratory.[25] In all cases irradiated samples were employed. Measurements of ^{26}Al in natural samples by the accelerator technique have not yet been made. This is mainly due to the fact that standard negative ion sputtering techniques produce rather low intensity aluminum beams. It will probably be necessary to start with positive ions and then charge exchange to the negative ion in a sodium vapour cell.

Accelerator mass spectrometry is not required for measuring ^{32}Si in natural samples since measuring the beta decay of the daughter ^{32}P is relatively straightforward. However, until recently the half life of ^{32}Si was rather poorly known, the accepted value being 330±40 years. Two groups recently combined the measurement of the beta decay rate of an artificially produced sample of ^{32}Si with the tandem accelerator mass spectrometry measurement of the ratio $^{32}Si/^{28}Si$ to obtain half lives of 108±18 years[26] and 101±18 years[27] respectively. The fact that the half life of ^{32}Si is three times shorter than previously believed has important consequences in several fields including glaciology and oceanography.

^{36}Cl is an important cosmogenic radionuclide for determining the age of ground water[7,28,29,30] and when combined with the measurement of other cosmogenic radionuclides for determining the terrestrial age and extraterrestrial cosmic ray exposure time of meteorites.[31,32] ^{36}Cl in natural samples has so far only been measured at Rochester.

^{129}I has been measured at Rochester both in artificial[33] and natural[32,34] samples. In the latter cases the samples were meteorites.

The new accelerator mass spectrometry, of course, is not confined to radionuclides. It can equally effectively measure trace amounts of stable elements in various matrices of other much more abundant elements. At Rochester ^{193}Ir, ^{194}Pt and ^{195}Pt have been detected at ppb levels in a variety of geological samples.[35,36] In particular both platinum and iridium were shown to be substantially enhanced in Danish Fish Clay at the Cretaceous-Tertiary boundary.[35,36] The iridium enhancement confirms measurements previously reported.[37]

In summary the MP tandem Van de Graaff accelerator at the University of Rochester has been employed as an ultrasensitive mass spectrometer to detect the radionuclides ^{10}Be, ^{14}C, ^{26}Al, ^{32}Si, ^{36}Cl and ^{129}I with limits of

detection of the measurement of the radionuclide to the stable isotope in some cases approaching one part in 10^{16}. ^{14}C, ^{36}Cl and ^{129}I were measured both in artificial and natural samples while the others have been measured only in artificial samples. The stable elements ^{193}Ir, ^{194}Pt and ^{195}Pt have been measured both in artificial and natural samples at ppb levels.

As a result of this work a great many other nuclear physics accelerator laboratories throughout the world have begun work in this field. Most of these groups are presenting papers at this conference. In addition there are under construction five accelrator systems based on the system described above which will be dedicated to this field of accelerator mass spectrometry.[6]

Thanks are due to T. Lund and the crew of the Rochester tandem for the measurements reported here.

---

†This material is based upon work supported by the National Science Foundation under Grant PHY-78-22698 and in part under Grant PHY-79-23307.

[1]K. H. Purser, General Ionex Corporation.

[2]R. P. Beukens, K. H. Chang, L. R. Kilius, H. W. Lee and A. E. Litherland, Department of Physics and J. C. Rucklidge, M. P. Gorton and G. Wilson, Department of Geology, University of Toronto (supported in part by a grant from the National Science and Engineering Research Council of Canada).

[3]D. Elmore and H. E. Gove, Nuclear Structure Research Laboratory and Department of Physics and Astronomy, University of Rochester (supported by grants from the National Science Foundation).

[4]H. E. Gove, D. Elmore, R. Ferraro, R. P. Beukens, K. H. Chang, L. R. Kilius, H. W. Lee, A. E. Litherland and K. H. Purser, Nucl. Instr. and Meth. 168, 425 (1980).

[5]H. E. Gove, D. Elmore, R. Ferraro, R. P. Beukens, K. H. Chang, L. R. Kilius, H. W. Lee, A. E. Litherland, K. H. Purser and M. Rubin, Radiocarbon, 22, 785 (1980).

[6]K. H. Purser, a paper included in the Proceedings of this conference.

[7]D. Elmore, a paper included in the Proceedings of this conference.

[8]T. S. Lund, Proc. 1980 SNEAP Conference, University of Wisconsin, ed. J. H. Billen, p. 141.

[9]K. H. Purser, R. B. Liebert, A. E. Litherland, R. P. Beukens, H. E. Gove, C. L. Bennett, M. R. Clover and W. E. Sondheim, Revue de Physique Appliquée, 12, 1487 (1977).

[10]C. L. Bennett, R. P. Beukens, M. R. Clover, H. E. Gove, R. B. Liebert, A. E. Litherland, K. H. Purser and W. E. Sondheim, Science 198, 508 (1977).

[11]C. L. Bennett, R. P. Beukens, M. R. Clover, D. Elmore, H. E. Gove, L. R. Kilius, A. E. Litherland and K. H. Purser, Science 201, 345 (1978).

[12]In most of the ^{14}C work at Rochester, M. Rubin of the U. S. Geological Survey has been a collaborator and has provided much valuable advice and assistance.

[13]D. Elmore, H. E. Gove, R. P. Beukens, A. E. Litherland, K. H. Purser and M. Rubin, Proceedings of the Second International Congress on the Shroud and Science, page 428, published by the International Center of Sindonology Turin, Italy (1978) ed. Piero Coero-Borga.

[14]K. H. Purser, P. Williams, A. E. Litherland, J. D. Stein, H. A. Storms, H. E. Gove and C. M. Stevens, Nucl. Instr. and Meth. (to be published).
[15]L. R. Kilius, R. P. Beukens, K. H. Chang, A. E. Litherland, H. W. Lee, D. Elmore, R. Ferraro, H. E. Gove and K. H. Purser, Nucl. Instr. and Meth. 171, 355 (1980).
[16]G. M. Raisbeck, F. Yiou, M. Lieuvin, J. C. Ravel, M. Fruneau and J. M. Loiseaux, papers included in the Proceedings of this conference.
[17]J. Thomas, K. Cochran, S. Krishnaswami, A. Mangini, P. Parker and K. Turekian, a paper included in the Proceedings of this conference.
[18]R. Middleton, J. Klein and H. Tang, a paper included in the Proceedings of this conference.
[19]G. W. Farwell, P. M. Grootes and F. H. Schmidt, a paper included in the Proceedings of this conference.
[20]T. H. Kruse, R. Moniot, G. Herzog, T. Milazzo and G. Hall, a paper included in the Proceedings of this conference.
[21]E. J. Stephenson, T. S. Mast and R. A. Muller, Nucl. Instr. and Meth. 158, 571 (1979).
[22]G. C. Ball, H. R. Andrews, R. M. Brown, N. Burn, W. G. Davies, Y. Imahori and J. C. D. Milton, a paper included in the Proceedings of this conference.
[23]G. M. Raisbeck, F. Yiou and C. Stephan, Le Journal de Physique Lettres 40, L241 (1979).
[24]L. R. Kilius, R. P. Beukens, K. H. Chang, H. W. Lee, A. E. Litherland, D. Elmore, R. Ferraro and H. E. Gove, Nature 282, 488 (1979).
[25]M. Paul, W. Henning, W. Kutschera, E. J. Stephenson and J. L. Yntema, Phys. Letts. 94B, 303 (1980).
[26]D. Elmore, N. Anantaraman, H. W. Fulbright, H. E. Gove, H. S. Hans, K. Nishiizumi, M. T. Murrell and M. Honda, Phys. Rev. Letts. 45, 589 (1980).
[27]W. Kutschera, W. Henning, M. Paul, R. K. Smither, E. J. Stephenson, J. L. Yntema, D. E. Alburger, J. B. Cumming and G. Harbottle, Phys. Rev. Letts. 45, 592 (1980).
[28]The measurement of ^{36}Cl in ground water at Rochester has involved a collaboration with H. W. Bentley, Department of Hydrology and Water Resources, University of Arizona.
[29]Workshop on Dating Old Ground Water Y/OWI/SUB-78 55412, ed. S. N. Davis, University of Arizona, March 1978.
[30]H. W. Bentley and S. N. Davis, a paper included in the Proceedings of this conference.
[31]The measurement of ^{36}Cl in meteorites at Rochester has involved a collaboration with J. R. Arnold and K. Nishiizumi, Department of Chemistry, University of California, San Diego.
[32]K. Nishiizumi and J. R. Arnold, a paper included in the Proceedings of this conference.
[33]D. Elmore, H. E. Gove, R. Ferraro, L. R. Kilius, H. W. Lee, K. H. Chang, R. P. Beukens, A. E. Litherland, C. J. Russo, K. H. Purser, M. T. Murrell and R. C. Finkel, Nature 286, 138 (1980).
[34]The measurement of ^{129}I in meteorites at Rochester has involved a collaboration with K. Nishiizumi and J. R. Arnold, Department of Chemistry, University of California, San Diego.
[35]J. C. Rucklidge, N. M. Evinsen, M. P. Gorton, R. P. Beukens, L. R. Kilius, H. W. Lee, A. E. Litherland, D. Elmore, H. E. Gove and K. H. Purser, Fifth International Conference on Ion Beam Analyses, February 1981, Sydney, Australia.
[36]J. C. Rucklidge, a paper included in the Proceedings of this conference.
[37]L. W. Alvarez, W. Alvarez, F. Asaro and H. V. Michel, Science 208, 1095 (1980).

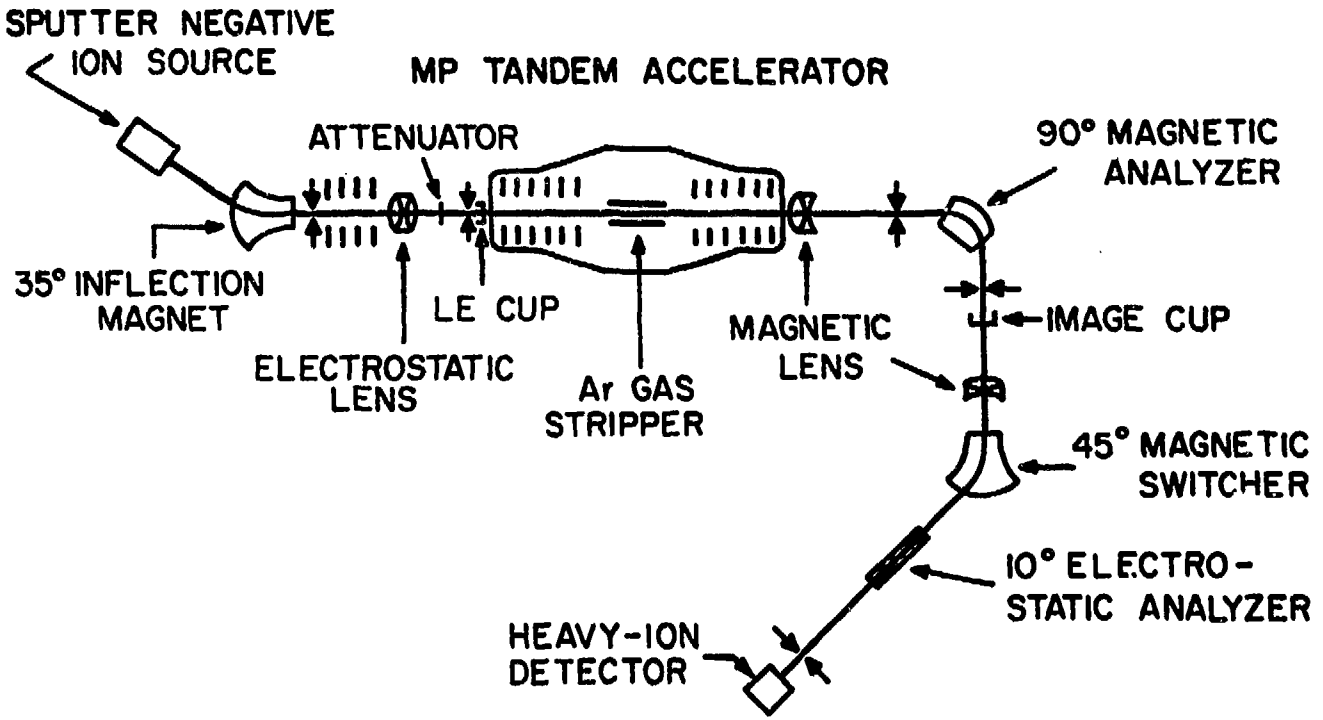

Figure 1. A schematic diagram of the system for ultrasensitive mass spectrometry employing the University of Rochester's MP tandem Van de Graaff accelerator.

ACCELERATOR MASS SPECTROMETRY WITH THE GRENOBLE AND ORSAY CYCLOTRONS

G.M. Raisbeck and F. Yiou
Laboratoire René Bernas, Centre de Spectrométrie Nucléaire et de Spectrométrie de Masse, B.P.1, F. 91406 Orsay.

1. Introduction

Three and one half years ago, at the Rochester meeting, we presented our first accelerator mass spectrometry measurements of ^{10}Be using the external ion source of the Grenoble cyclotron (1). Since that time the technique has been used to measure ^{10}Be in more than 100 geophysical samples, as summarized in another paper in these proceedings. We have also used the ALICE accelerator facility (linear accelerator plus cyclotron) at Orsay to detect ^{26}Al (half-life 730,000 years)(2) and ^{41}Ca (100,000 years) (3). While the latter measurements have so far been carried out only with enriched samples, they did demonstrate the feasibility of eliminating interference from lower atomic number isobars by analyzing fully stripped ions of the species being sought.

We describe here the present experimental status of these two techniques, following closely two papers presented recently at another conference (4) (5). We would like to stress that these techniques have not been developed arbitrarily, or as goals in themselves, but rather with certain applications in mind. It is therefore perhaps useful to first briefly outline these applications, which can be divided into three areas.

2 - Motivation

2a) Secular variation in cosmogenic isotope production rate : The production rate of cosmogenic isotopes produced in the earth's atmosphere depends essentially on three factors ; (i) the primary cosmic ray intensity, (ii) the strength of the geomagnetic field, (iii) solar activity (through the modulating effect of the solar wind). The study of cosmogenic nuclide profiles in appropriate geophysical reservoirs can thus potentially give information about these parameters in the past. For various reasons, including its abundance, half-life, and chemical behaviour, we have concluded that ^{10}Be is the best suited nuclide for such studies. The appropriate geophysical reservoirs include polar ice cores, marine and lacustrine sediments. The reason this aspect of our program has such high priority is that we feel accelerator mass spectrometry provides a powerful, and in many ways unique, possibility of inves-

tigating these effects, and their implications.

2b) Dating : Much of the early excitement regarding accelerator spectrometry has centered around dating, particularly with ^{14}C, and the potential extension to other, longer lived isotopes. It is important to realize, however, that the application and interpretation of these other isotopes is much less straight forward than with ^{14}C. In addition to the secular variation in production rates mentioned above, (which are strongly damped for ^{14}C) these other cosmogenic isotope are not necessarily homogenized with their stable isotopes before being incorporated into a reservoir. Measurement of the radioactive to stable ratio does not therefore automatically give the age of a sample. A potentially more powerful procedure is the combining of measurements of a pair of cosmogenic species. For example, in deep ice cores one can use the ratio of $^{36}Cl/^{10}Be$, which will decay with an apparent half life of 370,000 years. Because the nuclides are expected to remain fixed in the ice, the difference in the chemical behaviour of the two elements in this case is not important. In contrast, for sediment reservoirs the influence of chemical properties is likely to be very important. For this reason, the ratio $^{26}Al/^{10}Be$ is particularly interesting, because these two elements have similar chemical behaviour under many conditions. This is our primary motivation for trying to develop a capability for measuring ^{26}Al.

The isotope ^{41}Ca is produced primarily by neutron capture on ^{40}Ca at the earth's surface. There is thus perhaps a somewhat better chance for initial homogenization, although this must still be tested. However, the potential applications of this isotope, particularly for dating fossil bones, are so important, that we believe an experimental investigation is well warranted (6). It should be emphasized that, even if this ratio is not able to give absolute dates (because of a variable initial ratio in time or space), it should be useful in testing whether various samples found in the same location are contemporous or not. Such knowledge can often be very critical in studies of prehistoric sites.

2c) Environmental tracer : Knowledge of the behaviour of a cosmogenic isotope between the time it is produced and the time it is incorporated into one of the "permanent" reservoirs mentioned earlier is essential for the two applications mentioned above. It is for this reason that such studies have formed an important part of our initial measurements with ^{10}Be. While making such investigations, however, we have gradually come to realize that such

measurements of ^{10}Be, either alone or in conjunction with its shorter lived isotope ^{7}Be, can also be used as a tracer of various geophysical and geochemical transport processes in the atmosphere, precipitation, ocean etc... This aspect is thus likely to continue to play an important role in our program.

3 - Experimental Procedures

3a) Grenoble cyclotron

The first step in making measurements from natural samples is, of course, to extract the ^{10}Be. The method of doing this varies considerably, depending on the nature of the sample. In general, however, we first add a known quantity of ^{9}Be carrier to the sample. This ^{9}Be ($\sim$1.5mg) is always much larger than the "natural" ^{9}Be in the sample. Once they have become homogenized, the ^{10}Be and ^{9}Be are recovered with the same efficiency, so that by measuring only the final $^{10}Be/^{9}Be$ ratio, it is possible to calculate the initial number of ^{10}Be atoms in the sample. During much of our early work, we also added ^{7}Be to the initial sample, to act as tracer in following the Be through the various chemical steps. We have recently established, however, that at least some commercial sources of ^{7}Be contain measurable amounts of ^{10}Be. It is thus very important to check these solutions before using them for such a purpose. Once the Be has been chemically purified, it is converted to BeO, and made into sintered pellets, as described in Ref. (7). Similar pellets, having a known $^{10}Be/^{9}Be$ ratio, are made by mixing together solutions of known concentration of pure ^{9}Be and nearly pure ^{10}Be (whose concentration and isotopic composition have been established by a mass spectrometer in our laboratory). The $^{10}Be/^{9}Be$ ratio of the unknown sample is then determined by comparison with the known "standard".

A schematic diagram of the accelerator setup is shown in Fig. 1. The external ion source, cyclotron, and beam lines are first tuned up using $^{20}Ne^{+4}$, which has approximately the same charge/mass ratio as $^{10}Be^{+2}$. During this step the detectors are moved out of the beam, and the current reaching the chamber is measured with Faraday cup FC-2. A fine tuning is then accomplished by using ^{10}B from a BN sample. For this step it is necessary to use Ar as a support gas, so as to avoid interference from the $^{20}Ne^{+4}$ while measuring the $^{10}B^{+2}$. The final tuning for ^{10}Be is made by adjusting the radio frequency of the cyclotron in proportion to the mass difference between ^{10}Be and ^{10}B. The support gas is changed back to Ne, the detectors and absorber foil are moved into position, and the machine is now ready for ^{10}Be measurements.

In principle, all the parameters should remain fixed for the rest of the run. In practice we sometimes find that during the run the transmission changes, and that we need to repeat one or more of the above steps to optimize it. We have operated with overall transmission (from the ion source to detector) from 1 to 6.7%, with $\sim$ 3% considered typical. By measuring ^{7}Be in a sample before and after a run, we have established that the conversion efficiency of BeO to Be^{+2} in the ion source is $\sim 10^{-3}$. The overall detection efficiency is thus a few times 10^{-5}. The ^{10}Be (and any contaminating ^{10}B) ions are accelerated in the cyclotron to $\sim$ 30MeV. An Al absorber foil (13.2mg/cm^2) is used to absorb the ^{10}B ions while letting the ^{10}Be pass. These ions are detected in a detector telescope (ΔE=8.2μm, E=100μm), connected through standard electronics to a two dimensional (64x64) multichannel analyzer.

The samples (and standards) are mounted on a wheel, which is located near the ion source. By rotating this wheel, any one of ten samples can be introduced into the ion source chimney in a few seconds, without extinguishing or changing any parameters of the ion source discharge. The wheel itself is isolated from the ion source, and the sample is then biased by a voltage of typically-1000 Volts, so as to attract gas ions from the source plasma, and cause sputtering of the sample. The output of the ion source can be rapidly and reproducibly switched between $^{9}Be^{+2}$ and $^{10}Be^{+2}$ by changing the extraction voltage.

A typical measuring sequence is thus the following. With a standard in place, the Faraday cup FC-1 is inserted, and the ^{9}Be current measured (typically about 5μA). The extraction voltage is then set for ^{10}Be, FC-1 retracted and a 100 second count of ^{10}Be events in the detector telescope recorded. During the counting period, both the extraction voltage and the dynode voltage are continuously monitored. If they deviate by more than a certain amount from their nominal values, (for example, due to "sparking") the ^{10}Be acquisition and counting sequence are automatically blocked until the nominal values are reestablished. At the end of the counting period the extraction voltage is changed back to the value for ^{9}Be, and its current again measured. An average of the two ^{9}Be readings is thus used to established a (relative) $^{10}Be/^{9}Be$ value. An unknown sample is now rotated into the ion source, and the above sequence repeated (usually several times). Finally, after one or several unknowns have been measured in this way, the standard is again measured to insure that there have been no large changes in the transmission during the measurements. The $^{10}Be/^{9}Be$ of the unknown is then calculated by comparing

with the average of the before and after standards. The uncertainty on the measurement is estimated both from the statistics of the number of ^{10}Be events counted, and the reproducibility of the $^{10}Be/^{9}Be$ ratio of the standard. In order to give some idea of this reproducibility, we show in Fig. 2 the results of measurements on three separate (but having identical $^{10}Be/^{9}Be$) standards during a 10 hour running period. The standard deviation of the measurements (5.9%) is comparable to the statistical uncertainties on the individual measurements (as given by the error bars). Thus, during this period at least, other sources of random error must have been small in comparison. (This is not always the case however, and we do sometimes have significant drifts in transmission with time).

By measuring blank samples containing only ^{9}Be, immediately after a concentrated standard, we have shown that the cross contamination between samples is less that 1 part in 10^{3}, even a few seconds after changing samples.

Once all the samples on a given wheel have been measured in this way, the sample wheel itself is changed. While the ion source must be shut down to do this, the time necessary for such a change is less than 30 minutes, and the cyclotron parameters are not touched. The lifetime of the ion source itself is usually $\sim$24 hours. A change of the complete ion source takes only about 30 minutes.

The present practical sensitivity of our procedure is $\sim 10^{7}$ atoms of ^{10}Be, although the machine background is considerably less than this.

3b) ALICE

Because the interfering isobars for ^{26}Al and ^{41}Ca have longer ranges than the nuclide to be measured, the technique of preferential absorption cannot be used. We have therefore developed a procedure which consists of accelerating the nuclides to be measured to a sufficient energy that a significant fraction of them can be fully stripped of electrons, and then separating them from the isobar by magnetic analysis (2) (3).

The energy available at the Grenoble cyclotron is presently insufficient to permit a significant probability of fully stripping ^{26}Al or ^{41}Ca (although a "booster" stage soon to be installed may make such experiments feasible). We have therefore used the accelerator facility ALICE (linear accelerator + cyclotron) at Orsay for this work. A schematic diagram of the experimental setup for ^{41}Ca is shown in Fig. 3. A similar setup for ^{26}Al has been given in Ref. (2). The samples for ^{26}Al consisted of proton irradiated Al foils

in which the ^{26}Al had been determined (2). For ^{41}Ca we used neutron irradiated Ca metal in which the ^{41}Ca content was calculated both from an independent neutron monitor, and from counting ^{49}Ca (half-life = 8.72 min), and taking into account the relative isotopic abundances and cross sections for the reactions ^{40}Ca (n,γ) ^{41}Ca and ^{48}Ca (n,γ) ^{49}Ca. In both cases, samples having concentrations $^{26}Al/Al$ or $^{41}Ca/Ca$ of 10^{-9} to 10^{-11} were used. For Al a sputtering type ion source was used, while for Ca a heated furnace was used to evaporate the Ca into the ion source. Currents at the ion source of Al^{+3} (or Ca^{+4}) were typically 30-40μA. The ions of interest were initially accelerated in the linear accelerator to 1.15 MeV/nucleon. They were then partially stripped and further accelerated in the cyclotron. At the exit of the cyclotron the ions were passed through a thin foil to complete the stripping, before being passed through a 120° magnetic analyzer. The accelerator and beam line parameters were initially tuned up using ^{26}Mg (or ^{41}K). These beams also served to calibrate the magnetic analyzer, which then could be further adjusted using an NMR probe. The detector consisted of a pair of silicon surface barrier detectors (ΔE=17μm ; E=200μm) connected through standard electronics to a two dimensional (64x128) multichannel analyzer. Count rates of the ^{26}Al or ^{41}Ca were normalized to the current of ^{27}Al or ^{40}Ca at the ion source.

Based on our present work, we have estimated that we could measure samples having concentrations of $^{26}Al/Al$ or $^{41}Ca/Ca$ of $\sim 10^{-12}$. This value however, is still several orders of magnitude larger than the cosmogenic produced concentrations in some interesting "natural" samples. To reach the necessary sensitivity, one alternate is to "enrich" the original sample using an isotope separator. Our work along these lines has been described elsewhere (8).

It was clear to us from early in this work that ALICE was far from optimally suited as regards to making precise or numerous measurements of cosmogenic isotopes in natural samples. One reason for this is its rather poor transmission efficiency ($\sim 10^{-4}$). A second limitation for the moment is the long time that it takes to change from one sample to another using the normal source. At the present time both an oven source and a sputter source allowing multiple samples to be exchanged rapidly are being tested.

It should be noted that our primary objective in these experiments was to demonstrate that the technique of complete stripping to eliminate isobars is a viable procedure for accelerator spectrometry. Such a technique is of course not limited in principle to cyclotrons. It was thus gratifying for us to note at this meeting that several other groups using tandem accele-

rators with "booster" stages are also considering using this procedure.

Acknowledgements

The experimental procedure at the Grenoble cyclotron has been developed in collaboration with J.M. Loiseaux, M. Lieuvin, M. Fruneau and J.C. Ravel. The work at ALICE has been carried out with the help of C. Stephan. It is a pleasure to acknowledge our indebtedness to these colleagues.

References

1 - G.M. Raisbeck, F. Yiou, M. Fruneau, M. Lieuvin and J.M. Loiseaux, Proc. 1st Conf. Radiocarbon Dating with Accelerators, University of Rochester 38 (1978).

2 - G.M. Raisbeck, F. Yiou and C. Stephan, J. Phys. Lett. 40, L241 (1979).

3 - G.M. Raisbeck and F. Yiou, Proceedings of 20th Int. Symposium for Archaeometry, Paris 1980, Revue d'Archéométrie N°4, P. 121.

4 - G.M. Raisbeck and F. Yiou, Proc. 2nd Int. Conf. on Low Level Counting, High Tatras, Czechoslovakia, Nov. (1980) (in press).

5 - F. Yiou and G.M. Raisbeck, ibid.

6 - G.M. Raisbeck and F. Yiou, Nature 277, 42 (1979).

7 - G.M. Raisbeck, F. Yiou, M. Fruneau, and J.M. Loiseaux, Science 202, 215 (1978).

8 - G.M. Raisbeck and F. Yiou, Proc. 10th Int. Conf. Electromagnetic Isotope Separators, Zinal, Switzerland, Sept. (1980). Nucl. Inst. Meth. (in press).

Figure captions

Fig. 1 - Schematic diagram of experimental layout at Grenoble.

Fig. 2 - Measured ratio (normalized to average value) of 3 standards (represented by different symbols) having $^{10}Be/^{9}Be = 8.24 \times 10^{-12}$, measured periodically over 10 hour running period. Dashed lines correspond to standard deviation of all points. Error bars on points are one standard deviation statistics. Sample wheel was changed at time corresponding to $\sim$5 hours.

Fig. 3 - Schematic diagram of experimental layout at ALICE.

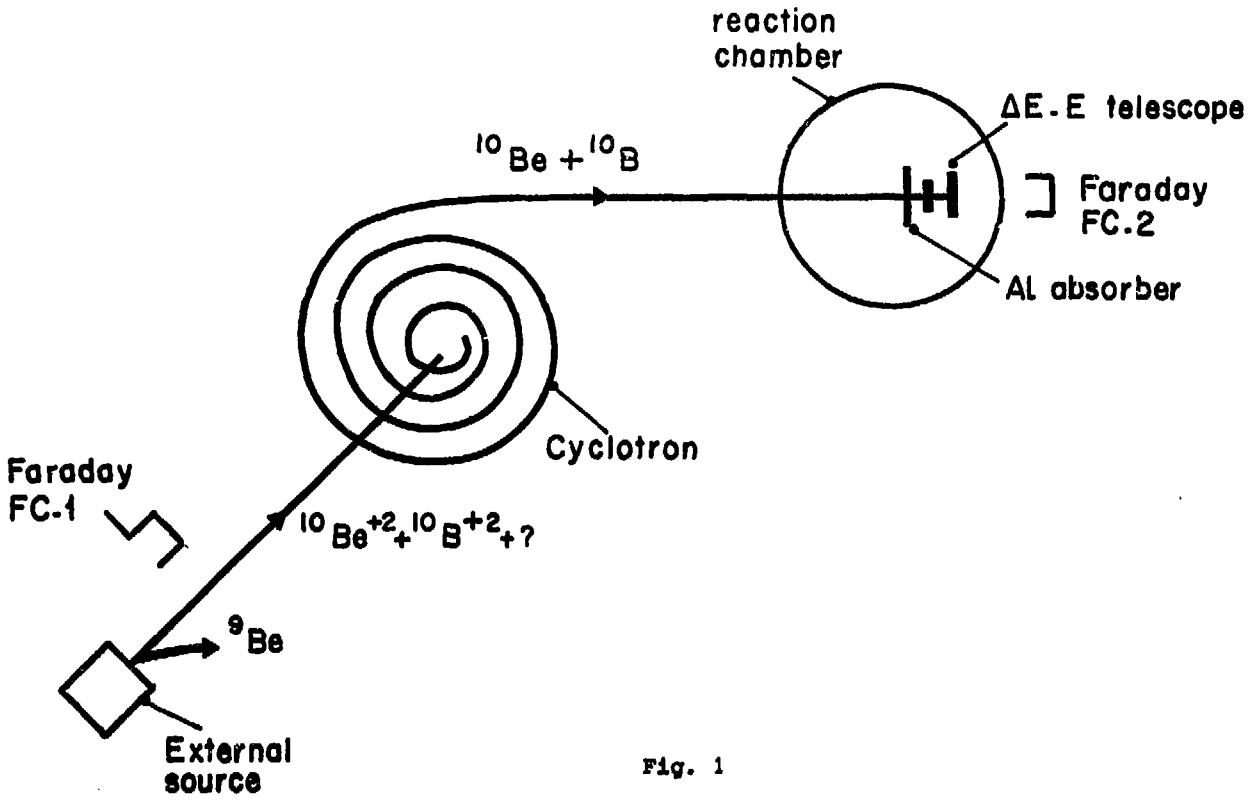
reaction
chamber
ΔE-E telescope
$^{10}Be + ^{10}B$
Faraday
FC.2
Al absorber
Cyclotron
Faraday
FC-1
$^{10}Be^{+2} + ^{10}B^{+2} + ?$
^{9}Be
External
source

Fig. 1

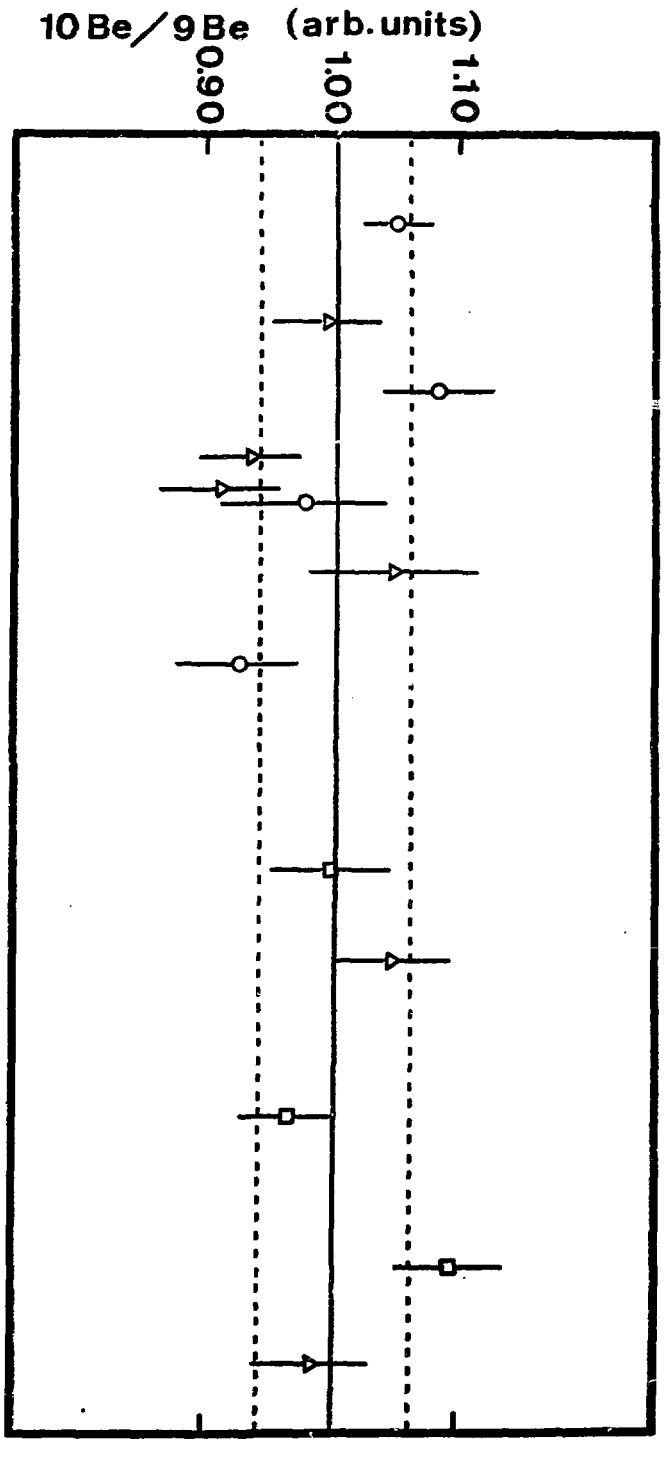

Fig. 2

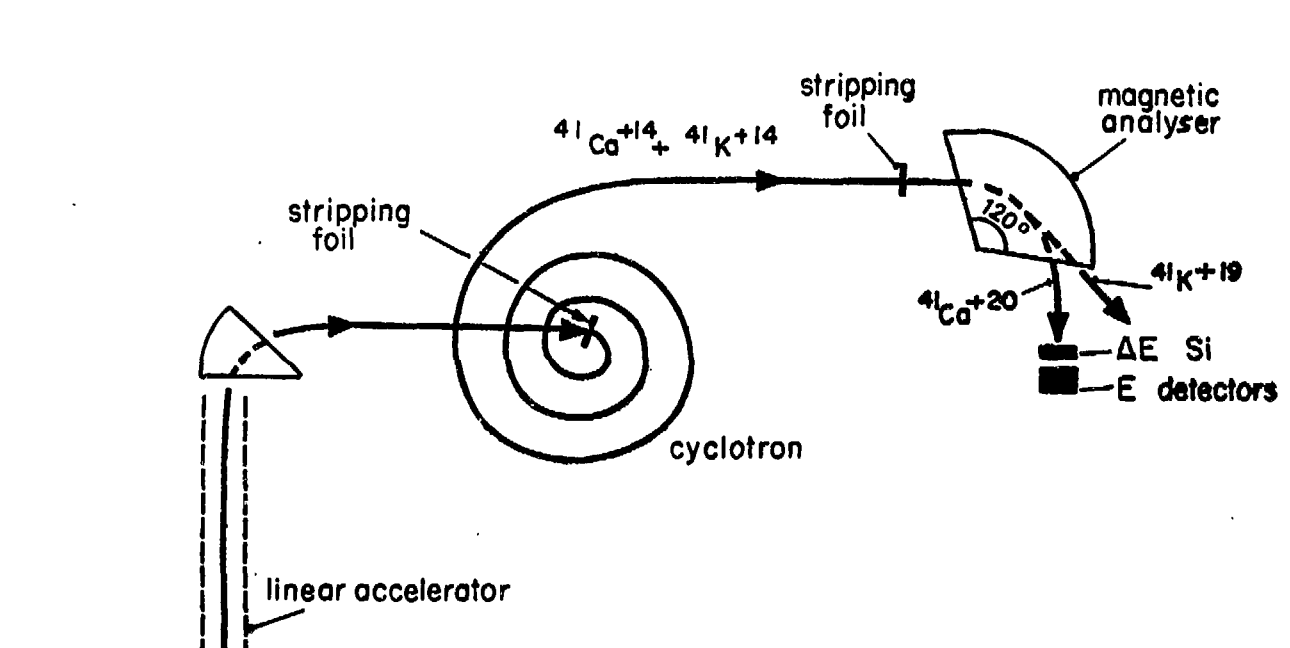
stripping foil
magnetic analyser
$^{41}Ca^{+14}$ + $^{41}K^{+14}$
stripping foil
120°
$^{41}K^{+19}$
$^{41}Ca^{+20}$
ΔE Si
E detectors
cyclotron
linear accelerator
$^{41}Ca^{+4}$
$^{40}Ca^{+4}$
Ca sample
ion source

Fig. 3

RADIOCARBON DATING WITH THE CHALK RIVER MP TANDEM ACCELERATOR

G.C. Ball, H.R. Andrews, R.M. Brown, N. Burn,
W.G. Davies, Y. Imahori and J.C.D. Milton
Atomic Energy of Canada Limited
Chalk River Nuclear Laboratories
Chalk River, Ontario, Canada K0J 1J0

I. INTRODUCTION

During the past three years an automated radiocarbon dating system based on the MP Tandem accelerator has been developed for the analysis of ^{14}C in groundwater samples from the nuclear waste disposal research program and other small samples of scientific interest. At the present time $^{14}C/^{12}C$ ratio measurements can be determined with an accuracy of about 5% and the system background levels ($\sim$ 35000 - 45000 years) are totally determined by sample and/or ion source contamination.

Our goal has been to develop a dedicated reliable system for routine analysis that will produce accurate results with a minimum expenditure of human resources and accelerator beam time. Improvements required to operate the tandem accelerator as a quantitative tool have also benefited the rest of the experimental nuclear physics program. The early evolution of the dating facility was described previously[1,2]. This paper is a brief report of the current status at Chalk River; recent detailed descriptions have been published elsewhere[3,4].

II. EXPERIMENTAL TECHNIQUE

A schematic layout of the dating system is shown in Fig. 1. Forty MeV $^{14}C^{4+}$ ions from the Chalk River MP Tandem accelerator are analyzed by two (90° and 56°) bending magnets followed by a Wien cross-field velocity filter and are detected in a gas proportional-ΔE, silicon surface barrier-E counter system.

Two stages of magnetic analysis are required[2] to eliminate background ions resulting from the macroscopic beams of 38.9 (39.4) MeV $^{13}C^{4+}$ ($^{12}C^{4+}$) ions that are injected as $^{13}CH^-$ ($^{12}CH_2^-$) molecular ions, stripped at the terminal and subsequently undergo charge exchange collisions in the residual gas of the first (90°) magnet box to emerge into the exit beam line.

Carbon and/or oxygen ions of the same magnetic rigidity that arise from charge exchange with residual gas in the accelerator tubes are removed by the

velocity filter. When this filter is set for $^{14}C^{4+}$ ions the vertical displacement, Δy, produced at the counter slits for other ions is given by:

$$\Delta y \simeq 20 \left(\frac{M}{q} - 3.5\right) \text{ mm}$$

where M and q are the mass and charge of the ions. Typical spectra obtained with and without the velocity filter are shown in Fig. 2. It can be seen that with the velocity filter off, $^{13}C^{4+}$ ions present in the residual energy spectrum gated on a ^{14}C ΔE window would limit the ^{14}C sensitivity for old samples. However, the 5 mm vertical displacement produced by the velocity filter reduces the transmission of these ions by $\sim 10^{4}$.

The $^{14}C/^{12}C$ ratios were determined by periodically injecting $^{12}C^{-}$ ions and adjusting all magnetic elements to transmit 40 MeV $^{12}C^{4+}$ ions to the counter cup located in front of the ΔE-E detector telescope. All measurements were made relative to a standard, NBS oxalic acid, that is 105% of modern. In earlier measurements an irradiated graphite cone was used to optimize all system parameters for the transmission of ^{14}C. However, this procedure is no longer necessary.

III. AUTOMATIC DATA ACQUISITION AND CONTROL SYSTEM

A versatile 24 channel laboratory programmer was used to provide regular updating of the system parameters for $^{14}C(^{12}C)$ counting, control and sequencing of the event recorded data and automatic GVM stabilization. The programmer, which is modeled after an original concept by Schwender et al.[5] consists of the following basic elements: a 10 kHZ internal clock capable of being prescaled to provide 1 HZ - 10 kHZ clock pulses, a 50 x 40 matrix plugboard, 24 independent device control (BNC) outputs, individual inhibit inputs for each channel, 6 ac power channel outputs and provisions for internal and/or external resets.

The outputs from each channel go to specialized local controllers, to the on-line PDP-1 computer or to the data acquisition control system. Most of the magnetic elements are controlled through relay-selected preset reference potentiometers. The exact fields for the 90° analyzing magnet are obtained by a digitally-controlled locking NMR system that acts through a magnet trim coil.

During periods of ^{14}C counting the generating voltmeter (GVM) must hold the terminal voltage to within ±5 kV. Stability somewhat better than this requirement has been achieved by improving the bearings in the GVM, by positively grounding the rotor with a brush and by periodic careful cleaning. However, small unexplained jumps in the GVM calibration still occur and therefore it has been necessary to provide automatic correction to the GVM as part of the measurement sequence. This was done by digitizing the integrated currents from a pair of pneumatically-driven retractable slits located ∿ 1 m in front of the regular image slits which are permanently retracted to provide a broad system energy acceptance.

The automatic measurement sequence is summarized in Table I. It is divided into "cycles" and "epicycles" and the cycle number is used to label all event recorded data. In this manner, the time evolution of the various quantities can be monitored and periods of malfunction or instability can be identified. The "cycles" which last one minute are used for direct ^{14}C counting and also monitor the ^{12}C beam current transmitted to the object cup (see Fig. 1). Every N(usually 10) cycles the ^{12}C beam is transported to the counter cup and the transmission measured before and after the GVM stabilization is updated. Representative yield spectra are shown in Fig. 3.

TABLE I

AUTOMATIC MEASUREMENT SEQUENCE

CYCLE (60 sec.)

[Beam transport and terminal volts set for ^{14}C to detectors.]

1. Advance cycle counter.
2. Inject ^{12}C; integrate ^{12}C at object Faraday cup 6 sec. (See Fig. 1)
3. Inject mass 14; count ^{14}C at detector 45 sec.
4. Every N (usually 10) cycles enter epicycle.

EPICYCLE (210 sec.)

[Beam transport and terminal volts set for ^{12}C at counter cup.]

1. Inject ^{12}C; change beam transport to bring ^{12}C to Faraday cup at counter position. (See Fig. 1)
2. Integrate ^{12}C on counter cup 50 sec. [Pre-update transmission.]
3. Update GVM reference (20 sec.) by signal from retractable stabilization slits.
4. Integrate ^{12}C on counter cup 50 sec. [Post-update transmission.]
5. Return to cycle.

[All particle events and integrator pulses labelled by cycle number.]

IV. SAMPLE PREPARATION

At the present time, our standard source material is 5 mg of carbon black mixed with 20 mg of reduced Fe powder to give improved cohesion and thermal conductivity. This material is pressed into a ring within the base of an aluminum source holder. The carbon black is obtained by oxidation of the carbonaceous material to CO_2 followed by reduction with an excess of Mg metal at 900°C. With our existing Cs^+ ion sputter source, a "burn in" time of $\sim$ 1-2 hours is required before the C^- beam reaches a stable output current of $\sim$ 1 μA. Other source materials such as iron carbide and pyrolytic graphite[6] have been tried. No improvements were obtained with the iron carbide samples; however, preliminary results with pyrolytic graphite show a significant reduction in the "burn in" time ($\sim$0.5 hr.) and a $\approx$ 50% increase in beam current. A more detailed discussion of our source preparation techniques is given elsewhere[3].

V. SYSTEM PERFORMANCE

As mentioned previously, a graphite sample enriched to $\sim$ 25 times modern ^{14}C was used to facilitate setting up and testing the system performance. The short term stability determined from eight successive 0.5 hr. runs was 3.7% for the standard deviation of a single ratio measurement. However, the long term reproducibility observed over a period of several days was significantly worse, $\sim$ 5.2%. We believe that this increase results primarily from the lack of reproducibility in positioning the sample cones. The absolute $^{14}C/^{12}C$ ratio determined from direct ^{14}C counting for NBS oxalic acid standard was $(1.17 \pm 0.03) \times 10^{-12}$ in good agreement with the accepted radiometric value[7], $(1.236 \pm 0.006) \times 10^{-12}$.

Known samples prepared from a series of quantitative dilutions of atmospheric CO_2 with ^{14}C-free CO_2 were used to test for ^{14}C contamination as well as other systematic errors in our direct counting technique. The results are summarized in Table II. A comparison of conventional (liquid scintillation counting) and accelerator ^{14}C determinations for two groundwater samples is also shown in Table II. The agreement obtained for the EMR-1 sample is excellent. For the Pebble Creek Hot Spring sample the large discrepancy is believed to result from contamination of the sample after the aliquot for radiometric analysis was removed.

TABLE II

SYSTEM PERFORMANCE WITH KNOWN SAMPLES

Sources: 5 mg carbon black + 20 mg reduced Fe powder.

KNOWN DILUTIONS

Spike CO_2 (2.5 x NBS oxalic acid) in ^{14}C-free CO_2.

Nominal		Measured	
% Spike	Equiv. Age	% Spike	Equiv. Age
26.3 ± .21[a]	3040 ± 100	24.4 ± 1.5[b]	3660 ± 508
18.2 ± .36	6090 ± 150	14.5 ± 0.9	7960 ± 513
6.57 ± .19	14500 ± 250	6.2 ± 0.6	14990 ± 800
1.13 ± .03	29060 ± 250	1.0 ± 0.3	30070 ± 2480
0.52 ± .02	35480 ± 320	0.57 ± 0.1	34720 ± 1450

GROUNDWATER CARBONATE SAMPLES

	(% Modern ^{14}C)	
	Liq. Scint. Ctg. (U. of Waterloo)	Accel. Meas.
Pebble Creek Hot Spring	1.5 ± 0.5 [b]	3.7 ± 0.6[b]
Meagher Creek EMR-1	5.4 ± 0.5	4.6 ± 0.7
Values obtained over several years using a new source for each run, made from a common preparation of carbon black.		6.1 ± 0.9
		6.8 ± 1.0
		5.3 ± 0.8
		Wt. Ave. 5.5 ± 0.5

a) Estimated dilution error
b) 1 Std. Deviation counting statistical error

A fundamental limitation of the present accelerator dating system is the high background level which varies from run to run in the range of ∿ 35000 - 45000 yr. The background level for each run is determined using samples of industrial graphite or carbon of petroleum or limestone origin. Fortunately, the background has been found to remain constant during a run (i.e. for 3-4 days). Tests with the irradiated graphite sample have shown no evidence of cross contamination within the source. Small C^- beams are produced when the Cs^+ beam is allowed to impinge on a pure Al cone and the absolute ^{14}C count rate (i.e. $^{14}C^{4+}$ ions/sec) is approximately equal to that of a graphite or

or limestone sample. This suggests that the background results from the cracking of modern carbonaceous molecules onto the sample surface by the Cs^+ beam. However, when the source pressure was reduced by the addition of a cold trap, no change in the background level was observed.

VI. FUTURE PLANS

Until mid 1982 when the tandem will be shut down for the installation of the Superconducting Cyclotron post accelerator, work will continue to improve accuracy, to develop new sample preparation techniques and to understand and reduce the system background. After the cyclotron installation the program is expected to continue at a new target location where it can be extended to other isotopes of interest.

ACKNOWLEDGEMENTS

The success of this program would not have been possible without the assistance of the entire Tandem support group and operations staff. We would especially like to thank R.L. Brown for invaluable help with the electronics, R.B. Walker for the design and construction of several specialized controllers, J.P.D. O'Dacre for improvements to the GVM and NMR, R.E. Howard for design changes and construction of the new laboratory programmer and M.G. Steer and N.C. Bray for the mechanical construction of the velocity filter.

REFERENCES

1. H.R. Andrews, G.C. Ball, R.M. Brown, N. Burn, W.G. Davies, Y. Imahori and J.C.D. Milton, Proc. 1st Conf. on Radiocarbon Dating with Accelerators, University of Rochester, H.E. Gove (Ed.) 114 (1978).
2. H.R. Andrews, G.C. Ball, R.M. Brown, W.G. Davies, Y. Imahori and J.C.D. Milton, 10th Int. Radiocarbon Conf., Berne/Heidelberg, Radiocarbon 22, 822 (1980).
3. R.M. Brown, H.R. Andrews, G.C. Ball, N. Burn, W.G. Davies, Y. Imahori and J.C.D. Milton, IAEA Symposium in Methods of Low-Level Counting and Spectrometry, West Berlin, Paper IAEA-SM-252-61 (1981) to be published.
4. H.R. Andrews, G.C. Ball, R.M. Brown, N. Burn, W.G. Davies, Y. Imahori and J.C.D. Milton, 3rd Int. Conf. on Electrostatic Accelerator Technology, Oak Ridge, Tennessee, IEEE Trans. on Nucl. Sci. (1981) to be published.
5. G.E. Schwender, D.R. Goosman and K.W. Jones, Rev. Sci. Instr. 43, 832(1972).
6. R.E.M. Hedges, J.O. Ward and N.R. White, Nucl. Instr. and Meth. 173, 409 (1980).
7. I. Karlen, I.U. Olsson, P. Kallberg and S. Kilicci, Arkiv fur Geofysik 4, 465 (1964).

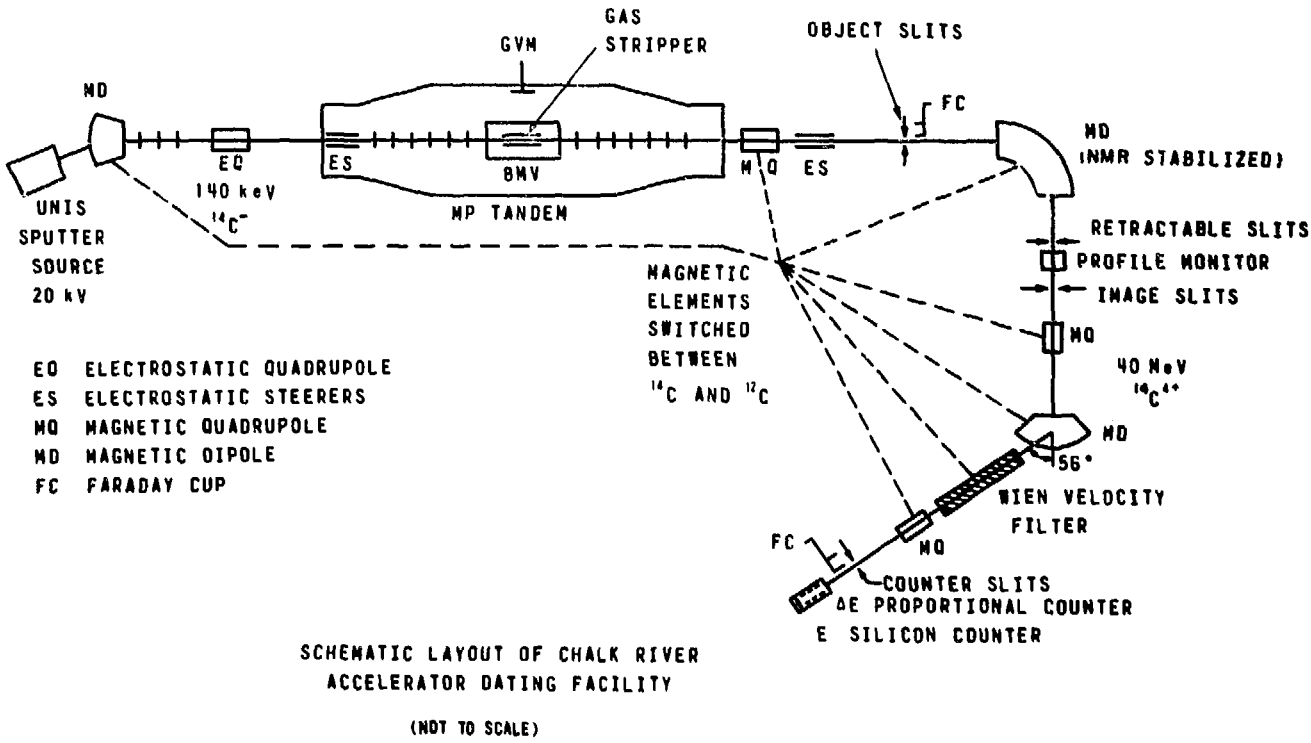

Fig. 1 A schematic layout of the Chalk River Accelerator Dating Facility

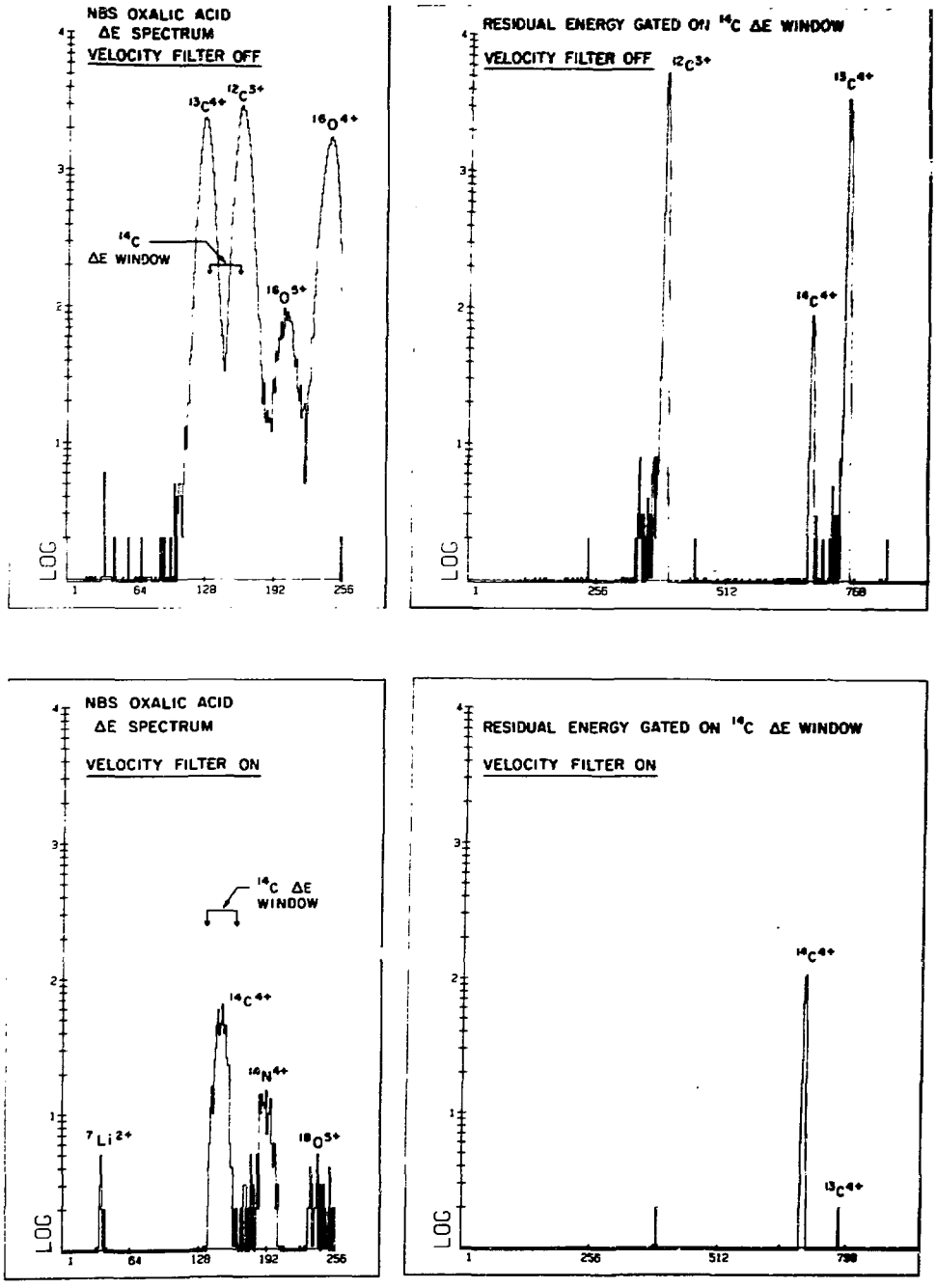

Fig. 2 Particle spectra obtained with and without the velocity filter in operation.

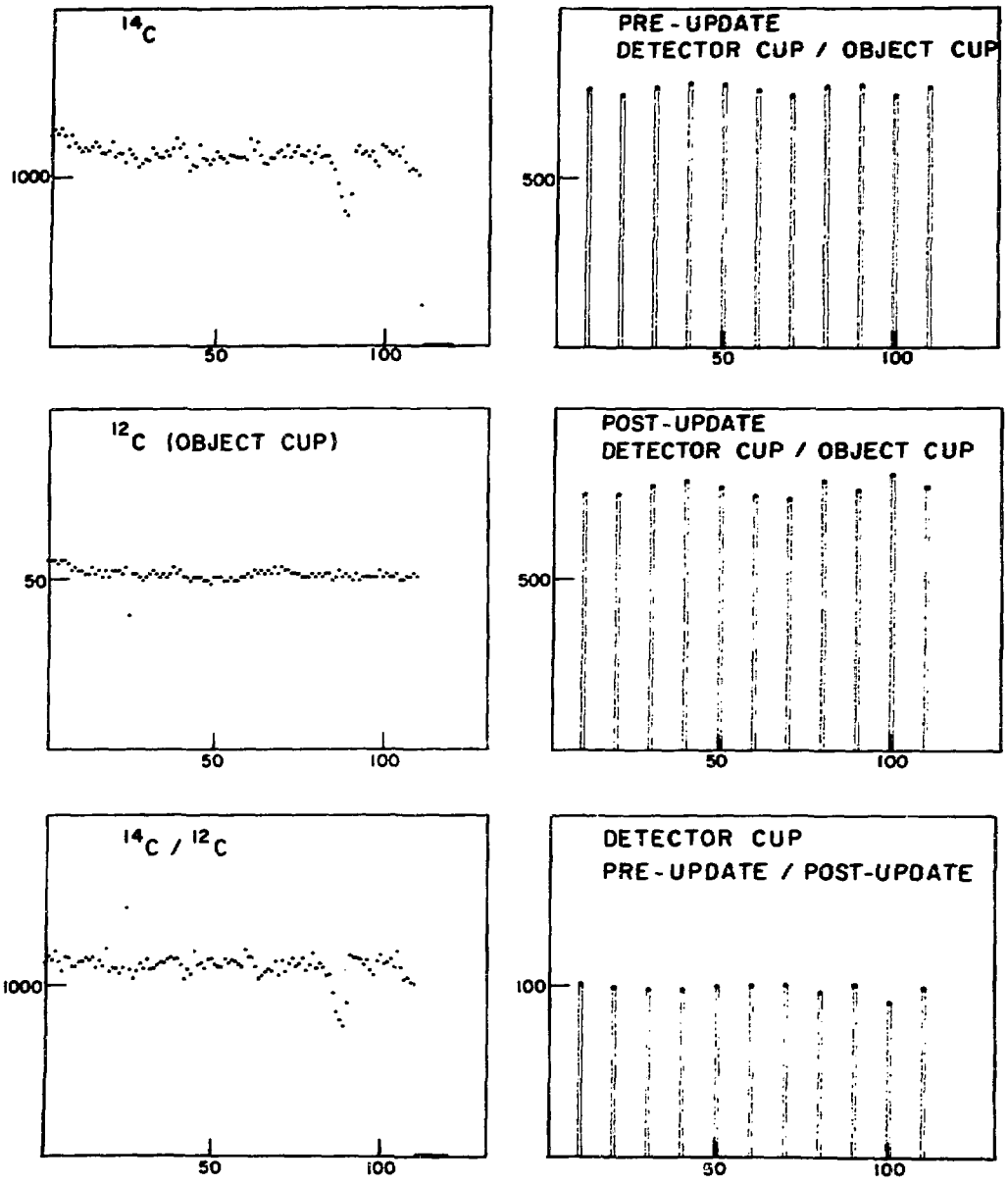

Fig. 3 Representative yield spectra from the automated data acquisition system.

THE ROLE OF ACCELERATOR MASS SPECTROMETRY IN NUCLEAR PHYSICS

W. Kutschera
Argonne National Laboratory, Argonne, IL 60439

1. Introduction

Accelerator Mass Spectrometry (AMS) was developed in nuclear physics laboratories and up to now all experiments were performed at these places. However, AMS is being applied to a variety of fields which have very little to do with nuclear physics. It may therefore be interesting to ask what the implications are for its original field. I think they can be divided in two domains. First, there are clearly instrumental implications. The overall demand of AMS for high efficiency ion sources, great stability, flexibility, and control of the entire accelerator system is certainly beneficial for the performance of any nuclear physics program. An example will be discussed in section 2. Second, AMS can be conveniently used to determine nuclear quantities of interest when the measurement involves very low radioisotope concentrations. Examples are the half-life measurement of ^{32}Si and the cross section measurement of the $^{26}Mg(p,n)^{26}Al$ reaction which will be discussed in sections 3 and 4, respectively. As the overall detection efficiency will improve there are some interesting problems in nuclear physics and elementary particle physics which are tempting to try. These include light and heavy ion capture cross section measurements, double β-decay studies, search for exotic particles (quarks and heavy hadrons), and possibly geologic solar neutrino detection measurements. Although most of these experiments are beyond the present capability of AMS, some general aspects will be discussed in section 5.

2. A ^{64}Ni Beam for the Argonne FN Tandem-Superconducting Linear Accelerator System

A general trend in AMS is to keep the sample size small. This meets very well the conditions of producing beams from enriched and therefore expensive isotopes. At Argonne we are using for our AMS experiments[1] the inverted Cs-beam sputter source.[2] This source allows an easy mounting of almost any shape of sample. We are frequently using pellets of 6 mm diameter pressed from metal powders with a standard laboratory press. Since there was a demand from nuclear physicists for a ^{64}Ni beam from the tandem-linac system, we utilized this technique with isotopically enriched material (93% ^{64}Ni). Two hundred mg of nickel metal powder were pressed into a pellet and mounted in the inverted sputter source. With average running conditions of the ion source such a pellet provided a $^{64}Ni^-$ beam of 300 nA for 50 hours, losing about half its mass. From this one calculates a total sputter rate of 2 mg/h and a negative ion efficiency of 3.6×10^{-4}. With current prices for enriched ^{64}Ni material the beam costs are 30 \$/h. Up to now this beam has been used with the tandem-linac system for a total running time of ten days. 10 - 20 nA of $^{64}Ni^{19+}$ ions at 290 MeV energy were used at the target for γ-ray spectroscopy experiments.

It is apparent from the above numbers that the negative ion efficiency is quite low. Improvements would be most desirable, both to lower the beam costs for nuclear physics experiments and to increase the sensitivity for our AMS experiments[3] with ^{59}Ni. The recent development of negative-ion sources with very high output[4] look very promising and may provide efficiencies of up to a few per cent.

3. The Measurement of Long Half-Lives

It is well established that with increasing half-life the counting of ions eventually becomes a more efficient detection method of radioisotopes than the counting of decays. However, where this transition occurs is difficult to define, since the detection limits of the two methods depend strongly on the specific radioisotope. In any case, we expect that this transition will be pushed towards shorter and shorter half-lives with improved detection efficiency of AMS. If we arbitrarily choose a half-life of one year for this limit, we are left with about 140 radioisotopes plotted in Fig. 1. They cover a range of eighteen orders of magnitude. Out of these only nine have been used for AMS so far: ^{3}He, ^{10}Be, ^{14}C, ^{26}Al, ^{32}Si, ^{36}Cl, ^{41}Ca, ^{59}Ni and ^{129}I. Basic to any practical use of radioisotopes is the knowledge of its half-life. There exist still a few interesting isotopes whose half-life is poorly known. One of those was, until recently ^{32}Si. At the time we got interested in remeasuring its half-life with AMS, the generally accepted value was around 300 yr.

Long half-lives are conveniently measured by the radioactive decay law,

$$\frac{dN}{dt} = -\lambda N \qquad (1)$$

where dN/dt is the disintegration rate and N the number of radionuclei. If both numbers are measured, the half-life can be calculated from the relation

$$T_{\frac{1}{2}} = \ln 2/\lambda \qquad (2)$$

In our experiment[5] a $^{32}Si/Si$ ratio of $(2.82 \pm 0.50) \times 10^{-8}$ was measured from a sample material (K_2SiF_6) enriched in ^{32}Si through the $^{30}Si(t,p)^{32}Si$ reaction. In order to separate a strong ^{32}S background from the ^{32}Si ions we used an energy loss dispersion technique in conjunction with a split-pole magnetic

spectrograph.[1,5] The specific activity of the same material was measured with a liquid scintillation technique to be 7883 ± 250 (dis/min)/mg Si. From Eq. (1) we then obtain

$$T_{\frac{1}{2}} = 101 \pm 18 \text{ yr}$$

This is a factor of three shorter than previously measured values (see Fig. 2). A similarly short value for the half-life, $T_{\frac{1}{2}} = 108 \pm 18$ yr was found in an independent AMS measurement by the Rochester group.[6]

Fig. 2 summarizes past and present ^{32}Si half-life measurements. There is a clear trend towards shorter half-lives in recent years. The data points labelled as "σ estimated" utilized relation (1), however, without measuring N explicitly. N was calculated from estimates on the respective production cross section (For details see Ref. 5). A serious discrepancy exists between the two geophysical measurements labelled "ice" (Ref. 7) and "sediment" (Ref. 8), and the accelerator measurements.[5,6] Both geophysical results were obtained from the depth distribution of cosmic ray produced ^{32}Si in terrestrial reservoirs, ice from Greenland and sediment from the Gulf of California, respectively. A key assumption in these measurements is a constant influx of cosmogenic ^{32}Si into these reservoirs. If neither the geophysical nor the accelerator measurements are subject to unknown experimental errors then the apparent discrepancy in half-life values indicate that the transport of ^{32}Si from the origin to the respective reservoirs is not understood. A somewhat less likely explanation would be variations in the cosmogenic ^{32}Si production caused by fluctuations in the cosmic-ray flux. It would be very desirable to perform another measurement of the half-life by an independent method. With a sufficiently large amount of ^{32}Si it seems feasible to do a decay measurement following the decrease in activity over a period of a few years.

The AMS technique to measure long half-lives can obviously be applied to other radioisotopes. We are presently concentrating our efforts to measure the half-life of ^{60}Fe where only a single value was measured.[9] A method to detect ^{60}Fe with the Argonne tandem-linac system is described in a contribution to this symposium.[3]

4. The Measurement of Nuclear Cross Sections

A simple way of measuring the total cross section of a nuclear reaction is to measure the radioactivity of the product nucleus. Usually, the total number of product nuclei is not very large and the method is therefore restricted to relatively short half-lives. If the product nuclei are analyzed by AMS this limitation does not exist and the method can be extended.

At Argonne we have recently performed such an experiment to measure the cross section of the $^{26}Mg(p,n)^{26}Al$ ($T_{1/2} = 7.2 \times 10^5$ yr) reaction near threshold.[10] In short, the procedure was as follows (For details see Ref. 10):

1. ^{26}Mg foils were bombarded with protons yielding about 10^{10} ^{26}Al nuclei per foil.
2. ^{27}Al was added as carrier and for normalization.
3. The combined material was converted into $MgO + Al_2O_3$.
4. The oxide was mixed with Zn powder and pellets pressed for the sputter source.
5. $^{26}Al/^{27}Al$ ratios in the range from 10^{-10} to 10^{-11} were measured with the tandem-split pole spectrograph system.

The results of these measurements are shown in Table 1 below. The third column in Table 1 gives the number of ^{26}Al ions detected. Since $10^{10} - 10^{11}$ ^{26}Al nuclei were produced in the irradiation of the ^{26}Mg foils the fraction of nuclei actually measured turned out to be only 10^{-9}. On the other hand, a

comparison of column 3 and 7 shows that the number of ^{26}Al decays in the same time period is a factor of 10 smaller. For a decay counting experiment this number would be further reduced by the efficiency of detecting the decay radiation. The comparison shows that even for a very unfavorable condition of AMS detection, the ion counting technique can be more efficient.

Table 1. Results of the $^{26}Mg(p,n)^{26}Al$ cross section measurement

Center-of-mass proton energy (MeV)	Running time (min)	$^{26}Al^{11+}$ ions (counts)	$^{27}Al^{8+}$ current (nA)	$^{26}Al/^{27}Al$ (10^{-11})	σ (mb)	^{26}Al decays
5.0	68	11	0.39	1.8 ± 0.6	7.4 ± 2.5	1
5.5	100	74	0.37	8.5 ± 1.3	37.3 ± 6.3	4
6.0	102	102	0.47	9.2 ± 1.3	28.2 ± 4.5	11
6.4	51	92	0.57	13.6 ± 2.0	42.6 ± 6.9	14
6.7	67	172	0.54	20.4 ± 2.6	65.2 ± 9.4	17
blank	33	0	0.32	< 0.4		

The cross sections covered in the present experiment lie in the millibarn range. It is conceivable to push this technique to the microbarn range or even lower with more favorable elements and/or improved ion sources and sample preparation techniques. In the present experiment the limiting factor was the extremely low output of Al^- ($\sim$ 1 nA). It is well known that other elements like carbon, silicon or chlorine yield up to 10^4 times higher negative ion currents.

The demonstration of a cross section measurement with AMS was only part of the motivation for choosing the $^{26}Mg(p,n)^{26}Al$ reaction. In recent years ^{26}Al has gained great interest in astrophysics since, despite of its cosmologically short half-life of 7.2×10^5 yr, it was apparently present in early condensates of the solar system. This was discovered through a ^{26}Mg

isotopic abundance excess correlated with the Al content of certain inclusions in the Allende meteorite.[11] Relating the measured ^{26}Mg excess to the in situ decay of ^{26}Al yields the ^{26}Al abundance at the time of forming these inclusions. Attempts have been made [12,13,14] to calculate the primordial ^{26}Al abundance of fresh stellar matter, since the decrease of primordial to meteoritic abundance would establish an interesting time scale in the early solar system. These calculations involve both, reactions which produce and destroy ^{26}Al. One of the crucial destructive reactions seems to be $^{26}Al(n,p)^{26}Mg$. Since this requires a radioactive target, the cross section has not yet been measured. Instead one can obtain at least partial information by measuring the inverse reaction $^{26}Mg(p,n)^{26}Al$ and calculating cross sections of the forward reaction through the principle of detailed balance. However, even the inverse reaction was poorly studied when we performed our experiment. The result of our measurement established[10] the approximate validity of Hauser-Feshbach calculations for this reaction, widely used in nucleo-synthesis calculations, whenever experimental data are missing. Very recently more detailed measurements were performed using the $^{26}Mg(p,n\gamma)^{26}Al$ reaction[15] and a thick-target yield technique to measure total neutron yields in the $^{26}Mg(p,n)^{26}Al$ reaction.[16]

Unfortunately, the study of the inverse reaction lacks information on important reaction channels for the forward reaction. In particular, the $^{26}Al_{5+,g.s.}(n,p)^{26}Mg_{2_1^+}$ channel can only be measured with an ^{26}Al target. The production of such a target is therefore of great interest. It seems possible to produce ^{26}Al in quantities of around 0.1 to 1 mg using, for example, the intense-proton-beam spallation facilities available at some medium and high-energy accelerators.

5. Out-look on Some Experiments Related to Nuclear Physics

AMS has developed into one of the most sensitive tools we have for isotope analysis. The sensitivity of isotope ratio measurements is extremely high and often only limited by the ion source current and not by background events. On the other hand the total efficiency of detecting atoms from the sample in the final detector is still low. We have studied this situation recently for the detection of ^{7}Be with our AMS system.

^{7}Be is a relatively short-lived radioisotope with a half-life of 53.3 d. It decays through electron capture with a 10% branch emitting a 478 keV γ-ray. Therefore, decay counting seems to be the obvious method for a ^{7}Be detection. However, if the total number of ^{7}Be atoms available for detection is below 10^{5} the ion counting technique may become competitive. The measurement of such a low ^{7}Be yield is of interest to study the $^{3}He(\alpha,\gamma)^{7}Be$ reaction at extreme subcoulomb energies relevant for the ^{7}Be production in the interior of the sun.

^{7}Be test samples were prepared via the $^{9}Be(\alpha,\alpha 2n)^{7}Be$ reaction bombarding thick Be metal discs with 42 MeV alpha particles from the Argonne cyclotron. Figure 3 shows ion spectra from an irradiated and a blank sample measured in the focal plane detector of the Enge split-pole spectrograph. Running conditions were as follows: $^{9}BeH^{-}$ (from Be metal plus NH_3 spray) = 200 nA; 40 nA current in the spectrograph target chamber for 32.7 MeV $^{9}Be^{4+}$; $^{7}Be^{4+}$ counting rate = 0.33 sec^{-1}. From this one calculates a $^{7}Be/^{9}Be$ ratio of 5×10^{-12}. The blank sample gave only one ^{7}Be count in 20 min corresponding to a $^{7}Be/^{9}Be$ detection limit of 10^{-14}.

Although the sensitivity and cleanness of detection is very good, the overall efficiency is still too low to push the method into the desired range of below 10^{5} ^{7}Be atoms. From the sputter rate measured via the weight

loss of the samples a total detection efficiency of 1.7×10^{-5} was determined. By far the biggest loss is due to the low BeH^- yield. The BeH^-/Be (sputtered) ratio was measured to be 3×10^{-4}. Therefore, it appears that the low negative ion efficiency is the bottleneck for a high-efficiency detection of ^7Be. Improved ion source technology will hopefully change this situation in the near future.

Table 2: Experiments for High-Efficiency AMS

Reaction to be Studied	Typical Reaction Rate	Quantity to be Measured (Range)
1. Radiative capture:		
$^{48}Ca(^{12}C,\gamma)^{60}Fe$	10^3/hr	$\sigma(10^{-8}$ b)
$^3He(\alpha,\gamma)^7Be$	5/hr	$\sigma(10^{-10}$ b)
2. Double β decay:		
$^{82}Se(\beta\beta)^{82}Kr$	60/hr kg(^{82}Se)	$T_{1/2}(10^{19}$ yr)[a]
$^{76}Ge(\beta\beta)^{76}Se$		
3. Geologic solar ν detection:		
$^{41}K(\nu,\beta^-)^{41}Ca$	10^4/ton (KCl)	ν capture rate (7 SNU)[b]

[a] Ref. 17
[b] Ref. 18

Table 2 lists some interesting experiments which could be performed if a substantial improvement of AMS efficiency can be achieved. In fact, most of the experiments listed would only be meaningful if a close to 100% efficiency can be reached. This seems rather far down the road. However, once this goal is achieved AMS would be an extremely powerful instrument to investigate basic questions in nature.

I should like to thank W. Henning, B. Myslek-Laurikainen, M. Paul, R. C. Pardo, R. K. Smither, E. J. Stephenson, J. L. Yntema, D. E. Alburger, J. B. Cumming, and G. Harbottle for a very encouraging collaboration on the AMS experiments at Argonne.

This research was supported by the U.S. Department of Energy under Contract W-31-109-Eng-38.

References

1. W. Henning, W. Kutschera, M. Paul, R. K. Smither, E. J. Stephenson, and J. L. Yntema, Nucl. Instrum. Meth. 184, 247 (1981).

2. K. R. Chapman, IEEE Trans. Nucl. Sci. NS-23, 1109 (1976).

3. W. Henning, W. Kutschera, B. Myslek-Laurikainen, R. Pardo, R. K. Smither, and J. L. Yntema, contribution to this Symposium.

4. R. Middleton, Proc. Symp. Northeastern Accelerator Personnel, SNEAP 80, Madison, J. H. Billen, ed., p. 134 (1980).

5. W. Kutschera, W. Henning, M. Paul, R. K. Smither, E. J. Stephenson, J. L. Yntema, D. E. Alburger, J. B. Cumming, and G. Harbottle, Phys. Rev. Lett. 45 (1980) 592.

6. D. Elmore, N. Anantaraman, H. W. Fulbright, H. E. Gove, H. S. Hans, K. Nishiizumi, M. T. Murell, and M. Honda, Phys. Rev. Lett. 45, 589 (1980).

7. H. B. Clausen, J. Glaciology 12, 411 (1973).

8. D. J. DeMaster, Earth Plan. Sci. Lett. 48, 209 (1980).

9. J.-C. Roy and T. P. Kohman, Can. J. Phys. 35, 649 (1957).

10. M. Paul, W. Henning, W. Kutschera, E. J. Stepehenson, and J. L. Yntema, Phys. Lett. 94B, 303 (1980).

11. T. Lee, D. A. Papanastassiou, and G. J. Wasserburg, Geophys. Res. Lett. 3, 109 (1976); Astrophys. J. 211, L 107 (1977).

12. J. W. Truran and A. G. W. Cameron, Astrophys. J. 219, 226 (1978).

13. W. D. Arnett and J. P. Wefel, Astrophys. J. 224, L 139 (1978).

14. M. Arnould, H. Norgaard, F. K. Thielemann, and W. Hillebrandt, Astrophys. J. 237, 931 (1980).

15. E. B. Norman, K. T. Lesko, T. E. Chupp, and P. Schwalbach, Nucl. Phys. A 357, 228 (1981).

16. E. B. Norman, T. E. Chupp, K. T. Lesko, and P. J. Grant, preprint University of Washington, Seattle, 1981, to be published.

17. M. K. Moe and D. D. Lowenthal, Phys. Rev. 22C, 2186 (1980).

18. W. C. Haxton and G. A. Cowan, Science 210, 897 (1980).

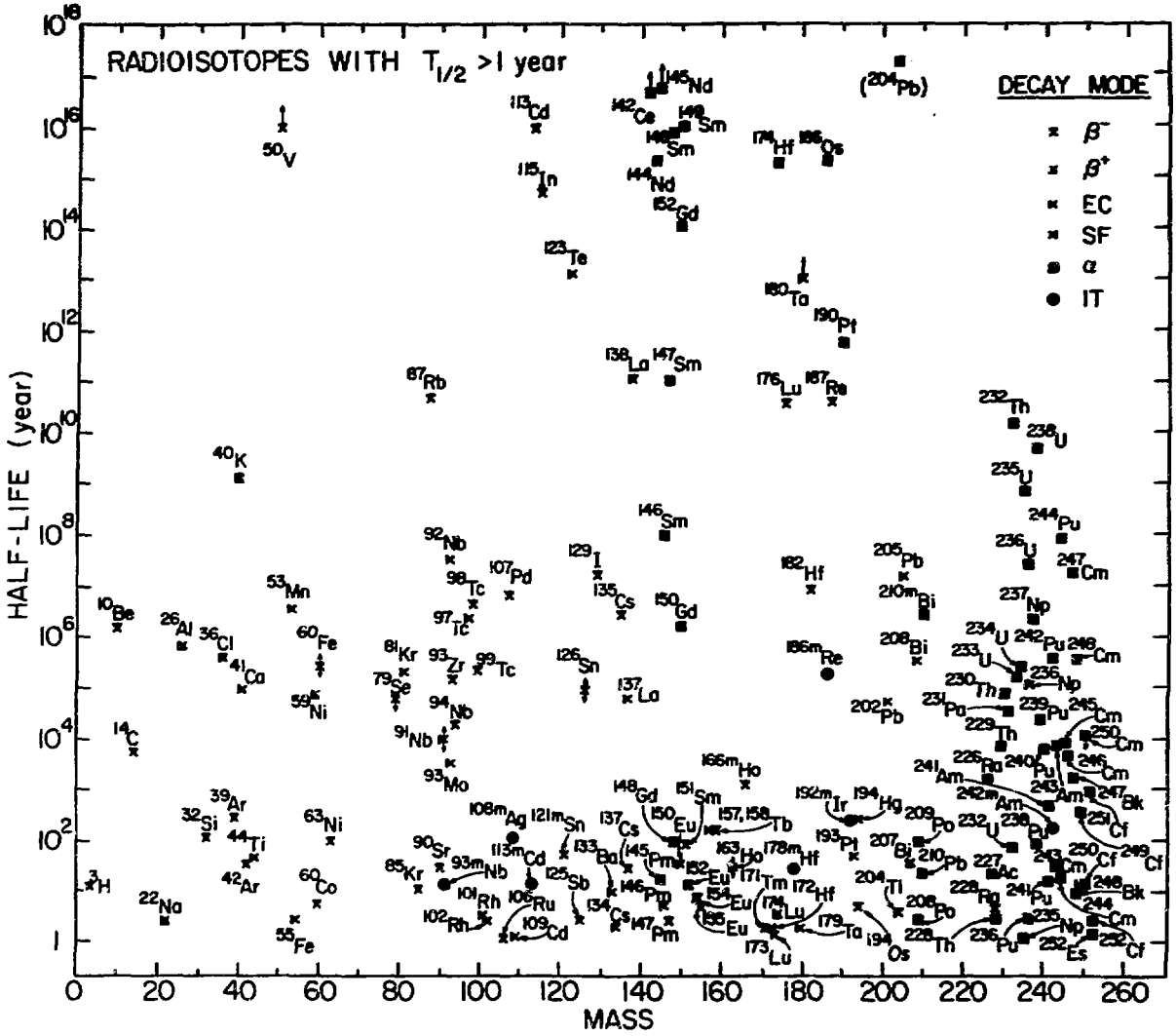

Fig. 1: Long-lived radioisotopes. Data points are marked by symbols indicating single or multiple decay mode. Arrows mean that the half-life is only approximately known in the respective direction. Isotopes in brackets indicate that their assignment is questionable.

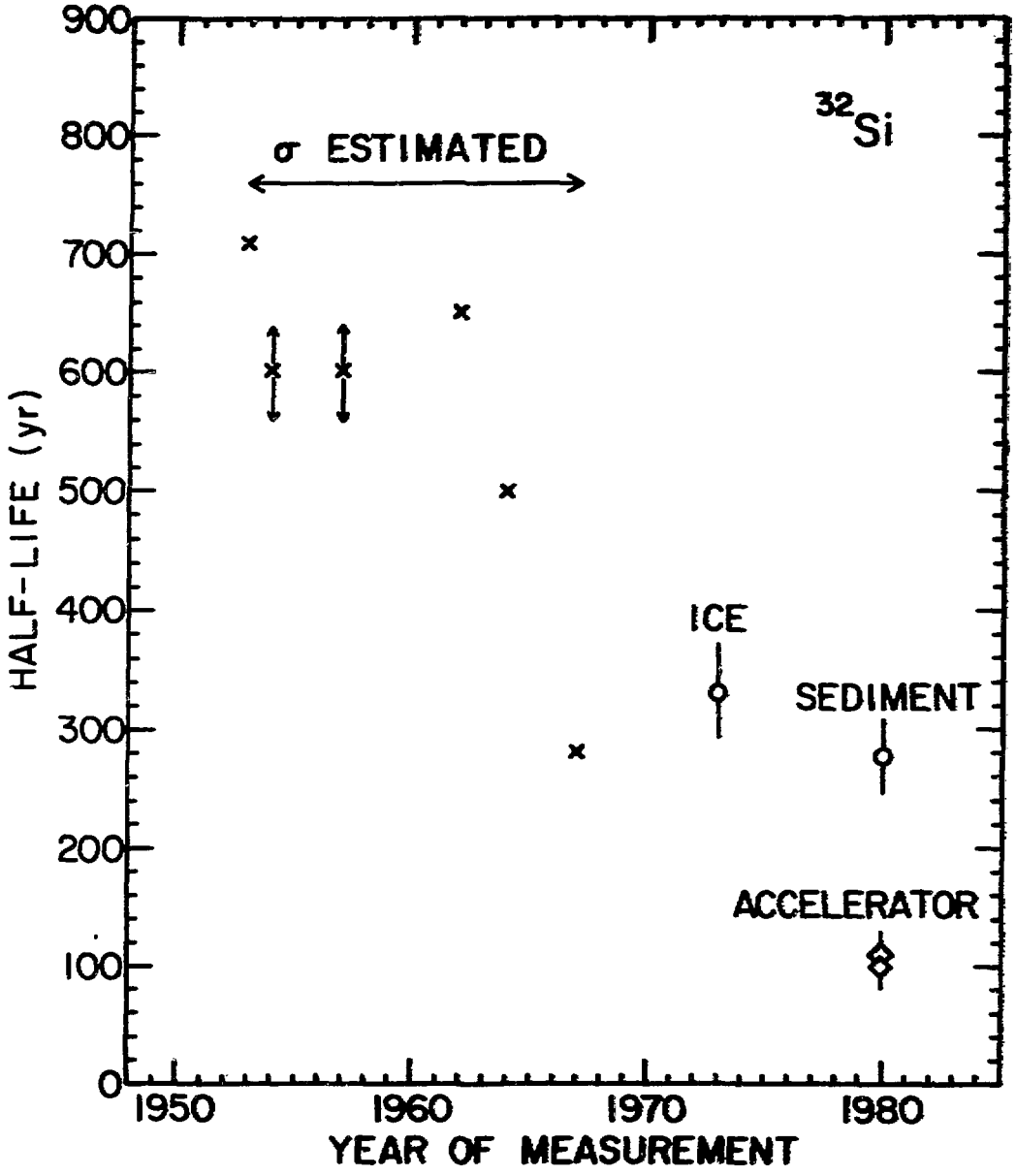

Fig. 2: History of ^{32}Si half-life measurements.

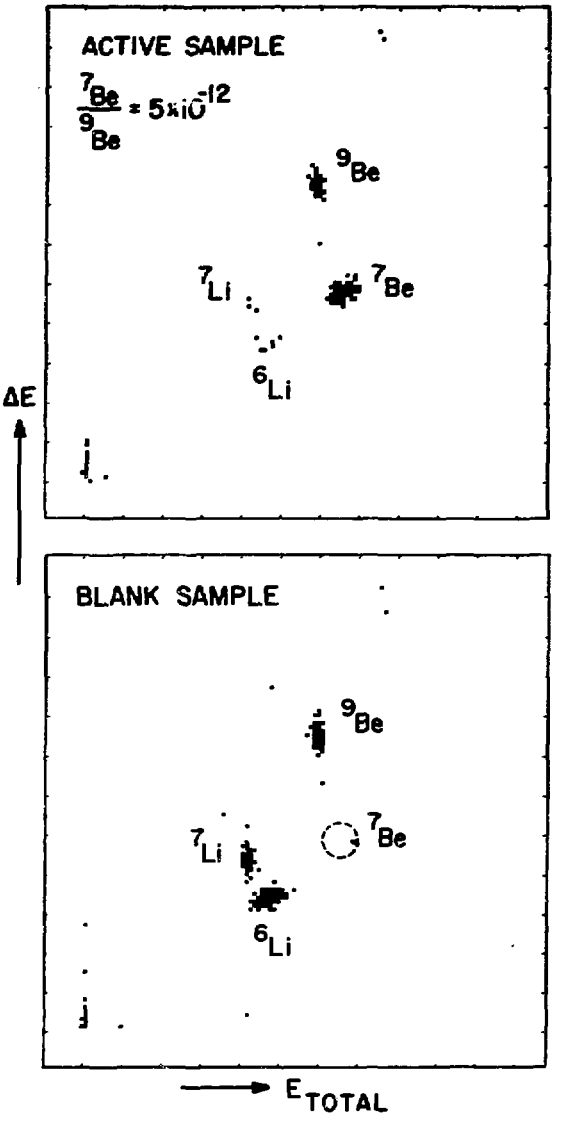

Fig. 3: Two-dimensional density plots of the total energy, E_{total}, versus energy loss, ΔE, measured with the split-pole focal plane detector for two metallic Be samples. The upper spectrum was accumulated for 10 min the lower one for 20 min.

INSTRUMENTATION OF AN FN TANDEM FOR THE DETECTION OF ^{10}Be*

R. Middleton, J. Klein and Hongqing Tang
Physics Department, University of Pennsylvania

1. INTRODUCTION AND OVERVIEW

Although the tandem accelerator at the University of Pennsylvania has been used to make a variety of mass spectroscopic measurements, about 18 months ago we decided to concentrate exclusively on ^{10}Be. Since then we have worked in close collaboration with L. Brown, I. S. Sachs and F. Tera from the Carnegie Institution of Washington – our efforts being mainly directed at instrumentation, which is the subject of this talk, while they were concerned with applications and the chemical preparation of samples. It is my intention to begin by giving a brief overview of the modifications that have been made to our FN tandem, then discuss in more detail certain specific components and conclude with an assessment of our present precision and sensitivity limits.

Fig. (1) shows the modified negative ion injector that was used throughout this work. Negative ions from the cesium sputter source are focussed by an einzel lens onto the object slits of a 30 cm radius double focussing 90° magnet -- the latter has

* Work supported by National Science Foundation.

a mass resolution $\Delta m/m \sim 1/50$, largely determined by the relatively large slit opening, but which is more than adequate to resolve $^{9}BeO^{-}$ from $^{10}BeO^{-}$. Note that an auxiliary Faraday cup has been added to the system so that $^{9}BeO^{-}$ can be monitored and integrated while $^{10}BeO^{-}$ ions are being injected into the accelerator. I would also draw attention to the alignment telescope which is not only invaluable for the precise positioning of samples in the source but also for observing the quality of the focus of the reflected cesium beam. After magnetic analysis, the injected beam passes through a 1 cm diameter aperture, through a passive magnet, and is brought to a focus in the object plane of the accelerator by a second einzel lens. The injected energy is low and for most of this work was 20 keV. Low energy injection is facilitated by the presence of an entrance grid in the low energy acceleration tube.

Fig. (2) shows the beam transport system at the high energy end of the accelerator. The emerging beam is focussed by a magnetic quadrupole doublet onto the object slits of the high energy 90° analyzing magnet. Immediately following the quadrupole is an E x B velocity selector which is described in more detail later. The dispersive plane of the latter is vertical, and to optimize the resolution, the vertical object slits are usually adjusted to ±1.5 mm – the horizontal slits are usually generously wide ~ ±5 mm. After magnetic analysis in the 1 m radius double focussing 90° magnet the beam passes through a

fixed 6 mm diameter aperture located a few inches in front of the image slits (not used in this work). Between the aperture and the image slits is the retractable counter telescope used to detect ^{10}Be. To tune the accelerator for ^{9}Be, the counter telescope is lifted and the beam passing through the 6 mm aperture is measured in the accelerator's standard Faraday cup.

2. INSTRUMENTATION DETAILS

The cesium sputter source used in this work was basically similar to that shown in Fig. (3), but slightly modified (described later) to improve performance with a reflected beam. One of the most important features of the source is that it can house up to 18 samples which can be changed within minutes without breaking the vacuum system.

At the outset of this work we made a fairly extensive study of the negative ions of beryllium which forced us to conclude, in spite of other difficulties, that BeO^- is the best choice for accelerator mass spectrometry. Using a beryllium metal sputter cone, we were surprised to obtain between 20 and 50 nA of elemental negative ions — suggesting that the electron affinity might be small but positive and not negative as previously reported. We also attempted to produce hydride beams by ammonia spraying a metallic cone. BeH^- proved to be the most intense hydride and the best current was 0.4 μA with 0.25 μA being typical. Although the intensity of BeH^- is adequate for most mass spectrometric measurements, the necessity of having to reduce a small

sample, usually oxide, to metal and then having to shape it to fit into a sputter target is far from attractive. On the other hand, we found that from small (~ 4 mg) samples of pressed beryllium oxide we could relatively easily obtain about 1 μA. These considerations caused us to adopt the latter ions for all subsequent measurements.

Fig. (4) shows the most important modifications that were made to the source shown in Fig. (3) to optimize performance with the reflected cesium beam. The primary cesium beam passing through an 8 mm diameter hole drilled in the 'sputter cone', is reflected and focussed onto the small sample mounted in a hole in the center of a thin tantalum strip mounted diametrically across the 8 mm aperture. Focussing of the reflected beam is accomplished by placing a variable positive bias voltage on the negative ion extraction electrode – in our case optimal at about 4.2 kV.

We also paid particular attention to the design of the region close to the sputter target to minimize the build-up of sputtered material which might give rise to sample cross-talk. In this regard, we have been quite successful and after hours of measurements on samples containing ^{10}Be at the 10^{-11} levels, we have made many a 40 minute measurement on a beryllium oxide blank without detecting a single ^{10}Be count. Fig. (5) shows an $E_T - \Delta E$ spectrum made on such an occasion – the run was of 20 minute duration and the average $^{9}BeO^{-}$ current was 1 μA. Most

measurements reported here were made using sample holders similar to that shown in the lower half of Fig. (4). Recently we have begun to experiment with a new type of sample holder as shown in Fig. (6). Lack of experience with the new holders prevents us from drawing any conclusions but, it is our belief that the improved symmetry close to the point of negative ion formation will favor this design.

A typical negative ion spectrum from 99% pure beryllium oxide is shown in the upper half of Fig. (7). Of particular interest is the peak corresponding to m = 26 since this is injected into the accelerator when ^{10}Be is being counted. Acceleration through the tandem confirmed our suspicions that the m = 26 peak corresponded almost entirely to $^{9}BeOH^{-}$ and, in our case, is the major source of a white $^{9}Be^{3+}$ spectrum.

The lower spectrum in Fig. (7) was obtained with a sample containing equal weights of beryllium and boron oxides. Intensities are consistent with BO^{-} ions being formed with about twice the efficiency of BeO^{-} ions.

Fig. (8) shows a negative ion spectrum from a typical geological sample (deep sea sediment). The initial sample weighed $\sim$ 1 g and, prior to chemical processing, was spiked with 0.5 mg of ^{9}Be – the processed sample loaded into the source weighed between 4 and 5 mg. Typically such a sample, after about a 15 minute break-in period, yields between 0.5 and 1.0 μA and will last for 6 – 8 hours. The efficiency of $^{9}BeO^{-}$ formation is in

the range 0.1 – 0.4%.

There are two disadvantages associated with the acceleration of a molecular rather than an elemental negative ion. One is, that for a given terminal voltage the energy available at the stripper is less, resulting in a lower average charge state – this causes us to work with Be^{3+} ions rather than the preferred fully stripped Be^{4+}. The other is that transmission through the accelerator is usually appreciably poorer. The reasons for the latter are not fully understood, but far from insignificant is the effect of the Coulomb explosion that occurs when a high velocity molecule passes through a stripper foil. To some extent, the effects of the Coulomb explosion can be minimized by using a thin gas stripper to dissociate the molecules prior to striking the stripper foil.

Table I summarizes the results of some transmission measurements that we made while injecting $^{9}BeO^{-}$, $^{12}C^{-}$, and $^{12}C_2^{-}$ ions using various stripper combinations. These values are lower than usual and this may be attributable to the use of an abnormally thick stripper foil ($\sim$ 15 $\mu g/cm^2$). Nonetheless they illustrate that the transmission of molecular ions, even with a gas/foil stripper combination, is significantly poorer than that of elemental ions. Also that the transmission loss cannot be attributed to the pressure rise in the high energy acceleration tube caused by the use of gas.

Typically our absolute transmission for $^{9}Be^{3+}$ ions from

$^{9}BeO^{-}$ at 6 MV using a combination of foil and gas stripping is 10%. For reasons which are not presently understood this does vary from one running period to another, and can be as low as 7.5% and as high as 14.5%.

Fig. (9) shows a cross section through the home-built E x B velocity selector which has an effective plate length of 52 cm. Typical operating parameters for 20.3 MeV $^{10}Be^{3+}$ ions are: B = 900 gauss, E = 18 kV/cm. It is difficult to quantify the resolution of the selector and possibly is best illustrated by Fig. (10). This shows the transmission of $^{9}Be^{3+}$ and $^{10}B^{3+}$ ions, at the same terminal voltage (6 MV), plotted as a function of the magnetic field strength (electric field constant). It is evident from the figure that when the field is adjusted for the maximum transmission of $^{10}B^{3+}$ ions (which simulate $^{10}Be^{3+}$ ions) $^{9}Be^{3+}$ ions are very effectibly attenuated.

Fig. (11) shows $E_T - \Delta E$ spectra measured with and without the velocity selector for a processed sample of river sediment. The velocity selector attenuates the ^{9}Be count rate arising from the white spectrum by a factor of 10^3. The importance of the selector is that it reduces the number of scattered ^{9}Be particles that otherwise might fall into the ^{10}Be window.

Fig. (12) shows a schematic drawing of our ^{10}B absorber system and the $E_T - \Delta E$ counter telescope. Since the counter telescope incorporates no unusual features it will not be

described in detail here. The absorber, however, is far from conventional and includes a ^{10}B ion chamber which has proved to be the most valuable element in our ^{10}Be detecting system.

A little over a year ago it occurred to us that since ^{10}Be and ^{10}B have almost the same mass ($\Delta m/m \sim 6 \times 10^{-5}$) and that the energy loss difference in the stripper is negligible (6.6 keV for a 5 $\mu g/cm^2$ carbon foil) these ions would track identically through the tandem and analysis systems. Thus if the ^{10}B ion current could be measured while ^{10}Be is being counted, the former could be used as a pilot beam to tune the tandem for the latter. This has been accomplished by incorporating into the absorber an ion chamber with a current amplification factor of 10^3 to 10^4. Since typical boron currents from geological samples are in the pico-ampere range this provides a several nano-ampere current with which to adjust the accelerator and beam transport system. It has been experimentally verified on many occasions that peaking the ^{10}B current also maximizes the ^{10}Be count rate.

Routine use of the ^{10}B ion chamber has revealed a significant source of error in our early work. Previously we optimized tandem transmission for ^{9}Be and assumed, that by resetting all magnetic elements to calculated values, that transmission for ^{10}Be would be the same. Not only has the ion chamber shown this to be wrong but, more importantly, that the 20 to 100% gain usually obtained in ^{10}B current (and ^{10}Be count rate) after

all of the tandem controls have been optimized is variable from one sample to another. We are presently unable to account for this variability but, clearly, it casts doubt on the procedure of using a standard of known ^{10}Be content alone to determine the ^{10}Be transmission.

3. SENSITIVITY AND PRECISION

The ^{10}B ion chamber has eliminated our largest source of (sample to sample) variability and we are now able to make a single measurement of ^{10}Be concentration with a precision of better than 7%, and possibly as high as 4% in back to back measurements. The major factor limiting absolute accuracy results from uncertainties in multiple scattering losses in the ^{10}B absorber. It is difficult to measure these losses directly, but from indirect measurements, we have determined it to be between 50 and 70%.

Table II shows a comparison of measurements we have made on the accelerator with those determined by β-counting on a series of four samples supplied by J. R. Arnold and K. Nishiizumi. The excellent agreement between the measurements made by these two techniques is demonstrated by the constant value of the ratio in the last column, and its average value of 2.57 ± 4% is in good agreement with our estimate of 2.3 ± 30% for the systematic error due to loss of ^{10}Be through multiple scattering. Consequently, the use of standards, independently measured by β-counting, allows us to determine $^{10}Be/^{9}Be$

ratios to an absolute accuracy of better than 12%.

Sensitivity is limited by beryllium produced by ^{10}B induced nuclear reactions in the absorber foils. Since the Z's of the absorbers were chosen to lie well above the Coulomb barrier of the boron, only impurities in the foils contribute. The only significant reaction resulting in beryllium end products is the reaction $^{1}H(^{10}B,^{7}Be)^{4}He$ (Q = 1.146 MeV) with the hydrogen, ever present in metal foils. Vacuum baking of the foils reduces backgrounds by about a factor three, but a sensitivity of 10^{-15} requires that the concentration of boron in the sample be less than 25 ppm if the nuclear reaction produced background is to be less than 10% of the counting rate. Backgrounds produced by all other sources are at least two orders of magnitude less than those resulting from nuclear reactions.

We have made measurements thus far on a variety of samples including ocean sediments, alluvial deposits, soils, rain, various types of rocks and a number of biological materials. Most of these will be reported elsewhere, however two rather interesting biological results will be presented by way of illustration of our current capabilities. Fig. (13) shows an $E_T - \Delta E$ spectrum obtained from some maple leaves from my garden. No chemistry was performed on the sample — the leaves were simply ashed and then baked in a vacuum system at a temperature of about 1300°C and the residue pressed into one of our standard

tantalum holders. Since the sample had not been spiked with ^{9}Be, the white spectrum contribution was relatively weak and the E x B velocity selector was not used while obtaining the spectrum shown in Fig. (13). The ^{10}Be count rate was low and only 12 counts were obtained in 100 minutes, nonetheless the counts are readily discernable above the background. A similar measurement with wood failed owing to an overwhelmingly strong ^{10}B beam.

Very recently we were fortunate to receive from our collaborators at the Carnegie Institution of Washington a wood sample chemically extracted from a 100 g piece of oak. Fig. (14) shows an $E_T - \Delta E$ spectrum obtained during a 10 minute run – since the sample had been spiked with ^{9}Be the E x B velocity selector was used on this occasion. As is evident from the figure, the ^{10}Be peak stands out very clearly above the background and was quite strong. Interestingly, the number of ^{10}Be atoms per gram of oak turns out to be 2×10^{6} which is about two orders of magnitude greater than the number normally present in a gram of rain water – indicating that considerable concentration has occurred. It is intended to explore wood further and, in particular, attempt to correlate ^{10}Be content with variations in the cosmic ray flux.

Table I

Particle	Be^{3+}/BeO^- (Foil)	Be^{3+}/BeO^- (Foil + Gas)	Be^{3+}/BeO^- (Gas Alone)
Trans.(absolute %)	4.8	7.5	5.4
Trans.(normalized %)	9.8	16.3	11.7

Particle	C^{4+}/C^- (Foil)	C^{4+}/C^- (Foil+Gas)	C^{4+}/C_2^- (Foil)	C^{4+}/C_2^- (Foil+Gas)
Trans.(absolute %)	29	25	5.2	8.7
Trans.(normalized %)	51	44	13.2	22.5

1) All measurements were made at a terminal voltage of 6 MV.

2) Trans.(absolute) is the analyzed particle current divided by the negative ion current measured in the low energy Faraday cup.
Trans.(normalized) is the transmission corrected for charge state distribution and a 10% negative ion loss in the tube grid.

3) The transmission figures tabulated here are somewhat lower than average. This might in part be due to an unusually thick stripper foil – estimated ~15 $\mu g/cm^2$.

Table II

Sample	Counts ^{10}Be Window	Bkg.	Accel.* $^{10}Be/^{9}Be$ ($\times 10^{-12}$)	β-Counted $^{10}Be/^{9}Be$ ($\times 10^{-12}$)	Ratio β/Accel.
BE03	1799	24	2.24 ± 9%	5.53	2.47
BE04	227	14	0.42 ± 4%	1.05	2.50
E4	760	0	1.04 ± 4%	2.75	2.64
E5	538	40	0.41 ± 7%	1.09	2.66

NOTES:

1) Average $^{9}BeO^{-}$ current ~900 nA.
2) Background almost entirely due to ^{10}B induced nuclear reactions producing Be. ^{10}B levels 10 to 100 X that of typical samples. (~1000 ppm, ~1 μA in ion-chamber)
3) Errors on accelerator measurements represent estimates of precision from replicate runs.
4) Sample BE04 was obtained from BE03 by dilution — estimated error 2%. Similarly for E5 and E4. Series BE0 and E related by β-counting — error ~ 10%.
5) Anticipated ratio of β/accel. from multiple scattering considerations was 2.3 ± 30% as compared with the measured average value of 2.57 ± 4%.

* Uncorrected for multiple scattering losses — see note (5).

Figure Captions

Fig. 1 - A schematic drawing of the negative ion injector used for tandem mass spectrometry.

Fig. 2 - A schematic drawing of the high energy analysis system.

Fig. 3 - The cesium sputter source used in the present work was basically similar to that shown above with the exception that the negative ion extraction electrode was insulated and could be positively biased.

Fig. 4 - The upper figure shows the modifications that were made to the existing cesium sputter source to improve performance with a reflected cesium beam. The lower sketches are of the sputter target holder used to hold the 4 to 5 mg. pressed powder samples.

Fig. 5 - A $E_T - \Delta E$ spectrum obtained during 20 minutes from a 99% pure sample of beryllium oxide believed to contain no ^{10}Be. The $^{9}BeO^-$ current from the source was about 1 μA.

Fig. 6 - A new sputter target holder that is currently being tested. It is hoped, by preserving symmetry close to the point of negative ion formation, that the yield and stability will be improved.

Fig. 7 - The upper negative ion spectrum was measured in the accelerator's low energy Faraday cup from a sample of 99% pure beryllium oxide. The lower spectrum

Fig. 7 (con.) - was similarly measured using a sputter target containing equal weights of beryllium and boron oxide.

Fig. 8 - A typical negative ion spectrum from a 1 g deep sea sediment sample which was spiked with 0.5 mg. of beryllium and chemically processed. The total sample weight loaded into the source was ~4 mg.

Fig. 9 - A cross section of the E x B velocity selector located at the high energy end of the accelerator.

Fig. 10 - The full curve shows the transmission of the velocity selector as a function of magnetic field strength for $^{9}Be^{3+}$ injected as $^{9}BeO^{-}$ at terminal voltage of 6 MV. The broken curve, measured with the electric field of the selector unchanged, and at the same terminal voltage, shows the transmission of $^{10}B^{3+}$ injected as $^{10}BO^{-}$.

Fig. 11 - Typical $E_T - \Delta E$ spectra obtained with and without the velocity selector from a sample of river sediment.

Fig. 12 - Schematic vertical and horizontal sectional drawings showing the fixed aperture, absorber, ^{10}B ion chamber, and the $\Delta E - E$ telescope.

Fig. 13 - A $E_T - \Delta E$ spectrum, obtained with the velocity selector switched off, showing the presence of a small amount of ^{10}Be in maple leaves. The sample was prepared by ashing and a high temperature vacuum bake with no subsequent chemistry or addition of ^{9}Be.

Fig. 14 - A $E_T - \Delta E$ spectrum obtained from 100 g of oak which had been ashed, spiked with ^9Be and chemically processed.

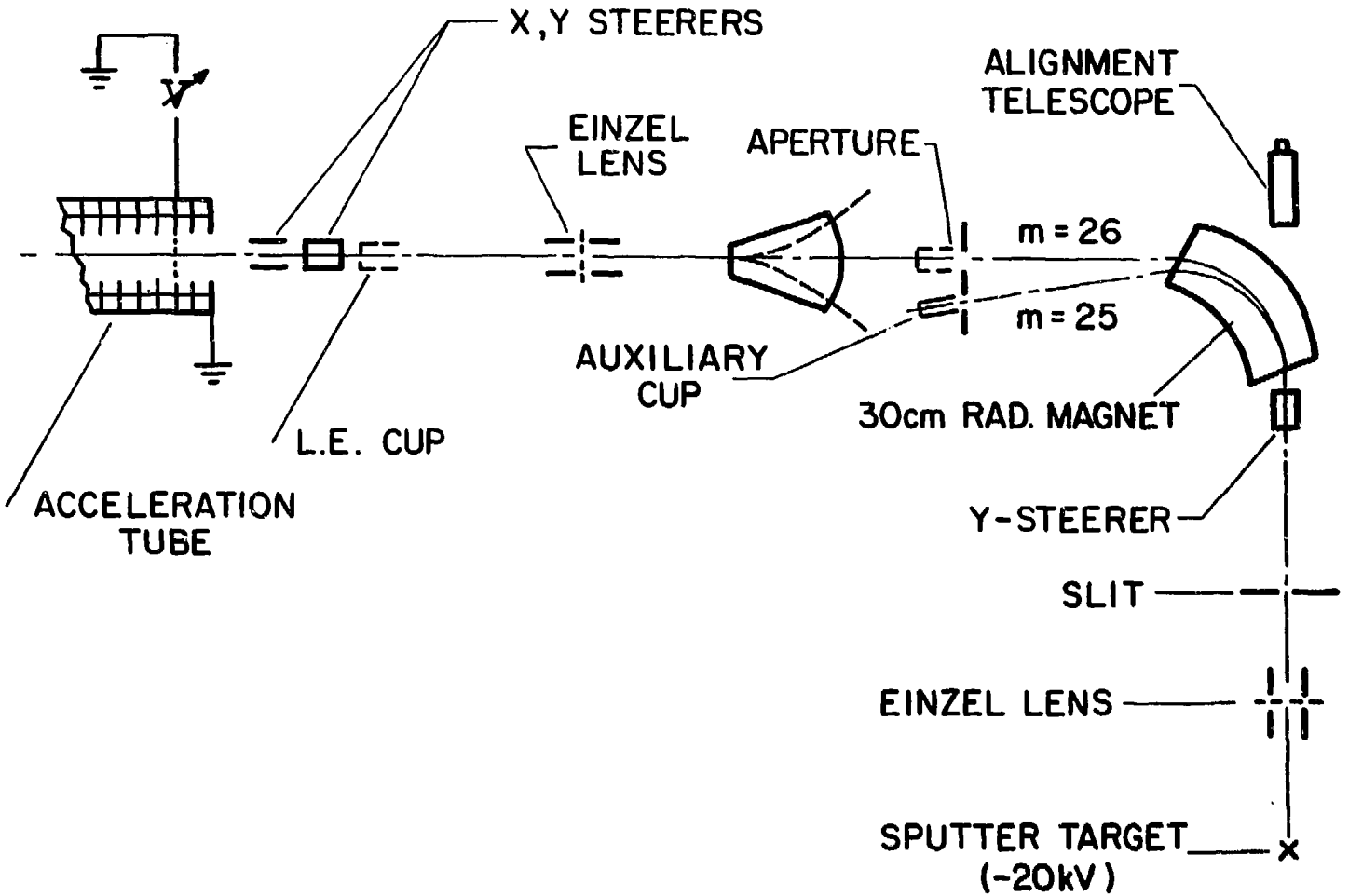
X,Y STEERERS
ALIGNMENT TELESCOPE
EINZEL LENS
APERTURE
m = 26
m = 25
AUXILIARY CUP
30cm RAD. MAGNET
L.E. CUP
ACCELERATION TUBE
Y-STEERER
SLIT
EINZEL LENS
SPUTTER TARGET (-20kV)

Fig. 1

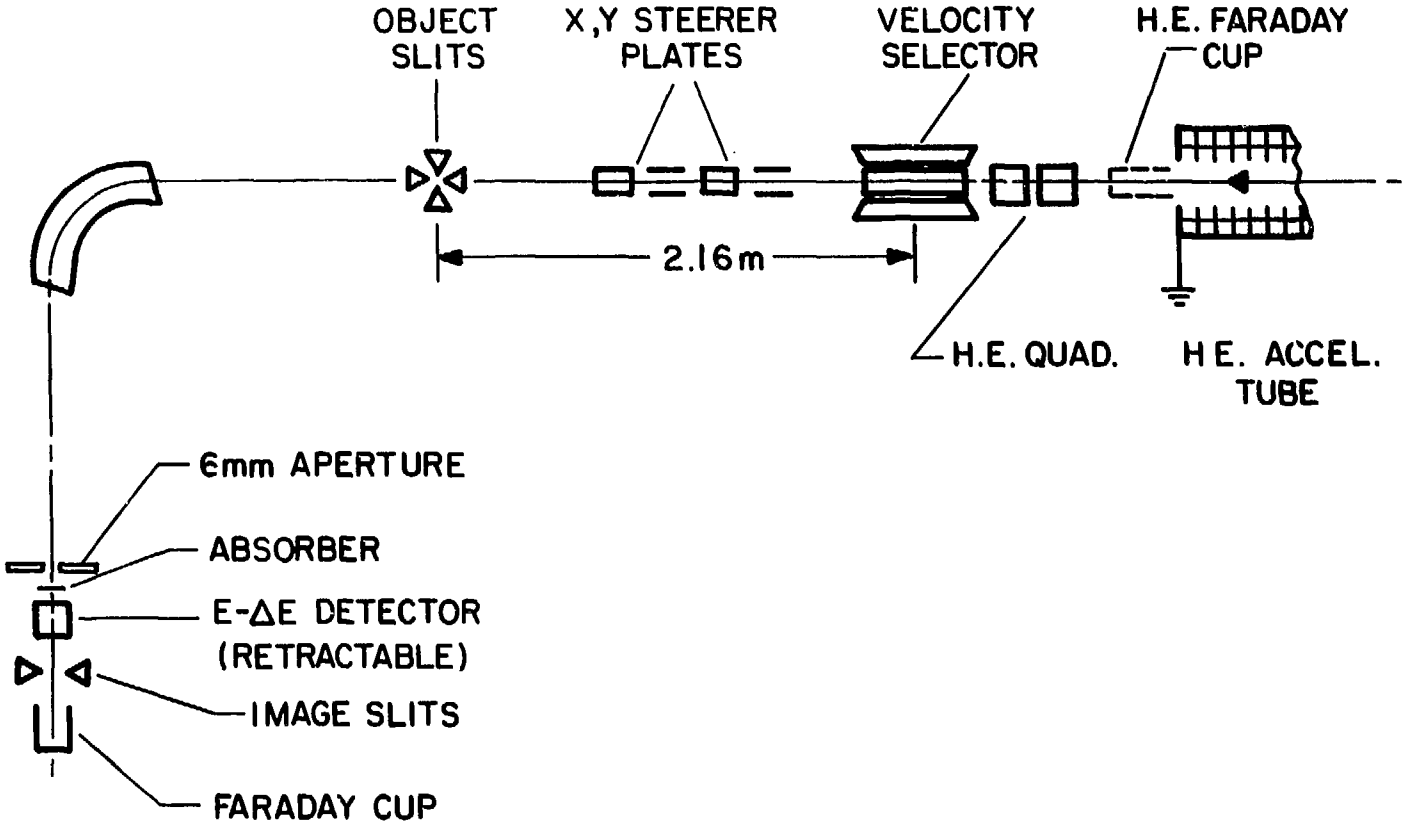
OBJECT SLITS
X,Y STEERER PLATES
VELOCITY SELECTOR
H.E. FARADAY CUP
2.16m
H.E. QUAD.
H E. ACCEL. TUBE
6mm APERTURE
ABSORBER
E-ΔE DETECTOR (RETRACTABLE)
IMAGE SLITS
FARADAY CUP

Fig. 2

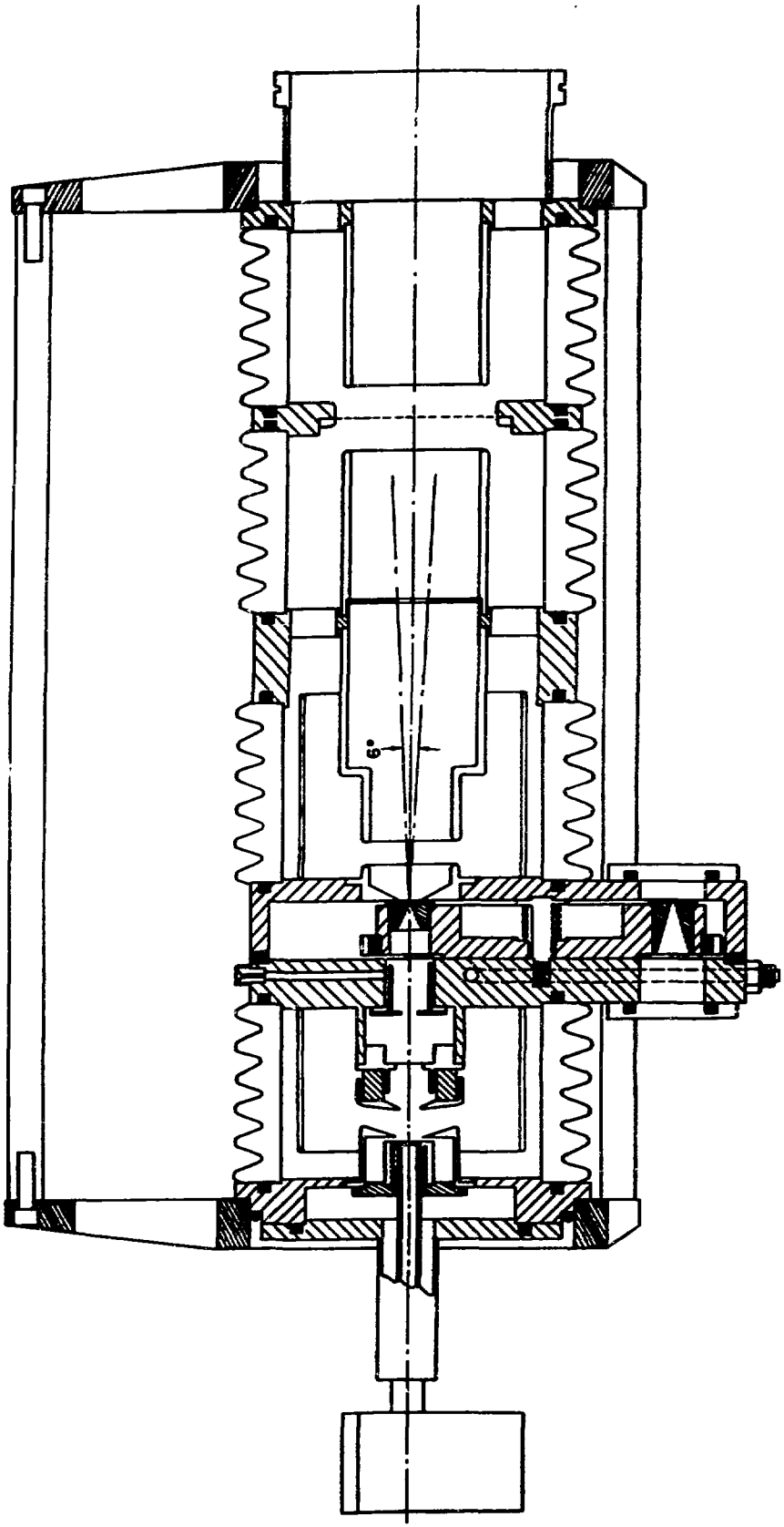

Fig. 3

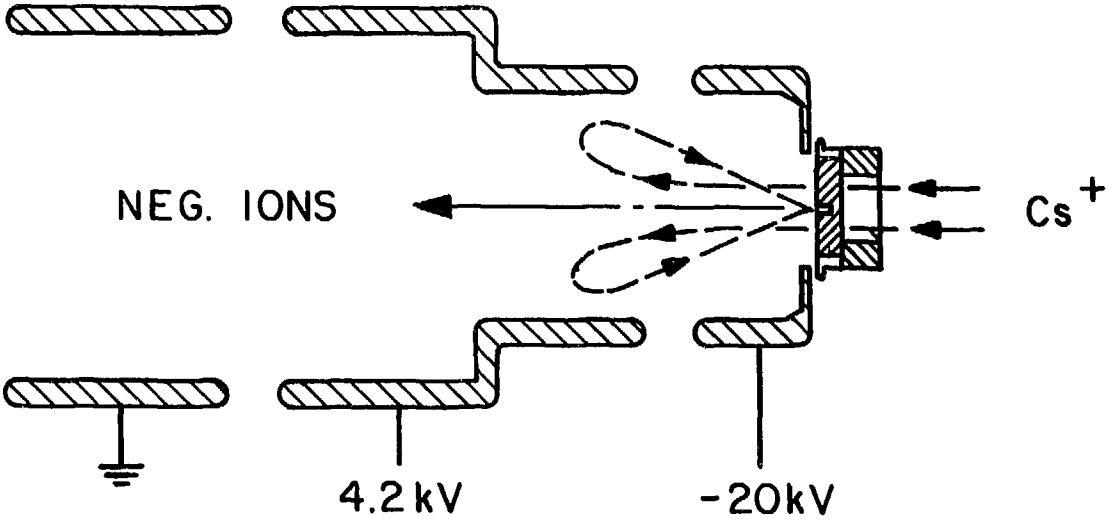
NEG. IONS
Cs+
4.2 kV
-20kV

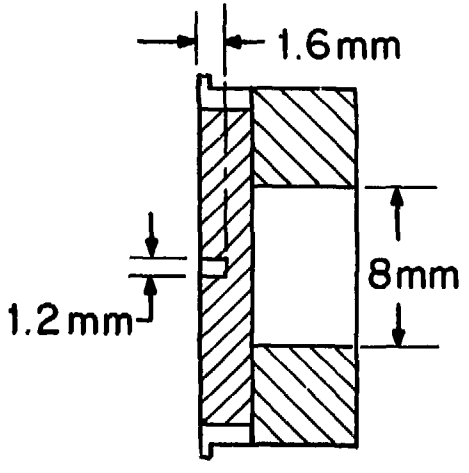
1.6mm
8mm
1.2mm

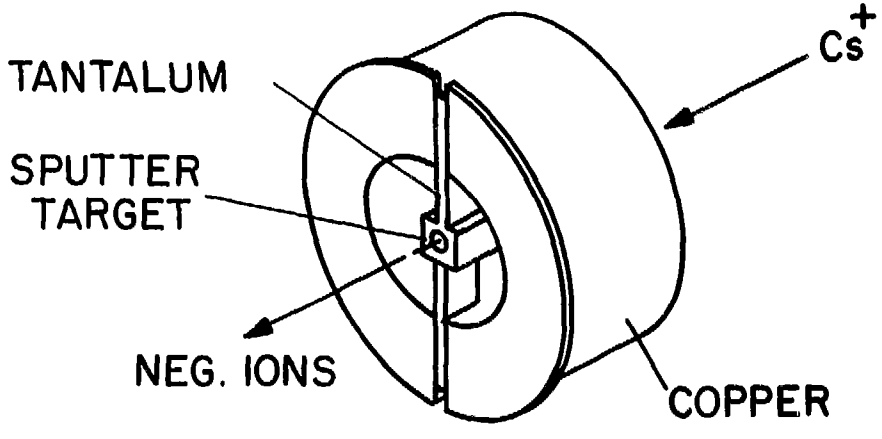
TANTALUM
SPUTTER
TARGET
Cs+
NEG. IONS
COPPER

Fig. 4

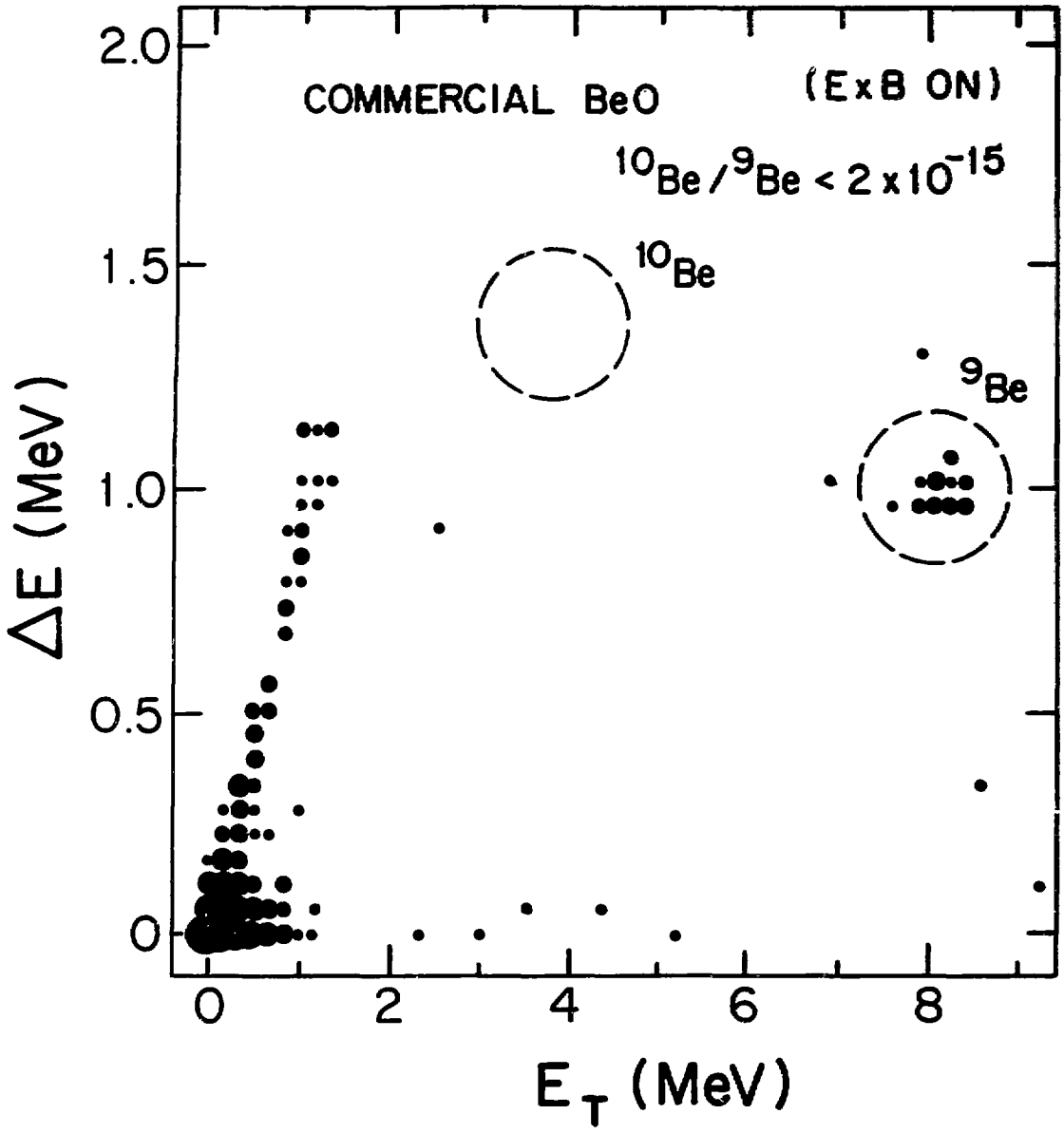
COMMERCIAL BeO
(ExB ON)
$^{10}Be/^{9}Be < 2 \times 10^{-15}$
^{10}Be
^{9}Be
ΔE (MeV)
E_T (MeV)
2.0
1.5
1.0
0.5
0
0
2
4
6
8

Fig. 5

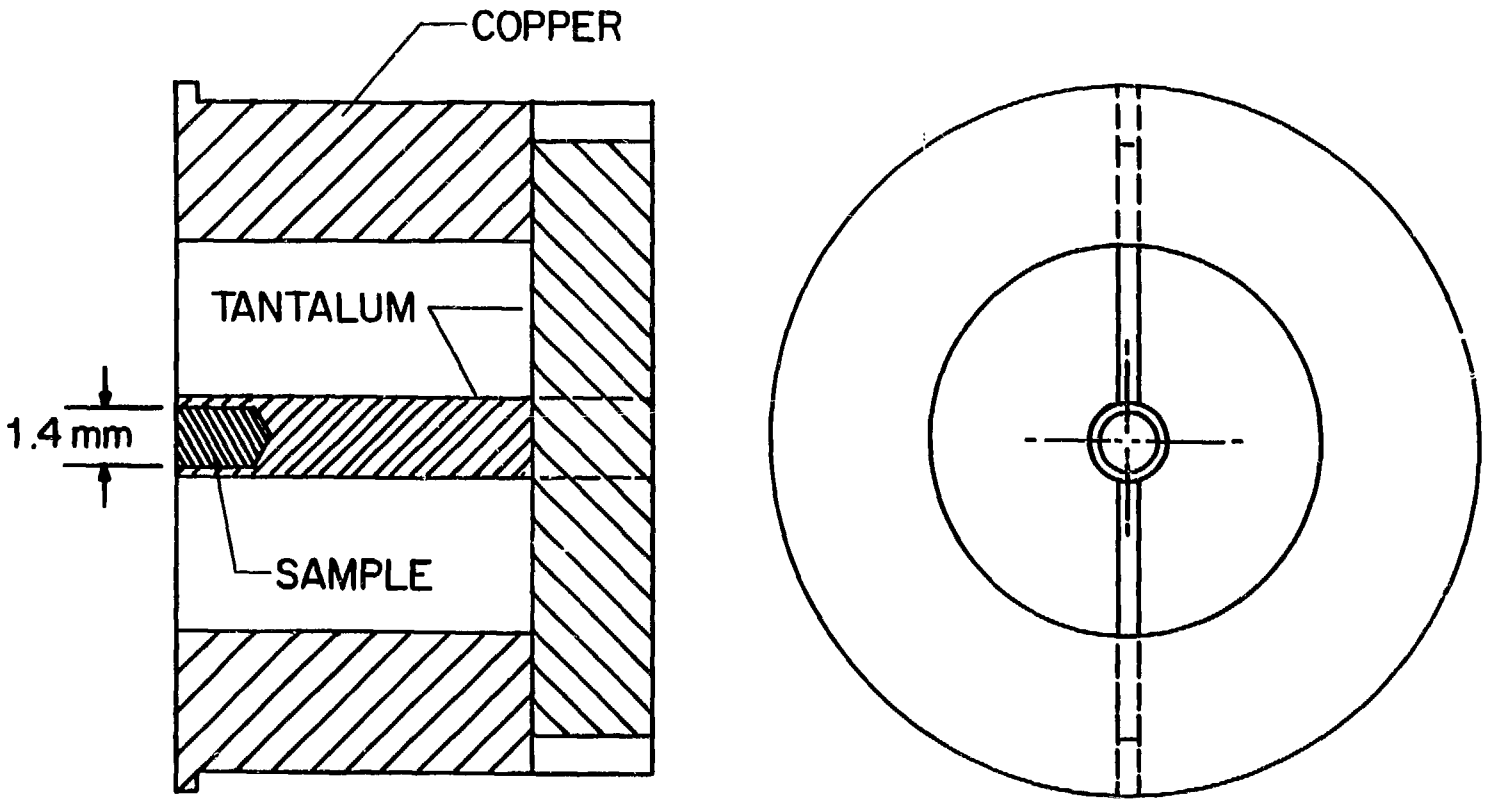

Fig. 6

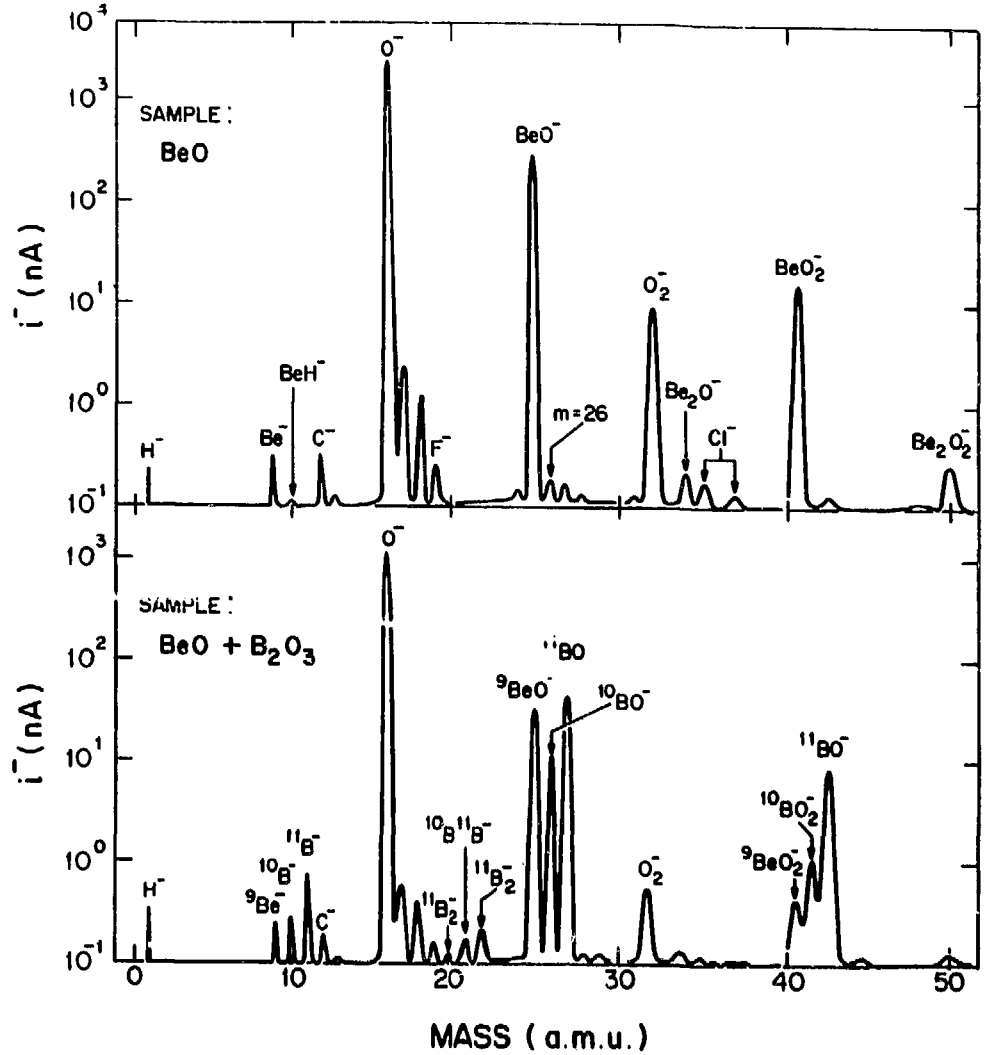
SAMPLE :
BeO
i⁻ (nA)
H⁻
Be⁻
BeH⁻
C⁻
O⁻
F⁻
BeO⁻
m=26
O₂⁻
Be₂O⁻
Cl⁻
BeO₂⁻
Be₂O₂⁻
SAMPLE :
BeO + B₂O₃
i⁻ (nA)
H⁻
⁹Be⁻
¹⁰B⁻
¹¹B⁻
C⁻
O⁻
¹¹B₂⁻
¹⁰B¹¹B⁻
¹¹B₂⁻
⁹BeO⁻
¹¹BO
¹⁰BO⁻
O₂⁻
⁹BeO₂⁻
¹⁰BO₂⁻
¹¹BO⁻
0
10
20
30
40
50
MASS (a.m.u.)

Fig. 7

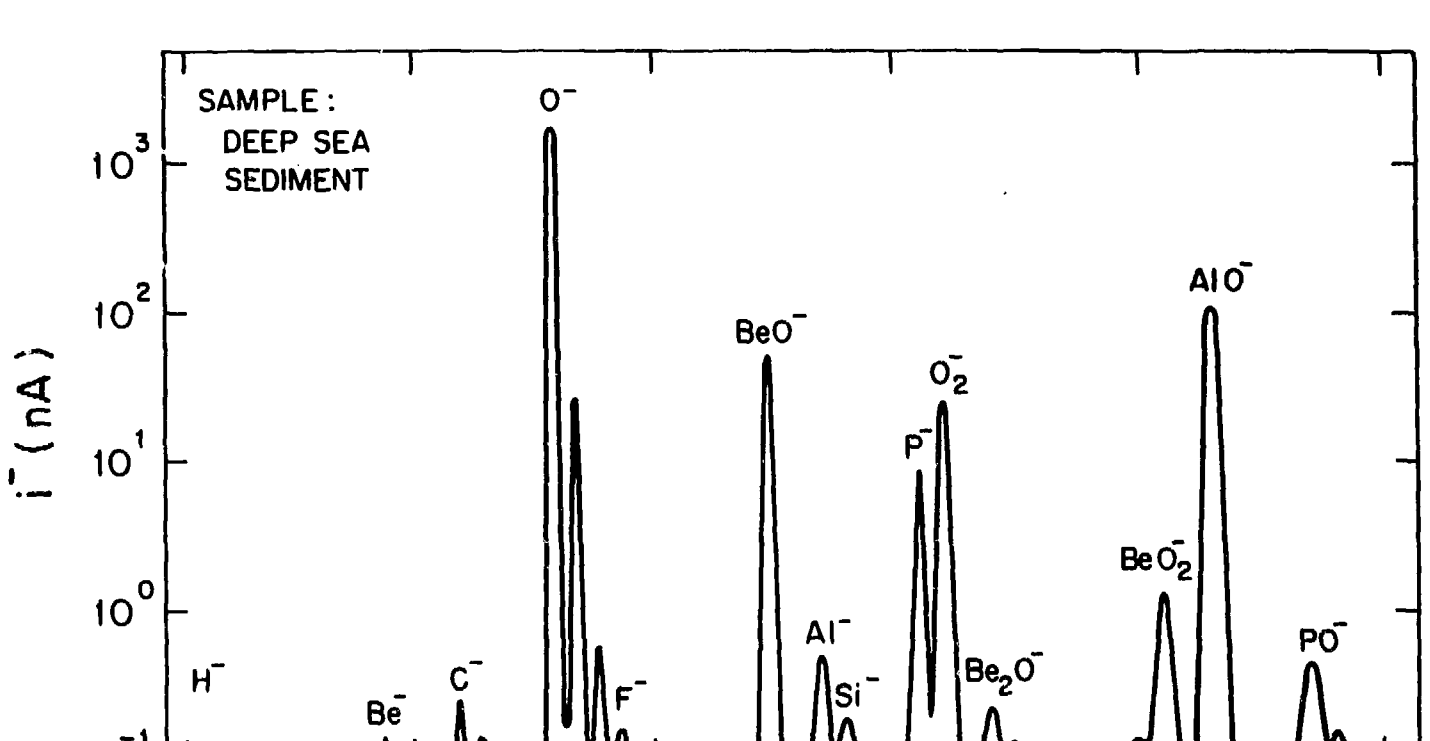
SAMPLE :
DEEP SEA
SEDIMENT
10^3
10^2
10^1
10^0
10^{-1}
i⁻ (nA)
H⁻
Be⁻
C⁻
O⁻
F⁻
BeO⁻
Al⁻
Si⁻
P⁻
O₂⁻
Be₂O⁻
BeO₂⁻
AlO⁻
PO⁻
0
10
20
30
40
50
MASS (a.m.u.)

Fig. 8

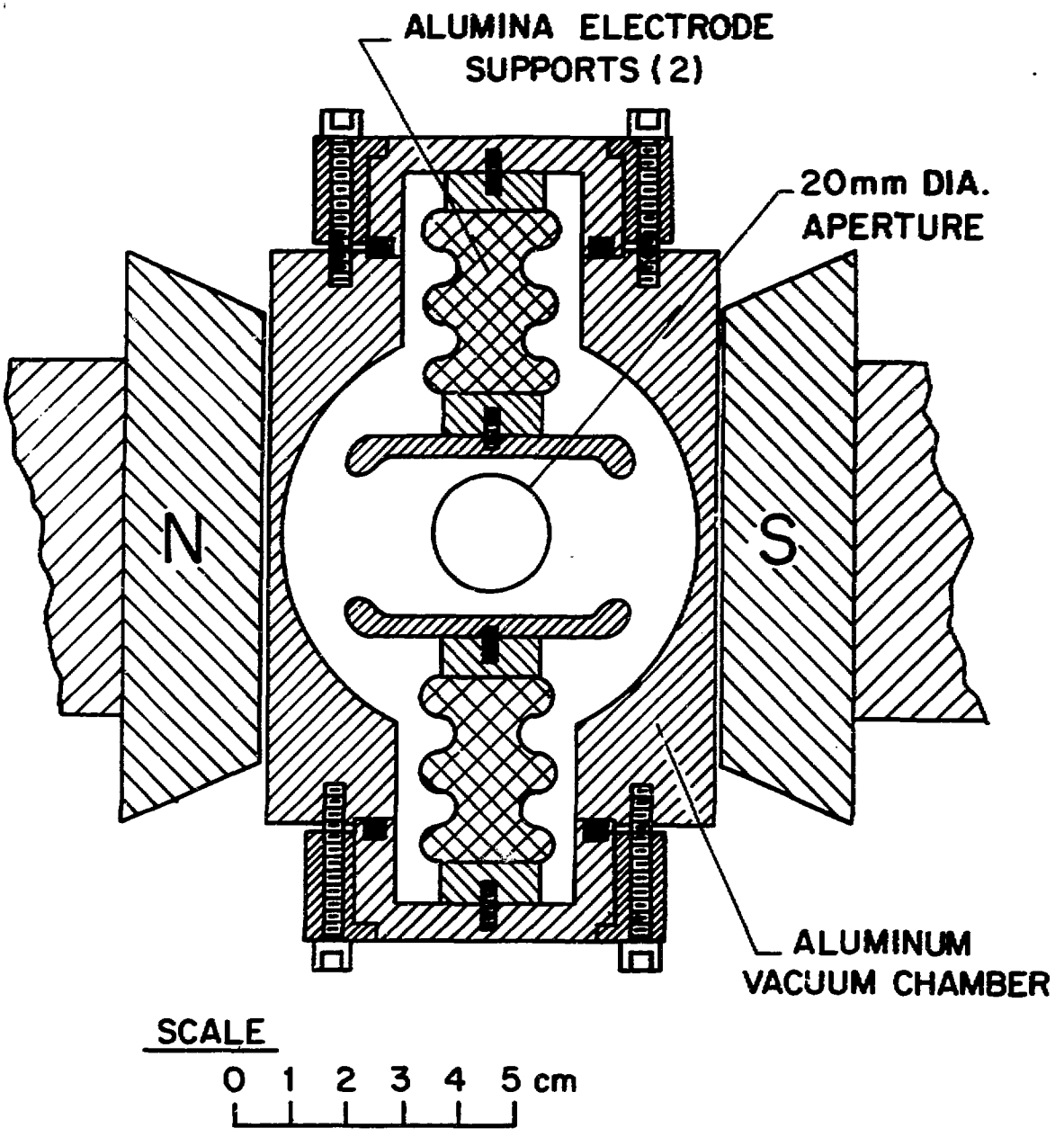
ALUMINA ELECTRODE
SUPPORTS (2)
20mm DIA.
APERTURE
N
S
ALUMINUM
VACUUM CHAMBER
SCALE
0 1 2 3 4 5 cm

Fig. 9

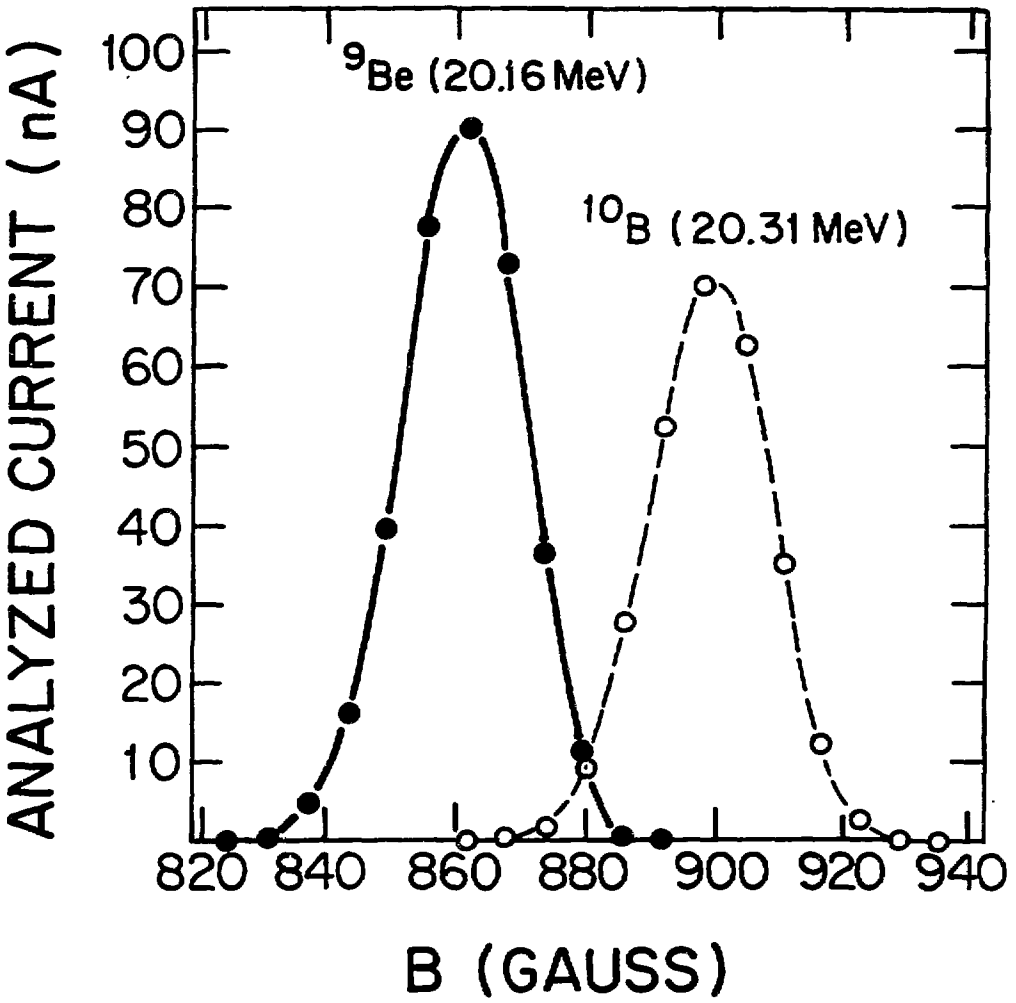
ANALYZED CURRENT (nA)
100
90
80
70
60
50
40
30
20
10
^{9}Be (20.16 MeV)
^{10}B (20.31 MeV)
820 840 860 880 900 920 940
B (GAUSS)

Fig. 10

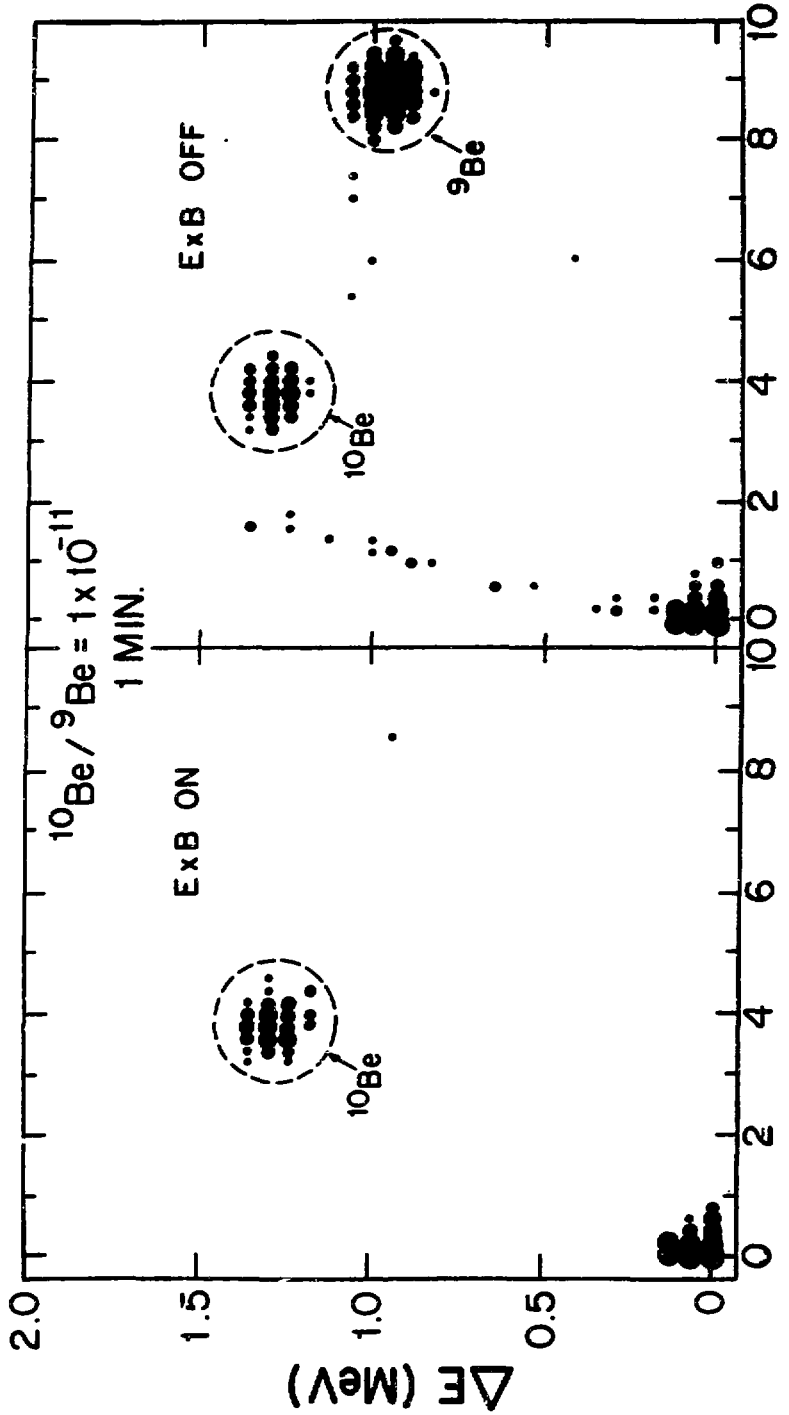
ΔE (MeV)
2.0
1.5
1.0
0.5
0
E x B ON
E x B OFF
$^{10}Be / ^{9}Be = 1 \times 10^{-11}$
1 MIN.
^{10}Be
^{10}Be
^{9}Be
0
2
4
6
8
10
100
E_T (MeV)

Fig. 11

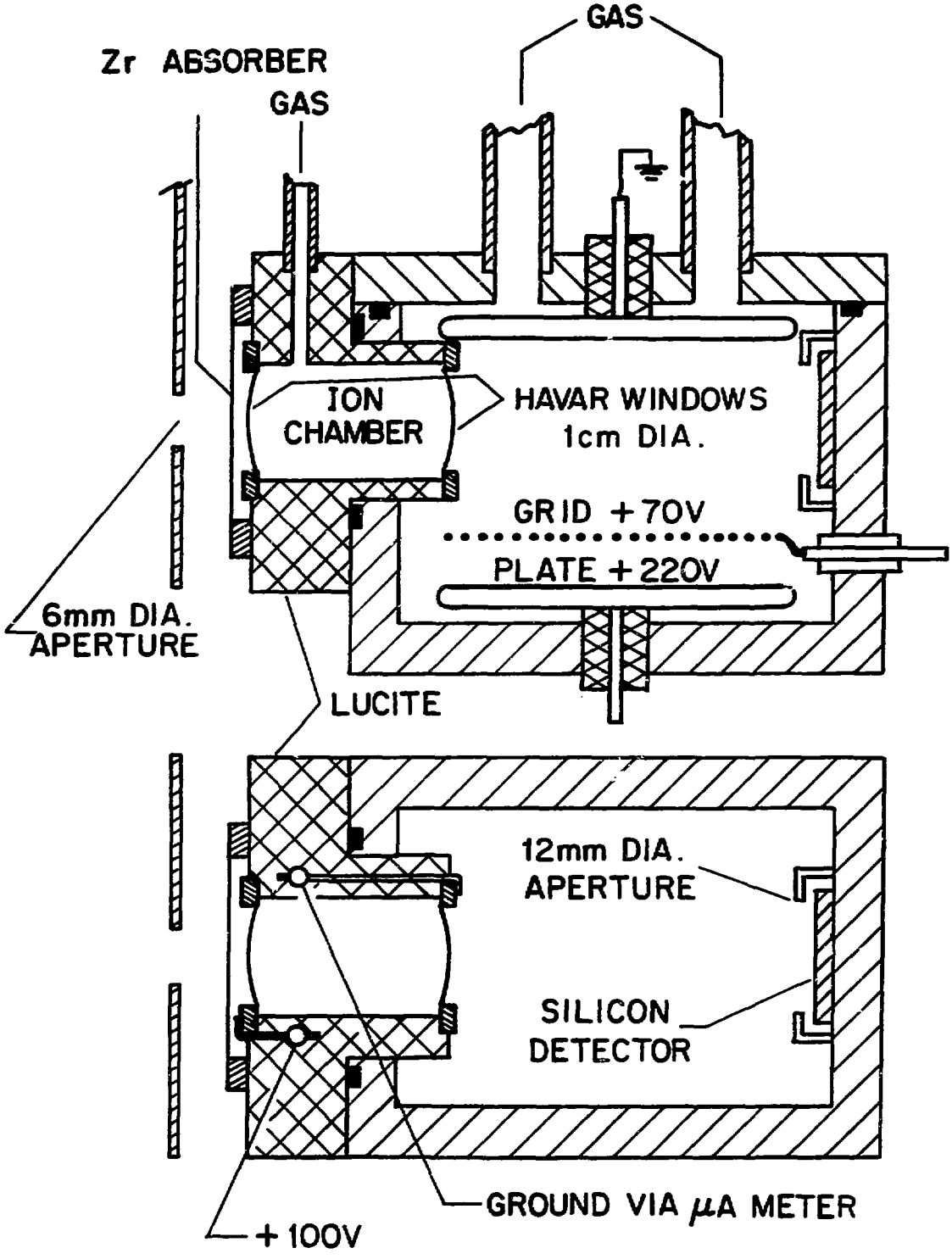
GAS
Zr ABSORBER
GAS
ION
CHAMBER
HAVAR WINDOWS
1cm DIA.
GRID +70V
PLATE +220V
6mm DIA.
APERTURE
LUCITE
12mm DIA.
APERTURE
SILICON
DETECTOR
GROUND VIA μA METER
+100V

Fig. 12

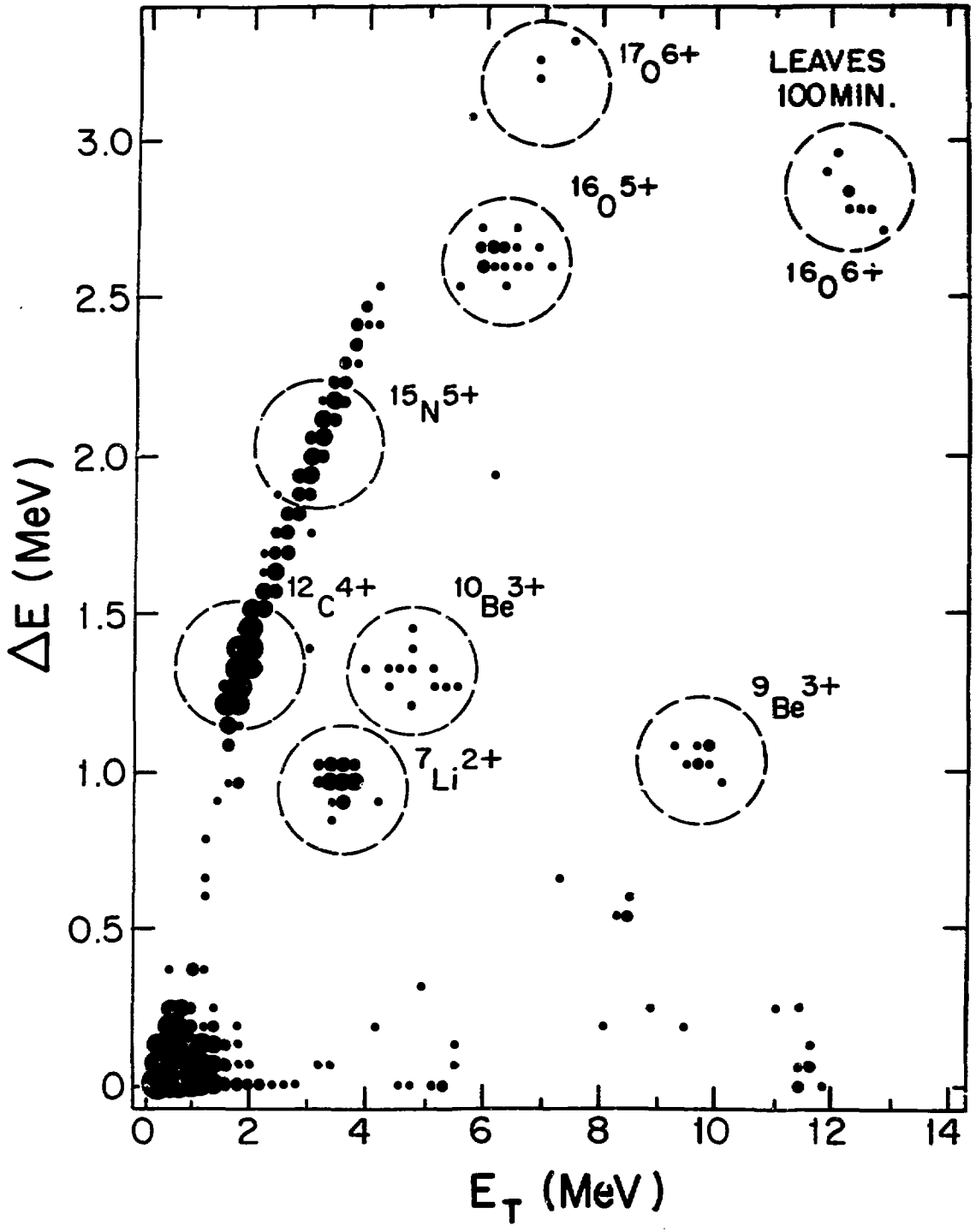
$^{17}O^{6+}$
LEAVES
100 MIN.
$^{16}O^{5+}$
$^{16}O^{6+}$
$^{15}N^{5+}$
$^{12}C^{4+}$
$^{10}Be^{3+}$
$^{9}Be^{3+}$
$^{7}Li^{2+}$
ΔE (MeV)
E_T (MeV)
0
0.5
1.0
1.5
2.0
2.5
3.0
0
2
4
6
8
10
12
14

Fig. 13

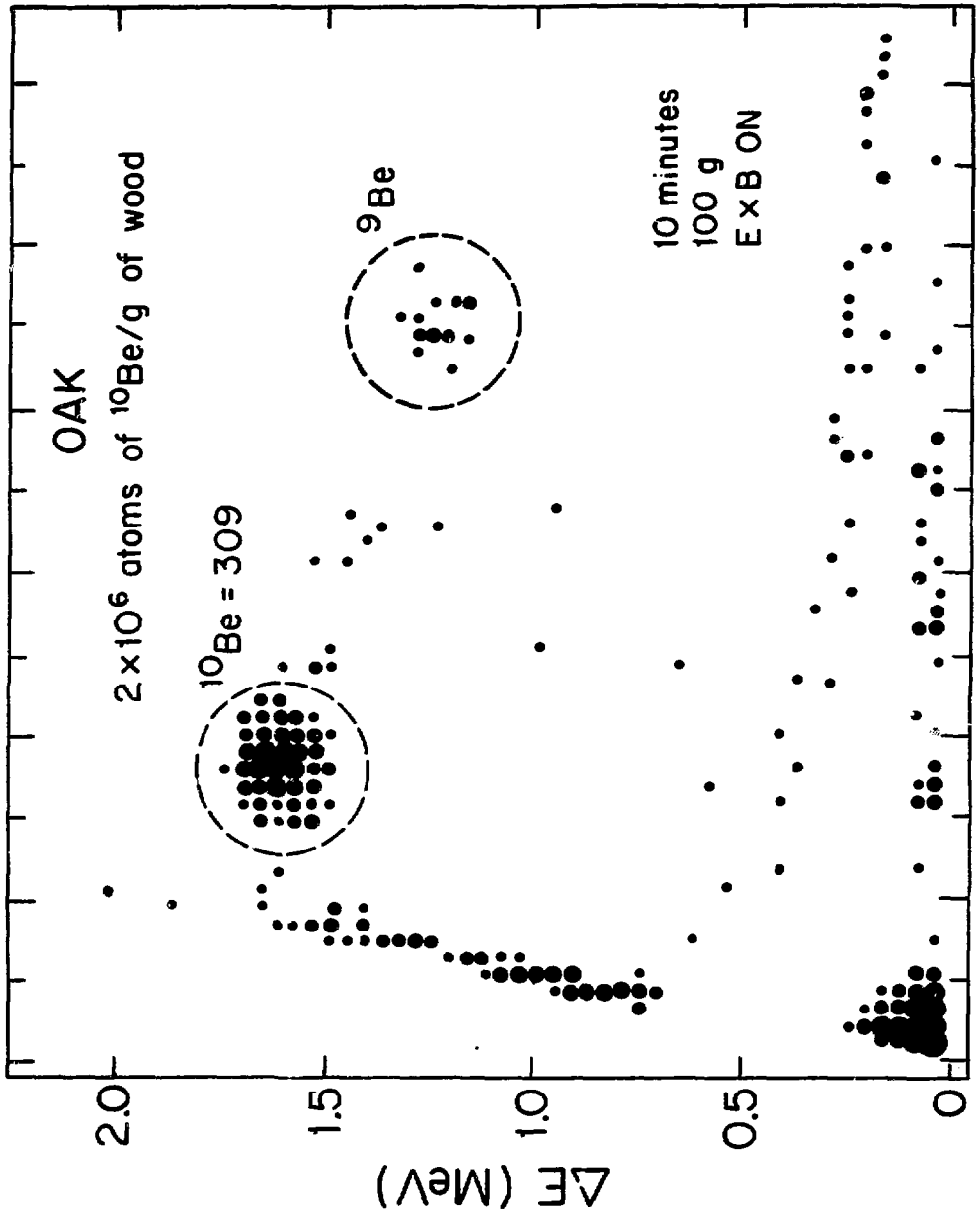
OAK
2×10⁶ atoms of ¹⁰Be/g of wood
¹⁰Be = 309
⁹Be
10 minutes
100 g
E×B ON
ΔE (MeV)
E_T (MeV)
0
0.5
1.0
1.5
2.0
2
4
6
8
10
12

Fig. 14

IMPROVEMENTS IN THE APPLICATION OF A TANDEM VAN-DE-GRAAFF ACCELERATOR FOR ULTRA-SENSITIVE MASS SPECTROMETRY

M. Suter, R. Balzer, G. Bonani, Ch. Stoller and W. Wölfli
Laboratorium für Kernphysik, Eidg. Technische Hochschule 8093 Zürich, Switzerland

J. Beer, H. Oeschger and B. Stauffer
Physikalisches Institut, Universität Bern, 3012 Bern, Switzerland

1. INTRODUCTION

In 1979, when this project was started, several other laboratories had already demonstrated that ^{14}C and other rare radioisotopes present in concentrations of 10^{-10} - 10^{-16} can be detected with existing tandem accelerator facilities[1]. These experiments have shown that the existing facilities are neither suited for these high precision measurements nor efficient in routine applications. Therefore, specifically designed facilities for highly sensitive mass spectrometry were proposed at the First Conference on Radiocarbon Dating with accelerators[2] and are now under construction.

A modification of the EN-Tandem facility existing at the ETH was undertaken applying a concept similar to that used for the dedicated facilities. First an isotope analyzer system consisting of an electrostatic deflector, a magnetic spectrometer and a ΔE-E counter was set up on a separate beam line at the high energy end of the accelerator. After replacement of some unstabilized power supplies, first measurements were performed in 1980 using the existing ion sputter source with cone geometry[3]. These measurements gave reproducible results within 5-10%. Subsequently, a new ion source arrangement was installed including a vacuum lock for sample loading and a new high resolution 90^{0}-inflection magnet. For measuring isotopic ratios accurately, a fast cycling system is now under development. Furthermore an electronic control system has been designed which allows to tune the ion beam in a reproducible way and continuously monitor it during operation.

2. EXPERIMENTAL ARRANGEMENT

The new ion source is installed on a separate entrance port to the inflection magnet, and the analyzing system on the high energy side is on a separate beam line, so that most of the components used for mass spectrometry are independent of other experiments performed with the same accelerator.

A schematic diagram of the arrangement is given in Fig. 1. Only those components which were used for the experiments described here are indicated. The negative ions are produced by a Cs-sputter source. The ions extracted at energies of 30-60 kV are focussed with a first single lens onto the object slits of the 90° inflection magnet. One essential part of the fast cycling system is the magnet chamber which is insulated, so that a high voltage can be applied to it. The acceleration and deceleration gaps are located symmetrically to the magnet and are close to the object and image slits. High voltage pulses up to 10 kV can be applied to the magnet chamber box in order to change the energy of the ions entering the magnet. This allows rapid switching from the measurement of one isotope to another one leaving the magnetic field constant. A special Faraday cup is set up behind the inflection magnet to monitor the ^{12}C beam while ^{14}C is measured. Two single lenses and electrostatic steerers are used to direct the beam into the accelerator. The accelerator can be used with a gas or a foil stripper. At present, a magnetic quadrupole lens is used to focus the beam at the high energy side of the accelerator. This leads to different focussing conditions for the various isotopes having the same energy. Therefore this lens has to be replaced by an electric quadrupole lens. After passing the degaussed analyzing magnet which is not used in this experiment the ions enter a 15°-electrostatic deflector which selects ions heaving a certain energy and charge state. The ions are then analyzed by a 90°-magnetic spectrometer having a resolution of $p/\Delta p=500$. Several apertures had to be mounted in front of as well as behind the magnetic spectrometer in order to eliminate

scattered particles. The Faraday cups and the ΔE-E gas counter are mounted on supports which can be adjusted in a reproducible way for the various isotopes of one element and rearranged easily for the measurement of the isotopic composition of other elements of interest.

3. ION SOURCE

Fig. 2 shows the ion source box in detail. The source was specially designed for low contamination between specimens (cross talk) and convenient loading of samples[4]. The arrangement is constructed in such a way that single components can easily be replaced. The basic layout follows the arrangement proposed by Mueller and Hortig[5]: A cesium beam produced by a porous tungsten surface ionizer (same type as in the Extrion source) impinges on a sputter target at an angle of 30°.

The ion source is enclosed in a stainless steel box pumped by a 2000 l/s diffusion pump (Pumpoil: SANTOVAC 5). A vacuum of 2-4 10^{-7} bar can be reached under operating conditions. On one side of the box the targets are stored in a cassette, which can be moved on a rail by means of a rotatable shaft. The cassette can be transported through a valve into a vacuum lock, so that the whole cassette containing up to 25 samples can be exchanged or loaded during full operation of the ion source. The samples located in the cassette are well shielded from the sputtering region in order to minimize contamination by sputtered material. The individual samples are mounted in the middle of a copper disc 25 mm in diameter and 3 mm thick. A particular sample can be brought to the sputter position with a manipulator which picks it up from the cassette and swings it onto the target holder. The exchange of targets takes place within a few seconds during full operation of the source. All steps of the procedure can be controlled manually or by a digital electronic system, which can be connected to the computer.

The cesium ion gun is mounted on a flange attached to the side of the vacuum box. The extracted negative ions are focussed by a single lens

onto the object slits of the inflection magnet. Electrostatic steerers are present for small angle corrections of the beam.

Using graphite samples, this ion source produces steady beams in the range of 10-20 μA C^-. Background beams obtained from a blank copper disc are less than 1 nA under equal conditions.

4. FAST CYCLING SYSTEM

In order to determine isotopic ratios accurately, it is advantageous to measure periodically the stable isotopes on the high energy side of the accelerator, so that all isotopes do have almost the same path from the ion source to the detector. When ^{12}C is monitored in addition at the low energy side during the time intervals, in which ^{14}C is injected into the accelerator, transmission variations can be recognized immediatly. By measuring periodically the ratio of the stable isotopes, fractionation changes can be monitored. All the additional information obtained by this technique, can significantly improve the reliability of the system.

It is a problem, that most existing tandem accelerators are neither designed to handle large beam intensity variations occuring when switching from a rare radioisotope to a abundant stable isotope, nor capable to handle intense beams of more than 10 μA continuously. Therefore the intense beams have to be attenuated or they can be injected only in very short pulses, so that the voltage variations on the terminal of the accelerator are insignificant.

At our Laboratory a fast cycling system is in preparation. It is planned to apply pulses of 200-500 μsec duration for isotopes producing intense beams. Since the intense beams can not be injected continuously, the beam transport elements have to be adjusted during the pulsed mode operation. For this purpose special current integrators with start/stop and reset features have been developed. In Fig.3 a schematic diagram of

the beam monitoring system is shown. A time sequence controller produces all the signals which are required to switch the high voltage power supply connected to the source magnet chamber, to control the current integrators and to start and stop the ^{14}C-data acquisition.

All Faraday cups and slits along the beam line are equipped with current integrators, which are capable to integrate the ^{12}C and ^{13}C beam current during short well defined time intervals. The integrated values are transmitted individually for ^{12}C and ^{13}C to the control room, where they are displayed on panelmeters and stored in the computer. With this system it is possible to tune lenses and steering elements in the pulsed mode operation and to see immediately the effect on both stable isotopes.

5. RESULTS

Recently first tests with the described arrangement have been performed. The main purpose of these tests was to check the stability of the improved system. Since the power supply for the fast switching was not yet ready, only $^{14}C/^{13}C$ ratios were measured using a slower switching sequence. ^{13}C was injected in pulses of about 20 msec duration and ^{14}C was measured during intervals of 700 msec. $^{14}C/^{13}C$ ratios were calculated for each 40 sec measuring interval. One run lasted about 14 minutes and consisted of 20 measuring intervals. For each run the standard deviation was calculated.

Three graphite samples have been used; two of them were furnished by H.A. Polach[6]. These were produced under high pressure (20 kb) and high temperature (700-1400°). Sample A was made from a sucrose dating standard (150% M) and sample B was extracted from a wood sample. Sample C was normal graphite prepared from old carbon and used for ^{14}C background measurements.

A summary of the results is given in Table 1. Sample B was used for the tuning of the system and at the beginning gave a beam of about 13 µA.

TABLE 1: Stability test, $^{14}C/^{13}C$ ratios and the corresponding errors.

RUN	SAMPLE	^{12}C-CURRENT (μA)	Stat. Error ^{14}C %	$^{14}C/^{13}C$ Counts/μC	Standard Dev. %
1	B	5.2	1.6	207.0	1.9
2	B	5.8	1.7	210.6	2.5
3	B	4.4	2.0	192.1	2.4
4	B	3.9	2.0	204.8	2.2
5	B	3.5	2.1	203.7	2.4
6	B	3.4	2.1	205.2	2.5
7	A	14.5	0.7	273.0	0.6
8	A	14.7	0.7	272.3	0.7
9	A	14.6	0.7	277.0	0.6
10	B	3.4	2.1	197.6	2.9
11	B	3.3	2.1	194.5	2.1
12	B	3.2	2.1	202.0	1.6
13	A	14.0	0.8	273.1	0.8
14	A	14.7	0.7	274.0	0.8
15	A	14.1	0.8	275.8	0.8
16	C	12.0	27	0.1	27
17	C	12.6	38	0.05	36
Mean Value					
	A		0.3	274.3	0.7
	B		0.7	201.9	3.0

However at the time of the actual runs this sample was almost burned out and delivered an unstable beam of only 3-5 μA. In contrast to this a very stable beam of 14-15 μA from sample A was obtained during the whole experiment. A few runs with sample A and B were performed in the order listed in Table 1. Except for some small corrections on the terminal voltage stabilisation system no adjustments were made during all runs listed. For sample A the standard deviations for the individual runs are 0.7-0.8%, which is consistent with the statistical uncertainty calculated from the number of ^{14}C counts. The mean value of the $^{14}C/^{13}C$ ratio determined from 6 runs performed with sample A has a standard deviation of 0.7%, which is larger than the corresponding statistical error (0.3%). This means that at this level of accuracy the systematic errors dominate. The unstable beam obtained with sample B effected the results considerably. Here the standard deviation of the mean value (3%) is significantly larger than the corresponding statistical error (0.7%). These tests show, that the system has the stability to reach 1% accuracy. But they also show clearly the problems: minor changes in the phase space of the emitted beam in the ion source can lead to transmission variations, which can cause changes in the fractionation. For the background runs performed with sample C, the runtime was 3 times longer than for sample A and B. A ^{14}C count rate of 7-15 counts per hour was registered, which corresponds to a $^{14}C/^{12}C$ ratio of about $5\ 10^{-16}$.

Fig. 4 shows a spectrum observed during a run of sample A. Only two well separated peaks are visible, which can be assigned to ^{14}C and ^{14}N. For modern carbon the ^{14}N peak is about 2 orders of magnitude less intense than the ^{14}C peak. This clean spectrum demonstrates the high rejection efficiency of the electrostatic and magnetic analyzing components.

6. SUMMARY

The tests performed have shown that the described system has the capability to reach 1% accuracy. To obtain reproducible results it is important to have stable sputtering conditions in the ion source, so that

the position and the emittance of the beam are constant. Otherwise changes in the fractionation have to be expected. It has been recognized, that fractionation effects depend very critically on the settings of the focussing and bending elements. Further tests have to be undertaken to understand these effects in detail.

It was possible to obtain very clean spectra from the ΔE-E counter by using appropriate antiscattering slits and assuring a good vacuum ($3 \cdot 10^{-7}$ bar) in the beam lines at the low and the high energy side of the accelerator. Beams with higher intensity and better emittance can be produced with the new ion source geometry, improving the transmission of the accelerator system by a factor of 2. In order to achieve 1% accuracy routinely several improvements have to be made. The fast cycling system has to be completed, so that also ^{12}C can be measured at the high energy end. The magnetic lens used on the high energy side has to be replaced by an electrostatic one. The terminal voltage regulation system needs some modifications so that it corrects automatically for slow drifts. Computer supported procedures have to be developed to adjust the beam reproducibly. We intend to begin measurements of other radioisotopes such as ^{10}Be, ^{26}Al and ^{36}Cl. For the measurement of ^{10}Be the fact, that ^{10}Be and ^{9}Be do not have the same energy when BeO or other Be molecules are injected into the accelerator, has to be taken into account. As a consequence, the electrostatic focussing and bending elements at the high energy side have to be modulated when switching from ^{10}Be to ^{9}Be.

We thank H.A. Polach for furnishing some graphite samples. This work was supported by the Swiss National Science Foundation.

References

1) Proc. First Conference on Radiocarbon Dating with Accelerators, University of Rochester, ed. H.E. Gove, 1978
2) K.H. Purser and P.R. Hanley, p.165-185, R.P. Benkens, p. 251-256, ref.1

3) M. Suter, R. Balzer, G. Bonani, W. Wölfli, J. Beer, H. Oeschger, and B. Stauffer, IEEE Nucl. Sci, NS-28 (1981) 1475
4) R. Balzer, G. Bonani, M. Suter, J. Beer, Paper presented at the Third International Conference on Electrostatic Accelerator Technology, Oak Ridge, 1981. To be published in IEEE Nucl. Sci.
5) M. Mueller and G. Hortig, IEEE Nucl. Sci NS-16 (1969) 38
6) H.A. Polach, Radiocarbon Dating Research Laboratory, The Australian National University, Canberra, Australia

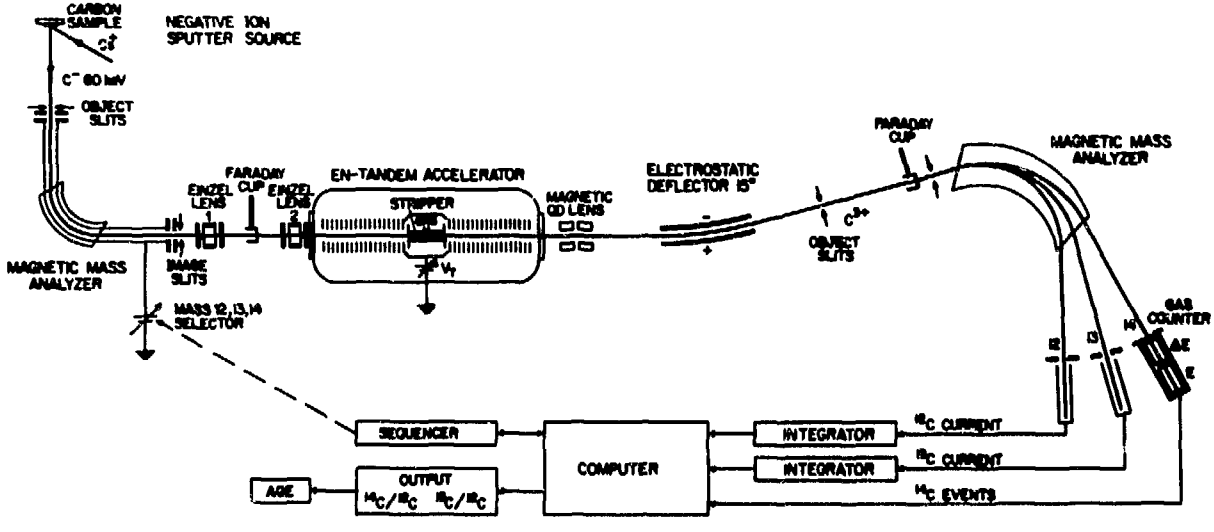

Fig. 1. Schematic diagram of the arrangement used for mass spectrometry

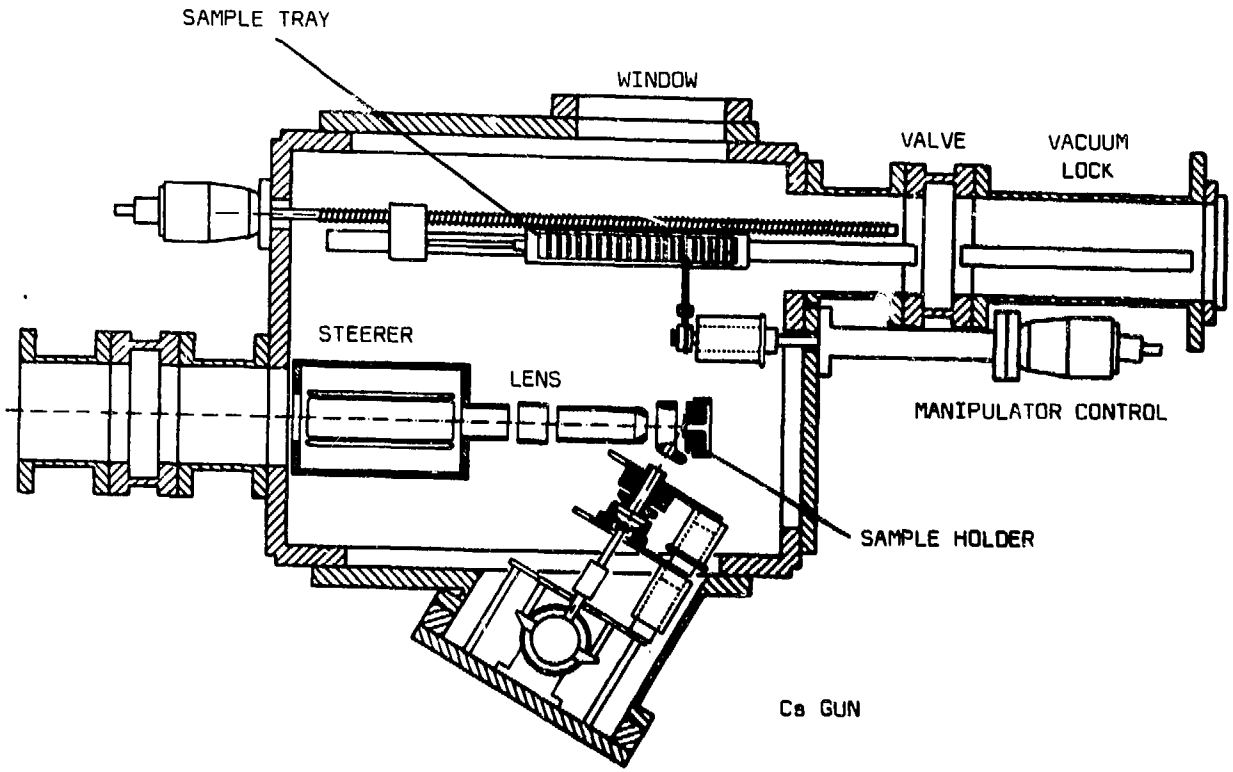

Fig.2. Negative ion sputter source arrangement, designed for mass spectrometry.

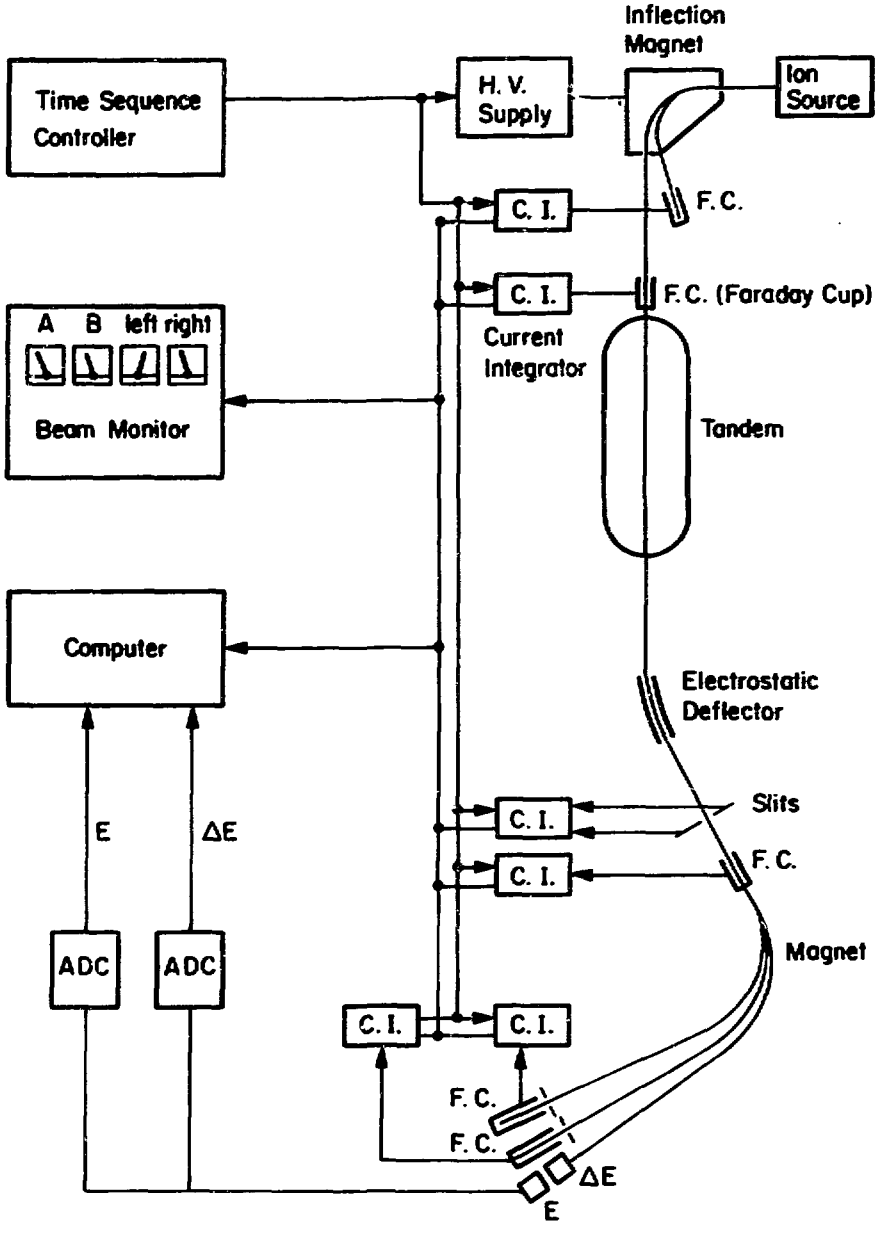

Fig. 3. Beam monitoring system.

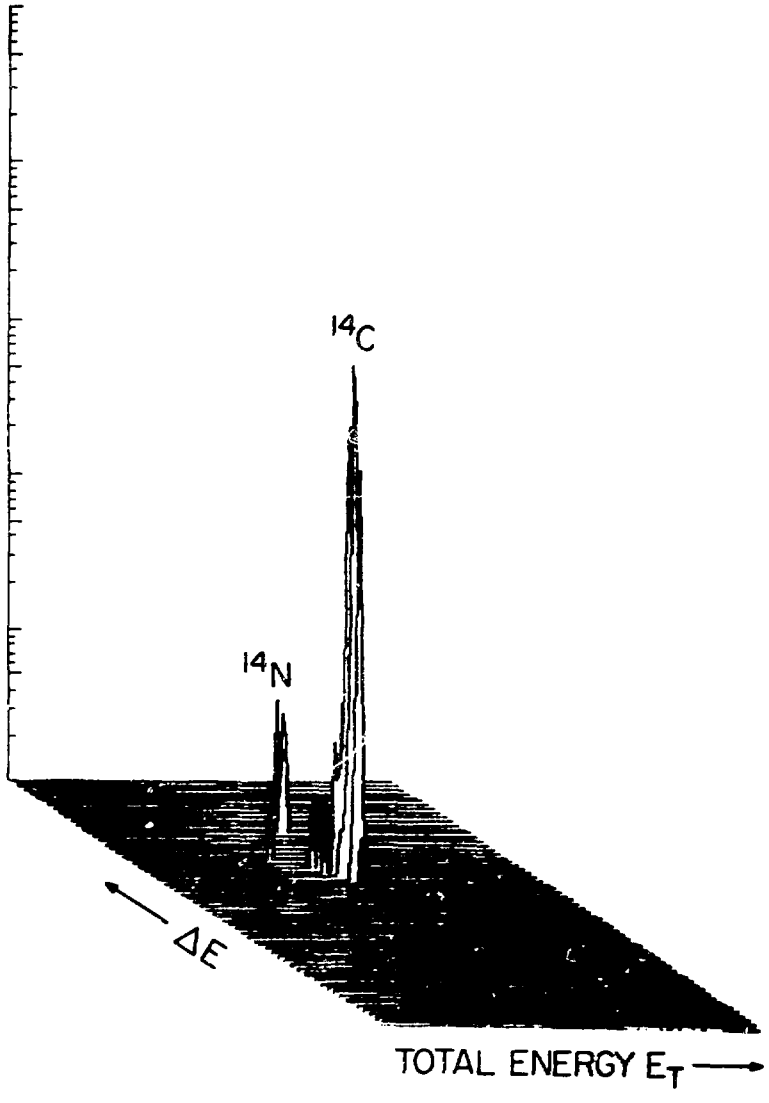

Fig. 4. A two parameter logaritmic plot of a spectrum obtained with the ΔE-E heavy ion counter, while the accelerator was set at a voltage of 4.5 MV and particles were selected having an energy of 18 MeV and charge state 3^+ (sample A).

ACCELERATOR MASS SPECTROMETRY AT THE UNIVERSITY OF WASHINGTON

George W. Farwell and Fred H. Schmidt
Nuclear Physics Laboratory and Department of Physics

Pieter M. Grootes
Quaternary Isotope Laboratory
University of Washington, Seattle, Washington 98195

1. INTRODUCTION

Our program is directed toward measurement of ^{10}Be and ^{14}C using the FN Tandem accelerator of the Nuclear Physics Laboratory.

We began work in June, 1977. Our progress and results up to August, 1979, were reported at the Tenth International Radiocarbon Conference[1,2]. The present report covers chiefly our work since then.

For ^{14}C, we are in the final stages of testing a new sample changer and alternator and are comparing three systems of normalizing the rare and abundant ion beams to give isotope ratios. We have successfully prepared graphitized carbon source samples from contemporary and other material; while the graphitized sources have given the largest carbon beams, we are exploring other possibilities, among which the use of C/Ag combinations appears very promising.

For ^{10}Be, we have begun testing and measuring samples prepared from Antarctic and Peruvian snow and ice.

In both the carbon and the beryllium programs various technical developments are in progress in addition to those reported here.

2. EXPERIMENTAL ARRANGEMENT

Fig. 1a shows the general features of our system. The sputter ion source is an Extrion-UNIS (universal negative ion source). Cs ions are reflected onto the sample after passing through six equally-spaced holes equidistant from the axis, as shown in Fig. 2.[3] A fixed Faraday cup, displaced from the main beam line as shown, serves in one mode of operation to provide a constant monitor for $^{12}C^-$.

The remainder of our system (Fig. 1b) has elements common to many other tandem Van de Graaff arrangements. We operate at 7 MV on the terminal, stabilizing the terminal voltage to within ±0.003 MV or better during data runs. The

image slit aperture at the focus of the 90° analyzing magnet is set quite narrow (0.200").

Generally, we accelerate $^{14}C^{+4}$ ions, or $^{10}Be^{+3}$ ions, to a detecting system consisting of a ΔE, E Si (Li) solid state counter telescope. Final beam cleanup by ion velocity selection is provided by a Wien filter located a short distance upstream from the detector.

Sample changer and alternator

Our recent normalization studies have pointed up the need for very precise positioning of ion source samples, including a capability for rapid alternation between two samples without loss of accuracy and reproducibility in source position. To meet this need we have designed and constructed a precision sample changer and alternator. Because of its innovative character we provide some details of its construction here. Other recent improvements are summarized below in Section 3.

Fig. 3 is a schematic diagram showing the chief features of the new sample changer; the actual device is somewhat more complex than indicated. To simplify the design of the detent wheel a new sample wheel was constructed having 20 instead of the original 18 sample positions so that only 2 detent notches are required. The pinion and ring gears have the same pitch diameter as the original ones, but the number of teeth has been increased to 32-pitch in order to reduce backlash. (This turned out to be insufficient, as discussed below in Section 6.)

The detent arm carries a ball-bearing detent. The ball-bearing slips smoothly into the notch despite the close clearance required to achieve precise radial positioning (± 0.001") of the sample. The motor drive (with gear reduction) is coupled to the pinion gear shaft by means of a slip-clutch (a rubber O-ring). This prevents damage to the mechanism should the internal sample wheel jam, and provides the necessary resilience when the detent falls abruptly into the detent wheel notch.

The sample changer can be operated either forward or backward by a manually-initiated motor drive mechanism, or automatically by an industrial-type programmable controller (5TI 2301) which carries the system through a timed cycle.

Low-energy Faraday cup for ^{12}C monitoring

To provide for continuous monitoring of the ion source output while measuring ^{14}C, a Faraday cup (FC, Fig. 1a) was placed on the low-mass side of the beam tube at the intermediate image plane produced by the inflection system. The transmission function (beam magnitude vs. inflection magnetic field) of the monitor beam is determined by the character of the image formed at the aperture in front of the fixed Faraday cup. This transmission function should match that of the primary beam (before acceleration) at the virtual entrance pupil (EP, Fig. 1a) of the accelerator. By observing a $^{13}C^{+4}$ beam to the Faraday cup at the image position beyond the high-energy analyzing magnet, and by observing also the corresponding mass-13 beam (at a different inflection setting) to the monitor Faraday cup, measuring in both cases the transmitted beam as a function of inflection magnetic field, we determined that we had achieved the desired matching of transmission functions to within a few percent at all positions on the curves down to 1/30 of peak values.[4]

3. RECENT CHANGES AND IMPROVEMENTS

A substantial number of other alterations, additions, and improvements have also been made to our system during the past several years. Some of these, initiated by our group, have benefited other research in our laboratory as well as our own. Similarly, several key improvements that are of great benefit to our program have been made by others. A list of these improvements is presented in Table I. Specific benefits derived from each improvement are noted in the right-hand column.

One of the most important items in Table I is the grid lens (GR, Fig. 1a) in the first accelerating electrode of the tandem accelerator. The grid lens has improved the carbon beam stability by a factor of 2 or 3, and the fraction of the C^- beam transmitted through the accelerator has been more than doubled. Our best measured particle transmission through the tandem is 65%; about 45% of these ions are stripped to the +4 charge state and reach the final Faraday cup. The best overall particle transmission is therefore about 30%.

The low-energy monitor cup and apertures were designed to match and to take advantage of the focusing conditions brought about by the grid lens. For some other tandem usage, however, the grid is undesirable. Therefore, it is necessary to schedule both types of operation, and to provide for easy insertion or removal of the grid.

As indicated in Table I, many of the improvements have led to better operational stability and reproducibility. For example, most ion source and beam parameters are now approaching "dial-set" capability; i.e., we need only set a particular focusing or steering element to a standard dial setting in order to obtain the same operation as pertained weeks or even months earlier. We hope to achieve this capability for every parameter in the beam system.

The improvement in terminal potential stability (Table I, item C.1) has been especially beneficial.

TABLE I

ALTERATIONS AND IMPROVEMENTS

Category and Item	Comment
A. Vacuum systems	
1. New liquid nitrogen traps:	Reduces ^{14}N with ^{14}C and raises beam currents.
a. above ion source diffusion pump	
b. on low-energy (L.E.) beam tube	
2. Cryogenic pump at high-energy (H.E.) end of tandem	Better vacuum in H.E. tubes reduces contaminant ions such as ^{13}C.
B. Sputter ion source	
1. New power supplies for source extraction and focus potentials	Provide great stability and reproducibility, with precision dial-set capability.
2. Symmetric 6-hole reflection geometry (reference 3)	Improved emittance of ion source.
3. New accelerating geometry (Fig. 4)	Increased ion output.
4. Improved Cs beam deceleration electrode shielding	Reduced ion source failures from voltage breakdown to this electrode from a serious level to zero.
5. Precision temperature control on Cs boiler	Provides beam magnitude adjustment capability with time constant of ~5 minutes.
6. Continuously-operating (rotating-coil) inflection magnet field readout.	Replaces intermittent duty cycle device which was very inconvenient.
7. Spark suppressor network for Cs ion reflection power supply	Stopped power supply failures.
8. 20-position sample changer and alternator	Enables precise positioning and rapid alternation of samples (Section 2, above).

Table I (cont'd)

Category and Item	Comment
C. Main tandem accelerator	
1. New type generating Voltracter corona control (Model I and II)	Essential to all operation. On test provided ±0.003 MV stability for >8 hours without adjustment.
2. Grid lens input to tandem	Raised transmission by factor 2.
3. New beam tubes (1978) and #2 beam tube (1981)	Accelerator was very unstable before changes.
D. Beam handling, low-energy	
1. New power supply (regulated) for L.E. beam tube Einzel lens	Provides greater stability and reproducibility, dial-set capability.
2. L.E. beam tube electric quadrupole lens replaced with a triplet, equipped with precision power supplies and biased steering	Gives increased ion transmission and provides dial-set capability.
3. Improved electrical feed-throughs on vertical and horizontal L.E. beam steering	Original arrangement was unreliable and caused days of outage.
E. Beam handling, high-energy	
1. New power supplies for H.E. beam tube and final beam tube magnetic quadrupole lenses	Provides greater stability and reproducibility, dial-set capability.
2. New image-slit beam monitor	Improved operational reliability and current-reading capability.
3. NMR monitor on switching magnet	Essential for reliable "blind" shift to rare isotope operation, and for monitoring magnetic field stability at all times.
4. Computer-assisted (but not -controlled) rapid field-shift for (coupled) analyzing and switching magnets	Saves time in moving from one ion to another.
5. Relocation of final beam line magnetic quadrupole (shifted downstream)	Provides sharper beam focus and reduced sensitivity to terminal voltage fluctuations (decreased dispersion).
F. Removal or reduction of contaminant ions	
1. Wien filter on final beam tube	Virtually eliminates ^{13}C (for ^{14}C) and ^{9}Be (for ^{10}Be) and most other beam contaminants.

4. OPERATIONAL PROCEDURES

For carbon, we generally align the entire beam and detector system using a $^{13}C^{+4}$ accelerated beam. The detector telescope is placed at ~45° from the beam direction and ^{13}C ions are scattered into the detector from a thin Au foil for energy calibration and alignment of the detectors, electronics and computer.

When it is desired to count the ^{14}C, all magnetic elements (inflection magnet, two quadrupoles, analyzing and switching magnets) are shifted to the calculated settings for mass 14 based on the observed ^{13}C settings. We have verified the validity of this procedure. The voltage on the velocity selector plates is similarly calculated and dial-set for ^{14}C transmission. Lastly, the detector is shifted by remote control into the zero degree position for ^{14}C counting.

Under normal circumstances we do not accelerate ^{12}C ions. Typically, the $^{12}C^-$ beam is from 5 to 12μA, which would result in from 10 to 30 μA at the H.E. Faraday cup. A beam current this large causes excessive loading on the tandem, with a long time-constant for recovery. The effect is possibly due to subtle alterations in the inclined field potentials in the accelerator tubes.

For beryllium our procedure is essentially the same. $^{9}Be^{+3}$ ions are used for beam and detector alignment. Magnetic elements are then shifted to appropriate settings for mass 10 (mass 26 for $(^{10}Be^{16}O)^-$ at inflection).

Sample preparation, ion source yields, and analyzed ion beam strengths for both carbon and beryllium are discussed in a companion paper (Grootes et al., this volume). We have found that only graphitized carbon produces C^- ion currents as large as can be obtained from commercial spectroscopically pure graphite. C/Ag composites appear very promising, however.

5. CONTAMINANT IONS

For ^{14}C measurements most of the contaminating ions arise from $^{13}CH^-$ and $^{12}CH_2^-$ molecular ions, generated in the ion source, which subsequently double-charge-exchange so as to produce a "white" background spectrum.

Our earlier work[1] showed that these contaminations could be reduced to a tolerable level by appropriate sample fabrication which reduced the hydrogen content of the sample material. However, once such "clean" samples were placed in the ion source they had to be used in measurements almost immediately,

and could never be removed and reinserted for additional measurement; otherwise they acquired hydrogen and the capacity to produce CH^- and CH_2^- ions in great abundance. This property severely limited the usefulness of samples.

To solve this problem, and to eliminate the analogous ^9Be ions in the case of ^{10}Be as well as other contaminants accompanying both ^{14}C and ^{10}Be, we have added ion velocity selection. A temporary Wien filter has been installed just upstream from the detectors. It has a velocity resolution $\frac{v}{\Delta v}$ of about 35/1 which is sufficient to reduce the contaminant ions by at least a factor 100. The temporary character of the filter derives from the fact that it is constructed from salvaged permanent magnets. The magnetic field is 1.1 kilogauss and the electric field is operated in the region of 23 KV/cm; both extend over an beam interval of about 46 cm.

While accelerating ^{14}C we also observe a small beam of $^{14}N^{+4}$ ions which pass through the entire beam handling and ion selection system. The ΔE, E detector telescope easily distinguishes these ions from the $^{14}C^{+4}$ ions, but their origin is nonetheless a matter of interest. We have shown that they arise from $^{14}NH^-$ ions generated in the ion source.

The inflected $^{14}NH^-$ beam is quite broad and has a low-energy tail. Thus, a few of the NH^- ions are accelerated to the terminal, arriving there with about 0.5 MeV less energy than $^{14}C^-$ ions. Some of them are stripped to $^{14}N^{+5}$. These +5 ions gain back the missing 0.5 MeV, and then acquire one additional electron in the residual gas present in the accelerator tubes. Thus, they form a "white" spectrum of particles, some of which pass the analyzing magnet with the same charge, momentum, and energy as $^{14}C^{+4}$ ions. We have verified the above sequence by tuning the inflection magnet to mass 15 and observing a considerable increase in the $^{14}N^{+4}$ component of the ΔE, E spectrum. We have also observed that the better the ion source vacuum, the smaller the magnitude of the ^{14}N contamination. Typically, the ^{14}N peak is less than 1/100 as large as the ^{14}C peak for contemporary carbon source material.

In the case of ^{10}Be beams the Wien filter easily removes beryllium (^9Be), carbon, and most oxygen and other contaminants that would otherwise enter the detector. However, it cannot remove the abundant ^{10}B ions that emerge from virtually every material we have studied. We have explored several methods for eliminating ^{10}B: (a) absorption by a foil placed just ahead of the detector, leaving a short residual ^{10}Be range with which to work; (b) differential

energy degradation of ^{10}B and ^{10}Be ions by a carbon foil (1,000 $\mu g/cm^2$) placed at the image slits just upstream from the switching magnet, whose dispersion at 30° for ^{10}Be then eliminates the ^{10}B; and (c) differential energy degradation of ^{10}B and ^{10}Be ions by a 400 $\mu g/cm^2$ carbon foil placed at the object slits upstream from the 90° analyzing magnet, whose dispersion then eliminates ^{10}B. The last option reduces the ^{10}B by a factor of 40,000 or better and appears to be the best choice if we consider both the need for maximum ^{10}Be beam intensity and the need for absolute particle identification in our ΔE, E detector system. (The short residual ^{10}Be range and the severe range straggling in the absorber foil make the particle identification more difficult in option (a).)

6. NORMALIZATION

A crucial element in the accurate measurement of isotopic abundance ratios is the normalization of one ion beam against another. During the past year we have worked with three systems of normalization. The first or "sequential transmission" method is based upon the sequential transmissions of radioactive (rare) and stable (abundant) isotope ion beams. This method provides a means of measuring directly the absolute isotopic abundance ratio for a given sample as well as for measuring the ratio indirectly by comparison with a sample of known isotopic composition. In the discussion that follows we shall refer to this as the sequential transmission method.

In the second or "concurrent L.E. monitoring" method, the stable isotope beam from a radioactive source — for example, ^{12}C for ^{14}C or ^{9}Be for ^{10}Be measurements — is monitored at the low-energy end of the electrostatic accelerator while the radioactive ion beam is measured simultaneously by particle detectors following acceleration to high energy and appropriate ion analysis (selection) in the beam handling system. We have built and are testing such a system; it includes the sample changer and alternator described in Section 2 (above). This permits rapid alternation of standard and unknown samples to minimize the effects of fluctuations in ion transmission through the accelerator.

In the third or "hybrid" method, the ion source sample alternator is used in measuring successively (a) the relative strengths (after acceleration and ion analysis) of the stable isotope ion beams from the two sources being compared, and (b) the relative strengths of the radioactive isotope beams from the same two samples. Both comparisons are made in the scattering chamber at the

terminus of the high-energy beam-handling system, the former through comparison of Faraday cup currents and the latter through comparison of detector counting rates.

Some of our experience to date with each of these methods is discussed below.

Sequential transmission method

The accuracy of the sequential transmission method depends critically upon constant ion source output during each measurement of both beams from one sample, and upon constant and equivalent ion transmission through the accelerator and beam handling system during the measurements of both samples. A rapid-sequencing system for switching all isotope-dependent beam parameters (six, in our case) would minimize the effects of fluctuations in ion source output and ion transmission, but we have not had the resources to develop such a system as yet. Nevertheless, reasonable precision has been achieved in the measurement of $^{10}Be/^{9}Be$ and $^{11}B/^{10}B$ ratios. Thus, in the $^{10}Be/^{9}Be$ results reported in ref. 1, the internal precision of measurements on various samples ranged from ±2% to ±5% (standard deviation) while isotopic ratio measurements made several weeks apart differed by 2%, 5%, and 15%, respectively, for three different samples. In tests with boron, in which both stable isotope beams (^{10}B and ^{11}B) were measured after acceleration and analysis, $^{10}B/^{11}B$ results with an internal precision of better than 1% were achieved several times but measurements made on different occasions sometimes differed by 5% to 10%. The absolute $^{10}B/^{11}B$ ratios determined by this method were always within 10% of the accepted range of values.

Because the hybrid method (see below) offers the same capabilities as the sequential method but is less sensitive to ion source and accelerator fluctuations, we shall probably abandon the latter in favor of the former for work on beryllium and on elements heavier than carbon. In the case of carbon another option is also being pursued, the concurrent monitoring method.

Concurrent L.E. monitoring method

This newly developed system permits monitoring of the ^{12}C ion source output from a carbon sample while, concurrently, the ^{14}C ions are injected, accelerated, analyzed, and counted. The required ^{12}C-^{14}C mass separation at low energy is achieved by utilizing the inflection magnet as a low-resolution

mass spectrometer ($m/\Delta m = 25$); the $^{12}C^-$ ion beam is continuously monitored at the Faraday cup (FC, Fig. 1a) placed on the low mass side of the main beam trajectory downstream from the inflection magnet. The system permits systematic alternation of unknown and standard samples, thereby minimizing the effects of fluctuations in ion transmission through the accelerator.

In practice the ^{14}C counts (normalized to the integrated $^{12}C^-$ beam) are measured both for an unknown sample and for a reference standard (e.g., carbon prepared from 1939 wood). The standard and unknown samples are alternated and counted numerous times, thus reducing the effects of variations in ion transmission by the square root of the number of measurement cycles.

In operation with carbon, the controller that facilitates this alternation of samples executes the following cycle:

Time (sec)	Operation
0	Mass-14 beam from sample #1 electrostatically deflected into tandem (deflector plates not shown in Fig. 1).
5	Computer on while routing to #1 set of counters and timers. On for 30 sec, counted only while terminal potential lies in the interval 7,000 ±2.5 KV.
35	Computer and counters gated off.
35.1	All beams deflected out. Changer starts shift to sample #2.
44.1	Sample change completed - sample #2 in position. Forward motion - no anti-backlash operation. Mass-14 beam deflected into tandem.
49.1	Computer on, routing to #2 set of counters and timers.
79.1	Computer and counters gated off.
79.2	All beams deflected out. Changer starts shift back to sample #1.
88.2	Sample change completed - sample #1 in position from final forward motion (anti-backlash operation).
88.2-0	Next cycle starts.

Note that 5 seconds is allowed for the ion output of the source sample to stabilize. During this time, if desired, the mass-14 beam (^{13}CH and $^{12}CH_2$) can

be quickly monitored at the high-energy exit of the tandem.

The fraction of time for sample counting is 60/88.2 = 73%. The counting time or the stabilization time can be altered quickly if desired. As yet, we have not made any studies to determine the optimum time intervals. The fractional counting time for the unknown sample is 36.5%.

Results obtained to date by this method will be discussed in a later section.

Hybrid method: sequential transmission with sample alternation

This method is capable of both relative and absolute measurement of isotopic abundance ratios.

In carbon work, the sample-changer cycle described above is used to measure the ratio of the respective ^{13}C beams from the two samples being compared. The beams are integrated at the final Faraday cup (Fig. 1b) over each 30-second counting cycle, and the individual measurements are averaged over at least 10 cycles in order to reduce the effects of transmission fluctuations. (These are typically 2 to 5% in any one 30-second period.) The ^{13}C sample ratio is measured both before and after a ^{14}C count. (If a $^{12}C^-$ measurement is also made during the ^{14}C count — the concurrent L.E. monitoring method — then results for the two approaches can be compared for the same ^{14}C measurement.)

Alternation of ^{13}C measurements with ^{14}C measurements requires manual shifting of five magnetic fields and one electric field (the Wien filter) and removal of the detector telescope by remote control, a total of seven operations. We also observed on one occasion a slight beam loading due to ^{13}C; this required an eighth operation, a small shift of the terminal voltage (a few KV).

At the time of reporting, a general tandem accelerator improvement program is in progress which includes full computer control of four of the five magnetic field parameters. This will greatly simplify normalization by this method.

Despite the relative awkwardness of the current methods of shifting from one isotope to another, the hybrid method has given results with a precision in the range of ±1 to ±3% in several recent tests (see below).

Comparison of methods

Among the methods discussed above, the sequential transmission and hybrid modes of operation offer the two alternatives of relative and absolute isotopic abundance ratio determinations, while the concurrent L.E. monitoring mode is restricted to relative measurements.

Absolute measurements are the most direct and in principle the most desirable. However, there are numerous caveats that must be observed. Corrections may be necessary for isotope fractionation in the ion source and at the terminal stripper. The Faraday cup must provide an accurate particle count of the abundant isotope with an efficiency matching that of the detector for the rare isotope. The transmission of the entire beam system must be isotope-independent; this imposes stringent requirements upon the accuracy and reproducibility of the alternation of all relevant beam parameters, as well as assurance that no stray or unknown magnetic fields are present that affect the transmission factor differently for different isotopes.*

It is possible to circumvent these effects, in both the sequential transmission and the hybrid modes of operation, by making relative measurements only, i.e., by comparing an unknown sample with a standard. To do so requires, however, that the unknown and standard samples be geometrically similar, be positioned accurately, and have comparable ion outputs. The fraction of operational time that can be devoted to sample counting will depend upon the frequency of the required shifts between isotopes; this in turn will be controlled largely by the long-term stability of the accelerator and beam-handling systems.

Relative measurements made by the concurrent L.E. monitoring method are also free of problems due to fractionation or stray magnetic fields. However, the sensitivity to small differences in sample geometry and to differences in ion output is apparently much greater than for the other methods.

Some of these considerations can be placed in clearer perspective through a simple argument involving source strengths and ion transmission factors, as follows:

For the concurrent monitoring method, the relative ^{14}C activity ratio, R, of unknown (2) to standard (1) is given by:

$$R = \frac{^{14}C(2)T_2/^{12}C(2)T_2^M}{^{14}C(1)T_1/^{12}C(1)T_1^M}, \qquad (1)$$

*The beam tubes of our FN tandem are equipped with a number of permanent magnets to suppress electron loading. The influence of these magnets becomes evident when the machine is first aligned on ^{12}C, then shifted to ^{1}H (a sputter source puts out a 1 to 5nA $^{1}H^-$ beam from graphite). The tuning parameters, especially the vertical steering, differ for the two masses. We infer from this that smaller, but not easily observable, effects probably exist for ^{14}C and ^{13}C. Recent experimental results for absolute ratios would suggest, however, that such effects are very small or negligible (see below).

where $^{12,14}C(1,2)$ are source strengths for samples 1 and 2 and $T_{1,2}$ and $T_{1,2}^{M}$ are the accelerator ion transmission factors and ion transmission factors to the L.E. monitor, respectively, for the two samples.

For an accurate determination of R a requirement imposed is therefore that

$$T_2/T_2^{M} = T_1/T_1^{M}, \tag{2}$$

i.e., the ratio of L.E. and H.E. transmissions must be sample-independent. This condition can be met if the samples are indistinguishable geometrically throughout the measurement period. The T^{M} factors also include effects due to non-linear secondary electron production in the monitor L.E. Faraday cup, so that the ion outputs from the two samples should be nearly equal. It is also likely that each sample should be subjected to the Cs sputtering beam for about the same length of time; consequently, one standard sample must be provided for each unknown, or possibly each pair of unkown samples. The transmissions, particularly T, fluctuate with time; for good results such fluctuations must be random and uncorrelated with the sample cycling time.

For relative ^{14}C measurements made with the hybrid method of sample comparison the transmission ratio requirement of Eq. 2 is eliminated. For this method, the ^{14}C activity ratio for samples 1 and 2 is

$$R = \frac{^{14}C(2)T_2/^{13}C(2)T_2'}{^{14}C(1)T_1/^{13}C(1)T_1'} \tag{3}$$

where the transmission T_1 (for ^{14}C) is not necessarily equal to T_1' (for ^{13}C) due, say, to stripper fractionation or stray fields (similarly for T_2 and T_2'). However, the two ratios T_2/T_1 and T_2'/T_1' can be expected in practice to be equal, unless the $^{13}C_{1,2}$ beams differ by enough to produce significantly different loading of the tandem. Thus, the measured activity ratio R should be reasonably independent of sample geometry, an important consideration.

At present the concurrent L.E. monitoring method has an advantage in regard to the fraction of time available for ^{14}C counting; this advantage will be significantly reduced as soon as arrangements can be made for a more rapid shift of the beam parameters between isotopes.

Both the concurrent monitoring and the hybrid methods are subject to uncertainties due to fluctuations in accelerator transmission; these affect the hybrid method more seriously since both the ^{14}C and ^{13}C measurements are influenced, while in the concurrent monitoring method only the ^{14}C beam is affected.

The best way to compare methods, of course, is to try them, and we have been engaged in an extended, though not yet completed, series of such tests.

Normalization tests and comparisons

An obvious and effective way to test normalization methods is to measure the ^{14}C activity ratio R for samples prepared from the same material, as, for example, graphitized carbon from wood from dated tree rings. For samples of identical origin R should be 1.00. We have used 1939 wood for this purpose. 1939 wood is known to contain 1.15×10^{-12} atoms of ^{14}C per atom of ^{12}C and thus can be used to assess the accuracy of absolute as well as relative isotopic ratio measurements. We have also used 1964 wood in our tests. Our sample of this wood has about 1.8 times the ^{14}C activity of 1939 wood; the activity is now being measured more exactly by beta-counting.

Results: concurrent L.E. monitoring method (relative)

Because a number of measurements by this method yielded valuable insights into the problems that must be faced in using it, we record here a succession of determinations that have, in some cases, far larger errors than one can accept in a proven system. The indicated uncertainties are from ^{14}C counting statistics only.

Comparison	R (measured)	R (expected)
(a) 1964 vs. 1939 wood	1.88 ±0.08	about 1.8
A repeat measurement	2.09 ±0.07	

Comment: The discrepancy was believed due to backlash in the sample-changer gear mechanism. A 5TI program was devised to eliminate backlash.

(b) 1964 vs. 1964 wood	0.978 ±0.013	1.00
A repeat measurement	0.815 ±0.009	

Comment: A vertical deflection power supply was found inoperative after the second measurement. These samples had concave surfaces, and it appears that non-flat surfaces result in greater sensitivity to tuning parameters.

(c) 1939 vs. 1939 wood	1.26 ±0.03	1.00

Comment: When these samples were removed, the distance from the sample surfaces to the accelerating electrode differed by 0.012".

Comparison	R (measured)	R (expected)
(d) 1939 vs 1939 wood	1.29 ±0.05	1.00

Comment: These samples differed in ^{12}C output by a factor of 4.5 (1 μA vs. 4.5 μA). A simultaneous measurement by the hybrid method was more successful (see below).

(e) 1964 vs 1939 wood	1.77 ±0.05	about 1.8

Comment: These samples differed in ^{12}C output by only about 20%, and both had what we consider to be optimum (flat) surfaces.

Results: hybrid method (relative)

Here we present our most recent results for comparison of $^{14}C/^{13}C$ ratios for samples of identical origin. Ion source and accelerator conditions were quite stable, and samples of optimum shape were used. The expected activity ratio R is 1.00 in all cases. Here, R is expressed as the ratio

$$R = \frac{^{14}C(1)}{^{14}C(2)} \Big/ \frac{^{13}C(1)}{^{13}C(2)} ,$$

where the ratio of ^{14}C count rates for samples 1 and 2 is taken with the standard deviation from counting statistics, and the ratio of ^{13}C beam currents is taken with the standard deviation representing fluctuations in measured ^{13}C currents over more than ten comparison intervals in each case.

Comparison	R (measured)
(a) 1939 vs. 1939 wood (4/10/81)	R = 0.920 ±0.022/0.922 ±0.010 = 0.998 ±0.026
(b) 1939 vs. 1939 wood (4/30/81)	1.023 ±0.045

Combined value: 1.01 ±0.03

Expected value: 1.00

Comment: Further measurements will be undertaken to validate these very favorable results.

Results: hybrid method (absolute)

Absolute $^{14}C/^{13}C$ ratios can also be calculated from the data taken on 1939 wood samples 1 and 2 on 4/10/81, and these can be translated into $^{14}C/^{12}C$ ratios. Here, for a given set of measurements on one sample,

$$\frac{^{14}C}{^{12}C} = \left(\frac{^{14}C \text{ count rate}}{^{13}C \text{ current}}\right)\left(\frac{^{13}C/C}{^{12}C/C}\right)$$

The results are as follows:

Date	Sample	Number of Determinations	Ratio $^{14}C/^{12}C(10^{-12})$
4/10/81	1939#1	2	1.152 ±0.045
4/10/81	1939#2	2	1.146 ±0.040
4/30/81	1939#1	2	1.104 ±0.044
4/30/81	1939#2	1	1.176 ±0.059

Combined: $^{14}C/^{12}C = (1.145 \pm 0.010) \times 10^{-12}$ (1939 wood)

Expected: $^{14}C/^{12}C = 1.15 \times 10^{-12}$ (1939 wood)

Comment: The consistency of the results for a total of seven determinations made on two different samples during two accelerator runs several weeks apart is most encouraging, as is the accuracy of the average value obtained for the absolute ratio $^{14}C/^{12}C$.

A few further comments and generalizations can be made, or reemphasized, in the light of the normalization tests discussed above.

(a) Accurate positioning of ion source samples is extremely important; reproducibility within ±0.002" is probably good enough for lateral and radial positioning.

(b) Sample shape, configuration, and ion yield are also very important. For a comparison by the ^{12}C concurrent monitoring method, samples should be geometrically identical (a flat surface works well and is easy to reproduce). Sample surfaces should be similarly positioned with respect to the accelerating electrode within about 0.002". Ion yields should not differ by more than about 20% lest there be monitoring errors due to secondary electron production at the L.E. Faraday cup.

(c) Voltage supplies for the ion source and for all elements of the beam system must be extremely stable.

(d) Normalization of ^{14}C count rates to the accelerated ^{13}C beams gives results that are very consistent within the estimated uncertainties (these are based principally upon counting statistics and observed beam fluctuations). Probable errors as low as ±1 to ±3% in relative isotopic ratio measurements demonstrate the excellent long-term stability of the system and the reproducibility of the beam parameter settings. The success of the absolute $^{14}C/^{12}C$

determinations on 1939 wood suggests that fractionation effects are small; that our tranmission factors are not significantly isotope-dependent; and that the petroleum pitch used in our carbon sample preparation (Grootes et al., this volume) disappears during high-temperature graphitization of the samples and therefore is not a source of error.

We believe that the capability for routine relative measurements of isotopic abundance ratios accurate to ±1%, apart from counting statistics, can be achieved with our system, and that the steps yet required to accomplish this goal are relatively minor in comparison to those already taken.

ACKNOWLEDGEMENTS

It is a pleasure to acknowledge the contributions of colleagues in the Nuclear Physics Laboratory and the Quaternary Isotope Laboratory. Dr. William G. Weitkamp, Technical Director of the Nuclear Physics Laboratory, Mr. Harold Fauska, Dr. Derek Storm, Dr. Thomas A. Trainor, Mr. John Amsbaugh, Mr. Gervas M. Hinn, Mr. Donald Leach and Mr. Carl Linder have given especially significant support in the accelerator aspects of the program. We are grateful to Professor Minze Stuiver, Director of the Quaternary Isotope Laboratory, for making the outstanding facilities of that laboratory available to us and for providing ^{14}C materials, valuable information and advice, and personal encouragement in our endeavors.

This work has received support from the National Science Foundation (Grant EAR-7904523, Geochemistry Program) and from the U.S. Department of Energy

REFERENCES

1. G.W. Farwell, T.P. Schaad, F.H. Schmidt, M.Y.B. Tsang, P.M. Grootes, and M Stuiver, Radiocarbon 22, 487 (1980).
2. P.M. Grootes, M. Stuiver, G.W. Farwell, T.P. Schaad, and F.H. Schmidt, Radiocarbon 22, 838 (1980).
3. F.H. Schmidt and G.W. Farwell, Bull. Am. Phys. Soc. 24, 650 (1979).
4. F.H. Schmidt, G.W. Farwell, and P.M. Grootes, Bull. Am. Phys. Soc. 26, 593 (1981).

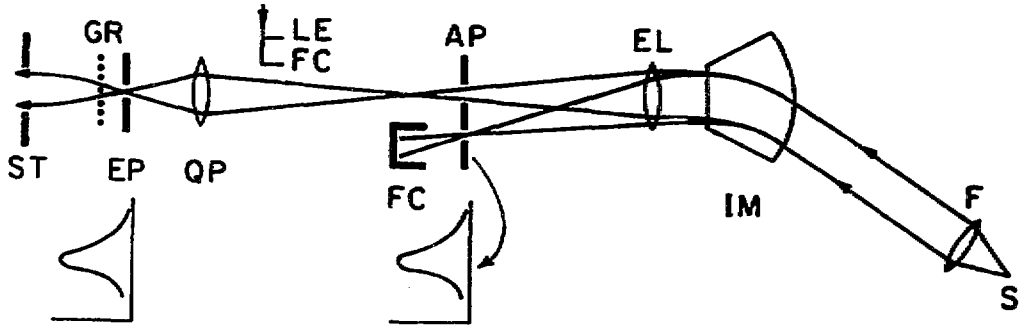

Fig. 1a: Disposition of elements in the low energy (L.E.) beam system. Two Faraday cups are shown: a fixed monitor for $^{12}C^{-}$, and a removable one farther downstream. Focusing and steering elements are electrostatic. GR is a grid lens on the first electrode of the accelerator tube; EP is the virtual entrance pupil due to the real pupil of the stripper ST.

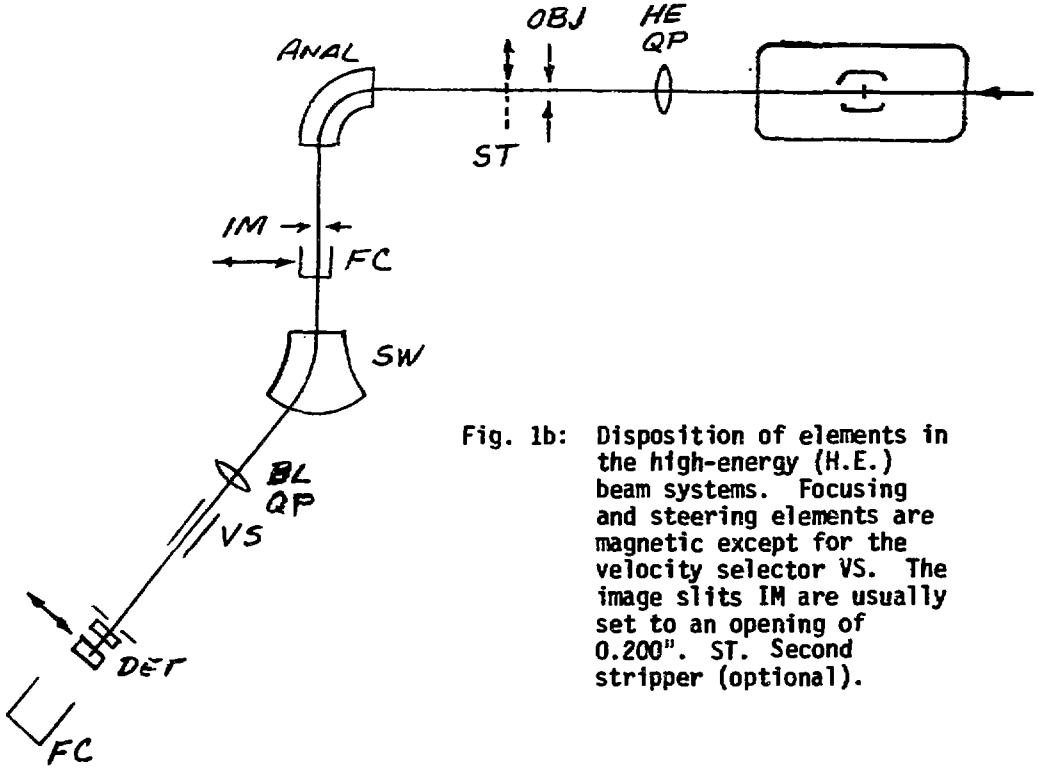

Fig. 1b: Disposition of elements in the high-energy (H.E.) beam systems. Focusing and steering elements are magnetic except for the velocity selector VS. The image slits IM are usually set to an opening of 0.200". ST. Second stripper (optional).

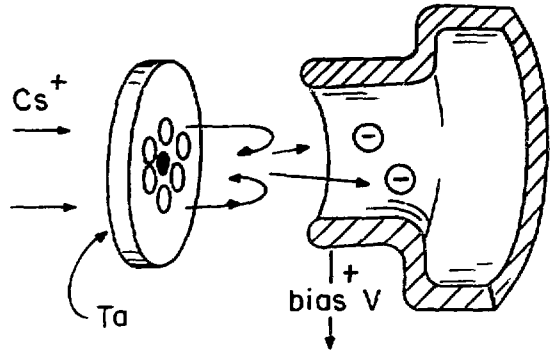

Fig. 2: Six hole reflection geometry. The bias voltage varies from 150 to 270 volts, depending inversely on extraction current in the range 2.5 mA down to 0.2 mA. The sample is 3/32" in diameter, and each of the six Cs beam holes is also 3/32" D.

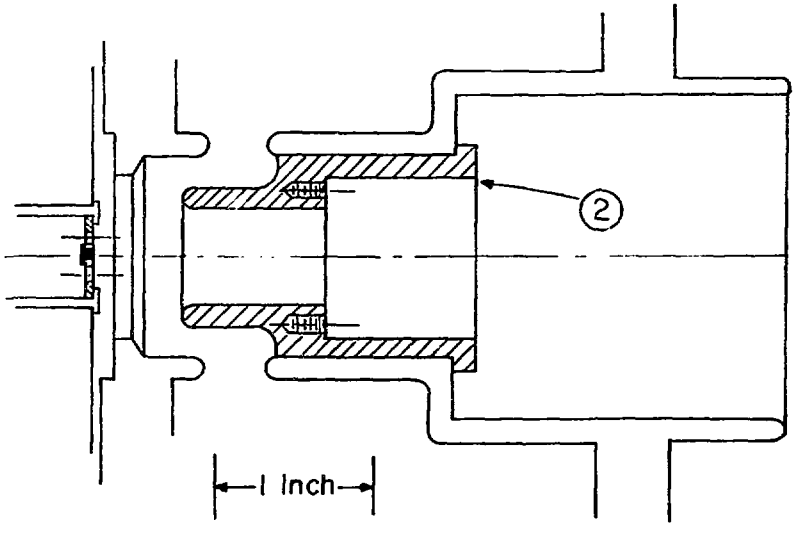

Fig. 4: New accelerating geometry. The electrode, 2, is made of aluminum. It can be inserted or removed without disassembling the source by means of long rods which screw into the threaded holes.

Fig. 3: Simplified diagram of Sample Changer Mechanism. The original 18 positions were increased to 20. The belt drive provides a clutch and cushioning action. Positioning accuracy ±0.001" with anti-backlash program for controller.

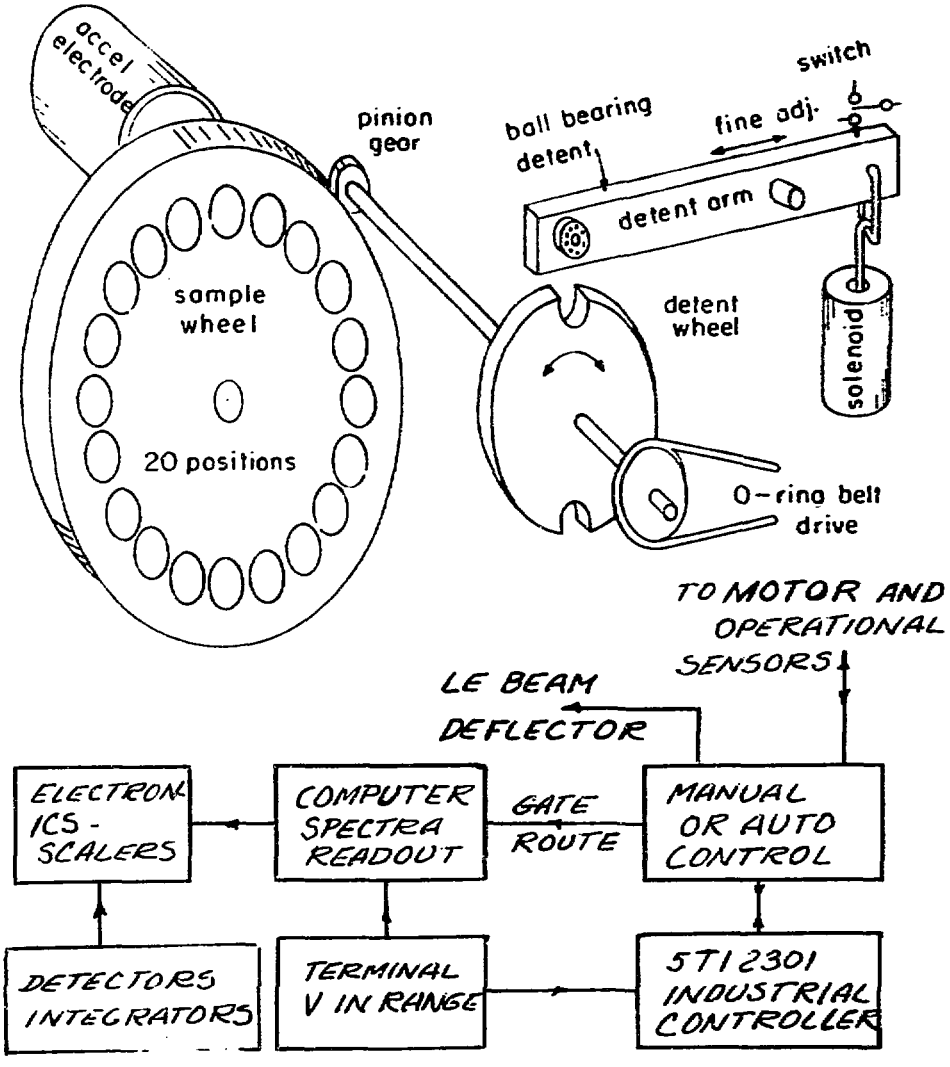

PLAN FOR MASS ACCELERATOR SPECTROMETRY AT GIF-SUR-YVETTE AND SACLAY

B. BERTHIER[+], L. BIANCHI[+]

[+]D.Ph.N/BE, Centre d'Etudes Nucléaires de Saclay, 91191 Gif-sur-Yvette

[++] G. DELIBRIAS[++], V. KOECHLIN[++]

C.F.R., Laboratoire mixte CNRS-CEA, 91191 Gif-sur-Yvette

1 - INTRODUCTION

From early 50', a carbon 14 dating laboratory was created at the Centre des Faibles Radioactivités de Gif-sur-Yvette (C.F.R.). From this time, more than 5,000 archaeological and geological samples were measured with the Libby method by this laboratory (1).

C.F.R. is in the way to actualise its dating activities with the new accelerator method. A 3 MV General Ionex Tandetron is planed to be located at Gif-sur-Yvette next year and shared with Orsay University for ^{14}C, ^{10}Be and ^{36}Cl mass spectroscopy measurement. During the same time atemps have been made to adapt the Super FN Tandem of the Centre d'Etudes Nucléaires de Saclay for ^{14}C dating.

2 - THE SACLAY TANDEM BEFORE MODIFICATIONS

In its conventionnal configuration (Fig. 1), the Saclay Tandem accelerator tank was connected with :

1) a negative ions injection section consisting mainly in a duoplasmatron gas filled ion source, a lithium oven device where negative ions are created by charge-exchange from positive ions in lithium vapour, and a 20° deflection magnet.

2) a high energy extension consisting in a deflection magnet analyser with no opportunity to analyse multiple beams, a QDDD analyser and at last a heavy ion identifier is a gas filled detector with associated

electronics for separating isobars and different elements.

During last year, some experiments were conducted with this configuration for ^{14}C dating and showed us the next important points :

a) The ability of a good isotopic separation of the output counts in the heavy ions counter.

b) A lack of stability in the terminal high voltage with a slow shift but large enough to produce a disappearance of the analysed ^{14}C beam after a certain time.

c) A poor transmission efficiency due mainly to the duoplasmatron ion source.

d) A strong memory effect from sample to sample was found, power law time dependent, and remaining more than 2% over 2 hours after the precedent sample was removed. Introduction of the CO_2 sample gas directly within the expanding plasma location reduces considerably this memory duration to 1% in a few seconds. Unfortunately, due to the broader emission angle of the beam, the intensity must be limited to a very low level to be valuable for ^{14}C dating purpose.

3 - MODIFICATIONS DURING 1980

This year, some modifications were introduced to this Super FN Tandem as to get better ^{14}C dating experiments.

First of all, the conventionnal analysing 90% deflection magnet was removed and replaced by a Brown Buechner type magnet analyser whose large momentum range allows simultaneous measurements of different beams as ^{14}C, ^{13}C and ^{12}C. A special analysing chamber was designed, connected with a precision Faraday cup mounted on an adjustable socket (fig. 2) so as to fit exactly with the beam to be analysed.

A new Sputter ion source was mounted with an entire new injection part comprising a 20° deflection magnet and focalisation quadrupole. The

Sputter ion source and the 20° magnet are placed upon a 60 Kv isolated platform.

The Sputter ion source is an ANIS ion source (2), a cesium vapour plasma type where the carbon sample could be a thin layer of approximately 10 µm deposit graphite on the concavity of the metallic cathode (fig. 3).

4 - THE CH SECONDARY BEAM

The ANIS Sputter ion source is especially planed to operate, if necessary, with addition of gas at low pressure within the plasma location room and the idea had come to us to create with this opportunity a controlled $^{12}CH_2^-$ secondary accelerated ion beam which could be available for stabilisation and monitoring purposes. With controlled addition of hydrogene gas in the ANIS ion source a mass 14 $^{12}CH_2^-$ molecular ion beam is created entering into the accelerator tube with the same rigidity as the $^{14}C^-$ ions do. After passing through the low energy section of the accelerator tubes the $^{12}CH_2^-$ molecular ions are stripped at the terminal stripping foil and gives a secondary $^{12}C^{4+}$ ion beam which is accelerated in the high energy section of the accelerator tubes. Arriving to the 90° Brown Buechner magnet chamber, it is curved just to be collected by the precision Faraday cup provided with adjustable slit assembly.

The slit assembly is connected to a slit feedback amplifier and allows us to achieve a terminal voltage stabilisation as usual in the FN tandems. In the same time the $^{14}C^{4+}$ ions are collected as usual by the high energy extension : the QDDD analyser and the heavy ion counter (fig. 4). During experiments performed at a 6 MV terminal high voltage a typical few nA intensity $^{12}C^{4+}$ secondary beam was obtained from the $^{12}CH_2^-$ mass 14 molecular ions. This beam is much larger than needed to start the feedback stabilisation system and 0.02% terminal voltage stabilisation was obtained easily and continuously. The adjustment of the overall accelerator line is drastically simplified with this secondary beam utilisation. The magnetic field of the 20° injection magnet is

tuned to maximise the intensity of the secondary $^{12}C^{4+}$ beam on the Faraday cup. At last the position of adjustable slits on the secondary $^{12}C^{4+}$ beam line is tuned to adjust the terminal high voltage in order to maximise the counting rate of the ^{14}C ions.

5 - MONITORING OF THE ^{14}C ION COUNTING RATE WITH THE $^{12}CH_2$ SECONDARY BEAM

We have tried to use the $^{12}CH_2^-$ secondary beam as a monitor of the ^{14}C counting rate. A recent experiment performed as Saclay shows that a reliability exits between the ^{14}C integrated counting in the heavy ion counter and the integrated Coulombs charges of the $^{12}C^{4+}$ secondary beam. The main parameter seems to be the partial pressure of the Hydrogen gas in the ion source. With a very precise hydrogen filling device, this reliability lies within 3% accuracy over a night.

6 - MEMORY EFFECT WITH ANIS ION SOURCE

When using a copper sample just after a 125 time enriched ^{14}C carbon sample *, the memory in ^{14}C counting drops down to less than 0.1% within the 15 minutes needed to change the samples (at that moment, there is not yet a multiple samples loader on the ANIS source).

7 - IMPROVEMENTS

a) Due to the addition of hydrogen gas in the ion source, the counting rate of ^{13}C ions which reach the counter increases dramatically. In order to avoid this effect we plan to install an electrostatic deflector after the analysing 90° magnet.

b) A part of the 3% accuracy observed up to now is due to the error of measurement with the Faraday cup. We plan to monitor our experiments by measuring the elastic scattering of the $^{12}C^{4+}$ beam with a silicon detector, located in the analysing magnet vacuum chamber.

* *This carbon sample is a reactor irradiated carbon whose activity in ^{14}C is 125 times the activity of a contemporary natural charcoal.*

8 - SUMMARY

a) An ANIS sputter ion source, with extra filling gas opportunity, connected with a Brown Buechner type 90° deflection magnet analyser allows to use a steady and controlled $^{12}CH_2$ secondary beam extremely useful for high stabilisation of the FN tandem when the main beam is too weak as the ^{14}C one in ^{14}C dating experiments.

b) A monitoring of the ^{14}C counting rate by this secondary beam seems realistic.

c) Memory effect in the ANIS ion source observed with a blank sample (i.e. : copper cathode) is less than 0,1%.

REFERENCES

1 G. DELIBRIAS et al., Radiocarbon 6, 1964, 233.
G. DELIBRIAS et al., Radiocarbon 16, 1974, 15.

2 a) P. TYKESSON and H.H. ANDERSEN, IEEE Trans. Nucl. Sci. NS 22, 1975, 1632.

b) P. TYKESSON et al., IEEE Trans. Nucl. Sci. NS 23, 1976, 1004.

FIGURE CAPTIONS

Figure 1 Schematic diagram of the Saclay F.N. Tandem.

Figure 2 Disposition of the precision Faraday cup at the output of the Brown Buechner magnet analyser.

Figure 3 Schematic drawing of the ANIS Sputter ion source.

Figure 4 CH secondary beam arrangement.

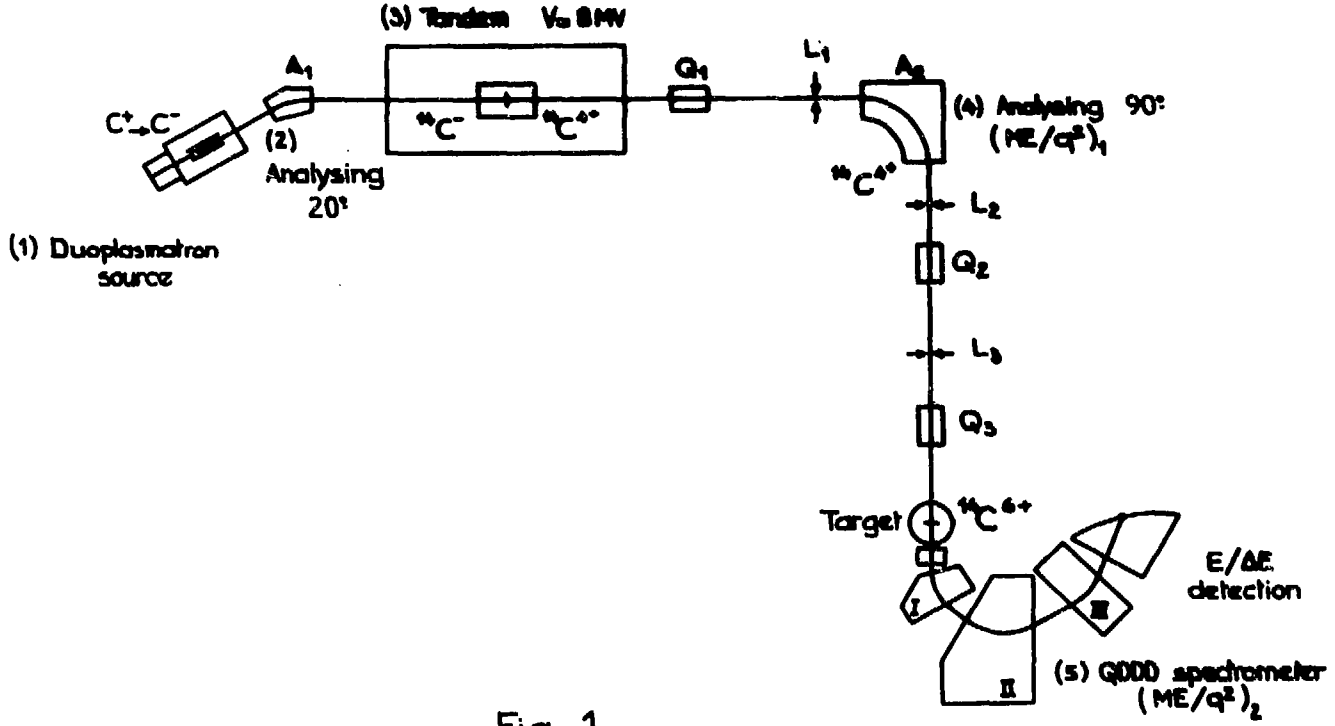
(3) Tandem V= 8 MV
A1
Q1
L1
A2
(4) Analysing 90°
(ME/q²)1
C+→C-
(2)
Analysing
20°
(1) Duoplasmatron
source
L2
Q2
L3
Q3
Target
E/ΔE
detection
I
II
III
(5) Q3D spectrometer
(ME/q²)2

Fig. 1.

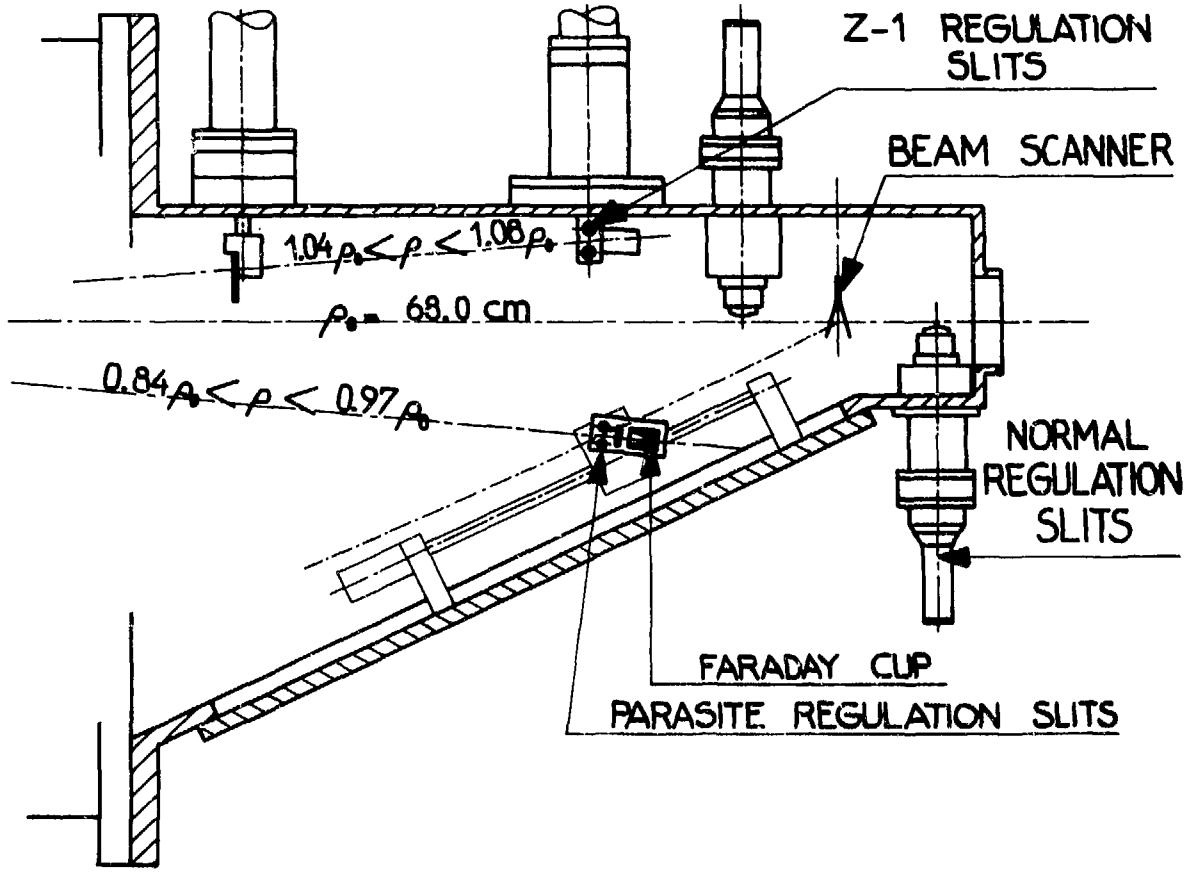
Z-1 REGULATION SLITS
BEAM SCANNER
1.04ρ₀ < ρ < 1.08ρ₀
ρ₀ = 68.0 cm
0.84ρ₀ < ρ < 0.97ρ₀
NORMAL REGULATION SLITS
FARADAY CUP
PARASITE REGULATION SLITS

Fig. 2 -

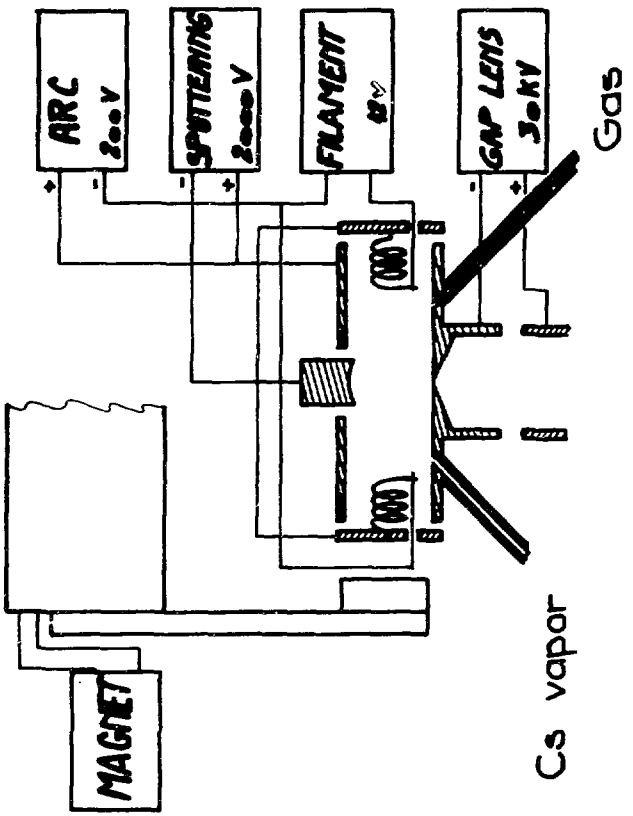
ARC
200 V
SPUTTERING
2000 V
FILAMENT
8 V
GAP LENS
30 kV
Gas
Cs vapor
MAGNET

Fig. 3-

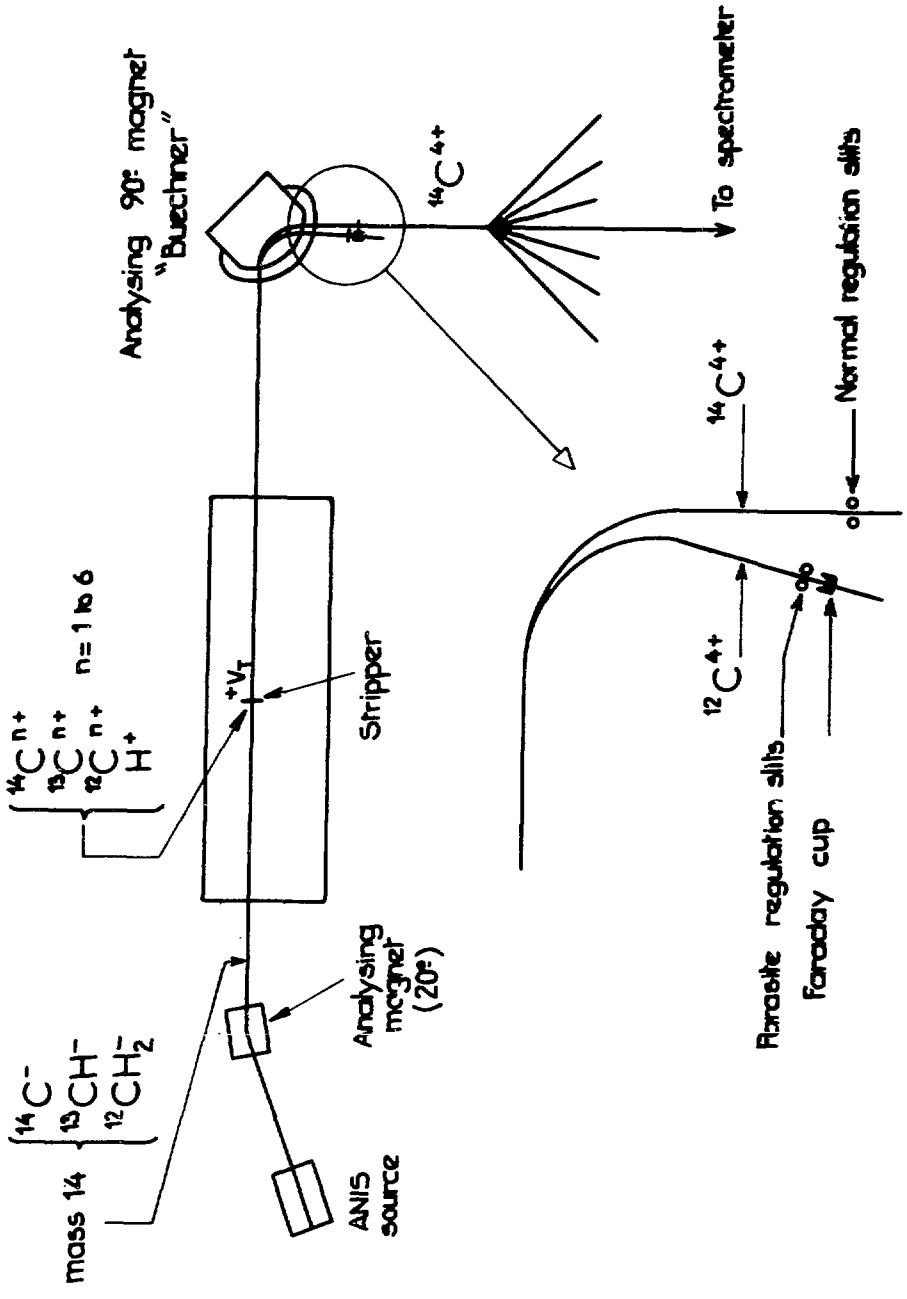
Analysing 90° magnet
"Buechner"
To spectrometer
$^{14}C^{4+}$
$^{14}C^{4+}$
Normal regulation slits
$^{12}C^{4+}$
Parasite regulation slits
Faraday cup
$^{14}C^{n+}$ $^{13}C^{n+}$ $^{12}C^{n+}$ $^{1}H^{+}$ n= 1 to 6
$+V_T$
Stripper
Analysing magnet (20°)
mass 14 $^{14}C^{-}$ $^{13}CH^{-}$ $^{12}CH_2^{-}$
ANIS source

Fig. 4 –

REPORT ON ACCELERATOR MASS SPECTROMETRY EXPERIMENTS AT THE REHOVOT 14UD PELLETRON†

M. Paul
Racah Institute of Physics, Hebrew University, Jerusalem, Israel
and
R. Kaim, A. Breskin, R. Chechik, J. Gerber*, M. B. Goldberg, N. Zwang
Nuclear Physics Department, Weizmann Institute of Science, Rehovot, Israel
and
A. Kaufman
Isotope Research Department, Weizmann Institute of Science, Rehovot, Israel

We report here on preliminary work on accelerator mass spectrometry performed at the Rehovot Accelerator Laboratory. The facility, whose principal component is a 14UD Pelletron, is mainly used for heavy-ion nuclear physics and fast molecular ion studies. Its general features, described below, are well suited for accelerator mass spectrometry and this encouraged us to start experiments to test the performance of the existing equipment under the special conditions of mass spectrometry measurements.

A schematic diagram of the facility is shown in Fig. 1. The negative ion source is a General Ionex Hiconex 834 sputter source. The injection of the negative ion beam is presently achieved by two magnets with 30° and 90° deflection angles. The maximum mass-energy product for the 90° magnet is mE = 28 MeV.amu.

The 14UD Pelletron accelerator is currently operated close to its maximum 14 MV terminal voltage and has shown excellent stability properties. Gas or foil can be used for terminal stripping. A second foil stripper is available in the HE section of the accelerator. The HE beam transport system, purely magnetic, consists of standard focusing and steering elements.

The detection system presently used in the accelerator mass spectrometry measurements is detailed in Fig. 2. Its main component is a magnetic spectrograph of the Browne-Buechner type. A bi-dimensional position-sensitive gas detector[1] provides a measure of both the magnetic rigidity of the ions ($B\rho$) and their angular spread (θ). This counter also provides a fast timing signal which, in coincidence with the light signal from a

* Guest scientist from CNRS, Strasbourg.

thin scintillator foil positioned at the spectrograph entrance slits, determines the time of flight of the ions through the spectrograph chamber.

Our work, devoted so far to tests of the experimental system, has been concentrated on the ^{14}C isotope. An enriched ^{14}C graphite sample[2] ($^{14}C/^{12}C = 5.1 \times 10^{-12}$) was mounted in the ion source together with natural graphite samples used for background measurements. Detection of the ^{14}C ions in the spectrograph was alternated with ^{13}C current measurements in a retractable Faraday cup in front of the spectrograph. Switching between ^{13}C and ^{14}C isotopes was achieved by tuning the injection magnets to mass 13 or 14 and keeping the magnetic rigidity constant after the acceleration stage; the terminal voltage was changed accordingly. From the first experiments it was found that, although the intrinsic stability of the terminal potential is excellent, the original GVM stabilization system was totally unsatisfactory for radioisotope measurements. The system has been modified in our laboratory and provides presently long-term stability to within ±3 kV[3]. The accelerator can be reliably operated in this mode at any terminal voltage in the working range.

Fig. 3 shows a time-of-flight spectrum obtained using the enriched ^{14}C sample. The ^{14}C ions are clearly resolved from ^{13}C ions originating from the dissociation of $^{13}CH^-$ in the terminal stripper foil and subsequent charge exchange in the residual gas of the HE tube. No ^{12}C ions were detected. It should be noted that the intensity of satellite beams is very low; background ions like ^{14}N, often present in mass 14 tandem beams[4], were not detected in our measurements. This low background rate is attributed to the good mass resolution of the injection system and the high vacuum throughout the machine. Using a natural graphite sample in the ion source, no ^{14}C count was recorded during the measurements. We cannot, however, quote at this stage the limit of sensitivity nor a value for the overall accuracy for the measurement of radioisotope concentrations.

Plans for future experiments include, together with further studies of the system properties, work on the ^{10}Be, ^{14}C and ^{36}Cl radioisotopes and dating applications.

† Work supported in part by the Israel Academy of Sciences and Humanities.

REFERENCES

1) A. Breskin, I. Tserruya and N. Zwang, Phys. Rev. Lett. 42, 369 (1979)

2) We thank Dr. W. Kutschera for providing us a sample of the "Fermi graphite" used at Argonne National Laboratory.

3) I. Ben-Zvi, M. Birk, E. Dafni, G. Hollos, R. Kaim, G.S. Sokolowski, Proceedings 3rd Int. Conf. on Electrostatic Accelerator Technology, 1981; to be published in IEEE Trans. Nucl. Sci.

4) See for example K.H. Purser, A.E. Litherland and H.E. Gove, Nucl. Instr. Methods 162, 637 (1979)

FIGURE CAPTIONS

Figure 1: Schematic diagram of the accelerator laboratory set-up, as used in mass spectrometry experiments. The 30^{o} deflection after the ion source and the switching magnet deflection lie in a horizontal plane; the 90^{o} injection and analysis deflections and the the magnetic spectrograph deflection are in vertical planes. The steering and focusing elements of the LE (HE) beam transport systems are purely electrostatic (magnetic) and are not detailed in the figure.

Figure 2: Schematic diagram of the detection system.

Figure 3: Time-of-flight spectrum of C^{6+} ions detected in the magnetic spectrograph, using an enriched ^{14}C sample in the ion source.

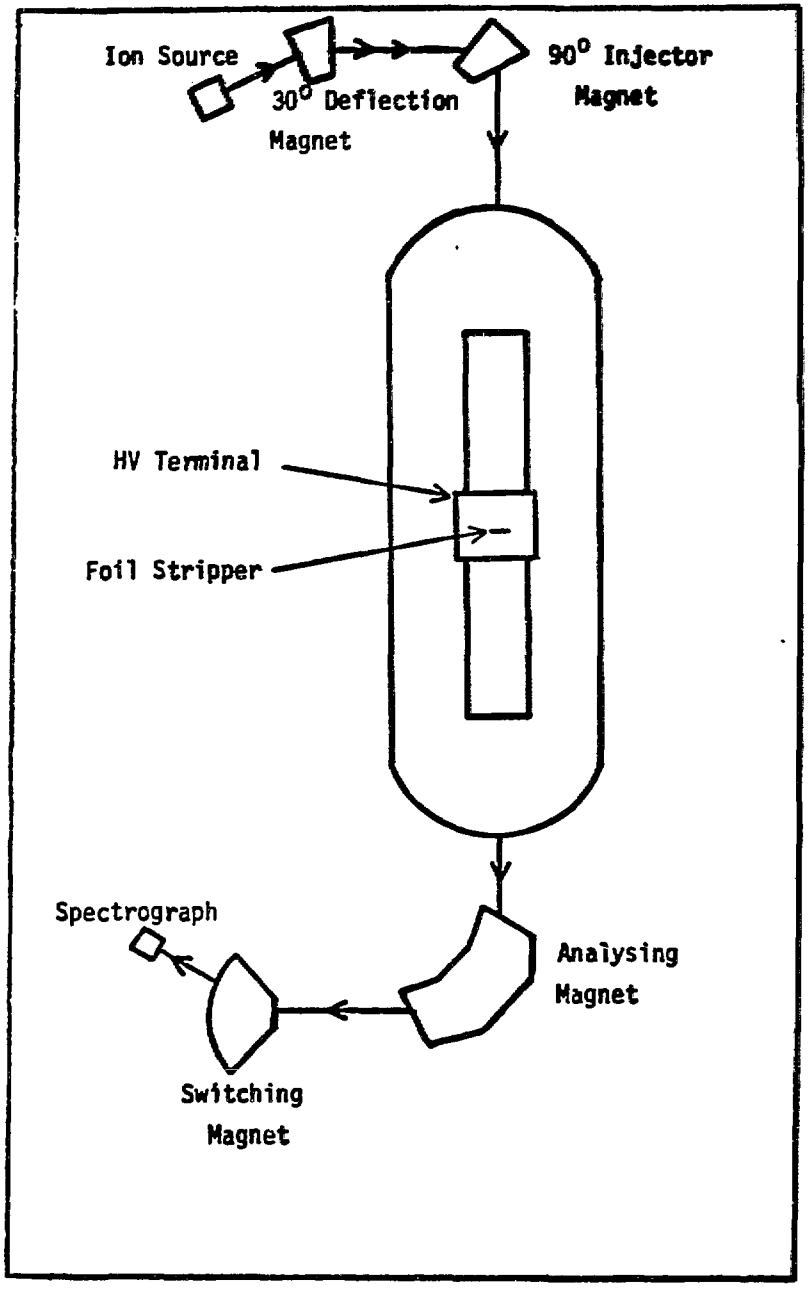
Ion Source
30° Deflection Magnet
90° Injector Magnet
HV Terminal
Foil Stripper
Spectrograph
Analysing Magnet
Switching Magnet

Fig. 1

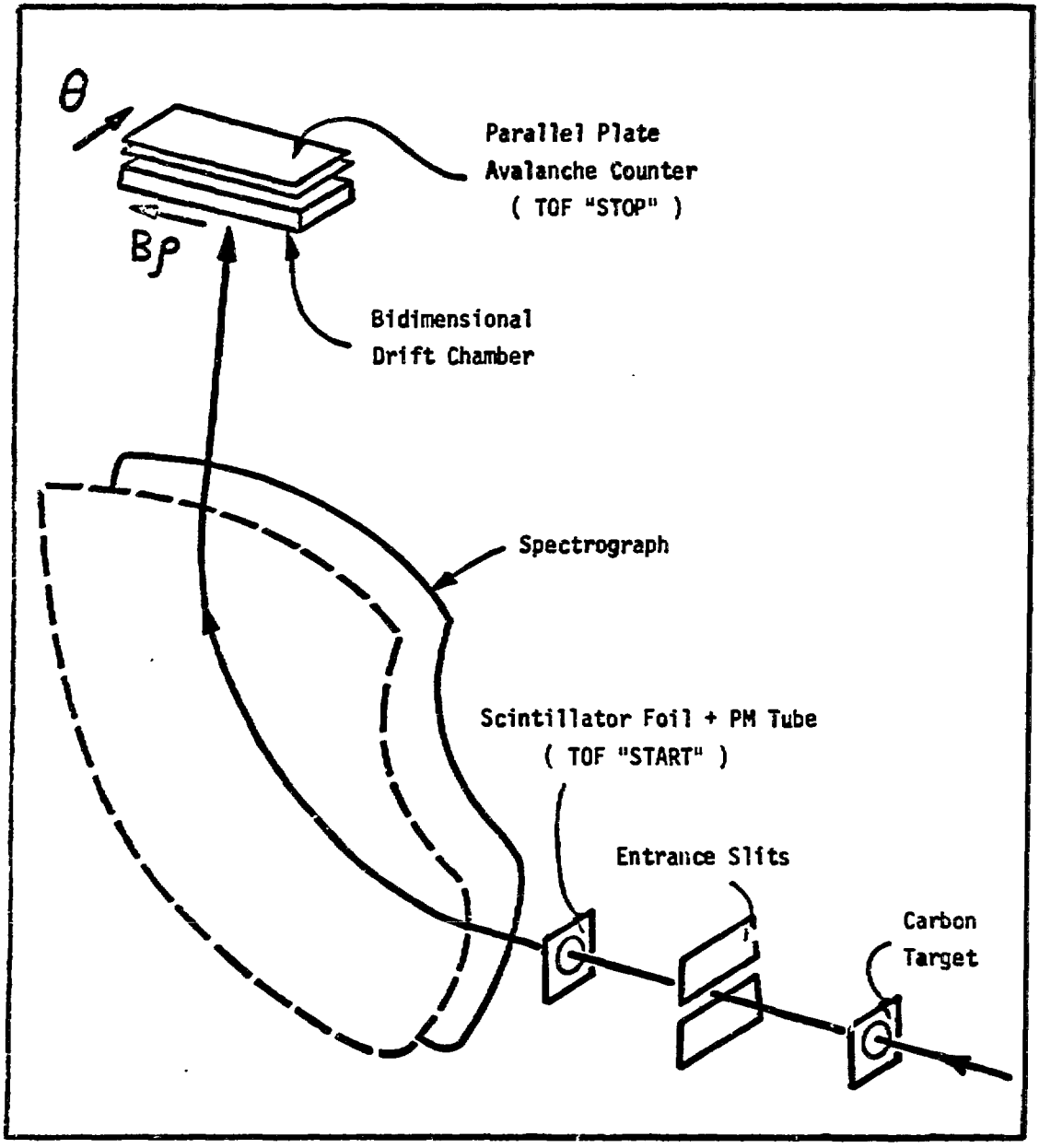
θ
Bρ
Parallel Plate
Avalanche Counter
(TOF "STOP")
Bidimensional
Drift Chamber
Spectrograph
Scintillator Foil + PM Tube
(TOF "START")
Entrance Slits
Carbon
Target

Fig. 2

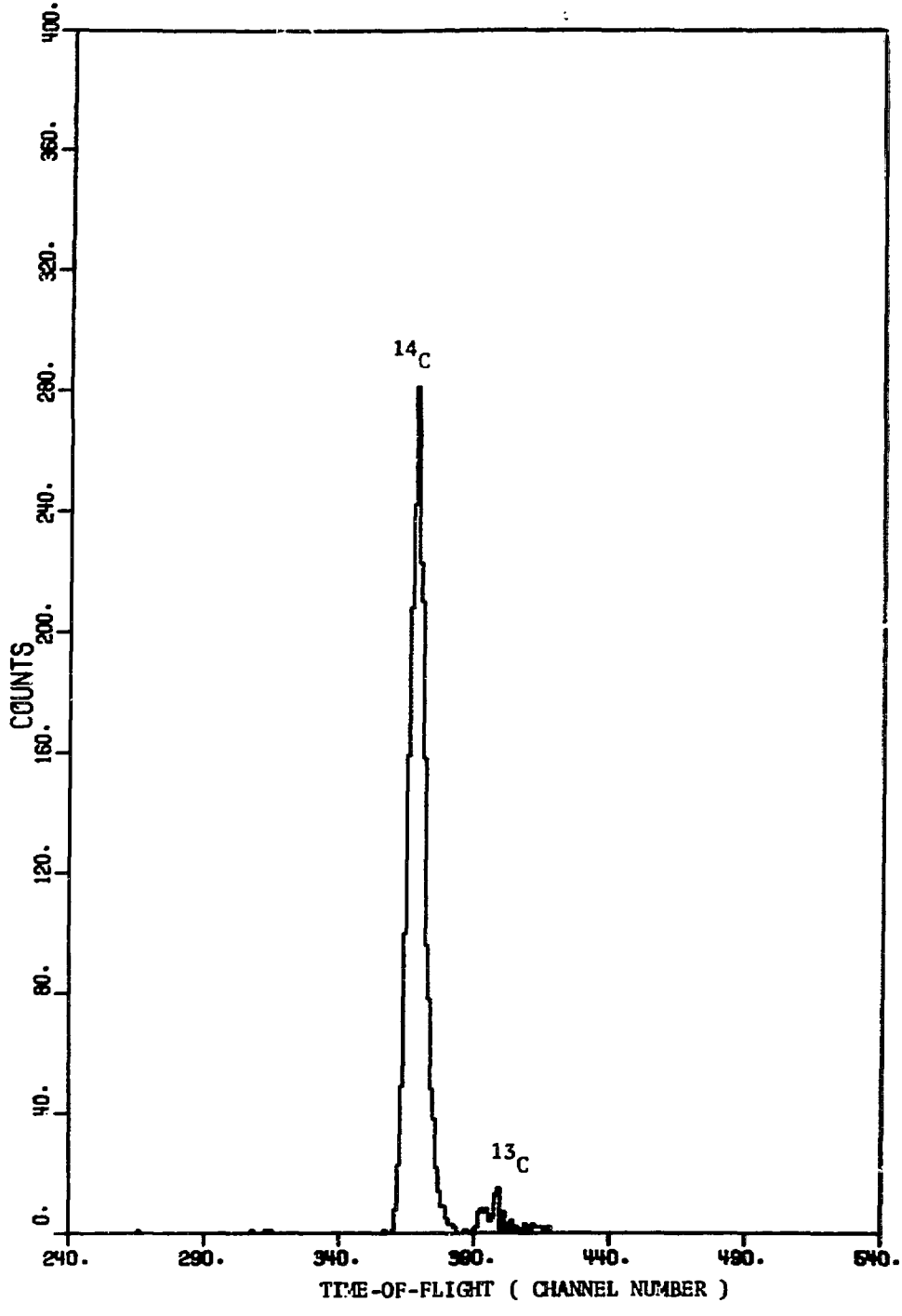
400.
360.
320.
280.
240.
200.
160.
120.
80.
40.
0.
COUNTS
^{14}C
^{13}C
240.
290.
340.
390.
440.
490.
540.
TIME-OF-FLIGHT (CHANNEL NUMBER)

Fig. 3

SEARCH FOR ANOMALOUSLY HEAVY ISOTOPES*

J. Klein, R. Middleton & W. E. Stephens
Physics Department, University of Pennsylvania

1. INTRODUCTION

In most previous searches, anomalously heavy nuclei have been sought in hydrogen — not only because of the ease with which it can be ionized and identified, but also since the use of deuterium automatically yields a factor of 7000 in sensitivity due to enrichment. For example, Alväger & Naumann[1]) set an upper limit of 3×10^{-18} on the existence of anomalously heavy hydrogen in the mass range 6 — 16 which was subsequently improved by Muller, Alvarez, Holley & Stephenson[2]) to 2×10^{-19} over the mass range 3 to 8.2 a m u. Recently, however, Dover, Gaisser & Steigman[3]) have suggested the possibility that the new stable heavy hadrons predicted by several elementary particle models should be present in $Z > 1$ nuclei at levels of the order of 10^{-10}. Since the particle is not expected to bind with a single proton to form a heavy isotope of hydrogen, the experimental searches, mentioned above, would, assuming its existence, have failed to detect it. These considerations prompted us to use our tandem accelerator as a supersensitive mass spectrometer to search for anomalously

*Work supported by National Science Foundation.

heavy isotopes of some elements with $Z > 1$.

Our first search was made with oxygen. This was chosen as it readily forms negative ions and as it was anticipated that we might gain a factor of at least 500 in sensitivity by use of ^{18}O, enriched by gaseous diffusion. Since this work has been published elsewhere[4]), it will not be described here.

Shortly after completing the above study, it occurred to us that the enormous chemical and biological processing of atmospheric oxygen might have seriously depleted an anomalously heavy isotope. After much consideration, we concluded that natural lithium might be a better choice since it is believed that between 10% and 50% of ^7Li is primordial. Several samples of 'natural' lithium were placed in our ion source where the $^6Li/^7Li$ ratio was measured and found to be abnormally low. Since it was clear that this lithium had been tampered with and, as it was uncertain what effect this might have had on an anomalously heavy isotope, we sought a sample of natural lithium with the proper $^6Li/^7Li$ ratio. Ultimately a sample supplied by the Lithium Corporation of America was used for this study.

While the lithium study was in progress we received a preprint of a paper by Dicus & Teplitz[5]) who, based on Dover et al.'s estimate of an H^o/proton ratio of 10^{-10}, calculated

the abundances of anomalous isotopes of various elements within the standard model of big-bang nucleosynthesis. This work confirmed our choice of lithium and predicted a $^{7}LiH^{o}/^{7}Li$ ratio of $\sim 3 \times 10^{-13}$, which though within our sensitivity range, was uncomfortably close to our lower limit. The same work, however, showed beryllium to be a much better choice, predicting a $^{8}BeH^{o}/^{9}Be$ ratio of $\sim 3 \times 10^{-6}$. In spite of difficulties associated with making negative ions from beryllium, it was decided to repeat the experiment once again, using beryllium metal as the source material.

Finally a limited search, over the mass range 3 – 8.12 a m u , was made for an anomalous isotope of helium, using atmospheric helium obtained as a by-product from argon manufacture. Atmospheric helium was chosen as it is believed to be approximately 3% primordial in origin.

2. EXPERIMENTAL PROCEDURE

Figure 1 shows the experimental setup used over the past two years for anomalous nuclei searches. The major modifications to the beam transport system of our FN tandem accelerator include a 90° injection system following a cesium sputter source, a crossed electric and magnetic field velocity selector following the high energy magnetic quadrupole lens, and a surface barrier detector following a series of absorber foils

mounted in front of the image slits of the positive ion 90° magnet.

Since the yield of Be^- ions is very low, it was decided that a molecular negative ion would have to be used, the most suitable being the hydride. These were generated by ammonia spraying following the technique described in Ref. 6. To minimize the partial pressure of ammonia in the source, the modifications in the gas delivery system shown in Fig. 2 were made. The sputter target was made by pressing a 1 cm long by 1 cm diameter piece of beryllium metal into one of our standard copper holders. A 1.5 mm diameter hole was drilled axially through the beryllium and then enlarged by a series of drills to have an approximately conical taper of 5°. A 1 mm diameter hole was then drilled radially through the copper and the beryllium for ammonia gas feed. Typically, this arrangement provided about 0.25 μA of $^9BeH^-$ negative ions. A similar arrangement was used for lithium, except that the sputter target was prepared by pressing, and oxygen gas was used to improve the yield of Li^- ions[7]). Throughout most of the lithium experiment the $^7Li^-$ current was in the range 0.4 to 1.2 μA.

Negative ions from the sputter source were extracted at 20 keV and, after being brought to a focus by an einzel lens, were momentum analysed in a 30 cm radius 90° double focussing magnet. With entrance and exit apertures of about 1 cm

diameter, the magnet had a mass resolution $\Delta m/m$ of about 1/50 with a transmission of about 90%. The lithium measurements were all made at a terminal voltage of 7.5 MV – yielding 30 MeV $^{*}Li^{3+}$ ions. The beryllium measurements were also made with 3+ ions, but at terminal voltages in the range 3 to 6.5 MV – the latter being dictated by the mass-energy product of the accelerator's 90° analyzing magnet. The mass resolution of this magnet, $\Delta m/m \sim 1/185$, was determined by a 12.5 mm diameter aperture located in front of the detector.

An absorber wheel was placed between the defining aperture and the surface barrier detector to stop beams of higher Z. The wheel had 8 apertures and 7 contained nickel foils ranging in thickness from 7.4 to 22 mg/cm^2. In the lithium experiment a 10.7 mg/cm^2 nickel foil was used throughout. This was chosen, for while it completely stopped 30 MeV oxygen and all higher Z ions, it caused a minimal energy loss for 30 MeV $^{*}Li$ – 8.7 MeV for ^{11}Li and 12.4 MeV for $^{3,4}Li$. Energy losses were calculated from the range-energy tables of Northcliffe & Schilling[8]). Because of uncertainties in extrapolating energy losses over such a wide range of masses, a generously wide window of ±3 MeV was set around the calculated energy. A similar procedure was used to select foils for the beryllium experiment but, owing to changes in terminal voltage, several different foils had to be employed.

Mass scanning was accomplished by incrementing both the negative ion injector and the high energy magnets after each integration period of 48 seconds. Step size was determined by the resolution of the high energy magnet and varied from 0.05 to 0.55 a m u over the mass range 11 to 93. These steps provided an overlap of greater than 20%. The accelerator's magnetic quadrupole lens was adjusted, using an empirically determined calibration curve, after every ten or so measurements. Since the absorber foils proved highly effective and backgrounds were usually zero, the E x B velocity selector was used only rarely.

A serious concern throughout this work was that the mass calibrations of the negative ion and high energy magnets might be in error and therefore cause a lack of synchronization. At the outset, it was assumed that the calibration of the high energy magnet was well established from prior nuclear studies and, it was thought that the largest error would arise from the negative ion magnet. To minimize this error we calibrated the negative ion injector using carbon molecular ions before each run. Through this calibration procedure, we were able to insure an accuracy of ~0.1% a m u over a range of ~60 mass units. Nonetheless, during the lithium experiment, it was discovered that a lack of synchronization was occurring at masses greater than 27 a m u. This was traced to saturation effects in the

high energy magnet at fields greater than 12 kg. Consequently, we determined a correction curve using low charge, high rigidity carbon beams for fields between 12 and 16 kg and remeasured the region between mass 27 and 34.5. In spite of this, we feel that a progressive loss of sensitivity is not unlikely at higher field strengths, and the broken line in Fig. 3 is our estimate of this effect. In the beryllium experiment, more attention was paid to maintaining magnet synchronization and checks were made (with no absorber) using the hydride beams of magnesium, aluminum, calcium and titanium.

The negative ions used in the helium search were made by charge exchanging in lithium vapor positive ions produced in a duoplasmatron. The helium gas (~50 liters) was obtained from Airco and was the non-condensing residue left over from the production of argon from air. Since only 10% to 20% of the sample was helium, purification was necessary before admitting it into the ion source. This was accomplished by passing the mixture over a liquid nitrogen cooled molecular sieve. Typical negative ion currents were about 1 μA. The rest of the analysis system was the same as used for lithium and beryllium with the exception that the helium was injected through a 40° deflecting magnet at 40 keV.

3. RESULTS

The results of the lithium search are shown in Fig. 3. During the vast majority of the run, no counts were obtained within the integration window of the energy display. It was only at the integral masses 11, 12, 14, 16, 17 and 18 that sufficient beam was injected into the accelerator to result in background from second order processes. The origins of most of these were identified and are indicated in the figure. It should be noted that in all of these cases, the counts falling within the window resulted from tails of strong peaks lying outside the window. The gradual loss in sensitivity from about 10^{-15} to 6×10^{-15} at mass 27 is due to a calculated loss in stripping efficiency of the slower moving heavier ions. The relatively sharp changes in sensitivity at masses 13, 17, 21 and the abrupt improvement between mass 26 and 27 result from changes in ion source output. As was mentioned earlier, the broken curve starting at about mass 27 is our best estimate of the sensitivity limit when allowance is made for saturation effects in the high energy magnet.

During the beryllium search no background was ever encountered within the integration window and the results are summarized in Table I. As can be seen from the table, measurements were made at five terminal voltages dictated by the mass-energy product of the high energy 90° magnet. The sensitivity

was calculated from the periodically measured $^{9}BeH^{-}$ current and the assumed transmission of $^{*}Be^{3+}$. The latter was obtained by correcting the measured $^{9}Be^{3+}$ transmission in accordance with the theoretical stripping curves presented in Marion & Young[9]) – these are shown in column three of the table.

The search for anomalous isotopes of helium was performed over the entire region from 3.06 a m u to 8.12 a m u except for a small window (± .040 a m u) around mass 4. As in both the lithium and beryllium searches, over most of this region no counts were observed within the integration window, and sensitivity was limited by ion source output. However, a substantial background was present between 4.63 and 4.86 a m u. This resulted from charge changing collisions ($^{4}He^{+} \rightarrow {}^{4}He^{o}$) occurring between the extraction electrode (at 26 kV) and the charge exchange canal (at 20 kV) and was eliminated by dropping the extraction voltage to 20 kV. Over the entire region, an upper limit of $\lesssim 6 \times 10^{-15}$ was established for the ratio of heavy hadron to nucleon in helium.

4. SUMMARY AND DISCUSSION

As was mentioned earlier the search for an anomalously heavy isotope of oxygen[4]) was prompted by a Phys. Rev. Letter by Dover, Gaisser& Steigman[3]). In this Letter these authors

suggest the possible existence of a stable heavy hadron in nuclei with $Z > 1$ at an abundance of $\sim 10^{-10}$. None was observed in oxygen over a mass range of 20 to 54 a m u and an upper limit for the heavy hadron to nucleon ratio was established at 10^{-16} over this entire region and over a large portion of it at 10^{-18}.

Since terrestrial oxygen has been the subject of very considerable chemical and biological processing, we were concerned that a very heavy isotope might have been depleted and decided to search elsewhere. We chose to repeat the experiment using natural lithium since it is generally believed that between 10% and 50% of terrestrial ^{7}Li is primordial. During this second search, we heard of the work of Dicus & Teplitz[5]) in which they calculated the abundance of anomalous light $Z > 1$ nuclei produced by primordial nucleosynthesis. These authors predicted ratios of $^{6}LiH^{o}/Li$ and $^{7}LiH^{o}/Li$ of $\sim 3 \times 10^{-14}$ and $\sim 3 \times 10^{-13}$ respectively. Our results place an upper limit on the $^{7}LiH^{o}/Li$ ratio of 1.5×10^{-14}, progressively rising to 7×10^{-14} over a lithium mass range of 11 to 32 a m u , and of about 4×10^{-13} over the range 32 to 34.5 a m u. Although our upper limits are generally somewhat smaller than their predictions, a factor of 10 uncertainty in the calculations, precludes the drawing of

meaningful conclusions.

Dicus & Teplitz pointed out that a much more favorable case existed in beryllium. Here the mass gap at 8 a m u and the low cosmic abundance of ^{9}Be make the predicted ratio of $^{8}BeH^{o}/^{9}Be \sim 3 \times 10^{-6}$. Our measured upper limit which progressively rises from 2×10^{-13} to 2×10^{-11} over the mass range of 16 to 93 a m u is considerably smaller than the predicted ratio. Thus it would appear that if a stable heavy hadron exists, then its mass must be greater than 85 a m u or its abundance with respect to protons must be $<10^{-15}$.

Fig. 4 summarizes the present status of searches for a stable heavy hadron, including the earlier searches (with deuterium) of Alvager & Naumann[1]) and Muller, Alvarez, Holley and Stephenson[2]). Not included in this figure are the results of a search for anomalous hydrogen in enriched D_2O by Smith, Bennett, Homer, Lewin, Walford & Smith[10]) which are included elsewhere in these proceedings. They establish a limit of 10^{-28} over the mass range 12 to 1200 a m u.

References

1) T. Alväger and R. A. Naumann, Phys. Letts. 24B(1967)647.

2) R. A. Muller, L. W. Alvarez, W. R. Holley, and E. J. Stephenson, Science 196(1977)521.

3) C. B. Dover, T. K. Gaisser, and G. Steigman, Phys. Rev. Lett. 42(1979)1117.

4) R. Middleton, R. W. Zurmühle, J. Klein, R. V. Kollarits, Phys. Rev. Lett. 43(1979)429.

5) D. A. Dicus and V. L. Teplitz, Phys. Rev. Lett. 44(1980) 218.

6) R. Middleton, Nucl. Instr. & Meth. 141(1977)373.

7) R. Middleton, Nucl. Inst. & Meth. 144(1977)373.

8) L. C. Northcliffe and R. F. Schilling, Nucl. Data Tables A7(1970)233.

9) J. B. Marion and F. C. Young, Nuclear Reactions Analysis: Graphs and Tables, American Elsevier Publishing Co., Inc. (1968)39.

10) P. F. Smith, J. R. J. Bennett, G. J. Homer, J. D. Lewin, H. E. Walford and W. A. Smith, Proceedings of Symposium on Accelerator Mass Spectrometry (1981) Argonne National Laboratory.

Table 1

Mass Range	Terminal Voltage (MV)	Be^{3+} Fraction[1]	$^{8}BeH^{o}/^{9}Be$[2]
16 – 42	6.5	~56 → 44%	2×10^{-13}
42 – 48	6.0	~ 39%	3×10^{-13}
48 – 51	5.5	~ 23%	5×10^{-13}
51 – 70	4.0	~ 8%	2×10^{-12}
70 – 93	3.0	~ 1%	2×10^{-11}

1) $^{*}BeH^{-}$ was stripped to $^{*}Be^{3+}$ with a carbon foil stripper.

2) The $^{9}BeH^{-}$ negative ion current was typically 0.2 μA throughout.

Figure Captions

Fig. 1 - Schematic drawing of the accelerator system used to search for anomalously heavy isotopes.

Fig. 2 - Details of the modifications made to the gas delivery system of sputter source. This arrangement significantly reduced the partial pressure of NH_3 gas in the source without impairing the formation of BeH^- ions.

Fig. 3 - Upper limit for heavy hadron to nucleon ratio, plotted as a function of mass, for natural lithium. The base line represents zero counts in a ±3 MeV energy window integrated over a 4.8 second period. The broken line represents our estimate of a decrease in sensitivity due to saturation of the high energy magnet.

Fig. 4 - Present status of heavy hadron searches. Log of the upper limit of the abundance ratio is plotted against hadron mass for various elements.

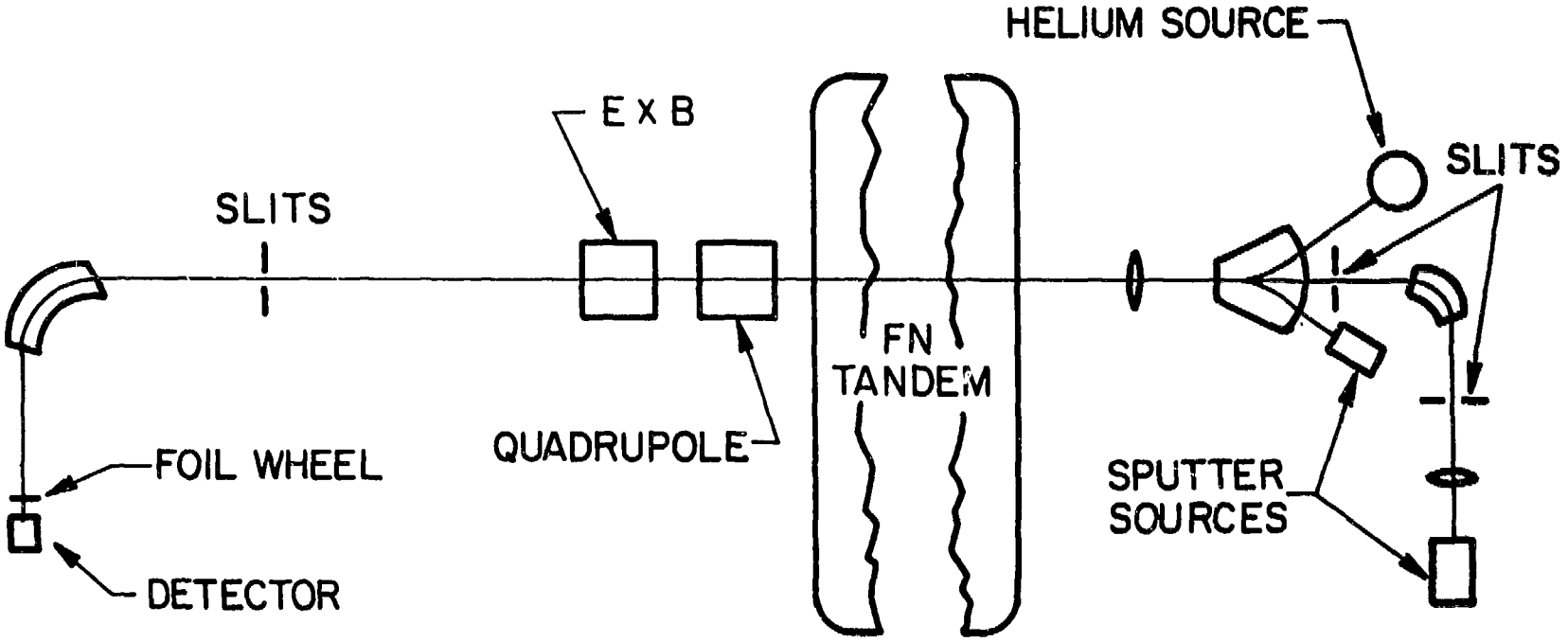
HELIUM SOURCE
E X B
SLITS
SLITS
FN
TANDEM
QUADRUPOLE
FOIL WHEEL
SPUTTER
SOURCES
DETECTOR

Figure 1

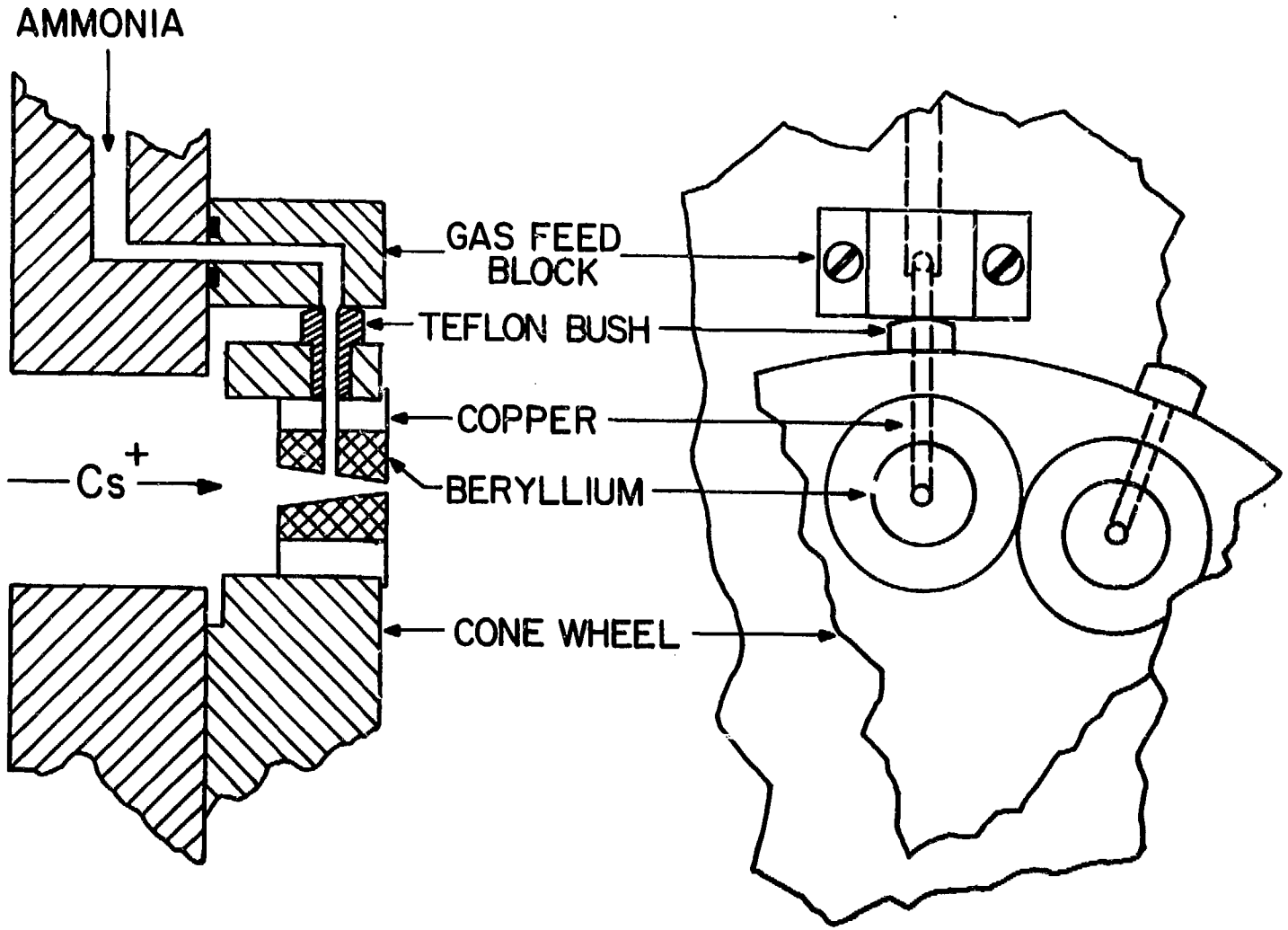
AMMONIA
GAS FEED BLOCK
TEFLON BUSH
COPPER
Cs+
BERYLLIUM
CONE WHEEL

Figure 2

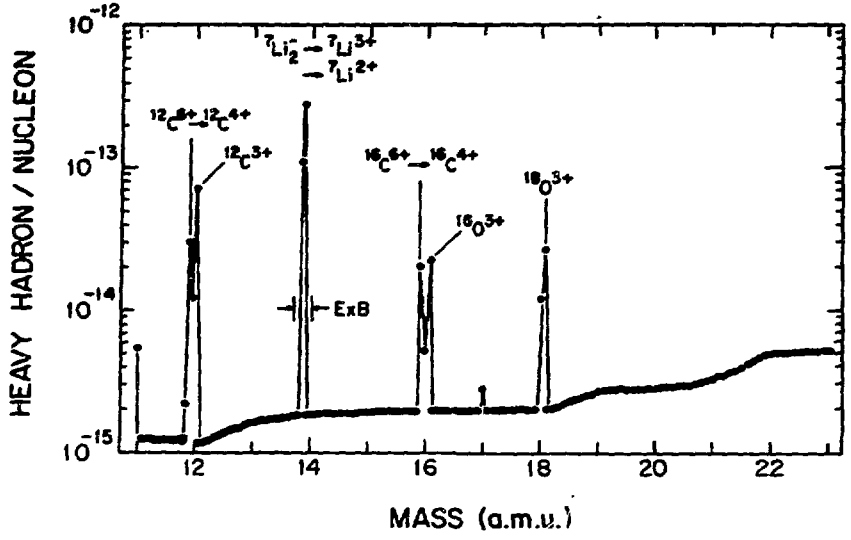
HEAVY HADRON / NUCLEON
MASS (a.m.u.)
ExB

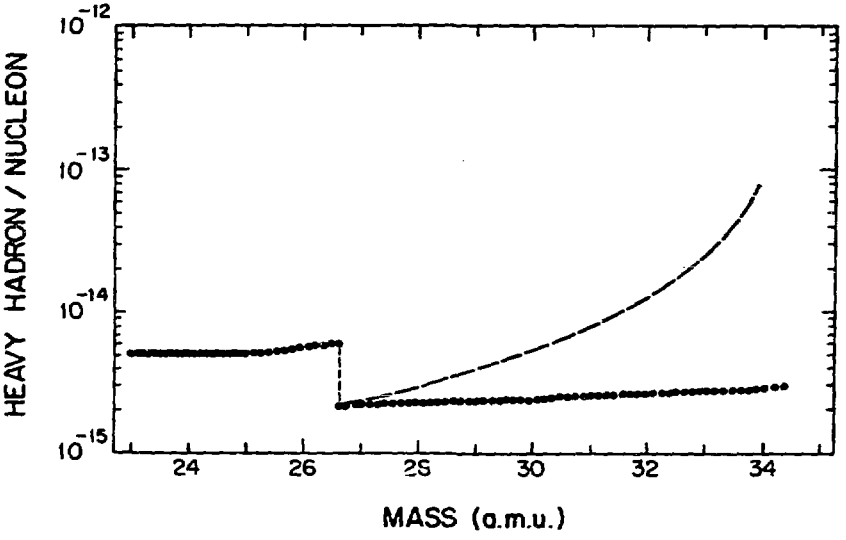
HEAVY HADRON / NUCLEON
MASS (a.m.u.)

Figure 3

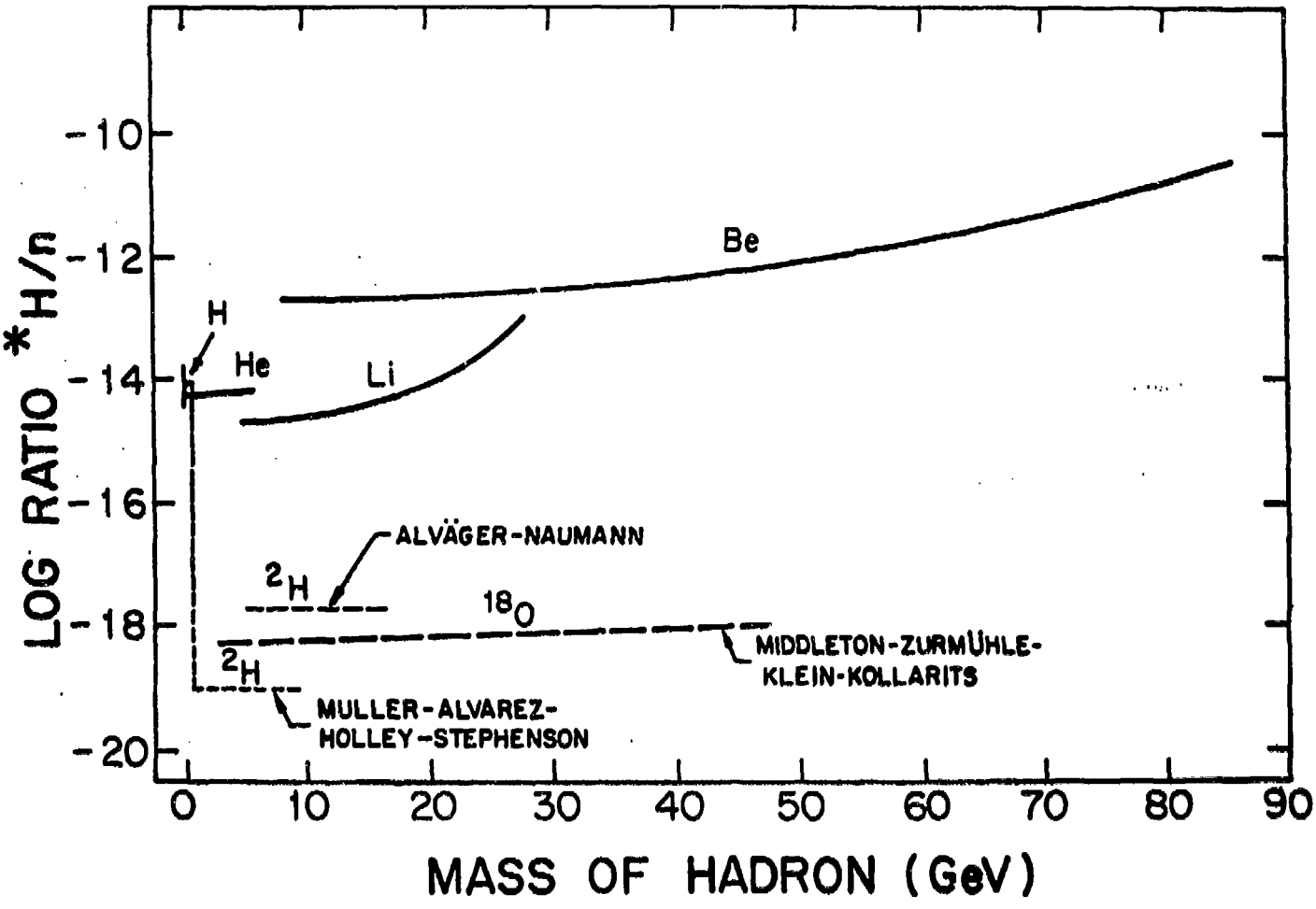
LOG RATIO *H/n
-10
-12
-14
-16
-18
-20
0
10
20
30
40
50
60
70
80
90
MASS OF HADRON (GeV)
Be
H
He
Li
ALVÄGER-NAUMANN
2H
18O
MIDDLETON-ZURMÜHLE-
KLEIN-KOLLARITS
2H
MULLER-ALVAREZ-
HOLLEY-STEPHENSON

Figure 4

RECENT SEARCH FOR QUARKS AND VERY HEAVY HYDROGEN ISOTOPES USING AN (ALMOST) ALL-ELECTROSTATIC SYSTEM

J. P. Schiffer, H. Ernst, W. Henning and W. Kutschera
Argonne National Laboratory, Argonne, IL 60439

A number of early searches for fractionally-charged stable particles produced negative results.[1] More recent work by the Stanford group,[2] consisting of measurement of charges on magnetically-levitated, superconducting Nb spheres, shows a number of spheres with fractional +1/3 or -1/3 charges. These charges seem to change randomly between successive measurements, indicating that whatever gives rise to the phenomenon is easily added or removed when the Nb sphere is allowed to touch a surface. The statistics on the largest Nb spheres studied is given in Table 1.

Table 1

Distribution of fractional charges on R = 140 μm Nb spheres from Ref. 2

Neutral	15
+1/3e	9
-1/3e	3
Total studied	27

Clearly the majority of these spheres had integral charge, and three times as many showed +1/3e charge (above integral multiple of e) as -1/3e. If a single type of particle is responsible for this phenomenon then it appears that it is likely to be (+1/3e) in charge; the (-1/3e) observations could be two such particles on one sphere.

A particle with (+1/3e) charge would be bound to electrons by only 1.5 eV and could have very high mobility, thus accounting for the frequent changes. It would be kept away from nuclei, under normal conditions, by Coulomb repulsion.

In order to search for +1/3e particles in metals we adapted the Argonne Dynamitron to accelerate particles from a metal filament. The particles, after being accelerated, were bent by an electrostatic deflector, passed through a foil which dissociated any molecules, and bent by a second electrostatic deflector to eliminate molecular fragments, through a slit system into a Si surface-barrier detector. Only charged particles that originated at the terminal of the accelerator and did not change their mass or charge state throughout, could reach the detector. The energy deposited in the detector was then a direct measure of the particle's charge: a +1/3e particle would have one third the energy of a singly charged one. But all particles were accepted, independent of their mass. These experiments were performed with negative results.[3]

Recently we adapted this technique to a search for anomalously heavy isotopes of hydrogen. A limit on such particles would be useful on quite general grounds.[4] In order to do the measurement, however, the technique of Ref. 3 had to be modified in several ways.

1.) To eliminate the known isotopes of hydrogen a small magnetic field was introduced, sufficient to deflect the light isotopes onto a beam stop, but leaving very heavy isotopes essentially undeflected.

2.) The solid state detector was replaced by a ΔE-E telescope, that provided charge identification, and

3.) The two elements in the telescope were separated sufficiently to allow time-of-flight measurements to be carried out, in order to search for heavy particles.

4.) In addition a nickel foil was placed in front of the detector of sufficient thickness to stop any normal ions (with $Z \geq 2$) but thin enough to readily transmit hydrogen-like particles of any mass.

From preliminary tests we anticipate no problems in observing a heavy hydrogen isotope which is 10^{-15} of the primary hydrogenic beam, and with minor improvements we might be able to reach 10^{-17}.

The prior isotopic enrichment of the hydrogenic material is a key argument in the limits quoted in earlier experiments.[5] Hydrogen, strongly enriched in deuterium (from heavy water) was used, with the assumption that this would also have led to the enrichment of very heavy hydrogen-like

species. Such enrichment, however, may be subject to some question. Most heavy water enrichment plants start with fresh water, and it is well known that deuterium is depleted by up to 25% in fresh water as compared to sea water. Is it possible that a very heavy hydrogen isotope, perhaps a hundred times the proton mass, will be depleted in fresh water by many orders of magnitude? We hope to be able to look at hydrogen beams starting with ocean water, and are considering the possibility of examining water from salt beds on the ground that very heavy hydrogen atoms in ancient oceans may have concentrated in the water of crystallization rather than evaporate.

References

[1]L. W. Jones, Rev. Mod. Phys. 49, 717 (1977); C. M. Stevens, J. P. Schiffer, W. A. Chupka, Phys. Rev. C 14, 716 (1976).

[2]G. S. LaRue, J. D. Phillips, and W. M. Fairbank, Phys. Rev. Lett. 46, 967 (1981).

[3]J. P. Schiffer, T. R. Renner, D. S. Gemmell, and F. P. Mooring, Phys. Rev. D 17, 2241 (1978).

[4]P. H. Frampton and S. L. Glashow, Phys. Rev. Lett. 44, 1481 (1980).

[5]T. Alvager and R. Naumann, Phys. Lett. B24, 647 (1967); R. A. Muller, L. W. Alvarez, W. R. Holley, and E. J. Stephenson, Science 196, 521 (1977); P. F. Smith and J. R. J. Bennett, Nucl. Phys. B149, 525 (1979).

A MASS-INDEPENDENT SEARCH FOR FRACTIONALLY CHARGED PARTICLES

K.H. Chang, A.E. Litherland, L.R. Kilius, R.P. Beukens, W.E. Kieser, E.L. Hallin

Department of Physics, University of Toronto, Toronto, Canada M5S 1A7

ABSTRACT

A proposed mass-independent search for fractionally charged particles with the all-electrostatic line of the IsoTRACE Laboratory at University of Toronto is described. Sensitive measurement of the fractional charge is accomplished by (1) a judicious choice of ion source and ion species, (2) charge changing and electrostatic analysis before injection into the tandem accelerator, (3) molecular destruction, charge changing, and acceleration by the tandem, (4) charge state selection and E/q analysis after acceleration, and (5) particle energy measurement with a Si surface barrier detector. In addition, the mass of the fractionally charged particles can be determined by a time of flight spectrometer. Specific cases involving $\pm(1/3)e$ and $\pm(2/3)e$ particles are discussed. Also included in the discussion are: integral charge background rejection, the procedure of the search, the signature of the fractionally charged particles, the resolutions of the analyzers and detectors, and the expected energy and time of flight spectra.

I. INTRODUCTION

The quest for the elusive fractionally charged free quarks started soon after the quark model was proposed by Gell-Mann[1] and Zweig[2] in 1964. The experimental searches took a variety of forms[3] but with the exception of a Stanford magnetic levitation experiment[4] no other experimental evidence exists for free quarks of fractional electric charge. However, since the spring of 1977 the Stanford group has repeatedly claimed the observation of fractional $\pm(1/3)e$ charge on superconducting niobium spheres levitated in a magnetic field and their experimental evidence for fractional charge is getting stronger. To resolve this apparent conflict of the Stanford results with those of other experiments, fresh experimental approaches are needed and several new investigations are already

planned.[5] In this paper we will describe a proposed experiment using the 3MV electrostatic tandem accelerator and the all-electrostatic line of the IsoTRACE Laboratory at the University of Toronto (see Fig. 1) to search for fractionally charged particles (FCP) in stable matter. Our experimental goal is to measure the charge of a very large number of atomic particles($\gtrsim 10^{20}$) independent of their mass and with a detection sensitivity for FCP comparable to that of the Stanford experiment ($\simeq 10^{-18}$ N(FCP)/N(Particles)). The principles of this ultrasensitive mass-independent charge spectroscopy using electrostatic accelerators are outlined in the following sections.

It is perhaps appropriate here to point out some of the differences between our proposed experiment and a number of accelerator-based charge spectroscopy searches for FCP. Our philosophy is to make as few assumptions as possible about the mass, the physical and chemical properties of FCP and yet achieve a high detection sensitivity for FCP. The existing experiments are either mass-dependent[6,7] or relying on some physical or chemical properties of FCP[8,9] so that when a negative result is obtained, it becomes somewhat inconclusive. We hope that with fewer assumptions made, our experiment can provide a more definitive conclusion about FCP even if the result is negative.

II. ULTRASENSITIVE MASS-INDEPENDENT CHARGE SPECTROSCOPY

A. General Considerations

In accelerator mass spectrometry the atomic particles are accelerated by the same electric potential drop and thereafter they are analyzed by a combination of electrostatic and magnetic analyses. The magnetic analyses are momentum- and hence mass- selective while the electrostatic analyses are not. Therefore, to achieve a completely mass-independent charge spectroscopy one has to use purely

electrostatic analyses.

One simple way to measure the charge of the atomic particles independent of their mass is to measure the energy E of the particles with a particle energy detector immediately following an electrostatic analyzer (ESA) which defines the electric rigidity E/q (kinetic energy/charge) . The charge q of the particles can then be easily deduced from E/q and E. But there is one problem that severely limits the sensitivity of this method, namely, the limited count rate ($\lesssim 10^6$/s) of the particle energy detector. Thus to detect FCP with high sensitivity one needs to reject, as completely as possible, the integral charge background with an efficient filter which preferentially passes FCP. Our idea of the filter[10] is based on charge-changing collisions which cause atomic particles to lose or capture electrons without altering the energy of the particles (to any significant degree). There is in fact a good reason why we use a charge-changing filter: since we are only allowed to use E/q analyses and since E does not change unless the particles are accelerated through an electric potential drop, or they suffer molecular break-up or inelastic collisions, the only way to differentiate integral charges from FCP through E/q analyses is to make use of charge-changing collisions. In general, the change of electric rigidity of FCP after charge-changing collisions is different from that of most integral charges and this is the basis of charge-changing filters.

B. Charge-Changing Filter

Before we discuss the details of charge-changing filters we have to make the following and, we stress, the only assumption about FCP: A FCP is composed of a fractionally charged (positive) central core and Bohr-type electron orbitals surrounding the core. A FCP is similar in its electronic structure to that of

ordinary atoms. The central core of FCP may be a quark or a "quarkleus" which is a free quark saturated with nucleons as proposed by De Rujula, Giles and Jaffe.[11] In the following discussion we will only rely on some well-studied and well-understood charge-changing phenomena[12] which only involve Coulomb interaction and are valid for FCP as well as for integrally charged ions.

The charge-changing filter consists of a gas canal or a thin foil as the medium for charge-changing collisions followed by an electrostatic analyzer. We have studied the background rejection capability of the filter for more than two dozen cases involving the electron capture and electron loss (single and multiple) by the $\pm(1/3)e$ and $\pm(2/3)e$ FCP through the filter. In each case the major integral charge backgrounds that have the same electric rigidity as the FCP are examined and their likelihood assessed. We shall only discuss two particularly favorable cases for FCP in detail.

As example [1], let us consider the electron capture $+1/3 \rightarrow -2/3$ which is accompanied by the integral charge backgrounds $X^{+1} \rightarrow X^{-2}$ and $X_2^{+1} \rightarrow X^{-1}$. The background $X^{+1} \rightarrow X^{-2}$ is rare because the existence of doubly negative atomic ions is doubtful,[13] although large doubly negative molecular ions are known.[14] In any event, molecules are destroyed in the tandem terminal due to the stripping of electrons at high energy and the fragile doubly negative ions may not survive the high electric field of the accelerator due to field ionization. The main background then comes from the molecular break-up $X_2^{+1} \rightarrow X^{-1}$. This background can be greatly reduced if we choose a source which produces little X_2^{+1} beam and ion species for which X^{-1} does not form readily (for instances: group-IIA and -IIB elements, noble gases, N, Hf, Sc, etc.). On the other hand, +1/3 is the most abundant charge state produced by the ion source for the FCP in this case and the electron capture for the FCP $+1/3 \rightarrow -2/3$ is favored because of the strong

electron affinity of the +(1/3)e FCP. Also this electron capture cross section can be enhanced by using an alkali-metal vapor charge-changing canal.[15,16]

Example [2] is also of electron capture: +2/3 → -1/3 which has the integral charge background $X^{+2} \rightarrow X^{-1}$. We note that in this case the magnitude of the charge decreases through the filter and the resulting increase of the magnitude of the electric rigidity effectively eliminates the background due to the molecular break-up. Again, as in the previous example, the background can be reduced by a judicious choice of ion source and ion species. Both of these examples yield negative FCP which can then be injected into the tandem electrostatic accelerator and, as we will see later, this results in further background rejection. We also note here that the first example is sensitive to antiquarks of +(1/3)e and -(2/3)e since +(1/3)e FCP include +(1/3)e quarkleus-atom as well as -(2/3)e quarkleus-atom with one electron removed. Similarly, the second example is sensitive to quarks of -(1/3)e and +(2/3)e.

The electron capture yield of FCP can be estimated from the systematic behavior of maximum negative equilibrium fractions (in Cs) which, according to Ref. 15, are 0.3-9% for group-I elements; 8-12% for group-III elements; 15-60% for group-IV elements and 80-90% for group-V elements. The maximum negative fractions for group-I elements also monotonically increase with electron affinities. It was shown[15,16] that the maximum negative fraction approximately occurs at a projectile velocity $V_{max} = a\,\Delta E/h$ in accordance with the Massey adiabatic criterion[17] where $\Delta E = E_I$(target ionization energy)$-E_A$(projectile electron affinity) and a is the interaction distance. Thus V_{max} occurs at lower velocity for projectiles having a stronger electron affinity. Based on the systematics of Ref. 15 we estimate that the maximum negative fraction for FCP occurs at about 0.1 to 1.0 keV/amu. However because of the unknown mass of FCP it

is difficult to tune for the maximum negative FCP yield. Fortunately, the electron capture yield does not vary rapidly with projectile velocity so that a significant negative FCP yield after charge-changing can be obtained in nearly all circumstances.

In addition to the two favorable cases mentioned above there are other cases for which the integral charge background is greatly reduced by using the charge-changing filter. We shall list them here: $+5/3 \rightarrow -1/3$; $-2/3 \rightarrow +1/3$; $-2/3 \rightarrow +7/3$; $+4/3 \rightarrow +7/3, +13/3$; $+5/3 \rightarrow +8/3, +11/3$. The background rejection of these cases relies on (a) the paucity of multiply charged positive or negative ions and (b) the paucity of some molecular break-up processes. For some of the above cases, one can in principle use a single-ended Van de Graaff followed by a series of charge-changing filters (which consist of charge-changing canal or a thin foil and an ESA) and a particle energy detector to search for FCP. However the sensitivity of the search may not be very high due to possible higher background, lower efficiency (at the ion source and the charge-changing filter), problems associated with measuring relatively low particle energy and higher energy resolution needed.

We also wish to point out that, according to our extrapolations of the isoelectronic series electron binding energies, $-(4/3)e$ FCP probably only exist for $-(1/3)e$ or $+(2/3)e$ Cl quarkleus-atom and $-(5/3)e$ FCP probably do not exist. In the case of Cl the filtering $-4/3 \rightarrow -1/3$ removes nearly all the backgrounds.

III. MASS-INDEPENDENT SEARCH OF $\pm(1/3)e$ AND $\pm(2/3)e$ FCP

We shall now describe the search for FCP using examples [1] and [2]. The proposed experimental set-up (see Fig. 1) is described in detail in Ref. 18 and it includes a positive ion source, a charge-changing filter, a 3MV electrostatic

tandem accelerator, a high energy ESA, a particle energy detector plus a high resolution time of flight spectrometer ("isochronator").

The positive ion source can be a field-ionization liquid-metal electrohydrodynamic source.[19,20] The reasons for this choice are: (a) high absolute efficiency (50% to 90% charged particles)[19,21] and even higher extraction efficiency (approaching 100%) for charged particles, (b) high current (up to 100 μA or more), (c) good beam optical properties (small emitting area and high brightness), and (d) cleanness. The field-ionization source is particularly suited for FCP search because FCP should desorb or field ionize at a lower extraction voltage than integrally charged ions. Although this is not essential in our scheme of background rejection it will be a very interesting effect to observe. A greatly reduced integral charge background should also be possible for negative FCP search if one applies a negative voltage below the field emission threshold to the tip of the source so that only negative FCP and few negative ions are emitted.[22]

ESA1 is used to "clean up" the beam from the source so that only the ions originated in the source are passed through the charge-changing filter. In addition the spherical ESA1 also serves as a lens which focuses the beam at the charge-changing canal. The charge-changing filter consists of an alkali-metal vapor charge-changing canal and ESA2 whose role in background rejection has already been discussed. After the charge-changing filter, the negative FCP and their background ions are accelerated toward the positive terminal where they are stripped of a few electrons by a charge-changing canal and are then further accelerated as they emerge out of the terminal. The tandem, besides accelerating particles to a conveniently high energy, also acts (together with high energy analyzer ESA3) as an efficient charge-changing filter which further rejects

integral charge background in much the same way as before. At a sufficiently high terminal voltage ($\simeq$ 3MV) molecules are also broken up in the terminal charge-changing canal. Although, in principle, to detect FCP it is not necessary to break up the molecules, in practice large molecules could give erroneously low energy signal due to the enhanced importance of energy loss in the detector window and pulse-height-defect of the detector.

ESA3 selects the desired charge state and makes the final E/q analysis before the energy of the particles is measured. The energy detector can be a Si surface barrier detector which is located right after ESA3. The energy signal derived from the Si detector is somewhat less than what it should be because of energy loss effect, nuclear collision effect and incomplete charge collection. This is called 'pulse-height-defect' (PHD). The PHD is relatively larger at lower energy (and heavier mass) and this is one of the reasons why higher energy is favored for FCP search. It suffices to say that the response of Si detector to heavy ions is well studied and a reliable calibration curve exists.[23]

Let us consider example [1] and choose FCP charge state +2 1/3 at ESA3 (assuming that FCP have enough electrons to strip, this is close to the most abundant charge state at about 2MV to 3MV). The background ions that have the same electric rigidity all the way through the source, ESA2, terminal and ESA3 must be: $X_2^{+1} \rightarrow X^{-1} \rightarrow X^{+8} \rightarrow X^{+7}$ which is an exceedingly unlikely process. The background rejection ratio of much greater than 10^{12} can easily be achieved. Of course, in addition, there will be integral charge background due to the charge-changing in the accelerator tube which results in an E/q continuum. The energy spectrum after ESA3 (see Fig. 2(a)) should consist of equally spaced energy peaks which come from the E/q continuum and correspond to different charge states q. The q=+7 peak is also due to the above-mentioned charge-changing

sequence. There is also a small E continuum which is due to the imprecise definition of the electric rigidity caused by charge-changing and scattering within ESA3. If FCP exists then its energy peak should be at 3e*(terminal voltage) which is separated from the nearest integral charge energy peak (q=+2) by 14.3%. Thus in order to see the FCP peak clearly the energy resolution must be better than 14% and the FCP peak should be above the E continuum. As the figure shows, the background peaks provide a rather good way of calibrating and tuning for FCP peak.

Similarly, for example [2] the charge-changing sequence of the FCP from the source, ESA2, to ESA3: $+2/3 \rightarrow -1/3 \rightarrow +2\ 2/3$ corresponds to the background $X^{+2} \rightarrow X^{-1} \rightarrow X^{+8}$ with a background rejection ratio of perhaps $\simeq 10^{10}$. If X^{-1} does not form easily this ratio could be much greater than 10^{12}.

From the foregoing discussion we see that the detection efficiency for FCP is the product of source efficiency, filter efficiency, stripping efficiency, and transmission and this is of the order of $> 1\%$. Thus with a source current of 100 μA running for one day a sensitivity of $\simeq 10^{-18}$ N(FCP)/N(Particles) can be reached if the E continuum in the energy spectrum is small enough. In principle, the E continuum can be greatly reduced by improving the vacuum and by proper collimation since the charge-changed and scattered particles arise from the collisions with residual gas molecules within ESA and their trajectories are different from that of the particles with the correct electric rigidity.[24] An additional ESA after ESA3 can also help reducing the E continuum significantly.

The signature of FCP must include (a) FCP energy peak appears only at the correct E/q values (i.e. ESA voltage settings), (b) FCP energy peak has the correct E value, and (c) FCP energy peak should be clearly above any E continuum background in the energy spectra. If all three criteria are met then we can

conclude that FCP exists and provide a rough estimate of the concentration of FCP. Otherwise, FCP does not exist at the level of the sensitivity of the experiment. The results should be clear-cut and few interpretations are needed. We should mention that examples [1] and [2] can be made to work for H or He quarkleus and diquarks[25] by an appropriate choice of lower charge state at ESA3 to reduce the integral charge background. Also, examples [1] and [2] work particularly well for low-Z elements ($2 < Z < 8$) since certain integral charge background is avoided.

At the second phase of the experiment, the mass of FCP can be measured by a time of flight spectrometer. A possible E vs. time of flight spectrum (in log scales) for example [1] is shown in Fig. 2(b). The FCP lies between the equally spaced energies of the background ions and, because of the anomalous mass of FCP, also between the $E \propto M/T^2$ lines (where M is the integral mass (in units of amu) and T the time of flight of the background ions). The time of flight spectrometer can be a high mass resolution "isochronator"[18] in which ion flight times are essentially isochronous with respect to small variations in ion energy, incident angle and initial displacement at the start detector. A very valuable piece of information about the effective core charge Z of FCP can also be obtained from the rate of energy loss (dE/dx) measurement by a ΔE detector.

REFERENCES

1. M. Gell-Mann, Phys. Lett. 8, 214 (1964)
2. G. Zweig, CERN Report 8419/Th, 412 (1964)
3. L.W. Jones, Rev. Mod. Phys. 49, 717 (1977)
4. G.S. LaRue, W.M. Fairbank, and A.F. Hebard, Phys. Rev. Lett. 38, 1011, (1977); G.S. LaRue, J.D. Phillips, and W.M. Fairbank, ibid, 42, 142 and 1019E (1979) and 46, 967 (1981)
5. A.L. Robinson, Research News, Science 211, 1028 (1981)
6. R.N. Boyd, D. Elmore, A. Melissinos, and E. Sugarbaker, Phys. Rev. Lett. 40, 216 (1978)
7. R.N. Boyd, S.L. Blatt, T.R. Donoghue, L.J. Dries, H.J. Hausman, and H.R. Suiter, Phys. Rev. Lett. 43, 1288 (1979)
8. J.P. Schiffer, T.R. Renner, D.S. Gemmell, and F.P. Mooring, Phys. Rev. D17, 2241 (1978)

9. C.M. Stevens, J.P. Schiffer, and W. Chupka, Phys. Rev. D14, 716 (1976)
10. A.M. Sandorfi, L.R. Kilius, and A.E. Litherland, "Search for Quarklei- A New Form of Matter?", Proceedings 3rd International Conference on Clustering Aspects of Nuclear Structure and Nuclear Reactions, Paper I1, June 19-23, 1978, University of Manitoba.
11. A. De Rujula, R.C. Giles and R.L. Jaffe, Phys. Rev. D17, 285 (1978)
12. H.-D. Betz, Rev. Mod. Phys. 44, 465 (1972)
13. L. Frees, E. Heinicke, and W.S. Koski, Nucl. Instr. and Meth. 159, 105 (1979)
14. J.H. Bowie, and B.J. Stapleton, J. Am. Chem. Soc. 98, 6480 (1976)
15. P. Tykesson, Proc. Symp. Northeastern Accelerator Personnel (SNEAP 78), (Oak Ridge,1978) pg.187
16. J. Heinemeier and P. Hvelplund, Nucl. Instr. and Meth. 148, 65 and 425 (1978)
17. J.B. Hasted, Advance Electronics Electron Phys. 13, 1 (1960)
18. L.R. Kilius, E.L. Hallin, K.H. Chang, A.E. Litherland, Proc. Fifth Int. Conf. Ion Beam Analysis, Sydney, Australia, 16-20 Feb. 1981, to be published in Nucl. Instr. and Meth.
19. R. Clampitt and D.K. Jefferies, Nucl. Instr. and Meth. 149, 739 (1978)
20. R. Clampitt, Proc. Third Int. Conf. Ion Implantation, Kingston, 1980, to be published in Nucl. Instr. and Meth.
21. G.L.R. Mair, Nucl. Instr. and Meth. 172, 567 (1980)
22. M. Anbar, and G.A. St. John, Science 190, 781 (1975)
23. S.B. Kaufman, E.P. Steinberg, B.D. Wilkins, J. Unik, and A.J. Gorski, Nucl. Instr. and Meth. 115, 47 (1974)
24. K.H. Purser, P. Williams, A.E. Litherland, J.D. Stein, H.A. Storm, H.E. Gove, and C.M. Stevens, Tenth Int. Conf. Electromagnetic Isotope Separators, Zinal, Switzerland, Sept. 1980, to be published in Nucl. Instr. and Meth. (1981)
25. R. Slansky, T. Goldman, and G.L. Shaw, submitted to Phys. Rev. Lett. (1981)

FIGURE CAPTIONS

FIGURE 1. The University of Toronto IsoTRACE Laboratory. The all-electrostatic line consists of a positive ion source, a charge-changing filter which includes ESA1 (a spherical electrostatic analyzer), an alkali-metal vapor charge-changing canal and ESA2, a 3MV tandem electrostatic accelerator, ESA3, and a time of flight "isochronator" which includes ESA4 and ESA5. The Si surface barrier particle energy detector is located right after ESA3.

FIGURE 2(a). A possible energy spectrum for example [1]. The charge-changing sequence for FCP from the source, ESA2, terminal, to ESA3 is $+1/3 \rightarrow -2/3 \rightarrow +2\ 1/3 \rightarrow +2\ 1/3$ and that of the integral charge is $X_2^{+1} \rightarrow X^{-1} \rightarrow X^{+8} \rightarrow X^{+7}$ which contributes to the q=+7 energy peak. All other integral charge energy peaks (spaced equally) are due to charge-changing in the accelerator tube. The small E continuum is due to charge-changing and scattering within ESA3. If FCP exists its energy peak should be at 3e*(terminal voltage) and separated from q=+2 peak by 14.3%.

FIGURE 2(b). A possible E vs. time of flight spectrum (in log scales) for example [1]. FCP lies between the equally spaced energies of the background ions and between $E \propto M/T^2$ lines where M is the integral mass (in units of amu) and T is the time of flight of the background ions. Open and solid circles denote FCP and integrally charged background ions respectively.

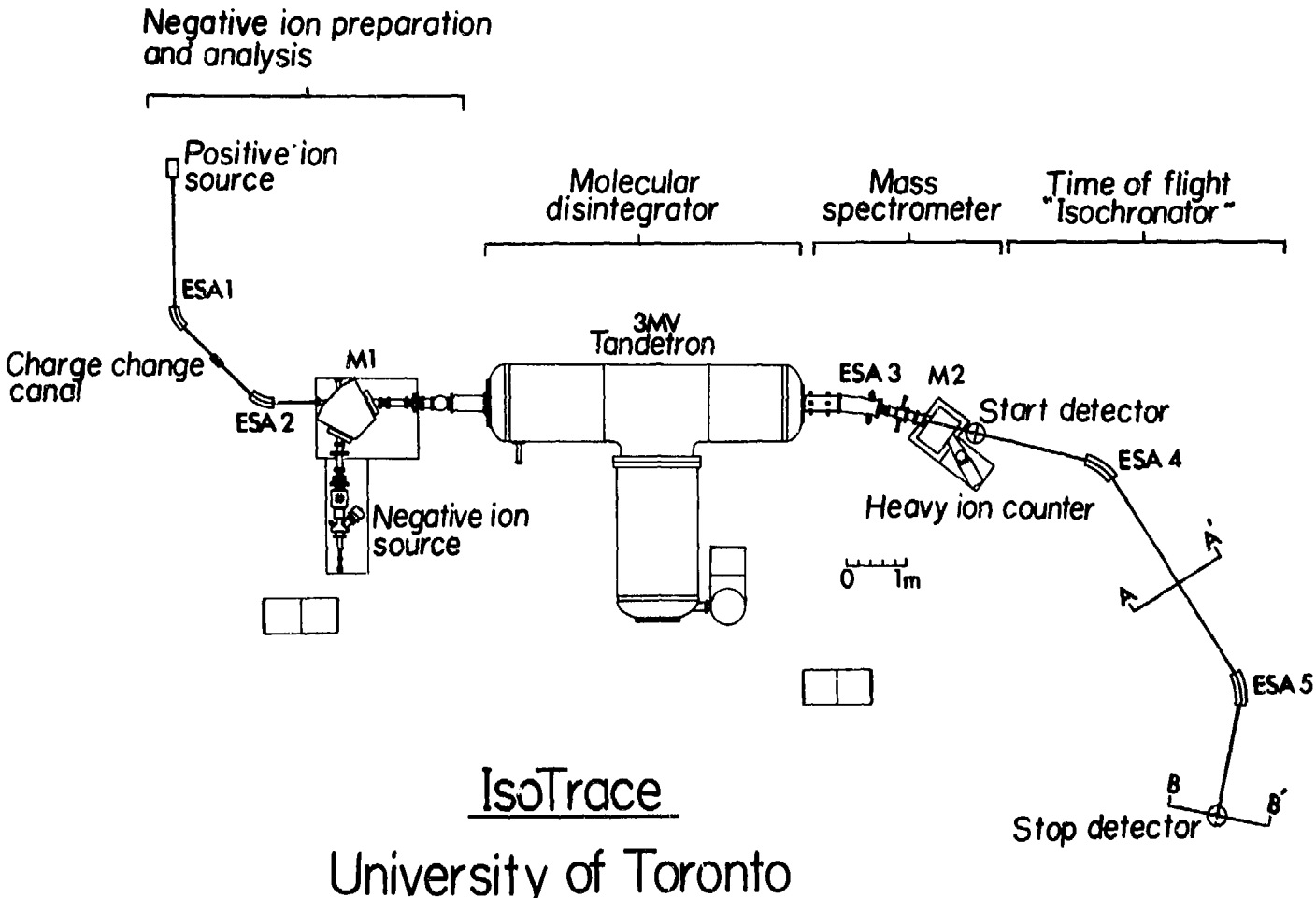
Negative ion preparation and analysis
Positive ion source
Molecular disintegrator
Mass spectrometer
Time of flight "Isochronator"
ESA1
3MV Tandetron
Charge change canal
M1
ESA 3
M2
Start detector
ESA 2
ESA 4
Negative ion source
Heavy ion counter
0 1m
A
A'
ESA 5
B
B'
Stop detector
IsoTrace
University of Toronto

FIGURE 1

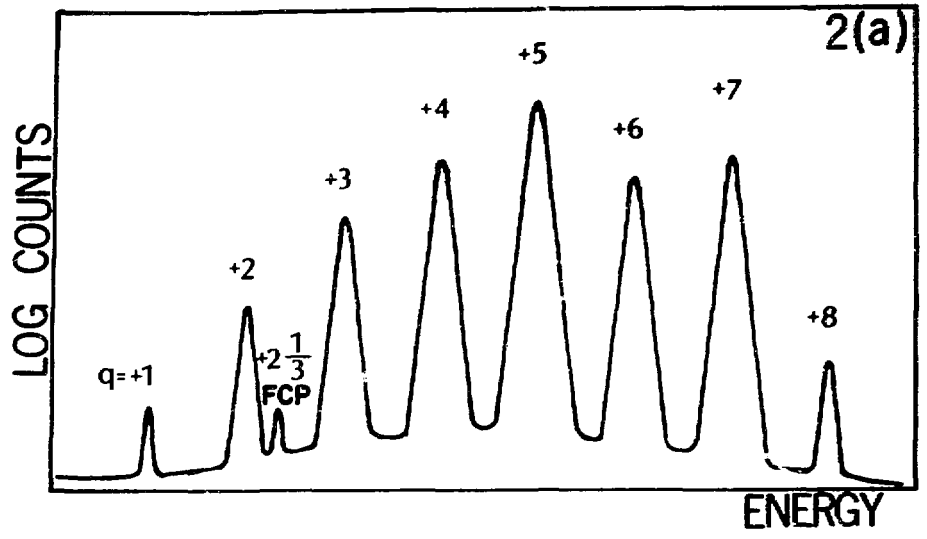
2(a)
LOG COUNTS
q=+1
+2
+2 1/3
FCP
+3
+4
+5
+6
+7
+8
ENERGY

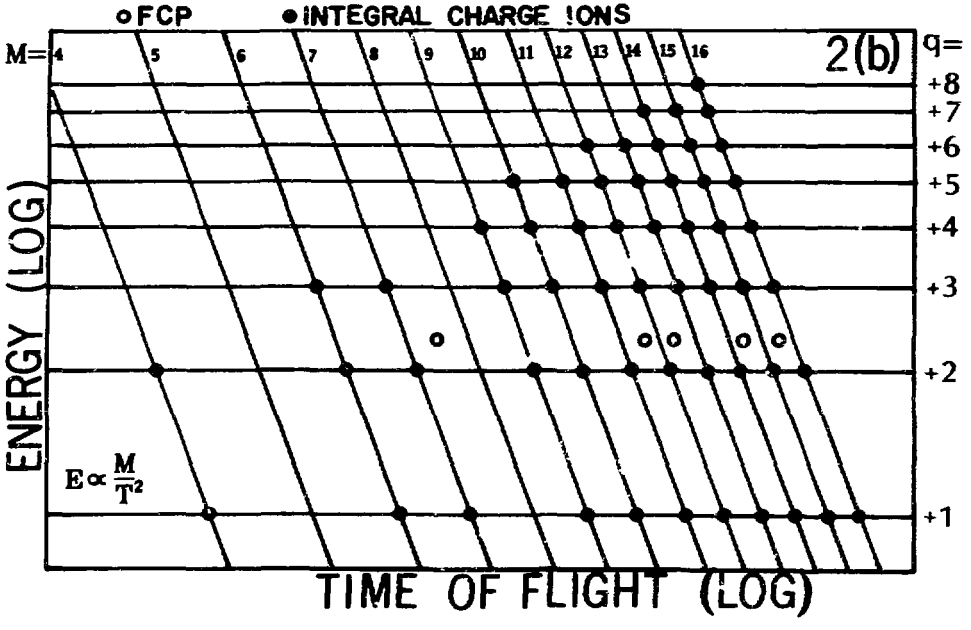
o FCP
● INTEGRAL CHARGE IONS
2(b)
M=
4
5
6
7
8
9
10
11
12
13
14
15
16
q=
+8
+7
+6
+5
+4
+3
+2
+1
ENERGY (LOG)
E∝ M/T²
TIME OF FLIGHT (LOG)

FIGURE 2

A SEARCH FOR ANOMALOUS HYDROGEN IN ENRICHED D_2O, USING A TIME-OF-FLIGHT SPECTROMETER

P F Smith, J R J Bennett, G J Homer, J D Lewin, H E Walford, W A Smith
Rutherford and Appleton Laboratories, Chilton, Oxon, U.K.

I. INTRODUCTION

We report on a search for stable charge +1 particles in the form of anomalously heavy hydrogen-like atoms in natural water. The objective of this experimental programme was to investigate the concentration range 10^{-20} to 10^{-30} which would be expected for cosmic ray production of 10-200 GeV mass particles during the lifetime of the earth.

In a previous paper[1] we described the production of a highly enriched sample of heavy water (itself produced by the enrichment of natural water), and the analysis of part of that sample in a conventional mass spectrometer to reach concentration levels of order 10^{-21} to 10^{-22} in the mass range 6 to 350 GeV. In the present paper we describe the analysis of the remainder of the enriched sample in a time-of-flight spectrometer designed specifically to identify individual low-Z heavy particles. No events corresponding to such particles were observed, giving concentration limits of order 10^{-28} to 10^{-29} over the mass range 12 to 1200 GeV.

In Section II we briefly summarise the production of the enriched sample and the factors limiting sensitivity in the mass spectrometer experiment. In Sections III and IV we describe the design, theory, and performance of the time-of-flight spectrometer. The experimental runs with enriched and control D_2O samples are summarised in Section V, and the detection sensitivity and concentration limits are calculated as a function of particle mass. Finally in Section VI we discuss the application of the spectrometer to other stable particle searches, in particular fractional charge and anomalous nuclei.

II. D_2O ENRICHMENT; MASS SPECTROMETER SEARCH

The production of the enriched D_2O sample was described in the previous paper[1]. The starting point was 6000ℓ commercial D_2O which had been manufactured from 1.2×10^8ℓ natural water[2] and thus provided an initial enrichment factor 2.10^4 for any heavy hydrogen-like atoms. Over a 3 year period the 6000ℓ was progressively reduced in volume by electrolysis to give two main samples:

Sample	Volume	Enrichment (relative to D_2O)	Overall Enrichment (relative to H_2O)
(a)	0.012mℓ	1.5×10^7	3×10^{11}
(b)	0.021mℓ	3.0×10^7	6×10^{11}

Sample (a) was used for the previous mass spectrometer search, and 0.016mℓ of sample (b) for the time-of-flight runs described in this paper. The remainder of sample (b) (0.005mℓ) remains unused, together with a number of samples with smaller enrichment factors.

Measurements of the increasing tritium concentration were used to provide a continuous check on all stages of the enrichment programme. The numerical enrichment factors can be calculated with a high degree of confidence since, for masses >10 GeV, they have only a second order dependence on the assumed isotopic separation factor α. For the expected value[3] $\alpha(X/D) \sim \alpha(D/H) \sim 8$ a volume reduction R produces a concentration increase R^p where p lies between 7/8 (no recombination) and 1 (100% recombination and reprocessing of evolved gases). The latter limit is approached in continuous commercial processes ($p \sim 0.98$ for tritium enrichment in D_2O production) but for batch processes it is difficult to do better than $p \sim 0.90$ to 0.92, and the estimated enrichment factor is thus nearly an order of magnitude less than the overall volume reduction ($\sim 4.10^{12}$). Using the theoretical mass-dependence of α[3], $\ln(A/B) \propto \ln(1/M_A - 1/M_B)$, we have also made an estimate of the slight mass-dependence of the enrichment factor, and this is included in the sensitivity estimates of Section V.

For the mass spectrometer runs, sample (a) was converted to D_2 gas, and

compared with D_2 from unenriched D_2O in several mass scans from 6 to about 350 proton masses. The detection sensitivity $\sim 7.10^{-11}$, divided by the 3.10^{11} enrichment factor, gave an overall sensitivity $\sim 2.10^{-22}$ over most of the mass range. It was evident, however, that the conventional mass spectrometer provided a very inefficient way of analysing a limited sample volume, only 10^{-5} to 10^{-4} of the input particles being ionised and a further factor $\sim 10^4$ being lost by the necessity to scan the mass spectrum. The possibility of retrieving these factors, by means of a high efficiency ion source together with a non-scanning particle identification scheme, provided the objectives of the time-of-flight spectrometer now described.

III. DESCRIPTION OF SPECTROMETER

The principal features of the system are shown in Fig. 1. D_2O vapour (plus any impurities and DXO) from the sample is released into the source where it is ionised and accelerated to 130 kV. The beam is then magnetically mass-separated to allow removal of low mass components, including the main D_2O beam. Everything remaining is then recombined into a single beam which is passed through a carbon foil to attenuate or remove high-Z nuclei. Any surviving particles are then individually recorded by a time-of-flight channel formed by three thin carbon foils and electron multipliers. From the flight times t_1 and t_2, before and after passage through the central thin foil, events due to low-Z heavy particles would be clearly distinguishable from those due to normal ions as discussed in Section IV. The separation of the time-of-flight foils is 10cm, and the overall length of the spectrometer is about 300cm. A general view of the spectrometer and control equipment is shown in Fig. 2.

We now discuss the principal components of the system in more detail:

A. Sample Injection System

The D_2O samples are initially stored in glass capillary tubes. For injection into the spectrometer the tube is broken, placed in a larger tube, and frozen by a liquid nitrogen cooled shield. D_2O vapour is then released into the ion source at a constant pressure of 50 microns by a servo operated

temperature controller. Alternatively the D_2O sample is first absorbed into about ten times its volume of 'molecular sieve', from which it can again be released by controlled heating. To run as D_2 gas, the procedure described previously[1] is used, the D_2O being first reduced to D_2 in a uranium furnace, stored as UD_3 in a tube of uranium powder, and subsequently released at a controlled pressure by heating. These processes are not expected to involve any significant isotopic discrimination[3] but, as a safeguard, the samples were finally heated strongly until the required ion source pressure could no longer be maintained.

B. Ion Source

The ion source is of the duoplasmatron type, operated at a pressure of 40-50 microns to give an ion current of 8μA. Under these conditions the measured ionisation efficiency for D_2O is about 2½%. Higher efficiencies were attainable, but resulted in excessive background counting rates. However, since the diffusion rate of unionised gas out of the ion source would be inversely proportional to (molecular weight)$^{\frac{1}{2}}$, the corresponding ionisation efficiency for DXO would be higher by a factor $[(M_X + 18)/20]^{\frac{1}{2}}$, ie 6% at 100 GeV and 17% at 1000 GeV. After extraction from the ion source the beam is accelerated to an operating voltage of normally 130 kV, which can also be set to values down to to 60 kV for test purposes. Electrostatic lenses are used to bring the beam to a focus at the mass separation plane, and again in the time-of-flight channel.

The mass spectrometer chamber is pumped by two 100 ℓ/sec. triode pumps and a liquid helium operated cryopump with a speed of 200 ℓ/sec. for D_2. The system pressure is normally in the region of 10^{-7} Torr when running. The cryopump was included in the system so that with the ion pumps switched off it could be used to collect and recycle the unionised gas to obtain higher effective efficiency. It was not brought into operation for the experiment since there was no indication of a positive result to justify the factor ∿5 increase in running time which would have been necessary.

C. Magnetic Mass Selection

Since the 8μA beam current corresponds to $\sim 5 \times 10^{13}$ ions per second, it is necessary to remove the majority of the unwanted components of the beam before it reaches the time-of-flight channel, both to obtain acceptable counting rates $<10^3$/s and to prevent foil burn-out. This is achieved by a symmetrical arrangement of magnets which separates the mass components of the beam and then recombines them into a single beam following its original path. Where the beam is separated, a scraper is positioned to remove all masses up to some value M_L, which can be selected by varying the magnetic field strengths. For example, by setting M_L to mass 24 we remove the main D_2O^+ beam, together with dissociated D_2^+, O^+, and other low mass contaminants, but retain DXO^+ for all $M_X > 6$. A more satisfactory operating point is $M_L = 29$, which eliminates an inconveniently large N_2^+ component and still retains all $M_X > 12$.

In practice, it has also been necessary to introduce a small 'hurdle' on the original beam axis at this point, to prevent ultra-violet light from the ion source reaching the foil system and producing excessive electron noise. This produces a field-dependent upper limit M_U to the mass range accepted by the system, related to the lower limit by $M_U = 22M_L$. Thus with M_L set to 29 the recombined beam would contain all masses in the range 30 to 660, ie. $12 < M_X < 640$. The maximum setting allowed by the magnet system is $M_L \sim 55$, giving $M_U \sim 1200$. This is not at present a significant restriction, since, as discussed below, the foil system itself becomes insensitive for mass numbers $>10^3$; the limitation could be overcome, if required, by the alternative solution of an electrostatic bend or 'joggle' in the beam path, to take the foil system out of the line of sight from the ion source.

The magnetic separation plane is also utilised for setting-up and diagnostic purposes. Movable slits can be introduced to scan the individual components of the mass spectrum, and to calibrate the M_L settings. To monitor beam size and position, Faraday cups on the beam scraper allow current measurements of the principal beam components.

D. High-Z Attenuating Foils

Removal of the D_2O^+ and other low mass ions reduces the beam current from 5×10^{13} ions/s to about 10^9 ions/s. This is reduced to a level 10^3/s by passing the beam through one or more carbon foils whose total thickness (60-100μg cm^{-2}) is sufficient to stop most of the high-Z ions, but is less than the range of hydrogen-like (Z = 1) ions, which are thus transmitted, though with some loss of energy. Moreover, at these energies (10-100 keV), the computed range of hydrogen isotopes increases with mass up to several hundred AMU (~GeV)[4], so that, having verified the transmission of test beams of H and D through the foil system, we can be confident that any heavier Z = 1 particles would also be transmitted with negligible loss.

However, the foil does introduce some angular scattering, which can exceed the acceptance angle of the final time-of-flight foil and thus reduce detection efficiency. For this reason the lowest thickness compatible with acceptable counting rates is used, and to allow this optimum thickness to be selected under running conditions a fixed foil of less than optimum thickness is used, together with a selection of additional foils which can be moved into the beam by an externally controlled mechanism.

The fixed foil is subject to damage due to heating by the absorbed particles, giving a lifetime in the region 10-100 hours running time. To give a longer lifetime, the beam is usually slightly defocused, to give a spot size ~2mm diameter. This does not significantly affect the acceptance of the time-of-flight channel since the foils themselves are 20mm diameter.

It should be noted that the attenuating foil also ensures the break-up of all molecules into their constituent atoms, sharing the original ion energy in proportion to their mass. Thus a DXO molecule will break up into D, X, and O atoms or ions, the O being stopped by the foil and the D and X transmitted with appropriate fractions of the original 130 keV energy. They may emerge from the foil either as ions or neutral atoms but this does not significantly affect their subsequent detection in the time-of-flight system, since the majority of the energy resides in the nucleus.

E. Time-of-flight Channel

Particles which survive the attenuating foil (mainly D and H atoms of various origin and energy, together with residual heavy ions and any new particles X) then pass through a system of three 10μg/cm^2 carbon foils, separated by 10cm flight paths. Secondary electrons released from the foil surfaces are directed into adjacent electron multipliers by a 200V positive potential, and these signals are used to measure the flight times t_1 and t_2 before and after the central thin foil.

The logic operates as follows: beginning the timing with a count on foil 1, the next count on foil 2 is assumed to correspond to t_1, after which the next count on foil 3 is assumed to correspond to $t_1 + t_2$, completing the event. If the event is not completed within a specified period, usually set at 5000 ns, timing is restarted with the next count on foil 1. This allows for particles which stop in one of the foils, or have a scattering angle too large to reach the final foil. The completed events are recorded by an on-line computer and simultaneously displayed as individual points with axes t_1 and t_2. The majority of events have 50 ns $< t_1 <$ 150 ns, with $t_2 > t_1$ by an amount depending on the energy loss in the central thin foil. The limit chosen, $t_1 + t_2 \leq 5000$ ns, is sufficiently long to allow the recording of heavy particles up to several thousand GeV in mass, but sufficiently short to ensure a very low probability ($\sim$1 event in 10^5) that t_1 and t_2 are produced by different particles.

To provide additional or confirmatory information on possible heavy particle events the time-of-flight channel can be terminated by a solid state detector. This was not required in the D_2O runs, since no candidate events were observed. It may, however, be necessary for future fractional charge searches, as discussed in Section VI.

IV. THEORY AND PERFORMANCE OF TIME-OF-FLIGHT SYSTEM

The computation of energy loss for heavy charged particles, using the standard theory established for normal ions, has been discussed in a previous report[4]. The principle of the time-of-flight identification scheme can be

seen from Fig. 3, in which the computed rate of change of velocity in a carbon foil is shown as a function of particle velocity for (a) a range of low-Z heavy particles, (b) protons and deuterons, and (c) a selection of heavy ions. Since the curves for (a) are well separated from those for both (b) and (c), it follows that any anomalous heavy particle events recorded in the time-of-flight channel will appear in a different area of the t_1t_2 plane.

The expected location of events in the t_1t_2 plane is indicated in Figs. 4 and 5. The curves of Fig. 4 show how t_2 varies with t_1 for the most probable energy loss in the central foil. (Note that, although the accelerating voltage is fixed, a range of t_1 will occur for a given type of particle, owing to energy straggling in the attenuator foil and the production of lower energy particles by various scattering and molecular dissociation processes). These curves illustrate in a general way the separation of events due to heavy particles from those due to normal ions, and also the existence of an effective upper limit to t_1 for the background ions; this arises from the fact that although longer values of t_1 may in fact occur, for sufficiently low energy D^+ ions say, such ions will be stopped by the central foil and no t_2 will be recorded to provide a completed event. Any high-t_1 events would, therefore, be a clear indication of a particle with abnormally low energy loss.

A more detailed prediction for a specific experimental foil system is given in Fig. 5, which shows computed contours within which 99% of events for a given type of particle would be expected to occur. The heavy particle contours are for X atoms released from 130 keV DXO^+ molecules incident on the thick foil. The background region is computed specifically for D^+ ions scattered into the time-of-flight system with various energies, but contours for other normal ions lie in the same region. The computations include an allowance for a $\sim$5ns timing error associated with variations in the transit time of the secondary electrons, and for this reason the contours drop slightly below the $t_2 = t_1$ line.

The observed performance of the system conforms exactly with these predictions. Fig. 6 shows a typical observed distribution of 1500 t_1t_2 events for a D_2O test sample, accumulated over a 5 hour running period.

Comparing this with Fig. 5, it is seen that all the events fall within the predicted boundary for normal ions, with no events in the heavy particle region. Similar agreement with predicted distribution is obtained for test beams of hydrogen and deuterium; Fig. 7 shows the on-line display during a test run with an H_2 - D_2 gas mixture, with four distinct clusters of points corresponding to (1) 120 keV H (2) 120 keV D (and 60 keV H from H_2^+) (3) 80 keV D from HD and (4) 60 keV D from D_2^+.

As explained above, the absence of any real events in region B of Fig. 6 is ensured by the fact that any low energy normal ions of long t_1 are stopped in the central foil, no event being recorded. It is, however, possible for accidental coincidences between the three foil counting rates to produce spurious points distributed at random over the t_1t_2 plane, occasionally falling in the heavy particle region; this effect can be readily produced by decreasing the low-mass limit M_L, or by reducing the thickness of the attenuating foil, to substantially increase the counting rates on the time-of-flight foils. The observed spurious event rate was found to be consistent with the expected value $\frac{1}{2}C_1C_2C_3t_m^2$, where C_1,C_2,C_3, are the foil counting rates and t_m is the maximum time (5000 ns) allowed for an event. Thus high counting rates in the region $C_1 \sim 3000$/s, $C_2 \sim 600$/s, $C_3 \sim 300$/s produced 25 spurious events per hour, but under the normal operating conditions, with $C_1 \sim 500$/s, $C_2 \sim 40$/s, $C_3 \sim 20$/s, the random event rate is reduced to <1 in 50 hours, (<1 in 100 hours for the region $t_1 > t_2$).

V. EXPERIMENTAL RESULTS

To take advantage of the procedures developed for the earlier mass spectrometer experiment, it was initially intended to convert the enriched sample to deuterium gas; but preliminary test runs with D_2 showed a significant current in the H_2O - D_2O mass region (probably formed in the ion source), causing excessive counting rates which could not be attenuated without damage to the thick foil. The sample was therefore injected as D_2O vapour, with the magnetic rejection stage set to a higher minimum mass number M_L. With various choices of M_L the following X mass ranges could be covered:

a) $M_L = 26$: $8 < M_X < 500$

b) $M_L = 30$: $12 < M_X < 600$

c) $M_L = 48$: $30 < M_X < 1000$

d) $M_L = 58$: $40 < M_L < 1200$

Only a short run was possible under condition (a) since the mass 28 N_2 peak produced a substantial increase in counting rate, but runs totalling about 65 hours were made under conditions (b), (c), and (d), the mass range 40 to 500 being covered for the whole of that time. Columns A and B of Table 1 show the total running time for various mass numbers. Extensive control runs were also made, using unenriched D_2O and D_2O samples of lower enrichment factor.

The experiment was carried out with 16μℓ of sample (b) (see Section II); 5μℓ was held in reserve and remains unused. Of the 16μℓ, 9μℓ was evaporated direct from the liquid state and 7μℓ from granules of 'molecular sieve' (the two techniques already outlined in Section III A).

To maximise detection efficiency lower attenuator foil thicknesses were used for the larger values of M_L, the background ion currents being much lower. For a given foil arrangement n, only some fraction f_n of incident particles of a given mass will be intercepted by the final foil F_3, owing to Coulomb scattering in the foils. Computed r.m.s. scattering angles for heavy Z = 1 particles passing through the system have been used to estimate f_n as a function of particle mass for each foil system used. These f_n values are multiplied by the corresponding running times T_n and the total $\Sigma f_n T_n$ (which is the equivalent running time in hours for 100% collection efficiency) is shown for each mass number in column C of Table 1. It should be noted that the computations of f_n included a normalisation factor 0.3 to bring the computed value for deuterium into agreement with a direct experimental measurement of f_n with a test deuterium beam. It is not known whether this factor represents a correction to the theoretical or to the experimental value, and we have simply assumed it to be constant over the mass range.

Two other efficiency factors are required. The increase of ion source efficiency η with mass has already been discussed in Section III B and the improvement factor relative to the D_2O beam is shown in column E of Table 1.

The other factor, shown in column D, arises from the decreasing probability of secondary electron emission as M_X increases (for fixed accelerating voltage). The measured secondary electron coefficient γ_D for ~100 keV deuterons is approximately 4 for foils orientated at 45°, and this is multiplied by the relative value γ_X/γ_D estimated as a function of mass and energy for heavier Z = 1 particles using the theoretical model developed by Firsov[5]. When γ_X drops below 1, some of the events will not be registered, and the detection probability will be approximately the product of the γ_X values for the three foils. We see from the table that the detection efficiency is not affected very much up to mass 100, but drops rapidly in the 100-1000 GeV mass range.

From the factors in columns C, D, and E we obtain the overall spectrometer sensitivity $(2NCDE)^{-1}$ where N is 1.7×10^{17}, the number of ions per hour at 8μA beam current, and the factor 2 converts the DXO/D_2O ratio to the X/D ratio. This figure (column F) is then divided by the overall enrichment factor (column G) to obtain the concentration limit X/H in terrestrial water (column H). Since no events were observed, the figure represents, by Poisson statistics, the 63% confidence level; multiplying by 2 gives the 86% level and multiplying by 3 gives the 95% level.

Figure 8 shows the concentration limits for both this experiment and the previous mass spectrometer search, the latter being updated to include the mass-dependent ion source efficiency and the (single foil) secondary electron efficiency. Also shown are typical theoretical concentration estimates for pre-stellar and cosmic ray production processes[6], and the current experimental mass limit for pair-production of charge +1 particles in e^+e^- collisions[7].

The line labelled 'D_2O density' represents a possible limit for ultra-heavy particles derived from the fact that the density of the enriched samples did not differ significantly from the density of unenriched D_2O. The accuracy of this comparison was limited to about 10% by the fact that the final enriched samples were held in capillary tubes and also contained ~30% NaOD from the final electrolysis stage. This particular limit depends on an additional assumption that the surface water from which the original D_2O was

extracted was not gravitationally depleted in heavy particles. Gravitational concentration gradients, governed by the factor exp(-Mgh/kT), would become significant in a static ocean for masses above 100-1000 GeV; but the equilibrium time constant would be $>10^8$ years so that, if there is a sufficient degree of mixing in the oceans on this time scale, the properties of enriched surface water provide a valid limit for the existence of anomalous hydrogen of very high mass.

TABLE I. Summary of running times, efficiency factors, and concentration limits

A	B	C	D	E	F	G	H
8	1	0.0004	1.0	1.14	5.8×10^{-15}	2.4×10^{11}	2.4×10^{-26}
10	1	0.0013	1.0	1.18	1.8×10^{-15}	3.2×10^{11}	5.7×10^{-27}
12	30	0.08	1.0	1.22	3.1×10^{-17}	3.6×10^{11}	8.5×10^{-29}
20	40	0.17	1.0	1.38	1.2×10^{-17}	5.0×10^{11}	2.4×10^{-29}
40	65	0.56	0.85	1.70	3.5×10^{-18}	6.0×10^{11}	6.0×10^{-30}
60	65	1.03	0.60	1.97	2.4×10^{-18}	6.4×10^{11}	3.8×10^{-30}
100	65	1.57	0.32	2.43	2.4×10^{-18}	6.8×10^{11}	3.5×10^{-30}
200	65	2.06	0.11	3.30	3.9×10^{-18}	7.0×10^{11}	5.6×10^{-30}
400	65	2.13	0.03	4.57	1.0×10^{-17}	$7.4.10^{11}$	1.3×10^{-29}
600	60	2.07	0.01	5.56	2.5×10^{-17}	7.6×10^{11}	3.3×10^{-29}
1000	25	1.20	0.002	7.10	1.7×10^{-16}	7.6×10^{11}	2.2×10^{-28}
1200	10	0.60	0.001	7.80	6.1×10^{-16}	7.6×10^{11}	8.0×10^{-28}

Column headings:

A. mass/proton mass (or ≈ mass in GeV)

B. total running time T (hours) at 8μA D_2O^+ beam

C. beam fraction at final foil x running time $\Sigma f_n T_n$ (hours)

D. secondary electron probability factor (3 foils) $\gamma_1\gamma_2\gamma_3$

E. relative ion source efficiency η_X/η_D

F. overall spectrometer sensitivity: $5.8\times10^{-18}/2CDE$

G. estimated overall enrichment $(DXO/D_2O)\div(HXO/H_2O)$

H. natural water X/H concentration limit
(Poisson statistics: 63% confidence level. Multiply by 3 for 95% level)

VI. APPLICATION TO OTHER PARTICLE SEARCHES

A. Fractional Charge

The principles of the time-of-flight detector apply to any low-Z particles and it is clear from the examples shown in Fig. 3 that heavy quarks of charge 1/3 or 2/3 would be similarly separated from normal ions in the $t_1 t_2$ plane. Since such particles, either alone or with an attached electron, are already charged, the normal ion source would not be required and would be replaced by a means of heating or evaporating the source material in the accelerating field. Nevertheless some normal background ions will still be present, produced by thermal or surface ionisation, or by electrons emitted from high voltage elements in the system; and the high-Z attenuator foils may therefore still be required.

This experimental arrangement would be applicable principally to the detection of positively-charged quarks, since negatively-charged quarks are most likely to be bound to the high-Z nuclei removed by the attenuator foil. Even for positive charge, it will be necessary to run with both signs of accelerating voltage, since the quarks may be released in the form of negatively-charged quark-plus-electron atoms (binding energies 1.5 eV for Z = 1/3, 6.0 eV for Z = 2/3).

The overall detection efficiency will be comparable to that of the charge +1 experiment for masses up to about 100 GeV since, although the secondary electron coefficient is lower for $Z < 1$, this is compensated by the reduced angular scattering and the now 100% 'ionisation efficiency' for all fractionally charged particles evaporated from the material. Above 100 GeV, the reduced secondary electron efficiency becomes dominant and it will be necessary to utilise additional foil surfaces, add supplementary (eg. solid state) detectors, or increase accelerating voltage, to maintain an acceptable sensitivity in the high mass region.

It may also be noted that, in principle, the apparatus is also suitable for the detection of quarks of very low mass (ie. < 1 GeV) which would give rise to events to the left of the deuterium region in Fig. 5. In this case the

magnetic separation stage would be modified to remove all masses greater than a specified value, say 1 GeV.

We are at present developing the preceding ideas to search for fractionally-charged particles in niobium samples at a sensitivity level equivalent to that obtained in the Stanford levitation experiments[8].

B. Anomalous Nuclei

Stable, heavy, low-Z particles bound to ordinary nuclei[9], or other types of quark- nucleon complex[10] would result in high-Z nuclear systems with anomalous mass values. For a sufficiently large mass difference, such nuclei could in principle be detected by the presence of distinctive large t_1 events in the time-of-flight spectrometer. The principal experimental difference is that the total foil thickness transversed must be reduced by about an order of magnitude to allow passage of the high-Z particles, ie. from the 100-150 $\mu g/cm^2$ used in the low-Z experiments to <20 $\mu g/cm^2$ (at 120 kV accelerating voltage). This could, for example, be achieved in our present system by using two 5-10 $\mu g/cm^2$ time-of-flight foils, collecting electrons from the front face of the third foil, and eliminating the attenuator foil. Since searches for anomalous nuclei involve principally the mass range above 60-100 GeV, where the background of normal ions is very small, the absence of an attenuator foil should not prove a serious problem. Nevertheless it would clearly be advantageous to use a higher accelerating voltage, to increase the range of the high-Z nuclei and provide greater flexibility in the choice of thickness and number of foils.

Extraction of the atoms containing anomalous nuclei will in general require evaporation of the source material. In the case of non-integral Z (fractionally-charged quarks attached to nuclei) the resulting atoms will be already charged and may be either positive or negative, although surface ionisation is likely to remove the weakly bound additional electron to favour the positively-charged state, so acceleration of positive ions should in general be sufficient. Alternatively the source material may be ionised to ensure a positively-charged state, and this also covers the case of abnormal nuclei with integral Z.

More detailed studies of the problem of detecting anomalous high-Z states are in progress.

REFERENCES

1. P F Smith, J R J Bennett, Nucl. Phys. B149, 525 (1979)

2. This figure is misprinted as 1.2×10^5 in Table 1 of Ref. 1

3. The application of the Biegeleisen isotopic substitution theory to heavy hydrogen is discussed by P F Smith, A H Spurway, Rutherford Laboratory Report RL-73-023 (1973)

4. J D Lewin, Rutherford Laboratory Report RL-77-128/A (1977)

5. O B Firsov, Sov. Phys. JETP 9, 1076 (1959). We assume the energy threshold appropriate to electron emission from a solid surface to be the work function of the surface, rather than the ionisation potential. Several mechanisms contributing to electron emission are discussed in "Ion Bombardment of Solids" by G Carter and J S Colligon (Heinemann, 1968) chapter 3. More detailed calculations are in progress, which may modify the provisional figures in column D of table 1.

6. S Wolfram, Phys. Lett. 82B, 65 (1979)
   N Isgur, S Wolfram, Phys. Rev. D19, 234 (1979)

7. Jade collaboration Z. Phys C 6, 295-302 (1980)

8. G S LaRue, J D Phillips, W M Fairbank, Phys. Rev. Letters 46, 967 (1981)

9. R N Cahn, S L Glashow, LBL preprint 12010 (1980)

10. A de Rujula, R C Giles, R L Jaffe, Phys. Rev. D17, 285 (1978)
    D A Dicus, V L Teplitz, Phys. Rev. Letters, 44, 218 (1980)

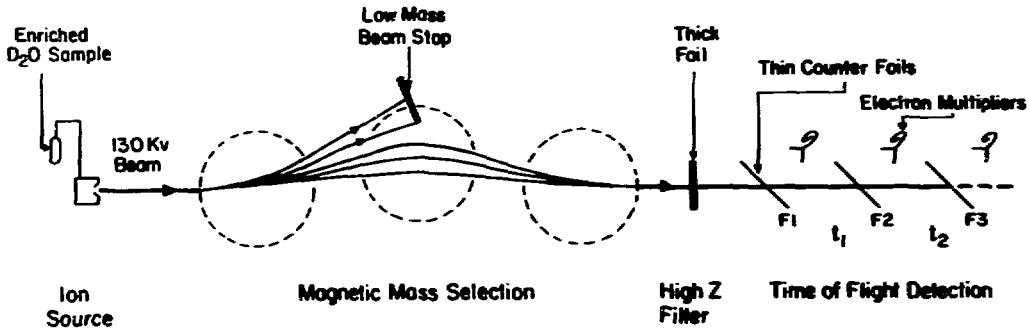

Fig 1 Principal components of time-of-flight spectrometer

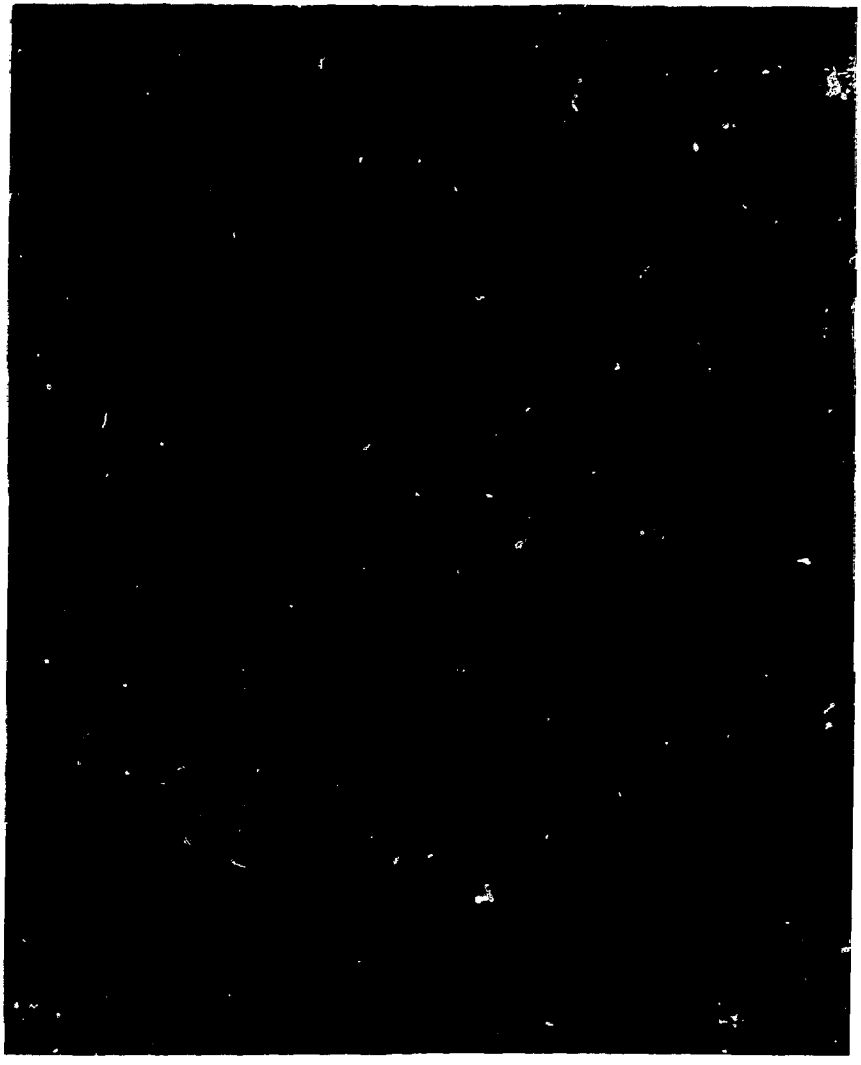

Fig 2 General view of spectrometer.

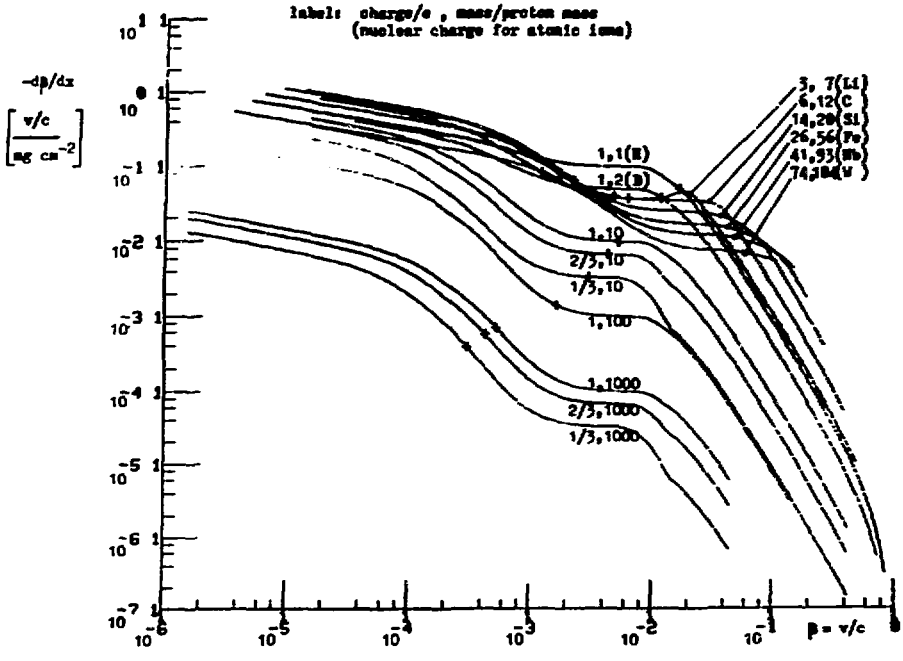

Fig 3 Computed dβ/dx in carbon foils (x = density x thickness, β = v/c) for atomic ions, protons, deuterons, and low-Z heavy particles. The crosses correspond to acceleration of the particle (or singly charged atomic ion) through 130kV.

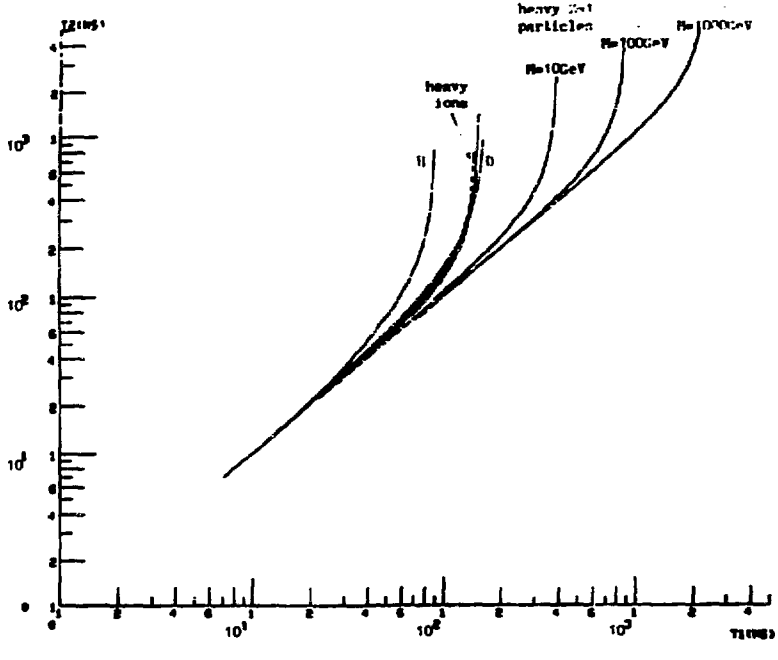

Fig 4 Computed $t_1 t_2$ curves for most probable energy loss in central foil, showing separation of hypothetical Z=1 heavy particles from normal ions.

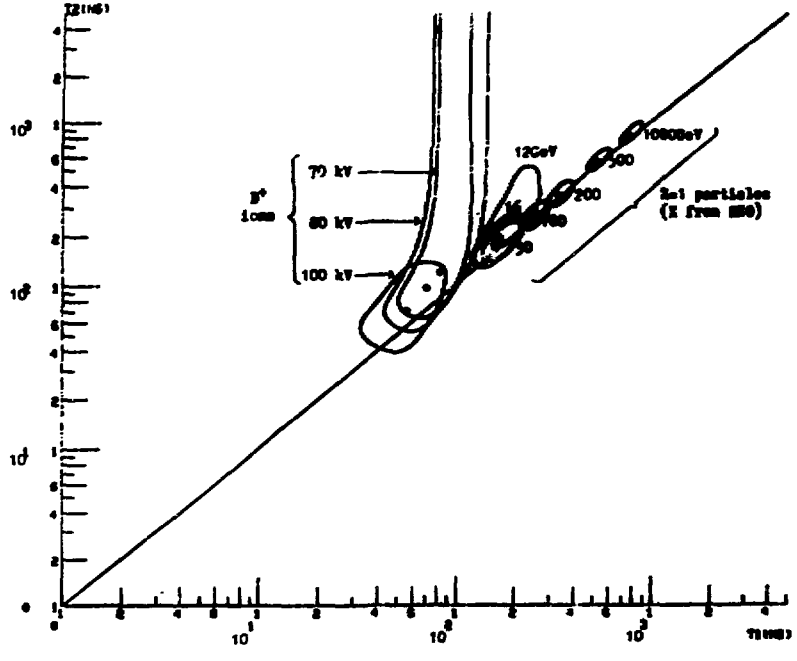

Fig 5 99% probability contours for (a) Z=1 particles, 12GeV<M<1000GeV
(b) background D^+ ions, various energies

(open circles show peak of probability distribution)

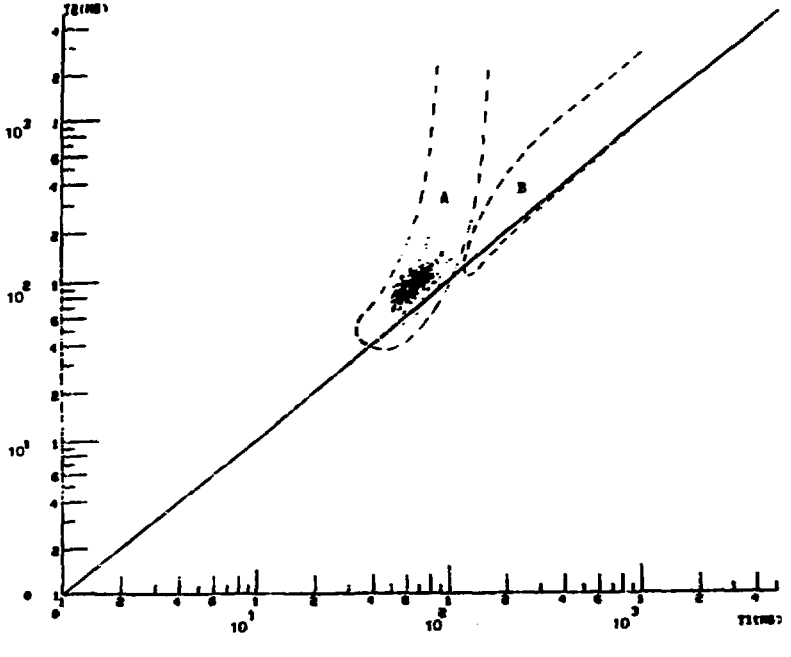

Fig 6 Results of 5 hour experimental run: 1500 background events are recorded, falling in predicted region A. No events are observed in heavy particle region B.

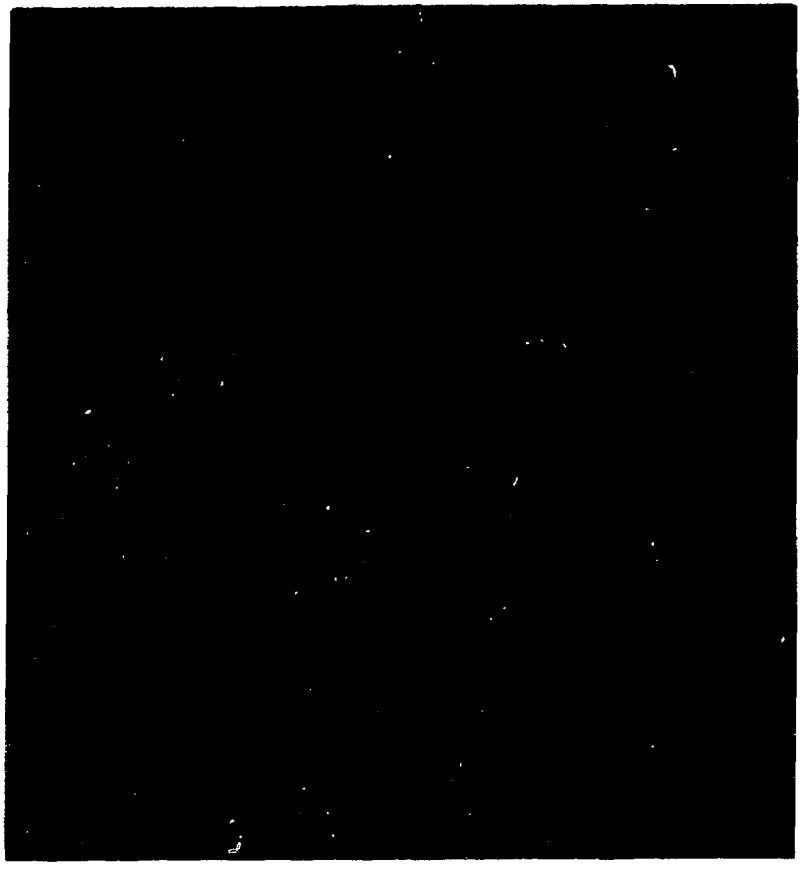

Fig 7 On-line display of events produced by 120kV test beam of deuterium + hydrogen. The axes are 100ns full scale and linear, with a lower cut-off at 20ns. The four clusters are identified in the text.

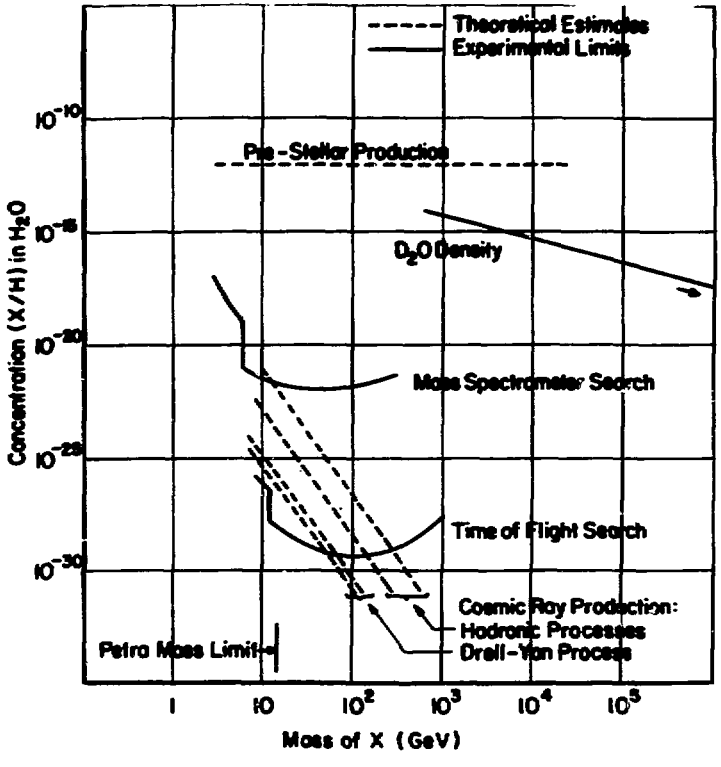

Fig 8 Concentration of anomalous hydrogen in natural water: summary of theoretical estimates and experimental limits as a function of mass.

APPLICATIONS OF AMS TO HYDROLOGY

Harold W. Bentley
Stanley N. Davis
University of Arizona

Introduction

The evaluation and management of water as a resource requires an understanding of the chemical, and geological interactions that water effects or undergoes in the hydrologic cycle (Fig. 1). Delivery of water to the land surface by precipitation, subsequent streamflow, circulation in surface waters and evapotranspiration, infiltration, recharge, movement of waters in the subsurface, and discharge are of interest. Also important are the quality of water, water's role in mineral dissolution, transport, and deposition, and the various water-related geotechnical problems of subsidence, tectonics, slope instability, and earth structures.

Mathematical modeling techniques are available and are being improved which describe these phenomena and predict future system behavior. Typically, however, models suffer from substantial uncertainties due to insufficient data. Refinement, calibration, and verification of hydrologic models require expansion of the data base. Examination of chemical constituents of water which act as tracers can often supply the needed information. Unfortunately, few tracers are available which are both mobile and chemically stable. Several long-lived radioisotopic hydrologic tracers exist, however, which have received little attention in hydrologic studies to date because of low concentration, low specific activity, or sample size limitations. Recent development of ultra-sensitive accelerator mass spectrometry techniques (AMS) by Purser and others (1977), Nelson and others (1977), Bennett and others (1978), Muller and others (1978), Raisbeck and others (1978) is now expected to provide access to many of these tracers.

Table I presents long-lived isotopes of possible interest to hydrology which may also be amenable to AMS analysis. The following discussion of these isotopes and their possible applications is necessarily speculative. The uses of ^{36}Cl, for which data have recently been obtained, will be deferred to a later section of this

Table I. Long Lived Radioisotopes of Potential Use in Hydrology

Isotope	Half-life(years)	Source
^{14}C	5730	Cosmogenic neutrons $^{14}N(n,p)^{14}C$ Fission and secondary alpha neutrons
^{36}Cl	3.01×10^5	Cosmogenic spallation ^{40}Ar Neutron activation of ^{35}Cl, ^{36}Ar
^{39}Ar	265	Cosmogenic spallation Neutron activation on ^{39}K
^{41}Ca	8×10^4	Neutron activation of ^{40}Ca
^{81}Kr	1.75×10^5	Cosmogenic spallation on ^{83}kr, ^{84}Kr, ^{86}Kr
^{99}Tc	2.1×10^5	^{235}U, ^{238}U fission
^{129}I	1.7×10^7	^{235}U, ^{238}U fission

paper.

Specific Hydrologic Problems of Interest to AMS

1. Water Dating

Dating is an obvious hydrologic use of radioisotopes. Dating is feasible if isotopic input is known and geochemical complexities can be resolved. Decay of the isotope is then a function of the residence time of the water. Replacement rate of water resources can be estimated from water age. Velocities of ground water gained from dating are important in calibration of numerical models. Velocity is also an important parameter in assessing the movement of nuclear or chemical wastes through the subsurface.

The most commonly used isotope for water dating is ^{14}C. Fontes and Garnier (1979) review various approaches to modeling ^{14}C's complex geochemistry. The models, and therefore the accuracy of ^{14}C ground water dating, will be improved by carbon isotope analysis of samples from the unsaturated soil zone and from mineral surfaces along the flow path. These experiments require analysis of very small (milligram) samples.

There is currently great interest in evaluating ^{14}C content of brines found in a variety of geologic media. Crystalline rocks in Canada, Sweden, and the United States have been found to contain highly saline waters of uncertain origin. These brines are often depleted in inorganic carbon due to high pH or high calcium content. AMS's ability to handle samples that are orders of magnitude smaller than those required for conventional ^{14}C counting apparatus suggests its application in both of the above study areas.

AMS may be sensitive enough to double the range of ^{14}C dating. If not limited by in-situ production (Zito and others, 1980), (Alweis, 1981), ^{14}C ground-water dating can be extended from 50 to 100 thousand years. This extension is particularly important when ^{14}C dates are used to calibrate other age-dating methods for which 50,000 years is the lower limit. Here too the ability of AMS to measure small samples may contribute. Contamination of the usual large-volume water samples obtained for ^{14}C water analysis is a

difficult field problem which could be avoided by using the 1 liter samplers normally used for gas analysis in water.

Ground-water dating has already been accomplished for ^{39}Ar (Loosli and Oeschger, 1978) but involved large sample sizes and difficult collection techniques. Natural concentrations of ^{39}Ar are about $3x10^{3}$ atoms per liter. Successful AMS techniques would simplify experimental difficulties and contribute to use of the ^{39}Ar dating tool, which covers an age range of 50-2000 yrs. Important questions concerning possible subsurface ^{39}Ar production (Loosli and Oeschger, 1978, Zito, 1980, personal communication) and observed discrepancies between ^{14}C and ^{39}Ar ground-water dates (Loosli and Oeschger, 1978) could be investigated.

^{41}Ca has never been observed in natural systems. However, cosmogenic neutrons should produce low $^{41}Ca/Ca$ ratios of about 10^{-14} in natural water (Davis, 1981, Elmore, 1981, both personal communications). Previous ^{14}C studies have made available sophisticated geochemical models which could also be applied to ^{41}Ca data. ^{41}Ca data from selected ground-water systems should provide insight into the role played by calcium in carbonate geochemistry and a more detailed understanding of corrections to ^{14}C data. Information about the age of a water sample can be determined from the decay rate of the geochemically-corrected ^{41}Ca concentrations.

^{81}Kr is probably the ideal dating tool for very old ground waters. The $^{81}Kr/Kr$ atmospheric ratio of $5.9x10^{-13}$ (Oeschger, 1978) is expected to have been nearly constant for millions of years. No important subsurface sources of the unstable or stable isotopes have been identified. Changes in the subsurface ratio would therefore be due only to decay of ^{81}Kr as a function of the water's residence time. Unfortunately, accelerator mass spectrometers have not yet been able to analyze for ^{81}Kr. Imposing sampling problems also exist; the extraction of ten milliliters of Kr (STP) requires about one million liters of water. Obtaining this quantity from the low-permeability formations of interest without introducing atmospheric contamination would be extraordinarily difficult.

^{129}I may be useful in dating waters of extreme age, such as oil-field brines. Knowledge of historical flow patterns obtained from ages might be useful in the exploration for oil. Waters of very low iodide content could also be dated; the $^{129}I/I$ input ratio of about 10^{-12} (Edwards and Rey, 1968; Elmore and others, 1980) is calculated to double in about 25,000 years in waters of the Madison Limestone (Wyoming). Large increases in atmospheric ^{129}I from nuclear weapons testing and power plants over the last thirty years suggest its use as a tracer for very young waters.

^{129}I may provide information about the degree of hydrologic isolation and stability of salt domes, currently being considered as repositories for nuclear wastes (Fabryka-Martin, 1981). The Louann formation is the mother bed for Gulf Coast salt domes, and dates to the Jurassic period (about 150 million years ago). Halite is depleted in uranium; the original ^{129}I should have significantly decayed. ^{129}I-depleted waters found in the dome could possibly be identified as having been trapped since dome formation. Iodide exchange between the halite and infiltrating waters, however, might negate this hypothesis. In any case, a choice might be made between the possible sources of the water found in mine openings. These include formation water, juvenile waters from dehydration reactions, leakage from the surface through man-made openings, and leakage from adjacent aquifers. Each source is postulated to possess a characteristic $^{129}I/I$ ratio.

2. Assessment of Nuclear Waste Repositories

Sorption or ion-filtration mechanisms, matrix diffusion, and chemical precipitation are processes which slow the transport of nuclear wastes to the biosphere. Each of the geochemical parameters has been evaluated in the laboratory. However, duplication of a natural chemical environment in the laboratory is a questionable exercise. Moreover, scale effects are controversial and difficult to quantify. From laboratory experiments evaluation of the transport of radionuclides away from natural repositories, (i.e., uranium deposits) located in a variety of geochemical environments would provide a

rigorous test of present geochemical models. In some cases, the natural repositories have been "breached" by a geologically recent catastrophic event. Examples include the entry of brines through fractures, increase in Eh by weathering and exposure, and magmatic intrusions. Table II lists some long-lived radionuclides found in nuclear wastes. Each nuclide presents an interesting and timely analytical problem possibly amenable to solution by AMS techniques. A typical detection limit of interest is 10^4-10^5 atoms (N. Hubbard 1980, private communication).

Table II. Long-Lived Radioisotopes of Interest to Nuclear Waste Repository Studies

Isotope	Half-life (years)
^{79}Se	6.5×10^4
^{99}Tc	2.13×10^5
^{107}Pd	7.0×10^6
^{129}I	1.7×10^7
^{226}Ra	1.6×10^3
^{230}Th	7.7×10^4
^{234}U	2.44×10^5
^{236}U	2.34×10^9
^{238}U	4.47×10^9
^{237}Np	2.14×10^6
^{239}Pu	2.41×10^4
^{240}Pu	6.54×10^3
^{242}Pu	3.8×10^5
^{241}Am	4.32×10^2
^{243}Am	7.37×10^3

Monitoring for leaking nuclear wastes will increase in sensitivity as new analytical techniques become available. Background concentrations of most of the radioisotope constituents in Table II

are presently too small to measure. In the near future, before wastes are actually emplaced, it will be important to determine their background levels so that any measured concentration increases could be attributed to waste leakage.

3. Identification of sources

A third use of isotopic hydrologic tracers is the identification of the source of waters or of the solutes therein. ^{129}I has already been discussed as a potential identifier of halite dissolution. ^{36}Cl will be shown to have several applications in this area. Both ^{129}I and ^{99}Tc are postulated to be indicators of upgradient uranium deposition. Both isotopes are major uranium fission products, and both are mobile in ground water although ^{99}Tc retardation may be a function of reducing conditions. About 90% of commercial uranium ore exists as roll-front deposits, believed to result from hydrochemical processes. The typical deposit is found in confined sandstone aquifers and is precipitated on sand-particle surfaces. Soluble fission products would be expected to escape easily from the microcrystalline uranium deposit but not in general from the sand-grain matrix. Therefore, the efficiency and strength of a roll-front source would greatly exceed that of the minerals elsewhere in the aquifer. We calculate for instance, that ^{129}I should increase its concentration by three orders of magnitude in ground water traversing a typical uranium roll-front deposit. The down-gradient ^{129}I plume could be used to prospect for uranium. Reasonable sample volumes would probably require the addition of iodide carrier. AMS techniques are useful because of their ability to handle small samples quickly and with high sensitivity.

^{36}Cl as a Dating Tool and Environmental Tracer

Chloride is unreactive and is regarded as the least sorbed of ions. Natural levels of ^{36}Cl in ground water have been measured by

acceleration (Bentley, 1978; Elmore and others, 1979; Bentley and Davis, 1981). Because of chloride's simple geochemistry, interesting prospects arise for the use of ^{36}Cl as a dating tool and environmental tracer. If parameters controlling ^{36}Cl concentration in rain water can be quantified, ^{36}Cl concentrations in ground water will reflect physical rather than chemical influences, i.e., the effects of time, evapotranspiration, ion filtration, and mixing. In addition to age, differences in ^{36}Cl concentrations in a regional aquifer might reflect the effects of historical climatic conditions on the recharging waters. One could determine whether mechanisms involved in increasing Cl concentrations down-gradient were leakage from other aquifers or the concentrating effects of outward leakage through shales or clays. Where ion filtration is taking place, its effects could be quantified by a careful comparison of ^{36}Cl concentrations with those of other ground-water constituents. Although such studies have been performed in the laboratory (Coplen and Hanshaw, 1970; Kharaka and Berry, 1970), they have not yet been attempted in the field.

^{36}Cl results obtained from the Carrizo Sand Aquifer in southeastern Texas and the Fox Hills Basal Hell Creek Aquifer in North Dakota demonstrate possible uses of ^{36}Cl as a dating tool and environmental tracer and will be discussed below.

1. Theory of ^{36}Cl ground-water input. The likely ^{36}Cl content in ground water can be described in terms of a ratio of ^{36}Cl to total chloride (Bentley, 1978). Neglecting anthropogenic sources, average tropospheric concentrations of both chloride and ^{36}Cl should remain relatively constant at a particular geographic location. Atmospheric chloride is mainly of oceanic origin, thus low in ^{36}Cl (Lal, private communication), and varies exponentially with distance from the ocean; wind direction and orogenic effects are also important (Eriksson, 1960). ^{36}Cl is produced in the stratosphere and troposphere by cosmic-ray spallation on ^{40}Ar and neutron activation of ^{35}Cl and ^{36}Ar (Lal and Peters, 1967). Seasonally-affected mixing

produces a maximum ^{36}Cl concentration at 40° geomagnetic latitude (Fig. 2). Chloride and ^{36}Cl should both become associated with aerosols which are rapidly removed from the troposphere by rainfall and dry deposition with a mean residence time of about one week (Turekian and others, 1977). Thus, the fallout of ^{36}Cl atoms per m^2-yr (calculated from data in Lal and Peters, 1967) divided by Kg chloride/m^2-yr (from Eriksson, 1960) should be constant at any one location. Converting to units convenient to mass accelerometry, the $^{36}Cl/Cl$ ratio is written:

$$^{36}Cl/Cl\ (\times 10^{15}) = 5.89 \times 10^{-11} \frac{^{36}Cl\ atoms/m^2\text{-}yr}{Kg\ Cl/m^2\text{-}yr} \qquad (1)$$

Weathering of most rock minerals produces negligible chloride; the chloride content of shallow ground waters normally originates from rainfall and dry fallout. The $^{36}Cl/Cl$ ratio should therefore be that calculated from eq. 1 and should be independent of climate. Fig. 3 shows calculated $^{36}Cl/Cl$ ratio isopleths for the United States.

^{36}Cl has also been produced by neutron activation of oceanic ^{35}Cl by nuclear weapons testing. Fig. 4 (Bentley and others, in preparation) shows the ^{36}Cl fallout pulse calculated on the basis of a box model.

Pre-bomb $^{36}Cl/Cl$ input ratios

Table III contains data collected from shallow waters expected to be free from ^{36}Cl originating from nuclear weapons testing ^{14}C and/or tritium data were used to establish non-contamination from the bomb pulse in all cases. Predicted $^{36}Cl/Cl$ values were calculated with eq. (1). Chloride delivery to the Madrid basin was extrapolated from data taken in Scandanavia (Eriksson, 1960), where wind patterns and topography similar to those in northern Spain are found. Although considerable scatter exists in the data at any particular location, the agreement of mean values with predicted values is good. Due to dispersion, older waters would be expected to approach mean input values.

Non-meteorogenic sources of ground water ^{36}Cl

^{35}Cl has a large thermal-neutron cross-section of 38 barns. Subsurface neutrons are produced both from uranium fission and from α-capture reactions as a result of uranium and thorium decay. (Bentley, 1978) calculated that subsurface production of ^{36}Cl limits the range of water dating by this isotope to approximately one million years. Table IV (Bentley, 1978) shows neutron production and buildup of ^{36}Cl in various average rock types. For a particular aquifer, the measurement of neutron flux would be necessary if it were important to precisely quantify ^{36}Cl buildup.

In general, ^{36}Cl buildup in older ground waters is likely to be significant. Sources of chloride in the subsurface, from leakage, diffusion, or weathering reactions, carry in ^{36}Cl. If known, the contributions of these subsurface sources can be subtracted from and thus correct the observed ^{36}Cl value in order to determine the initial meteoric input value. Work is presently in progress to determine low-level neutron fluxes in the subsurface, calculate ^{36}Cl production, and obtain samples for comparison to calculated values.

Table III

^{36}CL IN PRE-NUCLEAR WEAPONS TESTING GROUND WATER.

	$^{36}Cl/Cl$ ($\times 10^{15}$)	$^{36}Cl/l$ ($\times 10^{-7}$)	Average $^{36}Cl/Cl$ ($\times 10^{15}$)	Predicted $^{36}Cl/Cl$ ($\times 10^{15}$)
S.E. ARIZONA				
St. David	400 ± 40	6		
Tucson Well	320 ± 50	6		
Monkey Springs	478 ± 19			
Tucson Well B-8	365 ± 18	11.7	364.5 ± 78	400
C-13	379 ± 22	9.6		
A-3'	245 ± 16	6.6		
MADRID BASIN				
535-7-b	231 ± 21	-	254 ± 36	
535-7-9	295 ± 12	-	254 ± 36	250
535-5-c	235 ± 7	-	254 ± 36	
S.E. TEXAS				
AT 68-51-803	32 ± 3	2.7	32 ± 3	30

Table III (continued)

	$^{36}Cl/Cl$ ($\times 10^{15}$)	$^{36}Cl/l$ ($\times 10^{-7}$)	Average $^{36}Cl/Cl$ ($\times 10^{15}$)	Predicted $^{36}Cl/Cl$ ($\times 10^{15}$)
S. ALBERTA				
M.R. 42	538	14.4	453 ± 111	-
M.R. 41	327	3.7	453 ± 111	560
M.R. 26	494	50.3	453 ± 111	-

Table IV Neutron Production Calculated for Typical Granite, Sandstone, Limestone, and Shale by the Methods of Feige, Oltman and Kastner (1968) and the Resultant Steady-State 36Cl/Cl ratios for <1000 mg/ℓ Chloride Groundwaters

Neutron Production of Various Rock Types

Rock Type	U (ppm)	Th (ppm)	Natural fission neutron/kg-yr	u-α neutron/ kg-yr	Th-α neutron/ kg-yr
Granite	2.8	11	1,306	6,776	7,755
Sandstone	1.0	3.9	467	935	1,482
Shale	4.5	13	2,100	4,110	5,579
Limestone	2.2	0.2	1,027	1,408	57

Rock Type	Total neutrons/ kg/yr	Steady-State ^{36}Cl ratio ($\times 10^{-15}$) at t = 00
Granite	15,837	30.1
Sandstone	2,884	4.68
Shale	11,789	12.5
Limestone	2,482	10.9

In those few locations away from significant cosmogenic or radiogenic neutrons, chloride should lose its ^{36}Cl. Subsurface massive halite deposits older than a few million years should be depleted in ^{36}Cl as should ocean water. Two samples from Texas salt mines (provided by C. Kreitler), ocean water (provided by V. T. Bowen), and commercial reagent-grade salt have all shown $^{36}Cl/Cl$ ratios less than

1×10^{-15}. This value is the present tandem accelerator background level and is significantly less than the saturation $^{36}Cl/Cl$ ratios shown in Table IV. The presence of $^{36}Cl/Cl$ ratios lower than these saturated values then might be an indication of chloride coming from salt dome dissolution or salt water intrusion.

Velocity and mixing of a halite dissolution plume could be determined from its ^{36}Cl buildup, as might movement of waters between lithologies showing a significant contrast in neutron flux.

$^{36}Cl/Cl$ ratios of mineral (non-mobile) chloride should be useful in determining average neutron fluxes. Thus, the velocity of a uranium roll-front deposit or the levels of neutrons in deep mines (of interest in several physics experiments) should be ascertainable from mineral $^{36}Cl/Cl$ values.

Ocean basalts are low in uranium and thorium, as is ocean water. Sea bed sediments contain about 3 mg/kg uranium and 10 mg/kg thorium. If ocean water in the sediments were static, its $^{36}Cl/Cl$ ratio would exceed that of the overlying water or underlying basalt by more than an order of magnitude. Flow through the sea bed, which is being studied as a potential nuclear waste repository, would distort the $^{36}Cl/Cl$ ratio. Analysis of ^{36}Cl in deep ocean cores should enable the question of vertical flow to be answered.

We are presently investigating steady-state saturation $^{36}Cl/Cl$ by tandem analysis and measurement of subsurface neutron fluxes.

^{36}Cl concentration in "well-understood" aquifers

^{36}Cl results have been obtained from two regional aquifers which were selected for their "simple" hydrogeology. Analysis of these data will be based on the foregoing discussion.

1. The Carrizo Sand Aquifer.

The Carrizo Aquifer outcrops in an extensive belt five to twelve kilometers wide. In the study area (Fig. 5), the outcrop is about 200 km northwest of the coastline, toward which the formations dip at about 25 meters per kilometer. The Carrizo is composed almost

entirely of sand which unconformably overlies shale, sand, and clay of the Eocene Willcox group. Flow in the Carrizo is in the direction of dip; the aquifer is controlled by leakage through overlying Reklaw and Queen City formations, composed of shale and sand. A saline no-flow boundary can be found about 100 km down-dip. Fig. 6 shows the unusual isochlors, which are generally perpendicular to flow. These isochlors were based on chloride data points from only those wells which exhibited little chemical change over an extended sampling period. ^{36}Cl sampling points are represented on the figure as triangles. Age of Carrizo waters in the study area has been estimated by a three-dimensional finite difference model (Brinkman, 1981) and 95% confidence limits on ages are shown in Fig. 5. These show fairly good agreement with ^{14}C ages (Reardon and White, 1967).

$^{36}Cl/Cl$ values, are plotted against hydrodynamic ages taken from ^{14}C results where possible and from model results (Fig. 7). The "modern" sample collected in the recharging outcrop shows the highest $^{36}Cl/Cl$ ratio, probably due to ^{36}Cl fallout from nuclear weapons testing. The remainder of the data, which according to theory in the previous discussion should be nearly constant at this time scale, show a distressing curvature. On the assumption that "dead" chloride had entered the aquifer and distorted $^{36}Cl/Cl$ ratios, the ^{36}Cl/liter input was replotted on the same time scale (Fig. 8). The "modern" post-bomb ^{36}Cl/liter value stands out, but a smooth increase in pre-bomb ^{36}Cl with time is observed for the other samples. This increase could represent variable ^{36}Cl input to the aquifer, which could occur due to climate-induced changes in recharge, to changes in cosmogenic ^{36}Cl production, or to induced upward migration of old water containing dead chloride from lower aquifers. The first hypothesis is possible, although 60,000 years B. P. represents an interglacial period with temperatures similar to today. The second is unlikely; cosmogenic ^{36}Cl production should vary by less than ten percent (S. Kline, private communication). The third is not demonstrated in the chemical sampling history.

A fourth reasonable possibility is concentration of the ^{36}Cl by ion filtration. The aquifer exhibits considerable upward leakage, and most of the overlying Reklaw is buried deeper than the 500 meters (Berry, 1969) thought necessary for clay compaction sufficient to cause ion filtration. Assuming that ion filtration were responsible for ^{36}Cl increases, ^{36}Cl input concentration were constant with time, and no subsurface sources of chloride exist, then observed chloride concentrations can be converted to chloride concentrations that existed at recharge. Fig. 9 was constructed on the basis of these assumptions.

Part a of the figure is the chloride cross-section AB from Fig. 6. Part b is that same profile corrected for the effect of presumed ion filtration by assumption of constant ^{36}Cl input. The intriguing part of the figure is part c, the sea level relative to present, which shows strong similarities to part b. Chloride content of rainfall is known to vary strongly near coastlines, falling off rapidly as distance to the coast increases. At the height of the Wisconsin Glaciation, the distance of the study area Carrizo outcrop from the coast is estimated to have been 160 km greater than the present-day 200 km. Downdip variation of chloride in the Carrizo may well be a function of previous ocean water levels.

The foregoing data and discussion provide some support to the following statements:

1. Variation in chlorinity of aquifers near the coast may be a useful indication of water age.
2. Variations in ^{36}Cl concentration may indicate, perhaps even quantitatively, the concentration of solutes by ion filtration.
3. In the Carrizo, ^{36}Cl input concentration are likely to have been nearly constant for at least the last 60,000 years. If this assumption is true, then ^{36}Cl concentration rather than $^{36}Cl/Cl$ ratios may prove to be independent of climate and can be used to date very old ground waters.

The Fox Hills-Basal Hell Creek Aquifer

Hydrogeology and geochemistry of the Fox Hills-Basal Hell Creek Aquifer in southwestern North Dakota have been recently described (Thorstensen and others, 1979). Mack Croft, USGS, provided samples from locations shown in Fig. 10. The aquifer is composed of the Late Cretaceous Fox Hills Formation marine deltaic sandstone, grading upward into the fluvial and deltaic Hell Creek Formations. The Fox Hills conformably overlies the thick fissile Pierre Shale which in turn overlies the saline Dakota Sand Formation. Fig. 12 shows a cross section (from Thorstensen and others, 1979). Exposures include the Cedar Creek Anticline to the west and the Missouri River Valley to the east, in central North Dakota. Potentiometric data indicate that leakage, if present, is downward near the recharge area and upward from the Dakota as the Missouri River is approached.

^{36}Cl data are presented in Table V. Hydrodynamic ages were calculated from length (Δx) of flow lines, porosity (θ) of 3.4% and hydraulic conductivity (K) of 0.7 meters/day. Pre-pumping head data (h=head) were estimated from Fig. 10. From these parameters, age (Δt) is calculated by Darcy's Law.

$$\Delta t = \frac{\theta(\Delta x)^2}{K\Delta h} \qquad (2)$$

Instead of ratios, ^{36}Cl concentrations were utilized because a significant amount of chloride leaks into the aquifer from the Pierce Shale at the "transition zone", about one-third of the distance across the aquifer system. $^{36}Cl/Cl$ ratio data could therefore not be utilized directly. Fig. 12 shows $^{36}Cl/\ell$ plotted versus Darcy Law age. These data are encouraging but have not been corrected for ^{36}Cl carried into the aquifer by the chloride leakage.

Table IV - ^{36}Cl data - Carrizo Sand Aquifer

Well	$^{36}Cl/Cl$ ($x10^{15}$)	Cl^-(mg/ℓ)	$^{36}Cl/ℓ$($x10^{-7}$)
AL68-51-803	90 ± 9	129.1	20 ± 2
AL68-59-504	32 ± 3	52.0	2.9 ± .2
AL78-05-104	64 ± 6	32.5	3.5 ± .4
AL78-12-201	80 ± 8	40.4	5.3 ± .6
SU78-36-201	59 ± 6	72.9	7.3 ± .7
SU78-51-201	18 ± 2	233.3	7.1 ± .7

Table V - ^{36}Cl data - Fox Hills Basal Hell Creek Aquifer

Well	$^{36}Cl/Cl$ ($x10^{15}$)	Cl^-(mg/ℓ)	$^{36}Cl/ℓ$($x10^{-7}$)
Bowman 131-102-14AAB	262 ± 9	42	18.7 ± .6
Medora Fish Pond 140-102-22DCD	150 ± 8	54.5	13.8 ± .7
Mandan 139-081-09AAA1	10 ± 2	505.2	9.9 ± 2
Hettinger	31.4 ± 3	183.5	9.8 ± 1
Carson 136-87-36AAB	19 ± 4	255.9	8.3 ± 1.7
Cartwright Mackenzie 151-04-0YAAA	22 ± 3	185.6	6.9 ± 1.0
Shultz 144-85-1DCCA	11.9 ± 3	279	5.6 ± 1.4
Starston #400	7.1 ± 2.3	230.7	2.8 ± 0.7

Chloride in equilibrium with a standard shale neutron flux is calculated to contain 2.13 x 10^5 ^{36}Cl atoms/mg Cl. 30 mgCl/ℓ was the assumed input, to the recharge zone, and excess chloride above that value was assumed to have leaked in from or through the underlying Pierre Shale.

Corrected $^{36}Cl/ℓ$ are plotted against Darcy Law Age in Fig. 13. Clearly these corrected values drop to zero about halfway down the aquifer. Thorstensen and others (1979) discussed implications of their geochemical data on the flow of this system. Two flow patterns were proposed:

1) Less than 5% leakage from the Pierre Shale or below, a model supported by mass balance arguments using chloride content of the Dakota Sand, Pierre Shale, and Fox Hills-Basal Hell Creek.

2) Massive leakage, perhaps enough that Dakota water supplements the Fox Hills-Basal Hell Creek, a conclusion supported by excess He and, though not explicitly mentioned, excess I.

The ^{36}Cl data in Fig. 13 clearly supports the latter model; meteoric ^{36}Cl has apparently disappeared from the distal half of the aquifer system. For this much leakage to occur without substantially increasing chloride content of the Fox Hills, an ion rejection mechanism must be postulated. The data, then, are consistent with the Pierre Sahle acting as an ion filtration membrane, with a rejection efficiency for chloride about 95%. The water resource, if this model is valid, is much more extensive than previously thought.

The above data and discussions are consistent with the following:

1) mixing of recent ground water, tagged with ^{36}Cl, with older waters can in principle be quantified by determination of ^{36}Cl content of the older waters and of the mixture.

2) determination of ^{36}Cl brought in by chloride from weathering, diffusion, or convection should enable the conversion of observed ^{36}Cl concentrations to meteoric - origin ^{36}Cl concentrations. These "corrected" ^{36}Cl concentrations would vary with residence time in the aquifer and might allow dating of very old ground waters.

3) establishing proper subsurface neutron-flux saturated levels of ^{36}Cl should enable detection of chloride sources which are depleted in ^{36}Cl.

^{36}Cl Originating from Nuclear Weapons Testing

The ^{36}Cl fallout pulse is calculated to have peaked in 1956, to have exceeded natural fallout levels by about four orders of magnitude, and to have dropped back to natural levels (Fig. 4) (Bentley and others, manuscript in preparation).

Experiments are ongoing to identify the time and dimensions of the pulse in shallow groundwater and in glacial ice from Greenland. Possible application of the fallout ^{36}Cl to hydrology can be briefly summarized:

1) Ground-water flow rates and aquifer parameters, possibly even dispersion, may be calculated from a ^{36}Cl profile. Toxic waste movement in the same aquifer would then be predictable.

2) Movement of long-lived radionuclides in the natural system could be compared with that of chloride, which is not retarded by sorption.

3) Recharge rates in arid areas could be obtained by determining the velocity of the ^{36}Cl and the water content of the unsaturated zone by conventional techniques.

Tritium has been used in the past for similar purposes but suffers from possible sorption, a very broad pulse, and a short half-life of 12.7 years which hampers interpretation.

^{36}Cl as an Artificial Hydrologic Tracer

^{36}Cl is inexpensive, nonsorbed, and refractory. The maximum permissable concentration (MPC) of 8×10^{-5} μCi/ml exceeds natural ground-water levels by a factor of 10^{8}. As detection costs decrease and accelerator techniques become more widely used, the use of ^{36}Cl to evaluate hydrologic parameters will be feasible. However, political and legal barriers constrain use of any radioisotope as a hydrologic tracer. These barriers may be overridden when the radioisotope is added to toxic wastes.

^{36}Cl as a Monitoring Tracer

Subsurface disposal of wastes now requires major efforts in design, construction, and monitoring. The addition of a hydrologic tracer to wastes is a convenient way to simplify and quantify the monitoring process and give early warning of waste leakage.

Tracing wastes is a non-trivial exercise, however, because a hostile and complicated chemical environment often degrades tracers or influences their transport properties. ^{36}Cl should be neither sorbed nor degraded and should thus give early warning of waste leakage.

In the case of nuclear wastes, enough ^{36}Cl is usually present to serve as a tracer. Existing repositories could be better evaluated by investigation of ^{36}Cl in their ground waters. Future repository monitoring efforts should be designed to use ^{36}Cl as a tracer by measuring its concentrations in the wastes and in the surrounding ground water.

Conclusions

There are many applications of accelerator mass spectrometry to hydrology, the above discussion includes only a few. This is not surprising; increases in analytical sensitivity lead to advances in many fields, and AMS promises increases of orders of magnitude.

Because ^{36}Cl is now detectable by AMS techniques, it shows excellent promise as a tracer useful for dating old and young waters and for identification of source and mixing, and for monitoring leakage. In the near future, ^{36}Cl should become one of the principal weapons in the isotope hydrologist's arsenal.

Many have contributed to the above ^{36}Cl research. We would particularly like to thank Dave Elmore and Harry Gove from the University of Rochester and Ted Litherland, Rolph Beukens, and Linus Kilius from the University of Toronto for their contributions and encouragements in all phases of the work. Seth Gifford, Gerald Swannik and Tom LaMarche of the University of Arizona and Fred Phillips, now at the New Mexico Institute of Mining and Technology have contributed to research and discussion of ^{36}Cl in hydrology. Charles Kreitler, Texas Economics Board of Geology, Mack Croft, U.S. Geological Survey, North Dakota, and Donald Whittamore, Kansas Geological Survey have contributed their time and counsel in field and experimental investigations.

This work was s[illegible]rted by the Office of Nuclear Waste Isolation, Contract Number E512-u.900.

REFERENCES

Alweis, S. J., Possible subsurface production of carbon-14 in groundwater. Unpublished Masters Thesis. University of Arizona. 1981.

Bennett, C. L., R. P. Beukens, M. R. Clover, D. Elmore, H. E. Gove, L. R. Kilius, A. E. Litherland, K. H. Purser. Science 201, 345. 1978.

Bennett, C. L., R. P. Beukens, M. R. Clover, H. E. Gove, R. B. Liebert, A. E. Litherland, W. E. Sondheim. Science 198, 508. 1977.

Bentley, H. W., Some comments on the sue of chlorine-36 for dating very old groundwater. In: Workshop on dating old groundwater, S. N. Davis, ed., Subcontract 19Y-55412v, report to Union Carbide Corp., Nuclear Division, by Department of Hydrology and Water Resources, University of Arizona, 138 pp. 1978.

Brinkman, J., Unpublished Masters Thesis, University of Arizona Department of Hydrology and Water Resources. 1981.

Croft, M. G., The geochemistry of the Fox Hills-Basal Hell Creek Aquifer in southwestern North Dakota and northwestern South Dakota. Water Resources Research, 15 (6), 1479-1498. 1979.

Davis, S. N. and H. W. Bentley, Dating Groundwater--a Short Review. ACS. 1981.

Edwards, R. R. and P. Rey, Terrestrial occurrence and distribution of iodine-129. U.S. Atomic Energy Commission Report No. NYO-3624-3, Carnegie-Mellon University, Pittsburgh, Pa, 30 pp. 1968.

Elmore, D., B. R. Fulton, M. R. Clover, J. R. Marsden, H. E. Gove, H. Naylor, K. H. Purser, L. R. Kilius, R. P. Beukens, A. E. Litherland. Analysis of ^{36}Cl in environmental water samples using an electrostatic accelerator. Nature 277, 22-25. 1979.

Eriksson, E., The yearly circulation of chloride and sulfur in nature, meteorological, geochemical, and pedological implications, Part II. Tellus 12 (1), 63-109. 1960.

Fabryka-Martin, J. Iodine-129 as a tool for dating groundwater: applications to salt dome studies. Draft report to workshop on Isotope Assessment of Nuclear Waste Repositories, University of Arizona, October 1981.

Feige, Y., B. G. Oltman, and J. Kastner, Production rates of neutrons in soils due to natural radioactivity. J. Geophys. Res. 73, 3135-3142. 1968.

Fontes, J. C. and J. M. Garnier, Determination of the initial ^{14}C activity of the total dissolved carbon, A review of the existing models and a new approach. Water Resour, Research 15 (2) 399-413. 1979.

Krey, R. W. and Krajewski, Comparison of atmospheric transport model calculations with observation of radioactive debris. J. Geophys. Res. 75, 2901-2008. 1970.

Lal, D. and B. Peters, Cosmic ray produced radioactivity on the earth. Hanbuch der Physik XLVI/2, 551-612. 1967.

Loosli, H. H., Oeschger, H., Argon-39, carbon-14 and krypton-85 measurements in groundwater samples, in: Isotope Hydrology, Internat. Atomic Energy Agency, Vienna, 2, p. 931-945. 1978.

Muller, R. A., E. J. Stephenson, T. S. Mast, Science. 1978. 347 see also: Proc. of the first Int. Conf. on Radiocarbon dating with Accelerators, H. E. Gove (ed) University of Rochester. 1978.

Nelson, E., R. G. Korteling, W. R. Scott, Science 198 506. 1977.

Pearson, F. J., Jr., White, D. E., Carbon-14 ages and flow rates of water in Carrizo Sand, Atascosa County, Texas, Water Resources Research, 3 (1), 251-261. 1967.

Purser, K. H., R. B. Liebert, A. E. Litherland, R. P. Beukens, H. E. Gove, C. L. Bennett, M. R. Clover, W. E. Sondheim. Revue de Physique Appliquee 12 1487. 1977.

Raisbeck, G. M., F. Yiou, M. Fruneau, J. M. Loiseaux, Science 202 215. 1978.

Turekian, K. K., Y. Nozaki, and L. K. Benninger, Geochemistry of atmospheric radon and radon products. Ann Rev Earth Planet Sci, 227-55. 1977.

Zander, I.; and Araskog, R., Nuclear explosions 1945-1972: Basic Data: FOA-4, Report A-4505-A. 1973.

Zito, R., Donahue, D. J., Davis, S. N., Bentley, H. W., Fritz, P., Possible subsurface production of carbon-14, Geophys. Research Lett., 7 (4), 235-238. 1980.

FIGURE CAPTIONS

Fig. 1: The hydrologic cycle, is a diagramatic cross-section showing circulation of water to, through, and out of the earth's surface. Tracer techniques, aided by AMS analysis, can be applied to studies of the effects of the circulation on water resources, contamination, geotechnical and geologic processes.

Fig. 2: Cosmogenic ^{36}Cl Fallout as a function of geomagnetic latitude. The curve was constituted from ^{35}S and ^{32}P data reported in Lal and Peters (1967) Seasonal variations are neglected.

Fig. 3: $^{36}Cl \times 10^{15}/Cl$ ratio isopleths constructed from Fig. 2 and from data in Eriksson (1960). Neglecting seasonal variations these are the predicted $^{36}Cl \times 10^{15}/Cl$ ratios in young waters uncontaminated by nuclear weapons testing.

Fig. 4: Predicted ^{36}Cl bomb pulse (modeled from published nuclear explosion data in Zander and Araskoz (1973) and Carter and Mozhiosi (1977)).

Fig. 5: Carizzo Aquifer study area in S.E. Texas. Triangles show locations of well sampled for ^{36}Cl. Hydrodynamic ages (in years) are those predicted by a finite difference numerical model (Brinkman, 1981).

Fig 6: Isochlors of the Carizzo study areas. The line AB is a cross-section shown in Fig. 10a. Values are in mgCl/liter.

Fig. 7: $^{36}Cl/Cl$ ratios in well water sampled in the Carizzo Aquifer, Texas. These are plotted versus estimated age of the water taken from ^{14}C results of Pearson and White (1967) and the numerical finite-difference model of Brinkman (1981).

Fig. 8: ^{36}Cl concentrations ($\times 10^{-7}$) are plotted against the same time scale as in Fig. 7. The solid curve is the postulated increase in concentration of chloride species since recharge by ion filtration processes.

Fig. 9: Three parameters are plotted against the same time scale as in Fig. 7. Part a is the chloride cross-section AB taken from Fig. 6 part b is the chloride cross-section AB corrected for hypothesized ion filtration (see Fig. 8) Part c is sea level over the same time period. Historical distance from the coast to the Carrizo study area outcrop is proportional to sea level over the depth range.

Fig. 10: Sample locations and study area represented on a map plan of the Fox Hills-Basal Hell Creek Aquifer, North Dakota. Equipotential lines are in feet above sea level.

Fig. 11: A cross-section of the Fox Hills-Basal Hell Creek Aquifer System (taken from Thorstenson and others (1980).

Fig. 12: ^{36}Cl atoms/liter ($x10^{-7}$) versus Darcy's Law Age in the Fox Hills-Basal Hell Creek Aquifer.

Fig. 13: Corrected ^{36}Cl atoms/liter ($x10^{-7}$) versus Darcy's Law Age in the Fox Hills-Basal Hell Creek Aquifer, North Dakota. The corrections were made by subtracting $2.13x10^{5}$ ^{36}Cl atoms for each mgCl/ℓ greater than 30 at the sampling point.

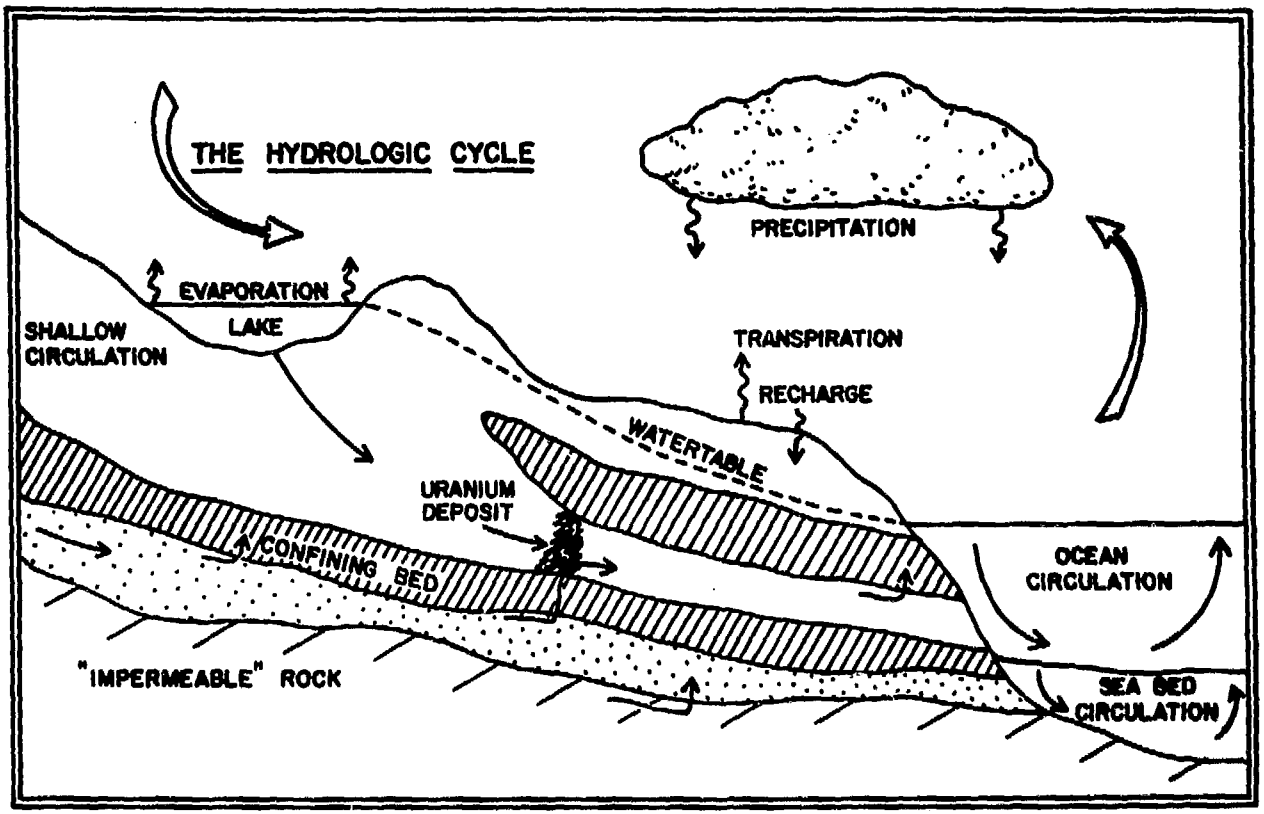

Figure 1. The Hydrologic Cycle

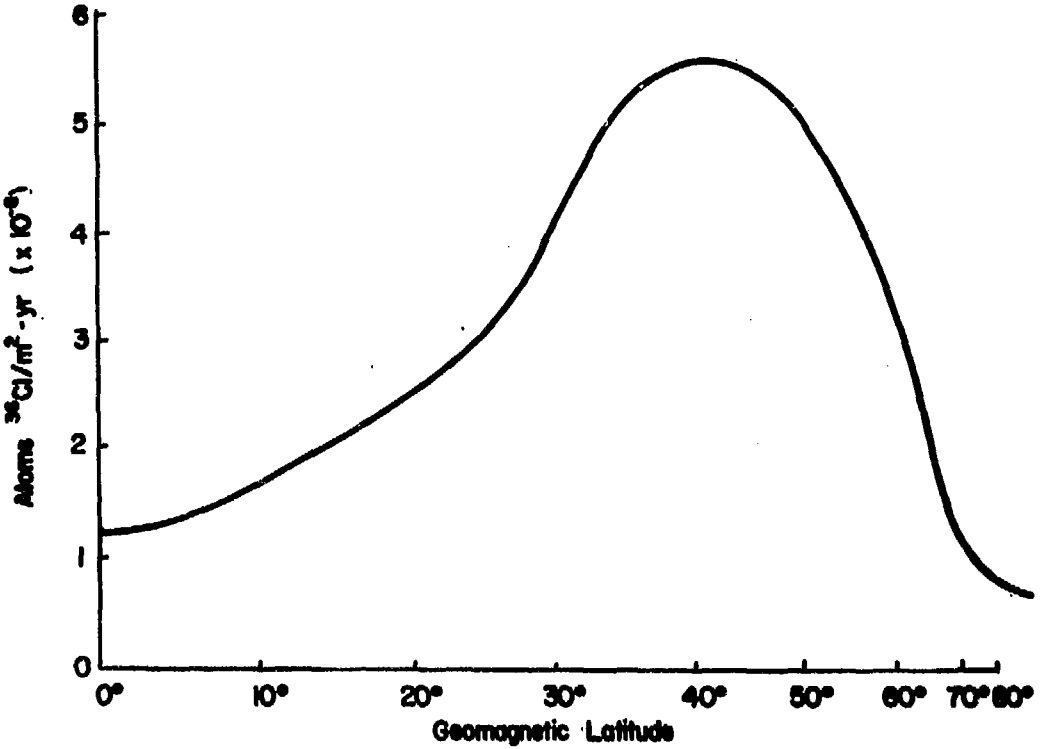

Fig. 2 Cosmogenic ^{36}Cl fallout as a function of geomagnetic latitude.

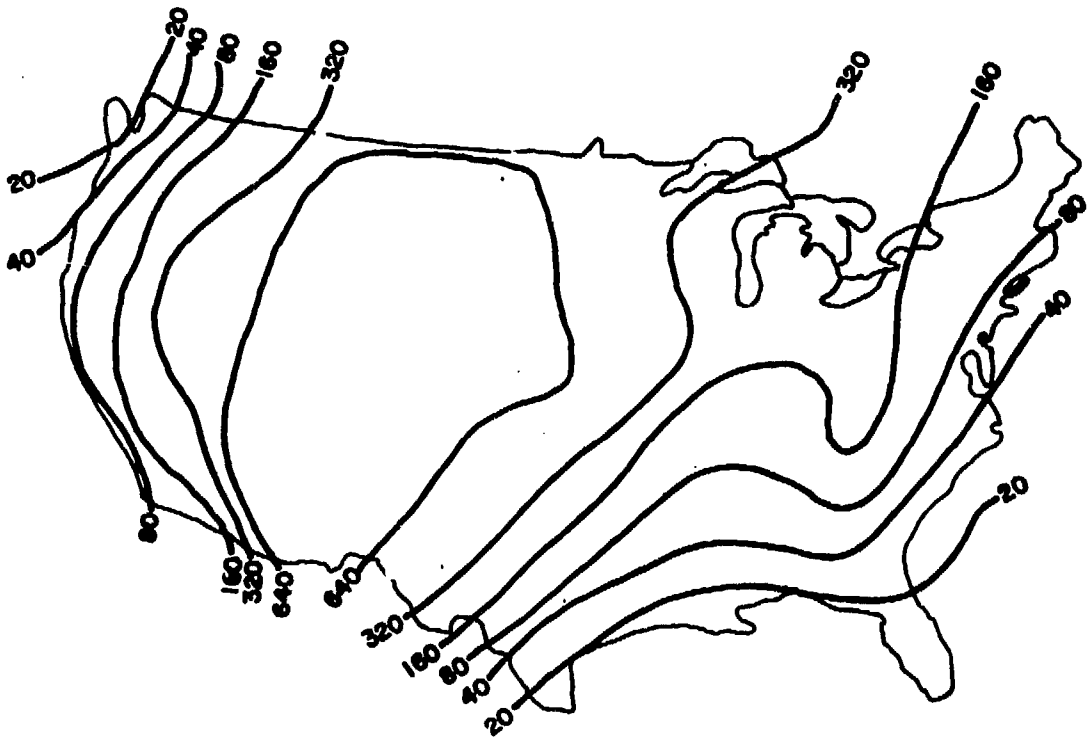

Fig. 3 Calculated $\frac{^{36}Cl \times 10^{15}}{Cl}$ Ratios in U.S. Pre-Bomb Ground Water

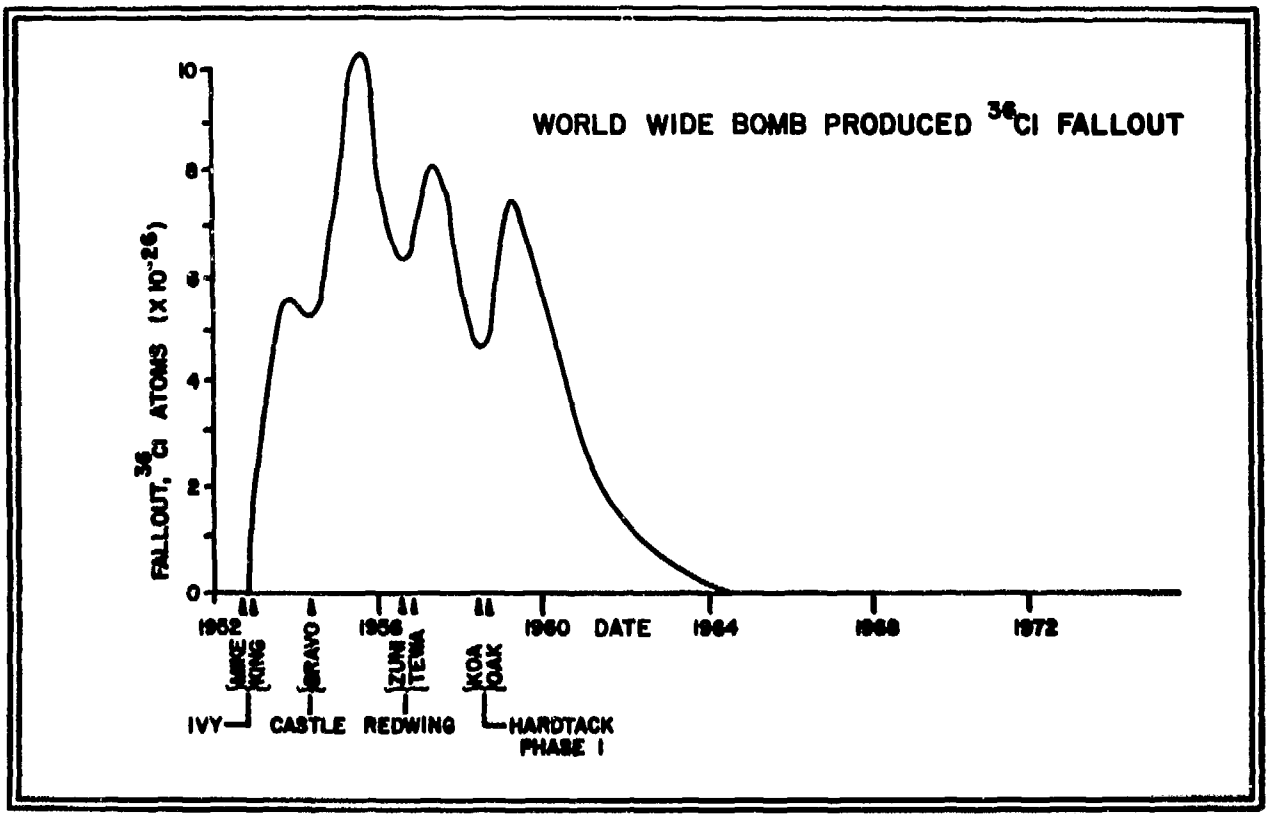

Fig. 4 Predicted ^{36}Cl fallout generated by nuclear weapons testing.

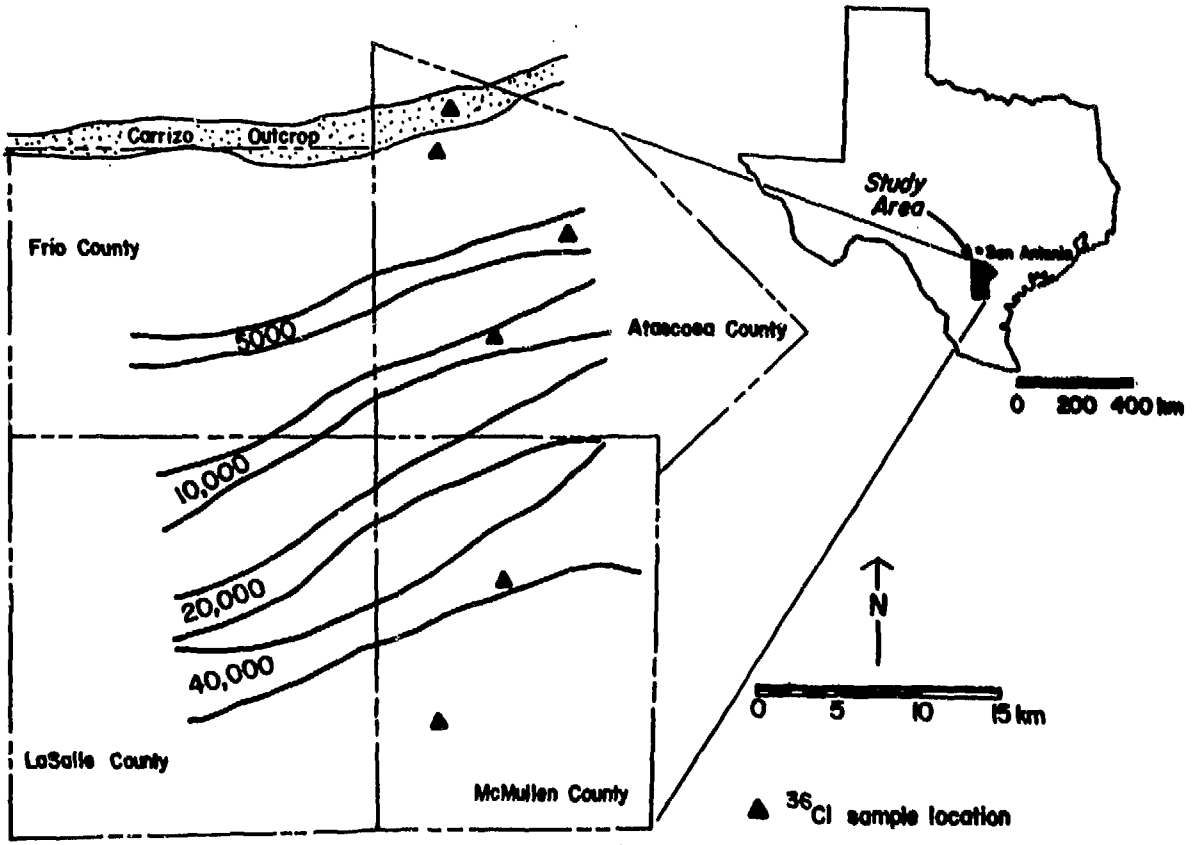

Fig. 5 Study area and calculated hydrodynamic ages, Carrizo Sand Aquifer, Texas

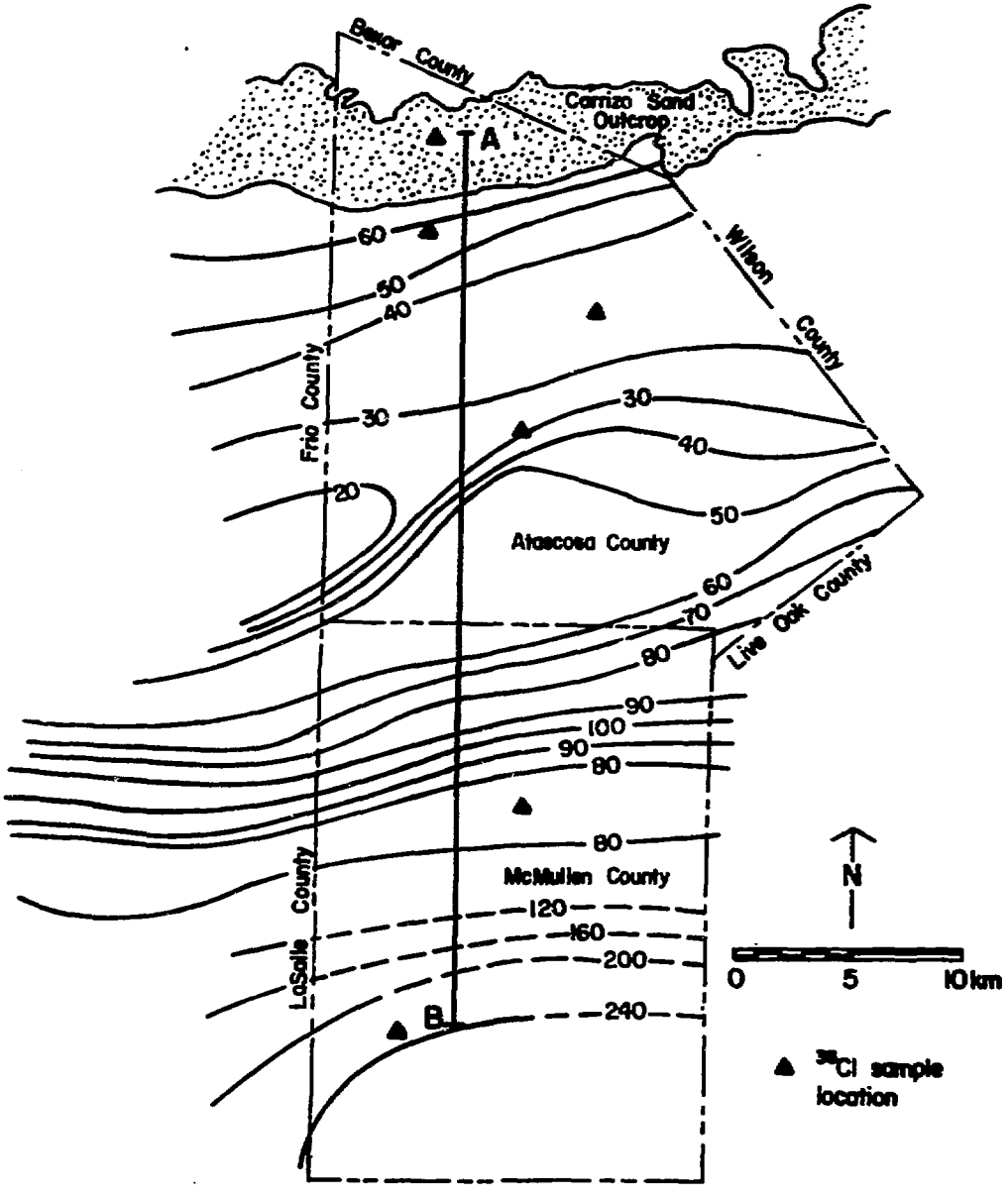

Fig. 6 Isochlors in the Carrizo study area.

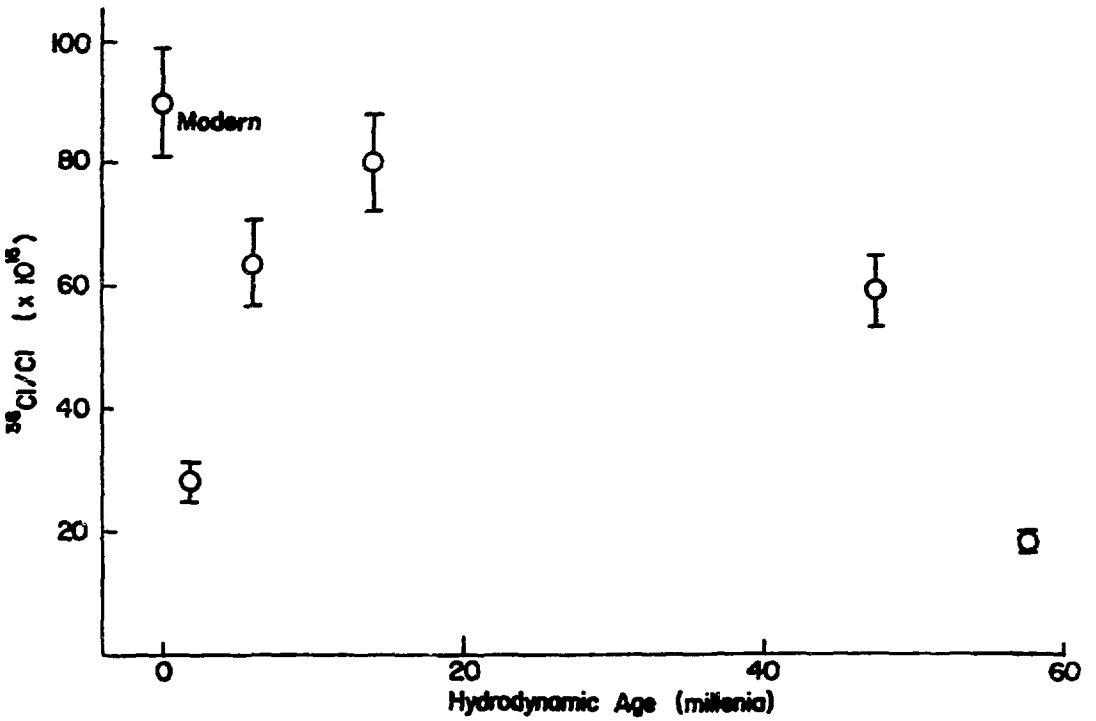

Fig. 7 $^{36}Clx10^{15}/Cl$ ratios in the Carizzo Sand Aquifer, Texas

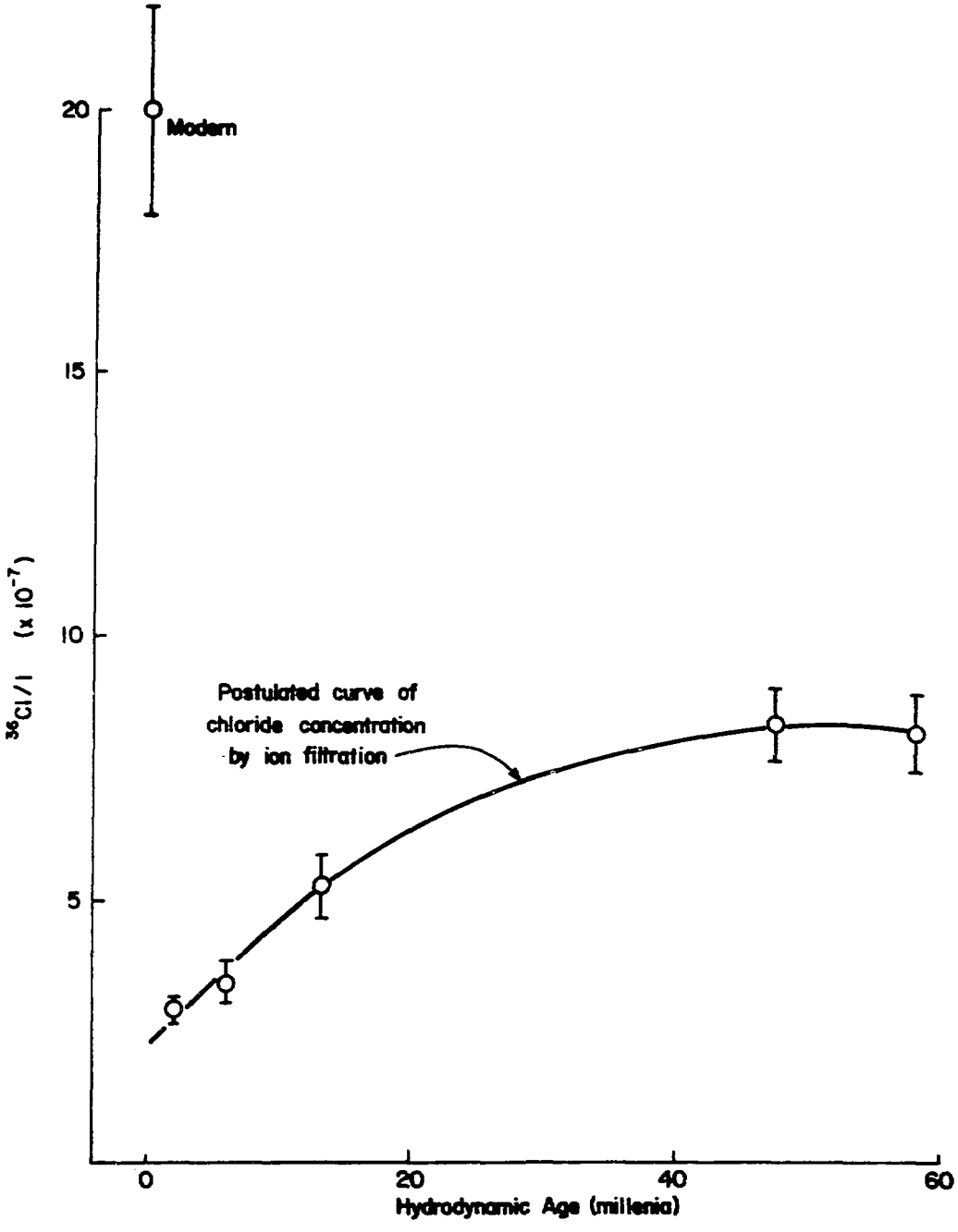

Fig. 8 ^{36}Cl concentrations versus estimated age, Carrizo Sand Aquifer, Texas

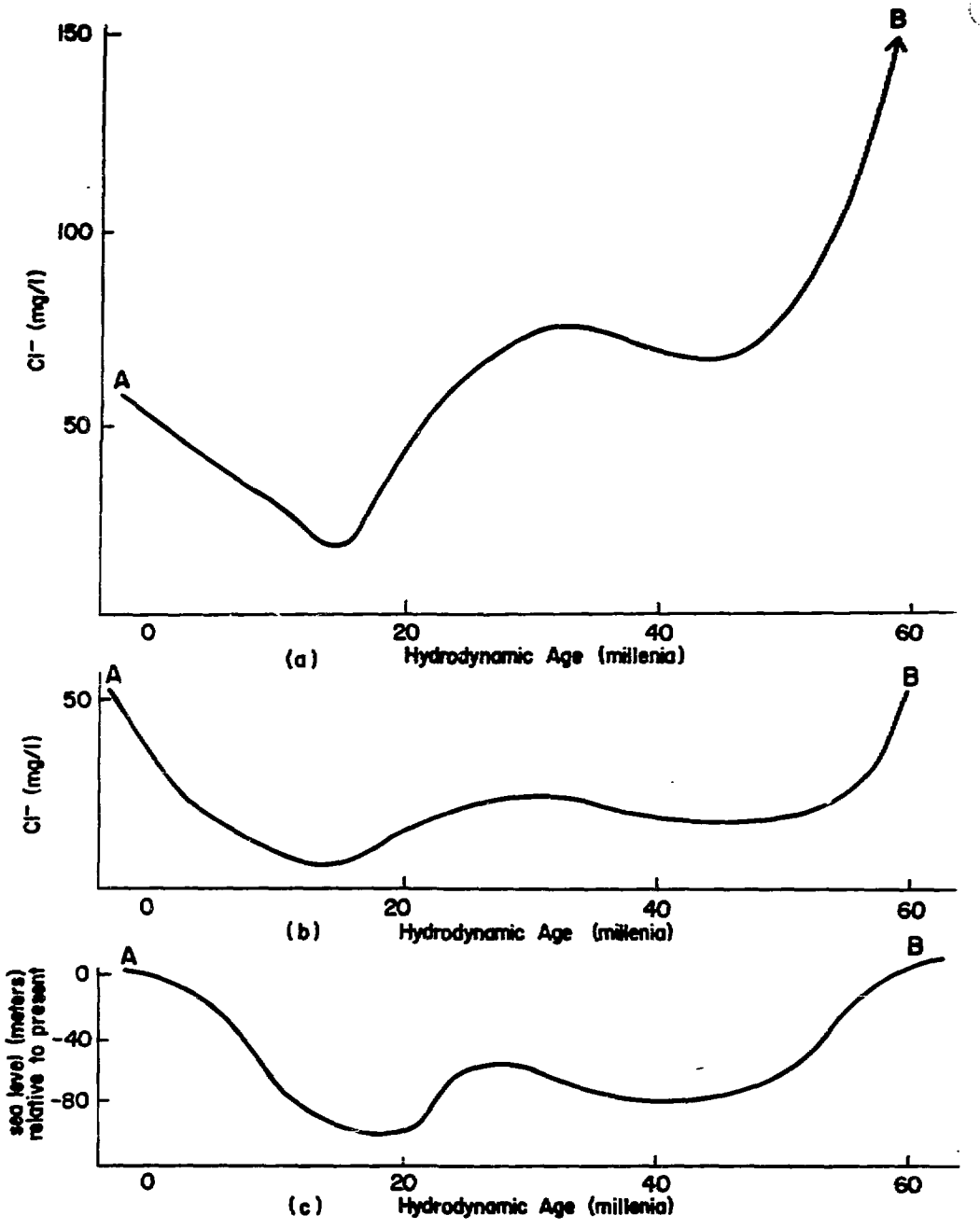

Fig. 9 Chloride concentrations/ocean level vs. time. (a) Chloride concentration cross section. (b) Corrected chloride concentration cross section. (c) Historical ocean water level.

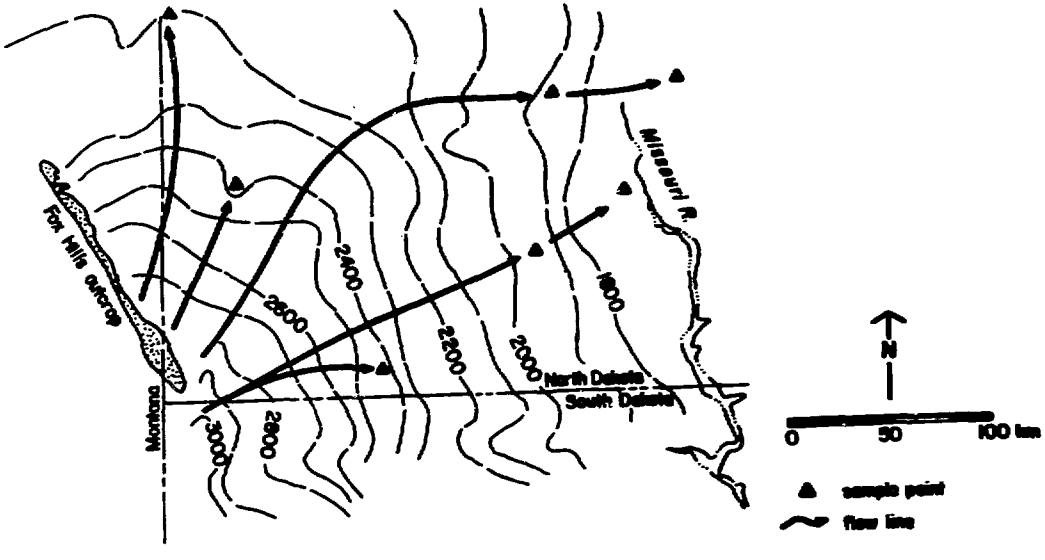

Fig. 10 Map view, ^{36}Cl sample locations, and equipotential lines, Fox Hills-Basal Creek Aquifer, North Dakota.

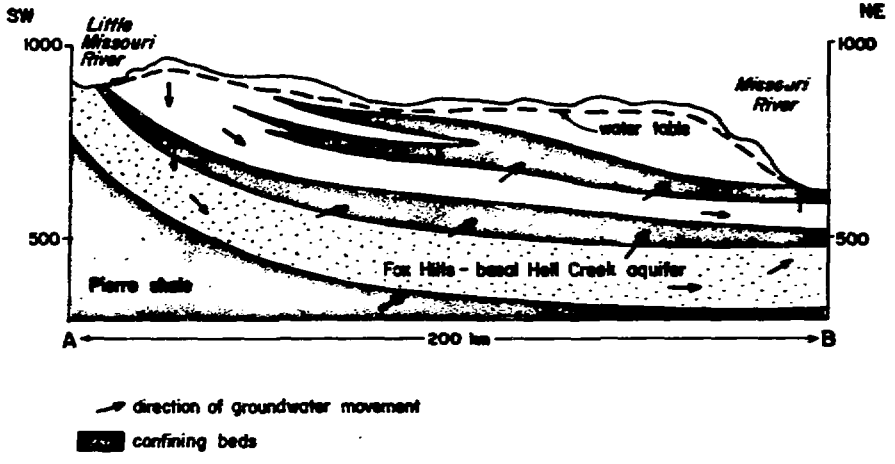

Fig. 11 Cross section. Fox Hills – basal Hell Creek aquifer

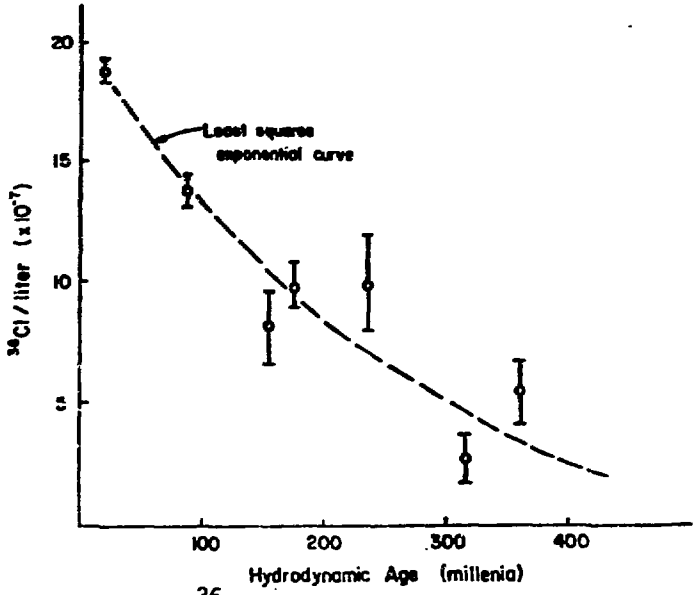

Fig. 12 ^{36}Cl concentrations in Fox Hills-Basal Hell Creek Aquifer, North Dakota

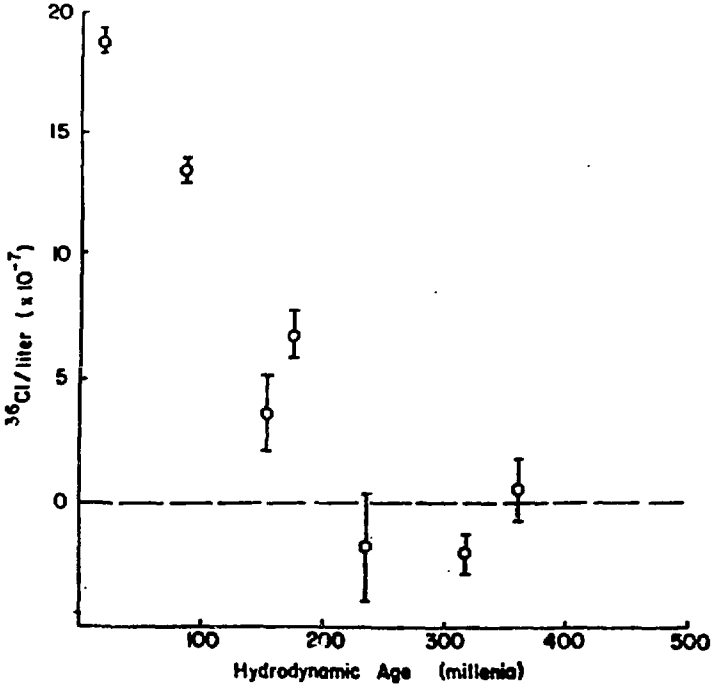

Fig. 13 ^{36}Cl concentrations vs. Darcy Age, corrected for ^{36}

^{10}Be IN THE ENVIRONMENT : SOME RECENT RESULTS AND THEIR APPLICATIONS

G.M. Raisbeck and F. Yiou
Laboratoire René Bernas, Centre de Spectrométrie Nucléaire et de Spectrométrie de Masse, F. 91406 Orsay.

M. Lieuvin, J.C. Ravel, M. Fruneau, J.M. Loiseaux
Institut des Sciences Nucléaires, F. 38026 Grenoble.

Using the Grenoble cyclotron, cosmogenic ^{10}Be has been measured in more than 100 environmental samples, including stratospheric and tropospheric air, precipitation, river water, ocean water, Antarctic ice, and lacustrine, inland sea, and deep sea, sediments. A summary of the results is given and some of their applications briefly mentioned.

At the first meeting on this subject, at Rochester, we presented the first quantitative results of ^{10}Be measurement by accelerator mass spectrometry, using the Grenoble cyclotron (1). Since that time our technique has evolved and improved significantly, as outlined in another paper in these proceedings. However, our main objective has been to determine ^{10}Be in actual geophysical samples, in order to understand its behaviour in the environment, and to begin to exploit its many potential applications. In Fig. 1 we show the pathway of ^{10}Be, from its initial formation in the atmosphere, through the "transient" reservoirs, such as precipitation, ocean water, rivers, and into its "permanent" reservoirs, such as polar ice cores, marine and lacustrine sediments. Our initial aim has been to make ^{10}Be measurements in as many different parts of this pathway as possible, and thus provide a solid base for further, more detailed, studies. To date, we have measured ^{10}Be in more than 100 environmental samples. Since most of these measurements are still unpublished, we thought it might be useful to summarize them here. While space limitations preclude any extensive discussion on the results, we do briefly comment on the most noteworthy points and, where appropriate, refer to other articles where certain aspects have been covered in more detail.

In Table 1 we show the ^{10}Be (and ^{7}Be) concentration in stratospheric and tropospheric air, as determined from measurements on air filters (2). One can notice the much larger concentration in the stratosphere, both because of a higher production rate there, and a longer residence time. We have discussed

how the ratio $^{10}Be/^{7}Be$ could be a very important tracer for movement of air masses, and in particular for transfer of stratospheric air into the troposphere (2). Such information could be important, for example, in deducing the sources of ozone at ground level. It will also be important for interpreting any ^{10}Be variations observed in polar ice cores.

We have previously reported an estimated ^{10}Be global production rate, based on the ^{10}Be deposited at Orsay for a period of one year (3). We now have made a similar measurement on a second sample collected over slightly more than one year. Making the same assumptions as in Ref (3), a global production rate has again been estimated, and both results are shown in Table 2. Although the actual deposition rate for the most recent measurement is within the experimental limits of the earlier result, the calculated global average production is about 25% less, in part because of a higher rainfall at Orsay during that period. Whether this difference is due to experimental uncertainties, natural variations, or actual decreased production due to solar activity,(the cosmic ray intensity was also lower during the second year) is not yet known.

In addition to yearly accumulation, we have for more than a year now, been making measurements of both ^{10}Be and ^{7}Be on precipitation samples collected at Orsay approximately every two weeks. In addition to providing more detailed information on seasonal variations of ^{10}Be, such as those reported in Ref (3), the $^{10}Be/^{7}Be$ ratio can be used to gain information on stratospheric-tropospheric exchange, as mentioned earlier for the air samples. The first results of this program are shown in Table 3. As can be seen, the $^{10}Be/^{7}Be$ ratio is quite similar to that observed in the stratospheric air samples, and considerably larger than the expected production ratio of $\sim$0.5. While more data are needed before any firm conclusions can be reached, this tendency, if confirmed, would favour a slow, almost continual leak of stratospheric air into the troposphere.

Most of the ^{10}Be that falls on the ocean is fairly rapidly transported to the sediment below, probably by particle scavenging. On the basis of the ^{10}Be concentration in ocean water (4), we have estimated the upper limit for this transport time as $\sim$600 years. The fate of ^{10}Be falling on the continents is less obvious. On the basis of some initial results on lake sediments (see below), we were led to conclude that at least a part of this ^{10}Be was being transported hydrologically. In order to test this directly, we measured ^{10}Be from an unfiltered sample of the river Seine, taken near the town of Fontainebleau. The result is given in Table 4. As can be seen, the ^{10}Be concentration

is several times less than in rain water. The upper limit established for ^{7}Be indicates that this ^{10}Be is not from recent runoff, but is at least several years old. From a single measurement, it is impossible to make any quantitative estimate of the fraction of ^{10}Be transported in this way. However, we can conclude that at least part of the ^{10}Be falling on the continents is being transported to the oceans in river water. Whether this ^{10}Be is in soluble form, or adsorbed onto particles, we cannot say from this measurement. The experiment is being repeated on a filtered sample, with the ^{10}Be being determined on both filtered and retained fractions. From measurements on "continental" sediments, Brown et al. (5) have also recently concluded that ^{10}Be is being transported by erosion, and they favour the adsorption mechanism.

We now look at ^{10}Be in the "permanent" reservoirs. In Table 5, we show some measurements on several deep sea sediments. There already exist in the literature, a number of ^{10}Be measurements in deep sea sediments made by conventional radioactive counting methods (6) (7). The difference with the present results (besides being made on much smaller samples) is that they are taken from regions of the ocean having relatively high biological activity, and thus higher sedimentation rates. Although coming from quite different regions, and sedimentation conditions, it can be observed that the ^{10}Be concentrations are remarkably similar. This is consistant with our suggestion that it is probably the ^{10}Be concentration, rather than its deposition rate, which is most constant in deep sea sediments (8). Indeed, the ^{10}Be deposition rates in these sediments are considerably larger than the average deduced from earlier work (6) and more consistant with the larger production rate estimated from our precipitation measurements. It should also be noted that even though the ^{10}Be concentrations are relatively constant, even in two quite adjacent cores such as MD 77215 and MD 77217, differences of almost a factor of two can exist. This demonstrates the uncertainties that can be expected if one wished to date samples simply by their ^{10}Be concentration.

An even more dramatic example of the influence of the deposition environment is shown by the results of a shallow water sediment from the Bay of Morbihan in the Kerguelen Archipelago (Table 6). Here, because of the very high sedimentation rate, the ^{10}Be concentration is about an order of magnitude less than in the deep sea, although the actual ^{10}Be deposition rate is larger.

In Table 7, we show some initial results for two cores from the Mediter-

ranean Sea. These cores were chosen because they have very high and apparently quite uniform deposition rates (9) and thus the potential for giving high time resolution results on possible production variations. Once again the ^{10}Be concentrations are remarkably constant, although about an order of magnitude lower than in the deep sea sediments. It is again noteworthy that the concentrations in the two cores appear about the same despite a difference in sedimentation rate of a factor of four. In contrast, despite being composed of very similar material, and being located only 75km apart, the estimated ^{10}Be deposition rates in the two cores are very different. This again emphasizes the danger in trying to estimate production rates on the bases of deposition rates in sediments.

We have previously discussed a search for a ^{10}Be concentration variation in a sediment at the time of a geomagnetic reversal (8). In Fig. 2 we show preliminary results of a similar search in a sediment that was deposited in the Mediterranean $\sim$ 6.5 My ago, and which is now uplifted on the island of Crete (10). Although the errors are still large, there appears to be an indication of some ^{10}Be increase $\sim$ 80cm above the reversal level. If confirmed this would give important information on the depth below the sediment surface at which remanent magnetism is "frozen in" (8). After correcting for age, we have included the average ^{10}Be concentration and deposition rate from this site in Table 7. Despite the many uncertainties it is interesting that the corrected concentrations are quite comparable (within a factor of $\sim$2) with the more recent sediments in the same region.

We are studying ^{10}Be in sediments from several lakes. One of the main objectives of these studies is to look for production variations caused by medium term (10^2-10^4 year) geomagnetic intensity variations (11). In Table 8, we give some results from two of these lakes. As mentioned earlier, it was the first results from lake Windermere (England), which suggested to us the importance of erosional transport of ^{10}Be. As can be seen, the ^{10}Be deposition rate in this lake is about an order of magnitude larger than measured directly by us in nearby France. We therefore conclude that a substantial fraction of the ^{10}Be falling in the lake's catchment area is arriving in the lake. Based on this evidence, it appears to us that the most suitable lakes for such a study would be those having the lowest possible catchment/surface ratio. Suitable candidates for such a characteristic are "crater" lakes, and this had led to our studies on lake Keilambete (Australia), which has a catchment/surface

ratio of only 1.5 and also has the advantage of having good magnetic stratigraphy and ^{14}C age control (12). Somewhat surprisingly, the deposition rates found here also seem somewhat larger than expected. The variations in the ^{10}Be deposition in the two lakes are not correlated, and are larger than expected for production variations. It is thus likely that at least part of these variations are due to other causes, such as changes in erosion rates. From this we conclude that considerable care will be necessary to extract production variations from lacustrine sediments.

In table 9 we show measurements of ^{10}Be in sediments below the Ross Ice Shelf. There is presently considerable controversy about when these sediments were last deposited. Our ^{10}Be concentrations, which are much lower than in any another recent sediments, suggest a rather old age for these sediments (13). More conclusively, the results indicate that ^{10}Be cannot be deposited from ocean water without particle sedimentation (this was in fact the original objective of the experiment), and that no bioturbation or mixing of the surface sediments is presently taking place (as demonstrated by the large difference between the surface sample and that at $\sim$7cm).

To conclude, we show in Fig. 3 and 4, a series of measurements in a 906m Antartic ice core (14). As we have expressed several times, we believe polar ice is potentially one of the most interesting reservoirs for ^{10}Be measurements. In Fig. 3 are shown ^{10}Be concentrations for the past $\sim$1000 years. It appears that there is evidence for enhanced ^{10}Be production during the Maunder Minimum (1645-1715). In Fig. 4 are shown some results over the whole length of the ice core. There is quite clear evidence that the ^{10}Be concentration in precipitation during the last ice age was greater than it is at present. Possible explanations for such an effect are discussed in Ref. (14).

We have presented here a series of measurements which begin to clarify the processes of production, transport and deposition of ^{10}Be in the environment. While much work remains to be done, we believe that these data, together with previously published results, will be helpful in planning and interpreting future experiments with this extremely promising geophysical probe.

ACKNOWLEDGEMENTS

We would like to express our sincere appreciation to the following people who have cooperated in providing us with samples : J.D. Hays, Lamont-Doherty Geophysical Observatory, L. Leclaire, Laboratoire de Géologie du Museum

National d'Histoire Naturelle, C. Lorius, Laboratoire de Glaciologie et Géophysique de l'environnement, D.S. Cassidy, Antarctic Research Facility, Florida State University, H. Volchok, H. Feely and R. Leifer, Environmental Measurements Laboratory, C. Laj, Laboratoire des Faibles Radioactivités, and C. Barton and R. Thompson, Dept. of Geology and Geophysics, Edinburgh University.
We thank also J. Lestringuez and D. Deboffle for their help in treating the samples.

References

1 - G.M. Raisbeck, F. Yiou, M. Fruneau, M. Lieuvin and J.M. Loiseaux, Proc. 1st Conf. Radiocarbon Dating with Accelerators, University of Rochester 38 (1978).

2 - G.M. Raisbeck, F. Yiou, M. Fruneau, J.M. Loiseaux, M. Lieuvin and J.C. Ravel, Laboratoire René Bernas report LRB-80-06, July (1980) (Submitted for publication).

3 - G.M. Raisbeck, F. Yiou, M. Fruneau, J.M. Loiseaux, M. Lieuvin and J.C. Ravel, Nature 282, 179 (1979).

4 - G.M. Raisbeck, F. Yiou, M. Fruneau, J.M. Loiseaux, M. Lieuvin, J.C. Ravel, J.L. Reyss and F. Guichard, Earth Planet Sci. Lett. 51, 275 (1980).

5 - L. Brown, I.S. Sacks, F. Tera, J. Klein and R. Middleton, preprint (1981).

6 - B.L.K. Somayajulu, Geochim. Cosmochim. Acta 41, 909 (1977), and references therein.

7 - S. Tanaka and T. Inoue, Earth Planet. Sci. Lett. 49, 34 (1980) and references therein.

8 - G.M. Raisbeck, F. Yiou, M. Fruneau, J.M. Loiseaux, M. Lieuvin, J.C. Ravel and J.D. Hays, Geophys. Res. Lett. 6, 717 (1979).

9 - N.D. Opdyke, D. Ninkovitch, W. Lowrie and J.D. Hays, Earth Planet Sci. Lett. 14, 145 (1972).

10 - J.P. Valet and C. Laj, preprint, (1981).

11 - G.M. Raisbeck and F. Yiou, Radiocarbon, 22, 245 (1980) ; EOS 62, 272 (1981).

12 - C.E. Barton and H.A. Polach, Radiocarbon 22, 728 (1980).

13 - F. Yiou and G.M. Raisbeck, EOS, 62, 297 (1981).

14 - G.M. Raisbeck, F. Yiou, M. Fruneau, J.M. Loiseaux, M. Lieuvin, J.C. Ravel and C. Lorius, Laboratoire René Bernas report LRB 81-03 May (1981) (Submitted for publication)

Table 1 - ^{10}Be AND ^{7}Be IN STRATOSPHERIC AND TROPOSPHERIC AIR (from Ref. 2)

Filter designation	Date of exposure	Latitude (km)	Altitude (km)	Volume (SCM)	^{10}Be in air sampled ($\times 10^4$ atoms/SCM)	^{7}Be in air sampled ($\times 10^4$ atoms/SCM) ::	$^{10}Be/^{7}Be$
10984	July 1978	65°N	19.2	73	1290 ± 210	533 ± 112	2.42 ± 0.64
10983	"	"	16.8	122	1190 ± 155	502 ± 55	2.36 ± 0.40
10975	"	"	13.7	148	791 ± 126	316 ± 57	2.50 ± 0.60
10978	"	"	10.7	189	663 ± 113	117 ± 12	5.67 ± 1.13
10899	"	9°N	16.8	152	181 ± 40	97 ± 18	1.86 ± 0.54
E 16956	July 1976	S.pole	2.8	16,010	3.31 ± 0.60	1.94 ± 0.05	1.71 ± 0.31
E 16747	Jan. 1976	S.pole	2.8	14,050	7.33 ± 1.17	4.83 ± 0.10	1.52 ± 0.24

Table 2 - ^{10}Be DEPOSITION AND ESTIMATED PRODUCTION RATE

Period	^{10}Be deposition at Orsay atoms/cm^2/sec	Estimated ^{10}Be global production atoms/cm^2/sec
03/04/78-06/04/79::	$5.5 \pm 0.8 \times 10^{-2}$	4.2×10^{-2}
02/08/79-29/08/80	$4.6 \pm 0.4 \times 10^{-2}$	3.1×10^{-2}

:: From Ref. (3)

Table 3 - ^{10}Be AND ^{7}Be CONCENTRATIONS IN PRECIPITATION AT ORSAY

Date	Vol. (l)	^{10}Be conc. ($x10^{4}$at/g)	^{7}Be conc. ($x10^{4}$at/g)	$^{10}Be/^{7}Be$
17/3 - 28/3/80	16.5	4.17	1.45	2.87
28/3 - 11/4/80	6.5	2.79	1.14	2.44
30/6 - 14/7/80	23.8	2.88	1.16	2.48
14/7 - 25/7/80	16.6	2.32	1.37	1.69
25/7 - 08/8/80	7.5	5.47	2.43	2.25
08/8 - 22/8/80	5.6	4.48	2.17	2.06
22/8 - 05/9/80	3.4	7.30	2.95	2.47
05/9 - 19/9/80	6.2	2.89	1.25	2.31
19/9 - 03/10/80	13.0	2.01	0.97	2.07
03/10- 17/10/80	28.2	1.51	0.97	1.56

Table 4 - ^{10}Be IN SEINE RIVER, NEAR FONTAINEBLEAU

24/07/80	30	0.73	< 0.005	< 0.007

Table 5 - ^{10}Be *IN DEEP SEA SEDIMENTS*

Reference	Location	Depth (m)	^{10}Be conc. at/g corrected for age	^{10}Be deposition rate at/cm^2/sec
AET 7606	38°26S-61°06E	5290	5.28×10^9	0.059
MD 76104	35°50S-58°27E	4860	5.95×10^9	0.076
MD 76106	38°43S-61°25E	5220	5.94×10^9	0.057
MD 77215	11°59S-78°56E	5120	4.46×10^9	0.035
MD 77217	11°56S-83°00E	4930	7.74×10^9	0.074
V20-108*	45°27N-179°14E	5200	5.58×10^9	0.10
V16-58 **	46°30S-31°16E	4731	7.6×10^9	- †

* Average of 6 samples (Ref. 8)

** Average of 7 samples

† Mass deposition rate not available

Table 6 - ^{10}Be *IN "COASTAL" SEDIMENT*

2EI	Kerguelen Islands (Morbihan Bay) ∿ 49°S-70°E	41	4.28×10^8	0.20

Table 7 - ^{10}Be IN INLAND SEA SEDIMENTS

Reference	Location (sedimentation rate)	Depth m	^{10}Be conc. at/g corrected for age	^{10}Be deposition rate at/cm^2/sec
V10-58 (235)	Agean (18cm/10^3y) 35°40N-26°18E	2283	5.51×10^8	0.24 *
V10-58 (340)	" "		6.11×10^8	0.26 *
V10-58 (345)	" "		7.79×10^8	0.33 *
V10-50 (81)	Agean (75.5cm/10^3y) 35°58N-27°05E	2547	4.35×10^8	0.78 *
V10-50 (85)	" "		4.36×10^8	0.78 *
V10-50 (239)	" "		4.68×10^8	0.84 *
V10-50 (245)	" "		5.90×10^8	1.06 *
KR	Crète (∿5cm/10^3y)		2.42×10^8	0.07

* assuming an "in situ" density of 0.75g/cm^3

Table 8 - ^{10}Be IN LAKE SEDIMENTS

Reference	Location	^{10}Be concentration at/g.	^{10}Be deposition rate* at/cm^2/sec
KO (50)	Lake Keilambete	1.04×10^9	0.29
KO (150)	Australia	0.80×10^9	0.22
KO (250)	38°13S-142°52E	1.40×10^9	0.43
KO (300)		2.31×10^9	0.70
KO (450)		0.76×10^9	-
WIND (20-25)	Lake Windermere	1.39×10^9	0.74
WIND (122-127)	England	1.48×10^9	0.42
WIND (172-177)	54°3N - 3°W	1.47×10^9	0.22
WIND (200-205)		1.60×10^9	0.20
WIND (262-267)		1.11×10^9	0.27

* based on preliminary estimates of mass sedimentation rates.

Table 9 - ^{10}Be IN ROSS ICE SHELF SEDIMENTS

Reference	Depth in sediment	^{10}Be concentration atoms/g.
RISP - 3	Surface	$9.6 \pm 1.4 \times 10^7$
RISP - 1	6-7.8cm	$0.57 \pm 0.10 \times 10^7$
RISP - 2	27-29cm	$1.3 \pm 0.4 \times 10^7$

Figure Captions

Fig. 1 - Schematic diagram of cosmogenic ^{10}Be production, transport and deposition.

Fig. 2 - ^{10}Be concentration during a geomagnetic reversal $\sim$ 6.5 My ago, as recorded in uplifted sediments on island of Crete.

Fig. 3 - ^{10}Be concentration in Antarctic ice at Dome C. The solid line corresponds to the Maunder Minimum, (1645-1715), according to Eddy (From Ref. 14).

Fig. 4 - ^{10}Be concentration (data points, left hand scale) and $\delta^{18}O$ (solid line, right hand scale) in ice at Dome C. The 20 points from Fig. 3 have been averaged, and are given by the open symbol (From Ref. 14).

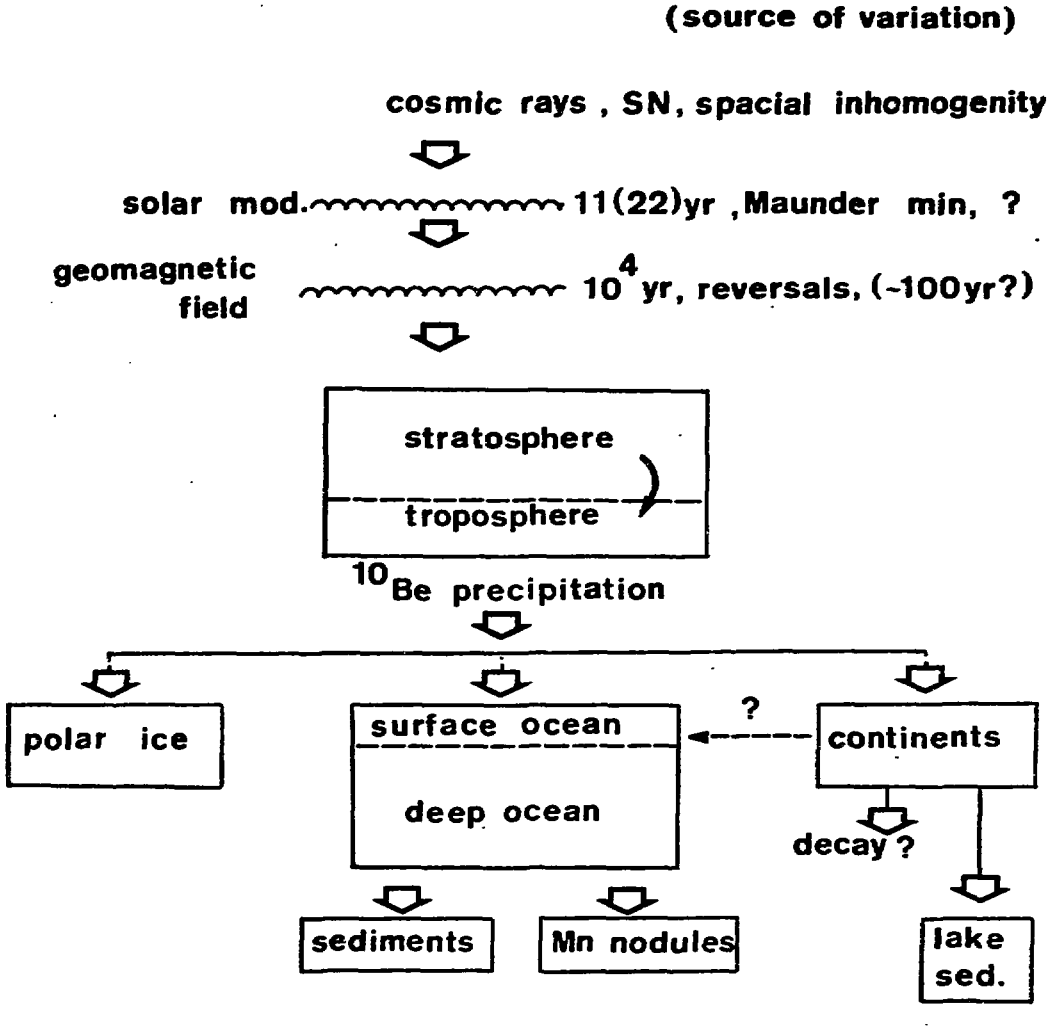
(source of variation)
cosmic rays , SN, spacial inhomogenity
solar mod.
11(22)yr ,Maunder min, ?
geomagnetic field
10^4 yr, reversals, (~100yr?)
stratosphere
troposphere
10Be precipitation
polar ice
surface ocean
deep ocean
?
continents
decay ?
sediments
Mn nodules
lake sed.

Fig. 1

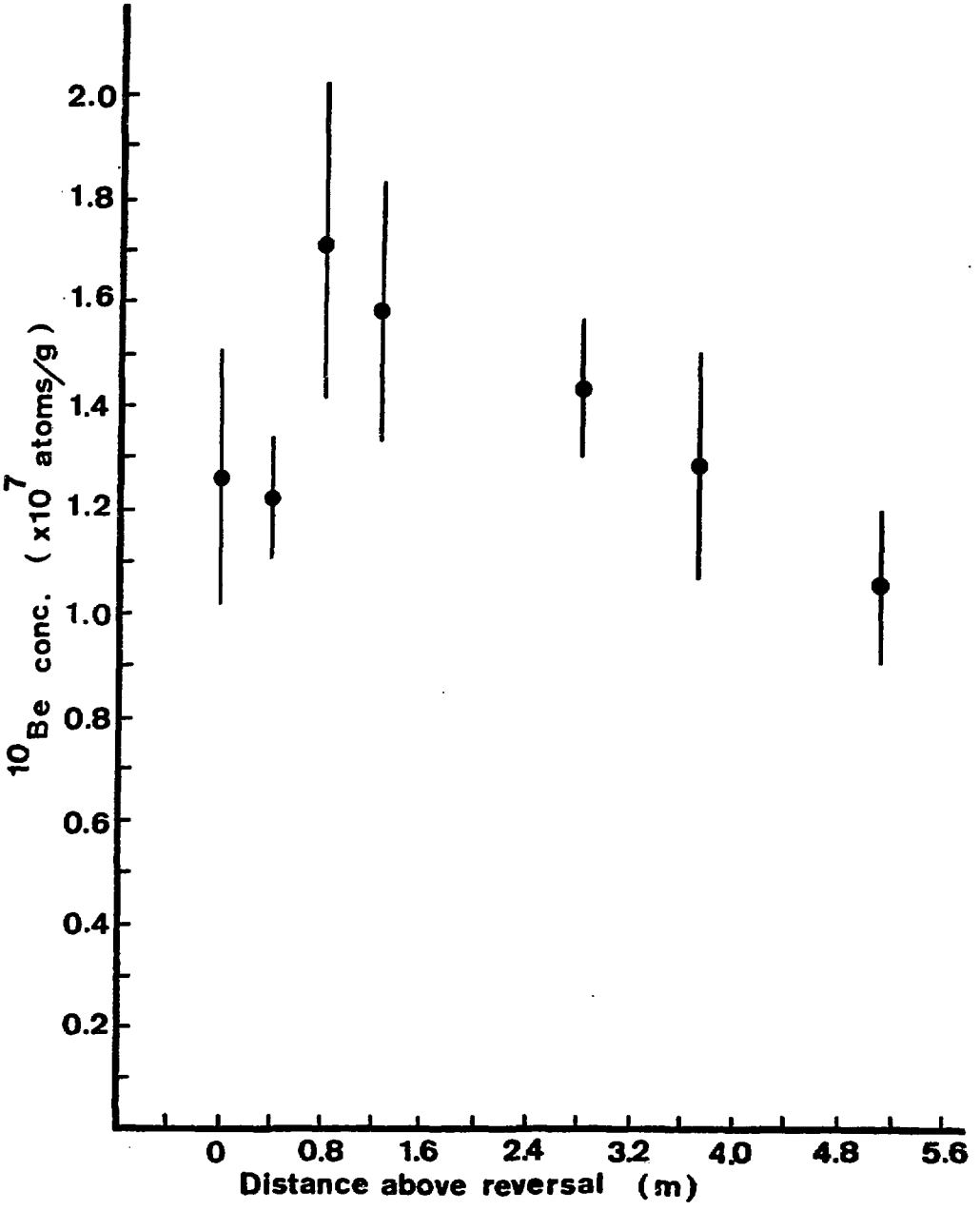
2.0
1.8
1.6
1.4
1.2
1.0
0.8
0.6
0.4
0.2
^{10}Be conc. (x10^{7} atoms/g)
0
0.8
1.6
2.4
3.2
4.0
4.8
5.6
Distance above reversal (m)

Fig. 2

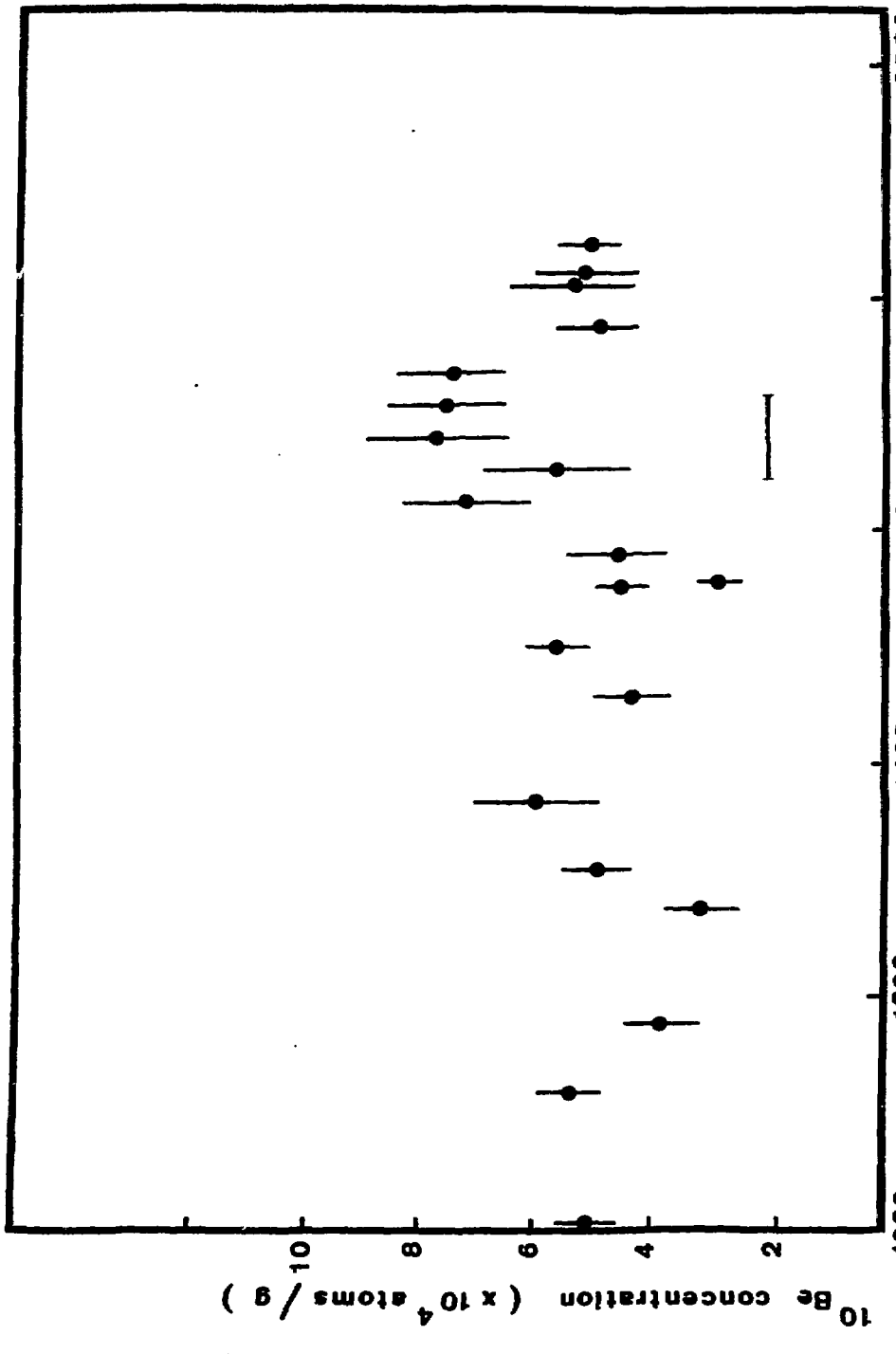
10Be concentration (x 10^4 atoms / g)
2
4
6
8
10
1000
1200
1400
1600
1800
2000
Year A.D.

Fig. 3

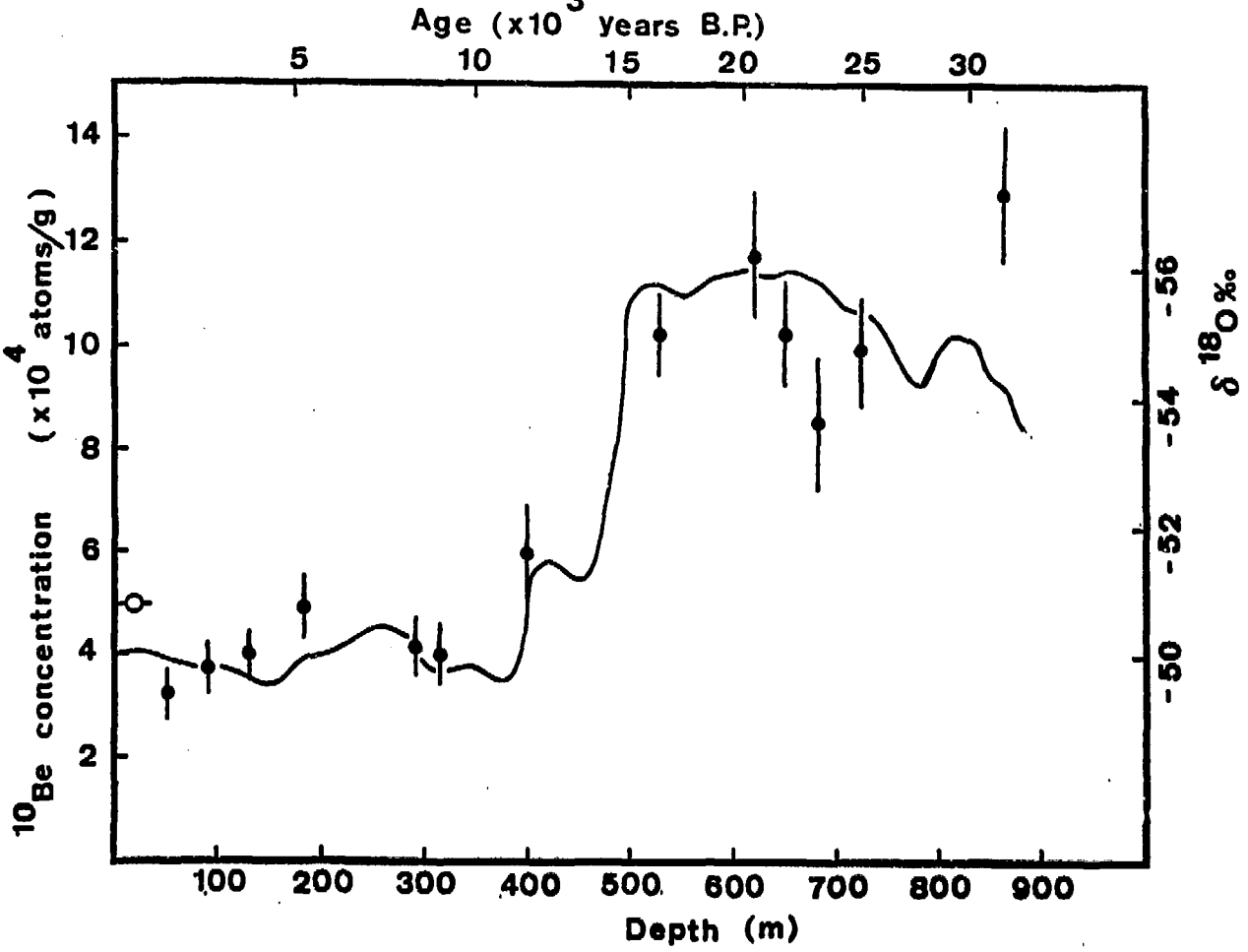
Age (x10^3 years B.P.)
5
10
15
20
25
30
14
12
10
8
6
4
2
10Be concentration (x10^4 atoms/g)
δ 18O ‰
-56
-54
-52
-50
100
200
300
400
500
600
700
800
900
Depth (m)

Fig. 4

^{10}Be IN MANGANESE NODULES

J. Thomas and P. Parker
Wright Nuclear Structure Laboratory, Yale University

A. Mangini, K. Cochran, and K. Turekian
Department of Geology and Geophysics, Yale University

S. Krishnaswami
Department of Geology and Geophysics, Yale University
and
Physical Research Laboratory, India

P. Sharma
Physical Research Laboratory, India

I. INTRODUCTION

^{10}Be ($t_{1/2}$ = 1.5 MY) is formed in the upper atmosphere by cosmic ray spallation on nitrogen and oxygen. It is transported to the earth's surface via precipitation. In the oceans it is eventually associated with solid phases depositing on the ocean floor such as manganese nodules and deep-sea sediments. One of the assumptions that is normally made in the analysis of such processes is that ^{10}Be has been produced at a relatively uniform rate over the past several million years. If we assume, in addition, that the initial specific concentration of ^{10}Be as it precipitates with a solid phase is invariant with time, then we would expect that the decrease of the ^{10}Be concentration as a function of depth in a deep-sea core or in a manganese nodule would provide a record of sediment accumulation rate in the former and of growth rate in the latter.

The possibility of using cosmic-ray produced ^{10}Be for the dating of marine deposits had been proposed 25 years ago by Arnold[1] and Goel et al.[2] The method of analysis used by these investigators, and those subsequently pursuing the problem, was low-level β counting. Though the potential of using ^{10}Be for dating manganese nodules was explored more than a decade ago[3], only a few measurements of ^{10}Be in nodules exist to date. This is largely because of the

difficulties associated with ^{10}Be measurements, which require large nodules, tedious radiochemical separation and high-sensitivity, low-background beta counters for their assay.

^{10}Be measurements in environmental samples, however, have gained considerable momentum during the past 3 - 4 years, after the development of accelerator mass spectrometry for its determination [4]. In 1979, the Yale-PRL group applied the accelerator mass spectrometric technique to measure a ^{10}Be profile in a manganese nodule from the Atlantic Ocean [5,6]. Since that time the Yale-PRL group has examined a number of other nodules in much finer detail, as well as a variety of other natural materials such as sediment cores from the Pacific Ocean floor, meteorites, deep ocean water, and ice. We are currently working to extend these techniques to the measurement of ^{26}Al in order to explore the use of the ^{10}Be/^{26}Al ratio as a dating tool particularly suited to certain types of problems. In this report we present our manganese nodule data.

II. TECHNIQUES

For the ^{10}Be measurements, the Yale Emperor Tandem Van de Graaff Accelerator is used as an ultra-sensitive mass spectrometer. The ^{10}Be concentration was measured by comparing the ^{10}Be count-rate to the ^{9}Be beam intensity. The procedure was calibrated periodically with ^{10}Be/^{9}Be standards.

The accelerator is shown schematically in Figure 1. Our techniques rely on electrostatic acceleration, magnetic analysis and $\Delta E - E$ particle identification. Since we use an Emperor Tandem Accelerator, we can fully strip the beryllium beam (Be^{4+}), and therefore we do not need any additional stages of analysis such as velocity filters or post-accelerator stripper foils.

We have a standard UNIS ion source which we use in a reflected beam geometry with a specialized cone shape (Figure 2) in order to optimize our efficiency and beam emittance [7]. In this geometry the cesium beam passes through the cone and then is reflected back to the sample by a bias electrode which is maintained at a few hundred volts. The samples are loaded in a cavity of $\sim$2 mm diameter and

~1 mm deep in the cones. Typically (for nodules) ~1 - 2 mg BeO was loaded in the cone. During the course of the work, improvements in the cone wheel designs were made so that the sample holders can be directly mounted on the wheel without the circular stainless-steel jackets shown in Figure 2. This new design was made to increase the thermal contact between the sample holder and cone wheel, which we hoped would reduce the waiting time (~1 hr) for a fresh sample to reach optimum source output. Although the new design increased the source output by ~40%, it did not reduce the warm-up time. We did find, though, that doping the samples with CsOH decreased the warm-up time by approximately a factor of two.

After the warm-up, a BeO beam is extracted from the source (typically a few hundred nA) and momentum analyzed by a 35 degree inflection magnet. It is then accelerated by a 10-million volt potential and stripped to charge state +3 in a nitrogen gas stripper canal. The beam is finally stripped to charge state +4 by a carbon foil located further down the accelerator tubes and then is momentum-analyzed by a high resolution 90 degree analyzing magnet. The beam at this point consists only of Be, B, and a few low-energy carbon and oxygen beams. We remove the carbon and oxygen by installing an Al absorber in front of our detector assembly. The boron beam is severely attenuated by the absorber, but it is allowed to pass into the ΔE detector for beam tuning purposes. The B and Be beams are easily separated by our ΔE (gas ionization) - E (Si(SB)) detectors.

The boron beam did present a problem for us once. Our aluminum absorber foils were accidentally contaminated with hydrocarbons and the boron beam produced copious quantities of ^{7}Be through the reaction ^{1}H(^{10}B, α)^{7}Be. When we replaced the absorber foils, the ^{7}Be went away, and we have had very clean ΔE-E spectra ever since (Figure 3).

Our procedure for measuring ^{10}Be/^{9}Be ratios starts with tuning the accelerator on a 44.4 MeV ^{9}Be guide beam. After tuning, we lower the terminal voltage so that the 40 MeV ^{10}Be beam can pass into the detector chamber without changing any of the magnet settings. However, we fine-tune the accelerator by

observing the ^{10}B count-rate in the detectors. (This is justified since the isobars ^{10}Be and ^{10}B have the same mass, energy and charge state.) The ^{10}Be counts are integrated for 400 seconds and then the accelerator magnet settings are readjusted to bring the much more intense ^{9}Be beam into a faraday cup after the 90 degree magnet. The ^{9}Be current is integrated at the faraday cup and, after several repetitions between ^{10}Be and ^{9}Be, the ratio of $^{10}Be/^{9}Be$ in the sample is determined. From the measured $^{10}Be/^{9}Be$ ratio, the ^{9}Be carrier added for extraction of ^{10}Be and the sample weight, the ^{10}Be atoms/g sample is calculated.

The ultimate sensitivity of an accelerator mass spectrometer is determined by how much of the stable beam can be produced in the ion source and then accelerated through the machine. We usually work with 100 to 500 nA of ^{9}Be beam out of the source, and we have accelerated as much as 30 nA of $^{9}Be^{4+}$ to the faraday cup after the analyzing magnet. The particle transmission efficiency through the accelerator is 1×10^{-2} to 2×10^{-2} while the overall efficiency, including the source, is about 10^{-5}. We have measured samples with as few as 10^{8} atoms, but we have not pushed the system to its ultimate capability. Our emphasis has been to analyze geologically interesting samples, and since most of the samples analyzed to date have had a relatively large amount of ^{10}Be, we have concentrated on refining our techniques in the direction of handling smaller samples. This has allowed us to make measurements on millimeter-thick layers of manganese nodules, for example, using about two hours of accelerator time for each sample.

III. RESULTS ON MANGANESE NODULES

Manganese nodules are accumulations of manganese and iron oxides that are found on the ocean floor. They occur in many sizes and shapes, although the object of our studies have been the small, spherical nodules which are only a few centimeters in diameter and are found in the deepest parts of the ocean (4-5 km deep). The area where these nodules occur typically accumulate sediments at a rate of a few mm per thousand years, whereas the nodules appear

to be growing at a rate of a few mm per million years based on a number of different techniques. The uniqueness of the ^{10}Be method of growth rate determination using the refined accelerator technique is that virtually the entire history of the nodule can be followed in detail. Such questions as the role of diffusion in influencing growth rate determinations by the ^{230}Th method and the changes in growth rate over time can thus be addressed.

Using the Yale accelerator, we have measured the depth porfiles of ^{10}Be in four nodules, RC-16-D10 (Atlantic, reported earlier in 5); A47-16(4) (North Pacific, 9°2.3'N; 151°11.4'W); R/V Vitiaz (Indian Ocean 26°48'S; 108°15'E) and TF-5 (S. Pacific 13°53'S; 150°35'W). The results of these measurements are given in Figures 4 - 7. In general, we have ascribed an error of $\sim$ 20% to these ^{10}Be concentrations, based on repeated measurements of a standard.

Nodule TF-5 shows an undisturbed exponential decrease of ^{10}Be with depth, yielding an accumulation rate of 1.0 mm/MY, in agreement with the growth rate of 0.9 mm/My measured from a ^{230}Th profile of the outer 0.5 mm of the nodule. (^{230}Th in excess of that supported by ^{234}U decreases with depth until secular equilibrium is attained.) The ^{10}Be measurements obviously extend much deeper into the nodule than the unsupported ^{230}Th ($t_{1/2}$ = 75,000 Y) and suggest that this nodule has been growing at a constant rate of 1 mm/MY for the past $\sim$5 MY.

Nodule A47-16(4) yields an average ^{10}Be growth rate of $\sim$2.2 mm/MY for the 1 - 7 mm of the nodule. The ^{230}Th - ^{231}Pa isotope data yield a growth rate of 4.55 - 7.5 mm/MY for the top 0.8 mm region. This is not inconsistent with the ^{10}Be results in the outer two layers (Figure 5), although the average ^{10}Be rate is lower than the ^{230}Th rate.

The samples from the nodule R/V Vitiaz were measured at various times over a period of one year. This nodule exhibits a growth rate of 1.6 mm/MY for the 0 - 6 mm region and ~3 mm/My for the 6 - 14 mm depth intervals. The ^{10}Be growth rate for the outer 6 mm is in agreement with the rate of 1.1-1.4 mm/MY deduced from the ^{230}Th - ^{231}Pa isotope data.

The agreement of the ^{10}Be and ^{230}Th rates over the past 400,000 years indicates that the ^{10}Be production rate has been roughly constant over at least the past several hundred thousand years. The authigenic source of the beryllium is indicated by a comparison of the $^{10}Be/^{9}Be$ ratio at the surface of the nodules with that in sea water. The surface $^{10}Be/^{9}Be$ ratios for the two Pacific nodules A47-16(4) and TF-5 are about 1.0 and 0.6×10^{10} atoms/μg Be. We have determined the ^{10}Be concentration in deep water from GEOSECS Station-500 in the North Pacific to be 6160 ± 1200 atoms/g. The ^{9}Be concentration in deep water from a nearby region was measured[8] to be ~1 ng/kg yielding a $^{10}Be/^{9}Be$ ratio of $\sim 6 \times 10^{9}$ atoms/μg Be, comparable to the observed values at the surface of nodules.

IV. CONCLUSIONS

The Yale MP Tandem Van deGraaff accelerator has been used successfully to measure ^{10}Be concentrations in a variety of natural materials. Our technique is capable of handling samples as small as 500 μg of BeO and can detect as little as 10^{8} atoms of ^{10}Be. We can routinely measure samples with $^{10}Be/^{9}Be$ ratios of the order of 10^{-13} in a couple of hours.

Thus far our measurements have concentrated on a study of the origin and nature of manganese nodules. All our data on ^{10}Be in nodules indicate that these deposits grow at rates of a few mm/MY. The agreement between ^{230}Th-^{231}Pa growth rates and the ^{10}Be rates, also suggests that the ^{230}Th-^{231}Pa profiles in these nodules are neither due to diffusion nor sampling artifacts, but represent nodule growth. The geochemical implications of these results are discussed elsewhere.

We have recently installed an electrostatic separator in a new beam line that will be dedicated in the future to mass spectroscopy. This separator will make it possible for us to utilize a higher intensity Be^{3+} beam, and it will also allow us to extend our measurement program to include other isotopes, in particular, ^{26}Al.

ACKNOWLEDGEMENTS

This work was supported by the U. S. Department of Energy contract number DE-AC02-76ER03074 and by a grant from the National Science Foundation OCE-79-11879.

REFERENCES

1. J. R. Arnold, Science 124 (1956) 584.
2. P. L. Goel, D. P. Kharkar, D. Lal, N. Narsappaya, B. Peters, and V. Natirajam, Deep Sea Research 4 (1957) 202.
3. B. L. K. Somayajulu, Science 156 (1967) 1219
4. See Proc. First Conf. on Radiocarbon dating with accelerators, 20-21 April 1978 ed. H. E. Gove (Univ. of Rochester) and references therein.
5. K. K. Turekian, J. K. Cochran, S. Krishnaswami, W. A. Lanford, P. D. Parker and K. Bauer, Geophys. Res. Lett. 6 (1979) 417.
6. W. A. Lanford, P. D. Parker, K. Bauer, K. K. Turekian, J. K. Cochran, and S. Krishnaswami, N. I. M. 168 (1980) 505.
7. J. Thomas, A. Mangini, and P. Parker, I. E. E. E. Transaction on Nuclear Science, NS-28 (1981) 1478.
8. C. Measures and J. Edmond, private communication.

FIGURES:

1. The Yale Tandem Van de Graaff accelerator. The ^{9}Be beam intensity is measured in the faraday cup immediately after the analyzing magnet. The ^{10}Be count rate is measured with a $\Delta E - E$ telescope in a detector chamber.

2. The inverted cone sample holder. The sample is mounted in a small dimple on the upstream side of the cone.

3. Typical spectra collected while measuring the $^{10}Be/^{9}Be$ ratio of a standard sample. The figure on the left illustrates the ^{10}B count rate as a function of time. The X axis extends from 0 to 400 seconds. The Y axis indicates the ^{10}B count rate. Since the ^{10}B and ^{10}Be count rates are proportional, we can evaluate the stability of a particular run in this way. The figure on the right illustrates how clean our $\Delta E - E$ spectra are. The ^{10}Be peak count rate was only a few per minute while the ^{10}B peak count rate was several hundred per second. The ^{9}Be peak is a background beam due to ^{9}BeH.

   Figures 4 to 7 (reading left to right)

4. Nodule RC16-D10 from the Atlantic Ocean. The horizontal bars in all of these figures represent depth intervals. The vertical bars indicate the assigned error for each point.

5. Nodule A-47-16-4 from the central Pacific.

6. Nodule R/V Vitiaz. The data points represented by open circles are averages. These samples were measured several times in different run periods. The vertical bars represent the deviations of the means. The data points represented by solid dots all come from one run.

7. Nodule TF5

YALE MP TANDEM ISOTOPE ANALYSIS SYSTEM

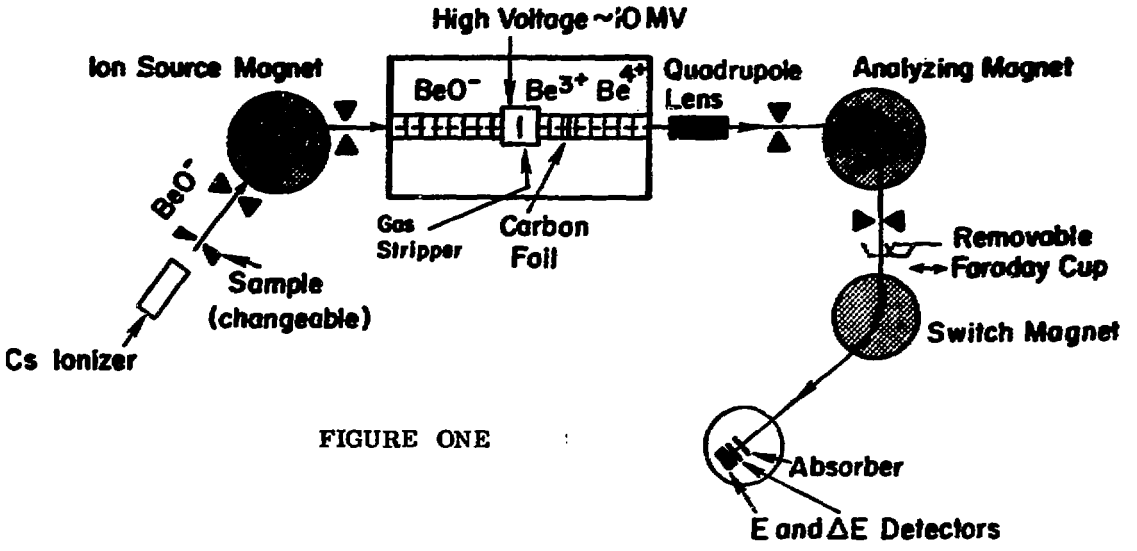

FIGURE ONE

INVERTED CONE SAMPLE HOLDER

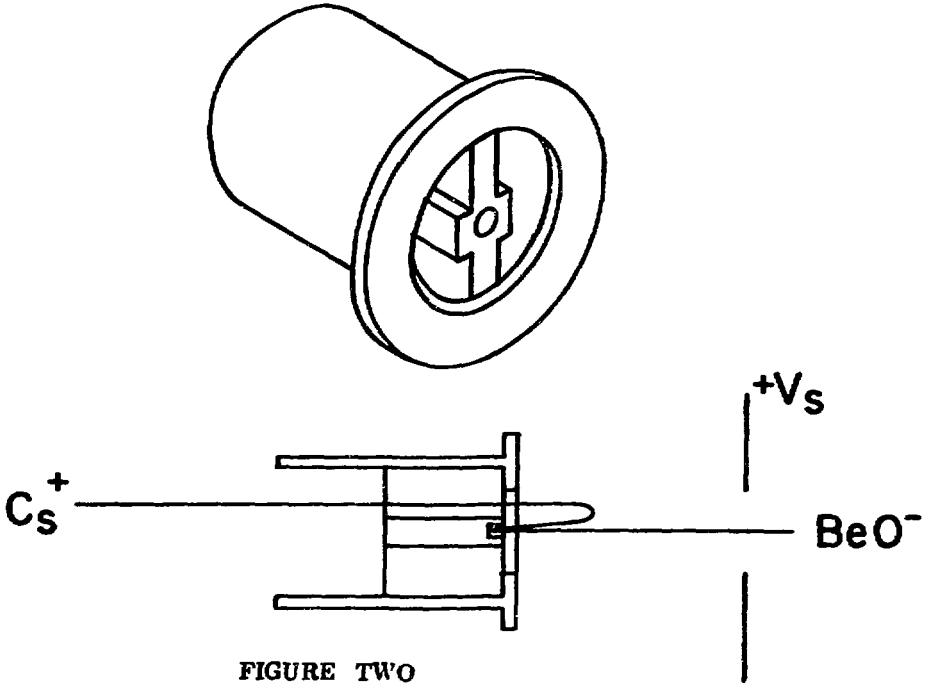

FIGURE TWO

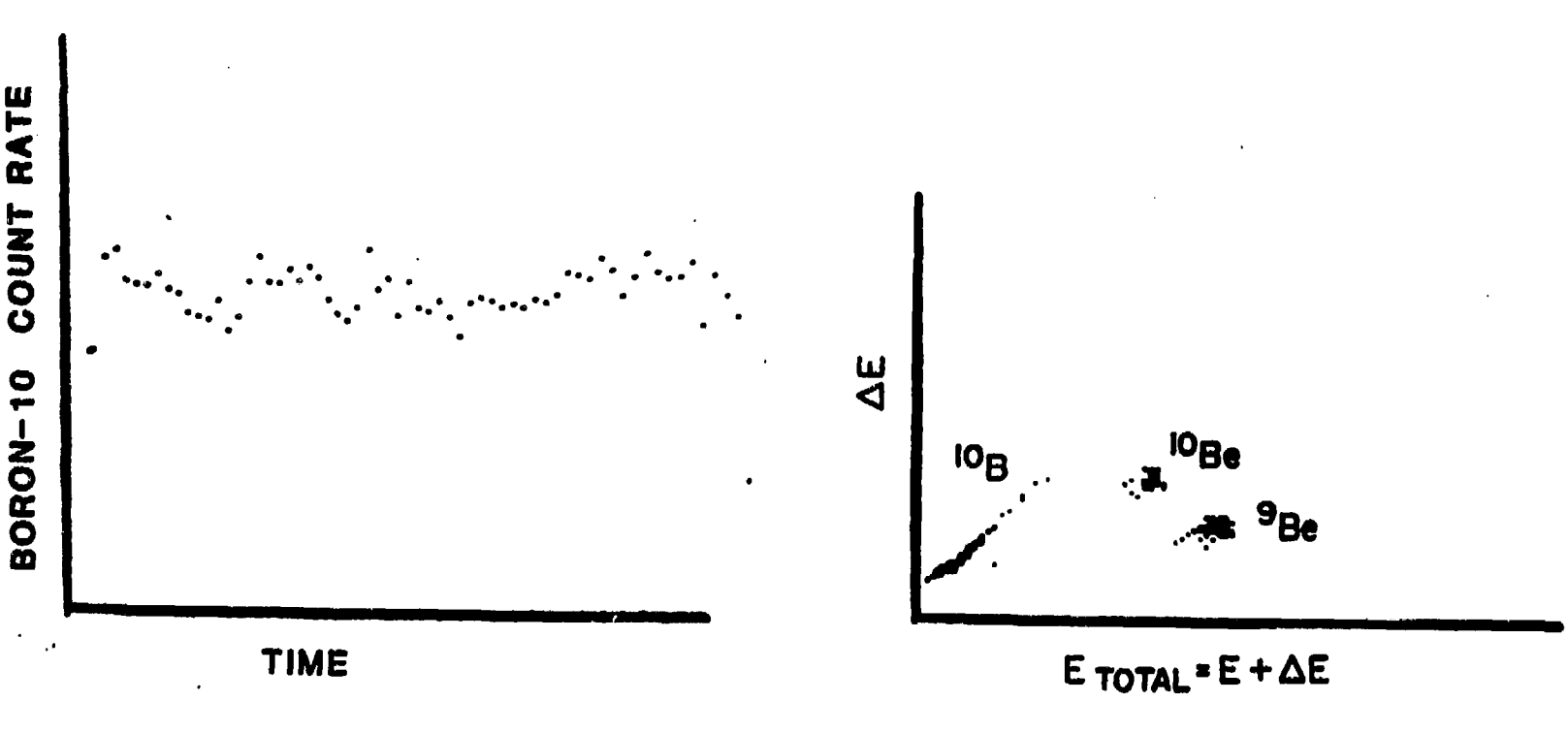

FIGURE THREE

FIGURE FOUR

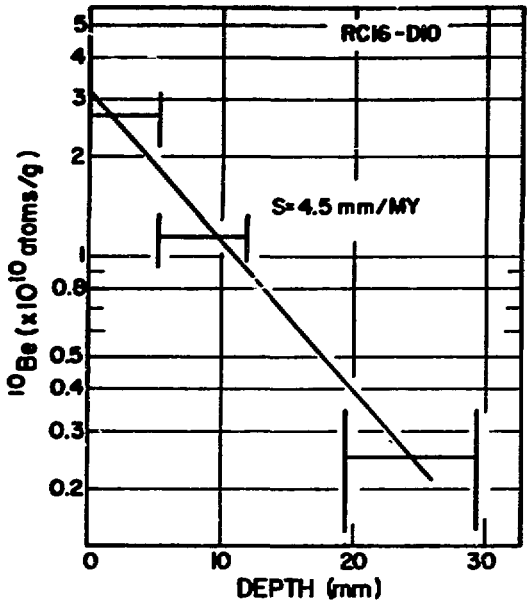

FIGURE FIVE

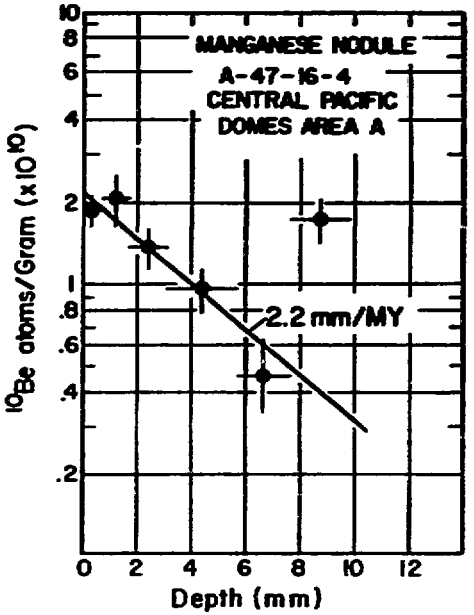

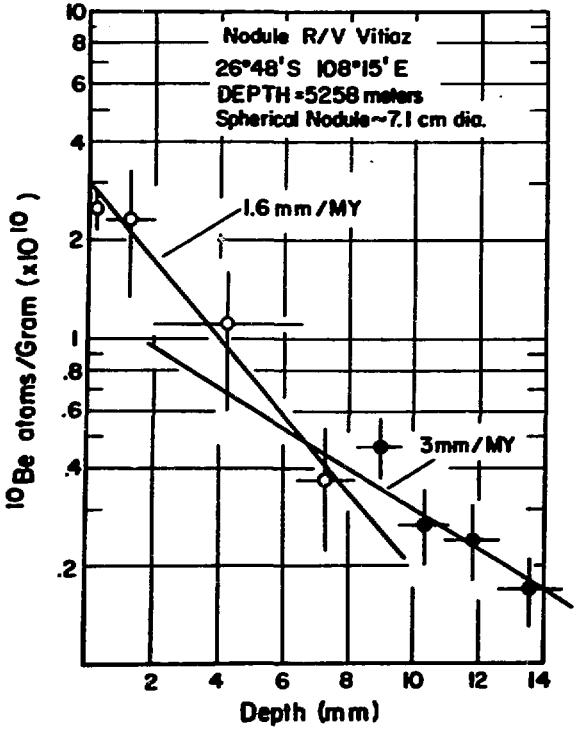

FIGURE SIX

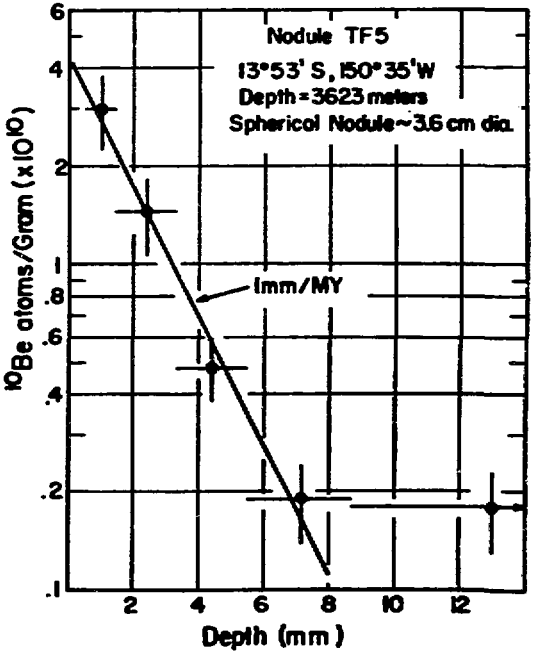

FIGURE SEVEN

THE PREPARATION OF A ^{10}Be STANDARD

J. Southon, I. Thorson, D.E. Nelson, R. Korteling and J.S. Vogel
Simon Fraser University, Burnaby, B.C., Canada, V5A 1S6

T.L. Ku and J.L. Reyss*
University of Southern California, Los Angeles, California 90007, U.S.A.

and

I. Nowikow
McMaster University, Hamilton, Ontario, Canada, L8S 4K1

INTRODUCTION

The recent development of accelerator mass spectrometry has reduced the difficulty of measuring the concentrations of long-lived isotopes such as ^{10}Be and hence led to increased interest in this isotope. Accelerator-based measurements are usually relative measurements made by comparing the isotope ratios from two or more samples. Absolute measurements are more difficult, as errors due to isotopic fractionation in the accelerator system must be corrected for. However, relative measurements can be converted to absolute isotope ratios if one of the samples is a standard containing a known concentration of the rare isotope. Thus a standard performs two functions:

i) it allows absolute isotope ratios (hence the abundance of the rare earth isotope) to be determined more easily by accelerator methods;

ii) it assists interlaboratory comparisons, including those between β-decay and ion-counting measurements.

Such a standard exists for ^{14}C, in the form of a quantity of oxalic acid prepared by the National Bureau of Standards, but no ^{10}Be standard is presently available. The purpose of this paper is to suggest some desirable properties for a standard and to examine a few of the possible production methods.

---

* On leave from: Centre des Faibles Radioactivités, 91190-Gif-sur-Yvette, France

PROPERTIES OF A STANDARD

An ideal ^{10}Be standard should satisfy the following criteria:

i) the ^{10}Be concentration (and activity) should be known precisely;

ii) this concentration should be close to those found in natural systems and sufficiently high for both ion-counting and β-decay measurements;

iii) the standard should be reliably uniform and available in sufficient quantities over a long period of time.

The ^{10}Be activity could be determined by the same procedure used for the ^{14}C standard: by simply adopting a mean value from the results of many careful β-decay measurements. Ideally, the standard should be prepared in such a way that its ^{10}Be concentration could be measured during the preparation by some well-established technique. Failing this, it could be determined from the specific activity, to an accuracy limited by the uncertainty in the ^{10}Be half-life -- currently about 10%[1-4]. Alternatively, it could be found from careful absolute ion-counting measurements corrected for fractionation. This could presumably be estimated from experiments with known mixtures of, say, ^{7}Be and ^{9}Be. However, even if the ^{10}Be concentration is poorly determined, a standard would at least ensure compatibility between ion-counting results from different groups.

The lower limit on usable ^{10}Be concentration is set by the requirements of β-counting. A BeO sample with a $^{10}Be/^{9}Be$ ratio of 3×10^{-10} has a specific activity of 6.4 dpm/g, assuming a ^{10}Be half-life of 1.5 MY. For a typical counter (sample size 40 mg of BeO, efficiency 40%, background .2 cpm), a 5% measurement of the ^{10}Be activity in the sample would take about two weeks. This $^{10}Be/^{9}Be$ ratio is therefore close to the lower limit.

The need for laborious calibrations of successive batches of standard against each other should be avoided if possible. Hence a large quantity of standard is required, or the production process should have good reproducibility.

METHOD OF PRODUCTION

Three possible ways of obtaining the ^{10}Be for such a standard are:

i) by homogenizing a large natural sample containing ^{10}Be and using this raw material as the standard;

ii) by artificially creating a relatively pure sample of ^{10}Be and subsequently diluting it with ^{9}Be as required;

iii) by irradiating a ^{9}Be sample with thermal neutrons to produce the required ^{10}Be concentration.

The homogenization method gives a check on the efficiency of the beryllium extraction from the sample as well as providing a standard. Natural materials with suitably high ^{10}Be concentrations exist: the outer layers of manganese nodules have ^{10}Be concentrations $\sim$ 10 dpm/kg[5,6], for example. If sufficient nodule material could be ground and properly mixed, several hundred samples (of $\sim$ 10 g size) with an activity of .1 dpm could be obtained from a few kg. The ^{10}Be concentration could only be determined from the specific activity or from absolute ion-counting measurements; a complete recalibration would be required for each batch of material.

An example of the second technique is given by Goosman[7], who irradiated enriched ^{13}C in a high flux of fast neutrons to produce .5 mg of 94% enriched ^{10}Be via the $^{13}C(n,\alpha)$ reaction. The ^{10}Be content in the extracted beryllium was determined to $\sim$ 1% accuracy in a mass spectrometer. The ^{10}Be concentra-

tion in a standard made by this method could therefore be formed independently of accelerator or β-decay techniques. The only uncertainties would be those of the mass spectrometer measurement and the procedures for diluting the sample to the required $^{10}Be/^{9}Be$ ratio. Also, while some of the sample would doubtless be lost in handling, a .5 mg ^{10}Be sample converted to BeO and diluted to a $^{10}Be/^{9}Be$ ratio of 10^{-8} would provide over one hundred kg of standard!

The production of ^{10}Be by this technique is a major undertaking, however, as very high neutron fluxes are involved. The irradiation and the subsequent beryllium extraction therefore require considerable expertise.

The neutron fluxes required for ^{9}Be irradiations are far lower and many groups including our own have already produced ^{10}Be samples by irradiating beryllium metal or oxide. In view of the relative ease of this technique, we have examined its accuracy and reproducibility with a view to preparing a working standard for our own laboratory.

Unfortunately some doubt has been cast recently[8] on the accepted value[9] of the ^{9}Be thermal neutron capture cross section. Although this ambiguity sets a limit on the absolute accuracy of the ^{10}Be concentration produced in a beryllium sample by neutron capture, the technique should be capable of yielding reproducible specimens providing that neutron flux monitoring is done accurately. Some of the requirements are outlined below.

The most important requirements for obtaining a reproducible standard are to establish the neutron density and spectrum in the bulk of the Be specimen during bombardment. To do this accurately, it is necessary to have an irradiation facility where the density gradients are small or the flux is "homogenized" by cycling the monitors and sample through a common volume. The

assaying of the spatially averaged neutron flux seen by the Be sample should be carried out using an auxiliary monitor reaction, such as neutron capture in cobalt to give ^{60}Co. The second requirement is to determine the neutron spectrum. For an epi-thermal/thermal neutron density ratio of a few percent (typical of many irradiation facilities in or near the cores of fission reactors) the epithermal/thermal capture fraction in Be would be roughly one-half the density ratio. For the $^{59}Co(n,\gamma)^{60}Co$ monitor reaction, this fraction is approximately twice the density ratio[10]. For neutron irradiation facilities with highly thermal fluxes (epithermal/thermal neutron density ratio $\lesssim$ 1%) the correction for spectrum effects can be determined to an accuracy of 1% or better.

Unfortunately, good thermalization requires that the reactor core and irradiation position be separated by a large quantity of moderator and the neutron flux is therefore rather weak. There may be a trade-off between the fraction of non-thermal neutrons which can be tolerated and the time required for the irradiation. For example, a thermal column at the Chalk River Nuclear Laboratory operates with a flux of 10^{10} neutrons/cm^2-sec. For a $^{9}Be(n,\gamma)$ cross-section of 9.2 mb, the time required to produce a $^{10}Be/^{9}Be$ ratio of 3×10^{-10} is 38 days.

The reproducibility of the irradiation is limited by the uncertainty in the total neutron fluence received. Any material used as a neutron monitor must be close to or embedded in the sample and, if any spatial variation in the flux exists, geometrically arranged to give the correct volume-averaged activation; it should have minimal shielding effect on either itself or the sample; and the radioisotope should have a half-life which is long compared to the irradiation time. Cobalt wire or foil can be used if the thickness is kept below .05 mm, as

even .1 mm of cobalt attenuates thermal neutrons by ∿ 3%. The 5.27 year half-life of ^{60}Co is sufficiently long that all but 1.4% of the ^{60}Co produced at the beginning of a 38-day irradiation is still present at the end, and the correction for variations in bombardment flux even smaller. Ten mg of cobalt irradiated for 38 days in a flux of 10^{10} neutrons/cm^2-sec produces 14 μCi of ^{60}Co. The activity of such a source can be readily determined with a calibrated Ge(Li) counter to an accuracy of perhaps 2%. If sufficient care is taken in cleaning and weighing the cobalt monitor before the irradiation, it should be possible to determine the total neutron fluence to a few percent.

The $^{9}Be(n,\gamma)$ and $^{16}O(n,\gamma)$ cross-sections are so small that there is no significant self-shielding effect for beryllium or beryllium oxide samples of 10 g or so. Sufficient material for several hundred β-decay or accelerator measurements can therefore be produced at one time.

Any standard produced in this way contains radionuclides created from trace contaminants in the original sample material and possibly from the container so radiochemical purification is required before β-counting can be undertaken. This should remove all contaminating radionuclides, but it would be desirable to minimize their formation by using ultra-pure sample material. It may also be advantageous to avoid containers made of chlorine-containing plastics to prevent ^{36}Cl contamination.

To summarize, this method can provide useful quantities of a standard with a suitably high ^{10}Be activity. The $^{10}Be/^{9}Be$ ratio can be determined from the specific activity to an accuracy of about 10%. Accurate absolute ion-counting measurements or a better determination of the ^{10}Be half-life or the $^{9}Be(n,\gamma)$ cross-section would be required to reduce this uncertainty. The

method should be reproducible to perhaps 5% at any reactor with a well-thermalized flux. It could therefore provide useful interim standards which would at least ensure ^{10}Be measurements from different groups to be compatible.

ACKNOWLEDGEMENTS

Much of this paper arises from discussions with many people active in the fields of ^{10}Be measurements and accelerator mass spectrometry. Their input is gratefully acknowledged.

REFERENCES

1. F. Yiou and G.M. Raisbeck, Phys. Rev. Letters 29 372 (1972).
2. E.M. McMillan, Phys. Rev. C 6 2296 (1972).
3. J.F. Emery, S.A. Reynolds and E.I. Wyatt, Nucl. Sci. Eng. 48 319 (1972).
4. T. Makino, R. Gensho and M. Honda, Mass Spectrosc. 23 33 (1975) (in Japanese).
5. F. Guichard, J.L. Reyss and Y. Yokoyama, Nature 272 155 (1978).
6. B.L.K. Somayajulu, Science 156 1219 (1967).
7. D.R. Goosman, Nucl. Instr. Meth. 116 445 (1974).
8. L.R. Kilius et al, Nucl. Instr. Meth. 171 355 (1980).
9. BNL-325 Neutron Cross-Sections, Third Edition, Vol. I (1973), S.F. Mughabghab and D.I. Garber, Compilers (1973).
10. C.H. Westcott, Effective Cross-Section Values for Well-Moderated Thermal Reactor Spectra, AECL Report #AECL-1101 (Rev) (1970) and A/Conf. 15/P1202 Effective Cross-Sections and Cadmium Ratios for the Neutron Spectra of Thermal Reactors, C.H. Westcott, W.H. Walker and T.K. Alexander, 1958.

MEASUREMENT OF COSMOGENIC NUCLIDES IN EXTRATERRESTRIAL MATERIAL

Kunihiko Nishiizumi and James R. Arnold
Dept. of Chemistry, B-017, Univ. of Calif., San Diego
La Jolla, CA 92093

1. INTRODUCTION

Meteorites are rocks and pieces of iron-nickel alloy which fall to earth from time to time. They were formed about 4.6 billion years ago when our solar system was started. Thus it has been said that meteorites are the Rosetta stones of our solar system.

We use the long-lived radioactive nuclides produced by cosmic ray bombardment, to study the history of the meteorites and also the history of the cosmic rays. When we have these historical facts in our hands, we hope we will be able to understand better how the solar system works, and how it got started. We can also learn more about the nature and origin of the cosmic rays.

We have also had about twelve years' experience now in studying lunar samples. At the beginning it was clear that we could see effects of solar particles in the surface layers of the lunar rocks and soil. These typically have energies around 10-100 MeV/n, and produce relatively few secondary neutrons and so on. So their effects are only seen in the top few centimeters of the moon. The galactic cosmic rays are in the GeV range of energy, so they penetrate much deeper. Also they produce many secondary neutrons and other particles which can go still deeper. Fig. 1 shows the depth profile of 3.7 million years half-life ^{53}Mn in the moon [1]. In the figure, the two regions are clearly seen. Production at depths below a depth of a few grams per cm^2 is due to galactic cosmic rays (GCR). The big increase of ^{53}Mn content near the surface is due to solar cosmic rays (SCR).

We don't see these solar cosmic ray effects in meteorites, not yet anyhow, because the meteorites suffer ablation when they pass through the earth's atmosphere. So they lose centimeters or tens of centimeters of surface stuff. If we could see the original surfaces, we would expect to find solar cosmic ray effects.

We are studying the later history of meteorites using cosmogenic nuclides. When the meteorite parent body broke up, it formed the small objects we see. The meteorite was then bombarded by cosmic rays in space and accumulated various cosmogenic nuclides until it was captured by the earth. This period is what we call the exposure age. If the exposure age is long in comparison with the half-life of the radioactive nuclide, the activity level is saturated. This means that the production rate of a given nuclide is equal to the decay rate. The terrestrial age is the time period between the date a meteorite fell on the earth and the present.

One new and exciting development in meteorite research is the discovery by Japanese and American scientists of more than 5000 new meteorites on the Antarctic ice sheet. This allows us, among many other things, to learn more about the rate of meteorite infall to the earth, and about the history of the big ice sheets themselves.

Why have so many meteorites been found to be concentrated only in certain regions, such as the bare ice field near the Yamato mountains and the Allan Hills? The terrestrial age of the Antarctic meteorites is of importance for understanding both the meteorite accumulation mechanism and the glaciology of the Antarctic continent. The terrestrial ages obtained range between 10,000 and 700,000 years [2, 3, 4]. Thus ^{36}Cl has a good half life ($t_{1/2}$ = 3.0x10^5 y) for terrestrial age determination.

Cosmic spherules are another form of extraterrestrial matter. They

are found in small numbers in deep sea sediments. They seem to represent a much broader class of material than the hard rocks which survive to form our meteorite collections. Surprisingly they can survive in seawater and in sediments for millions of years. Because we have sediments from many geological periods, we can study the meteorite influx in past time too. We have measured ^{53}Mn in a few spherule samples by the neutron activation method [5, 6]. We have not yet succeeded in measuring ^{10}Be, ^{36}Cl and other nuclides in collaboration with others. Because of the small mass of these spherules, sensitive methods are required to detect cosmogenic nuclides. It appears that we can make such measurements using accelerator techniques for several nuclides.

It is extremely valuable to be able to measure two or three or more cosmogenic nuclides on the same sample. We must make some assumptions about the history of each sample. These assumptions may be wrong, especially because we usually lack some basic information about each sample we study. Thus we may not know the size of the object before entering the earth's atmosphere, or the time during which it was exposed to radiation in space. With two or more isotopes, we can tell much more.

This brings us to another point which can't be said too often. For the nuclides we are discussing in this apaper, usually an accuracy of 10% is very useful, because it is hard to reach such accuracy by counting, even with fairly large samples. This is very different for ^{14}C, where several labs can approach 0.1% accuracy today.

The work carried out by our group has been entirely collaborative in nature, because we possess no accelerator facilities. Because of our experience with cosmogenic nuclides in meteorites and lunar samples, and because we are chemists, we have been able to contribute usefully to a

number of researches [3, 4, 7, 8, 9]. We are presently working actively with groups at Rochester and the University of Pennsylvania; we hope to continue joint work with these groups and others. In this paper, we do not show the published results again.

2. DISCUSSION

The accelerator mass spectrometry method helps not only reduce sample size, in most cases by two or three orders of magnitude, but opens another set of cosmogenic nuclides which have not been measured yet. Already ^{10}Be ($t_{1/2}$ = 1.6x10^6 y), ^{36}Cl (3.0x10^5 y) and ^{129}I (1.6x10^7 y) in meteorites have been measured by accelerator mass spectrometry [3, 4, 7, 10]. Possible new candidates for measurement in extraterrestrial materials are ^{26}Al (7.2x10^5 y), ^{41}Ca (1.3x10^5 y), ^{60}Fe ($\sim$10^5 y) and ^{59}Ni (7.6x10^4 y). We hope also to measure ^{146}Sm (1.0x10^8 y) and ^{92}Nb (3.3x10^7 y).

In Fig. 2, some cosmogenic nuclides are shown with various half-lives between 108 y for ^{32}Si and 1.28x10^9 y for ^{40}K. The figure also shows main target elements for extraterrestrial materials. Nuclides which were surrounded by a square have been measured by accelerator mass spectrometry. The right column in the figure shows the preferable methods for measurements of these nuclides in natural samples. The shorter half-life nuclides have higher activity than longer ones, if we compare the same number of atoms. Conventional counting methods are more sensitive than accelerator mass spectrometry for shorter half-life nuclides. On the other hand, the longer half-life nuclides, especially $t_{1/2}$ >10^9 y, are better measured by low energy mass spectrometry. In general, the accelerator mass spectrometry method is very useful for the nuclides whose half-lives are between 10^4 and 10^8 y. Some nuclides, such as ^{53}Mn and ^{81}Kr, can be

measured by other methods with high sensitivity.

The isotope ratio (ratio of radioactive nuclides to stable nuclides) in extraterrestrial material is much higher than the detection limit of the accelerator mass spectrometry, because these materials were exposed to low and high energy primary cosmic ray bombardment in space. On the other hand, the terrestrial material has been shielded by primary cosmic ray bombardment by the earth's very thick atmosphere and magnetic field. However, because of the limited amount of sample material, the absolute amount of the nuclides is very small. For example, we can use only less than a few hundred μg of deep-sea spherules for study.

The ratio of the radioisotope to stable isotope abundance ($N^*/\Sigma N$) in various samples is shown in Fig. 3. The ratio varies from 10^{-4} to 10^{-18} as shown on the vertical axis. The horizontal axis indicates the half-life of radioactive nuclides on a log scale. The hatched area shows a typical detection limit, less than 10^{-15}, at the present time. In the figure, the stars show the isotope ratio of cosmogenic nuclides in meteorites and lunar samples. These are measured values except ^{92}Nb and ^{146}Sm, which were calculated. The circled "S" indicates measured isotope ratios in the deep sea sediments. The radioactive nuclides ^{32}Si, ^{26}Al and ^{10}Be were produced by the interaction of cosmic rays with the earth's atmosphere [11, 12, 13]. Extraterrestrial materials entering the atmosphere contribute nearly all ^{59}Ni and ^{53}Mn [14, 15]. The circle for ^{3}H indicates the ^{3}H/H ratio of rainwater. ^{129}I, ^{236}U and ^{92}Nb indicate the values in nature. The filled triangle is a calculated cosmogenic isotope level which was produced by the interaction of secondary cosmic rays and terrestrial granite. The calculation was made by the Yokoyama et al. [16] method assuming the mean composition of granite, no surface erosion, longer exposure time,

sea level altitude and 8 GV cut off rigidity (La Jolla). It is clear that the cosmic ray produced nuclides in extraterrestrial materials are more concentrated than in terrestrial samples. This of course means easier measurements and a more extended range of possible experiments. The figure also shows the concentrations of many cosmogenic nuclides in terrestrial rocks are higher than the detection limit of this method. However, we will only discuss extraterrestrial materials in this paper.

Table 1 shows the comparison of the minimum extraterrestrial sample requirement for accelerator mass spectrometry and other methods. We assume that 5 mg of source material, as shown in the third column, is required to make a measurement. Based on this source size we could expect to measure the isotope ratio listed in the fourth column. Now we can calculate the minimum number of radioactive atoms in the source sample (column 5). Although the isotope ratio detection limit of some of the nuclides has not been reached, due to their low transmittance, low ionization efficiency or high background noise, we anticipate many improvements in the future. It is clear that accelerator mass spectrometry has provided more than two orders of magnitude improvement in detection limits for many long-lived nuclides.

Using the above nuclides, several applications for extraterrestrial materials will be discussed below.

Galactic Cosmic Rays (GCR)

The secular variation of cosmic rays is one of the important subjects of cosmic ray study. The ^{14}C concentration in tree rings is the most famous and well studied method. The ^{14}C method can reach up to 20,000; it is not sensitive to the rapid change of cosmic ray intensity because of the long residence time in the atmosphere and in the biological chain, although the accuracy reached $\pm 0.1\%$ level. On the other hand, ^{36}Cl and ^{10}Be have

longer half-lives and are made by bombardment of the atmospheric Ar or N and O, respectively. These nuclides are rapidly washed out by rain or snow. Ideally, the annual production rate of ^{36}Cl and ^{10}Be which represents the galactic cosmic ray intensity at the earth, as affected by solar modulation, will be measured in the same ice core using accelerator mass spectrometry. Using this technique, we may extend the study up to 10^5 years based on the age of ice cores. From 10^5 to 10^9 years, we may again use meteorites which have been studied since the 1960's. During the 10^9 year time period, our solar system has revolved around the galaxy several times. We have not resolved the many associated problems such as the cosmic ray intensity change in the galactic arms, local supernova remnants or unknown sources. We can continue to examine these problems using meteorites. In one of the methods, we are measuring nuclides with several different half-lives in iron meteorites which fell to the earth a million years ago. The meteorites contain the cosmic ray records of more than a million years ago.

Solar Cosmic Rays (SCR)

SCR produced nuclides can be directly measured so far only in lunar surface materials, because such low energy ($E \leq 100$ MeV/n) particles can not penetrate the geomagnetic field. We have measured ^{26}Al and ^{53}Mn depth profiles in a few lunar rocks. From these samples we have studied the constancy of SCR over a time scale of millions of years [17]. We may extend the time scale up to 10^7-10^8 y using precise depth profile measurements of lunar rocks and soils. Probes such as ^{129}I, ^{236}U and ^{146}Sm are possible nuclides for such a study. We also consider the solar α-particles interaction $^{56}Fe(\alpha, n)^{59}Ni$, in the surface lunar rocks.

Even though recent instrumental charge and mass identification techniques for current cosmic ray profiles are remarkably accurate and give us many exciting results, it is very important to measure the fossil cosmic ray record in various samples. Although exciting techniques are adequate for the high energy cosmic ray component, low energy resolution needs development. Then, for example, we could measure isotopic components in surface lunar rocks or soils, and long-exposed foils flown on the space shuttle.

Meteorite Bombardment History

Meteorites are very good probes for the study of the various cosmic ray produced stable and radioactive nuclides described above. We can also study the history of meteorites using these cosmogenic nuclides. The exposure ages are split into two groups, typically 3-10x10^6 y for stony meteorites and 5-6x10^8 y for iron meteorites. The cosmic ray bombardment history is a key to the investigation of meteorite origins. Although the multi-stage bombardment history of large iron meteorites is known, clear cases of two-stage bombardment of stony meteorites in space have been found only recently [18]. If we do a systematic survey of cosmogenic nuclides in meteorites, we expect to find more cases of such bombardment history. ^{26}Al, ^{53}Mn or longer half-life nuclides are important for this study. Using small sample sizes, we should measure many nuclides, because the production rate of cosmogenic nuclides is dependent on the size of the meteorite and the depth from which samples are taken. Again accelerator mass spectrometry is very useful for this study.

Cosmic Dust

Deep sea spherules or mini-meteorites, the so-called "cosmic spherules," which were collected from deep sea sediments, are probably a third category

of extraterrestrial materials, even though we are not sure that there are meteorite ablation droplets or true individual micrometeoroids. Several nuclides, which have different half-lives and were formed by various nuclear reactions, can provide information about the origin, the dynamics in interplanetary space and the distribution in space of those materials. We have measured ^{53}Mn in several deep sea spherules [5, 6] by a very sensitive neutron activation method. These spherules are too small, less than a few hundred micrograms, to measure by conventional low level counting methods. It is therefore ncessary to use accelerator mass spectrometry for these samples. In the future we hope to use this method to measure some cosmogenic nuclides even in the very tiny "Brownlee particles" which were collected in the stratosphere and probably have a cometary origin [19].

Acknowledgements

We have profited from discussions with many colleagues, but especially those with our collaborators M. Honda, D. Elmore, H. Gove, and R. Middleton. This work was supported by NASA Grant NGL 05-009-148.

References

1. Nishiizumi, K., Imamura, M., Kohl, C. P., Murrell, M. T., Arnold, J. R. and Russ, G. P. III (1979) The extent of lunar regolith mixing, Earth and Planet. Sci. Lett., 44, 409-419.

2. Fireman, E. L. (1980) Carbon-14 and Argon-39 in ALHA meteorites, Proc. Lunar Planet. Sci. Conf., 11th, 1215-1221.

3. Nishiizumi, K., Arnold, J. R., Elmore, D., Ferraro, R. D., Gove, H. E., Finkel, R. C., Beukens, R. P., Chang, K. H. and Kilius, L. R. (1979) Measurements of ^{36}Cl in Antarctic meteorites and Antarctic ice using a Van de Graaff accelerator, Earth and Planet. Sci. Lett., 45, 285-292.

4. Nishiizumi, K., Murrell, M. T., Arnold, J. A., Elmore, D., Ferraro, R. D., Gove, H. E. and Finkel, R. C. (1981) Cosmic ray produced ^{36}Cl and ^{53}Mn in Allan Hills-77 meteorites, Earth Planet. Sci. Lett., 52, 31-38.

5. Nishiizumi, K. and Brownlee, D. E. (1979) Measurement of cosmic ray produced ^{53}Mn in deep sea metallic spherules, Proc. 16th International Cosmic Ray Conf., Kyoto, OG 12-17.

6. Nishiizumi, K., Murrell, M. T., Davis, P. A. and Arnold, J. R. (1980) Cosmic ray produced ^{53}Mn in deep sea spherules, Meteoritics, 15, 342.

7. Elmore, D., Gove, H. E., Ferraro, R., Kilius, L. R., Lee, H. W., Chang, K. H., Beukens, R. P., Litherland, A. E., Russo, C. J., Murrell, M. T. and Finkel, R. C. (1980) Determination of ^{129}I using Tandem acceleration mass spectrometry, Nature, 286, 138-140.

8. Elmore, D., Anantaraman, N., Fulbright, H. M., Gove, H. E., Hans, H. S., Nishiizumi, K., Murrell, M. T. and Honda, M. (1980) Half-life of ^{32}Si using Tandem accelerator mass spectrometry, Phys. Rev. Lett., 45, 589-592.

9. Finkel, R. C., Nishiizumi, K., Elmore, D., Ferraro, R. D. and Gove, H. E. (1980) ^{36}Cl in polar ice, rainwater and seawater, Geophys. Res. Lett., 7, 983-986.

10. Moniot, R. K., Kruse, T. H., Savin, W., Hall, G. S., Milazzo, T. and Herzog, G. F. (1981) ^{10}Be in stony meteorites by accelerator-based mass spectrometry, (Abstract) Lunar Planet. Sci. XII, 711-713.

11. Lal, D., Goldberg, E. D. and Koide, M. (1960) Cosmic ray produced silicon-32 in nature, Science, 131, 332-337.

12. Reyss, J. L., Yokoyama, Y. and Tanaka, S. (1976) Aluminum-26 in deep-sea sediment, Science, 193, 1119-1121.

13. Arnold, J. R. (1956) Beryllium-10 produced by cosmic rays, Science, 124, 584-585.

14. Yamakoshi, K. and Yanagita, S. (1981) Cosmic ray produced ^{59}Ni in marine sediments, Earth Planet. Sci. Lett., 52, 259-263.

15. Imamura, M., Inoue, T., Nishiizumi, K. and Tanaka, S. (1979) ^{53}Mn in deep-sea sediment cores — An indicator of past solar activity, Proc. 16th International Cosmic Ray Conf., Kyoto, OG 12-21.

16. Yokoyama, Y., Reyss, J. and Guichard, F. (1977) Production of radionuclides by cosmic rays at mountain altitudes, Earth Planet. Sci. Lett., 36, 44-55.

17. Kohl, C. P., Murrell, M. T., Russ, G. P., III and Arnold, J. R. (1978) Evidence for the constancy of the solar cosmic ray flux over the past ten million years: ^{53}Mn and ^{26}Al measurements, Proc. Lunar Planet. Sci. Conf., 9th, 2299-2310.

18. Nishiizumi, K., Imamura, M. and Honda, M. (1979) Cosmic ray produced radionuclides in Antarctic meteorites, Mem. National Inst. Polar Res., Spec. Issue, 12, 161-177.

19. Brownlee, D. E., Tomandl, D. A. and Olszewski, E. (1977) Interplanetary dust: A new source of extraterrestrial material for laboratory studies, Proc. Lunar Sci. Conf., 8th, 149-160.

Nuclides	$T_{1/2}$ (yr)	Accelerator Mass Spectrometry: Chemical Form	Isotope Ratio	Atoms	Required Sample (g)	Others: Method*	Required Sample (g)
^{32}Si	108	SiO_2	10^{-13}	5×10^{6}	75	$\beta(^{32}P)$	$\gtrsim 20$
^{59}Ni	7.6×10^{4}	Metal	10^{-13}	5×10^{6}	2×10^{-3}	X	~ 2
^{41}Ca	1.3×10^{5}	CaO	10^{-14}	5×10^{5}	2×10^{-3}	X	$\gtrsim 25$
^{36}Cl	3.0×10^{5}	AgCl	10^{-14}	2×10^{5}	5×10^{-5}	β	~ 2
^{26}Al	7.2×10^{5}	Al_2O_3	10^{-14}	6×10^{5}	2×10^{-5}	γ-γ	$\lesssim 1$
^{10}Be	1.6×10^{6}	BeO	10^{-14}	1×10^{6}	5×10^{-5}	β	~ 1
^{53}Mn	3.7×10^{6}	Mn_3O_4	10^{-13}	4×10^{6}	2×10^{-4}	NAA	$\gtrsim 10^{-4}$
^{129}I	1.6×10^{7}	AgI	10^{-12}	1×10^{7}	2	NAA	< 5
^{236}U	2.3×10^{7}	?	--	10^{7}	10 (Euc) 1 (lunar)	Mass.Sp.	1 (lunar)
^{92}Nb	3.3×10^{7}	Nb_2O_5	10^{-12}	2×10^{7}	2	γ-γ	$>10^{5}$
^{146}Sm	1.0×10^{8}	Sm_2O_3	10^{-12}	2×10^{7}	10	α	$>10^{3}$

* X : X-ray counting
β : β counting
α : α counting
NAA : neutron activation analysis
γ-γ : γ-γ coincidence method

Table 1. Comparison of the minimum extraterrestrial sample requirement for accelerator mass spectrometry and other methods.

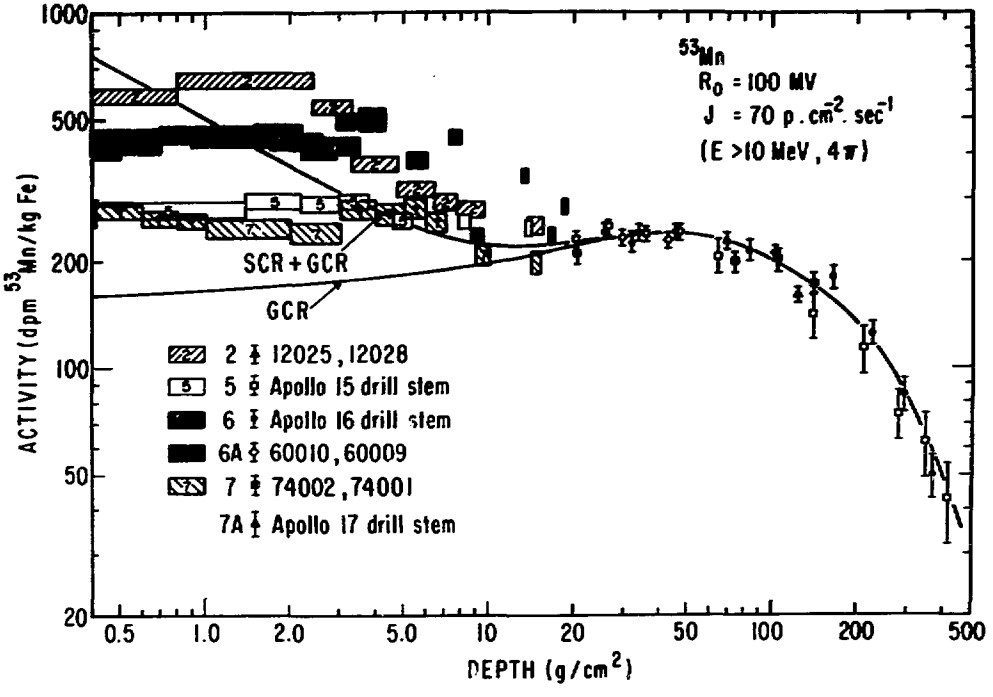

Fig. 1. ^{53}Mn data in lunar cores (Nishiizumi et al., 1979). The theoretical curves were calculated using the Reedy-Arnold model.

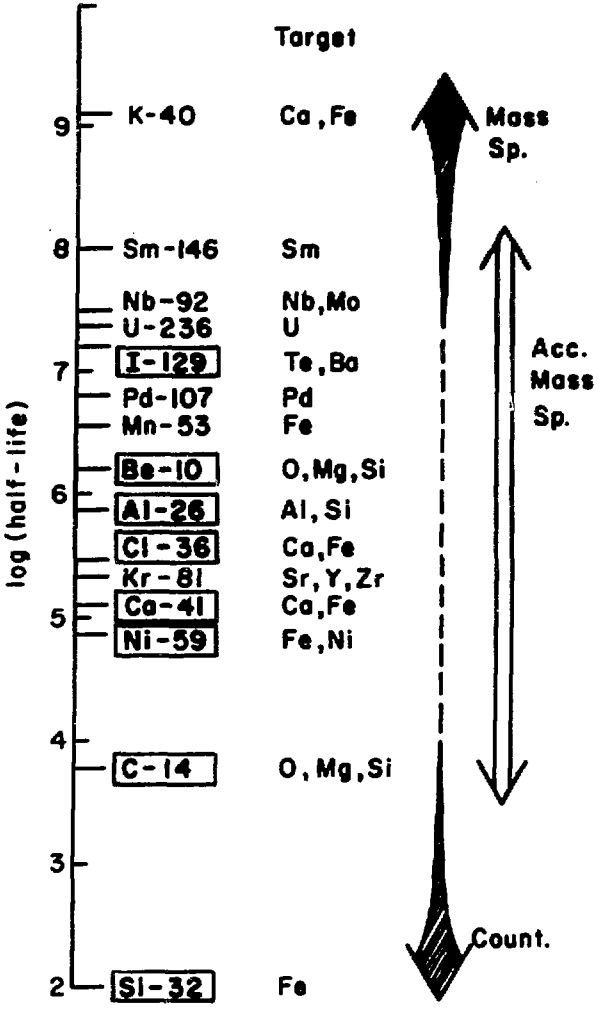

Fig. 2. Cosmogenic nuclides with various half-lives. Nuclides which were surrounded by a square have been measured by accelerator mass spectrometry.

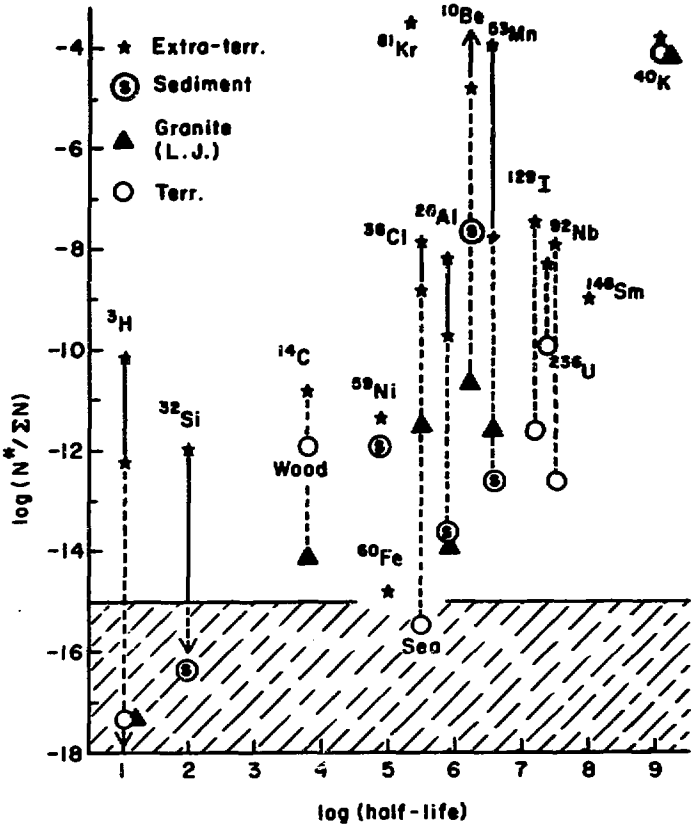

Fig. 3. The ratio of the radioisotope to stable isotope abundance ($N^*/\Sigma N$) in various samples. The hatched area shows a typical detection limit at the present time.

TANDEM VAN DE GRAAFF MEASUREMENT OF ^{10}BE IN METEORITES

T. H. Kruse, R. Moniot, Dept. of Physics and Astronomy
G. Herzog†, T. Milazzo, and G. Hall, Dept. of Chemistry
Rutgers University*, New Brunswick, N. J. 08903

W. Savin, Dept. of Physics
New Jersey Institute of Technology, Newark, N. J. 07102

1. METEORITES AS PROBES IN TIME AND SPACE

Meteorites represent the beginnings of the solar system, according to Sr-Rb and Pb-Pb ages of 4.6 billion years.[1] Their chemical and mineralogical properties are therefore instructive concerning conditions of formation.

Meteorites also represent integrating probes of cosmic ray intensities and variations in the solar system.

^{10}Be, with a half-life of 1.5 million years, can only provide information on cosmic ray interactions during the last 10 million years or so. The specific ^{10}Be content is an integral over time, the cosmic ray spectrum, nd the elemental composition of the samples, which fall into the general classes of stones (predominantly silicates) and irons (largely iron-nickel). In addition to compositional variation, ^{10}Be yield will depend on sample depth and size, i.e. shielding.

On atmospheric passage, the surface of a meteorite is ablated, removing the effects of solar and other low energy protons, and leaving the effect of high energy galactic protons and their secondaries. Most stony meteorites are recovered within a few hundred years of their fall, a time short compared to the ^{10}Be half-life, so that the ^{10}Be contents measured reflect their cosmic ray exposure in space rather than terrestrial decay.

With a constant cosmic ray flux, the shielding-corrected ^{10}Be content of a particular meteorite type should fall on a growth curve of the form $(1-e^{-\lambda t})$. If the rocks have persisted in space unaltered for longer than several half-lives, all samples would show the same equilibrium value of specific ^{10}Be content. In fact, some samples do have smaller than equilibrium values, implying "recent" collisional breakup.

A method of extending the range of determination of exposure ages is the measurement of the specific content of cosmic-ray produced stable rare-gas isotopes which, however, carry no intrinsic time scale. One of the objects of our ^{10}Be measurements is to apply the ^{10}Be time scale to a recalibration of the production rate of ^{21}Ne by comparing specific ^{21}Ne (linear buildup) and ^{10}Be ($1-e^{-\lambda t}$) measurements on the same meteorite. Another, more speculative interest, is to search for time variations in the galactic cosmic ray flux within the solar system, as might be evidenced by discrepancies between age measurements based on radioisotopes with different half lives.

2. METHODS

The Rutgers FN tandem Van de Graaff acceleration, beam handling, and detection scheme[2,3] are shown in Figure 1 (focusing devices omitted for clarity). The ion source is the earliest Extrion version of the Middleton cesium sputter source, operated in the reflection geometry.[4] Measurements involve several alternating ^{9}Be and ^{10}Be measurements, first on a standard, then on the unknown sample, then again on the standard. ^{9}Be is measured by counting 90° Rutherford scattering from a removable 1 mg/cm^2 gold foil near the image position of the analyzing magnet.

^{10}Be and ^{9}Be are analyzed in the 3^+ charge state after (oxygen) gas or gas + foil terminal breakup (6.2 MV) and stripping of the injected BeO^-. Near the analyzing magnet image position a 40 μgm/cm^2 carbon foil changes the magnetic rigidities, converting most of the 3^+ ^{10}Be and ^{9}Be to 4^+, most of the 3^+ ^{10}B isobar to 5^+, and most parasitic C and O beams to a new charge state which will not transmit further. Remaining beams are ^{10}Be (21 MeV), ^{10}B, and parasitic (double charge exchange) ^{9}Be, all in the 4^+ state. A nickel foil of 1.8 mg/cm^2 at the target position of the split-pole magnetic spectrograph disperses ^{10}Be, ^{9}Be, and ^{10}B in the focal plane by differential energy loss.

A thin window (0.06 mil Mylar) counter telescope (Figure 2) consisting of a proportional counter (90 mm Hg of argon-methane) (ΔE) and a position-sensitive silicon counter (xE and E) provides

computer input to a software identification of ΔE-E regions of interest, for x (position) gating.[5]

For typical stony meteorites, background (measured using a reagent grade ^{9}BeO sample) was a few percent of signal. Recent measurement shows no background counts in 15 minutes, after source overhaul.

Typical performance and results are shown in Tables 1 and 2. Higher currents are expected from an inverted (Chapman) sputter source under construction.

TABLE 1. Cleanup Factors

	^{10}B	^{9}Be	Other (^{12}C, ^{16}O)
Post-stripper Foil $^{10}Be^{+3} \rightarrow {}^{10}Be^{+4}$	50	1.0	$>10^4$
Energy-loss Foil + Spectrograph	10^4	10^2	--
ΔE, E Signal Windows	10^4	10^2	--
Position Signal	>10	10^4	--

TABLE 2. Typical Data

Sample*	^{10}Be Count Rate	^{9}Be Count Rate
Stony Meteorite	0.5 cps	200 cps
Iron Meteorite	0.05 cps	200 cps
Blank		
Reagent BeO	0.003 cps	400 cps
(or: Volcanic Rock, Gibeon Iron Meteorite)		
Standard $^{10}Be/^{9}Be = 10^{-8}$	40 cps	1200 cps (∿7 nA Beam Current)
Overall detection efficiency ($\frac{\text{Total Counts } ^{10}Be}{^{10}Be \text{ Atoms in Sample}}$)		∿10^{-6}

*From 0.25g of meteorite + 100 μg ^{9}Be carrier.

Prior chemical concentration of Be is performed by a process of acid digestion, solvent extraction, and ion exchange.[6] A few micrograms of ^{9}Be is added during this process, for recovery check by atomic absorption. About 100 μg additional ^{9}Be is added for handling before preparation of the final BeO sample by precipitation (ammonium hydroxide), centrifuging and drying.

BeO samples require conditioning by Cs bombardment for an hour or so. No oxygen gas flow is used in the source. The analyzed beam of ^{9}Be is then a few charge nanoamperes. A sample lasts for many hours and is not exhausted during data accumulation of an hour or two. A cycle of ^{9}Be-^{10}Be counting consists of a minute for ^{9}Be and a few minutes for ^{10}Be. Only the inflection and analyzing magnets and the high energy magnetic quadrupoles are varied. Magnetic dipoles and quadrupoles downstream from the analyzer transmit only ^{10}Be and background beams and are not varied.

Among the advantages of the acceleration method for ^{10}Be is that radiochemical purity is not required, merely concentration. A basic limitation in our data rate is the ^{9}Be dilution necessary for handling. The known amount of ^{9}Be carrier being much greater than the meteoritic content, the $^{10}Be/^{9}Be$ ratio measurement and knowledge of meteorite sample weight enables calculation of specific ^{10}Be content in the meteorite sample. The result is naturally expressed in disintegrations per minute per kilogram of sample, independent of half-life. The standard was prepared by dilution of a commercial ^{10}Be solution, the activity of which was determined independently by the supplier and by us, with agreement to within 2%.

Errors assigned to these ratio measurements are dominated by observed variations, rather than by statistics.

3. RESULTS

Comparison of the accelerator ^{10}Be results for long exposure ages (dpm/kg) with those of decay counting are shown in Tables 3 and 4. As expected from the production mechanism, the ^{10}Be contents of the irons are much lower than those of the stones.

TABLE 3. ^{10}Be in Meteorites of Long Exposure Age.
Stony Meteorites

	Meteorite	^{10}Be (This Work)	^{10}Be for Comparable Meteorite	
Ordinary Chondrites				
	ALHA 78084	17.9 ± 1.8	Y 7304	19 ± 2 (1)
	Seres	19.5 ± 1.0 21.3 ± 1.4	Bruderheim	19 ± 2 (2)
	Adrian	23.5 ± 3.8	Achilles	19 ± 2 (2)
Achondrite				
	Johnstown	27.3 ± 1.8	Consistent with higher O content	

(1) Nishiizumi et al. (1979)
(2) Honda and Arnold (1964)

TABLE 4. ^{10}Be in Meteorites of Long Exposure Age.
Iron Meteorites

Meteorite	^{10}Be (This Work)	^{10}Be for Comparable Meteorite	
Odessa	1.72 ± 0.08	Odessa	1 - 2 (1)
Butler	2.84 ± 0.63	Range for Iron Meteorites	0 - 6 (2)
Gibeon	<0.05 ± 0.02 (3)		

(1) Honda and Arnold (1964)
(2) Chang and Wänke (1969)
(3) Upper limit, equal to blank level.

A test of shielding effects was undertaken on samples from various depths of an Antarctic meteorite, ALHA 78084 (Allen Hills). Theoretical comparison is complicated by shape effects; however, results agree with general expectation that ^{10}Be production is not a strong function of depth, since ^{10}Be is mainly a high energy product.

The specific ^{10}Be content of one achondrite (Johnstown) was found to be higher than the equilibrium value for the general run of chondritic meteorites in accord with its higher content of

oxygen, the principal target for spallation production of ^{10}Be.

It is premature to draw any conclusion on variation of the high energy cosmic-ray flux as suggested by ^{26}Al and ^{53}Mn comparisons.[7,8] Progress is shown in Figure 3 toward use of the ^{10}Be time scale (short exposure age stony meteorites) to calibrate the "recent" ^{21}Ne cosmic-ray production rate in stony meteorites. More data and higher precision are needed, as well as checking of some discrepant results. There seem to be reasonable prospects of obtaining a calibration, relevant to the recent cosmic-ray flux, for this stable rare gas isotope which, in many cases, suffers neither from an excessive diffusion loss nor from contamination by an excessive primordial component.

REFERENCES

†Supported in part by the National Aeronautics and Space Agency.
*Supported in part by the National Science Foundation.

1. The Nature and Origin of Meteorites:
D. W. Sears, 1978, Oxford (New York).

2. W. Savin, T. Kruse, R. Moniot:
Bull. Am. Phys. Soc. 26, 543 (1981).

3. R. K. Moniot, T. H. Kruse, W. Savin, G. S. Hall, T. Milazzo, and G. F. Herzog:
Lunar and Planetary Science XII, 711-713 (1981).

4. F. H. Schmidt and G. W. Farwell:
Bull. Am. Phys. Soc. 24, 650 (1979).

5. M. E. Williams, T. Kruse, D. Bayer, N. Williams, and W. Savin:
Nucl. Instr. Meth. 102, 201 (1972).

6. J. Korkisch and A. Sorio:
Analyt. Chim. Acta 82, 311-320 (1976).

7. O. Müller, W. Hampel, T. Kirsten, and G. F. Herzog:
Geochim. Cosmochim. Acta 45, 447-480 (1981).

8. K. Nishiizumi, S. Regnier, and K. Marti:
Earth Planet. Sci. Lett. 50, 156-170 (1980).

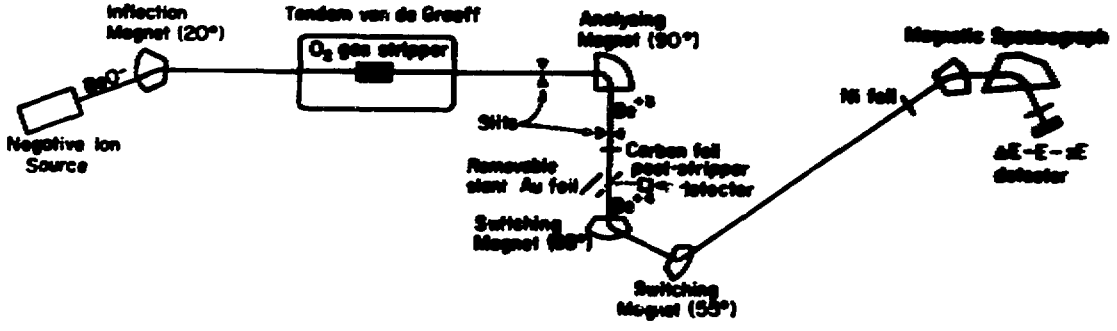

Fig. 1 Beam Layout

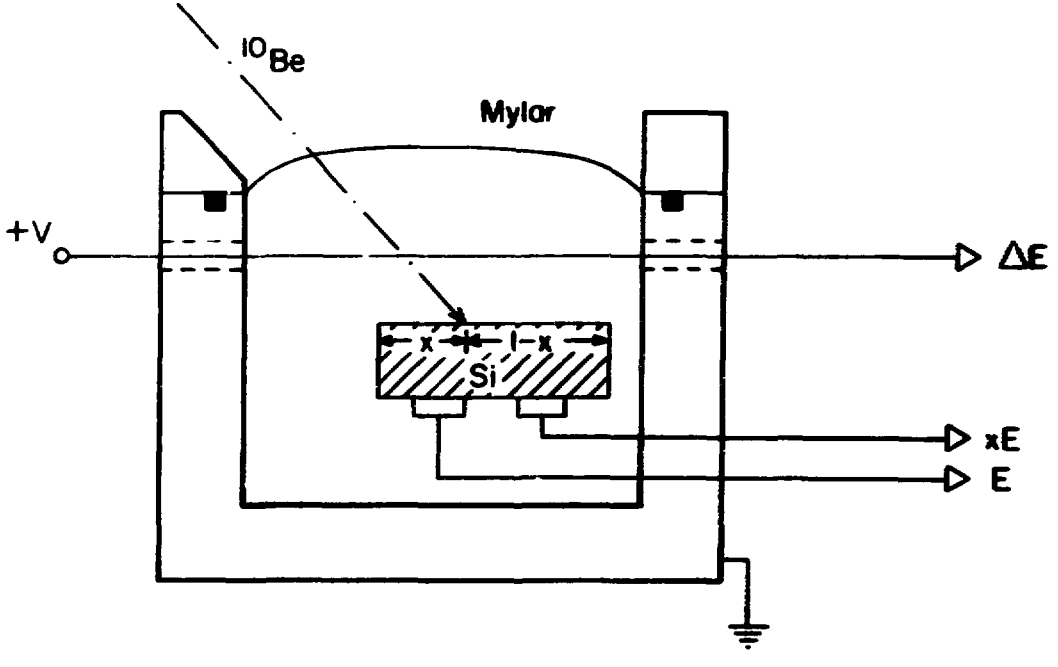

Fig. 2 Counter Telescope

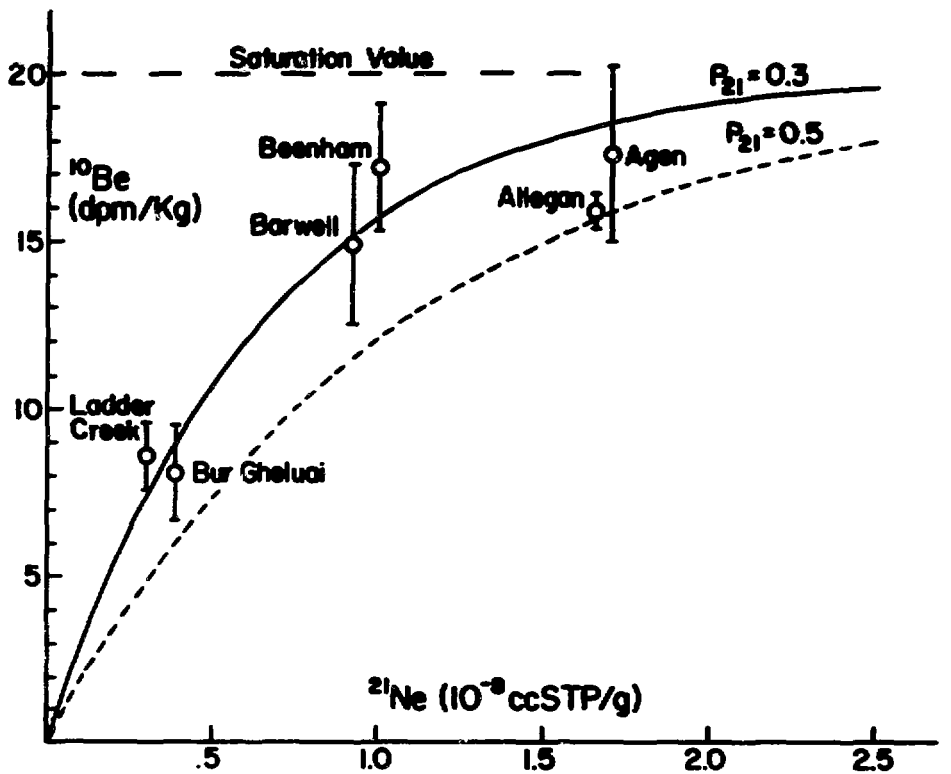

Fig. 3 $^{10}Be - ^{21}Ne$ Growth Curve

EARTHQUAKE DATING BY ^{14}C ATOM COUNTING

A. B. Tucker
Physics Department, San Jose State University
San Jose, California 95192

G. Bonani, M. Suter, and W. Woelfli
Laboratorium für Kernphysik, Eidg. Technische Hochschule
8093 Zurich, Switzerland

1. INTRODUCTION

In the absence of written records that go back more than 150 years, the frequency of major earthquakes in the seismically active regions of the western United States can only be deduced from geologic evidence. Scarps along the Wasatch fault near Salt Lake City, Utah exhibit cumulative surface displacements as large as 10 meters in alluvial deposits that post-date the recession of Lake Bonneville 12,000 years ago; although no damaging earthquakes have occurred since the area was settled. Recent trenching studies by Swan et al. (1) have exposed ancient surface soil layers in which discontinuities reveal a sequence of significant surface faulting events. Radiocarbon dates of detrital charcoal from these deposits would be a record of earthquake recurrence intervals, vital data for contemporary earthquake hazards assessment. Most of the samples collected so far have been too small for conventional beta-decay counting. We report a successful radiocarbon assay by direct atom counting of four milligram-sized specimens from the Wasatch study.

2. MEASUREMENTS

The specimens consisted of small flecks of charcoal, presumably residue form forest fires, separated from soil samples taken from exploratory trenches on the Wasatch fault at Little Cottonwood Canyon, 20 km south of downtown Salt Lake City. Sputter source targets were prepared by dissolving approximately 4 mg of each sample in 50 mg of iron melted under vacuum. The resulting material would adhere to small tungsten blades which could be mounted in standard cones. Similar calibration targets were prepared from four charcoal specimens with known ages between 250 and 10,000 years, as determined by beta counting at radiocarbon labs at the University of Bern and the U. S. Geological Survey in Menlo Park.

The measurements were made with the EN tandem Van de Graaff accelerator at the ETH, Zürich in the summer of 1980. This facility is described in ref. 2. Mass selection of negative ions from a cesium sputter source was made by the injection magnet, the only element changed during the isotope counting cycle. Following acceleration, 22 MeV 3+ ions were selected by a 15° electrostatic analyzer. After precise collimation by a double set of slits defining beam direction as well as position, the monoenergetic ions were sorted in a magnetic spectrometer. Separate ports were provided for masses 12, 13, and 14; the field strength being held constant. The abundant isotopes were counted by collecting their currents in long Faraday cups. Atoms at the mass 14 port were detected and identified by a two-stage (dE/dx - E) gas filled ionization counter. The spectrum in Fig. 1 shows the separation of ^{14}C from background ^{14}N and ^{13}C.

The data were taken in a series of counts alternating between calibration and unknown samples. Each run consisted of a sequence of 20 computer controlled 3-minute counting cycles, 15 seconds at mass 12 and at mass 13 then 150

seconds at mass 14. With this slow switching sequence, the $^{12}C^-$ beam had to be restricted to less than 200 nA to maintain stable accelerating voltage under the different beam loads. (In another paper, Suter reports the improvement achieved with faster switching.) Table 1 and Fig. 1 are typical data from one of the unknowns. The C13/C12 ratio was a monitor of system stability. The rms deviation of the C14/C12 ratios was compared to the fluctuation expected from the small number of total C14 counts; they were always consistent. Each sample was counted a minimum of three times during the 72 hours of the experiment. Repeated measurements agreed within the statistical accuracy of the C14 counts, approximately 10%.

Figure 2 displays the results. The four calibration points fall on a straight line with slope corresponding to a half-life of 5568 years, the vaule used in decay dating. All the geologic specimens produced countable beams. Unknown to us during the experiment, the geologists suspected sample WCC-4 to be modern material from a burned root. The data confirm this. Three specimens were ancient material, having C14/C12 ratios corresponding to ages of 7800, 8800, and 9000 years with counting statistical uncertainties of $\pm$ 600 years. These ages are consistent with the geologic evidence that this material was deposited after the recession of Lake Bonneville about 12,000 years ago. A larger charcoal sample from a nearby site had an age, as determined by beta counting, of approximately 5,600 years. Unfortunately, strata in the formation from which this sample was taken could not be correlated with those at Little Cottonwood Canyon, but the similarity of the ages of samples from the two sites was expected.

3. FUTURE APPLICATIONS

Atom counting offers the field geologist two advantages over the standard beta counting technique. First is the ability to analyze very small samples, a few milligrams compared to the grams required by commercial radiocarbon labs. If a fleck of charcoal can be seen, it can be counted. This capacity should lead to new data from strata in which no large specimens exist.

Second is the potential for prompt results. Decay counting takes weeks or, for small samples, months. The atom counting facilities being developed throughout the world will be able to date samples within days. Data can be available while a trench is still open and the geologists are still in the field. Preliminary judgements can be tested and revised while additional samples are still easily available.

The atom counting technique has been improved significantly during the past year. In another paper presented here, the ETH group report measurements of 1% accuracy requiring only a few minutes of accelerator time (3). The limit to the accuracy of dates from geologic specimens will be our understanding of contamination with "old" or "new" carbon.

Acknowledgments: This work was supported in part by the Swiss National Science Foundation, the U. S. Geological Survey Earthquake Hazards Reduction Program, and Chevron Oil Field Research Corporation.

REFERENCES

1) F. Swan III, D. Schwartz, and Lloyd Cluff, Bull. Seis. Soc. Am. 70, #5 (1980).

2) M. Suter, R. Balzer, G. Bonani, W. Woelfli, J. Beer, H. Oeschger, and B. Stauffer, IEEE Transactions on Nuclear Science, Vol. NS-28 #2, 1475 (1981).

3) M. Suter, R. Balzer, G. Bonani, W. Woelfli, J. Beer, H. Oeschger, and B. Stauffer. This report, p. 87.

Table 1. Typical raw data for sample WCC-2.

Cycle	C14[a]	C13[b]	C12[b]	C13/C12[c]	C14/C12[d]
1	7	3884	1221	1.060	0.382
2	5	4059	1258	1.075	0.265
3	7	4150	1304	1.061	0.358
4	5	4285	1355	1.054	0.246
5	5	4418	1347	1.093	0.248
6	2	4381	1284	1.137	0.104
7	11	4257	1321	1.074	0.555
8	8	4553	1295	1.172	0.412
9	3	4425	1409	1.047	0.142
10	5	4581	1420	1.075	0.235
11	10	4549	1411	1.075	0.473
12	8	4428	1336	1.105	0.399
13	8	4548	1431	1.059	0.373
14	3	4588	1443	1.060	0.139
15	5	4592	1436	1.066	0.232
16	4	4625	1415	1.089	0.189
17	6	4520	1412	1.067	0.283
18	4	4669	1466	1.062	0.182
19	7	4676	1465	1.064	0.319
20	8	4709	1476	1.063	0.361
Totals	121 (±9%)			1.077 (±0.6%)[e]	0.293 (±9%)[e]

a) Counts.
b) Integrated current, different normalizations for C12 and C13.
c) Percent.
d) Normalized to 1.0 for the expected ratio from contemporary material.
e) Standard deviations.

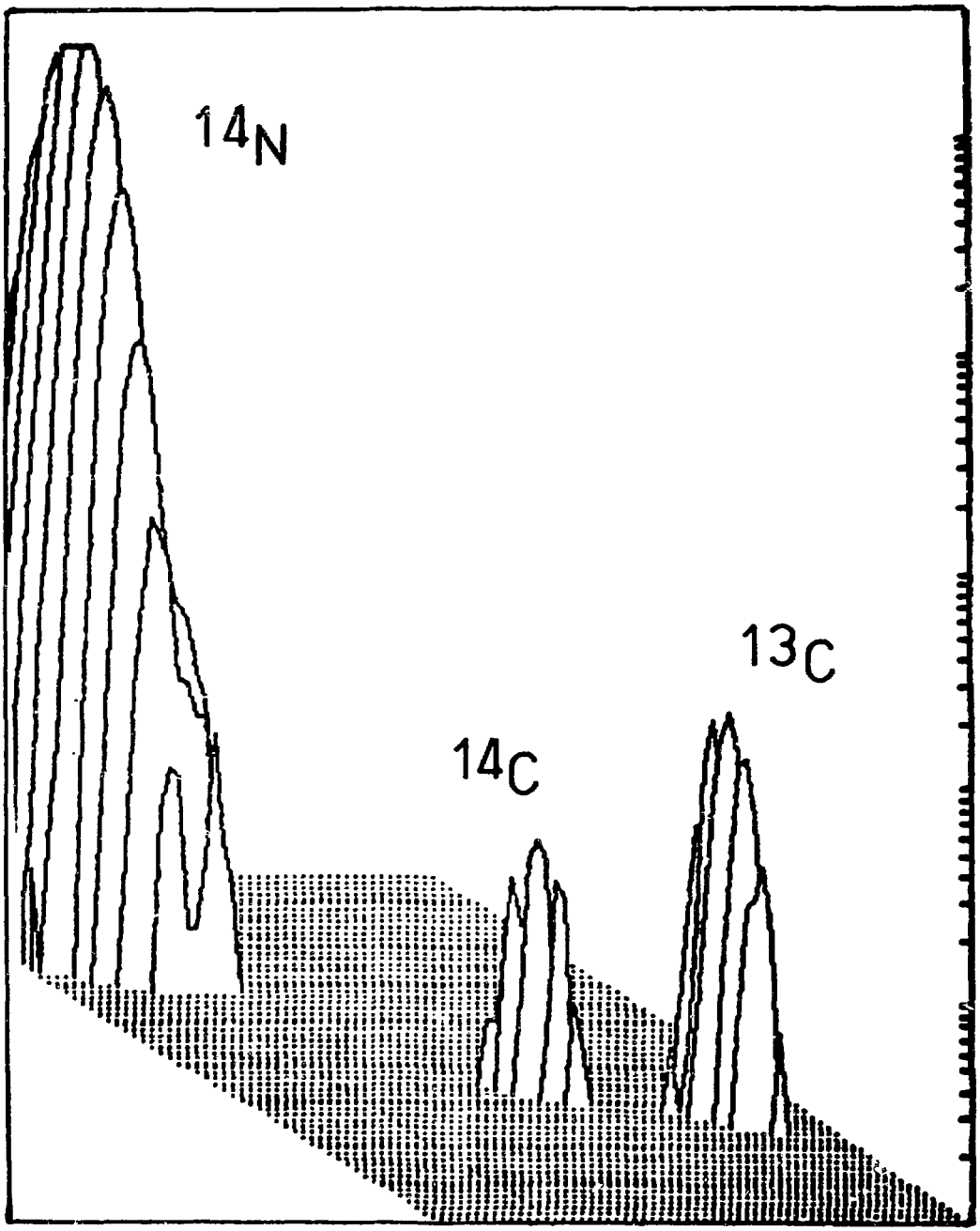

Figure 1. Expanded portion of the particle identification spectrum, ΔE vs $(E_{total}-\Delta E)$.

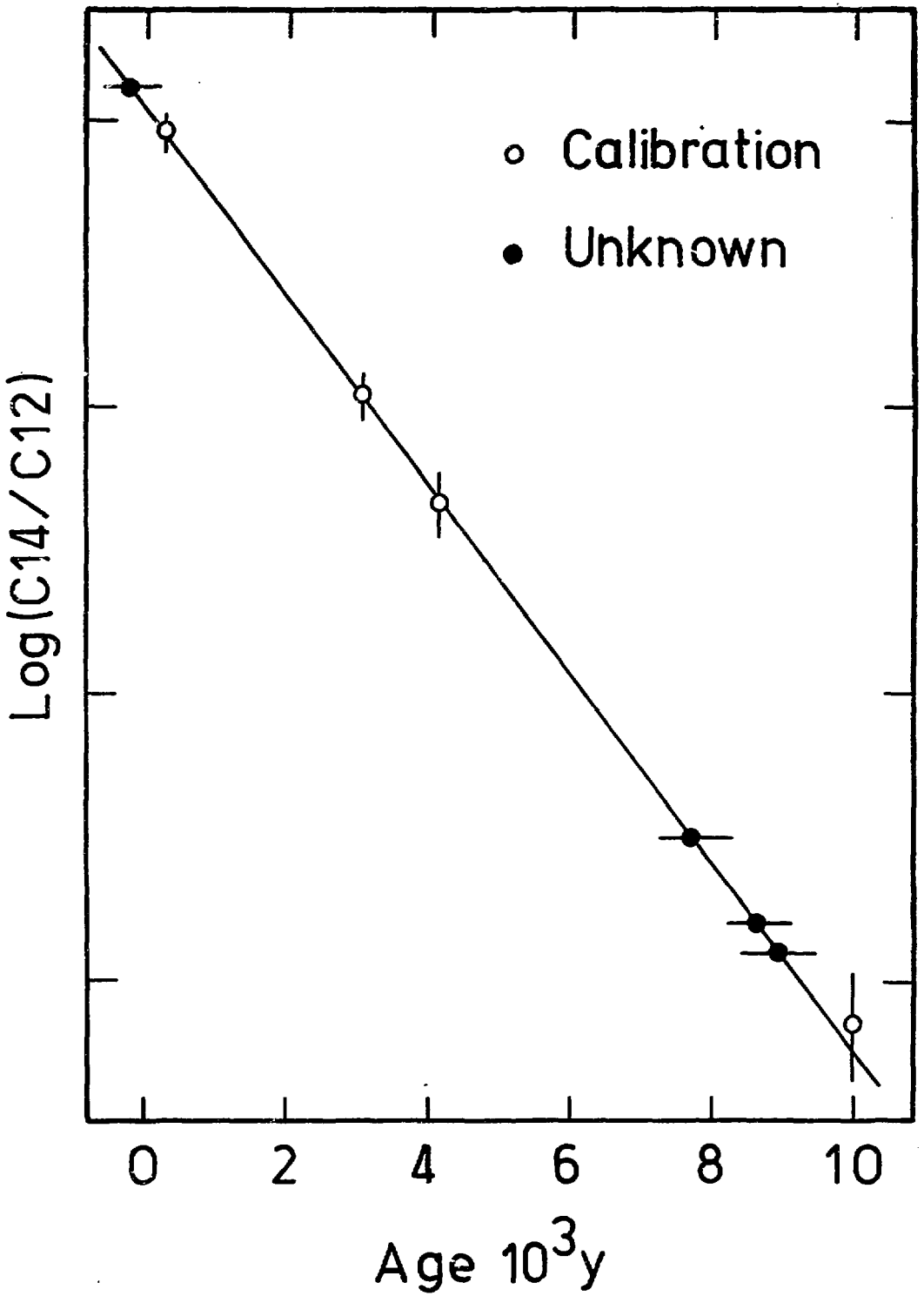

Figure 2. Results. Open circles are calibration points fit with a half life of 5568 years; solid circles are data from the unknowns.

STABLE ISOTOPE APPLICATIONS OF AMS IN GEOLOGY

J. C. Rucklidge
Department of Geology, University of Toronto
Toronto, M5S 1A1 Canada

1. INTRODUCTION

The subject of geochemistry has become increasingly concerned with the distribution of trace elements in and between mineral phases. Part per million detection is routine, but part per billion measurements are, for certain elements, beyond the range of such sensitive analytical methods as neutron activation analysis (NAA). Tandem AMS has the ability to extend this limit several orders of magnitude for those elements which readily form negative ions. There is no doubt that such information can be most valuable for elements which are partitioned strongly between different mineral phases. While bulk analyses may indicate trace levels of certain elements to be present in a rock, it has always been difficult to state with certainty whether the trace element occurs at a uniformly low level throughout the various phases, or whether it is concentrated at a high level in small grains of an extremely rare phase scattered through the rock. The milli- or micro-probe analytical capability, which can be part of AMS, enables such problems concerning ultra-low level element concentrations to be tackled. With the same approach isotopic ratios of both major and minor elements in microgram amounts of material may be undertaken.

2. TRACE ELEMENT ANALYTICAL METHODS

Some of the commonly used methods for trace element analysis in geological materials such as rocks and minerals are summarized in Table 1. The bulk method which has the greatest sensitivity is neutron activation analysis (NAA), and for suitable elements this is capable of approaching the ppt (parts per trillion) level. However, sensitivity may vary by several orders of magnitude between chemically comparable elements (e.g. a factor of 2000 between Ir and Pt is given by Crockett and Teruta [1]) and there may be elements for which analysis is not possible. The need to irradiate the samples and to handle them subsequently during counting adds an undesirable hazard to the measurements, especially if radiochemical separation has to be

undertaken. Further, the time required to perform the analysis may extend into periods of weeks because of the need to wait for decays to give optimum counting opportunities. On the other hand, data for many elements can be obtained with a single irradiation.

Table 1

Methods for trace element assay

Bulk methods	Limit	Comments
X-ray Fluorescence	1ppm	Spectral overlaps
Neutron Activation	1ppb	Selective, slow
Spark Source Mass Spec.	1ppm	Molecular interferences
		Ionization problems
Micro (milli) methods		
Electron Probe	100ppm	Bremstrahlung
Ion Probe	1ppm	Molecular interferences
Accelerator Mass Spec.	1ppb	Negative ions

X-ray fluorescence (XRF) has been the method widely applied to trace analysis in the ppm range. It is non destructive, and avoids many of the inconveniences of NAA, and sensitivity is more or less a continuous function of an element's position in the periodic table. Heavy elements, which are those most likely to be of interest at the trace level, have to be analysed by the complex L spectra, which frequently overlap. This problem, coupled with the ubiquitous presence of a certain level of background radiation limits detection, generally speaking, to the 1-10 ppm range [2].

Spark source mass spectometry, in which a few milligrams of rock are heated in an arc discharge, produces ions which are analysed in a mass spectrometer. This has the potential of extremely high sensitivity for measurement of both absolute amounts of an element, and isotope ratios. Unfortunately the yield of ions of a particular species is strongly temperature dependent, and large numbers of molecular ions are produced, which may interfere with the ions of interest. Thus, although broad band measurements are in principle possible, the promise of this technique does not seem to have been realized, and sensitivities around 1 ppm appear to be

as good as can be attained in practice [3].

The methods described above are used on homogenized rock powder, and give no information as to how the elements may be distributed between the different mineral phases present in a rock. Information regarding element partitioning is of vital importance in attempting to determine the origin and history of a rock, and also in understanding the behaviour of trace elements under various geochemical processes. For this type of information, mineral grains have to be analysed in the undisturbed rock, and a micro-analytical method is required. 'Micro' implies studying with probe of micrometer dimensions, while a less spatial demanding milli-probe (millimeter dimensions) may give appropriate information if the grain size is course enough. Typically the grain size of an igneous or metamorphic rock is a function of the rate of crystallization, with plutonic rocks having a size range of 1-5 mm, while volcanic rocks are much finer, with grains down to micron dimensions. These are very rough generalizations.

The electron micro-probe analyzer (EPMA) has been the tool which in the past twenty years has revolutionized our understanding of minerals as they relate to rocks [4]. A focussed beam of electrons is directed onto a polished section of a rock and the emitted X-rays contain the spectra of the elements present. The intensities of the principle spectral lines, when compared with standards, allow concentrations in micro volumes to be determined. By scanning the probe the concentration profile of an element in and between minerals can be found. This method is most valuable for major elements (>0.5%) because there is considerable background contributed by the ever-present bremstrahlung radiation. This limits the useful detection limit to about 100ppm for favourable elements in the first transition series. Elements lighter and heavier suffer through low emission and high matrix absorption for the former, and spectral complexity and overlap for the latter, as described for XRF. Consequently, for serious microanalysis of trace elements, this method has severe limitations.

Ion microprobe analysis, in which a focussed beam of ions (usually O^-) impinges on a micro-area of a polished target, and sputters secondary ions

which proceed thence into a mass spectometer. This has the potential to be much more sensitive than EPMA. Detection limits well below 1ppm may be obtained in favourable circumstances [5], but a major limiting factor is the presence of molecular interferences, which may discriminate strongly against certain isotopes. Partial solutions to this problem include using very high resolution (M/ΔM=5000) in the mass spectometer. This approach utilises the small mass differences which exist between molecules and isotopes of the same nominal mass. In this way molecules such as Zr_2O can be distinguished from ^{206}Pb using M/ΔM=1000 [6]. The price paid in this approach is reduced transmission efficiency, and even so there are many situations, such as those involving hydrides, where the resolution required would be impossibly high.

The molecular interference situation can also be improved by energy discrimination on the secondary ions. Shimizu et al [7] have shown that the range of kinetic energies of sputtered atomic ions is greater than that of molecular ions of the same mass. In selecting only the ions in the higher energy range the atomic/molecular ion ratio can be improved, but of course with an overall reduction in sensitivity. Both of these methods can be applied in the latest CAMECA 3F machine, and impressive sensitivities may be obtained, but it must be noted that neither high resolution nor energy discrimination eliminate the interferences, but merely reduce them at the expense of reduced transmission. Complete elimination of the molecules has so far only been obtained using accelerator mass spectrometry, and if a molecular disintegrator of this type is incorported in the beam line of an ion probe, it looks as if a much more effective instrument may be constructed. The requirement for tandem AMS is that the secondary ions be negative, which is opposite to that used in conventional ion probes. Of course those elements which do not form stable negative ions cannot be simply handled in this modification, and the characteristics of the sputtering of negatives appear to be rather different to that of positives, so that determination of element concentrations may not be straight forward. However, the enormous benefit bestowed by the ability to measure atomic ions without interference is such as to convince several groups that this is the way that ion probes must develop if their full potential is to be

realised. Ultrasensitive analysis of stable isotopes equal to and often exceeding that of NAA is thus available through AMS. The micro- or milli-probe capability allows the spatial variation of trace elements to be determined, but analysis of small homogenised samples can also be performed where necessary. This dual capacity does not be apply in reverse to those methods which are primarily intended for bulk analysis.

3. Pt and Ir MEASUREMENTS

The first attempts to apply AMS to geological problems were undertaken by the Toronto - Ionex - Rochester Group, using the Rochester MP Tandem. The elements selected for study were the heavy members of the platinum group (Pt, Ir, Os), which are eminently suitable for this intitial study for several reasons. From the analytical point of view, both Pt and Ir form negative ions readily, having electron affinities of 2.13 and 1.6 eV respectively. There are at least two unique isotopes of major abundance for both Pt and Ir (^{195}Pt, 33.8%; ^{194}Pt, 32.9%; ^{193}Ir, 62.7%, ^{191}Ir, 37.3%) so the isotopic ratios can be checked easily. Because of the importance of heavy elements in trace element geochemistry, it is also appropriate to establish the feasibility of making sensitive measurements in the upper ranges of the periodic table. From the geological point of view, the geochemical behaviour of platinum group elements (PGE) has long been the subject of debate. The solubility of these elements in oxide and silicate minerals has never been measured, falling, as it appears to, below the detection limits of conventional techniques such as NAA. PGE are known to be strongly siderophile or chalcophile, i.e. their natural occurrences are either in the native metal state or in sulphide type minerals, which includes arsenides and tellurides. In rocks where no sulphides can be seen but yet PGE can be measured, the question is - Are the PGE in solid solution in the silicates, or are there undetected grains of sulphides carrying high concentrations but present so sparsely as to evade detection?

In the initial feasibility experiments Pt and Ir bearing standards were prepared in nickel sulphide solid solution. It is believed that the PGE distribute themselves homogeneously through the NiS matrix, and so a Cs beam

directed at a polished surface of such a sample should sputter representative amounts of Pt and Ir secondary ions. Separate aliqots of the same standards were analysed by NAA for comparison, and those with concentrations of Pt in the range 5 to 100 ppb were studied by AMS. ^{195}Pt was added as spike to some samples so that isotope dilution measurements could be made. 2mm cylinders were removed from the NiS buttons with a core drill and impressed into the central hole of the Al 'cone' in the ion source. In later experiments finely powdered material was used instead of solid, with equally satisfactory results. The machine was aligned using a beam of pure Au, and settings for Pt and Ir were scaled from the settings for ^{197}Au. Typically currents of 1 to 2 μA were extracted from the ion source. Charge state +5 was selected at a terminal voltage of 3MV. At higher voltages or lower charge states it would not be possible to bend the ions at the 90° magnet of the Rochester machine. Time of flight detection was used at the end of the beam line.[8] To switch between isotopes the settings on the inflection magnet, terminal voltage and electrostatic analyser were changed.

Table 2

Pt in Nickel Sulphide Standards (see Figure 1)

(S denotes spiked with ^{195}Pt)

Standard	574II	$574S_5II$	--549SII--	*	$574S_{10}II$
^{195}Pt concentration ppb	155	325	63	46	684
^{194}Pt concentration ppb	151	155	31	14	217
$^{195}Pt/^{194}Pt$ expected	1.03	2.10	2.03	3.2	3.15
$^{195}Pt/^{194}Pt$ observed	1.12	2.42	3.17	3.2	3.46
CPM per ppb Pt isotope	20,18	20,18	11,7	15,16	19,17

* concentrations adjusted assuming correct isotope ratio

Figure 1 shows the results for Pt in four of the NiS standards. Three of the these contain the same material, #574, with different amounts of ^{195}Pt spike added, and the predicted and observed ratios and absolute levels show good agreement. The fourth sample, #549, has apparently less Pt than expected from the NAA data, and this isotope dilution experiment has given a

corrected value. Detailed analysis of the data in Figure 1 are shown in Table 2. It can be seen that under the operating conditions used the sensitivity is about 20cps per ppb of the Pt isotope measured. Translating this number to concentration of the element, including all isotopes, and taking into account an attenuation factor of 10 which was present when the measurements were made, the sensitivity works out at about 1cps per ppb of Pt. Thus 10% precision could be obtained in 1000 secs at a concentration of 0.1ppb. This is impressive when compared with the situation in NAA where, because of the low neutron capture cross-section of Pt, the detection limit is often quoted about 10ppb. The difference in electron affinities between Pt and Ir leads, under the same operating conditions, to Ir having a sensitivity less than Pt by a factor of about 1.6 [8].

Table 3

AMS Measurements of Pt and Ir Ultra-mafic rocks

Sample	Pt(NAA)	Pt(AMS)	Ir(NAA)	Ir(AMS)
1. PCC1 Alpine peridotite	6	0.14	5.0	n.m.
2. Cumulous dunite	11	0.29	1.3	n.m.
3. Cumulous pyroxenite	24.5	0.43	0.3	n.d.
4. Cumulous pyroxenite	48	0.04	0.38	.007

Notes: Samples 2, 3 and 4 from Thetford Mines, Quebec. Concentrations quoted in ppb. Standard = #574 NiS. 480ppb Pt, 217ppb Ir. n.m. = not measured. n.d. = not detected, less than .003ppb.

In order to attack the problem of PGE solubility in silicates four samples of ultra-mafic rock were analysed for Pt and Ir. These rocks had been previously analysed by NAA by J.H.Crockett [9], and were selected to span a broad range of Pt concentration. The materials were inserted into the ion source as powders pressed into 2mm holes in a multi-sample wheel, as used on the recently modified ion source at Rochester. With the exception of the Cs beam, which was a milliprobe 0.2mm diameter, experimental conditions were effectively same as in the earlier experiment. Using the NiS standard #574 for calibration, the data shown in Table 3 were obtained. It is seen that there is considerable divergence between the NAA and the AMS results: in fact there is no correlation at all, and the AMS data are less

by two orders of magnitude than the NAA. Bearing in mind that the sample size for NAA is usually of the order of tens of grams, while in AMS micrograms, at the most, are consumed, so there may be a volume ratio of 10 between the two methods. Homogeneity may have quite different meanings in the two cases. In this example the AMS results are saying that the PGE are present at considerably less than ppb levels in the silicates olivine and pyroxene, and the scattered sulphide grains, in which the PGE must reside, simply were not included in the volume of material sputtered by the primary Cs beam. This would appear to be the first instance of milliprobe experiment using AMS.

4. Pt and Ir AT THE CRETACEOUS-TERTIARY BOUNDARY

A specific problem where the method could be applied appeared in the curently active subject of the trace element anomalies at the Cretaceous-Tertiary boundary. Alvarez et al.[10] and others have shown that an Ir anomaly exists at this stratigraphic horizon at a number of different localities around the world, and they have ascribed it to the impact of an asteroid on the earth at this time. This event threw up a cloud of dust which encircled the earth and blocked off the sunlight for several years. This caused a catastrophic change in the state of life, with the most spectacular effect being the sudden extinction of the dinosaurs. The Ir anomaly arises because asteroids are assumed to be enriched in PGE relative to crustal rocks, and the dust which settled out of the cloud into the sediments contained a large proportion of meteoritic debris. The data presented by Alvarez et al.[10] include measurements for several elements, and while Ir is the critical one, no data for Pt itself have been gathered, presumably because of the poor sensitivity of their analytical method for this element.

A preliminary measurement of Ir in a pyritiferous shale is shown in an energy - time of flight diagram in Figure 2. The peak of Ir, corresponding to a concentration of about 3ppb is clearly resolved by energy discrimination from those of other ions with similar m/q. The Ir data shown in Figure 3 confirmed the data of Alvarez et al.[10] convincingly. However, Pt, which on the basis of the meteorite hypothesis and known chondrite

abundances should be present at a level of about twice that of Ir, behaved in a much more puzzling manner. In the most Ir-enriched clay layer Pt was also enriched, but at levels up to 100 times what would be expected, as shown in Figure 4. A further discovery was that Pt appeared to be inhomogeneously distributed in the clay, as seen from the spiky nature of the count rate compared with time of exposure to the Cs beam. The clay was known to contain considerable pyrite, and the inference was that as the Cs beam eroded the sample, different mineral grains were consumed, each giving off different amounts of Pt, though no obvious similarity was noted for Ir. Several subsequent sets of measurements have been made on other materials from different exposures of the Cretaceous-Tertiary boundary around the world. The AMS results suggest a strong correlation of PGE with sulphide content of the rocks though there also seems to be an association with organic remains in some of the black shales. The details of these measurements will not be discussed here, but this example serves to show that AMS can be an alternate and probably superior method of investigating directly the PGE variations in sediments.

5. FUTURE APPLICATIONS

So far, the practical applications of AMS to stable isotopes in geology have been restricted to ultrasensitive assay measurements of heavy elements in rock and mineral matrices. Because of the many uncertainties, which include sputtering yields, calibration and matrix unknowns, the measurements have been of low precision. However, even with only order-of-magnitude precision, the rapid milli-, and ultimately micro-probe, capability for ultrasensitive analysis will be of inestimable value in geochemical studies.

It is perhaps tempting to think of an AMS facility as offering solutions to a wide range of analytical problems for which adequate methods already exist. While it is certainly true that priority should be given to experiments where AMS has unique capability, the prime consideration is that a machine dedicated to making analytical measurements should be utilised as efficiently as possible. To achieve this, a wide variety of measurements will be made, for some of which there might be alternative, if less convenient methods. Of course, if precision is critical and AMS cannot

equal it, there is little point in attempting to use the new method.

Isotope ratios of the stable isotopes of Pt and Ir have so far been measured only with low precision, mainly for the purpose of confirming the identity of those elements. When higher precision isotope ratio measurements become feasible, as will undoubtedly happen with the aid of AMS, then there will be unique problems to be tackled in looking at the signatures of multi-isotope elements. Already, using conventional ion microprobes, ^{26}Mg excesses have been reported in anorthite from Allende inclusions [11], but the difficulties of making sufficiently precise measurements increase with heavier elements and the associated multiplicity of molecular interferences. Anomalous $^{107}Ag/^{109}Ag$ ratios have been found in iron meteorites [12], with ^{107}Ag being enriched by amounts exceeding 100‰ with respect to normal. This is due to the in situ decay of extinct ^{107}Pd. Those measurements on Ag have only been made using thermal ionization mass spectrometry on Ag separated from the meteorite. Direct measurement of ppb levels Ag in the iron meteorites using AMS should be able to reveal such swings in $^{107}Ag/^{109}Ag$, though because Ag has only two stable isotopes, the problem of correcting for isotope fractionation may be difficult. There will clearly be many elements occurring in both terrestrial and meteoritic rocks, whose isotopic concentrations can be usefully investigated by direct in situ measurement. Suitable candidates for such study could include Sn, Te, Pt, and Hg. In connection with the $^{187}Re/^{187}Os$ decay, Os isotope ratios are clearly of importance. $^{187}Os/^{186}Os$ has already been measured on separated Os, using an ion microprobe as a mass spectrometer [13], and AMS should offer a more efficient and convenient way of making these measurements.

Light element isotopes such as those of C, O, and S, which show temperature fractionation in rocks and ores, might be usefully studied using ion milli-probe and AMS. Precision better than 0.1% would be required for those data to be useful, and this may be some time off. None of these isotope ratios have been measured with conventional ion probes, primarily because of molecular interferences, of which hydrides are especially important. The ability to study these isotope ratios in relation to zoning

in minerals will be an immense step forward.

Patterns of enrichment or depletion within groups of chemically similar elements, such as the rare earth elements (REE) or PGE, are invaluable in understanding the origin of rocks. Crustal rocks have quite different patterns compared with mantle or meteoritic materials. At present such profiles can be obtained only with some difficulty, and often with gaps, by NAA. In the event that broad band measurements become possible with AMS we can expect that this could be a very useful area of application.

6. CONCLUSIONS

So far it has been shown that AMS can give rapid direct measurements of element concentration at the sub ppb level in rocks and minerals. Those elements which form negative ions readily may be tackled directly, while for others preliminary charge exchanging may be needed. Matrix variation may be expected to introduce errors in simple calibration comparisons of factors in the range 2 to 5. For accurate absolute measurements improved standards are required, and isotope dilution experiments, which are matrix independent, should be performed. Ion implantation methods would be another approach to the calibration problem, and with the appropriate use of short lived radioactive species, adjacent element ratios may be determined precisely. Without this, accurate inter-element comparisons will lack precision.

One extremely encouraging feature which has emerged in these early experiments is the fact that contamination between samples appears not to be a serious problem. Samples were measured in which no counts were recorded for ^{193}Ir in a period of twenty minutes. One count in twenty minutes would imply a level of about 1ppt so that contamination must be less than that. The reason for this remarkable fact must be that the sputtering process, by which the ions are removed from the sample, cleans the sample at the same time, constantly exposing virgin material. It may be that this feature alone could be the strongest argument for using this method in ultra-sensitive analysis in the future.

7. ACKNOWLEDGEMENTS

I wish to thank my many colleagues for assistance with experiments, providing materials for analysis, giving access to experimental facilities, and for much advice, guidance and stimulating discussion. At Toronto R.P.Beukens, N.M.Evensen, M.P.Gorton, W.E.Kieser, L.R.Kilius, A.E.Litherland, D.W.Strangway, and G.C.Wilson. At Rochester D.A.Elmore and H.E.Grove. J.H.Crockett of McMaster University kindly made analysed material available, and C.K.Brooks and T.D.Nielsen of Copenhagen University collected and donated a magnificent suite of Fish clay samples. The National Science and Engineering Research Council is acknowledged for operating and equipment grants. Some of the work reported was performed under a contract with the Department of Supply and Services, Ottawa.

8. REFERENCES

1. J.H.Crockett and Y.Teruta, Palladium, iridium and gold contents of mafic and ultramafic rocks drilled from the Mid-Atlantic Ridge, Leg. 37, Deep Sea Drilling Project. Can. Jour. Earth Sci. 14, 777-787 (1977).
2. K.Norrish and B.W.Chappell, X-ray Fluorescence Spectrometry. In: Physical Methods in Determinative Mineralogy, J.Zussman(Ed.) Academic Press, 201-272 (1977).
3. M.P.Gorton, Private communication
4. D.G.W.Smith and J.C.Rucklidge, Electron Microprobe Analysis in the Earth Sciences. Advances in Geophysics 16, 57-154 (1973).
5. I.M.Steele, R.L.Hervig, I.D.Hutcheon and J.V.Smith, Ion microprobe techniques and analyses of olivine and low-Ca pyroxenes. American Mineralogist 66 (1981).
6. R.W.Hinton and J.V.P.Long, High-resolution ion-microprobe measurement of lead isotopes: variations within single zircons from Lac Seul, N.W.Ontario. Earth Planet Sci. Lett. 45, 309-325 (1979).
7. N.Shimizu, M.P.Semet and C.J.Allegre, Geochemical applications of quantitative ion-microprobe analysis. Geochim. Cosmochim. Acta 42, 1321-1334 (1978)
8. L.R.Kilius, PhD Thesis, University of Toronto (1981).
9. J.H.Crockett, unpublished data, (1981).
10. L.W.Alvarez, W.Alvarez, F.Asaro and H.Michel, Extraterrestrial Cause for

the Cretaceous-Tertiary Extinction, Science 208, 1095-1108 (1980).

11. J.G.Bradley, J.C.Huneke, and G.J.Wasserburg, Ion microprobe evidence for the presence of excess ^{26}Mg in an Allende Anorthite crystal, Jour. Geophys. Res. 83B1, 244-254, (1978).
12. T.Kaiser, W.R.Kelly, and G.J.Wasserburg, Isotopically anomalous Ag in two iron meteorites, Lunar and Planetary Science, Abstracts XI, 527-529, (1980)
13. C.J.Allegre and J.M.Luck, Osmium isotopes as petrogenetic and geological tracers, Earth Planet. Sci. Lett. 48, 148-154, (1980).

9. Figure Captions

1. Tandem accelerator measurement of Pt in nickel sulphide standards. Repeated measurements of the count rate, for two isotopes on four samples, are shown on a time scale with an arbitary origin.
2. Total energy - time of flight - intensity spectrum for $^{193}Ir^{+5}$ in a pyrite concentrate extracted from a sample of a black shale from Oshawa, Ontario. Other isotopes appearing have the same m/q for charge states +2, +3 and +4.
3. Tandem accelerator measurement of ^{193}Ir in four samples across the Cretaceous-Tertiary boundary, Stevns Klint, Denmark. The stratigraphic level goes up in time from left to right. Bed 3, the critical 'Fish Clay' boundary shows the highest Ir content of about 5ppb.
4. ^{194}Pt from the same four samples described for Figure 3. In the critical layer the Pt count rate is extremely erratic, varying according to the presence or absence of sulphide grains under the Cs beam. The highest peak in Bed 3 corresponds to a Pt concentration of over 300ppb.

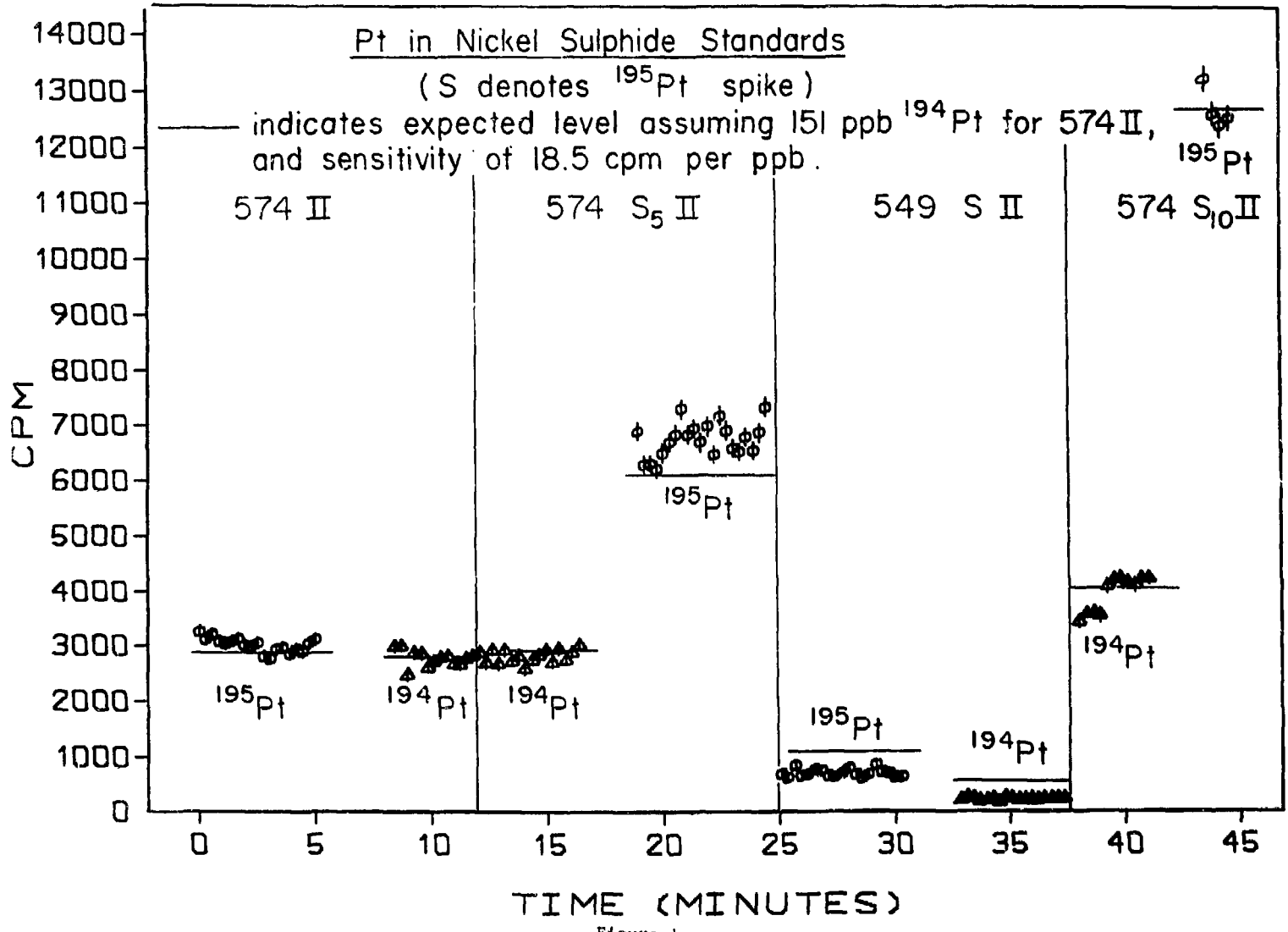
Pt in Nickel Sulphide Standards
(S denotes 195Pt spike)
—— indicates expected level assuming 151 ppb 194Pt for 574 II,
and sensitivity of 18.5 cpm per ppb.
574 II
574 S5 II
549 S II
574 S10 II
195Pt
194Pt
194Pt
195Pt
195Pt
194Pt
194Pt
CPM
TIME (MINUTES)
0
1000
2000
3000
4000
5000
6000
7000
8000
9000
10000
11000
12000
13000
14000
0
5
10
15
20
25
30
35
40
45

Figure 1.

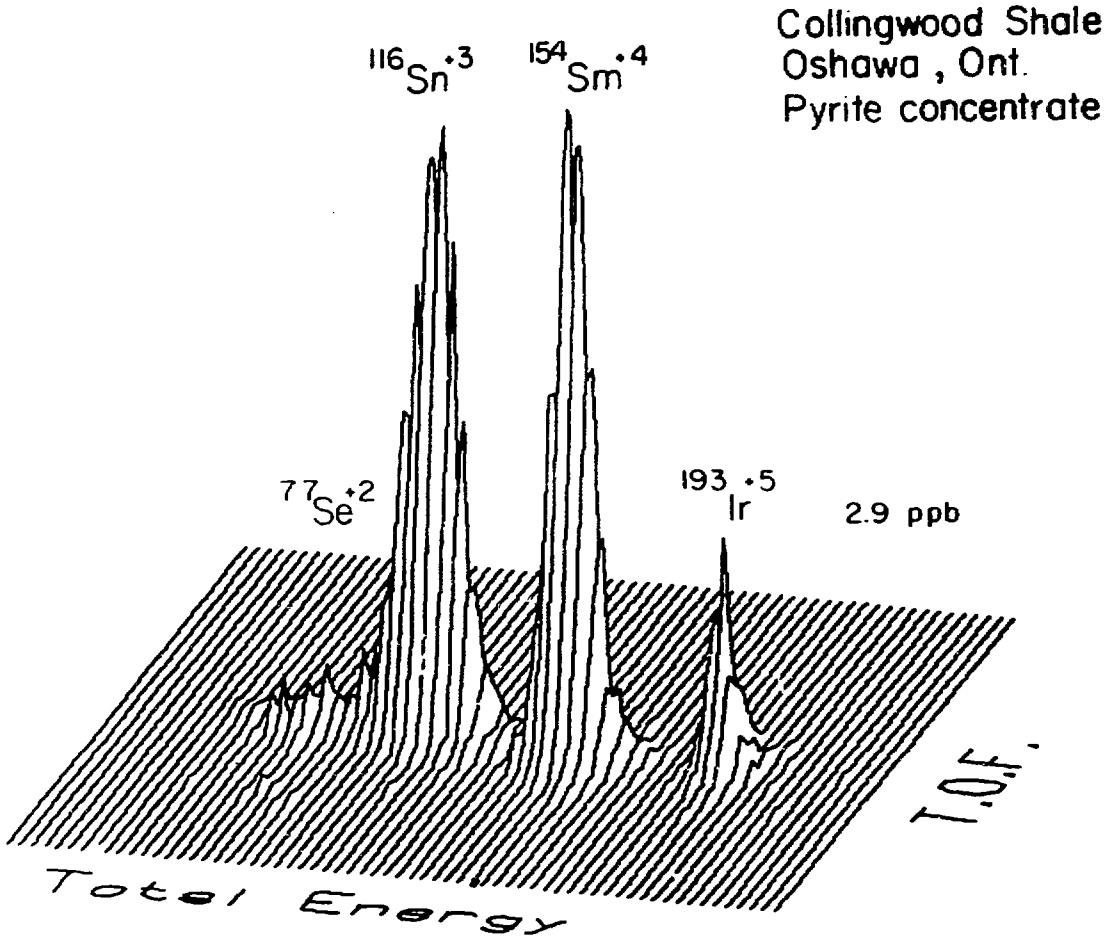
Collingwood Shale
Oshawa , Ont.
Pyrite concentrate
116Sn+3
154Sm+4
77Se+2
193Ir+5
2.9 ppb
Total Energy

Figure

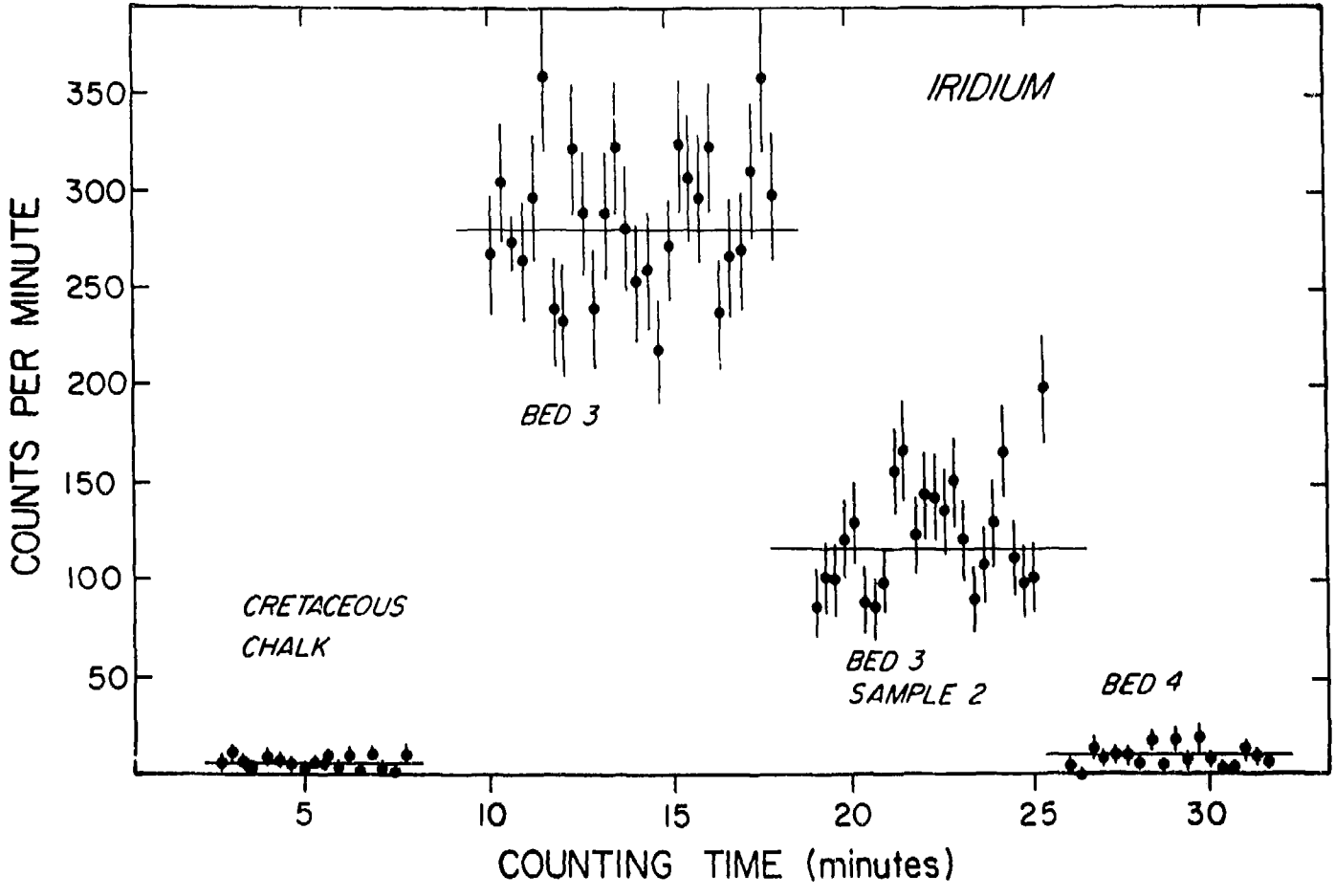
IRIDIUM
BED 3
CRETACEOUS
CHALK
BED 3
SAMPLE 2
BED 4
COUNTS PER MINUTE
350
300
250
200
150
100
50
5
10
15
20
25
30
COUNTING TIME (minutes)

Figure 3.

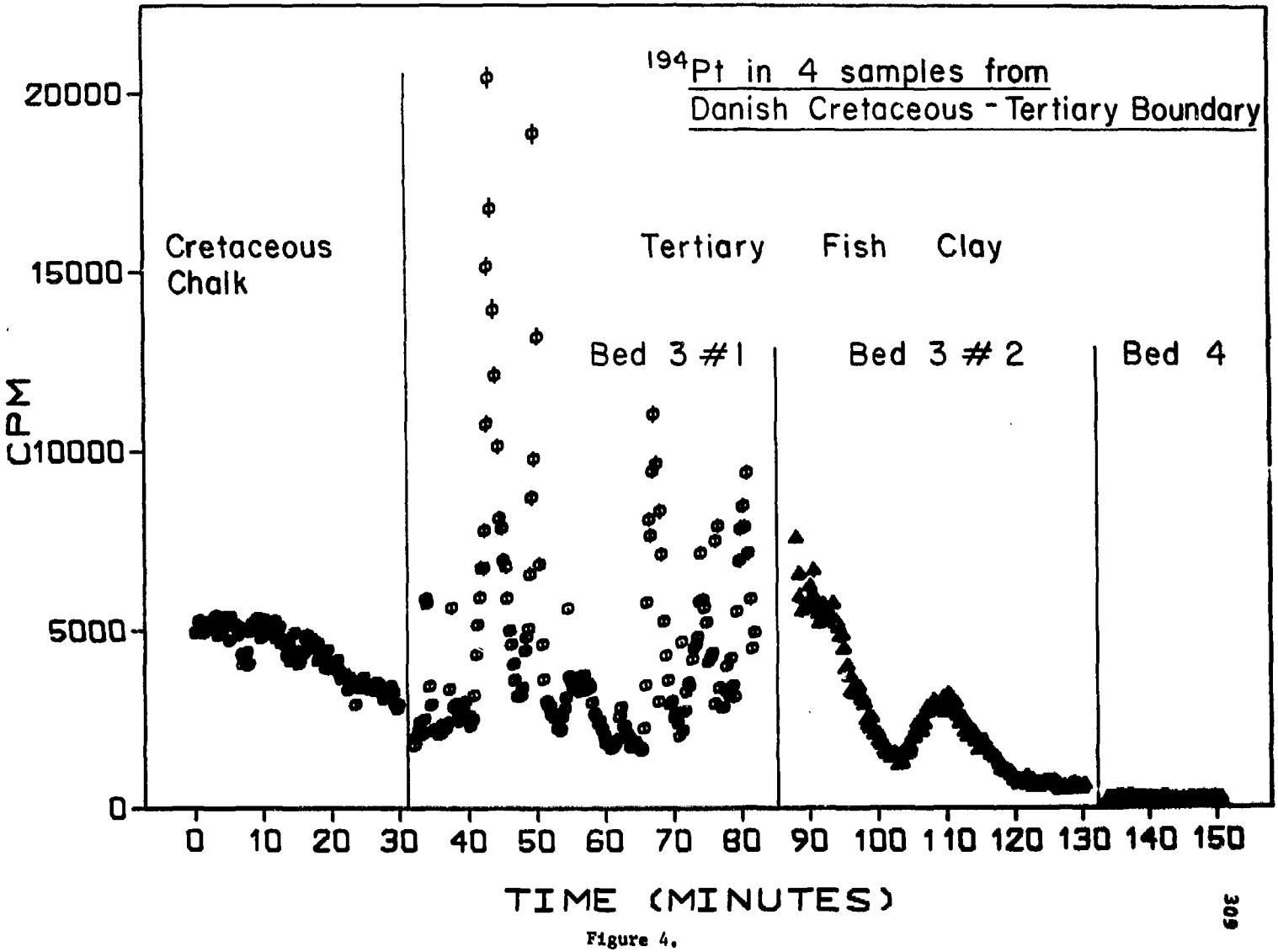
^{194}Pt in 4 samples from
Danish Cretaceous - Tertiary Boundary
Cretaceous
Chalk
Tertiary Fish Clay
Bed 3 #1
Bed 3 # 2
Bed 4
CPM
20000
15000
10000
5000
0
0 10 20 30 40 50 60 70 80 90 100 110 120 130 140 150
TIME (MINUTES)
309

Figure 4.

RARE STABLE ISOTOPES IN METEORITES

G.C.Wilson
Department of Physics,University of Toronto

ABSTRACT

Secondary Ion Mass Spectrometry (SIMS) using accelerators has been applied with success to cosmic ray exposure ages and terrestrial residence times of meteorites by measuring cosmogenic nuclides of Be, Cl, and I. It is proposed to complement this work with experiments on rare stable isotopes, in the hope of setting constraints on the processes of solar nebula/meteoritic formation. The relevant species can be classified as -

a)daughter products of extinct nuclides (halflife $\lesssim 2 \times 10^8$ y)
-chronology of the early solar system.

b)products of high temperature astrophysical processes
-different components incorporated into the solar nebula.

c)products of relatively low temperature processes, stellar winds and cosmic ray reactions
-early solar system radiation history.

The use of micron-scale primary ion beams will allow detailed sampling of phases within meteorites. Strategies of charge-state selection, molecular disintegration and detection should bring a new set of targets within analytical range. The developing accelerator field is compared to existing (keV energy) ion microprobes.

Two major attractions of accelerator SIMS are the high sensitivity and the ability to resolve interfering species. A third, given an ion microprobe 'front end', is spatial resolution able to provide two-dimensional data on the textural relations within the samples. In many applications this ability may govern the choice of technique for sub-ppm analyses; other options commonly including INAA, XRF and AAS, which all involve crushing/dissolution of samples. The spatial factor is especially significant in geology and metallurgy, where information from discrete phases (or portions of nonuniform phases) may help decipher crystallization and alteration sequences, partitioning of elements between different hosts, and genetic relations in complex materials. Ion sources, especially EHD models, are now developing a capability beyond earlier microsampling[1] and ion microbeam techniques. It

will be shown that SIMS with electrostatic accelerators can provide a tool for probing meteorite mineralogy,at concentrations orders of magnitude below the limits of the electron probe, and with a certainty of identification often impossible using a conventional ion probe. It is hoped to determine the isotopic composition of meteorites in elements where this may give clues to the early history of the solar system, roughly in the age range 4.5-5.0 Ga. This reflects on processes -

1)Producing evolved material prior to the existence of the solar nebula.

2)Leading to segregation during the condensation of the solar nebula.

3)Of modification following accretion into discrete planetismals, whether due to-

a)Gravitational or radioactive heating.

b)Collisional breakups

c)Cosmic ray / solar wind irradiation of exposed surfaces.

This last has already been explored (for the more recent events) by several groups using the Be and Cl dating methods. It is possible, using details of petrography, major element composition and thermodynamic phase relations, to identify such refractory minerals as might be expected to crystallize first during condensation of an initially hot gaseous nebula[2]. Lattimer et al[3] cite corundum, perovskite, spinel, melilite and pyroxene as possible containers of presolar material in C3 meteorites, and carbides,nitrides and sulphides in enstatite chondrites. A particularly interesting MeV SIMS application would be measurements constraining the meteoritic content of solar system precursors, a concept developed at length by Clayton[4]. MacPherson et al[5] described textural evidence for vapour-phase alteration of coarse-grained inclusions from Allende, supporting the viewpoint of Grossman[2,6]. Clayton[4]

details his contrasting model of condensation of refractory materials in expanding regions of supernova debris, and does not in consequence require an initially hot solar nebula. The crucial point here is whether or not solid presolar material was incorporated into the solar nebula, preserving unmodified evidence of its origins. In brief, components differing from homogenized nebular material (planetary samples,moonrock) may best be found as-

a)Inclusions bearing evidence of extinct radioactive species (formed 1-2 of their halflives before nebular condensation) in the form of anomalous isotope ratios due to the daughter products.

b)Stable isotopes from prior nucleosynthetic events[7], carried into the solar system as gas, dust and grain aggregates.

c)Products of irradiation early in the solar system, first postulated by 'FGH' as an intense proton flux bathing early planetismals. Analogous to the GCR spallation model for LiBeB.

Clayton[8] suggested from O isotope data that perhaps 1% of solar system refractory grains had prior existence. It is important to distinguish nuclear effects from solar system fractionation processes. To date remarkable results have been achieved by precision mass spectrometry, generally involving either high mass resolution or complex chemical separation procedures. Conventional ion probes such as the AEI IM20 and the Cameca 3F are capable of producing useful results in certain applications, such as measuring the ^{26}Mg anomaly. Currently however, they are unable to compete with specialised mass spectrometry in terms of precision; limits depend on application but $2\sigma \simeq 1o/oo$ is probably about the limit for favourable cases, almost two orders of magnitude behind state-of-art thermal ionization mass spectrometers.

Isotopic matrix effects, often suspected in the past, have recently been demonstrated in a variety of minerals, and may be up to a few percent of the measured ratios (much less than for elemental abundance measurements, but still substantial). This situation is often aggravated by the need to separate interferences by mass resolution and/or energy filtering, necessitating longer counting times and so increasing the potential effects of instrumental drift. Reproducibility of ±1% or so should be obtainable with accelerator SIMS. Initial reconaissance work should be aimed at determining isotope ratios previously inaccessible due to interferences, with the aim of constraining the nature and origins of the material represented by primitive meteorites. Isotope anomalies to date (excluding early, unreliable measurements) are mostly <5% or so, commonly in the o/oo region. There is a substantial database of astronomical, meteoritical and geochemical measurements of element and isotope abundances[9,10]. Sample preparation for microprobe work is generally a straightforward combination of sectioning, polishing and coating. Although a normal ion probe destroys the sample at an appreciable rate, this is commonly only in the ng/min to ng/hour range for sputtering by 2-20 nA O^- and Ar^+ primary beams at 5-30 keV energy. The beam diameter varies according to the application, but is commonly 5-50 μm. It is possible to raster a 50-500 μm wide area in order to sputter sufficiently slowly (about 1 monolayer per second) to record the variation in Si signal with depth in a variable target. In contrast, ion beam analysis by RBS or nuclear reaction depth profiling commonly use mm beams. Recently, experiments were carried out at Rochester in which the 100 μA, 30 keV Cs^+ beam was focused to a spot some 300 μm across on powdered rock samples, a polished section and the Al holder. For all sputter-removal techniques there is an initial period during which the implanted concentration of the primary ions in the target surface reaches an

equilibrium level. This depends on the range of the primary ions (typically a few hundred Å) and commonly involves transients in the secondary ion yield. Cs sources commonly deliver a greater dose of (heavier) ions than has been used with ion microprobes in the past. This should destroy near-surface crystallinity, minimizing yield variations due to structural as opposed to compositional effects. Thus a 100 μA primary beam 300 μm in diameter has a beam current density of 140 $mAcm^{-2}$, compared with 6 $mAcm^{-2}$ for a 10 nA beam 15 μm across. The ion flux of the 'milli'beam is some 8.8×10^{17} $cm^{-2}s^{-1}$, sufficient to amorphize a target in a fraction of a second (based on a Si target[11]). For isotopic measurements, terrestrial mineral standards with appropriate (ppm-ppb) levels of the relevant species should be used. If three or more isotopes can be measured, suitable corrections can be made for instrumental fractionations. A new generation of sources is likely to reduce the beam diameter by at least a factor of ten, and sample consumption by two to three orders of magnitude, from mg to μg. Destruction of rare material by direct sputtering is likely to be much exceeded by the act of section cutting; this however gives scope for later optical examination,EPM etc. At present, target selection must be constrained by a minimum grainsize in the 200-300 μm region. Accelerator SIMS will be subject to similar instrumental effects to normal ion probes-

1)Variation between designs due in part to variations in sputtering efficiency (with angle,energy and mass of incident ions).

2)Variation between experiments for one machine, caused e.g. by changes in residual gas pressures, efficiency in secondary ion (SI) tuning etc.

To these must be added analogous effects in the accelerator and the high E beam line. An empirical approach is currently desirable, using standards as

similar as possible to the unknowns, or at least well characterised in SI yield relative to the samples. Possible subjects for this kind of research are easy to find by review of the extensive literature[12] ,or indeed, by perusal of a chart of the nuclides (Tab. 1).

TABLE 1 : NUCLIDES OF POSSIBLE INTEREST IN METEORITICS

Isotopes	Electron affinity[25] (eV)	Isotopic abundance[26]	Comments
			Early solar system p irradiation
^{51}V	0.63	0.25	
^{138}La	0.55	0.089	
^{180}Ta	0.15	0.012	
			p process
^{112}Sn	1.03	1.01	
^{114}Sn		0.67	
^{115}Sn		0.38	
			Parent of halflife (y)
^{99}Ru	1.51	12.7	^{99}Tc 2.1×10^5
^{202}Hg	-0.19	29.8	^{202}Pb 3.0×10^5
^{97}Mo	1.18	9.6	^{97}Tc 2.6×10^6
^{182}W	1.23	26.3	^{182}Hf 9.0×10^6
^{205}Tl	0.32	70.5	^{205}Pb 1.4×10^7
^{92}Zr	0.45	17.1	^{92}Nb 1.6×10^8

This list includes some species of relatively high isotopic abundance : for these the precision needed to reveal minor nuclear components may well exceed the capabilities of accelerator SIMS in the near future. With the exception of ^{202}Hg, no significant variations have been reported for any isotope in the table[12].

Less obvious,however, are the means by which to measure the chosen ratios. Isobaric interferences are a major concern with regard to the heavier elements, as (dE/dx) and T.O.F. resolution is not adequate for isobars much above Z=20. Increasing E does not realistically overcome this problem. Extensive electron stripping can yield unambiguous results in some situations (e.g. Cl dating) but requires a large machine and is impractical for more massive species. Mass resolution and T.O.F. separation will be quite inadequate for the applications envisaged, generally precluding even the most

speculative data reduction (peak stripping) techniques. Possible strategies for removing interferences are shown in Tab. 2.

TABLE 2 : MEASUREMENT TECHNIQUES

A : MOLECULAR INTERFERENCES
1. Negative ion spectroscopy, electron stripping, and ion acceleration.
2. Negative (halogen) primary ion beam, charge exchange in alkali metal vapour, electron stripping and ion acceleration.

B : ISOBARS
1. Negative ion formation (compare electron affinities in Tab. 1), e.g. good probability of resolving La from Ba (E.A. -0.48) and Sn from Cd (E.A. -0.27).
2. Use of metastable states of positive ions following stripping, e.g.
   $KF^- \rightarrow (KF)^{2+}$:unstable
   $CaF^- \rightarrow (CaF)^{2+}$:metastable
3. dE/dx : not useful at low energies (a few MeV in this context) for $Z \gtrsim 20$.

A promising line of research concerns the light tin isotopes. $^{112,114,115}Sn$ are traditionally p process creations. Clayton[13] considers ^{115}Sn to be largely r process-derived, which may indicate that the p process is essentially one of photodisintegration reactions, suppressing odd-A nuclei due to their smaller binding energies, in contrast to the alternative p process model of radiative capture. The reluctance of Cd to form negative ions implies that the only possible significant interference on the three Sn isotopes will be isobaric In on ^{115}Sn. A second application relates to the rare light isotopes of V, La and Ta, whose abundance limits possible proton irradiation a la FGH of the early solar system[14]. ^{50}V may also be formed deep in a star near nuclear statistical equilibrium, and the others may form during C burning in a high n:p flux. Ba interference is unlikely due to the low electron affinity of the alkaline earth, but Ce may be a problem and requires study. Armstrong et al[15] reported V-rich hibonite (V_2O_3 ~1%) from the core of a Murchison inclusion. Both options are problematical by conventional mass

spectrometry / ion probes without extensive chemical preparation, both in terms of mass resolution (e.g. to resolve ^{138}La, $M/\Delta M$ of 77000 and 125000 is needed for the Ba and Ce isobars respectively) and sensitivity :mean chondritic abundances of about 1 ppm Sn and 0.3 ppm La imply some 1-10 ppb of the rare Sn trio and 0.3 ppb of ^{138}La, although enrichment is likely in some inclusions. Within the next year it should be possible to determine negative ion production efficiencies (and thus the magnitude of interferences) and to analyse for selected elements in appropriate material. Grain size will initially be a determining factor in this selection. The most promising materials for isotopic studies are mostly located in the carbonaceous chondrites[16].The CV3 group (which includes Allende) tend to be coarser than the rest[17]. Allende coarse-grained type B inclusions[6] have major phase grain sizes ranging from 3-4mm (pyroxene) down to 1-25 μm (hibonite). Fine-grained inclusions in Allende[18] and Murchison[19] may have grainsizes in the 10-50 μm range, although much smaller (μm size) particles may be enclosed within the major minerals. In this connection, a future target for fine-beam analysis are the fremdlinge of El Goresy et al[20,21], minute inclusions of possible primordial material of exotic mineralogy (Pt group metals, V-rich spinel, Ca/REE minerals etc). Consumption rates must be reduced before very rare material is studied, but there are ample supplies of primitive carbonaceous chondrite matrix,chondrules and inclusions (roughly 6:3:1 in Allende) for present purposes. Thus it is already possible to run comparisons between chondrules and matrix. If the SUNOCON[4] idea is valid then sputtering and reassembly in interstellar space may homogenize initial condensates, such that heavy refractories will only show peculiar FUN effects if somehow retained in discrete forms. Lighter gaseous elements (e.g. ^{16}O) may better retain initial anomalies. The ^{50}Ti anomaly may have been preserved by initial

condensation of this, the heaviest stable Ti isotope, in a separate metal phase in the next deeper ($\bar{V}$) zone of a supernova[22]. Endemic mixing of SUNOCONS in space would imply that the FUN inclusions are as rare as they now appear, and that lengthy searches for more will be entailed. Although this discussion is aimed primarily at isotope ratios,and associated anomalies[23] suitable standards can be provided to allow trace analysis of common minerals for a wide range of elements (REE etc) which have so far escaped SIMS analysis due to mass resolution restrictions. Many refractory elements are enriched 15-20,20-60 times in coarse- and fine-grained Allende inclusions respectively[6], and 4-100 times in hibonite-spinel inclusions from Murchison[24]. Their occurrence reflects on the origins of the host phases, and so the processes by which isotopically strange components are initially confined.

REFERENCES

1. T.Lee, D.A.Papanastassiou and G.J.Wasserburg, Geochim.Cosmochim. Acta 41, 1473-1485 (1977)
2. L.Grossman, Geochim.Cosmochim.Acta 36, 597-619 (1972)
3. J.M.Lattimer, D.N.Schramm and L.Grossman, Astrophys.J. 219, 230-249 (1978)
4. D.D.Clayton, Space.Sci.Revs. 24, 147-226 (1979)
5. G.J.MacPherson, Grossman,L, Beckett,JR and Allen,JM, Abs.Lunar Planet. Sci.Conf. 12, 648-650 (1981)
6. L.Grossman, Ann.Rev.Earth.Planet.Sci. 8, 559-608 (1980)
7. V.Trimble, Rev.Mod.Phys. 47, 877-976 (1975)
8. D.D.Clayton, Astrophys.J. 199, 765-769 (1975)
9. B.Mason (editor), Handbook of Elemental Abundances in Meteorites, Gordon and Breach, 555pp (1971)
10. A.G.W.Cameron, Space.Sci.Revs. 15, 121-146 (1973)
11. F.F.Morehead and B.L.Crowder, In Ion Implantation (editors F.H.Eisen and L.T.Chadderton),Gordon and Breach, 25-30 (1971)
12. G.C.Wilson, University of Toronto ISOTRACE report 81-M01 (1981)
13. D.D.Clayton, Astrophys.J. 224, L93-L95 (1978)
14. D.D.Clayton, E.Dwek and S.E.Woosley, Astrophys.J. 214, 300-315 (1977)
15. J.T.Armstrong, G.P.Meeker, J.C.Huneke and G.J.Wasserburg, Meteoritics 15, 259-260 (1980)
16. W.R.Van Schmus and J.M.Hayes, Geochim.Cosmochim.Acta 38, 47-64 (1974)
17. T.V.V.King and E.A.King, Meteoritics 13, 47-72 (1978)
18. J.T.Armstrong and G.J.Wasserburg, Abs.Lunar Planet.Sci.Conf. 12, 25-27 (1981)
19. J.D.Macdougall, Earth.Planet.Sci.Lett. 42, 1-6 (1979)

20. A.El Goresy, K.Nagel, B.Dominik and P.Ramdohr, Meteoritics 12, 215-216 (1977)
21. A.El Goresy, K.Nagel, B.Dominik and P.Ramdohr, Meteoritics 13, 448-449 (1978)
22. D.D.Clayton, Abs.Proc.Lunar Planet.Sci.Conf. 12, 151-153 (1981)
23. F.Begemann, Rep.Prog.Phys. 43, 1309-1356 (1980)
24. W.V.Boynton, R.M.Frazier and J.D.Macdougall, Meteoritics 15, 269 (1980)
25. R.J.Zollweg, J.Chem.Phys. 50, 4251-4261 (1969)
26. F.W.Walker, G.J.Kirouac and F.M.Rourke, Chart of the Nuclides, General Electric Co., edition 12 (1977)

ACCELERATOR MASS SPECTROMETRY OF ^{59}Ni AND Fe ISOTOPES AT THE ARGONNE SUPERCONDUCTING LINAC

W. Henning, W. Kutschera, B. Myslek-Laurikainen,* R. C. Pardo,
R. K. Smither and J. L. Yntema
Argonne National Laboratory, Argonne, IL 60439

ABSTRACT

We have obtained initial results in an attempt to use the Argonne tandem-linac system for accelerator mass spectrometry of medium-heavy nuclei. Nuclei of the radioisotope ^{59}Ni ($T_{1/2} = 7.5 \times 10^5$ yr) and of the stable isotope ^{58}Fe at low concentrations have been accelerated and clearly identified. The latter experiment is in preparation of a measurement of the half-life of ^{60}Fe($T_{1/2} \approx 3 \times 10^5$ yr).

I. INTRODUCTION

In order to extend the use of heavy-ion accelerators to mass-spectrometric measurements of medium-heavy and heavy nuclei, higher ion energies are desirable. The reason is, of course, that the higher energies greatly improve the capability of nuclear-charge identification through a differential energy-loss measurement, and increase the stripping probability for very high charge states. Both properties can be used to separate a radioisotope of interest from a contaminant isobaric background, though the second property is only useful if the radioisotope has a greater nuclear charge than the isobaric contaminant. In that case, complete electron stripping will produce the radioisotope in a charge state at least one unit higher than the contaminant, and then the higher charge state can be ion-optically separated. This has been successfully demonstrated for the ^{26}Al and ^{41}Ca radioisotopes.[1]

We present here results of a first attempt to use the Argonne tandem-linac system for accelerator mass spectrometry of ^{59}Ni ($T_{1/2} = 7.5 \times 10^5$ yr) and ^{60}Fe($T_{1/2} \approx 3 \times 10^5$ yr). For ^{59}Ni, complete stripping to the maximum charge state $q_{max} = 28^+$ was employed to separate it from its ^{59}Co isobaric background ($q_{max} = 27^+$). For the study of ^{60}Fe, preliminary tests were performed with the stable radioisotope ^{58}Fe by using a

passive absorber foil for, essentially, a differential energy loss measurement.

II. EXPERIMENTAL SETUP

The Argonne tandem-superconducting linac accelerator system presently provides beams of ≈ 5 MeV/nucleon in the mass region investigated here, approximately a factor of three higher in energy than the tandem alone. The advantage of higher energy from the linac comes at the expense of a higher isobaric ion-beam background, since the superconducting linac is an rf structure whose phase needs to be locked to the beam-pulse phase by actually sensing the arrival time of these pulses at the entrance of the linac. This requires a measureable beam of at least a few tens of picoamperes current. Therefore in order to accelerate radioisotopes of much lower intensity, we have developed the technique of an isobaric carrier beam, which then needs to be separated after acceleration. Although the carrier beam presents a difficult problem in separation, it can be used in three rather useful functions: i) tuning of the accelerator system with the measurable beam; ii) stabilizing the accelerator by slit-current (tandem) and phase-lock control (linac); and iii) normalizing beam currents vs ion counts. Although the latter poses a number of problems (as, for example, the constancy of the relative negative-ion output of different elements from the sputter source) it has the great virtue of allowing a continuous normalization without retuning the accelerator system.

Figure 1 shows the essential components of the tandem-linac system[2] used in the present studies. In normal operation the ions get stripped twice, once in the terminal of the tandem (stripper #1) and a second time between tandem and linac (stripper #2) in order to provide a high charge state for more effective acceleration in the linac. The tandem-linac bunching system,[3] indicated by prebuncher, chopper and superconducting postbuncher in Fig. 1, provides a narrow pulse of ≈100 psec width for injection into the linac and also locks the beam-pulse phase to a reference phase at the linac entrance by means of the phase-detector. The latter unit requires a beam of at least several tens of picoamperes and thus leads to our use of an isobaric carrier beam. The accelerated beam from the linac is passed through two analyzing magnets with a stripper foil (#3) placed between them. This latter foil has

the function either to completely strip the ions of interest (^{59}Ni) or to introduce a differential energy loss (^{58}Fe). The ions of interest are then selected by the second magnet at a 45° deflection angle and identified in a ΔE-E silicon surface-barrier telescope placed at 0° with respect to the direction of the analyzed beam. Also shown in Fig. 2 is the location of the Enge split-pole magnetic spectrograph, which will be used in future AMS experiments in a way similar to that used at the tandem.[4]

III. RESULTS FOR ^{59}Ni

To separate the ^{59}Ni radiosotope from its isobaric background of stable ^{59}Co, we chose to completely strip ^{59}Ni to its maximum charge state q = 28^+, which does not exist for ^{59}Co. The expected ^{59}Ni^{28+} charge-state fraction for Ni ions of approximately 314 MeV and for a 100-μg/cm^2 carbon stripper foil was determined with a ^{58}Ni beam. The results are listed in Table I, together with the results of previous measurements obtained with the aim of using the same technique for the following other isobaric pairs:

^{36}Cl($T_{1/2} \approx 3.0 \times 10^5$ yr) - ^{36}S (carrier),

^{41}Ca($T_{1/2} \approx 1.0 \times 10^5$ yr) - ^{41}K (carrier).

Table I shows that, for the lighter ions (^{35}Cl and ^{40}Ca) at ≈5 to 6 MeV/nucleon incident energy, an appreciable fraction (~10%) is fully stripped. On the other hand, similar incident energies per nucleon for ^{59}Co and ^{58}Ni yield only a very small fraction of fully stripped ions (~0.01 - 0.02%). This reflects the Z^2 dependence of the binding energy of the last electron which requires that the ion velocity increase proportionally to Z for equal stripping probability. It is conceivable that with the final linac configuration the stripping efficiency for the heavier ions of interest here can be increased by a factor of ≈100.

For the present measurement, we prepared a 150 mg sputter pellet composed of approximately equal amounts of Co and Ni. It contained ^{59}Ni from neutron activation in a ^{59}Ni/Ni ratio of 1.3×10^{-7}. The tandem-linac system delivered a ^{59}Co-^{59}Ni beam of 328 MeV with about 2×10^9 ^{59}Co ions/sec. This beam was passed through stripper #3 (See Fig. 1) and the second analyzing magnet (#2), set to select ^{59}Ni^{28+} ions at 45°. The particle energy spectrum measured under this condition with a Si ΔE-E telescope is shown in Figs. 2 and 3. In Figure 2 the total ^{59}Co background is seen. Since slit scattering and

charge exchange reactions will produce a low but continuous background in energy of essentially all charge states of ^{59}Co ions reaching the second analyzing magnet, the finite momentum bite of the magnet will result in the selection of discrete energy peaks of ^{59}Co ions reaching the $\Delta E/E$ detector telescope. Figure 3 shows an expanded view of the region of the highest charge states, and in particular the $^{59}Ni^{28+}$ peak at the expected position. For comparison the energy spectrum of a non-irradiated sample with a similar Co-Ni composition is shown. Although the ^{59}Ni counting rate was low (0.7 counts/min) due to the small stripping efficiency (See Table I), ^{59}Ni ions are clearly identified and separated from the ^{59}Co background.

Due to the multiple stripping involved in the present measurement, the sensitivity for detecting ^{59}Ni radioisotopes, $^{59}Ni/Ni \approx 10^{-8}$, is rather low. Optimistically one might hope for two orders of magnitude improvement from an increased stripping fraction at higher incident energy, for another one to two orders of magnitude from an increased ion-source output, and of course for some increase in sensitivity from a longer measurement. Measurements in the range of $^{59}Ni/Ni \approx 10^{-12}$ seem feasible in the future.

IV. RESULTS FOR ^{58}Fe

The ^{58}Fe tests were performed in preparation for a $^{60}Fe(T_{1/2} \approx 3 \times 10^5$ yr) lifetime measurement by accelerator mass spectrometry, similar to our recent measurement of the ^{32}Si half-life.[5] Ni-Fe mixtures, of natural abundance as well as depleted by a factor of 10^2 in ^{58}Fe (already only 0.3% natural abundance), were used as the sputter source materials. Only the terminal stripper was used in the accelerator system, resulting in an $^{58}Fe(^{58}Ni)$ beam of 169 MeV energy. The beam was again passed through the two analyzing magnets with a 1.7 mg/cm^2 aluminum foil placed approximately halfway between them. In this measurement the foil acted as a passive differential absorber resulting in a difference in energy loss for the ^{58}Fe and ^{58}Ni ions. The absorber foil thickness was chosen in such a way that the energy loss difference places the ^{58}Fe ions, with various charge states, halfway in magnetic rigidity between corresponding charge states of the ^{58}Ni ions. In this way the ^{58}Ni carrier beam background could be strongly suppressed by optimizing the second analyzing magnet setting for $^{58}Fe^{20+}$. The ΔE and E signals, and also the time-of-flight with respect to the pulsed beam structure

of the linac, as recorded by the silicon detector telescope are shown in Fig. 4 for a pure Ni, a pure ^{58}Fe, and a mixed Fe-Ni sample. The ^{58}Fe ions are unambiguously identified, with a sensitivity at present of $^{58}Fe/Fe \approx 1 \times 10^{-7}$.

V. SUMMARY AND CONCLUSION

The higher energies from the tandem-linac system allow us to extend the methods of accelerator mass spectrometry to medium-heavy nuclei. The multiple stripping involved severely limits the sensitivity, although limits of 10^{-12} should be possible, in particular when the spectrograph becomes available for particle analysis. The half life measurements of ^{60}Fe seems feasible with the present sensitivity.

We should like to thank the tandem and linac staff for their continuous assistance in these measurements, which required considerable skill and patience in machine operation. This work was supported by the U. S. Department of Energy under Contract W-31-109-Eng-38.

References and Footnotes

*On leave from Institute of Nuclear Structure, Swierk, Poland.

[1]G. M. Raisbeck, F. Yiou and C. Stephen, J. Phys. Lett. 40, L241 (1979); G. M. Raisbeck and F. Yiou, 20th Int. Symp. for Archeometry, Paris, March 26-29, 1980, to be published in Rev. d'Archéometrie.

[2]See for example: K. W. Shepard, IEEE Trans. Nucl. Sci. NS-26, 3659 (1979); L. M. Bollinger, Proc. Symp. on Heavy Ion Physics from 10 to 200 MeV; Brookhaven (1979); and references therein.

[3]F. J. Lynch, R. N. Lewis, L. M. Bollinger, W. Henning, and O. D. Despe, Nucl. Instrum. Meth. Phys. Res. 159, 245 (1979).

[4]W. Henning, W. Kutschera, M. Paul, R. K. Smither, E. J. Stephenson, and J. L. Yntema, Nucl. Instrum. Meth. Phys. Res. 184, 247 (1981).

[5]W. Kutschera, W. Henning, M. Paul, R. K. Smither, E. J. Stephenson, J. L. Yntema, D. E. Alburger, J. B. Cumming and G. Harbottle, Phys. Rev. Lett. 45, 592 (1980).

TABLE I. Charge state distribution of various medium-heavy ion beams from the linac, after stripping in a 100 μg/cm^2 carbon foil.

Charge state	Charge State Fraction (%)				
	^{35}Cl 165 MeV	^{40}Ca[a] 170 MeV	^{40}Ca 260 MeV	^{59}Co 328 MeV	^{58}Ni 314 MeV
12	.30				
13	1.3				
14	9.6				
15	37.8	6.4	.40		
16	39.5	18.0	1.9		
17	11.5	36.8	14.1		
18		32.1	41.2		
19		6.3	33.7		
20		.41	8.7	.36	.075
21				3.0	.81
22				13.5	5.2
23				31.5	18.7
24				36.0	35.5
25				14.7	29.9
26				.97	9.4
27				.023	.45
28					.014

[a]40 μg/cm^2 carbon foil.

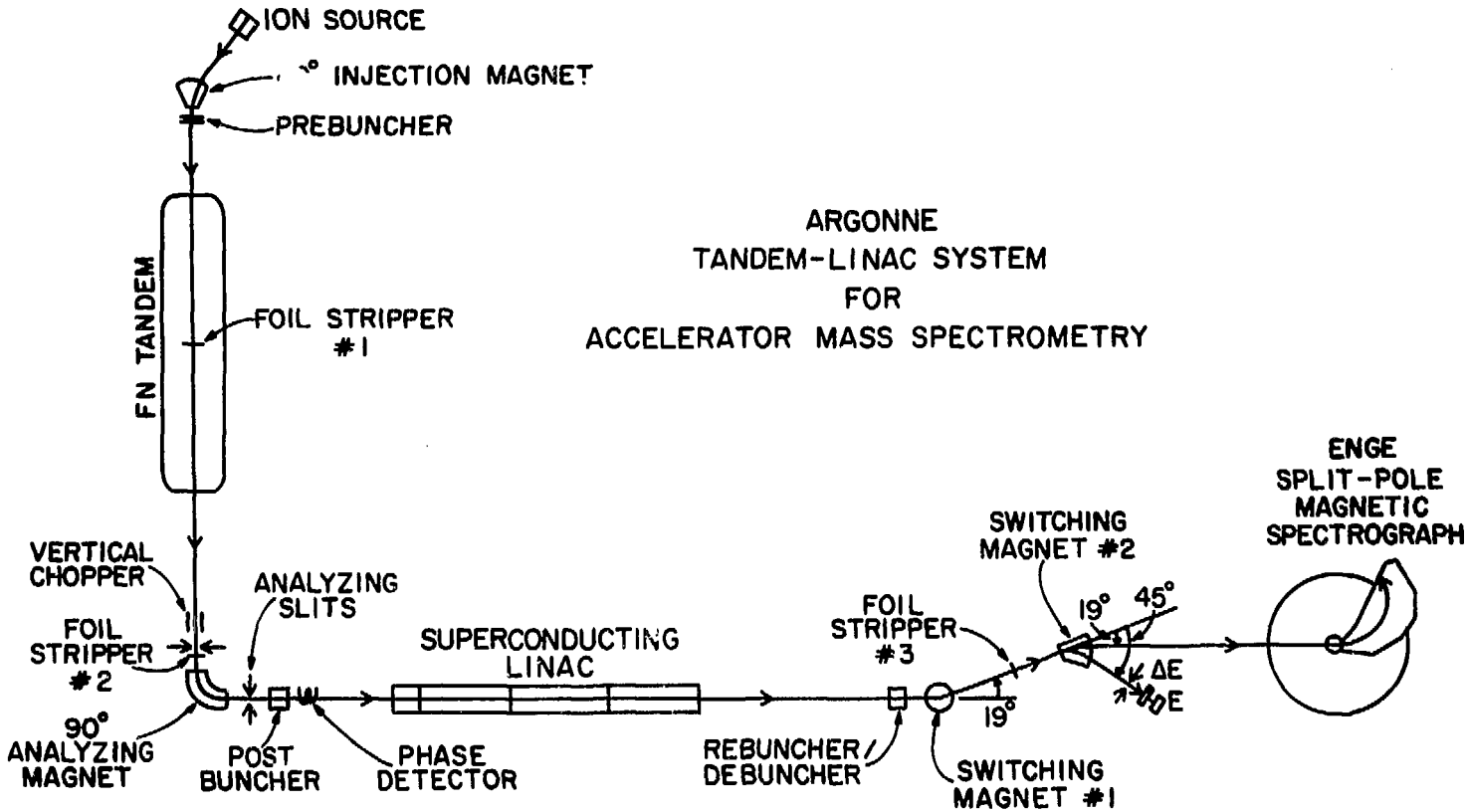

Fig. 1. Schematic layout of the Argonne tandem-linac system, showing the essential components for accelerator mass spectrometry. The magnetic spectrograph was not yet used in the present measurements.

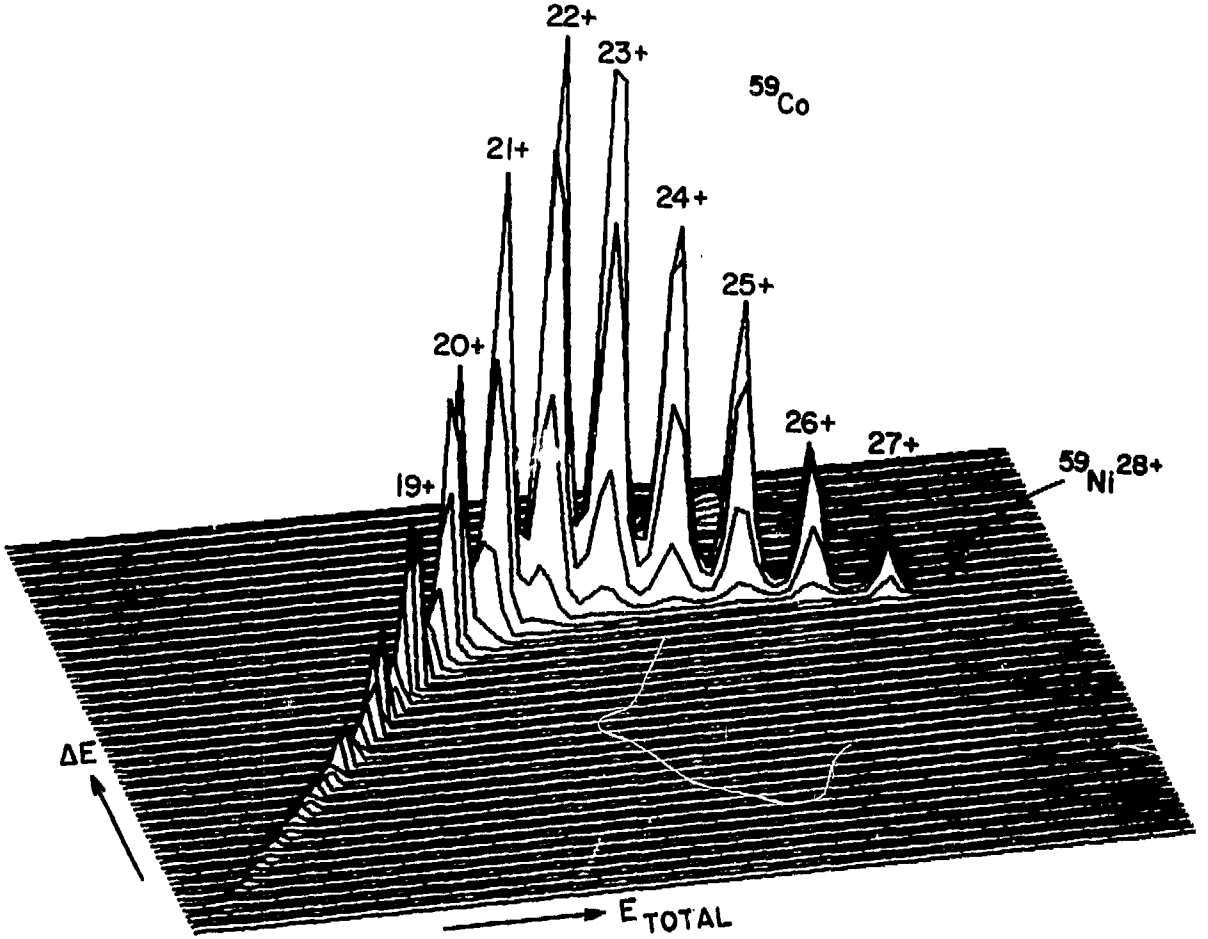

Fig. 2. Isometric plot of total energy, E_{total}, versus differential energy loss, ΔE, for $^{59}Co(^{59}Ni)$ ions as measured with the Si ΔE-E telescope. The vertical scale is linear.

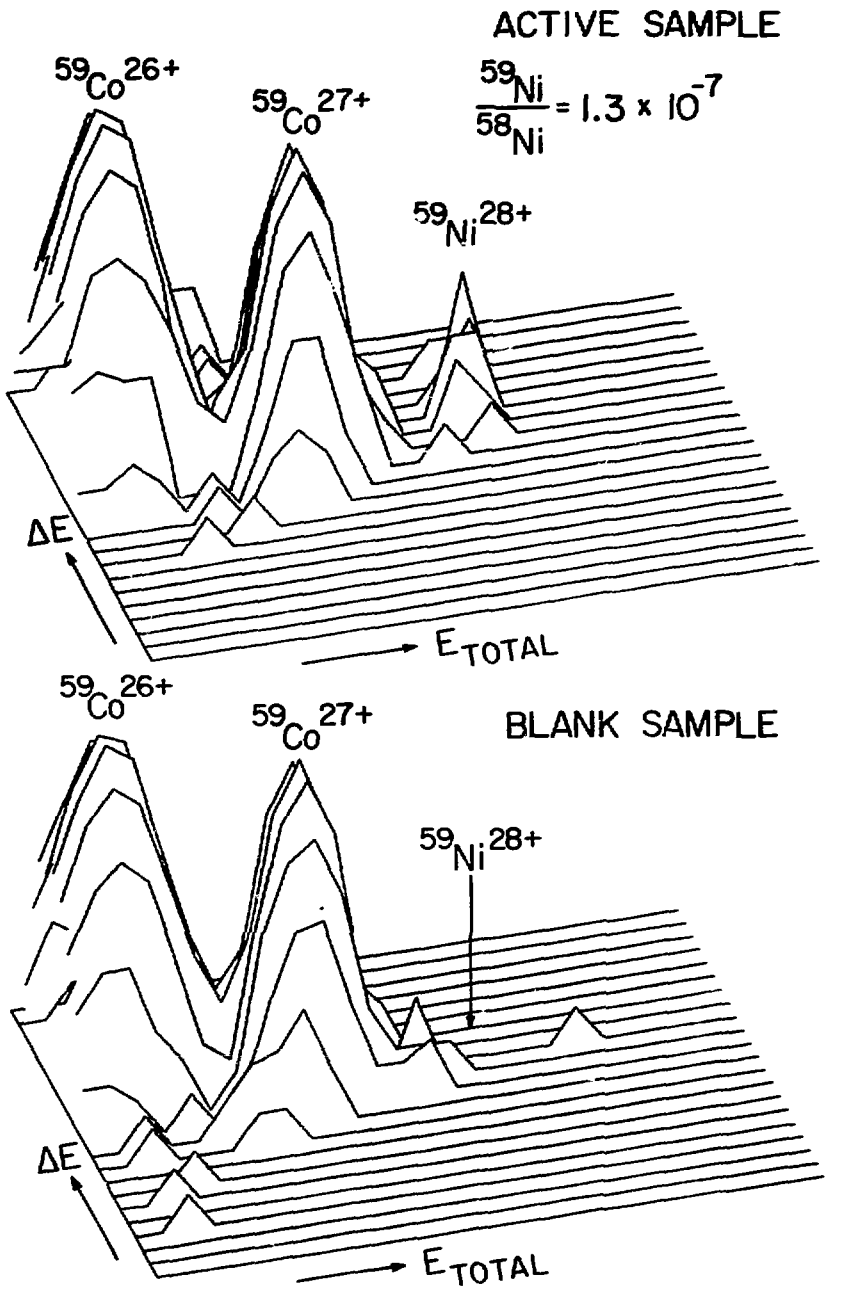

Fig. 3. Expanded view of the area of the three highest charge states in Fig. 2, for two different samples. The vertical scale is logarithmic, offset by 1 count such that a single count is showing.

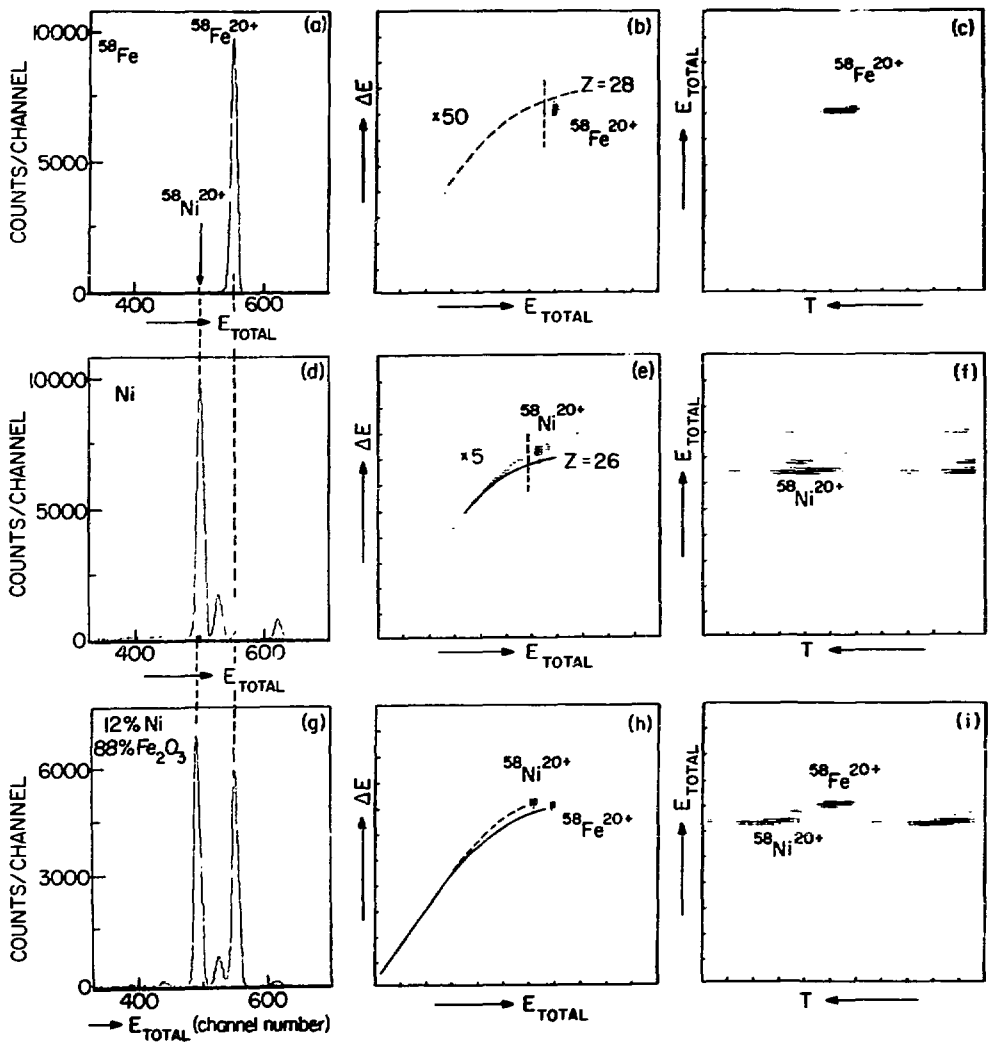

Fig. 4. One- and two-dimensional spectra for ^{58}Fe and ^{58}Ni ions of the total energy, E_{total}, energy loss, ΔE, and time-of-flight, T, measured in the Si ΔE-E telescope for three different ion source samples. The background peak in spectrum d), at the position of the ^{58}Fe 20+ peak, arises mainly from slit-scattered ^{58}Ni ions of a different charge state as deduced from the ΔE signal (not visible in e)). The time-of-flight spectra c), f), i) cover a range of approximately two beam-pulse periods (20 nsec).

SEARCH FOR THE ^{36}Cl ISOTOPE IN NATURAL SAMPLES BY CYCLOTRON OR TANDEM ACCELERATORS

I. Brissaud, J. Kalifa, H. Laurent, J.C. Roynette and C. Zaidins[x]
Institut de Physique Nucléaire, BP 1 91406 Orsay-Cedex

J.C. Fontes and J.M. Garnier
Laboratoire de Géologie et d'Hydrologie Isotopique
Université Paris-Sud Orsay

J. Guillot[xx], A. Peghaire[xxx], S. Plattard and J. Uzureau
Service de Physique Nucléaire et Neutronique,
Centre d'Etudes de Bruyères-le-Châtel

INTRODUCTION

Because of the Half-life of ^{36}Cl (305.000 years), the measurement of the concentration of $^{36}Cl/Cl$ in natural samples is essential to the dating of very old ground waters[1]. Thus, this measurement can provide an unique tool in fundamental research (such as knowledge of slow ground water movements) or in applied research (such as the evaluation of fossil water natural ressources... etc...). We are more especially involved in age determination of groundwaters from confined aquifers in regions with presently arid or semi-arid climates where deep aquifers were recharged during post pluvial episodes.

Accelerators as mass spectrometers have been used for approximately three years for the detection of different isotopes[2] and especially ^{36}Cl[3]. As a first step our group has tried to evaluate the possibilities of different accelerators by measuring the concentration $^{36}Cl/Cl$ of different samples prepared artificially. Then, we have begun to measure the ^{36}Cl presence in Sahara ground water samples.

To reduce the presence of impurities and especially of sulphur, we chose the silver chloride as chemical form to prepare the samples. These experiments were performed at different accelerators facilities of the Institut de Physique Nucléaire at Orsay and of Commissariat à l'Energie Atomique at Bruyères-le-Châtel.

x on leave from University of Colorado, Boulder
xx present address : IPN-Orsay
xxx on leave from CSNSM-Orsay

1. LINAC AND HEAVY IONS CYCLOTRON (ALICE-Orsay)

In 1979, we have done our first experiment using the heavy Ions Cyclotron + injection linac. Because of the magnetic field and the High-Frequency of these two accelerators, we could select perfectly mass 36. The background due to charge exchange was eliminated. The parameters of the two machines were adjusted by the acceleration in a first step of ^{27}Al for which the charge q^+ is chosen to keep similar the ratio M/q for ^{36}Cl and ^{27}Al. The final energy of ^{36}Cl was $E = K\,q^2/M$ = 252 MeV corresponding to a charge 12^+; the charge in the injection linac was 4^+ and energy ($E = \lambda M$) 42 MeV.

The detection of Cl was performed by a E.ΔE solid state detector telescope which separated the 3 isobares ^{36}Ar, ^{36}Al and ^{36}S. Sulphur originates principaly from the samples, but Argon is very abundant because this gas is very often used for the source plasma and this contamination of the machine is very important. The measurement was done for 10^{-8} and 10^{-10} concentration samples. We estimate that a concentration limit of few 10^{-11} could be reached. But the use of a detector having a more selective discrimination (for instance the multianode ionisation chamber used below) could certainly reduce the concentration limit to near 10^{-13}. Figure 1 shows a typical spectrum corresponding to 10^{-8} concentration. The poor beam transmission in whole accelerator (1 %) is another drawback because a large volume of sample is needed. That means that major improvements of these facilities are necessary.

2. EN TANDEM (Bruyères-le-Châtel)

Different measurements have been done at Bruyères since 1980. The 834 Genionex sputtering source was used at the beginning with a classical direct cesium beam and very recently with the reverse bombardment procedure. Different samples of 10^{-10} to 10^{-13} concentration have been used in the barrel. The particle detector is an ionization chamber with 3 or 5 anodes giving different ΔE signals; the cathode induces the total energy signal. The geometry of this detector is quite near to that of Rochester and Argonne[4]. A flow of isobutane at 28 torr is used; the energy resolution is about 4 % for each ΔE and 1 % for E. This detector is mounted on the beam line, in the focal plane of a split pole spectrometer.

The tandem operated at the maximum voltage (V = 6 MV) and the charge of chlorine was 7^+ to avoid the ambiguity of the detection induced by M/q (see

reference 3). The background due to charge exchange of ^{35}Cl and ^{37}Cl is reduced because the source magnet has a mass resolution of 2 %. In the first experiment, we saw that a cross-contamination between the source cones was important. To reduce this effect we now make use of a mixture ClAg + Zn with only 4 % of chloride in it. The mechanical and thermical stability of the samples are sharply improved by the use of this mixture and of the reverse procedure. The source magnet and the tandem voltage were tuned by means of the 35 and 37 chlorine acceleration and detection to obtain the same magnetic rigidity of these isotopes in the analyzing spectrometer. Thus the machine parameters were deduced for the equal rigidity ^{36}Cl by interpolation. The acquisition and reduction of data is done by a Mitra 225 computer with a Pericolor system. A typical spectrum is shown in figure 2 for the sample of concentration 10^{-10}. We could see two contaminations peaks by ^{35}Cl and one by ^{37}Cl. The contamination by ^{36}S is due to the sample and by an intermittent leakage of SF_6 in the accelerator tube. The simultaneous analysis of data in the different identification spectra E.ΔE improves sharply the separation of the 4 isotopes. For instance figure 3 shows in the $\Delta E_1 \times \Delta E_2$ space the identification of ^{36}S and ^{36}Cl for a concentration of 10^{-8}. Figure 4 shows the $E_T \times \Delta E_f$ spectra for a 10^{-12} concentration prepared sample and a sample from Sahara groundwater.

Up to now we have detected the 3 chlorine isotopes by switching simultaneously the source magnet field and the tandem voltage. We have designed two Faraday cups to be installed in the focal plane of the analyzing spectrometer to measure the 35 and 37 chlorine isotopes currents and 36 Chlorine after switching the source magnet only, the tandem voltage remaining tuned for the mass 36. The concentration limit obtained up to now is about 10^{-13}, but we have to improve the tuning of the machine, the cleanliness of the source and especially the preparation of the samples. For these reasons it is difficult today to give the ^{36}Cl concentration of Sahara groundwater with a good accuracy. We are planning to resume these experiments very soon and improve the recent measurements.

3. MP TANDEM (Orsay)

At the tandem of IPN Orsay a preliminary test showed that the background due to charge exchange of Cl in the accelerator tube is excessive due to the fair mass resolution of the source magnet (only 6 %). Thus, we have designed and built a 2 meters and 23° electrostatic deflector. Its mass disper-

sion is about 6 mm for $\Delta M/M = 1$ %. This deflector will be installed just after the analyzing magnet at the 70° out-put and the detector will be fixed at the extremity of the deflector to detect ^{36}Cl. Two Faraday cups at the entrance of the electrostatic spectrometer measure simultaneously the ^{35}Cl and ^{37}Cl beams passing through the injection magnet. A new type of halogene source due to Pomot et al[5] could select Cl isosopes from sulphur because of the different electronic affinity in a porous material (ZrC). The selectivity could be about 10^4. The design of such a source is underway at Orsay (see figure 5). The tandem voltage will be stabilized by a classical slits system on the 35 Chlorine beam.

In conclusion we hope to use very soon the electrostatic spectrometer and the specific source to measure ^{36}Cl abundance in natural samples. We are planning to use our different facilities at Orsay to detect ^{81}Kr (underway at the Orsay cyclotron) and ^{129}I. A preliminary detection of ^{14}C is planned at Bruyères-le-Châtel by Uzureau et al.

Figure captions

1) Typical spectrum of 36 isobares accelerated by Heavy Ions Cyclotron (ALICE).

2) $\Delta E_{final} \times E_{total}$ identification spectrum showing the 36 mass isobares and the 3 peaks of 35 and 37 chlorine background. ΔE_{final} is the signal coming from the third anode and corresponding to the residual energy.

3) $\Delta E_1 \times \Delta E_2$ identification spectrum of ^{36}Cl and ^{36}S for a 10^{-8} concentration sample; ΔE_1 and ΔE_2 are the two first anodes signal from the ionization chamber.

4) $\Delta E_{final} \times E_{total}$ spectra a) for a 10^{-12} concentration sample
b) for a Sahara ground water.

5) MP tandem and detection set-up at Orsay.

References

1) Proceeding of the Workshop on dating old ground water Tucson (Arizona) 1978, S.N. Davis editor.

2) T.S. Mast and R.A. Muller, Nucl. Science Appl. 1 (1980) 7 and references inhere.

A.E. Litherland, Ann. Rev. Nucl. Science 20 (1980) 437 and references in here.

G.M. Raisbeck and F. Yiou et al., Nature 275 (1979) 731, Earth Planet Sci. Lett. 43 (1979) 237, J. Phys. Lett. 40 (1979) 241 and references in here.

3) D. Elmore et al., Nature 277 (1979) 22, K. Nishiizumi et al., Earth Planet Sci. Lett. 45 (1979) 285. See T.S. Mast and R.A. Muller, and A.E. Litherland Reference 2.

4) D. Shapira et al., Nucl. Inst. Meth. 129 (1975) 123.
J.P. Erskine et al., Nucl. Inst. Meth. 135 (1976) 67.
H.W. Fulbright et al., Nucl. Inst. Meth. 162 (1979) 21.

5) I. Rachidi, J. Monte, J. Pelletier, C. Pomot and F. Rinchet, App. Phys. Lett. 28 (1976) 292.

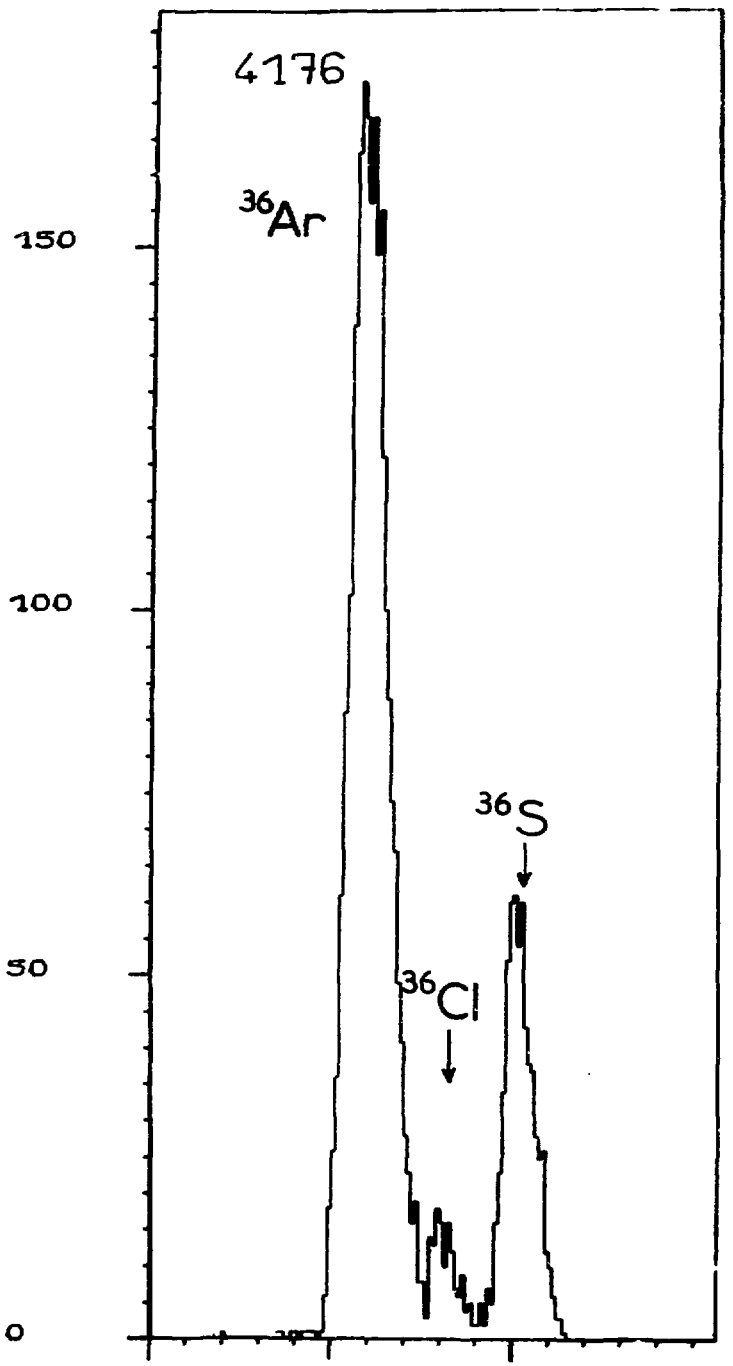

Fig. 1

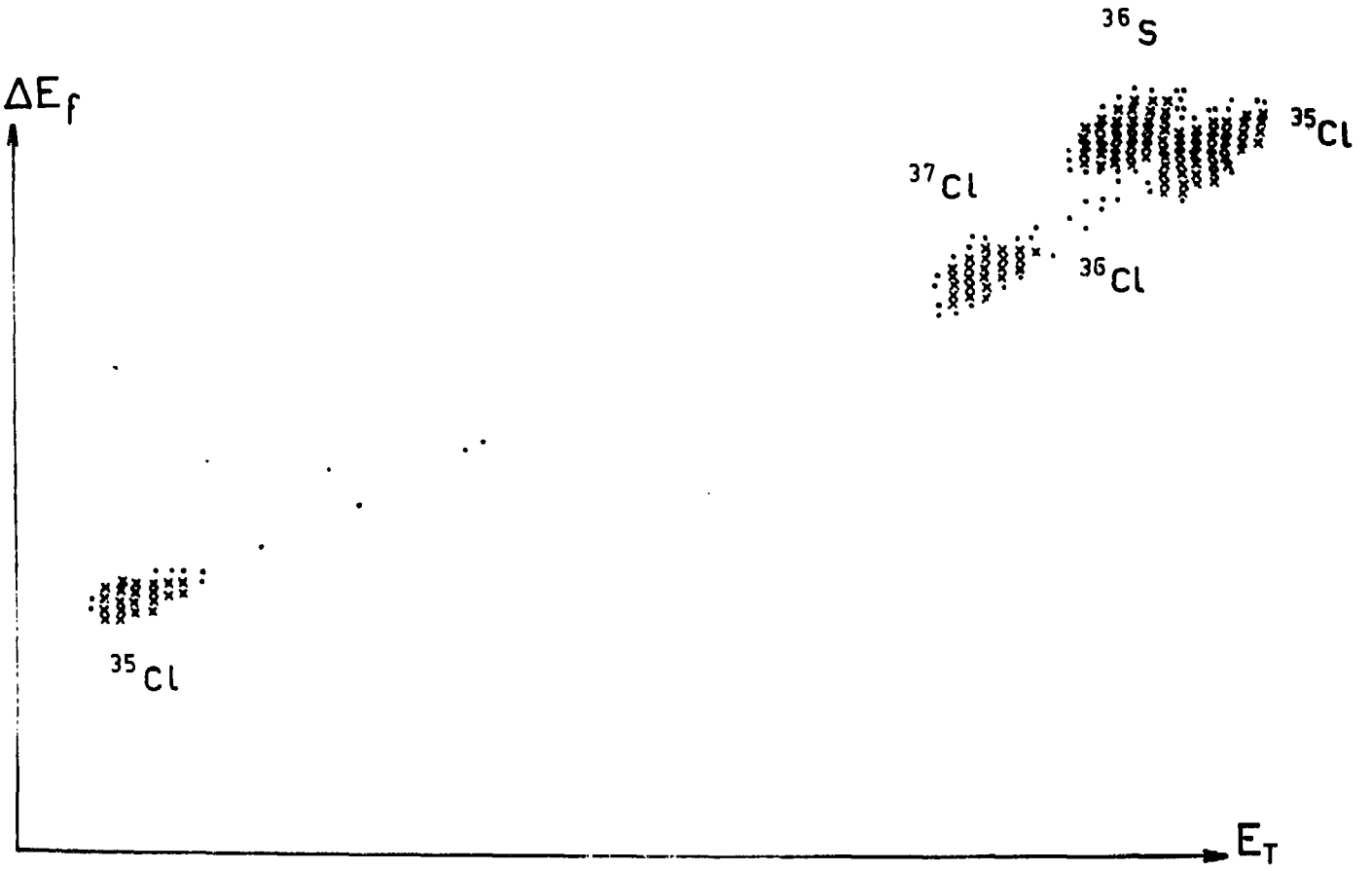

Fig. 2

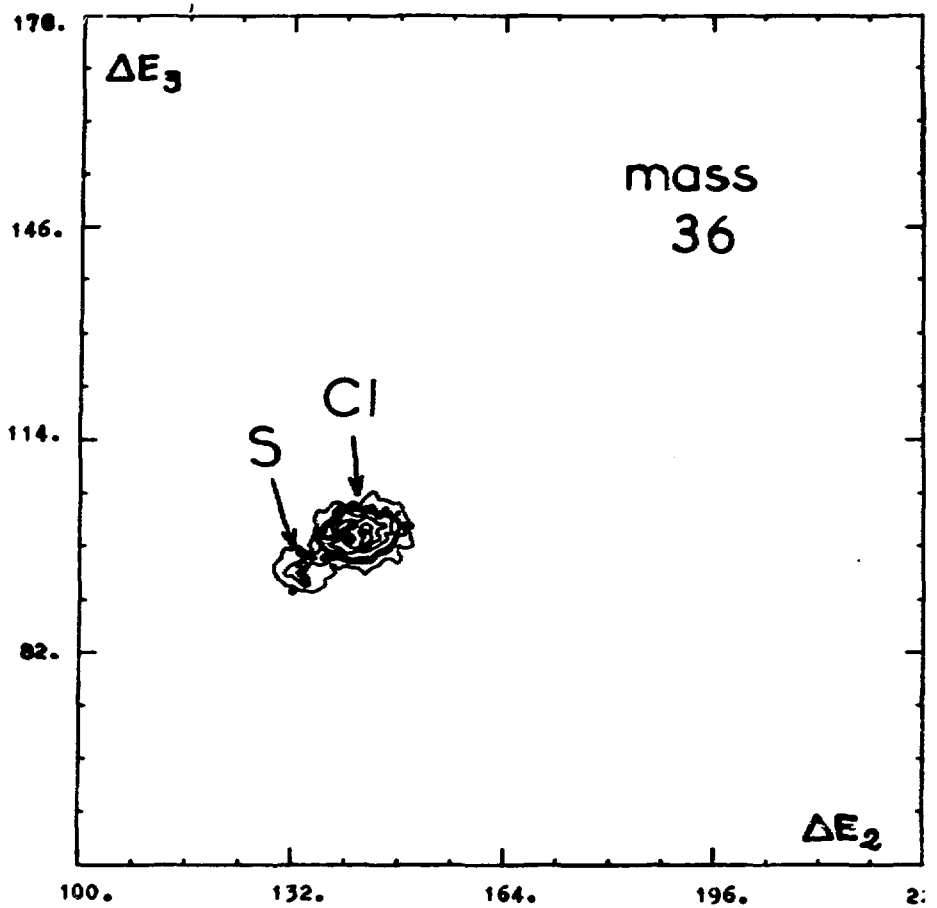

Fig. 3

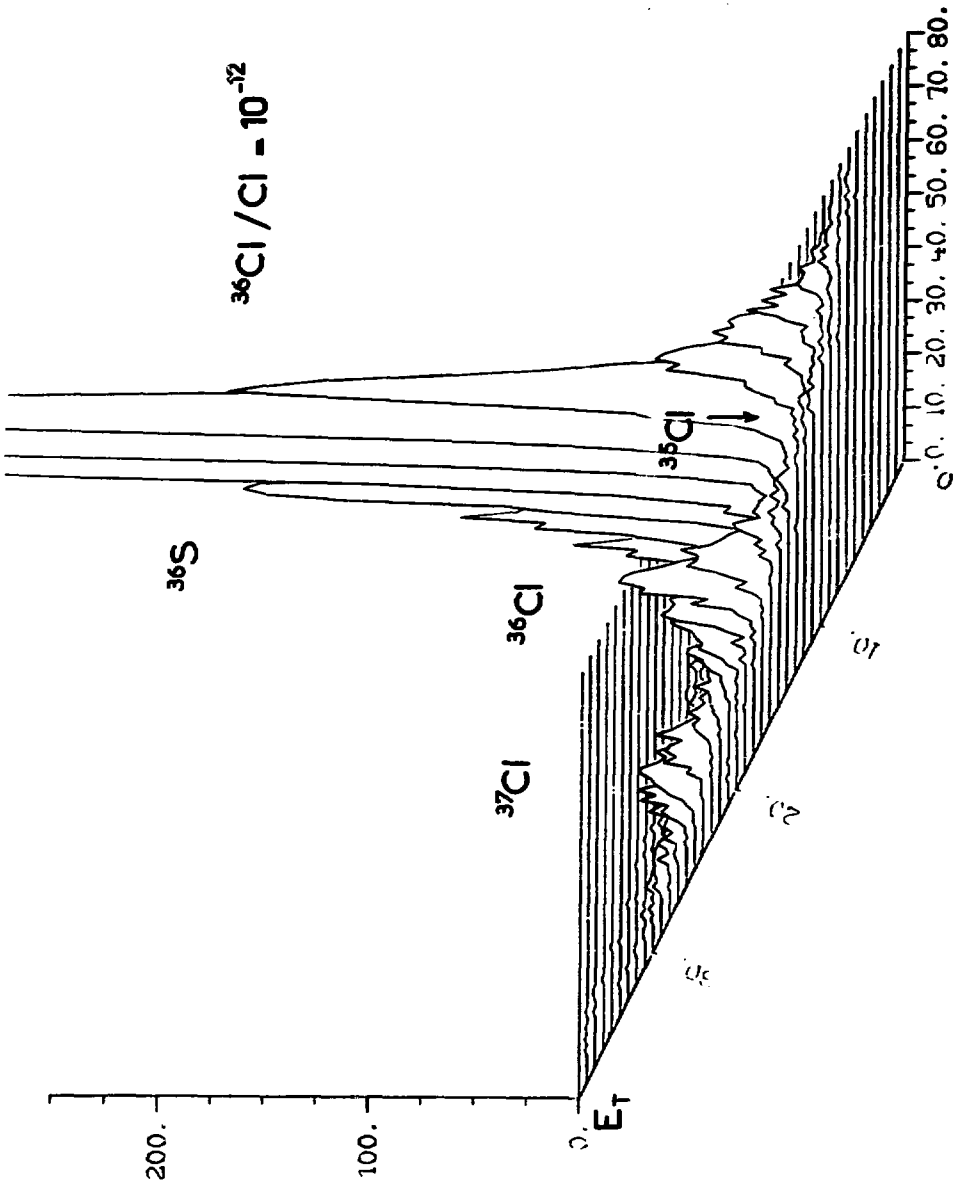
$^{36}Cl/Cl - 10^{-12}$
^{36}S
^{35}Cl
^{36}Cl
^{37}Cl
200.
100.
0.
E_T
0. 10. 20. 30. 40. 50. 60. 70. 80.
ΔE_f

Fig. 4.a

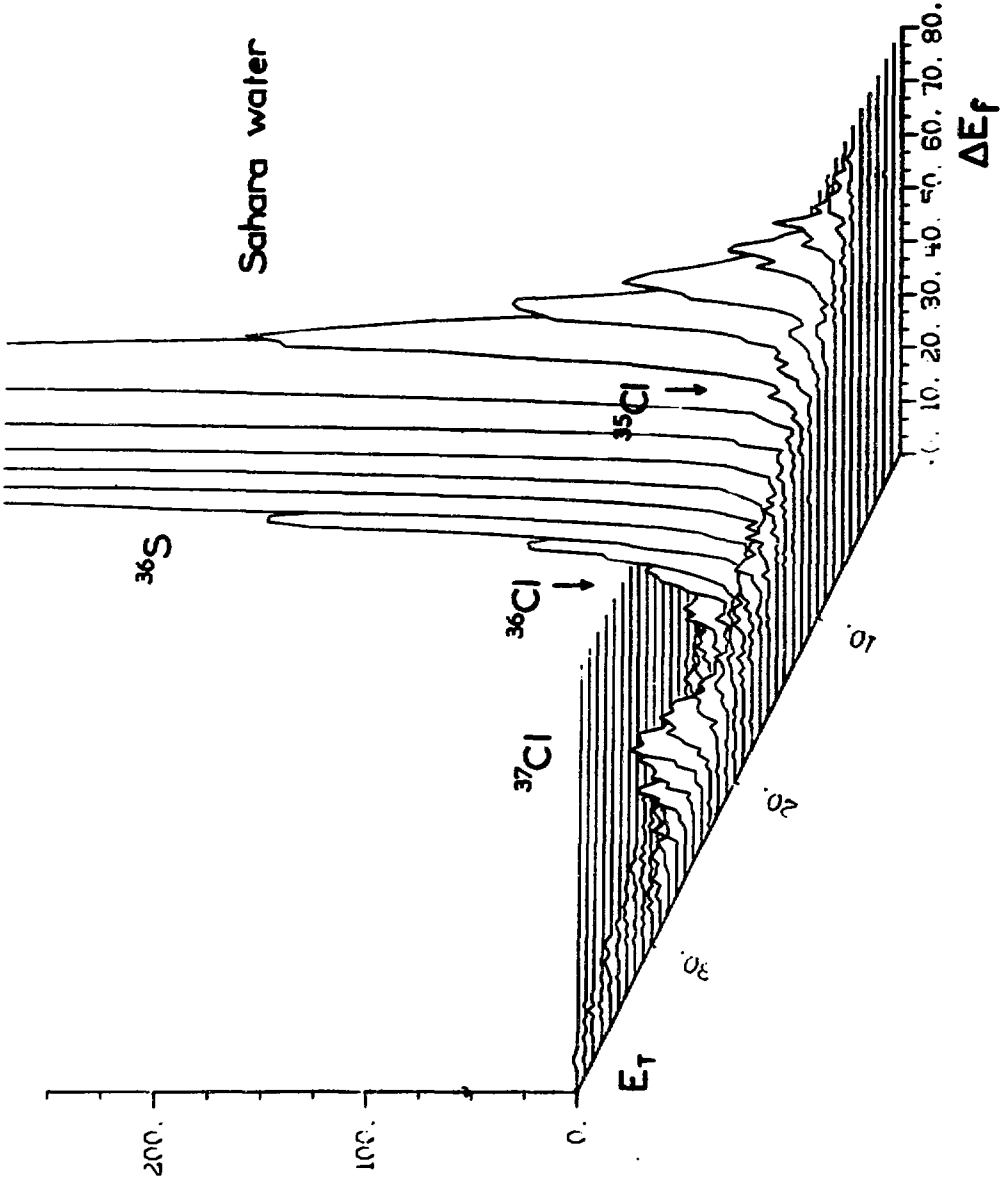
Sahara water
^{36}S
^{36}Cl
^{35}Cl
^{37}Cl
E_T
ΔE_f
0
10.
20.
30.
40.
50.
60.
70.
80.
100.
200.

Fig. 4.b

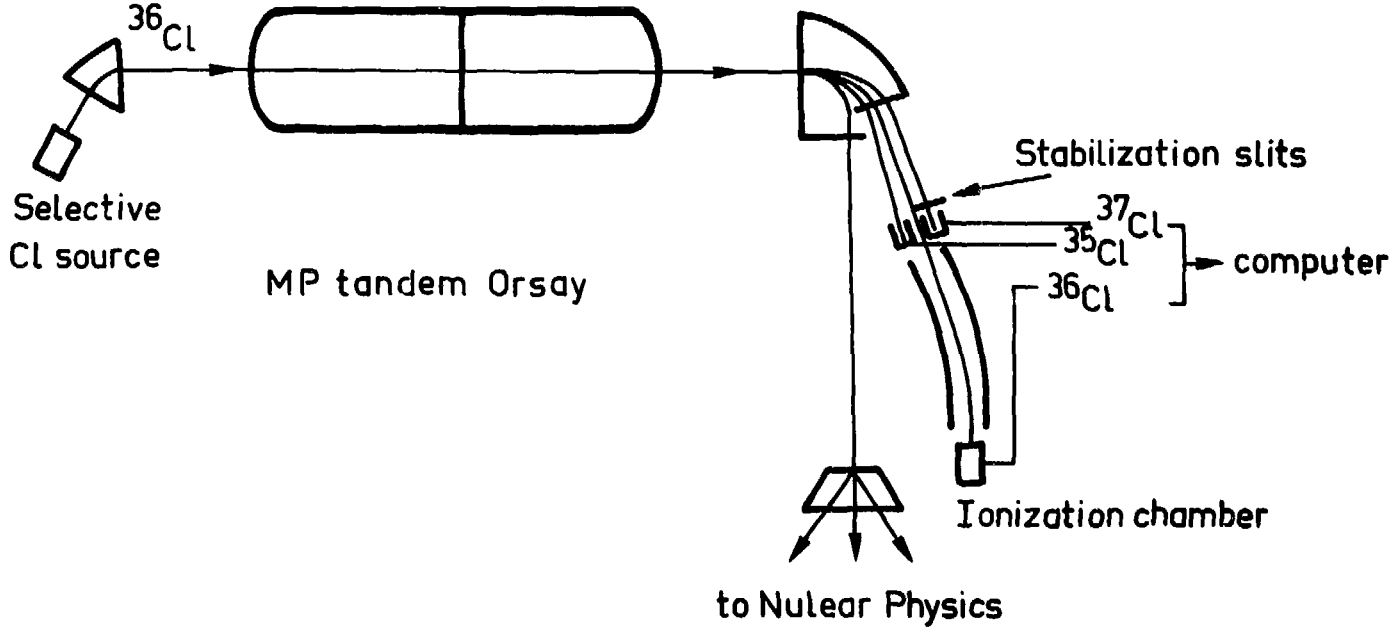
^{36}Cl
Selective
Cl source
MP tandem Orsay
Stabilization slits
^{37}Cl
^{35}Cl
^{36}Cl
computer
Ionization chamber
to Nulear Physics

Fig. 5

THE MUNICH ATTEMPT TO DETECT ^{36}CL

P.W. Kubik, G. Korschinek, E. Nolte, M.S. Pravikoff, H. Morinaga
Fachbereich Physik E17, Technical University Munich, W.-Germany

ABSTRACT

The Munich MP-tandem-postaccelerator facility is suitable for the detection of traces of ^{36}Cl making use of the fact that postaccelerated ^{36}Cl ions can be stripped to a good portion to naked $^{36}Cl^{17+}$ ions and can be separated from the disturbing isobar $^{36}S^{16+}$ by magnetic deflection. Since the beam line system of the Munich MP-tandem and the postaccelerator[1] is rather long - about 110 m from the ion source to the detection place - it is necessary to use an auxiliary beam in order to stabilize the tandem and to transport the ghost beam. In the case of a ^{36}Cl beam the auxiliary beam will be $^{18}O_2^-$ injected into the tandem. The postaccelerated ghost beam and the auxiliary beam are separated by a stripper foil and a successive magnetic deflection.

First trials, using a ^{36}S test-beam instead of ^{36}Cl, show that it is possible to postaccelerate the ghost beam and the auxiliary beam at the same time.

1) E. Nolte, G. Geschonke, K. Berdermann, M. Kress, W. Schollmeier, Y. Shida, H. Morinaga; IEEE Trans. on Nucl. Sc.. Vol. NS-26, No. 3, June 1979 and E. Nolte, G. Geschonke, K. Berdermann, R. Oberschmid, R. Zierl, M. Feil, A. Jahnke, M. Kress and H. Morinaga; Nucl. Instr. and Meth. 158 (1979) 311-324

Dup

MASS SPECTROMETRY WITH A VERY SMALL CYCLOTRON

Richard A. Muller, Pieter P. Tans
Terry S. Mast, James J. Welch

Lawrence Berkeley Laboratory
University of California
Berkeley, California
94720

Abstract: We propose that direct detection of natural radioisotopes can be accomplished by using a very low energy (20-100 keV) cyclotron accelerating negative ions.

The multi-MeV energy of cyclotrons and tandem Van de Graaff accelerators has played a central role in the development of direct dating techniques. The high energy has been necessary in order to allow the use of particle identification detectors which measure dE/dx and total energy, and for range filtering.[1] It also facilitates the disintegration of molecular backgrounds in the tandem machines.[2]

Also important has been the discovery that certain potential background ions (^{14}N for ^{14}C detection; ^{36}Ar for ^{36}Cl detection) do not form negative stable ions, and are therefore not accelerated in the tandem machines. This suppression has not been exploited with existing cyclotrons, which were all designed to accelerate positive ions.

Cyclotrons have a different feature which has proven useful in direct radioisotope detection: The great selectivity of the resonant acceleration process. This suppression arises from the requirement that the ion stay in phase with the applied electric field for the 100 to 200 or more cycles of acceleration. Ions which differ in charge-to-mass ratio by only a part in a thousand can be <u>totally</u> suppressed. Detuned by 1% from a 10 microampere beam, we once observed no counts in a half hour, a suppression factor better than 10^{-17}. Although ordinary mass spectrometers can achieve resolutions equal to or superior to that of the cyclotron, they cannot match the total suppression of background ions with different charge-to-mass ratios.

We believe that by combining the high selectivity of the cyclotron with the suppression of certain backgrounds by using negative ions, that one can achieve the sensitivity necessary for direct detection of natural radioisotopes without the need for

high energy. When all backgrounds are suppressed, particle identification is unnecessary.

We propose a negative ion cyclotron with a magnetic field of a few kilogauss. The maximum energy would be less than 100 kilovolts, and perhaps as low as 20 kilovolts. By using many turns to accelerate the ions, we should be able to obtain selectivity comparable to or better than that obtained with high energy machines. Good vacuum (less than 10^{-7} torr) may be necessary to achieve good efficiency, and we probably wish to use sector focussing. External ionization with axial injection would minimize space charge effects from non-resonant background ions. For the lighter ions (^{3}H, ^{10}Be, ^{14}C) the entire instrument should be smaller than a desk. Accelerated ions never reach sufficient energy to induce radioactivity, and in many ways the machine would be like a mass spectrometer rather than like an accelerator. (Perhaps it should be called a "cyclometer" rather than "cyclotron".) Detection with a dynode detector supresses scattered beam which had not been accelerated to its threshold energy of 15 to 20 keV. Solid state high bandwidth power supplies can easily provide the less than one thousand volts required on the Dees. Pulse shapes other than the usual sine-wave can be used. Normalization can be accomplished by rapidly switching the cyclotron frequency to accelerate a stable isotope, or by switching from the sample to a standard of known concentration.

On the Berkeley 88" cyclotron our resolution has been better than 20,000 : 1, and have resolved (although not completely separated) the isotopes ^{10}Be and ^{10}B. Our goal for the small cyclotron is a resolution of about 50,000 to 1. Small mass spectrometers based on the cyclotron principle have already achieved excellent resolution. The "Omegatron" of Sommer, Thomas, and Hipple[3] achieved a mass resolution of 1 part in 10,000 and had a radius of less than one centimeter. The "mass synchrometer" of Lincoln Smith and C. Damm[4] achieved a resolution of 1 part in 25,000 and was 15 inches in diameter. It combined slits with three turns of cyclotron acceleration. Negative ions and resolution of 50,000:1 should be sufficient to allow measurement of the following naturally occurring radioisotopes: ^{3}H, ^{10}Be, ^{14}C, ^{26}Al, ^{32}Si, ^{36}Cl, and ^{129}I. With other separation techniques or better resolution, other radioisotopes could be measured. In the table we list several of the interesting radioisotopes, and the properties of potential backgrounds. It is clear from the table that for certain radioisotopes, positive ions could be used as well. Not included in the table is the "higher harmonic" background. If ^{3}H is accelerated, ^{9}Be, ^{15}N, and molecules of the same mass are also accelerated, the dee frequency being the third, fifth, etc. harmonic of the approximate particle frequency. Most of these backgrounds are suppressed by the cyclotron resolution; further suppression

occurs at the deflector at the exit of the acceleration region because they have lower energy than the radioisotope.

Compact magnets of the size and field required for dating have been designed and built for microtrons (cyclotron-like devices for electrons). A typical microtron electromagnet, including return yoke, fits in a space 1.5 meter in diameter and 0.5 meter high, and gives a magnetic field of 2 kilogauss over a circular region with diameter 1 meter.[5] It may be possible to use permanent magnets by using rare-earth alloys such as Samarium-Cobalt.

The proposed low energy negative ion cyclotron is based on the extensive experience gained in the last five years with high energy systems. If successful, it may bring down the cost of detection, and make the direct detection technique more accessible to many scientists.

Acknowledgments

This work was supported by the U.S. Department of Energy under contract W7404ENG48

REFERENCES

1. R.A. Muller, LBL-5510 (1976), SCIENCE 196, 521 (1977).
2. D.E. Nelson, R.G. Korteling, W.R. Stott, SCIENCE 198, 507 (1977): K.H. Purser, R.B. Liebert, A.E. Litherland, R.P. Beukens, H.E. Gove, C.L. Bennett, M.R. Clover, W.E. Sondheim, 2nd Int. Conf. Electrostatic Accel. Tech., Strasbourg France, 1487 (1977); C.L. Bennet et al., SCIENCE 198, 508 (1977).
3. J.A. Hipple, H. Sommer, and H.A. Thomas, Phys. Rev. 78, 332 (1950).
4. L.G. Smith and C.C. Damm, Rev. Sci. Instr. 27, 638 (1956).
5. S.P. Kapitza and V.N. Melekhin, The Microtron (Harwood, London 1978), Chap. 5.

TABLE

Selected Radioisotopes for Small Cyclotron Dating

Radioisotope	Background	Required Resolution	Comments
^{3}H	^{3}He	150,000	Eliminate with (-) ions
	HD	230	Easily resolved
	H_3	400	Easily resolved
^{10}Be	^{10}B	17,000	Resolvable
	^{9}BH	1,500	Easily resolved
^{14}C	^{14}N	83,000	Eliminate with (-) ions
	^{13}CH	1,800	Easily resolved
	$^{12}CH_2$	1,100	Easily resolved
^{26}Al	^{26}Mg	6,000	Easily resolved
^{32}Si	^{32}S	15,000	Resolvable
^{36}Cl	^{36}Ar	47,000	Eliminate with (-) ions
	^{36}S	29,000	Possible (?)
^{39}Ar	^{39}K	64,000	Very difficult; (+) ions required
^{41}Ca	^{41}K	89,000	Use CaH_3^- ions
^{53}Mn	^{53}Cr	82,000	Difficult
^{129}I	^{129}Xe	62,000	Eliminate with (-) ions

REPRODUCIBILITY OF ISOTOPE RATIO MEASUREMENTS

D. Elmore
Nuclear Structure Research Laboratory
University of Rochester
Rochester, New York 14627

The use of an accelerator as part of a mass spectrometer has improved the sensitivity for measuring low levels of long-lived radionuclides by several orders of magnitude. However, the complexity of a large tandem accelerator and beam transport system has made it difficult to match the precision of low energy mass spectrometry.[1] Although uncertainties for accelerator measured isotope ratios as low as 1% have been obtained under favorable conditions, most errors quoted in the literature for natural samples are in the 5-20% range. These errors are dominated by statistics and generally the reproducibility is unknown since the samples are only measured once.

Radiocarbon dating by decay counting is a well developed technique — typical uncertainties are at the 1% level and 0.2% is possible with large modern samples.[2] The $\sim 10^3$ improvement in sensitivity with the accelerator technique reflected in reduction of sample size is not always useful with modern samples unless 1% (80 years) reproducibility is obtained, although 10% measurements can be very useful for old samples. A similar detailed chronology has not yet been established for ^{36}Cl dating of groundwater, but even here the use of ^{36}Cl profiles to study old acquifers benefits from a reproducibility of a few percent or better. The radioisotopes ^{10}Be, ^{26}Al, and ^{129}I have only one stable isotope. For reasons discussed below it may be difficult to obtain ratios to better than a few percent in such cases.

In this paper, I will try to identify some of the problems in obtaining reproducible isotope ratios at the 1% level when using an existing tandem accelerator facility. The experience gained at Rochester and elsewhere is being used to design a new generation of tandem-accelerator mass spectrometers — it is hoped that these new machines[3] will be able to reduce uncertainties in isotope ratios to well below the 1% level.

APPARATUS AND PROCEDURE

The apparatus at Rochester has been described elsewhere[4,5] so only the details relevant to normalization of isotope ratios will be given here. Refer to Figure 1, reference 4 (H. E. Gove, this proceedings) for a diagram of the present system. The basic normalization features are (1) to cycle the magnetic elements to alternately select each isotope over a few minute time scale, (2) to measure currents after the accelerator and (3) to normalize isotope ratios to a standard.

Until recently a HICONEX[6] model 834 Cs sputter ion source was used. Here a twelve sample cassette allows switching between an unknown sample and a standard in a few seconds. The reflection geometry[7] was used: the positive cesium, after passing through a hole 3 mm off axis, is reflected back by the positive extraction electrode to sputter the sample located on axis. The Cs optics are not ideal; a cusp is formed in the Cs beam spot which results in an irregular beam profile. Also, it was difficult to orient the sample holders precisely.

A new source[3,6] has been used to obtain the results in this paper. As with the old source, the cesium beam is formed external to the negative ion extraction region (in the Cs "gun"). However, in the new source, the cesium is directed at the front of the sample with an angle of 45° to the negative ion axis, more like a conventional microprobe. The cesium beam is steered and focused to a small (0.1-1 mm) uniform spot on the sample. The Cs and negative ion extraction supplies are independent so that load changes in the Cs gun will not affect the beam energy, resulting in a stable beam (less than ±1% variation is typical over a period of 10 minutes). Up to eighteen samples can be mounted on a 23 mm diameter disc (5 mm separation between samples) and this can be loaded into the source through a vacuum lock. A two dimensional computer controlled manipulator is used to both select the desired sample and to position it to about 50 μm. Beam currents of 15 μA C^- from graphite and 22 μA Cl^- from AgCl have been obtained. For the results presented in this paper the source has been mounted on the 35° inflection magnet of the original injector. A new injector with a 90° magnet is under construction.[8]

The beam transport system, shown in Figure 1 of ref. 4 incorporates six beam waists. The two (circular) apertures located before the accelerator as

well as the 8.6 mm diameter stripper canal at the terminal are filled by the beam and are not easily enlarged. The three slits following the accelerator are adjustable and for the lighter isotopes can be made three or four times larger than the beam without allowing appreciable interference to pass to the detector. A Ni mesh attenuator with ~10% transmission is inserted before the low energy Faraday cup to keep intense beams from loading down the accelerator and possibly changing its transmission efficiency.

Normalization is accomplished by switching three magnetic elements (the inflection magnet, the high energy quadrupole, and the 90° analyzer) to alternately select the stable and radioactive isotopes. The stable isotope current is measured in the image Faraday cup. The radioisotopes pass through three additional fixed elements and are then counted in the gas-filled ionization detector.

The inflection magnet field is set with a computer controlled stepping motor and is monitored with a Hall-effect probe. The high energy quadrupole doublet and 90° analyzing magnet are controlled by three independent sets of potentiometers which are manually adjusted but selected by computer controlled relays. An NMR probe is used to set the magnet field, and beams with the appropriate magnetic rigidity are used to set the quadrupole fields. The magnets take from 2 to 15 seconds to stabilize depending on the magnitude of the change in field.

Once everything is adjusted, the computer takes over control of the measurements. The detector, magnets, Faraday cups and attenuator are interfaced to a PDP-8 computer which is connected by a fast link to a DEC-10 computer where the FORTRAN program URSULA resides. URSULA is given an arbitrary sequence of commands to be carried out for each cycle. Typically, the attenuation factor, $i_{LE}(\text{att. in})/i_{LE}(\text{att. out})$, and accelerator transmission efficiency, $(i_{IMAGE}/q)/i_{LE}$, are measured the first cycle and every fifth cycle thereafter. The inflection magnet field is set with a closed-loop beam optimization method which is carried out with the stable isotopes every 1-3 cycles. To do this, beam current readings in the image cup at five different field settings near the mass peak are fit with a Gaussian shape to determine the location of the maximum and width. The field is then set to the maximum and the current is read for typically five consecutive 5 sec intervals to provide a measure of the source and accelerator stability. An

increase in width is an indication that the source needs to be retuned. Normally no changes are made in the system when changing samples.

After the stable isotope currents are read, the cups are removed and the radioactive isotope is counted. URSULA accepts up to six parameters for each event (e.g. five energy loss and one total energy) and applies a digital gate to each parameter and/or an arbitrary two-dimensional gate to any pair of parameters. This procedure can provide rejection factors over 10^6 for interfering isotopes.[5] The experimenter is warned if the location of a peak within its gate changes. Deadtime losses are corrected for by normalizing to a 60 Hz pulser (connected to the preamplifiers) that runs during data acquisition. In addition to the usual one-and two-dimensional data displays showing the current setting of the gates, URSULA plots on a CRT the isotope ratios and beam current for each cycle as shown in Figure 1. This graphic representation of the results helps the experimenter distinguish between statistical fluctuations and step function changes caused by instabilities in accelerator parameters. At the end of a series of cycles (a cycle includes one measurement of each isotope), a statistical summary is typed out which includes the mean value of the ratios and the standard deviation of the mean (the so-called external error).

RESULTS

The figures show results for the stable chlorine isotopes obtained with several AgCl samples. The ratios in Figure 1 are for individual cycles on one sample and were obtained in about 20 min. The mean values for many similar series of cycles are plotted in Figure 2. The standard deviation of the mean is less than 0.3% in all cases and averages about 0.15%. However, the value of the ratio varies from 3.45 to 3.56, a 3% range. The ratio differs from the expected natural ratio, 3.13, primarily because of mass fractionation in the terminal stripper and beam transport system. The change in the ratios when going from one sample to the next and when tuning the beam (vertical lines in Figure 2) are due to changes in this mass fractionation, as will be explained more fully below.

DISCUSSION

For the purposes of this discussion I will divide errors into random errors, those that contribute to the standard deviation of the mean, and

systematic errors, those that shift the mean from the expected value. The data (Fig. 1) show that automated cycling has reduced the random errors, excluding counting statistics, to below the 0.5% level. It can be reasonably assumed that counting statistics are the main additional contribution to the random error for radioisotope ratios. Improvements below 0.5% can almost certainly be made by decreasing the cycle period below the 3-5 minute minimum for the present apparatus.[3] Errors much lower than this will be difficult to establish for the radioisotope ratios, however, because of the large number of counts required. Since systematic errors seem to be a problem above the 1% level (Fig. 2), the rest of the paper will be devoted to them — first those that affect the isotopes independently, then errors in the correction to mass fractionation.

Independent Systematic Effects

These effects result in an incorrect value of either the stable isotope current or the radioisotope counting rate. To a large extent, the resulting change in the ratio of radioisotope to stable isotope will be the same for the standard and unknown so that much of the errors will cancel when the data is normalized to a standard. Non-linearities, zero offsets, and changes with time (especially infrequent step function changes) will still introduce errors, however. Errors from non-linearities and unknown zero-offsets can be minimized by choosing a standard with an isotope ratio and source output close to those of the unknown.

There are many effects that contribute to the problems of reproducibility of isotope ratios, especially when complex existing accelerators are used. Since the relative importance of these effects depends on which radionuclide is being studied, on the magnitude of the ratio and the source current, and on the stability of power supplies, I cannot do more than list the possible causes. The data presented in this paper does not support or contradict any of the statements made about the magnitude of the errors in the following independent effects. Based on experience with ^{14}C and ^{36}Cl measurements at Rochester, each of these effects can be kept below 1% after comparison to a standard. More experiments will be required to establish whether the sum of all such errors can be kept below 1%.

1. Current measurement: The beam current is measured in a Faraday

cup with a negatively biased shroud for electron suppression using a commercial current integrator.[9] Drifts are unlikely but a zero offset can result from bias leakage and ground loop currents.

2. Attenuation factor: Transmission through the attenuator will increase slowly with time due to sputtering of the Ni mesh. Also, the attenuation will become non-uniform so that changes in the beam position will affect the transmission. The attenuation factor is therefore measured at least once for each sample.

3. Particle loss: There are three mechanisms that tend to lower the counting rate but do not affect current measurements. Drifts in beam elements between the Faraday cup and detector is one of them. If the pulser derived dead-time correction is not accurate, errors can result from a difference in counting rate (^{36}S rate for example) between standard and unknown. A third source of loss occurs when a change in counter gas pressure causes peaks to shift outside of the gates in the computer (for ^{36}Cl, gates are set tight to minimize background contributions so that small shifts can change the rate by 1%).

4. Extra contributions to the radioisotope rate and stable isotope current: Radioisotope contamination in the sample, sample holder, and residual gas in the source and also stable isotope interference in the detector not only set the limit of detection but also introduce an uncertainty for higher level samples. For example, ^{14}C contamination that limits dating to 40,000 years contributes 1% to modern $^{14}C/^{12}C$ ratios. This can be measured with a chemistry blank but the correction is approximate and may vary with both time and the particular sample used. Cross contamination is particularly troublesome because it depends on sample arrangement in the source as well as the recent history of sample use. An upper limit for cross contamination has recently been determined for our new source to be 10^{-4} for neighboring samples.

A similar systematic error arises from extra contributions to the stable isotope current measurement. Such contributions could originate in the sample holder[10] or in the residual gas of the source. Similarly, other isotopes could scatter into the Faraday cup or could be selected by the magnet following various charge changes in the accelerator.

Mass Fractionation

In processes where an element or compound is selected with less than 100% efficiency there is an opportunity for isotope fractionation[11] to occur. This fractionation is seen as a change in isotope ratios and is independent of the isotope abundance. For tandem accelerator mass spectrometry mass fractionation can originate in five places: (1) in nature before the sample is obtained, (2) in the sample preparation stage, (3) during sputtering and negative ion formation, (4) in the tandem terminal stripper, and (5) in the beam transport system. It is not possible, with only two or three isotopes, to separate the different origins with only the accelerator measurements. A precision mass spectrometer could be used to measure the stable isotope fractionation arising in nature and in sample preparation if these values are required, however they will provide little additional improvement in the uncertainty of the radioisotope ratio since the inseparable stripper and transport fractionations will dominate.

Much of the fractionation can be corrected for by comparing the radioisotope ratio to a standard that has been prepared and measured identically. The correction can work well even in cases where the fractionation is not linear with mass. However, this correction will not be adequate if conditions causing fractionation are not identical for the standard and unknown or if the fractionation is time dependent. In these cases fractionation can be accounted for only if there is more than one stable isotope. Thus, if the mass dependence of this variable fractionation is known (which is unlikely) or it is assumed to be linear (often a good approximation), then a correction can be made based on the measured stable isotope ratio for ^{14}C and ^{36}Cl. The five types of fractionation will now be considered in more detail.

In general, natural fractionation cannot be corrected for by comparison to a standard. The fractionation will be nearly linear, however, so that it can be lumped together with the machine fractionation and corrected for with the stable isotope ratios.

Mass fractionation in the sample preparation stage may be significant although it should be small and nearly linear. Radiofrequency cracking of small carbon samples can lead to a depth dependence of the isotope ratios. In this case, the isotope ratio will depend on the time the sample has been run, requiring frequent measurement of the stable isotope ratios.

Fractionation in the sputtering process is probably quite small and again the linear correction should be adequate.

The yield into a given charge state from the terminal stripper depends primarily on the ion's velocity and therefore on its mass since the energy is constant. Fractionation is minimized by choosing a charge state and terminal voltage that result in a charge state yield near the maximum. Fractionation cannot be eliminated and is not linear especially at the maximum. If the stripper is thick enough for the desired charge state to be in equilibrium, the fractionation is relatively insensitive to small changes in thickness and in nonuniformities so that comparison to a standard should provide an excellent correction even when the fractionation is large (10-30%). Stripper gas is preferred over foils because (1) the increased (and variable) emittance from a foil may lead to additional fractionation in the rest of the transport system and (2) partial tears and pin holes give a positional dependence to the transmission which will lead to fractionation if the beam position depends on mass (see below).

Mass fractionation results from magnetic fields in the beam transport system that are not changed in proportion to the square root of the isotope mass in the cycling procedure. Such fields shift the beam position according to its mass resulting in fractionation at apertures. This fractionation can arise from non-linear fringing fields in the magnetic elements that are switched, electron suppression magnets in the accelerator tubes, the earth's magnetic field, and magnetic steerers. The fractionation can be minimized by removing the magnetic fields or by making the apertures significantly larger than the beam waists. These are difficult remedies in existing accelerators; in particular, the accelerator tube apertures and stripper canal cannot be increased in size easily. If the sample position, sample physical properties, and beam transport parameters do not change, this fractionation can be corrected for by comparison to a standard. But small changes cannot be avoided: the beam profile will change as the sample is sputtered away, and physical properties, such as the packing density distribution of the sample in its holder, will affect the beam profile. To first order, changes in fractionation due to changes in the beam profile with time and differences between standard and unknown can be corrected for using the stable isotope ratio measured <u>after</u> the accelerator (the fractionation is

probably most significant at the tandem terminal).

The results in Figure 2 illustrate these points. The change in isotope ratio when going from one sample to another "identical" one is two or three standard deviations. These changes cannot be due to a random drift in some independent parameter or else they would contribute to the random error. The samples are positioned to about 50 μm, a small displacement compared to the Cs spot size of about 1 mm. However, some of the samples had been used during source start-up and beam tuning so the negative ion beam profiles were probably different. If ^{36}Cl measurements were being made under such conditions, the $^{36}Cl/^{37}Cl$ ratio could be corrected to first order: the 2-3% shifts in $^{35}Cl/^{37}Cl$ ratios would result in errors of less than 1% in the $^{36}Cl/Cl$ ratio.

Calculations have been made to estimate the magnitude of this beam transport fractionation. A 6 G field acting over 1 m at the base of the tandem would produce a relative shift in the isotopes of a Cl^- beam by 0.4 mm/amu. If ^{36}Cl was centered in the terminal stripper, there would be little fractionation. Assume a Gaussian beam profile with 85% transmission through the stripper. Then if the sample is moved by 0.4 mm, resulting in a 0.8 mm shift at the terminal, the fractionation will become 1% per amu. Although the sample can be positioned to better than 0.4 mm, a shift in the point of origin of the negative ions of this magnitude is likely, and this explains the results of Figure 2. Note that these effects will be three times greater for the carbon isotopes.

There is another similar problem that we have seen recently with AgCl samples. If the sample material is not packed tightly into the Al sample holder, heat conduction will be poor resulting in high temperatures that force some of the AgCl to decompose. Then Cl^- ions will form from the resulting Cl gas surrounding the sample and this will lead to ar increased beam emittance. This is one case where the amount of fractionation depends on the physical properties of the sample.

The solution to these fractionation problems is to have close to 100% transmission through the accelerator (excluding stripper losses) and beam transport system and in addition to be flat-topped through all apertures. It is especially important to have a constant transmission with small changes in sample location and Cs spot size and location. To do this the beam must

be prepared by optimizing through small apertures then opening them up for the measurements. This is not possible for existing tandems where the beam fills the stripper canal; a partial solution that we are trying is to center the beam in the canal with steerers for each sample.

FUTURE PROSPECTS

We are presently installing a new injector and Cs sputter ion source on the Rochester tandem for improved mass spectrometry performance.[10] Although the primarily goal is improved mass resolution ($M/\Delta M \approx 300$ expected), there are several features that may improve reproducibility of isotope ratios. Stabilized power supplies and computer control through light links will improve stability and provide the ability to monitor changes. The advantages of the new Cs sputter source have already been described. A 25% reduction in the magnification will result in a smaller beam waist at the terminal. Improved vacuum and an easily cleaned environment will help reduce contamination.

We hope that these and other improvements will enable us to routinely obtain overall uncertainties of 1%, although we realize that it may be impossible to do much better than this with existing accelerators. Measurements that require higher precision can be left to the dedicated machines being built, while the larger existing machines can utilize their assets (higher energy, larger magnets, sophisticated and general purpose detectors and computers, and large and experienced staff) to tackle new problems in nuclear physics and other fields that require these assets but do not need the better precision.

ACKNOWLEDGEMENTS

This work represents a collaborative effort of many people including R. P. Beukens, L. R. Kilius, K. H. Purser, K. H. Chang, H. E. Gove, H. W. Lee, and A. E. Litherland. I thank T. S. Lund and A. K. Hamann for designing the computer control hardware and the rest of the NSRL staff for technical assistance. This work is supported by the National Science Foundation under grants PHY-77-27943 and PHY-78-22698.

---

[1] G. J. Wasserburg, elsewhere in this proceedings.

[2]M. Stuiver, Science 202, 881 (1978).
[3]K. H. Purser, elsewhere in this proceedings.
[4]H. E. Gove, elsewhere in this proceedings.
[5]D. Elmore, et al., Nature 277, 22, 246 (1979).
[6]General Ionex Corporation, Newburyport, Massachusetts 01950.
[7]K. Brand, Nucl. Instr. and Meth. 141, 519 (1977).
[8]T. S. Lund, Proc. 1978 SNEAP Conf., University of Wisconsin.
[9]Ortec, model 439.
[10]D. Elmore, et al., Phys. Rev. Lett. 45, 589 (1980).
[11]W. A. Russell, et al., Geochim. Cosmochim. Acta. 42, 1075 (1978).

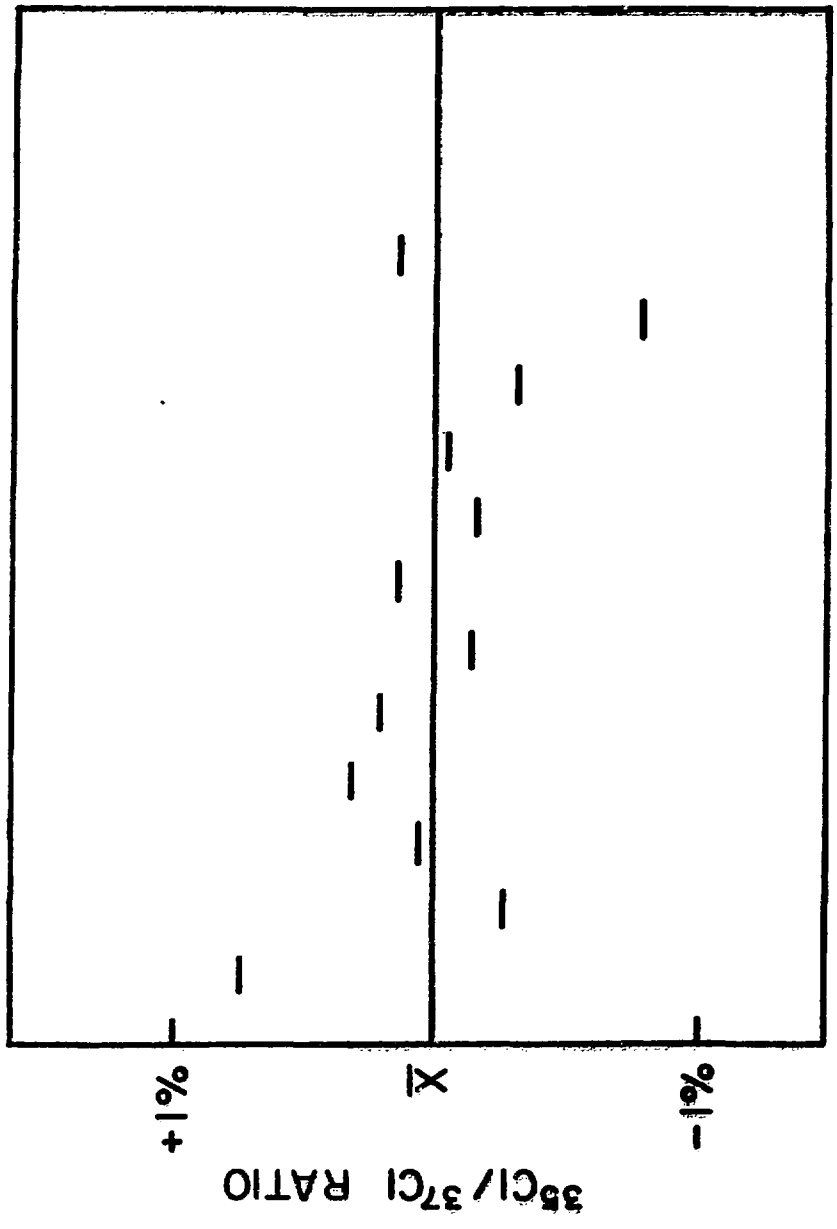

Figure 1. Stable Cl isotope ratios for individual cycles on a single AgCl sample measured in the image cup. The mean value for this series was $^{35}Cl/^{37}Cl = 3.506 \pm 0.003$. This 0.09‰ error is the standard deviation of the mean.

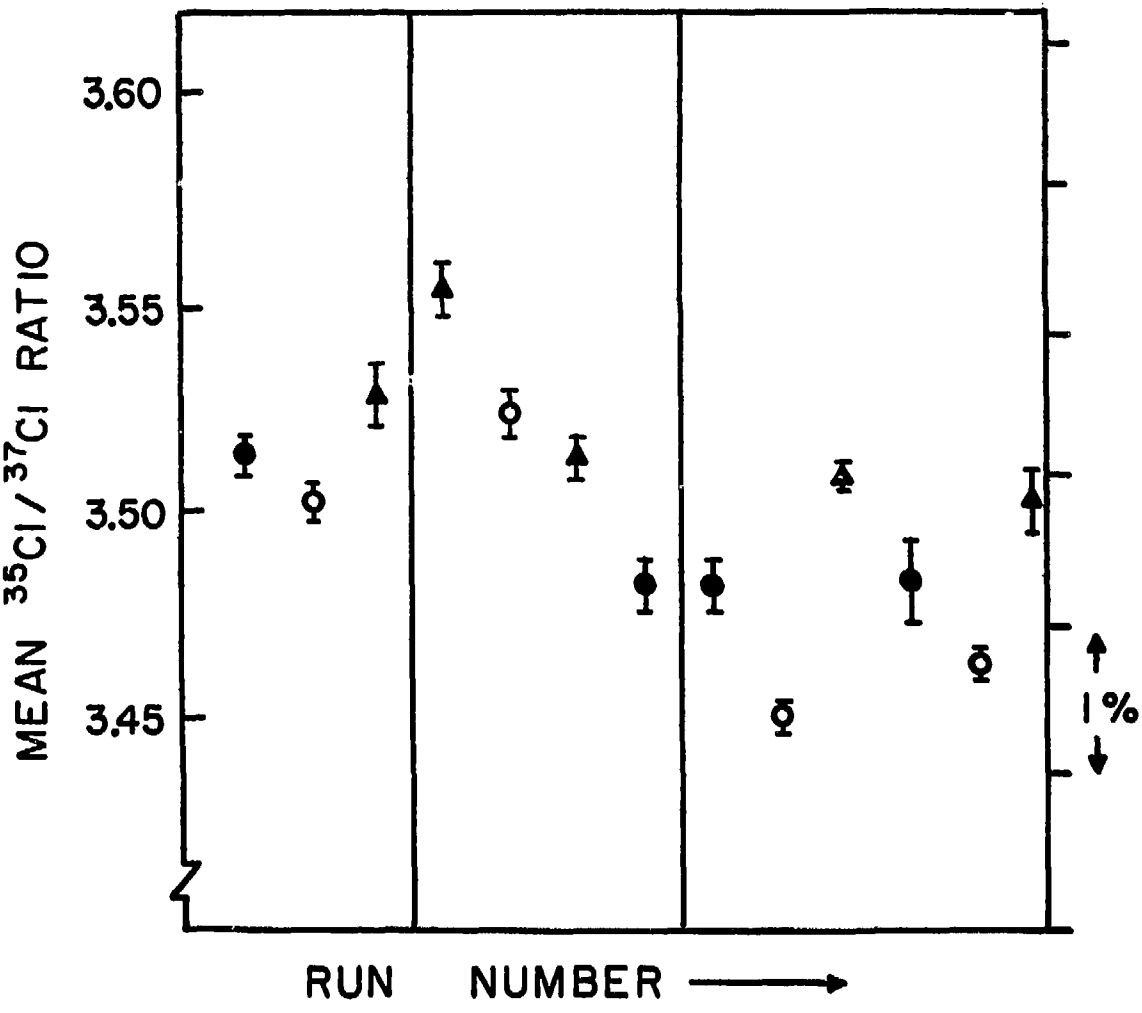

Figure 2. The mean $^{35}Cl/^{37}Cl$ ratios obtained for separate series of 8-15 cycles each as shown in Figure 1. The three symbols indicate different samples of the same AgCl material. Vertical lines show when the source was tuned.

ISOTOPIC FRACTIONATION IN ACCELERATOR BASED RADIOCARBON DATING

N.R. White
Oxford University Research Laboratory for Archaeology
and the History of Art, 5 Keble Road, Oxford, OX1 3QJ, England

1. INTRODUCTION

Isotopic fractionation is a potential source of error in the age of a sample as calculated from the measured ratio of ^{14}C to ^{12}C. The fractionating processes that must be considered occur at all times in the history of the sample: Photosynthesis, metabolic processes, combustion and extraction in the chemical preparation, ionisation, acceleration and transmission, and final measurement. Many of these processes can be approximately allowed for, by assuming that isotopic fractionation at mass 14 is calculable from that at mass 13, and normalising all ^{14}C measurements to a given $^{13}C/^{12}C$ ratio. If the fractionating process can be approximated by an expression of the form:

$$Q' = Q_o \left(1 + A\left(\frac{\Delta m}{m}\right) + \text{terms of higher order in } \frac{\Delta m}{m}\right) \qquad (1)$$

where m represents the mass of the reference isotope, here 12 a.m.u., Q represents the fraction of an isotope present in a reservoir that participates in a given process, the suffix o refers to the reference isotope (here ^{12}C), and the prime to an isotope of higher mass, then the fractionation at mass 14 will to first order be twice that at mass 13, and a correction is easy to make. Such processes will be referred to as exhibiting linear fractionation. It will be seen that some processes are present which exhibit strictly non-linear fractionation; since the correction is then very difficult it is necessary to identify such processes and understand them as well as possible. Accurate dating requires that the conditions under which such processes occur do not change.

The procedures for dealing with fractionation in beta-counting laboratories have been standardised (1). Since it is very difficult to make measurements of absolute isotopic ratios to high precision, all work is referred to standards. The PDB standard (a cretaceous belemnite) is adopted for $^{13}C/^{12}C$ ratios. The quantity $\delta\ ^{13}C$ is defined as:

$$\delta\ ^{13}C = \left(\frac{R - R_o}{R_o}\right) \times 1000 \qquad (2)$$

where R is the measured isotope ratio for the sample, and R_o the measured ratio for the standard. The value of $\delta^{13}C$ for the atmosphere is fairly constant at - 6.3‰ PDB with a very small long term decrease due to the combustion of fossil fuels, whilst for many plants it is close to -25‰ PDB. The age BP (Before Present, i.e. 1950 a.d.) of a sample in Standard Radiocarbon Years is defined by convention (2) to be:

$$\text{Age} = \left(\frac{5568}{\log 2}\right) \log \left(\frac{A_{on}}{A_s}\right) \qquad (3)$$

where A_{on} is related to the NBS (old) oxalic acid standard by the expression:

$$A_{on} = 0.95\, A_{ox} \{ 1 - 0.002\, (19 + \delta^{13}C) \} \qquad (4)$$

and the measurement of the activity of the standard has been corrected to first order for isotopic fractionation (see below) from an assumed initial level of - 19‰ PDB. A_s is the measured activity of the sample after correction for isotopic fractionation according to the approximate expression:

$$A_s = A_m \left(1 - 2\, \frac{\delta - \delta_o}{1000}\right) \qquad (5)$$

A_m is the measured activity of the sample. The $\delta^{13}C$ values are obtained by means of a separate stable isotope mass spectrometer, and are preferably obtained by burning a small fraction of the prepared counting medium (benzene in the case of liquid scintillation), as this takes into account all fractionation. Equation (5) is only a first-order approximation for:

$$A_m = A_s \left(1 + 2\, \frac{\delta - \delta_o}{1000}\right) \qquad (6)$$

which is itself directly derived from equation (1); equation (1) can be regarded as a Taylor expansion of any monotonic function which truly describes the fractionation, in which second and higher order terms can be neglected. Thus equation (5), recommended by Radiocarbon, is only valid for small corrections.

The choice of δ_o vitally affects the validity of this approach. $\delta^{13}C$ levels in the samples submitted to radiocarbon laboratories range typically

from +5‰ to -30‰, and over this range significant error can be introduced through the use of equation (5). Marine organisms have $\delta^{13}C$ values close to PDB, and land organisms tend to have negative values. Different photosynthetic pathways exist in different plants, and these give rise to different $\delta^{13}C$ values. Plants which use the pathway known as C3 have $\delta^{13}C$ values of typically -26‰ PDB, whereas C4 plants have values of typically -12.5‰. Since most samples in fact originate from C3 plants, δ_o is chosen to be -25‰, and in most cases the correction is so small that the approximation causes no loss of accuracy; furthermore, in the case of marine samples, it has frequently been the practice to neglect the fractionation correction, as this is largely compensated by the effective age of the reservoir.

Fractionation introduced by the preparation of the sample for beta counting is small, since most of the processes involved have yields approaching 100%. However, in the accelerator technique the overall efficiency of the processes preceeding the final detection of the ions is low; it is estimated to be ~1 - 2% overall. Therefore it is possible for significant isotopic fractionation to be present in the system. The nature of some of the processes involved is such that the fractionation could change with time. For example, it has been established that the pyrolysis of acetylene fractionates, so that it is likely that the sputter targets have spatially varying isotopic composition. It thus becomes necessary to consider the algorithms used to make the correction in much more detail. Furthermore, since much of the fractionation occurs within the accelerator, it is not possible to meaningfully use a separate stable isotope mass spectrometer. The stable isotope ratio MUST be measured within the accelerator system itself, as closely as possible to the ^{14}C detector, in order to correct all the fractionation. It is then not meaningful to quote a single value of $\delta^{13}C$ for the sample, for the purpose of comparison with the results of another laboratory.

After a discussion of the individual fractionating processes, the proposed procedure for the accelerator technique will be presented in full.

2. THE ION SOURCE

There are two hypothetical sources of fractionation to be considered here: fractionation in the conversion of C to C^-, and fractionation due to beams of different mass having different beam optical properties, leading to fractionation in transmission. Both of these proved extremely difficult to quantify by measurement. The most significant obstacle was the need, in the absence of the accelerator, to obtain all the information from measurement of the absolute ratio of ^{12}C to ^{13}C! Carbon 13, present at about 1.1% was swamped in all beams from natural samples by $^{12}CH^-$, which has almost the same mass. No device capable of resolving the two beams would have had a sufficiently large acceptance to give a useful result. No useful experiment, in which the composition of a sample before and after ionisation could be measured under identical conditions, could be devised.

The only approach that was available at this time in the absence of an accelerator was to load enriched ^{13}C into the source, at about 93 atom%, and to compare the ratio of the $^{12}C^-$ and $^{13}C^-$ currents so obtained with the 'known' enrichment of the sample. It proved impossible to obtain an accurate absolute measurement of the initial isotopic ratio, since all accurate isotope ratio work is carried out with reference to a standard, and no standard was available at this degree of enrichment. In any case, it would be unwise to introduce enriched material into a highly accurate stable isotope mass spectrometer. The only conclusion that could be made from this experiment was that any fractionation present was less than the uncertainty in the initial isotopic abundances, about 1%.

What mechanisms could cause fractionation in the C^- production? Firstly it must be pointed out that in steady state sputtering no overall fractionation can occur, since 100% of the material in the surface layer is ejected. Any fractionation that does occur is in the partitioning of the sputtered material into neutrals, negative ions, and molecular ions. Since there is no thermodynamic equilibrium in the sputtering process (3), the distribution is not easy to calculate. Is the probability of forming a negative ion different for each mass? If so, what property of the isotope is the cause of the fractionation?

Differences in atomic electronic energy levels between isotopes are extremely small, and it is in any case unlikely that electronic transitions occur during sputtering. As a result, it may be safe to assume that the atoms behave as elastic spheres during the sputtering collisions. In this case, the only possible cause of fractionation is that the ionisation probability is determined by the velocity of the sputtered ion as it leaves the surface (4), this is determined by elementary ballistics.

In a target of pure carbon a particle which is sputtered has, neglecting for now the presence of caesium in the surface, a 99% probability of being ejected by an incident ^{12}C atom, 1% by a ^{13}C atom. This is true whatever the final particle might be. Considering motion along the line joining the centres of the atoms at the moment of impact, elementary mechanics yields the following results.

$$v' = v_o \frac{2m_o}{m_o + m'} \tag{7}$$

where the suffix o indicates the incident particle, and a prime indicates the sputtered particle. Clearly, for an incident ^{12}C atom, the sputtered particle has the same velocity as the incident particle if it is also a ^{12}C atom. It is useful to regard the sputtered atom as having mass $(m_o + \Delta m)$. It is now possible to write:

$$v' = v_o \left(\frac{1}{1 + \frac{\Delta m}{2m_o}}\right) \tag{8}$$

whence

$$p' = p_o \left(1 + \frac{\Delta m}{2m_o} - 2\left(\frac{\Delta m}{2m_o}\right)^2\right) \tag{9}$$

and

$$U' = U_o \left(1 - \left(\frac{\Delta m}{2m_o}\right)^2\right) \tag{10}$$

where U refers to the kinetic energy of the atom due to motion in the stated

direction. So far no approximations have been made. For the case of an incident ^{13}C atom it is readily seen that the velocity and momentum terms are little changed, and that the change could be approximated by a constant factor. The incident particles have a distribution of velocities, and it is a good approximation to regard equations (8), (9) and (10) as describing the mean properties of all sputtered carbon atoms, relative to ^{12}C. Thus the heavier isotopes are slower, have higher momentum, and have almost identical energy to the ^{12}C; the energy of a ^{14}C atom is 0.993 of that of a ^{12}C atom, before acceleration.

Doucas has experimentally measured the energy distribution of sputtered negative ions from the inside of a cone in a Middleton sputter source (5). The high energy tail of the energy spectrum of sputtered neutrals from a monatomic target is predicted (6) to be:

$$\frac{dN}{dU} \alpha \frac{1}{U^2} \tag{11}$$

Doucas found the negative ion data fitted such an expression well, with an exponent of 2.29, implying that the probability of a negative ion forming was not strongly dependent on the velocity of the sputtered particle. If this data can be safely taken to imply a dependence of the negative ion formation probability on $(U^{-\frac{1}{4}})$ or on the square root of velocity, we could use (8) to write:

$$S^- \alpha \left(1 + \frac{\Delta m}{4m_o}\right) \tag{12}$$

This speculative expression would predict a 4% greater yield of $^{14}C^-$ than $^{12}C^-$ but should not be taken very seriously, since the measured slope of the energy dependence could be affected by other factors. If the negative ionisation probability depends on velocity, this would tend to imply ionisation whilst passing through a given zone (4), but as discussed below, this description may not correspond with reality.

Although no definite conclusion has been reached about fractionation in the ion source, it is likely that equation (12) represents the worst possible case, and if so, then the fractionation is linear, and correction is possible. It is stressed that measurements of ^{14}C relative to a standard

are used in the calculation of dates, and it is only necessary that CHANGES in fractionation are small and linear for adequate correction to be possible.

Equation (10) predicts almost identical energy spectra for the three isotopes. This implies that the beam envelopes have the same shape, provided that the handling and accelerating of the beams is purely electrostatic. If this is indeed the case (except in the case of analysing devices) it is safe to conclude that no fractionation occurs through clipping of the beams.

3. THE STRIPPING PROCESS

The more serious fractionating effect is the stripping process itself. There is no good published experimental data on charge state fractions for carbon. There are two sources of semi-empirical calculated data: the published curves of Marion and Young (8) (fig. 1), and the expressions of Sayer (9) which fit excellently to data on atoms of $Z > 8$. There is substantial disagreement between these two sources with regard to carbon, and not enough experimental data to indicate which is more accurate. Fractionation will arise because the charge state fractions are velocity dependent, and the velocities differ because the three isotopes have the same energy. Unfortunately, because of the large second derivative of the charge state function, the fractionation of ^{13}C wrt ^{12}C is not simply related to the fractionation of ^{14}C wrt ^{12}C. This fractionation will not be corrected by the application of any algorithm of the form of equation (1). From an expression such as that in ref. (8) one could calculate the difference between the calculated fractionation at mass 14 according to Sayer's expression, and the result of a linear extrapolation of the calculated fractionation at mass 13. This fractionation error, Ef, is given by the expression:

$$E_f = (F_{14} - (F_{12} + 2D)) \qquad (13)$$

I have written a short computer program to calculate the charge state fractions, and hence Ef, and to plot the results, using a routine based on ref (9) by Greenway (10). The resulting plots, for the 3+ charge state, for gas and foil strippers, are shown in fig. 2. It can be seen that the error, which could be regarded as resultant fractionation, is ~ 1% in the

region of interest with a foil stripper, and ~ 2% with a gas stripper. Since measurements are to be made relative to a standard, the situation is not as serious as it first appears. It is vital that the voltage remains constant from sample to standard to within a few kV, and the characteristics of the foil or gas do not change significantly. It is likely that both are thick enough for the charge states to be in equilibrium, in which case small changes in stripper thickness will not have any significant effect. Before any absolute ^{14}C measurements can be made, good data on charge state fractions will have to be obtained.

4. COLLECTION AND MEASUREMENT

The stable isotopes will be collected and measured on two Faraday cups after acceleration and subsequent magnetic analysis. The ^{14}C is drifted through a Wien filter before entering a detector. Systematic errors will exist at this point in the system, in the form of transmission loss of the ^{14}C, and Faraday cup errors. The accuracy of measurement will be limited by the constancy of these measurements, as no corrections for changes could be calculated.

In subsequent calculations these errors will be lumped together with the residual fractionation from the terminal as an irreducible error, hopefully constant, from sample to standard. Its constancy will be tested as soon as the accelerator is available.

5. ON-LINE CORRECTION

The injection system has been designed to cause puleses of ^{12}C and ^{13}C to be transmitted through the accelerator, during which the ^{14}C will not be counted. A timer will cause these currents to be sampled on the appropriate high energy Faraday cup and digitised, after which ^{14}C will be counted for a longer fixed period. The cycle length will be between 15 and 40 mS, avoiding the mains frequency of its harmonics. Each cycle the ^{12}C and ^{13}C charges will be read by the computer and stored in arrays, along with the number of ^{14}C counts for that cycle (obtained by on-line computation from the detector data, and with error signals indicating the misplacement of the beam within the Faraday cups, for correction of the accelerator voltage.

Periodically during data collection, or else afterwards, an analysis routine will be run. After rejecting any data where, for example, the isotope ratio is manifestly wrong, subsets of data covering ~30 seconds will be averaged, and the following algorithms applied to the result to correct for fractionation, writing the corrected result into a new file. Finally a date can be calculated from the corrected final ratio of ^{14}C counts to ^{12}C charge.

In the allowance for fractionation and the calculation of the date, it is assumed that the only two forms of error which will affect the isotopic levels in the sample between its original formation and final measurement are:

(a) well behaved fractionation which may differ from sample to standard, which can be corrected at mass 14 by a suitable algorithm. For the present a simple factor of 2 is assumed, but this may be changed in the light of future knowledge.

(b) badly behaved changes in isotopic levels which cannot be corrected by calculation, but which are the same for sample and standard.

These assumptions will be seen to fit the data available: any errors which do not correspond to these assumptions will be irretrievable. A program of experiments will be needed to quantify such errors.

Let P_h and Q_h represent the ratios $^{13}C/^{12}C$ and $^{14}C/^{12}C$ as they would be in the sample today in the hypothetical absence of any fractionation. Thus P_h represents the initial atmospheric $^{13}C/^{12}C$ ratio, which is unknown, but probably close to -6‰ PDB.

Let P and Q represent these values corrected for isotopic fractionation to $\delta\ ^{13}C = -25‰$.

Let P_o and Q_o similarly represent the actual isotopic ratios of the NBS oxalic acid standard, corrected to $\delta^{13}C = -19‰$.

(A future version of this argument will probably use the new oxalic standard corrected to -25‰ , causing some numerical simplification in the following equations.)

By definition $P = 0.9939\ P_o$.

Let p, q. p_o, q_o represent measurements of P, Q, P_o, Q_o. There are time dependent correctable fractionation errors occurring, and constant uncorrectable errors such that p is reduced by a constant factor A, and q by a constant factor B. That is to say, the quantities Ap, Ap_o, Bq, Bq_o are related to P, P_o, Q, Q_o by a simple relationship correcting for fractionation, which is known, but the quantities A and B are unknown.

For the present, take the fractionation relationship to be that of equation (6), which may be slightly more accurate than that recommended by Radiocarbon. This can be written:

$$Bq = Q(1 + \frac{2(\delta^{13}C + 25)}{1000}) \tag{14}$$

As the fractionation is time dependent, pairs of values of p and q (also of p_o and q_o) are measured quasi-simultaneously, but a particular measurement of p or q can have no particular association with any particular value of p_c or q_o. The pairs of values are linked by the following equations:

$$Bq_o(t) = Q_o(1 + \frac{2(Ap_o(t) - P_o)}{P_o})$$

$$Bq(t) = Q\ (1 + \frac{2Ap(t) - P)}{P}) \tag{15}$$

$$= Q\ (1 + \frac{2.0123(Ap(t) - P_o)}{P_o})$$

These equations follow from (14); it is convenient in this context not to explicitly use delta values, but that notation could be used if desired. Time averaged pairs of values of p and q have equal validity in these equations, and these would be used in practice. Substitution into the age equation , (3), gives:

$$Age = \frac{5568}{\log 2} \log \left[0.95(\frac{Bq_o}{2Ap_o - P_o})(\frac{2.0123Ap - 1.0123\ P_o}{q}) \right] \tag{16}$$

which reduces to:

$$Age = \frac{5568}{\log 2} \log \left[0.95(\frac{q_o}{2p_o - (P_o/A)})(\frac{2.0123p - 1.0123(P_o/A)}{q}) \right] \tag{17}$$

Evaluation of this expression requires knowledge of the quantity (P_o/A). If the average fractionation introduced by the system during a particular run is arbitrarily included into the constants A and B (this involves no loss of generality) then (mean p_o) = (P_o/A). The age equation now becomes:

$$\text{Age} = \frac{5568}{\log 2} \log \left[0.95 \frac{q_o}{q} \left(2.0123 \frac{p}{p_o} - 1.0123\right)\right] \qquad (18)$$

Hopefully, with the introduction of a new oxalic acid standard, the fractionation of the standard will in future be corrected to the same level as that of the samples. If this is done the age equation becomes:

$$\text{Age} = \frac{5568}{\log 2} \log \left[S \frac{q_o}{q} \left(2 \frac{p}{p_o} - 1\right)\right] \qquad (18a)$$

If conditions between successive complete measurements alter, giving different values of (mean p_o), the factor by which the calculated date would change is of the order of:

$$\text{Error factor} = \left(\frac{\Delta p}{p_o}\right)^2 \qquad (19)$$

Thus a 2% change in the mean overall fractionation would lead to a change in the calculated date of 0.04%.

A thorough analysis of fractionating processes might indicate that some second-order term in equation (1) can be predicted with some confidence, or that the factor 2 in equation (5) is not the most suitable factor. If some suitable expression can be found and used in a similar manner to that outlined above, it is clear that sufficient information is available to allow the calculation, in principle to good accuracy, of radiocarbon ages relative to a standard, using this expression. For example, an alternative version of the fractionation algorithm which has been suggested gives:

$$\text{Age} = \frac{5568}{\log 2} \log \left[S \frac{q_o}{q} \left(\frac{p}{p_o}\right)^2\right] \qquad (18b)$$

hich gives the same answer for small fractionations. It will have to be determined experimentally how frequently it is necessary to run on a standard.

6. CONCLUSIONS

Systematic errors in accelerator dating can be minimised by transmitting in sequence the three isotopes of carbon through the accelerator. Many processes exist which cause isotopic fractionation, and the extent of these has been discussed, but is not predictable. Many are linear, that is, a first order correction of the ^{14}C fractionation can be calculated from a measurement of the $^{13}C/^{12}C$ ratio, but some processes are known to be not so well behaved. It has to be assumed that such processes remain unchanged between measurements on sample and standard; with this assumption it has been demonstrated that the technique, although failing to provide absolute isotope ratios, provides in principle sufficient data for the calculation of dates to an accuracy of better than 0.1%. Of course accuracy is not only limited by such fluctuations, but also for example by the Poisson statistics and by contamination, and this conclusion should only be taken to indicate that there is no need for further data in the form, say, of a separate $^{13}C/^{12}C$ measurement - there would be no way of using such data.

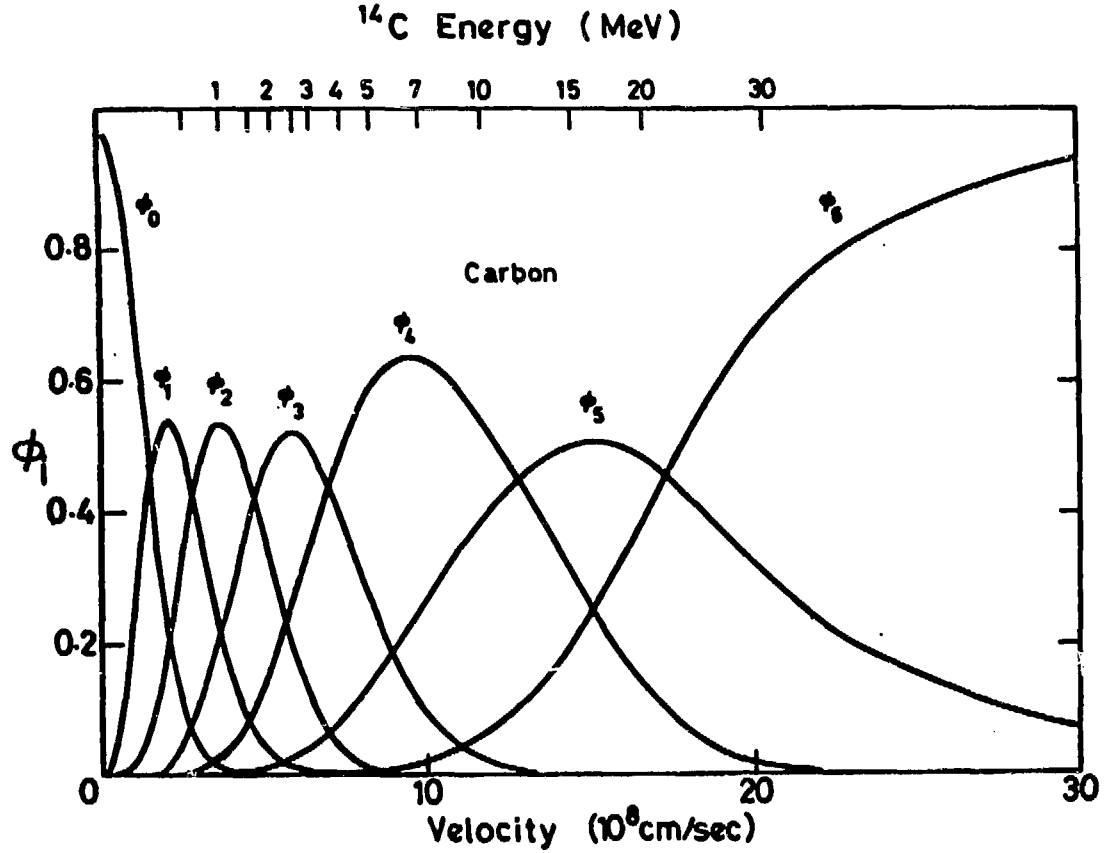

Fig. 1. Charge state fractions for 14C ions stripped with a carbon foil, according to Marion and Young(8).

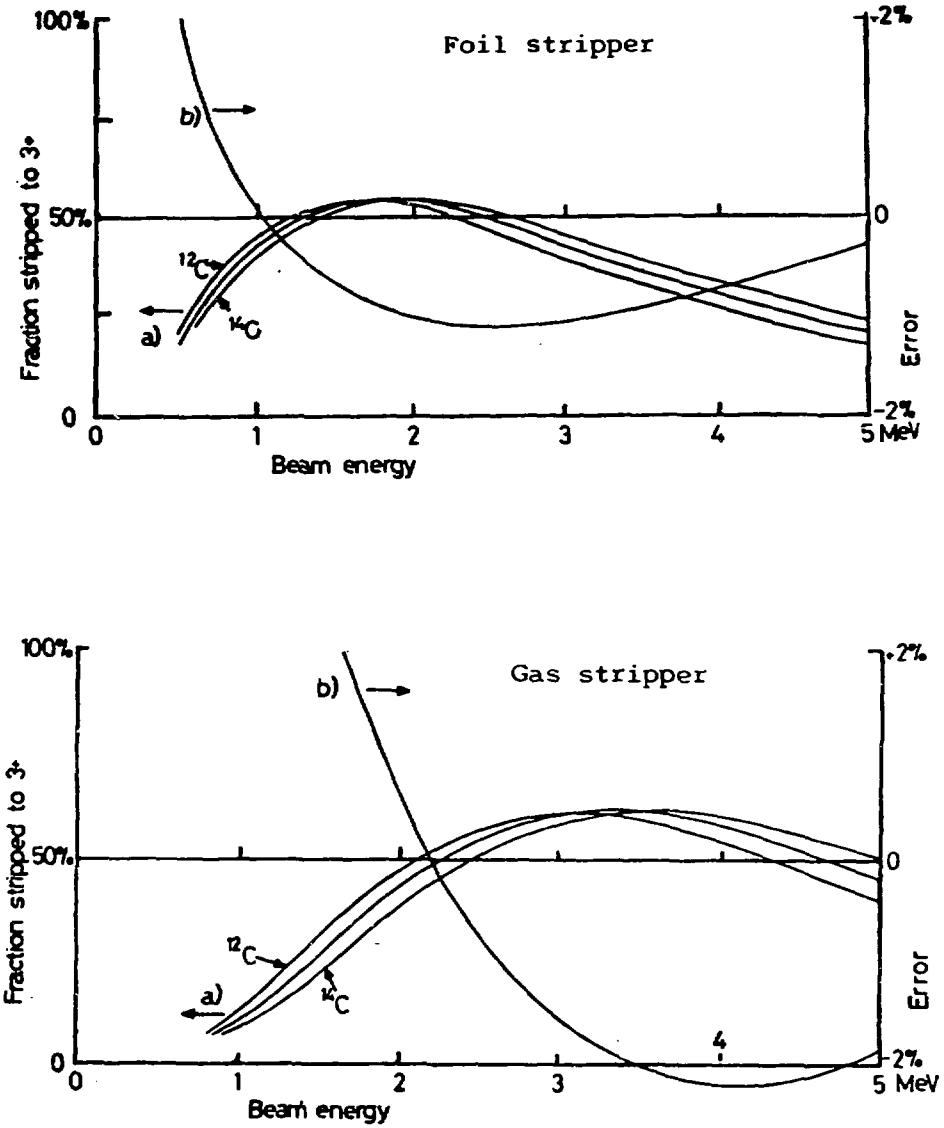

Fig. 2. Fraction of ions in the 3+ charge state, according to the algorithms of Sayer[9]. Also plotted is the residual ^{14}C uncorrected fractionation following the application of the Radiocarbon algorithm for fractionation correction.

THE INVERTED SPHERICAL IONISER SPUTTER ION SOURCE (IS3)

N.R. White
Oxford University Research Laboratory for Archaeology
and the History of Art, 6 Keble Road, Oxford, OX1 3QJ, England

1. INTRODUCTION

The reflected beam sputter ion source has been found to have an inherent need for frequent readjustment of several voltages during use. Its lack of cylindrical symmetry is reflected in the asymmetry of its beam (1), and the position and shape of the sputtering Cs^+ beam have been shown to depend strongly on the Cs^+ current because of space charge effects (2). There has been a tendency for ion source designs starting from a simple concept to be subjected to continual "improvement" a process which, whilst improving one feature, often complicates the originally simple concept, and makes operation more complex.

I felt that it was possible to describe fairly clear requirements for a caesium sputter ion source, which would make it ideal for the present work, and which might also find more widespread acceptance. These were:

1. The Cs^+ beam would be produced by surface ionisation, and its current would be controlled via the temperature of an oven, as at present.
2. The acceptance of the negative ion extract system should exceed the beam emittance.
3. The size of the Cs^+ focus should match the sputter target size, at about 1 to 2 mm dia, to give a suitable emittance.
4. There should only be a need for a single E.H.T. supply.
5. The electrode system should have cylindrical symmetry throughout.
6. The focussing conditions should be insensitive or independent of the beam currents.

It can be seen that some of these conditions (4,5), are met in the original Middleton ion source, but have been lost in the course of subsequent improvements; others (2,3) are met (approximately) in the reflected beam source. The inverted sputter source of Chapman (3) originally met

conditions 4 and 5, and seemed to me to be capable of modification to improve its correspondance to these requirements. Impetus to proceed was given by the fact that I had seen a dished porous tungsten ioniser made by Middleton, showing that flexibility in the design of this component was possible. A further condition could be added:

7. The ion source geometry should as far as possible be based on a simple concept, such as a known exact solution of the electric field equations.

This approach was used in the design of the ion source described below.

2. THE DESIGN

A computer program by Dimmikis whose ability to calculate accurate beam trajectories in the presence of space charge had been proved in previous work (4), was used to analyse existing designs and to evolve and test trial designs. It was found that negative ion extraction efficiency was low in many published geometries, because the electric field at the sputtered surface was neither strong enough nor suitably shaped to capture particles launched with several eV of kinetic energy in random directions. Only the reflected beam source gave essentially 100% efficiency.

Initially some time was spent trying to make arbitrary improvements to existing designs but this was found to be unprofitable. It was then decided to combine the following two well-known strategies in a form of inverted ion source:

(a) High perveance electron guns use a spherical sector cathode and accelerate the electrons radially towards the centre of the sphere (fig. 1). This suggested a spherical annulus as the ioniser surface with a central hole for transmission of the negative beam.

(b) A shallow immersion lens around the sputter target with a high electric field allows extraction and focussing of negative ions with several tens of eV of transverse kinetic energy (fig. 2).

Both these concepts are simple to execute, and can dovetail well, as shown in fig. 3. The high electric field near the centre of curvature increases the acceptance of the immersion lens, whose electrode shape in turn helps

maintain the sphericity of the equipotentials. The shape of the electrodes was refined using the computer program to make the equipotentials spherical over as wide a range as possible. The radius of curvature is 15 mm; the waist in the Cs^+ beam occurs at a point about 2 mm beyond this, and the program predicts a spot size smaller than that required. In practice, it is thought likely that manufacturing defects will enlarge the spot size to about 1.5 mm diameter. If necessary the position of the target could be empirically adjusted to give the required spot size. The immersion lens produces a waist just in front of the hole in the centre of the ioniser, and no negative particle should strike the ioniser surface.

3. THEORY

The well-known solution to Laplace's equation giving the potential between two concentric spheres is:

$$V \propto \frac{1}{r}$$

If there is a current flow between the two spheres, this introduces space-charge, and Poisson's equation must be used. If the current flow retains the symmetry, then so does the potential distribution, and the current flow remains radial. In other words, in such a system the focussing conditions are independent of the current.

In the realisation of this ideal the emitting area is a spherical annulus, and non-spherical perturbation of the field will occur at high currents at the beam edges, but the effect is found to be small. The electrode shapes are such as to maintain as near radial acceleration as possible over a large region. The charge density is greatest near the ioniser surface, since the ion velocities are low, and this is also the region in which the trajectories are most easily deflected. The sphericity of the equipotentials is upset near the immersion electrode around the target, but the high energy of the Cs^+ beam at this point makes the effect insignificant. Within the immersion lens there is a high axial field and field gradient necessary for focussing the negative ion beam.

For between 0 and 3 mA of Cs^+, computations at 20 kV revealed no detectable difference in focussing conditions. Above this current, as the space charge limit for emission from the ioniser was approached, the program had difficulty in handling the launching conditions. Because the negative ion

beam was almost entirely in the hollow centre of the cylindrically symmetrical Cs^+ beam, the space charge of the latter had no perceptible effect on the negative ion focussing conditions. In making the computations the negative ions were assumed to have an initial energy of several tens of eV, and to be travelling in quasi-random directions.

This geometry has been shown to be capable in principle of accelerating Cs^+ ions from a spherical annular surface onto a target of ~ 1 mm diameter, and of extracting essentially 100% of the sputtered negative ions through a hole in the centre of the ionising surface. Only one EHT supply is used The configuration is exceptionally compact. The focussing is independent of current or voltage, being determined solely by the geometry, and is tolerant of misplacing of components in an axial direction by $\pm$ ½ mm. Cylindrical symmetry of the electrode structure ensures a circular beam with a stable trajectory, and there should be insignficant movement of the virtual source position as sputtering proceeds. This geometry meets all the initial conditions, and should therefore provide a basis for an efficient, stable ion source.

4. CONSTRUCTION OF A PROTOTYPE

Precise axial alignment of the ioniser, electrodes and target is needed. The basic electrode structure was designed to consist of four turned pieces of stainless steel and three machinable glass ceramic insulators assembled to a concentricity of 0.05 mm. Into this unit, the ioniser is located on one side, and the target holder on the other.

The Cs oven and ioniser were based on existing practice; however the porous tungsten ioniser tip, which was machined to a radius of 15 mm, was electron-beam welded into a housing of tantalum, rather than the molybdenum used in smaller assemblies. The thermal expansions of these material match well. The expense of tantalum was necessary since molybdenum became too brittle during welding. The housing was designed to accept a commercially available heater. The thermal expansion of this unit was taken into account in its location (against knife edges) into the electrode structure and in the oven support. Provision was made for both heating and cooling the oven, since it was necessary to mount it within the vacuum enclosure.

The use of a rotating sample carrier seemed problematic, so a simple airlock was designed instead. Targets were pressed into a recess in the centre of aluminium target mounts, which were disposable, to avoid cross-contamination. These were mounted on an insulator, on the end of a probe designed to fit the airlock. The target and associated electrodes were connected to the -30kV EHT supply.

Difficulties were encountered in the welding of the ioniser components but the use of tantalum and the introduction of careful weld preparation seems to have overcome these.

5. TESTING

The porous tungsten ionisers performed very badly at first, but improved after ultrasonic cleaning in alternating dilute hydrochloric acid and sodium hydroxide solutions, and improved further after several hours of operation. They now produce more than sufficient Cs^+ current, at modest oven temperatures (ca. 200°C), giving a maximum total current (Cs^+ plus electrons) of more than 7 mA. Direct measurement of Cs^+ is not possible in this design at present, but on the basis of past measurements (2) is estimated to have reached 1 mA. In routine use, only ~ 100 μA is needed.

Samples of 1 mm diameter of graphite pressed into the target mounts gave currents of up to 10 μA of C^- at 20 to 25 keV. The sputter pit diameter was less than 1 mm. Estimates of efficiency were not made since it was clear that the target temperature was too high. The radiant heat from the ioniser was raising the temperature of the target mount and was believed to be causing loss of Cs from the target surface (see chapter 2). An alternative target probe with incorporated cooling was constructed, and now awaits testing. One prototype failed catastrophically, filling the vacuum system with hydrocarbon coolant and glass, but the cooling is only a minor engineering problem and should soon be overcome.

References

1. N.R. White - in preparation.
2. R.E.M. Hedges, J.O. Wand, N.R. White, Nucl. Inst. & Meth. 173 (1980), 409.
3. K.R. Chapman, Nucl. Inst. & Meth. 124 (1975), 299.
4. D. Dimaikis, Computer program for the numerical analysis of electron flow systems, Univ. of Sheffield, 1975.

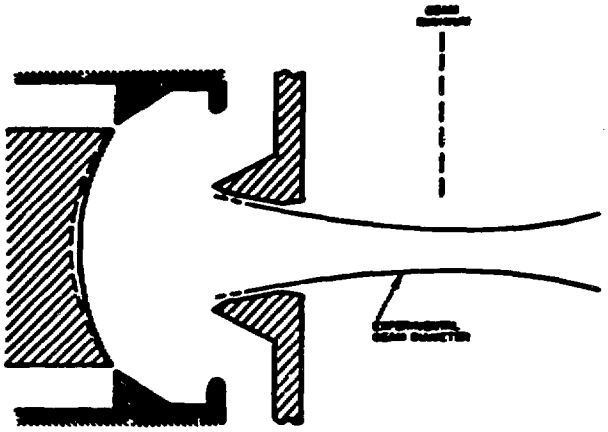

Fig.1 A high perveance electron gun.

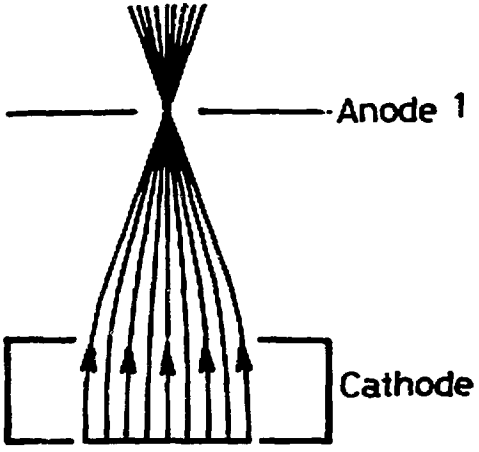

Fig. 2. A simple immersion lens, shown here converging an initially parallel zero emittance electron beam.

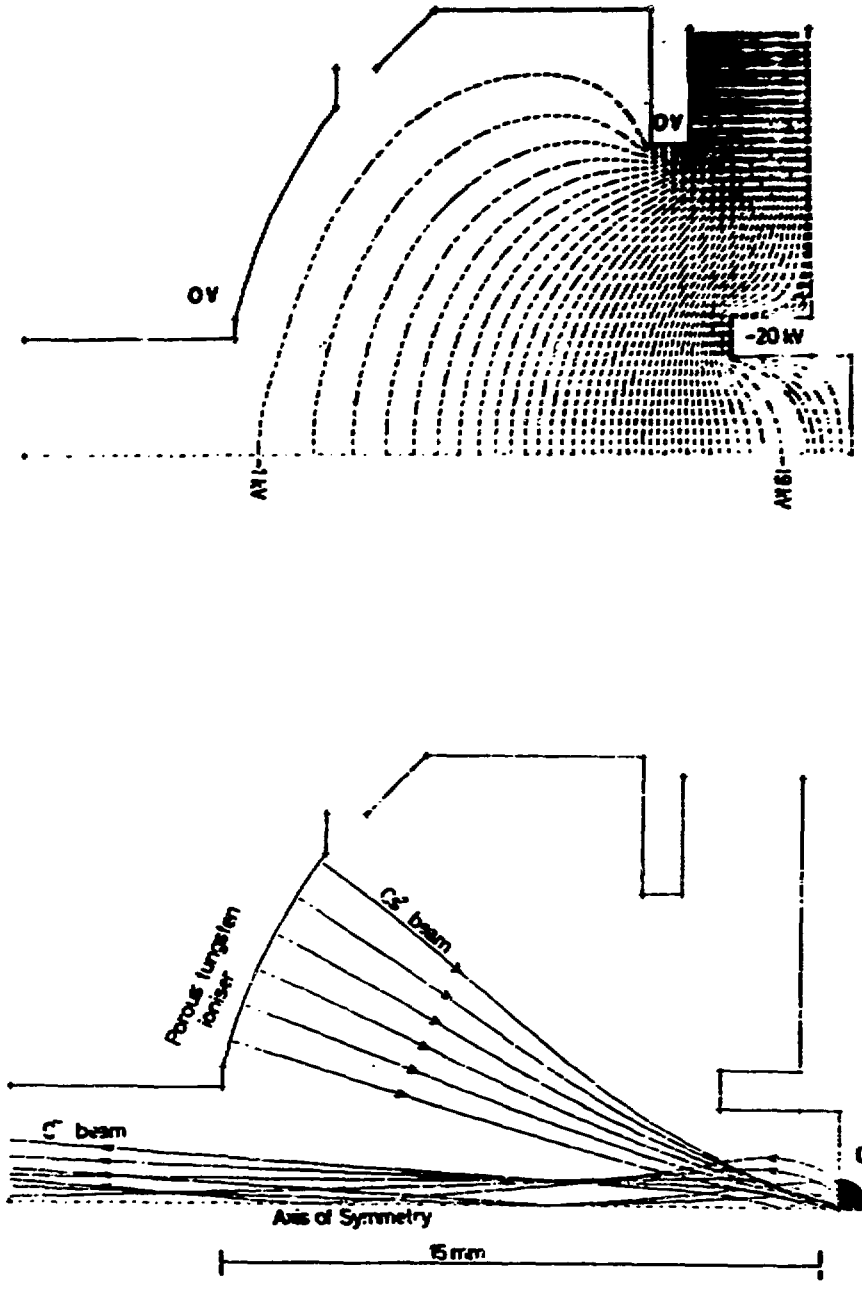

Fig. 3. Computer produced plots of the Inverted Spherical Ioniser Sputter Ion Source:

a) Equipotentials at 1 kV intervals (100V near cathode).

b) Computed trajectories of both primary and secondary particles. C^- ions have>10 eV energy spread.

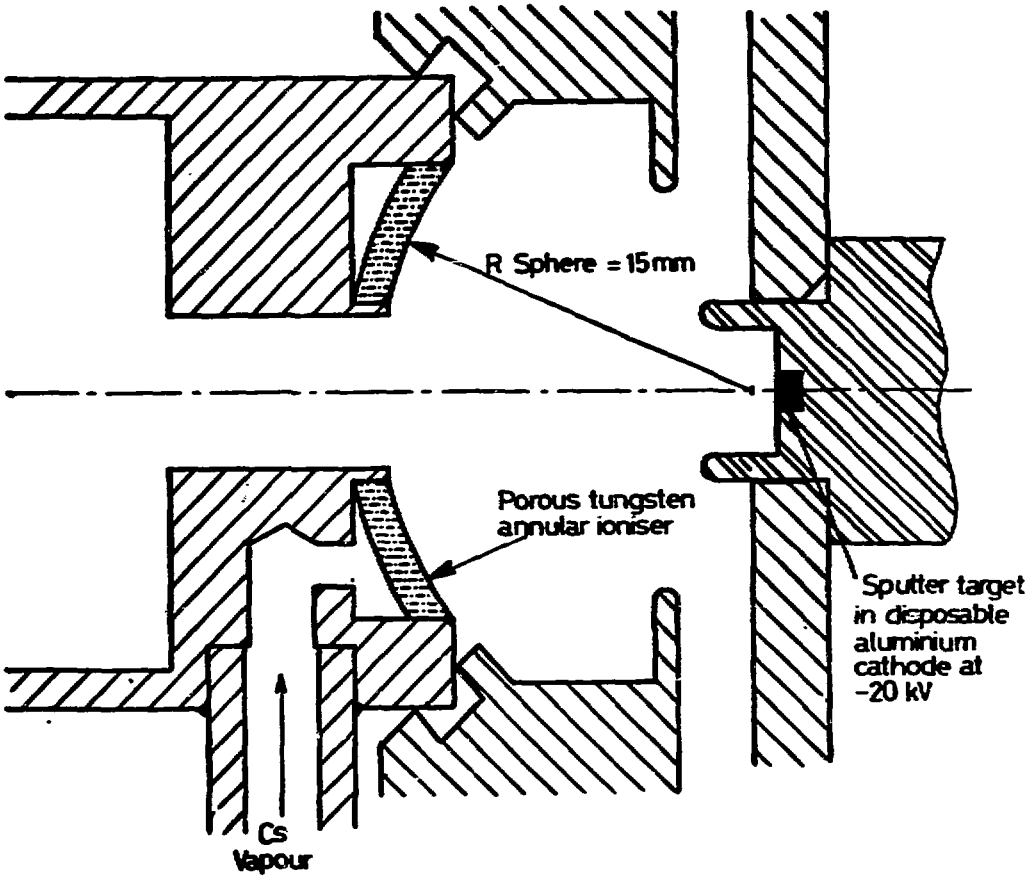

Fig. 4. Enlarged sectional drawing of the Inverted Spherical Ioniser Sputter Ion Source.

OSIRIS

S.H. Chew, E.F. Garman, T.J.L. Greenway and K.W. Allen
Nuclear Physics Laboratory, University of Oxford,
Oxford OX1 3RH, England.

1. INTRODUCTION

Ultrasensitive mass spectrometry using accelerators has been performed successfully by various laboratories with measurements of isotopic abundance ratios as small as 10^{-15} being achieved for light isotopes e.g. $^{10}Be/^{9}Be$[1] and $^{36}Cl/Cl$[2]. However, for heavy isotopes, such as $^{129}I/^{127}I$, the lowest abundance ratio measured[3] to date is of the order of 10^{-12}. The Oxford Supersensitive Injector for Radioactive Isotope Separation (OSIRIS) is being developed at the Nuclear Physics Laboratory with an emphasis on detection and separation of heavy isotopes. We hope to achieve better sensitivity for heavy masses than has so far been reported.

2. EXPERIMENTAL ARRANGEMENT

The OSIRIS system, which will be used as an injector with the Oxford EN tandem, consists of an ion source producing negative ion beams, a 100 kV accelerating section and a 180° deflection magnet for mass analysis.

The ion source at present installed is a model 834 Hiconex manufactured by the General Ionex Corporation. This consists of a tungsten surface ionisation source producing beams of Cs^+ ions which are focussed and deflected through a 3mm diameter, tapered, off-axis hole in a stainless steel target holder. The Cs^+ beam is then reflected[4] back to strike an on-axis target pellet, 2mm in diameter, and a negative ion beam of the target material is produced by Cs sputtering. Twelve different targets can be loaded on to a

wheel and individually selected by a pneumatic drive. The negative ion beam is extracted at 20-30 kV, focussed by an einzel lens, further accelerated by 100 kV and it then forms an image at the object position for the 180° magnet. For certain negative ions the Hiconex source will be replaced by an appropriate alternative; for example, a negative surface ionisation source is planned for iodine and the other halogens based on the use of hot lanthanum hexaboride as an electron donor.

The ion beam enters the analysing magnet of radius (R) 61cm which deflects the beam through 180° in the vertical plane. The magnetic field is double focussing with $N=\frac{1}{2}$ ($N=(R/B)(\partial B/\partial R)$); unit magnification is produced for object and image distances equal to $R/\sqrt{2}$. The dispersion is approximately 12mm for a relative mass difference ($\Delta M/M$) of 1% and the mass-energy product is 28 MeV amu.

This magnet was originally[5] used with a bending angle of 188° to allow the ion beam to follow a central trajectory in the magnet. The deviation from 180° was due to the extended fringing field from the coils. The equivalent sharp cut-off fringing field (SCOFF) was measured to be 4.5cm from the pole edge. After installing field clamps of low-carbon steel the SCOFF was measured to be (1.73±0.06)cm from the pole edge. Careful checks were made to ensure that there was no saturation in the field clamps at high magnetic fields. The magnet is now set to bend ion beams through 180° although for this situation the beam has to follow a slightly non-central trajectory.

A set of variable slits can be mounted at the magnet image position. Where there is an abundant isotope within ~4% of the mass of the ion of interest, the associated ion beam can be measured with an offset Faraday cup and used as a reference to monitor the main beam.

Negative ion beams from OSIRIS will be further accelerated by the Oxford EN tandem and the emerging positive high energy ions will be focussed by an electrostatic quadrupole doublet before being analysed by a 20° electrostatic deflector for energy/charge selection. This electrostatic deflector, of radius 320cm, is being designed to maintain a 50kV/cm field over a 4cm gap. Thus it will be capable of giving a 20° horizontal deflection to beams of energy up to 8 MeV/unit charge. The energy/charge selection will be made at a pair of analysing slits positioned some 300cm away from the exit face of the deflector. Beam optics calculations predict an energy resolution of the order of 1 in 400. At a later date, an additional 70° electrostatic deflector of similar gap width and radius will be added giving a total horizontal deflection of 90°. It is calculated that the energy resolution of the combined deflectors should be of the order of 1 in 2000 which is comparable with the energy spread of the beam from the accelerator.

In addition, a time-of-flight measurement is being planned to confirm the velocity of the ions. The "start" signal of this measurement will be obtained by using a microchannel plate to detect electrons which have been ejected from a thin carbon foil by the high energy beam ions. The "stop" signal will be provided by a solid state detector at the end of the beam line.

Figure 1 is a schematic diagram of the system.

3. MEASUREMENTS AND RESULTS

OSIRIS has been in operation now for about 2 months although the system has yet to be coupled to the EN tandem in our laboratory. Table 1 shows the intensity of negative ion beams that have been produced and studied. Beam currents are measured in a Faraday cup after the image slits at the focal

plane of the 180° magnet.

The Pt^- beams have been investigated closely. Figure 2 shows a spectrum of the intensity of negative ion beams against the field in the 180° deflection magnet. The separation of the peaks of masses 194 and 195 at constant magnetic field was determined by measuring the beam intensity as a function of the vertical image slit position. A slit width of 0.13mm was maintained throughout. A separation between masses 194 and 195 of (6.3±0.2)mm was obtained where the full width half maximum (FWHM) for each peak was measured to be (1.6±0.2)mm. From this, a mass resolution (FWHM) of 1 in 750 was determined. This is consistent with beam optics calculations for OSIRIS and also with the energy resolution measurements of Cohen et al[5] for the 180° analysing magnet used here. The background intensity in this mass region from the stainless steel target holder has been investigated and found to be less than 0.2nA with a 0.5mm slit.

4. EXPERIMENTS PLANNED

One application of OSIRIS will be to search for long-lived radionuclides resulting from nucleon decay eg ^{129}I from ^{130}Te since

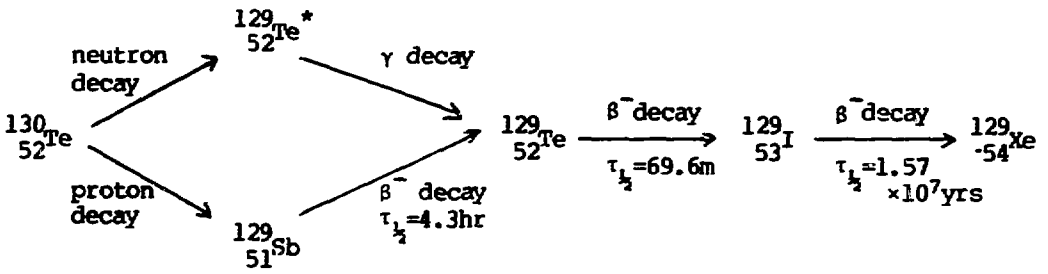

Therefore a measurement of the concentration of ^{129}I in samples of tellurium ore may enable us to determine a limit for the lifetime of the nucleon.

Assuming a nucleon half life of 10^{30} years, the yield of ^{129}I from nucleon decay is about 1.4 atoms per gram of natural tellurium, so a sensitive system is essential. It will also be necessary to know the depth and environment from which the tellurium samples are mined to enable us to correct for the background yields, for example $^{128}Te(n,\gamma)^{129}Te$ and $^{130}Te(\nu,n)^{129}Te$ will both result in ^{129}I as a decay product.

With the mass resolution and high sensitivity achievable with OSIRIS it would be interesting to measure the abundance and isotopic ratios of the Pt metals in geological samples. In particular, the clay boundary between the Cretaceous and Tertiary limestone beds has shown anomalous concentrations of Ir[6], and investigations of further samples from this and other similar layers will be investigated.

5. CONCLUSIONS AND ACKNOWLEDGEMENTS

It is difficult at this time to predict the sensitivity we could ultimately achieve with our system. Placing defining slits at the object position of the 180° analysing magnet could improve the mass resolution but at the cost of reduced transmission. Transmission efficiency through the system has yet to be measured. By the application of the selection methods described, it is expected that we should be able to measure isotopic ratios for heavy isotopes of the order of 10^{-15} or better.

We would like to thank A.B.Knox for preparation of the target samples and H.Dodd for his help in some of the data taking. One of us, E.F.G., acknowledges financial support from the Science Research Council.

6. REFERENCES

1) L.R.Kilius et al, Nucl.Instr.Meth. 171 (1980) 355

2) K.Nishiizumi et al, Earth Planet. Sci.Lett. 45 (1979) 285
D.Elmore et al, Nature 277 (1979) 22, 246

3) D.Elmore et al, Nature 286 (1980) 138

4) K.Brand, Revue de Physique Appliquée 12 (1977) 1453

5) A.V.Cohen et al, Nucl.Instr.Meth. 10 (1961) 84

6) L.W.Alvarez et al, Science 208 (1980) 1095

Table 1. 80 keV negative ion beams were collected in a Faraday cup at the exit aperture of the 180° analysing magnet. The image slits were 10mm by 5mm. The Cs oven temperature was set at 165°C. The extract voltage was 20 kV with an extract current of the order of 0.2 mA.

Target pellet	Mass	Natural isotopic abundance (%)	Faraday cup current	Identification of negative ions
C	12	98.89	5μA	$^{12}C^-$
PbS	32	95.0	860nA	$^{32}S^-$, $^{16}O_2^-$
	33	0.76	20nA	$^{33}S^-$, $^{32}SH^-$
	34	4.22	30nA	$^{34}S^-$
	35		10nA	$^{35}Cl^-$
	36	0.014	0.18nA	$^{36}S^-$
	37		2.4nA	$^{37}Cl^-$
Pt	194	32.9	380nA	$^{194}Pt^-$
	195	33.8	400nA	$^{195}Pt^-$, $^{194}PtH^-$
	196	25.3	320nA	$^{196}Pt^-$, $^{195}PtH^-$
Au	197	100	3μA	$^{197}Au^-$
Ir	191	37.3	220nA	$^{191}Ir^-$
	193	62.7	350nA	$^{193}Ir^-$
Si (cone)[+]	28	92.21	1.75μA	$^{28}Si^-$

[+] The Si beam was not measured in reflected mode but with a straight-through on-axis Si cone.

Figure Captions

Figure 1 Schematic diagram of the experimental arrangement to be used for ultrasensitive mass sepectrometry at the Oxford Nuclear Physics Laboratory.

Figure 2 Intensity of negative ion beams from a platinum target. The magnetic field is measured with a Hall probe. The beam was collected in a Faraday cup after the image slits of the 180° analysing magnet. The slits were set at 10mm by 1mm.

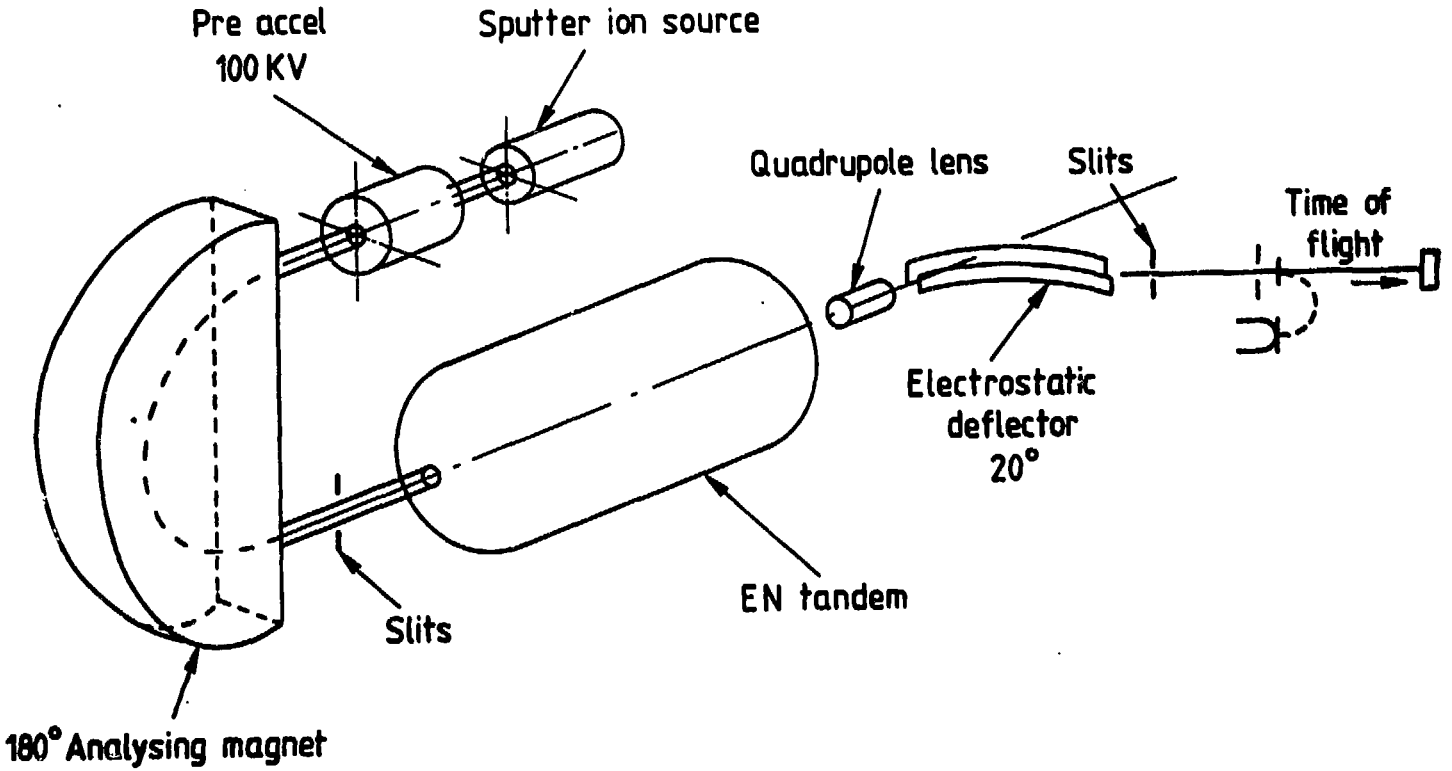
Pre accel
100 KV
Sputter ion source
Quadrupole lens
Slits
Time of
flight
Electrostatic
deflector
20°
EN tandem
Slits
180° Analysing magnet

Figure 1

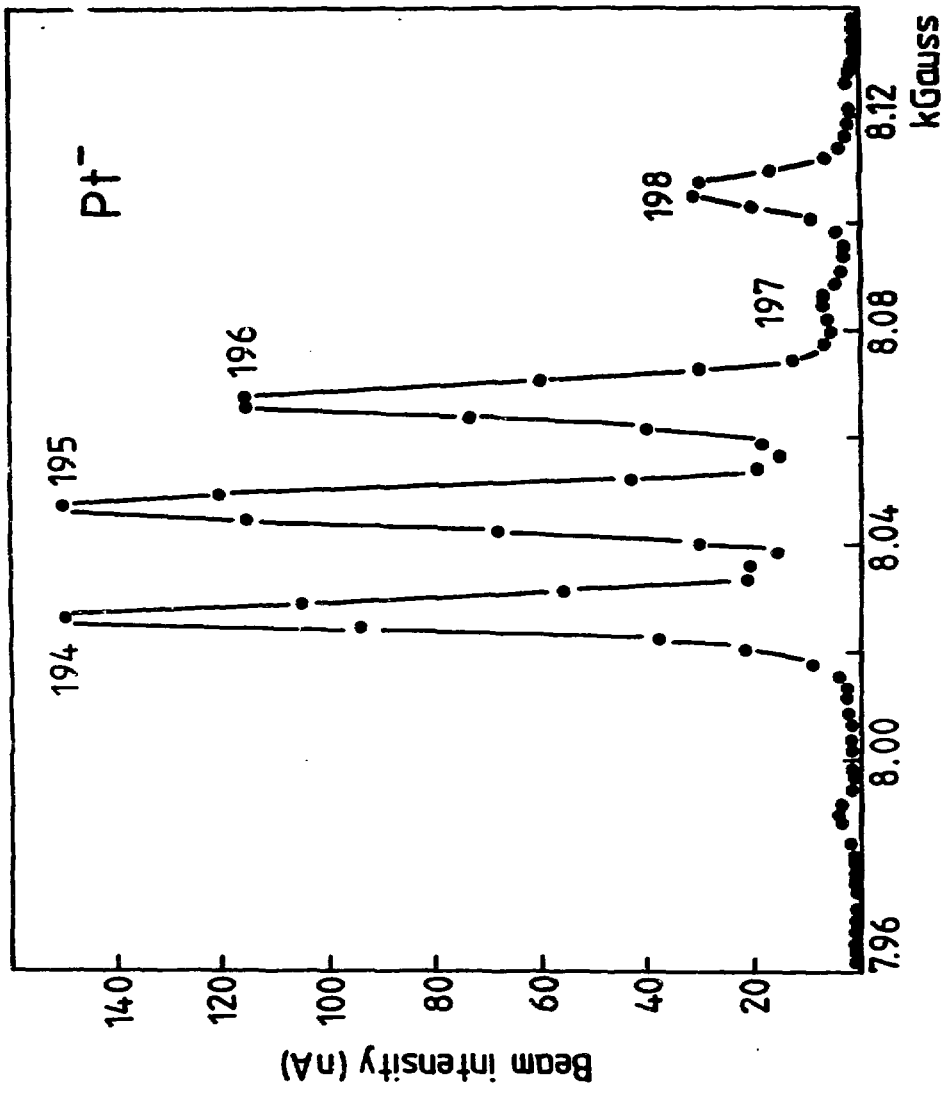
Pt⁻
194
195
196
197
198
Beam intensity (nA)
140
120
100
80
60
40
20
7.96
8.00
8.04
8.08
8.12
kGauss

Figure 2

Broad Band Mass Analysis at MeV Energies

L.R.Kilius, K.H.Chang, E.L.Hallin, A.E.Litherland
Dept. of Physics, University of Toronto

INTRODUCTION

The potential of tandem accelerator based mass spectrometry [TAMS] for the detection and measurement of rare isotopic abundances has been demonstrated consistently at numerous laboratories[1]. Based on these exploratory experiments, a number of dedicated facilities are presently under construction, primarily for the measurement of the radioisotopes ^{14}C and ^{36}Cl at natural abundances. To further increase the versatility of the University of Toronto Isotrace laboratory using TAMS, a series of modifications is being considered to make possible the detection of heavier ions, for example the rare earth elements, Pt, Pu, and to improve the precision of isotope ratio measurements.

Two fundamentally different modes of operation are compatible with TAMS for the measurement of isotopic abundances. The first, and the most commonly employed method, is based on the sequential selection of isotopes. However, the precision of this method is limited by the stability of the spectrometer components (power supplies, ion source etc.), ion transmission variations and the cycling frequency between isotopes. Because of the greater complexity of TAMS, greater effort will be necessary to approach the 0.02% level of precision attained by conventional mass spectrometry for some isotopes of geochronological interest[2]. Arbitrarily increasing the cycling frequency will not ensure higher precision as the optimum cycling frequency is restricted by the time scale for drift related errors in systems with inherently large response times and at higher bandwidths by random errors.

In contrast, the alternative method of simultaneous measurement of all relevant masses is insensitive to system instabilities. Simultaneous mass analysis has been applied successfully to high resolution conventional mass spectrometry using multiple detectors[3]. However, as molecular destruction requires the acceleration of ions to a few MeV, low mass resolution systems which will inject a band of masses are necessary. Without extensive mass filtration, greater use must be made of post acceleration ion identification techniques such as heavy ion detectors and time of flight (TOF). This latter option of simultaneous mass analysis is the method under consideration for the next phase in the development of Isotrace.

WIDE BAND MASS INJECTORS

Low detection limits (greater than one part in 10^{15}) and high sensitivity (efficiencies of greater than 1%) are the principal requirements for the detection and measurement of most radioisotopes at natural abundances or the search for rare and exotic particles such as superheavy elements of unknown mass. In the search for these particles using broad band mass spectrometry at least one or more stable isotope beams must be selectively removed or attenuated by at least 9 to 12 orders of magnitude to prevent damage of the heavy ion detectors due to an excessive counting rate. Magnetic systems which accept a band of masses ($\Delta M=0.1M$) would be appropriate for these searches. On the other hand, the typical ion microprobe experiment requires low sample consumption rates and hence low secondary ion intensities can be anticipated. Precise isotopic and elemental abundance information at the ppm or ppb level is the primary objective. Mass independent all electric systems are more suitable in this case.

1)-MAGNETIC INJECTION

The dispersion, selection of a band of masses and the reconstitution of the beam prior to acceleration must be made in a manner which minimizes the loss of ions of interest due to the finite acceptance of the accelerator and stripping canal. This is best accomplished with a non mass dispersive, achromatic system that has a plane of reflection symmetry along which masses

are initially dispersed. It is here that the appropriate band of masses can be selected. It is also necessary that the focal plane lie perpendicular to the median ray for each mass group to minimize mass dependent aberrations in the reconstituted beam and to reduce mass dependent transmission through the accelerator. Doubly achromatic magnetic systems with this property have been discussed extensively in the literature[4]. One of these configurations is shown schematically within figure 1a.

The three magnet system illustrated consists of a sequence of 45°, 180°, 45° sectors with a plane of symmetry midway through the 180° magnet. For a small momentum spread Δp or equivalently a small mass spread $\Delta M=0.1M$, the focal plane will coincide with the symmetry plane to second order[5]. Although the reduction or elimination of the more abundant isotopes can be made at this plane of maximum dispersion, a field free region would be more advantageous. Ion optical studies of four element spectrometers with this property are presently under study[5].

The additional flight path available for multi-magnet systems is advantageous also for the reduction of molecular fragments from the spontaneous dissociation of metastable molecules and dissociative collisions with residual gas molecules. Those fragments which are transmitted by the magnet are removed by a subsequent electric analysis, ESA1, which ensures that all ions originate from the ion source with a well defined energy. The versatility of the mass injector is further enhanced by the provision of a metal vapor charge changing canal. As has been demonstrated by Heinemeier and Hvelplund[6], it is more efficient to produce some negative ions by the charge changing of positive ions than by direct sputtering. This is especially true for the group III elements such as Al^- and the group II elements such as Be^- which form more abundant metastable negative ions. Since the production of negative ions by charge changing is a multistep process, the yield of metastable ions can be expected to be higher than by direct sputtering also.

The probability of a further dissociation of molecules during the charge changing process is also increased in the vapor canal. The second electric analyzer ESA2 ensures that only those ions which have not changed energy, only

charge, will be transmitted. The combination of both ESA1 and ESA2 will only be transparent to fragments which satisfy the relation:

$$m / M = + 1 / q$$

where m is the mass of the fragment and M,q are the initial molecular mass and charge. Fortunately, the majority of positively charged ions will be of charge state +1. This restricts the passage of all fragments. Although not abundant, the multiply charged molecules are usually metastable and will decay in flight prior to ESA1.

The positive to negative charge conversion also eliminates the positive ions that scatter into the acceptance phase space of ESA2. The scattering of negatively charged ions is not expected to be significant as the cross sections for collisional detachment are significantly higher than the neutralization of positive ions. Unfortunately the above filter does not exclude multiple scattering and dissociative processes which can generate a continuum of ions.

2-ALL ELECTRIC INJECTION

If an ion source immediately precedes the combination of ESA1 and ESA2, the injector will be mass independent and preserve the molecular filtering capabilities described previously. This configuration is particularly well suited for the search of fractionally charge particles as both ESA1 and ESA2 can be tuned to accept a unique charge signature. This portion of the spectrometer is discussed in greater detail within a preceding paper[7].

HIGH ENERGY ANALYSIS SYSTEM

Molecular fragments leaving the accelerator will have an energy spectrum determined by:

$$E = (q + m / M) Ve + K$$

where E is the fragment energy of charge qe and mass m, V the accelerating potential and K the injection energy. More stringent requirements on the resolving power (R) of ESA3, than ESA1 or ESA2, are necessary for the removal of these molecular fragments, for example $R=E/\Delta E=M(q+1)/\Delta M$. For the analysis

of ions up to and beyond uranium, a resolving power of R>1000 is required for the removal of hydride molecular fragments (ΔM=1). Even with sufficient resolution, electric analysis alone cannot remove all fragments as multiple charge changes within the accelerating tube will generate a continuum of ion energies. Magnetic systems can eliminate some of these ambiguities and could provide parallel processing of different mass groups with multiple detectors. Although suitable gas ionization and solid state detectors for the analysis of ions much lighter than calcium are available, TOF detectors have been shown to be essential for the detection of heavy isotopes such as ^{129}I. As TOF transmits all masses equally, this method is potentially simpler than using large magnetic sectors.

The mass resolution of conventional TOF spectrometers is limited by the energy loss straggling within the thin detector used to derive the start signal. After passage through thin foils, the ion energy distribution will be asymmetrical with a large tail on the low energy side typical to Landau-Symon scattering[8]. Adjacent masses will overlap due to this tailing effect and make separation of rare events or hydride fragments, impossible. At the 15-20 MeV operating energies proposed for TAMS, the time resolution Δt/t will be limited to 0.3% for ions passing through a 2 $\mu gm/cm^2$ carbon foil. As the time spread Δt due to energy loss is proportional to the flight path length in conventional TOF, increasing the length of the spectrometer will not improve the time or mass resolution. However, the detection efficiency will be reduced due to small angle scattering of ions in the start detector and the finite acceptance of the start detector.

The effects of ion energy degradation on the determination of TOF can be reduced by a class of spectrometers first proposed by Poschenrieder[9] for low energy ions and later extended to the analysis of ions at MeV energies[10]. The underlying principle is simply that the transit time for an ion which has lost or gained energy can be adjusted to be equal for all ions of the same mass, if an appropriately shorter or longer ion trajectory is chosen. In general the flight path length through a sector field increases in response to an increase in ion energy. As the opposite is true for drift spaces, a suitable combination of sector fields and drift spaces can always be found to

produce isochronous trajectories[10].

Although ion divergence away from the central ray affects the transit time through drift spaces in second order, it is a first order effect in sector fields as:

$$\Delta l = \rho(1 - \cos(p\theta))x'$$

where Δl is the change in the length of the ion trajectory for a bending angle θ and a divergence x', ρ and p are the radius of curvature and p the field index. Based on symmetry arguments, Penner[11] demonstrated that if all ions can be made to cross at a common point at the plane of symmetry, then these trajectories would also be isochronous. This implies that the first order matrix element to the symmetry point, a_{12}, is zero. Similarly if an identical system of sector fields is added but arranged asymmetrical with respect to a new symmetry plane, then the transit time variations with respect to the finite size of the beam is reduced. Equivalently the a_{21} matrix element is zero. These arguments apply equally to pure electric, magnetic or combined sector fields. However, as additional compensation is available in an electric field due to the change in kinetic energy of the ion, smaller deflecting angles will suffice. As electric analyzers are mass independent, the measurement of the TOF through electric sectors fields will retain broad band mass capabilities.

In first order, a spectrometer with the appropriate degree of isochroneity can be constructed by a sequence of drift space -analyzer- drift space arranged in a definite pattern of symmetry constrained by:

$$L/\rho = \cos(p\theta) \pm 1 \ ) \ / \ p \sin(p\theta)$$

where L is the length of the drift space. For a symmetrical system the + sign is chosen and the - sign for the corresponding asymmetrical system. Figure 1b illustrate schematically a symmetrical combination of two analyzers of bending angle, radius of curvature and drift length 43.42^{o}, 0.75 m and 1.88 m, which is isochronous for angle and energy divergences. An ion optics ray trace, figure 2a, confirms that this simple spectrometer is double focussing and achromatic. A similar ray trace of the transit time spread as a function of distance, figure 2b, confirms that the time differences between an arbitrary ray and the central trajectory is zero at the point of spatial focus.

The effects of the finite size of the beam are small and only limit the time resolution $t/\Delta t$ to <2000 for a beam diameter of 2mm. This can of course be improved by the addition of two similar electric analyzers arranged asymmetrically about ESA5. The vertical motion (y') of an ion out of the bending plane is also a second order effect as $\Delta t/t=1/2(y')^2$. Fringing fields and other second order effects do not appear to be significant. In principle, given the state of the art TOF detectors[12], spectrometers with a mass resolution >5000 are feasible.

To maintain an electric gradient below 20 kV/cm, at least charge state +11 must be selected by ESA4. Fortunately, the production of ions in this charge state is maximized as +11 is at the peak of the equilibrium charge state yield for 15 MeV ion in carbon foils. This choice of charge state is also fortunate for heavy ion mass analysis (M>100) as all ions lighter than sodium will be rejected by ESA4.

This form of broad band analysis will be limited by counting rate to 100 kHz due to the generation of false start and stop signals. In principle these ambiguities can be reduced by a second TOF measurement in coincidence with the first. A reduction in transmission efficiency from the production of a new distribution of charge state can be avoided as a conventional TOF measurement should be sufficient.

The realization of broad band mass spectrometry should open up a number of interesting possibilities for TAMS. For example, if a precision of at least one part in 10^4 can be attained, then the simultaneous measurement of the ^{147}Sm, ^{146}Nd, ^{143}Nd abundance distributions should make feasible dating in the range of $1\text{-}5\times10^9$ years. Many similar examples, such as ^{187}Re-^{187}Os, are available of geochronological, and cosmochronological significance[13]. Equally exciting will be the mass independent searches possible, at greater sensitivity, for superheavy elements and quarks.

REFERENCES

1) A.E.Litherland, Ann. Rev. Nuc. Part. Sci. 30(1980)437

2) R.K.O'Nions at al., Ann Rev. Earth. Planet. Sci. 7(1979)11

3) J.Esat private communication
4) J.J.Livingood, The Optics of Dipole Magnets, Academic Press (1969)
5) E.L.Hallin et al., Internal Report University of Toronto, 1981
6) J.Heinemeier et al., Nuc. Instr. Meth. 148(1978)65
7) K.H.Chang et al., these procedings
8) W.Landau, J.Phys (USSR) 8(1944)201
K.Symon High Energy Particles 32(1952)
9) W.Poschenrieder Int. J.Mass. Spect. Ion. Phys. 6(1971)413,
see also Int. J. Mass. Spect. Ion. Phys.,9(1972)357
10) L.R.Kilius Proc. 5th Int. Conf. Ion. Beam Ana. to be published
11) S.Penner, Rev. Sci Inst. 32(1961)150
12) J.Guard et al., Nuc. Instr. Meth. 140(1977)279
13) J.M.Luck et al., Nature 283(1980)256

FIGURE CAPTIONS

Figure 1a- A broad band mass analysis system is illustrated schematically. ESA are electric analyzers and ES quads are electric quadruples.

Figure 1b- An isochronator consisting of two 43.42° spherical electric analyzers (ESA) is illustrated schematically

Figure 2a- A first order ray trace through a two element isochronator is presented as a function of the transit time along the central ray. Trajectories are given for the following initial conditions: 1) an angular divergence of 10 milliradians and an energy spread of 0.5%(- - -),2) an energy spread of 0.5% only (.....) and an angular deviation of 10 milliradians only (___),

Figure 2b- The corresponding time deviations with respect to an ion travelling along a central ray are plotted.

Figure Ia

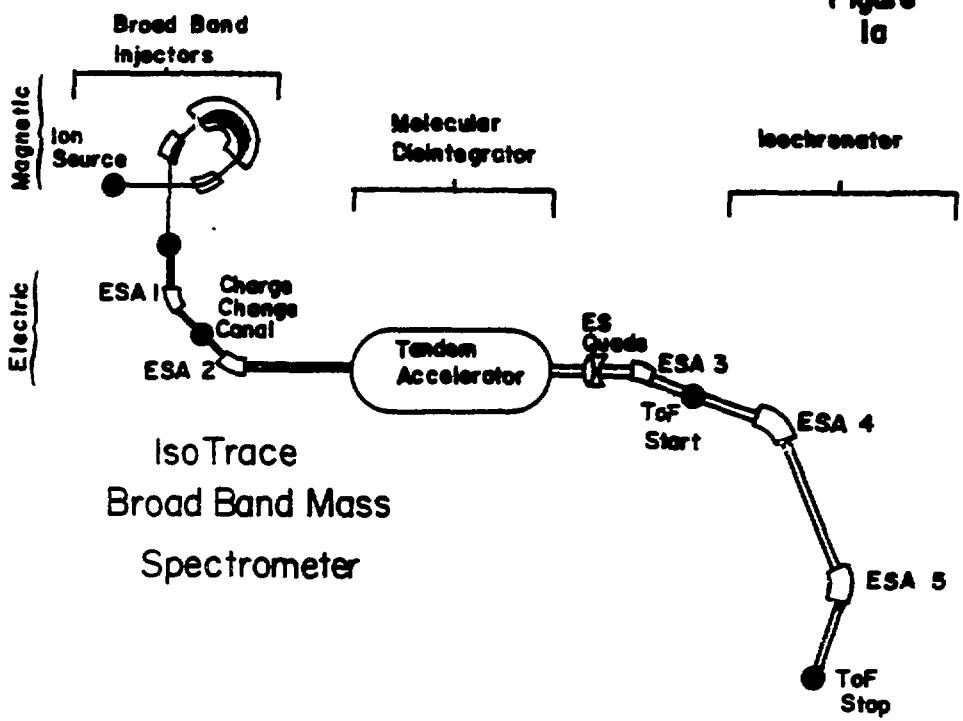

IsoTrace
Broad Band Mass
Spectrometer

Figure Ib

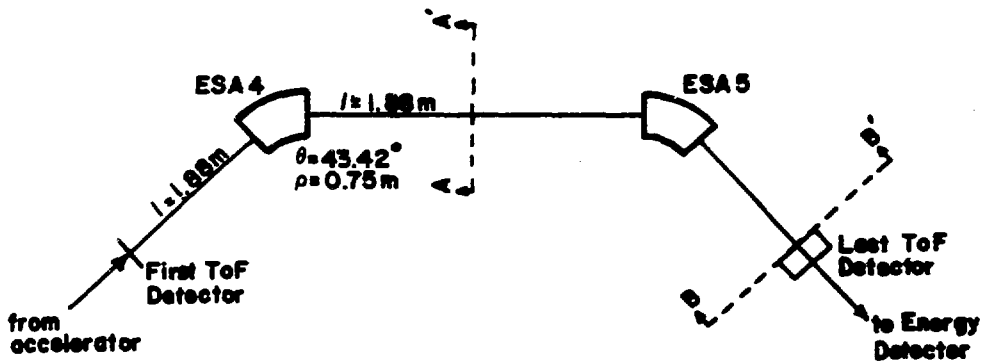

An Electrostatic
Isochronator

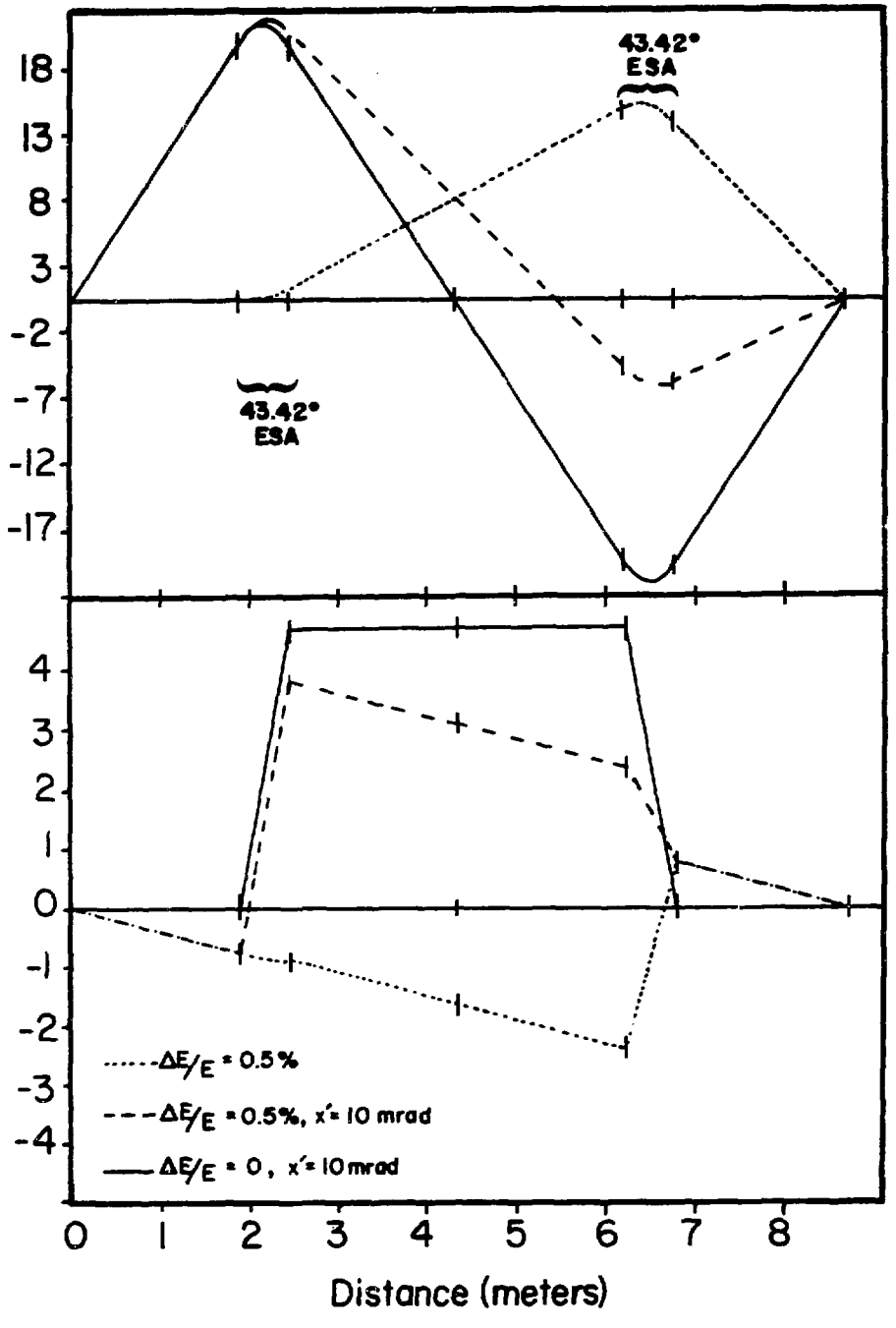

Figure 2a

Figure 2b

CALIBRATION SAMPLES FOR ACCELERATOR MASS SPECTROMETRY[+]

R. L. Hershberger, D. S. Flynn and F. Gabbard
University of Kentucky

Radioactive samples with precisely known numbers of atoms are useful as calibration sources for lifetime measurements using accelerator mass spectrometry. Such samples can be obtained in two ways: either by measuring the production rate as the sample is created or by measuring the decay rate after the sample has been obtained. The latter method requires that a large sample be produced and that the decay constant be accurately known. The former method is a useful and independent alternative, especially when the decay constant is not well known.

The facilities at the University of Kentucky for precision measurements of total neutron production cross sections offer a source of such calibration samples. The possibilities, while quite extensive, would be limited to the proton rich side of the line of stability because of the use of (p,n) and (α,n) reactions for sample production.

The 4π neutron detector, measurement techniques, and comparisons with other measurements have been described previously[1,2]. References 1 and 2 show that total neutron production cross sections can be measured with an accuracy of 3 to 4% and the efficiency of the 4π neutron detector, which is pertinent to the production rate measurements, is shown to be accurate to approximately 3%.

The experimental production rate is given by:

$$(PR)_{exp} = \frac{\text{Counting Rate}}{\text{Efficiency}}$$

where the counting rate can be made accurate to less than 1% and the efficiency has a systematic uncertainty of 3%. This means that if a series of samples were prepared at the Kentucky facilities the absolute number of atoms produced would be known to approximately 3%. However the relative number of atoms from sample to sample would be known to approximately 1%.

[+]Supported in part by the National Science Foundation and the Department of of Energy.

The calculated production rate for typical operating conditions is:

$$(PR)_{calc} = \frac{\sigma}{A} (3.76 \times 10^5) \quad \frac{Atoms}{Sec}$$

where σ is in mb and A is the atomic mass of the target. For example the reactions

$$^{26}_{12}Mg\ (p,n)\ ^{26}_{13}Al \qquad \text{and} \qquad ^{23}_{11}Na\ (\alpha,n)\ ^{26}_{13}Al$$

both have 100mb cross sections at E_p or E_α = 5 MeV. Hence for both reactions

$$(PR)_{calc} \simeq 1.5 \times 10^6 \quad \frac{Atoms}{Sec}$$

which means that in about two hours beam time an ^{26}Al sample of 10^{10} atoms could be produced. Table I is a partial list of useful samples which could be produced at the Kentucky facilities.

In summary, under the conditions of cross section, threshold energy, and per cent natural target abundance (p,n) and (α,n) reactions could be used to produce samples with the number of atoms known to 3% and with a sample to sample relative precision of 1%.

[1]K. K. Sekharan, H. Laumer, B. D. Kern and F. Gabbard, Nuc Instr. and Meth., 133 (1976) 253.

[2]R. L. Hershberger, D. S. Flynn, and F. Gabbard, Phys. Rev. C 21, 896 (1980).

Table I. Calibration Samples

Isotope Produced	$t_{\frac{1}{2}}$ [10^5 years]	Reaction	Natural Abundance [%]
$^{41}_{20}Ca$	0.8	$^{41}_{19}K$ (p,n)	6.88
$^{26}_{13}Al$	7.4	$^{23}_{11}Na$ (α,n)	100.
		$^{26}_{12}Mg$ (p,n)	11.2
$^{36}_{17}Cl$	3.1	$^{36}_{16}S$ (p,n)	0.014
$^{53}_{25}Mn$	19.	$^{50}_{23}V$ (α,n)	0.24
		$^{53}_{24}Cr$ (p,n)	9.55
$^{59}_{28}Ni$	0.75	$^{56}_{26}Fe$ (α,n)	100.
		$^{59}_{27}Co$ (p,n)	100.
$^{94}_{41}Nb$	0.2	$^{94}_{40}Zr$ (p,n)	17.4
$^{97}_{43}Tc$	26.	$^{97}_{42}Mo$ (p,n)	9.46

PRODUCTION OF CHARCOAL FOR ACCELERATOR TARGETS

S. W. Leavitt, D. J. Donahue, A. Long
University of Arizona

One method for preparing accelerator targets from carbon-containing materials is to produce charcoal from samples and to mix the charcoal with a binder. This mixture can then be used as a target in a sputter-type ion source. In the experiments to be described, we have measured yields and isotopic fractionations for several methods of preparing charcoal from wood, (assumed to be $(CH_2O)_n$), and cellulose $(C_6H_{10}O_5)_n$. Yields are defined as $\frac{\text{mass of charcoal produced}}{\text{mass of carbon in wood or cellulose}}$ and were determined by weighing the samples before and after reduction. Fractionations of ^{13}C relative to ^{12}C were determined by burning the charcoal to CO_2 and measuring $^{13}C/^{12}C$ ratios in a mass spectrometer. The ratios, $^{13}C/^{12}C$, are reported with respect to a standard and defined by the equation

$$\delta(^{13}C) = \left\{ \frac{(^{13}C/^{12}C)_{sample}}{(^{13}C/^{12}C)_{standard}} - 1 \right\} \times 1000 \ .$$

Results were obtained from pyrolizing wood in a vacuum and in an argon atmosphere, and from pyrolizing cellulose in a vacuum, in an argon atmosphere and in sealed tubes. Conversion to charcoal is essentially complete at temperatures greater than about 300°C. Best results were obtained when a fixed amount of cellulose was sealed in an evacuated glass tube and heated to about 600°C. Yields of greater than 60% were obtained, and fractionation from cellulose to charcoal was about -0.03%.

Targets were prepared by mixing charcoal with an equal number of atoms of copper and aluminum powder, and by melting a mixture of (15/1) by mass iron powder and charcoal. Negative-ion currents from these targets in a General Ionex sputter ion source were compared with currents from spectroscopic graphite and from a target made of graphite produced by cracking acetylene. Relative magnitudes of currents obtained from the various targets are: spectroscopic graphite, 1.0; cracked graphite, 0.4; melted Fe-C solution, 0.25; Al-C and Cu-C mixtures, 0.1.

SAMPLE PREPARATION FOR ACCELERATOR MASS SPECTROMETRY AT THE UNIVERSITY OF WASHINGTON

Pieter M. Grootes and Minze Stuiver
Quaternary Isotope Laboratory

George W. Farwell and Fred H. Schmidt
Nuclear Physics Laboratory and Department of Physics
University of Washington, Seattle, WA 98195

The adaptation of the University of Washington FN tandem Van de Graaff to accelerator mass spectrometry (AMS), as well as some of the results obtained, are described in another paper in this volume (Farwell et al., 1981). Here we discuss our experiences in preparing carbon and beryllium samples that give large and stable ion beams when used in our Extrion cesium sputter source with an inverted cesium beam geometry.

1. SAMPLE PRETREATMENT

Samples of cosmogenic isotopes first have to be concentrated and/or purified before their isotopic composition can be measured. The procedure depends on the geochemistry of the isotope and is different for the two isotopes we are working on (^{10}Be and ^{14}C).

^{10}Be has a short residence time in the atmosphere. It is transported with precipitation and particulate matter rapidly into snow deposits and sediments, where it is fixed. Because of this rapid fixation the probability of a later addition of ^{10}Be to sample material (contamination) is small and the pretreatment mainly serves to concentrate the ^{10}Be. We concentrated ^{10}Be from snow samples by ion-exchange filtration of the meltwater. The Be was eluted from the filter with 20 ml of 3M HCl and 5 mg of Be carrier was added as high purity metal flakes to the solution. The Be was then precipitated as hydroxide by neutralising with a minimum volume of concentrated NaOH solution and, by heating, converted into oxide. The elaborate radiochemical purification procedure used for β-decay measurements of ^{10}Be does not have to be followed, because the AMS system easily discriminates out the radioactive impurities otherwise eliminated chemically. The stable isotope ^{10}B, which has no effect on the decay activity measurement, however, has to be avoided, because it has virtually the same mass as ^{10}Be and, except by its

range, is very hard to separate from ^{10}Be. The Be sample chemistry must therefore be carried out in plastic or teflon labware (glass labware like "Pyrex" has a B_2O_3 content of 13% and a measurable solubility in acid and alkali).

^{14}C in CO_2 has an atmospheric residence time of several years and is cycled through atmosphere, biosphere and ocean sufficiently fast to give a more or less homogeneous distribution throughout these reservoirs. Therefore, unless the sample has been a closed system it is very common, that radiocarbon samples have received an admixture of carbonaceous material(s) with differing specific ^{14}C activity (contamination). Since the carbon concentration in samples is often high, the radiocarbon sample pretreatment is designed mainly to eliminate contaminants. For organic material this is accomplished by using differences in solubility in acid and alkali between the original sample material and the contaminants introduced later, frequently by infiltrating groundwater (carbonates, humic and fulvic acids). If we have an inorganic carbon sample, typically carbonate, elimination of contaminants is generally not completely possible.

The routine procedure for radiocarbon samples in the Quaternary Isotope Laboratory consists of: (i) extraction with 3% NaOH solution at about 60°C; (ii) washing with distilled water until almost neutral (pH<9); (iii) extraction with 4% HCl solution at about 60°C; (iv) again washing with distilled water until almost neutral (pH>5). Usually this extraction is sufficient to eliminate contaminants so that a reliable radiocarbon date can be obtained for the sample. It results, however, in a loss of 40 to 60% of the original dry and ash-free material. Although it may be tempting to use small, carefully selected and apparently clean samples directly for AMS, such a procedure may result in the effective loss of the complete sample, because the measured $^{14}C/^{12}C$ ratio is the resultant of the true sample ratio and that of a contaminant or contaminants.

The major advantage of AMS for radiocarbon dating is the very small sample size required. For samples in the range from 10 to 100 mg special precautions are necessary to minimize handling losses during the chemical extraction. This can be done by using a glass tube with a sealing fritted disc in the middle on which the sample is placed. This technique has been quite successful in the Quaternary Isotope Laboratory where it has been used to prepare pure

α-cellulose from 100 mg of wood for ^{18}O and ^{13}C measurements. The solution is poured onto the sample which is then stirred and allowed to react. When the extraction is complete, the sample is sucked dry with an aspirator and rinsed with distilled water. It is advisable to test the fritted discs before the extraction and to use only those that have a high permeability.

2. SAMPLE COMBUSTION

As discussed earlier in this volume (Farwell et al., 1981) precise measurements of isotope concentrations can be made, when the influence of isotope fractionation in the AMS system is eliminated by comparing samples with a standard. A necessary condition for this comparison is that the samples of unknown and reference material used to generate the ion beams be closely identical in everything except isotopic composition.

Natural radiocarbon samples contain many non-carbon compounds. These can only partly be eliminated from the sample and therefore lead to a variable composition of the unknown sample if the sample material is used directly for source preparation. Combustion of carbonaceous sample material to CO_2 with subsequent sample preparation from this gas ensures an identical composition for all samples and the reference. Small sample size, however, may preclude the use of the normal combustion technique for radiocarbon samples. For a research program to measure variations in the isotopic abundance of ^{13}C in tree rings the Quaternary Isotope Laboratory uses breakseal tube combustion. The sample (10 mg of cellulose) is placed in a 0.9 cm diameter, 10 cm long Vycor tube closed on one side with a breakseal, that has been preheated at 900°C for one hour. To the sample is added 1 g of a mixture of CuO and MnO_2 (5 to 1 by weight). The CuO has been preheated to 900°C for 20 min to eliminate organic contaminants. The tube is then narrowed near the end to enable vacuum sealing, pumped to high vacuum for 3 to 4 hours, and sealed with a blow-torch. Combustion of the sample is accomplished by placing the sample, marked with heat resistant paint, in a fire resistant brick in an oven at 900°C for 1 hour. The CO_2 (about 10 ml NTP) is extracted by breaking the seal with a magnet breaker inside a vacuum system. It is then purified by passing it through a dry-ice-alcohol water trap and a silver/copper oven at 450°C, and collected with liquid nitrogen. This method has been tested extensively for ^{13}C samples and shows a reproducibility in $\delta^{13}C$ of better than 0.1‰, where δ is the relative difference in

isotopic composition between the sample and a standard. If fritted disc tubes of Vycor are used it is possible to perform the whole chemical pretreatment and the combustion in the same tube without any further sample transfer with accompanying handling loss. For especially small and valuable samples this may be well worth the extra expense of the Vycor fritted disc tubes.

3. SPUTTER SOURCE SAMPLE PREPARATION AND ION YIELD

Once the carbonaceous sample material has been converted into pure CO_2 the problem is to bring this into a solid form suitable for use in a cesium sputter ion source. (Such sources have given the best results, so far, in AMS). A relatively simple and straightforward way to do this was reported by us at the Tenth International Radiocarbon Conference in Bern (Grootes et al., 1980). The CO_2 is reduced to CO by passing it over zinc powder at 400°C. The CO subsequently circulates thermally through a glow discharge, where it is partly dissociated (cracked) to C↓ and O, and over the same hot zinc where the oxygen liberated by the dissociation is taken up. This leads to near quantitative conversion of the CO_2 to carbon. From an initial pressure of 20 torr or more an end pressure of less than 0.2 torr is obtained. The cracking process requires a good circulation of the gas and even then is rather slow (it takes at least overnight).

Other gases like methane and particularly acetylene are less stable and therefore lend themselves better to cracking, either thermally or in a discharge. Their synthesis, however, is more elaborate; considering the very small samples and the high sensitivity for contamination that are involved, this means also less favorable. The development of highly efficient catalysts, like the one used in gas chromatography measurements of CO_2 which is capable of converting CO_2 into methane in just a single pass of a gas mixture, may change the situation in favor of the use of methane.

Initially we tried different forms of carbon and different carbon-binder mixtures to prepare samples for the sputter source. In general the ion beams obtained were only 10 to 20% of the one obtained from a commercial spectrographically pure graphite, which we adopted as our yardstick for good sample beams (table 1). Notable exceptions were laboratory made "graphitized" carbon pellets and a smooth, thin layer of cracked carbon deposited directly on a tantalum backing. The maximum beams obtained from these two were about the

same as for graphite. We have therefore pursued these two options.

Table 1. Comparison of $^{12}C^-$ ion beams obtained from different types of carbon samples in Extrion cesium sputter ion source with an inverted cesium beam geometry.

Type of Sample	Normalized $^{12}C^-$ beam[a] ($^{12}C^-$(sample)/$^{12}C^-$(graphite))
graphite[b]	1.0
charcoal from wood	≈0.045 (0.01-0.30)
charcoal from excavation	≈0.015
cast iron	0.05-0.16
carbon/iron mixture	0.08-0.12
calcium carbonate	0.015-0.035
pencil no. 1	≈0.23
anthracite	≈0.16
C/KBr mixture	0.02-0.20
wood charcoal/silver powder (1 to 8 by weight)	0.47
wood charcoal/silver powder (1 to 16 by weight)	0.48
charcoal briquet, pressed, heated to 2700°C	≈1.0
wood charcoal, pressed, heated from 750 up to 2500°C	0.09-0.17
cracked carbon, thin deposit	0.03-1.0[c]
cracked carbon, thick (lumpy) deposit	<0.2
cracked carbon, pressed, heated to 2700°C	0.06
wood charcoal/coal tar pitch (3 to 1 by weight), pressed, heated to 1000°C (carbonized)	0.06
wood charcoal/coal tar pitch (3 to 1 up to 6 to 1 by weight), pressed, heated to 1000°C in N_2, to 2500°C in vacuum (graphitized)	0.4-1.0
Ta blank in 10 min	0.11→0.018

[a]Measured in a removable Faraday cup at the low-energy end of the accelerator.

[b]Output up to 48μA depending on the beam intensity desired; controlled by cesium boiler temperature.

[c]Three samples started with 0.5, increased for a few minutes (up to 0.67), then fell off to 0.3 as cesium burned through deposit; one started at 1.0 and dropped to 0.3; changing source position gave back 0.8 immediately.

The original cracked carbon deposits were distributed evenly over the whole backing and were so thin that the cesium beam soon burned through the deposit so that no stable beam was obtained (decay constant of the beam about 7 min^{-1}). Following a suggestion of the Tononto group (Beukens pers. commun.; see also Purser et al., 1980) we limited the discharge area by shielding most of the sample backing with an insulator (fig. 1). Quartz was chosen as the insulator because it can be cleaned easily by burning off any carbon deposited during the cracking. The other parts were brass and spring steel (again to facilitate cleaning and to have no parts that can give off carbon). With the new setup we have obtained "thick" carbon deposits of 0.5 to 5 mg of carbon on the center part (about 3mm diameter) of a copper or tantalum backing. These thicker carbon deposits, however, have an irregular, "lumpy" surface (fig. 2) and seem to have a low density. The beam produced by them is generally only 10 to 25% of the $^{12}C^-$ beam from graphite.

The production of "graphitized" carbon pellets has been described before (Grootes et al., 1980). About 15 mg of a 3 to 1 mixture of sample carbon and coal tar pitch are heated under pressure in a mold to 1000°C in a nitrogen atmosphere. After cooling the pellets are taken from the mold and heated under vacuum to 2500°C. This procedure has been slightly modified. The ratio sample to binder of 3 to 1 is unnecessarily low and can be increased to 5 to 1. Furthermore a more homogeneous-looking carbon pellet is obtained when the first heating step is limited to 850 to 900°C. Pellets prepared by this method have consistently given $^{12}C^-$ beams that are similar to those of graphite and that last for many hours or even days. When run for the first time the beam output of these samples increases rapidly over the first few minutes. After perhaps 5 or 10 minutes the increase levels off and there is only a rather slow long-term drift.

The behavior of compacted mixtures of carbon and silver powder (1 to 8 and 1 to 16 by weight) is promising. After an initial gradual increase by a factor of 2 to 3 over a period of half an hour, the ^{12}C beam stabilizes at about 50% of the output of a graphite sample. The availability of carbon-free silver powder and the greater ease of preparation of the pellets may make this a viable alternative to the graphitized sample pellets. Further study is needed.

The maximum stable beams obtained from our Extrion source so far are 48μA $^{12}C^-$ in the low-energy cup and 190 nA $^{13}C^{+4}$, analyzed, in the image Faraday cup.

These beams were obtained using a graphite sample pellet and a cesium boiler temperature of 315°C. For a pellet made out of AD 1950 standard carbon ($^{14}C/^{12}C = 1.17 \times 10^{-12}$) these beam currents translate to a ^{14}C counting rate of about 1860 counts per minute. With a relatively cool ion source (250°C) and a $^{12}C^-$ beam of about 10μA, ^{14}C count rates of about 700 cpm have been obtained from a pellet made out of wood grown in 1964. This material has a ^{14}C activity of about 180% of the 1950 activity due to the extensive nuclear weapons tests of the early sixties.

With count rates such as these (and they will be increased further if the accelerator transmission can be improved) it is relatively easy to obtain 1% counting statistics for young (not older than 10,000 years) samples. Precision of the final $^{14}C/^{12}C$ ratio in these cases will depend on the stability of the ion source and the accelerator transmission rather than the counting rate. The uncertainty in the measured ratio should therefore be deduced from the distribution of the results of several measurements repeated at different times and, preferably, on different days.

After the automated sample changer described by Farwell et al. (1981) had been installed, quite sharp images of the cesium beam have been obtained on sample pellets that had undergone many alternations of sources (fig. 3). This proves that the sample changer provides the accurate positioning of the sample essential for the comparison of the isotopic composition of an unknown sample with that of a reference sample.

Because of the small size of the cesium beam spot we tried a smaller diameter pellet (1/16" diameter instead of the regular 3/32"). This produced a $^{12}C^-$ beam about 10% stronger than that from a regular size pellet, which proves that the amount of sample can be reduced by at least a factor 2 (from 15 to less than 7 mg). Further reduction in diameter and thickness may be possible, leading to a sample size as small as 1 mg. Here the difficulty of handling such extremely small samples may become a limiting factor.

For beryllium we have continued our studies of the production and detection of ions of the radioisotope ^{10}Be. Our best operation was originally achieved by using Be metal samples in the sputter ion source while maintaining a very small flow of O_2 gas through the ion source chamber (pressure with O_2 about 2×10^{-6}, without between 1 and 2×10^{-7}). Recently, acting upon a suggestion by colleagues at Simon Fraser University (Canada) (J.R. Southon,

pers. commun.), we found that a mixture of BeO powder and finely-ground silver, compressed into a pellet and used with O_2 gas, produces beams almost as large (up to 25 nA Be^{+3}, analyzed) as those from Be metal samples. The ^9Be beams obtained from the mixture depend strongly on the mixing ratio and seem to be maximum for ratios BeO/Ag between 1 to 4 and 1 to 8 by weight. Though we have not yet established the ultimate durability of sources made by this method, some have run very steadily for several hours. BeO/Ag is much easier to prepare than the metal, so this approach may be very advantageous.

ACKNOWLEDGEMENTS

This work has received support from the National Science Foundation (Grant EAR-7904523, Geochemistry Program) and the Department of Energy. We would like to thank Mr. Gervas Hinn for carrying out the beryllium chemistry and preparing the beryllium samples.

REFERENCES

Farwell, G.W., Schmidt, F.H., and Grootes, P.M., Accelerator mass spectrometry at the University of Washington, 1981 (this volume).

Grootes, P.M., Stuiver, M., Farwell, G.W., Schaad, T.P., Schmidt, F.H., 1980, Enrichment of ^{14}C and sample preparation for beta and ion counting. Proc. Tenth Int. Radiocarbon Conf. Bern/Heidelberg, 1979, Radiocarbon, v. 22, p. 487-500.

Purser, K.H., Liebert, R.B., Russo, C.J., 1980, MACS: An accelerator-based radioisotope measuring system. Proc. Tenth Int. Conf. Bern/Heidelberg, 1979, Radiocarbon, v. 22, p. 794-806.

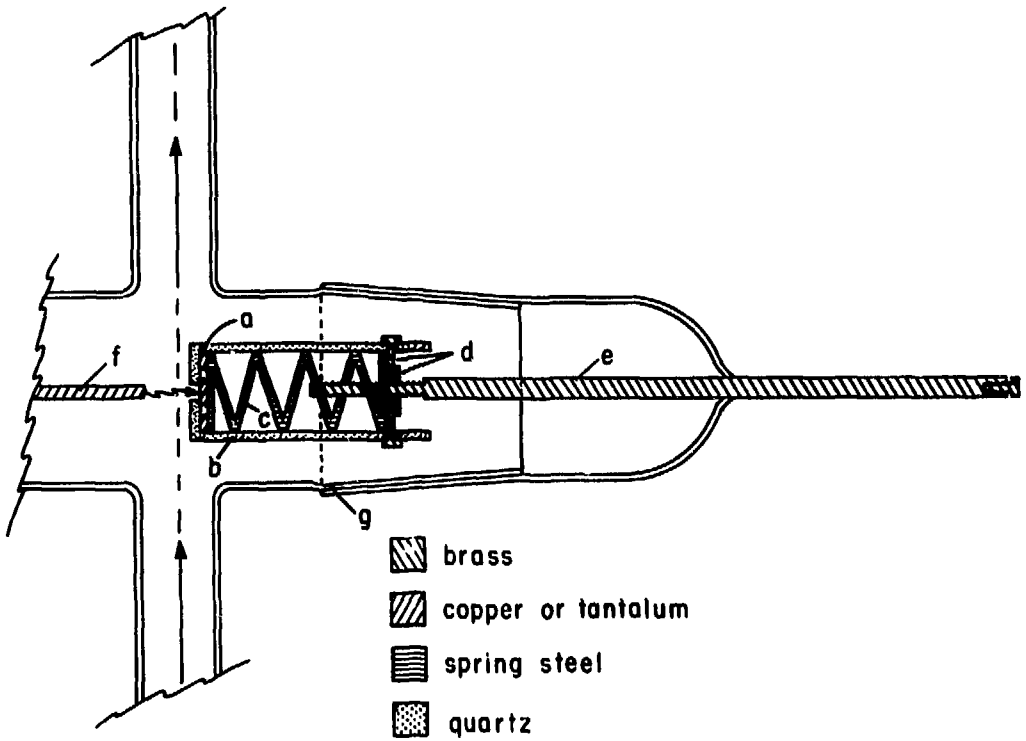

Fig. 1. Setup for localized deposition of carbon samples from CO in a glow discharge. Gas flows up through discharge region by thermal circulation. Discharge takes place between electrode (f) (+ in DC operation) and sample backing (a) mounted inside quartz insulator (b). Electrical contact to (a) is made by steel spring (c) compressed by the mounting (d), which consists of 3 brass bolts centering a brass nut in the insulator. The nut screws on support electrode (e) and allows adjustment of the electrode gap. The assembly is mounted in the vacuum system with 34/45 ground glass joint (g).

Fig. 2. Deposit of carbon cracked directly onto tantalum backing for insertion in cesium sputter ion source using the 6 hole inverted cesium beam geometry.

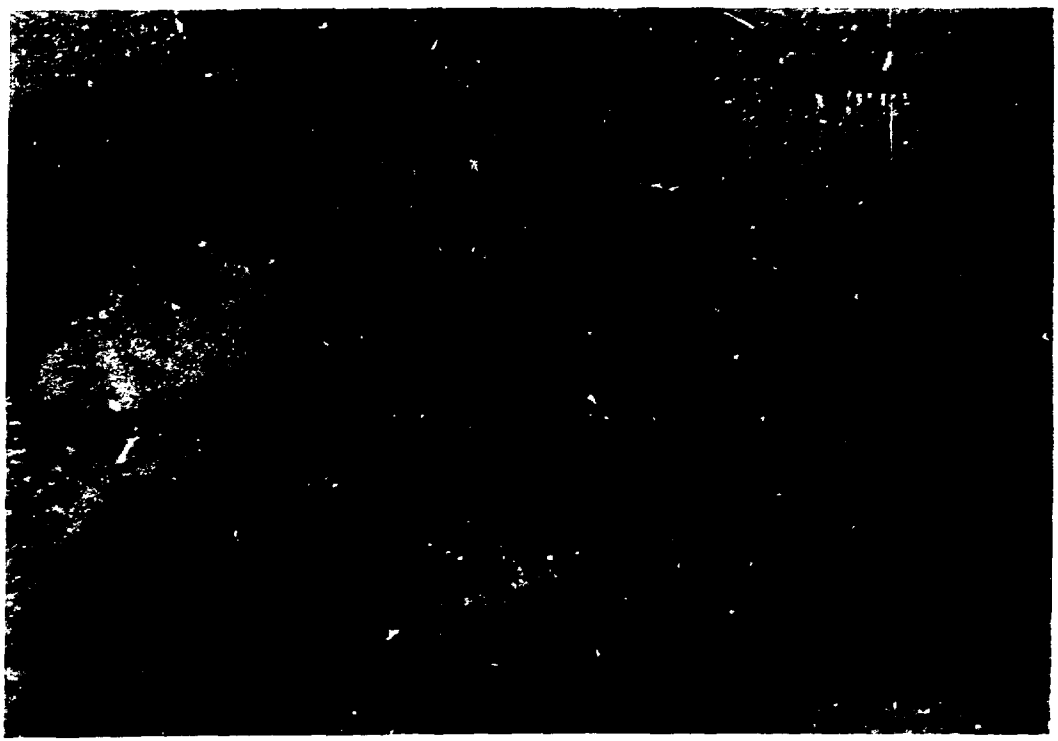

Fig. 3. Image of cesium beam spot on 3/32" diameter graphite pellet that has been switched into the beam a large number of times. The pellet is shown mounted in its 6 hole tantalum backing.

THE PRODUCTION OF SMALL CARBON SAMPLES BY R.F. DISSOCIATION OF ACETYLENE

Roelf P. Beukens and Henry W. Lee

University of Toronto, Toronto (Ont) Canada

INTRODUCTION

As gaseous ion sources cannot be used for radiocarbon dating with accelerators due to the extraordinary large amount of cross contamination, sputter sources with solid samples have commonly been used. A number of of small carbon samples have now been dated by the Toronto-Rochester-General Ionex group using the MP-tandem accelerator of the Nuclear Structure Research Lab. at the University of Rochester [1]. In the early experiments a variety of sample preparation techniques have been used including mixing with KBr, Cu and Ag binders. Although the currents from these samples were often adequate, the variations in C^- beam quality from sample to sample has caused some concern about the reproducibility of the data. Early in 1978 we started the development of a better sample preparation technique which meets the following criteria:

1) The source material should be in the form of graphite to produce good stable C^- beams.

2) Low loss sample conversion is essential as sample sizes are often 1 milligram or less.

3) The sample diameter should be of the same order as the caesium primary sputter beam for efficient use of the material. The HICONEX-834 in reflected geometry has a caesium beam spot size of approximately 500 microns while the new Tandetron sputter source has a spotsize of 200 microns.

The method which seems to meet these criteria the best is the pyrolysis or dissociation of a hydrocarbon gas such as acetylene (C_2H_2).

The synthesis of acetylene, from carbonates, CO_2 or charcoal, in small, contaminant-free quantities is well understood and has been described in detail by Tamers [2]. The carbonaceous material is first converted to Li_2C_2 at 900°C. The reaction with water subsequently produces C_2H_2 and Li_2O.

The conversion of acetylene to graphite samples which produce good C^- beams required more thought and experiments. Several methods using thermal pyrolysis, high voltage DC and RF discharge dissociation were investigated [3] and the RF discharge method appeared to satisfy the requirements the best. Thermal pyrolysis does not allow small sample spotsizes while the D.C. discharge dissociation cannot achieve a sample thickness of more than a few microns.

THE PRODUCTION OF ACETYLENE

The USGS Radiocarbon Laboratory produces acetylene routinely with a conversion efficiency of better than 94% from 2 grams of $SrCO_3$ (240 mg equivalent Carbon). However no measurable amount of acetylene was produced when 0.2 grams of $SrCO_3$ (24.9 mg equivalent Carbon) was used [4]. The reaction bomb used by the USGS for the 2 gram $SrCO_3$ samples was 1 litre. As we would expect to convert samples of approximately 1 mg equivalent Carbon a scaled down reaction bomb has been used in our setup with a volume of 6 ml. Figure 1 shows schematically the complete setup. The most notable features in addition to its small size are:

1) All the parts are made out of stainless steel and are degreased in hot chlorothene-v, rinsed and heat dried before assembly. Before use the setup is baked for at least an hour.

2) Only Vacsorp cryopumps and a zeolite trapped oil roughing pump are used to obtain an oil free system.

3) The reaction temperature of 900°C to produce the Li_2C_2 is generated

conviently by a 10kW radiofrequency induction furnace. The bomb volume provides good coupling with the radiofrequency field. The temperature is monitored with a chromel-alumel thermocouple.

4) The reaction bomb is manufactured cheaply from a rod of low carbon 316L stainless steel and therefore is replaced as often as required to prevent sample cross contamination.

RADIOFREQUENCY DISCHARGE DISSOCIATION OF ACETYLENE

The deposition mechanism of the dissociation products of gasses in a glow discharge is strongly dependent on the gas pressure. At pressures less than 7 torr the R.F.-excited plasma deposits on a substrate very hard insulating carbon films which have been variously termed "amorphous", "glassy" and "diamond-like". If the C-H bond is not sufficiently broken polymerization can take place. The production of carbon films in this pressure range has been studied by a large number of authors [5]. Samples produced by this process proved to be unsuitable as eratic current behaviour was observed while the C^- currents were in general less than 1 uA. At pressures above 10 torr a blue arc discharge is obtained and it is believed that the dissociation in this region takes place mainly through ion-molecule reactions. The products are in addition to Carbon and Hydrogen, other hydrocarbons such as CH_4, C_2H_4 etc. and the yields are less than 20%. The arc discharge is eratic and the deposition rate is low. The best pressure region, producing graphitelike carbon deposits, with an efficiency of better than 60%, was found to be the transition region of 7 to 10 torr where a spacially well defined discharge is obtained. Nitrogen filler gas has been added without an appreciable change to the discharge while Argon pushes the operation into the regime of an uncontrolable arc discharge.

The small discharge chamber is shown in Figure 2. It is a simple diode arrangement where one of the electrodes is grounded while the the other is connected to a high voltage R.F. generator with variable power output. The sample holders are mounted on the ends of the electrodes and all but a small opening of 1mm diameter is electrically insulated.

Hydrogen gas, produced in the dissociation, is pumped away through a hot Palladium foil. Figure 3 shows a photograph of a sample of approximately 1 mg and a diameter of 1mm produced with this apparatus.

RESULTS

Several samples have been produced successfully with this method from small slag samples from the L'Anse au Meadow site in Newfoundland, from carbonates from ground water samples and standards such as NBS Oxalic acid and a 1850 wood sample and have been used in dating attempts at Rochester during 1980. Figure 4 shows the current behaviour of a 1.2 mg and a 0.2 mg sample as compared to a charccal + KBr mixture, run under conditions where regular graphite yielded 10 uA of C^-. The C^- current of the two samples produced by R.F. dissociation of acetylene rose in approximately an hour to their maximum value of 7 uA (70% of graphite). The charcoal + KBr took longer to reach it maximum current of 5 uA. The beam quality (emittance) of the two samples was considerably better than that of the charcoal + KBr sample as more than 90% of the beam passed through the low energy aperture into the accelerator as compared to 50% of the beam from the C + KBr sample. The time of one hour necessary to obtain the maximum current from a fresh sample is about the same as that required for a fresh graphite sample. It is probable that this initial period of rising current is related to the crater which is produced in the sample by the Caesium beam which increases the emitting surface. The importance of cratering was also indicated by some of our earlier experiments with samples which were less than 100 microns thick. In these experiments the currents would rise in seconds to the maximum value and proceed to drop of exponentially. The average sputter efficiency was very low in those cases suggesting that the material was being blasted away by the cratering process.

FRACTIONATION

At this point some comments should be made about fractionation. In

the conventional carbon dating technique sample fractionation due the preparation is avoided by ensuring 100% conversion. As the end product is a gas in which homogenization will take place no additional fractionation will take place. In the case of the deposition of carbon from acetylene this unfortunately is not the case as homogenization is not possible even if complete conversion could be achieved. The solution of using the whole sample and averaging the end result is not practical even in case of a sample of 1mg. This problem can however be overcome as will be shown in the next example.

Lets assume we have an ideal primary 1950 wood standard with a δ_{13} of -25 per mill. The 13/12 and 14/12 ratios measured with an accelerator would then be:

$$R_{13}^{ms} = F_{13} * f_s * R_{13}^{s}$$

$$R_{14}^{ms} = F_{14} * f_s^2 * R_{14}^{s}$$

Two different kinds of fractionation factors have been used:

1) The fractionation factor f_s is the sample fractionation including the fractionation introduced due to sample preparation. This would normally have the general form of $f = (1 + \delta_1) * (1 + \delta_2) \ldots$. The important feature of this fractionation is that this fractionation in the 14/12 ratio is exactly the square of the fractionation in the 13/12 ratio.

2) The fractionation factors F are the fractionations due to the mass dependent transmission efficiency through the accelerator. The main cause for this fractionation seems to be the velocity dependent stripping efficiency in the terminal stripper and the energy dependent small angle scattering in the stripper combined with a limited acceptance of the high energy acceleration tube. No known simple relation exists between F13 and F14.

If we now have a sample with an unknown age of t years and an

unknown δ_{13} sample fractionation we can write its measured ratios, assuming that the transmission efficiencies remain the same, as:

$$R^m_{13} = F_{13} * f * R^s_{13}$$

$$R^m_{14} = F_{14} * f^2 * R^s_{14} * EXP(- \lambda t)$$

The sample fractionation f now is different from f_s of the standard as they are the product of the initial sample fractionation and the fractionation introduced due to preparation, which in general will be different from the standard. By eliminating the fractionations F and f from the four formulas we get the simple result for the age of the unknown:

$$EXP(- \lambda t) = \frac{R^m_{14}}{R^{ms}_{14}} * \left(\frac{R^{ms}_{13}}{R^m_{13}} \right)^2$$

If we have a less than ideal primary standard it is of course easy to see that by deduction we can obtain an equally simple result. The above discussion can be generalized by identifying the F's with any mass dependent fractionation which in good approximation remains constant from sample to sample, and identifying the f's with any fractionation which varies from sample to sample but is to a good approximation f^2 for the 14/12 ratio.

REFERENCES

1) R.P.Beukens; British Museum Occasional Papers Vol.21 (1980) 7
2) M.A.Tamers; Int.J.Appl.Rad.Iso. Vol.26 (1975) 676
3) R.P.Beukens et al; Atomic Energy of Canada Ltd. Report TR-39 (1980)
4) M.Rubin; USGS, Private communication
5) L.Holland and S.M.Ojha; Thin Solid Films Vol.58 (1979) 107
and references therein

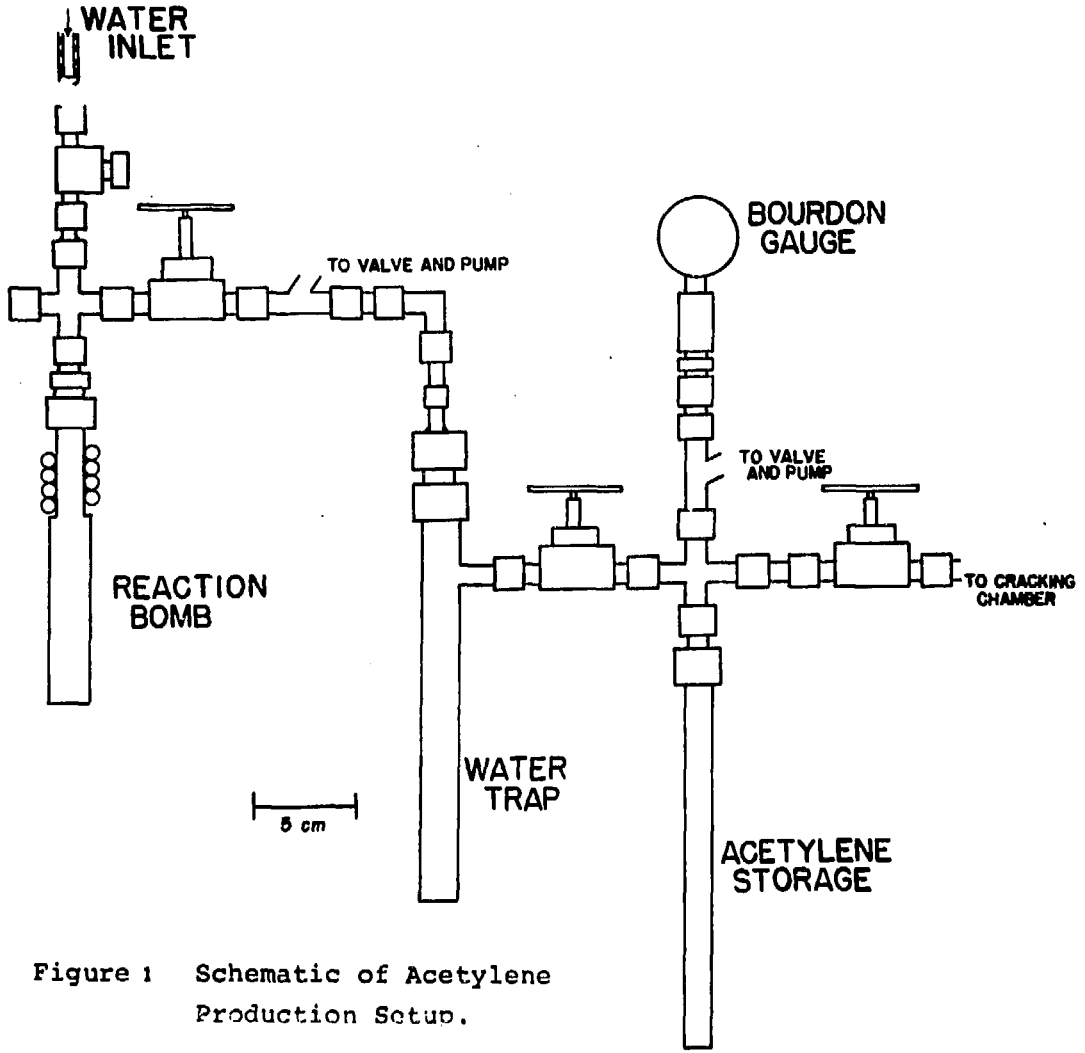

Figure 1 Schematic of Acetylene Production Setup.

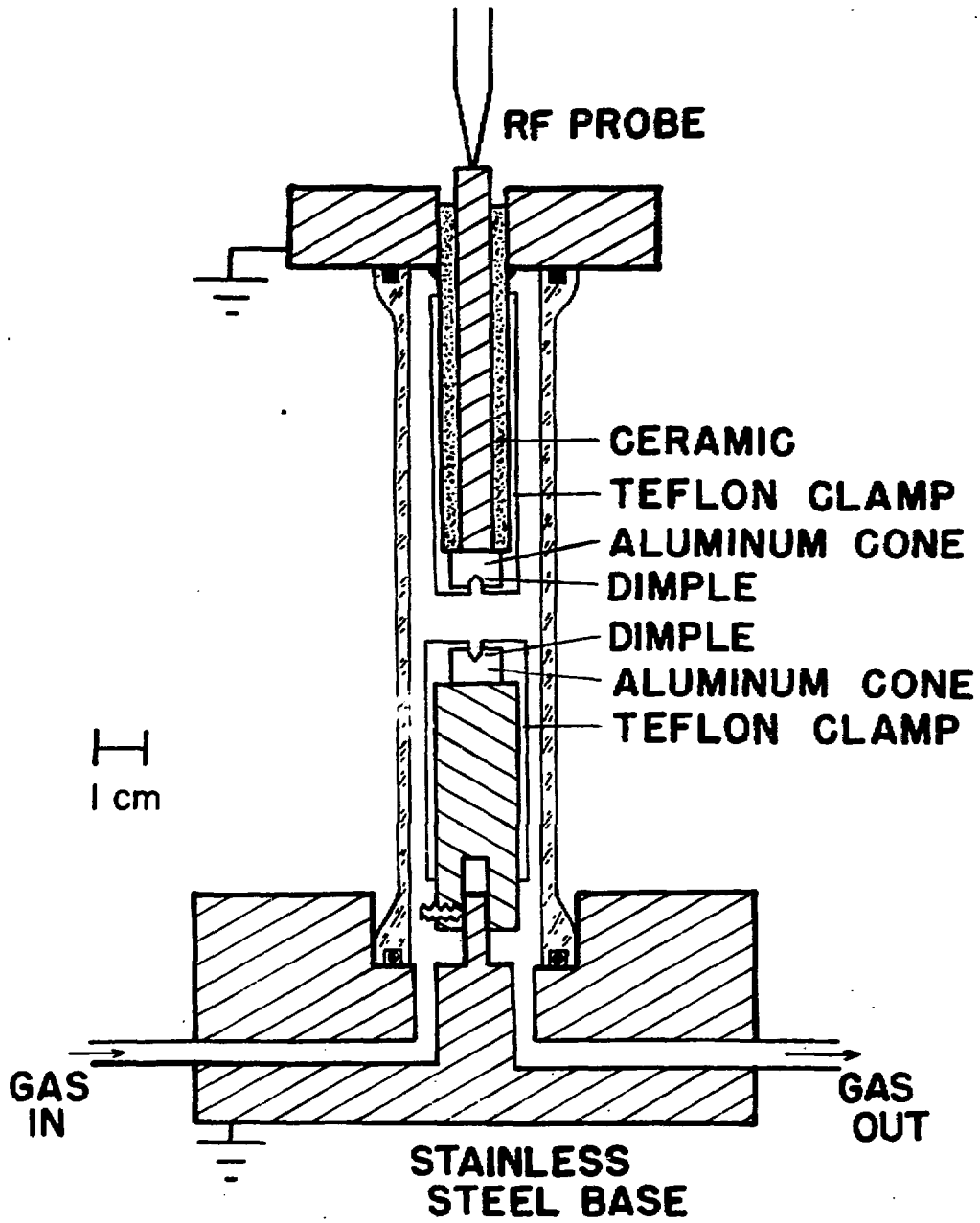

Figure 2 Radiofrequency Discharge with two Aluminum Cones (dimple).

Figure 3 Appearance of Cracked Carbon in an aluminum dimple (the spot size is about 1 mm across).

Figure 4. Current behaviour of two samples produced by R.F. cracking of acetylene as compared to a C + KBr mixture. The dotted sections represent the periods during which the caesium beam was moved around to improve the current output.

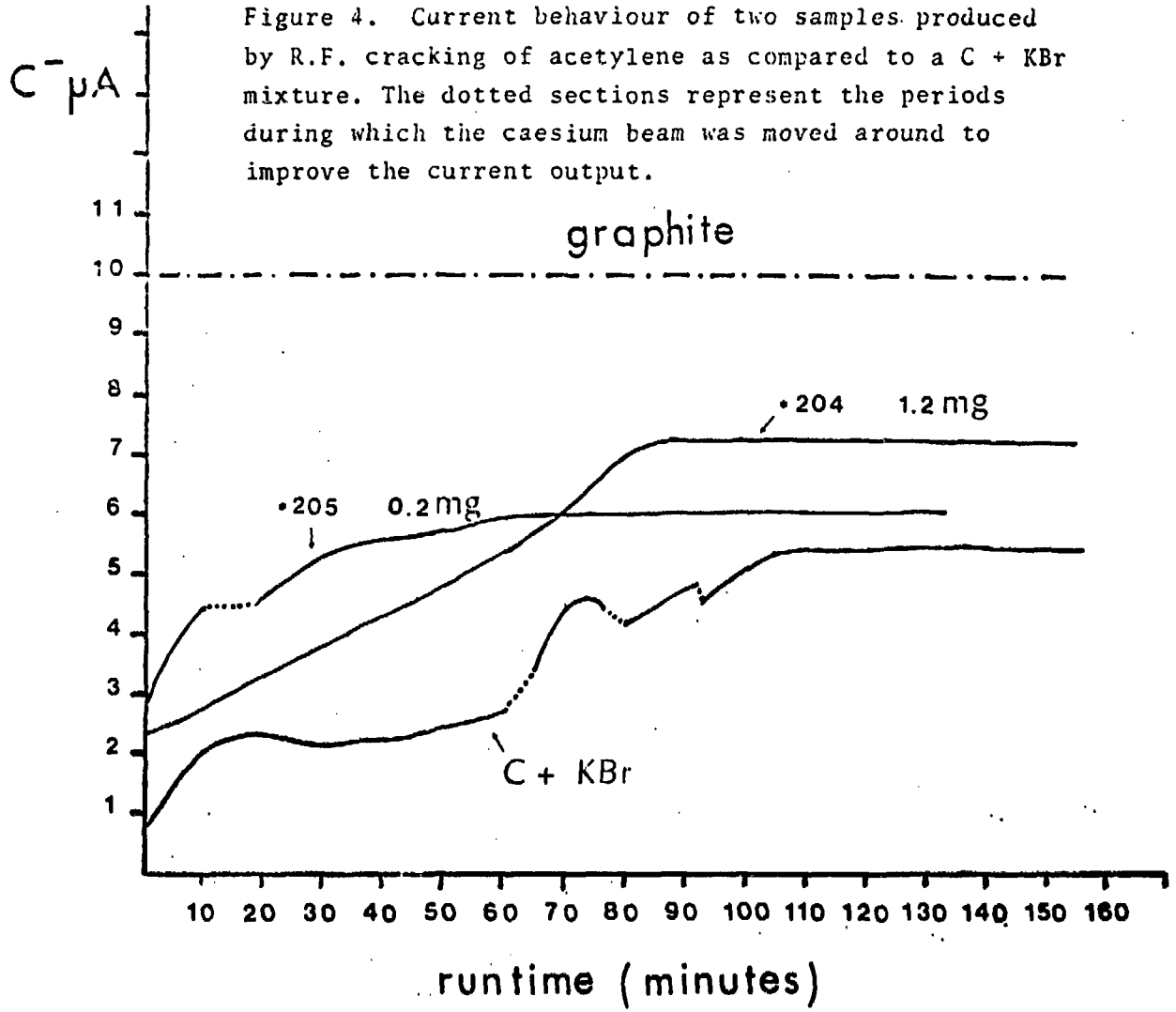

INSTABILITY OF KH_3^- AND POTENTIAL IMPLICATIONS FOR DETECTION OF ^{41}Ca WITH A TANDEM ELECTROSTATIC ACCELERATOR.

G.M. Raisbeck and F. Yiou
Laboratoire René Bernas, Centre de Spectrométrie Nucléaire et de Spectrométrie de Masse, Bât. 108, F. 91406 Orsay.

A. Peghaire, J. Guillot and J. Uzureau
Service de Physique Nucléaire et Neutronique, Centre d'Etudes de Bruyères-Le-Châtel, F. 91680 Bruyères-Le-Châtel.

Using a tandem Van de Graaff equipped with a moderately high resolution injector system ($M/\Delta M \sim 150$) we have investigated the stability of the negative hydride ions of potassium. We find that, using a Cs sputter source, and NH_3 gas appropriate for CaH_3^- emission, the ratio KH_3^-/K^- is $\leqslant 10^{-8}$ (and perhaps much less). These results are very favourable to the eventual detection of natural ^{41}Ca (half-life 10^5 years) using a tandem electrostatic accelerator.

Several years ago we pointed out the potential interest of ^{41}Ca as a radioactive dating isotope, and discussed its possible detection by accelerator mass spectrometry (1). We subsequently made measurements of this nuclide using the accelerator facility ALICE, and demonstrated that separation of the interfering isobar ^{41}K could be realized by analyzing completely stripped $^{41}Ca^{+20}$ (2). In Ref. (2), we also briefly mentioned an alternative method of eliminating ^{41}K, by accelerating a negative molecular ion of Ca which did not have a stable K analogue. We describe here an experiment to investigate such a possibility.

The most convenient method of producing Ca beams for tandem electrostatic accelerators is by spraying a Ca metal cone with NH_3 gas, thus forming the CaH^-, and CaH_3^- ions (3). It seemed therefore natural that the first investigations should be carried out on the stability of the K analogues of these ions.

The experiments were performed on the EN tandem Van de Graaff at Bruyères Le-Châtel. The principal advantage of this accelerator for the present work is a 90° injection magnet, which gives moderately good mass resolution ($M/\Delta M \sim 150$ under typical operating conditions). A schematic diagram of the experimental setup is given in Fig. 1. The injection magnet, which is equipped with a Hall probe, was first calibrated in the region of interest using peaks

of known mass. Then, using a Ca metal cone, the NH_3 gas flow was optimized to give maximum CaH_3^- emission, after which it was left constant. An example of the spectrum from the Ca cone is shown in Fig. 2. With the detectors and Au scattering foil in the "out" positions, the machine (with a terminal voltage of $\sim$ 5.7 MV) and beam lines were optimized to give a maximum $^{40}Ca^{+8}$ current in the Faraday cup at the reaction chamber. From this point on, all the high energy beam line parameters were left constant, and each change in beam was accompanied by an appropriate change in the terminal voltage, so as to give final ions of a constant magnetic rigidity.

A cone containing pressed KBr was then rotated into position and the injection magnet set for $^{39}K^-$. The $^{39}K^{+8}$ current was measured at the reaction chamber Faraday cup. The Au scattering foil was then inserted, and the movable ΔE(8μm) E (50μm) silicon diode detector telescope slowly rotated toward the beam. The Au scattering foil was used both to avoid a sudden and "catastrophic" increase of beam through the detectors, and also to allow comparison of beams having intensities too weak to measure with the Faraday cup, but too intense to measure with the detectors at zero degrees. By closing a pair of slits before the injection magnet, it was possible to measure the scattered K peak at any angle from 90 to 0°. The ΔE-E detector signals were recorded on a 256x256 channel display, and could be stored on magnetic disc for later analysis if necessary.

Once the ΔE-E coordinates corresponding to ^{39}K at various angles had been established, the injector magnet (and terminal voltage) was successively changed to the mass corresponding to $^{39}KH^-$, $^{39}KH_2^-$ and $^{39}KH_3^-$, and the count rate in the peak position determined (since the mass and velocity of the final ion was always the same, for a given angle, the ΔE-E signal in the detectors must remain fixed). For each case, both the injector magnet and terminal voltage were "scanned" in order to determine whether the observed signal was really peaked at the appropriate values. In between each run the beam from $^{39}K^-$ was also verified to check for any variation in source or transmission characteristics.

The results of the experiment were the following. The observed ratio of KH^-/K^- was $\sim 10^{-3}$. In several different experiments, this ratio varied, and probably is quite dependent on the source conditions. However, the count rate was maximum at the correct value for both injector mass and terminal voltage and there seems to be no doubt that KH^- does indeed exist. The upper limit of

KH_2^-/K^- was $\leq 10^{-5}$. We did not spend much time on this ion, since the corresponding CaH_2^- ion is much weaker than CaH^- or CaH_3^-. However, as pointed out by Ted Litherland at the meeting, a strong KH_2^- might have been significant, because of the potential interference of KHD^- for KH_3^- (although the natural abundance of deuterium is only $\sim 10^{-4}$). The upper limit for KH_3^-/K^- was $\leq 10^{-8}$. The events observed showed no indication of being a "peak", but rather from the tails of background peaks. This is supported by the fact that the count rate was not maximized at either the appropriate injection mass or terminal voltage. The source of the background, although not positively identified, is likely caused by injected $^{41}K^-$ or $^{41}KH^-$ which has charge exchanged in the tandem to give the correct magnetic rigidity to arrive at the detector. An electrostatic analyzer or Wien filter could of course be used to remove such events and thus lower the upper limit for KH_3^-. However, even the limit observed here seems sufficiently low to permit accelerator detection of ^{41}Ca if we take into account the following factors. i) The isotopic abundance of ^{41}K is 6.7%, ii) Using chemical procedures, it should be relatively straightforward to reduce K levels in Ca samples to $\sim 10^{-6}$, iii) It is not necessary to completely eliminate ^{41}K, but simply reduce its intensity to perhaps less than 10^3 times the ^{41}Ca. Using the above factors, one can see that ^{41}K interference should not constitute a significant problem down to $^{41}Ca/Ca$ concentrations of $\sim 10^{-18}$. This is several orders of magnitude lower than expected "natural" concentrations (1). Thus, we feel that the present results show considerable promise for the eventual detection of ^{41}Ca by means of electrostatic accelerators.

References

1 - G.M. Raisbeck and F. Yiou, Nature, 277, 42 (1979).

2 - G.M. Raisbeck and F. Yiou, Proceedings of 20th Int. Symposium for Archaeometry, Paris 1980, Revue d'Archéométrie N°4, P. 121.

3 - R. Middleton, Nucl. Inst. Meth., 144, 373 (1977).

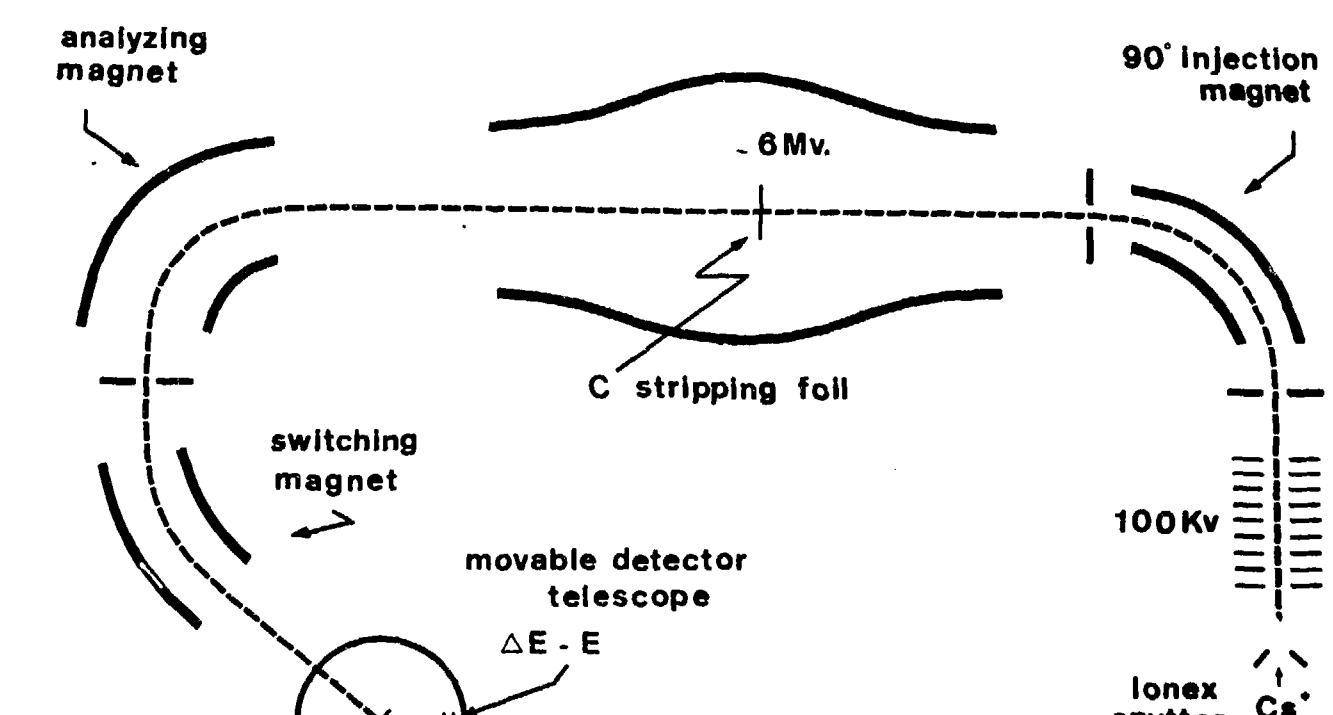

Fig. 1 - Schematic diagram of the EN tandem at Bruyères-le-Châtel.

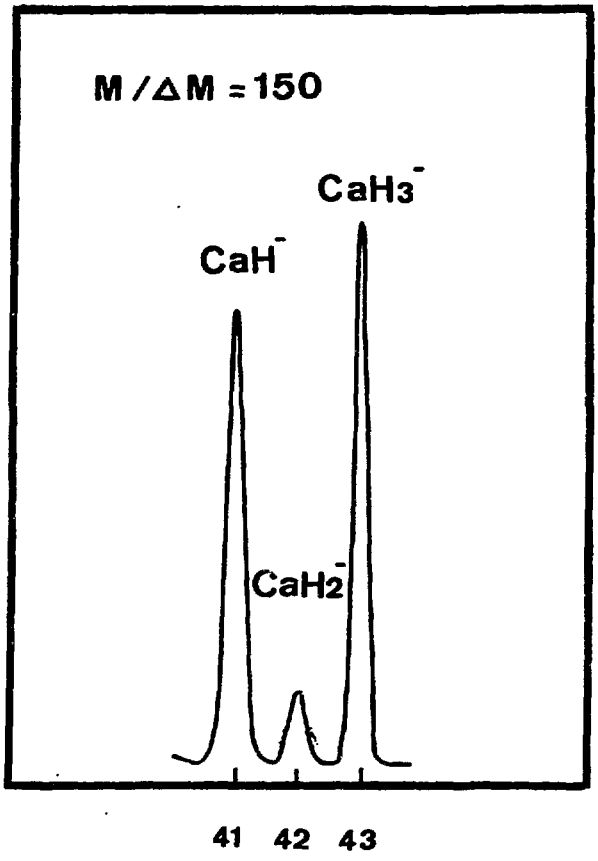

Fig. 2 - Mass spectrum from Ca metal cone with NH_3 gas.

A PRELIMINARY DESCRIPTION OF A DEDICATED COMMERCIAL ULTRA-SENSITIVE MASS SPECTROMETER FOR DIRECT ATOM COUNTING OF ^{14}C

K.H. Purser, R.J. Schneider, J.McG. Dobbs, R. Post
General Ionex Corporation
Newburyport, Mass. 01950

ABSTRACT

A description is presented of a commercial, tandem-accelerator centered secondary ion double mass spectrometer dedicated to $^{14}C/^{13}C/^{12}C$ ratio measurements. Some design philosophy of the instrument is presented and the performance is described. A scanning cesium ion source with primary beam diameters between 100-200 micrometers is used to produce C^- beam intensities of 10-20μA with the intensities remaining constant to better than 0.1% per minute after the source stabilizes. For recent carbon, these currents correspond to ^{14}C count rates from the ion source of 60-120 particles per second. Resolution of the first mass defining system, $M/\Delta M$, is greater than 120 with the capability of rapid mass switching between isotopes. The measured isotopic ratios at the ion source for carbon are constant to better than 0.25%. The virtues of the 3MV parallel-fed Cockroft-Walton accelerator supply are presented. At the operating voltage of 2.5MV, the stability is better than 1:4000 with a terminal ripple <200 volts. The desirable features of the second mass spectrometer which follows the accelerator are discussed. The measured beam width at the defining slits following the electrostatic analyzer is less than 1.4mm. At this same point, the dominant background $^{13}C^{3+}$ and $^{12}C^{3+}$ ions which originate from mass-14 molecular ions are measured to be 3.6mm away from the beam axis and so can be completely eliminated by the slits. Isotopic ratios have been measured beyond these slits, and it is shown that these ratios are constant to better than half a percent using recent samples. The final strong focusing magnet has a rejection ratio for unwanted carbon ions greater than 10^7. Finally, the operation of the detector is presented and a spectrum of ^{14}C atoms is shown. Measurements indicate that for recent samples a statistical precision better than 1%, limited only by counting statistics, can be achieved in a half hour period; it is anticipated that in the near future, a precison of 0.2% will be obtainable by counting for a ten hour period.

INTRODUCTION

Widespread interest has developed during the last few years in a secondary ion mass spectrometry technique which has the potential of permitting measurement levels close to single atom concentrations.[1-3] In this technique, nuclear physics detection methods are used in conjunction with a rather low voltage 2-3MV d.c. tandem accelerator which couples a double mass spectrometer to allow the detection of specific atoms at mass abundance sensitivity below $1:10^{15}$.

Compared to conventional mass spectrometery, the features of this new high energy technique include:

1. The elimination of the molecular interferences which frequently represent the ultimate sensitivity limit for conventional mass spectrometers.
2. A dramatic reduction of scattered ions into the final detector from the walls and the residual gas molecules.
3. The elimination of spurious counts in the final particle detector by overdetermining the kinematic parameters of each particle as it slows down.
4. Element identification of isobaric components up to Z=20 by the use of nuclear detection techniques.

Using these procedures, individual atoms from many parts of the periodic table have been identified with high efficiency and at concentrations as low as $1:10^{15}$ using little pre-chemistry.[3]

This paper describes an ultra-sensitive detection system developed by General Ionex Corporation. Four nearly identical instruments are being built for the Universities of Arizona (U.S.A.), Toronto (Canada), Nagoya (Japan), and the C.E.A. (France) with the first being delivered in June, 1981. While each of these systems is a versatile ultra-sensitive mass spectrometer capable of measuring a wide variety of stable and radioactive isotopic ratios, all of these instruments will be used at times for carbon-12-13-14 isotopic ratio dating and the problems of such measurements represent the form of the present document.

The direct counting of ^{14}C by classical mass spectrometry techniques is made difficult by the presence of large numbers of molecules such as $^{12}CH_2$ and ^{13}CH which have nearly the same mass as ^{14}C. Elimination of these molecular interferences on the basis of their small difference in mass from ^{14}C is not practical because, in contrast to conventional mass spectrometers, high resolution and tight collimation cannot be used to eliminate analyzer aberrations. At the $1:10^{15}$ level, each microampere of background is only accompanied by 0.4 wanted ions per minute. For adequate statistical accuracy in a reasonable counting period, the acceptance phase space must be large and high background currents must be accepted by the instrument.[4]

In contrast, accelerator-centered mass spectrometry eliminates molecular ions such as $^{12}CH_2$ and ^{13}CH by 100% dissociation in high velocity collisions with gas atoms such as argon. For the dissociation to be complete, at least three electrons must be removed from the neutral molecule. This requires a kinetic energy of about 2.6MeV. At this energy, 50% of the atoms become C^{3+} and no mass-14 molecules are left to interfere with the $^{14}C^{3+}$ ions.

In precision age determination, a measurement of the $^{12}C/^{13}C/^{14}C$ ratios must be compared to the same ratios for a standard such as 1850 wood. The subsidiary $^{13}C/^{12}C$ ratio is needed to correct for any isotopic

fractionation effects in the sample which occurred during formation or during the measurement phase. In this respect, fractionation due to the ion source and other parts of the accelerator is as much a problem in ultra-sensitive mass spectrometry as it is in conventional mass spectrometry. With the added complexity of the accelerator, there are other machine fractionation contributions which are not present in conventional mass spectrometry. For example, the electron stripping cross sections at the terminal of the accelerator are velocity dependent. Consequently, because the ions are stripped of electrons at constant energy rather than at constant velocity, the effect may not be the same for all isotopes. Figure 1 shows how this effect is avoided in the present design; at a negative ion energy of about 2.6MeV the correction is zero for the primary $^{14}C/^{12}C$ ratio with a small but finite (<2%) correction for an accurate value of the subsidiary $^{13}C/^{12}C$ ratio. Fractionation can be readily accounted for by comparing the ratios for each sample with an appropriate standard which is substituted into the source in an identical geometry to that of the sample.

Another issue that must be addressed in a precision instrument (<0.5%) is the feature of "flat-topping" the instrument transmission function. The concept of flat-topping, shown in Figure 2, is basically that the transmission function is insensitive over a small range to all instrument variables. For example:

1. Each parameter should operate about a flat transmission maximum rather than on the shoulder of a rapidly changing transmission curve.

2. Small shifts in sample location, alignment, etc., should have no effect on the source emittance and on the effective object point for the whole mass spectrometer system.

3. Defining apertures should be substantially larger than the natural width of the beam including the width contributed by power supply fluctuation.

4. The lens effects and the optical transmission of the accelerator section should be independent of small fluctuations of terminal voltage and accelerating tube field gradients.

APPARATUS DESCRIPTION

The instrument, shown schematically in Figure 3, divides itself naturally into four sections:

1. An ion preparation section where sequential bursts of $^{12}C^-$, $^{13}C^-$, $^{14}C^-$ ions, free of unwanted mass contaminants, are prepared in the form of ion beams of equal emittance.

2. A tandem accelerator region where the ions are accelerated to an energy of ∿10MeV and the molecular components $^{13}CH^-$ and $^{12}CH_2^-$ dissociated.

3. An electric and magnetic deflection stage where almost all of the unwanted particles are eliminated.

4. An ion chamber detector in which the final selection of events is made on the basis of mass, atomic number, and charge state.

The Ion Preparation Section

The ion source, which has been designed specifically for this new instrument, is shown schematically in Figure 4. The sample is inserted as one of several samples and standards at the anode of a cesium sputter source. A 30keV focused cesium ion beam of intensity ∿200μA, impinges at 45° on the surface of the sample, sputters the surface and produces negative ions, both molecular and atomic.

To generate the Cs^+ ions, a reservoir containing liquid cesium is heated to approximately 225°C. This causes cesium vapor to migrate along a heated feed tube to the rear of a porous tungsten plug, maintained at 1100°C, produced by etching a sintered tungsten-copper mixture. The cesium vapor diffuses through the plug and is ionized at the front surface with up to 99% efficiency. The resulting ions are then accelerated to an energy of 10keV, focused by a 4-sectored einzel lens and accelerated through a further 20kV onto the surface of the sample. The conceptual

simplicity and the stable operation of the Cs^+ ion gun[5] leads to very stable operation of the present ultra-sensitive mass spectrometer.

An important feature of the new source is the capability of measuring very small samples (<1mg). To do this conveniently, the Cs^+ beam can be focused to a diameter below 200 micrometers at the sample and be moved in both lateral directions to explore the surface and to maximize yield. Typically, a sputtered graphite sample which has been bombarded for several hours by the focused Cs^+ beam shows a cratered region with a FWHM diameter ∿100 micrometers.

The incident cesium ions not only sputter carbon atoms from the surface but also introduce a monolayer coating which acts as an electron donor for negative ion formation. For carbon, the efficiency of negative ion production is high; approximately 8-10% of the sputtered carbon atoms from a graphite sample is converted into C^- ions[6]. Under normal operation, the source consumes graphite at the rate of about 100μg/hour with a C^- yield of 10-20μA. For an 1850 graphite sample, this corresponds to a yield at the ion source of 60-120 $^{14}C^-$ ions/second.

An important feature of a mass spectrometry source is high stability, both in position and intensity. A feature leading to good stability in the present source is that the power supply for primary Cs^+ acceleration is completely independent of the power supply used for the secondary negative ions. Thus, minor fluctuations due to electron loading of the cesium gun are completely separated from the critical acceleration power supply. Figure 5 shows the stability of C^- current from the source. Measurements also show that the source output has no detectable high frequency oscillations or noise.

A vacuum-lock permits rapid sample change without breaking the main source vacuum or without shutting down the cesium gun. Individual samples are isolated to prevent sputtered cross-contamination from sample to sample and from sample to source. If necessary, metal O-rings can be substituted for the existing elastomer seals making possible an

occasional baking to eliminate contamination from adsorbed carbon monoxide.

For good reproducibility, a standard sample preparation technique is essential. Considerable work has been done at both Oxford[7] and Toronto[8] on the conversion of small carbon samples into graphite-like materials which efficiently produce negative ions. The University of Toronto workers have concentrated on the dissociation of acetylene (C_2H_2) into a graphite-like material. Acetylene can be produced by converting carbonaceous material into lithium carbide (Li_2C_2) which is subsequently reacted with pure water to produce C_2H_2 and lithium oxide. This part of the conversion process has a conversion efficiency greater than 95% and has been used extensively in the production of benzene for radiocarbon dating. The acetylene is finally converted into a graphite-like substance by electrical dissociation.

An alternative technique has been explored at Oxford University.[7] Here, ethylene is cracked onto a heated tantalum filament to produce a tough graphite coating which in minutes produces large C^- currents.

A high-speed turbomolecular pump is employed near the source to maintain a pressure $<10^{-6}$ torr during cesium bombardment. Cryogenic vacuum pumps operating at temperatures of about 14-18K provide the remainder of the vacuum pumping.

After formation into a useful beam, the C^- ions leaving the sample are focused to the object plane of high resolution 90° directionally double-focusing magnetic mass analyzer. This analyzer has a radius of curvature of 35cm and a maximum Mass·Energy product of 10 AMU·MeV. The magnetic field of this analyzer is tailored to allow beams of large angular spread to be accepted while still maintaining low aberration coefficients. For some systems, this tailoring is achieved by adding curvature to the exit and entrance double-focusing shims together with quadrupole components at the 45° symmetry plane. Figure 6 is a plot of the mass spectrum for the Arizona mass analyzer around mass-14. The contribution from the

adjacent masses $^{13}C^-$ and $^{14}NH^-$ is virtually zero.

As mentioned earlier, constancy of ion source output and constant transmission efficiency is vital for precision isotopic ratio measurements. Because the ratios $^{14}C/^{12}C$ and $^{13}C/^{12}C$ are the only quantities needed for an age determination, the effects of small changes in source efficiency and system transmission can be factored from the measurement by frequently normalizing the transmission of the system with $^{12}C^-$ and $^{13}C^-$ beams. To do this, the three carbon masses are accelerated sequentially through the whole system in a controlled time-sequence as shown in Figure 7.

A feature of the optics of the first magnetic mass analyzer is that the vacuum chamber within the magnetic field is insulated to allow it to be elevated from ground potential by several thousand volts. This design allows the energy of the particles within the magnetic field to be varied and different masses selected electrostatically. At constant magnetic field, the Mass·Energy product for a magnetic analyzer remains constant (see eqn. 1). Thus, increasing the ion energy causes lower masses to be deflected through identical trajectories.

$$M \cdot E = B^2 \rho^2 q^2 / 2 \quad \ldots\ldots\ldots\ldots\ldots\ldots\ldots\ldots (1)$$

(here M is the mass of an ion having energy, E. B, is the fixed d.c. magnetic field; ρ, the radius of curvature; q, the charge)

A simple voltage variation on the magnet vacuum box causes the analyzer to select different masses. Table I shows the voltages needed for mass selection of 20keV carbon isotopes.

TABLE I

MASS	VOLTAGE INCREMENT
12 AMU	3.33kV
13 AMU	1.54kV
14 AMU	0.00kV

The location of the accelerating gaps producing these changes in particle energy is close to the object and image beam waists. In this manner, the optical effects on the beam emittance is kept close to zero. Figure 8 shows a typical series of negative ion current ratio measurements made using a Faraday cup located beyond the defining aperture of the first mass analyzer when the system is switched repeatedly between $^{12}C^-$ and $^{13}C^-$.

The 3 Megavolt Tandem Accelerator Section

The 3 Megavolt accelerator power supply consists of a parallel-fed voltage multiplier consisting of a series of high voltage rectifiers energized by the 30kHz voltage coupled through the inherent capacity between a series of capacitor coupling rings and an r.f. driven grounded electrode. Figure 9 is a schematic of the circuit.

The 3MV power supply for the present instruments has just entered the final voltage test phase and has recently demonstrated operation at the full voltage of 3MV. It is capable of producing currents of several mA, an essential characteristic for making precision isotopic ratio measurements. High current capability allows the various machine voltages and gradients to remain stable throughout the complete mass spectrometer cycle of $^{12}C^-$, $^{13}C^-$, $^{14}C^-$ injection. During a single cycle, changes in injected currents $>10^{13}$:1 can occur. Voltage stability is achieved by draining large currents down the gradient control resistor chains. At

the low energy end of the accelerator, where the C^- ions are most susceptible to gradient fluctuations, the resistor grading currents exceed 300 microamperes; along the high-energy tubes, the resistor currents are approximately 200 microamperes at 3MV. These currents are approximately an order of magnitude greater than used in conventional accelerators.

The magnitude of the capacitively coupled 30kHz terminal ripple can be inferred by intercepting a portion of a stable d.c. beam on one of the slits which follow the 15^o electrostatic deflector and measuring the induced 30kHz beam intensity fluctuations. Such measurements indicated that 30kHz terminal fluctuations are less than 200 volts peak to peak.

A precision generating voltmeter, having a flat frequency response between d.c. and 200Hz, monitors and controls the terminal voltage.[12] During carbon-14 measurements this voltmeter serves the following functions:

1. To provide a stable feedback signal for the 3MV Power Supply independent of any tube loading. The measured stability is better than 1:4000 (less than 1kV terminal fluctuations).

2. To provide a gating signal to the data collection system so that if, for any reason, the terminal voltage moves more than $\pm$3kV from its assigned value, the data acquisition moves into a "halt" mode.

The reasons for such stringent voltage control is to ensure that at all times the transmission function remains "flat-topped". Also, to ensure that the $^{12}C^{3+}$ and $^{13}C^{3+}$ beam components inevitably present because of the mass-14 molecular species $^{12}CH_2^-$ and $^{13}CH_2^-$, are not unintentionally injected into the final detector section.

At 2.5MV terminal voltage these background molecular ions undergo the following acceleration sequence:

Stage (1) ... $^{13}CH^- \rightarrow {}^{13}CH^-$ (acceleration to 2.5MeV)
Stage (2) ... $^{13}CH^- \rightarrow {}^{13}C^{3+}+H$ (stripping; carbon energy 2.312MeV)
Stage (3) ... $^{13}C^{3+} \rightarrow {}^{13}C^{3+}$ (final acceleration to 9.812MeV)

These 3+ background ions are lower in energy by 188keV than the wanted $^{14}C^{3+}$ ions and intercept the slits which follow the electrostatic deflector stage. At this point, the physical width of the ^{14}C beam has been measured to be 1.4mm. The unwanted $^{13}C^{3+}$ particles arrive 3.6mm from the center of the defining slits at this point, reducing the molecular derived $^{13}C^{3+}$ and $^{12}C^{3+}$ ions to unmeasurable levels beyond the slits.

Because of the need for mass independent transmission, it is desireable that the acceleration tube structure be wholly electrostatic and have constant lens properties at both entrance and exit. To avoid fractionation, the lens strengths must be independent of any changes in beam current loading which may occur as the mass spectrometer is switched from $^{12}C^-$ to $^{14}C^-$. During the $^{12}C^-$ phase of each measuring cycle, 10-20 microamperes of $^{12}C^-$ are injected into the accelerator section for a fraction of a second. After settling the introduction of such current bursts causes terminal voltage changes less than 0.5kV.

If the electric field gradient is not constant along the length of the acceleration tube, additional lens effects are present. Upsets in gradient control along the acceleration tubes is minimized by electrostatic suppression of secondary electrons and other particles by the use of a spirally suppressed inclined-field tube design[13]. Furthermore, divider resistor currents are used about ten times greater than those drained along the grading resistors of classical tandem accelerators.

Finally, the flat-topped transmission function for the accelerator is produced by stripping the negative ions using argon gas rather than foils and by the use of a large diameter non-defining stripping canal. Figure 10 shows the ion beam envelope throughout the whole machine. It can be seen that at the terminal the diameter of the beam fills less than half the available diameter of the stripping canal.

The High Energy Mass Spectrometer Stage

The characteristics of conventional mass spectroscopy, which identifies particles by deflection through various combinations of electric and magnetic fields, are summarized as follows:

Magnetic Deflection

The magnetic rigidity of a particle ($B\rho$) is given by:

$$B^2\rho^2 \propto \frac{ME}{q^2}$$

Electrostatics

The electric rigidity of a particle ($E.\rho$) is given by:

$$\vec{E}.\rho \propto \frac{E}{q}$$

Velocity Selector (crossed electric and magnetic fields)

The velocity of a particle (V) is given by:

$$V^2 \propto \frac{E}{M} = \frac{E}{q} / \frac{M}{q}$$

(Here M is the particle mass, E the kinetic energy and q the charge)

These constraints only involve the two variables $\frac{E}{q}$, $\frac{M}{q}$. The effects of these field arrangements for $^{14}C^{3+}$, $^{13}C^{3+}$, $^{12}C^{3+}$ measurements can be seen in Figure 11, where transmission functions are plotted against the two variables $\frac{E}{q}$, $\frac{M}{q}$. The usefulness of such a diagram[14] is that loci can be drawn which represent the constraints imposed on individual particles by various static combinations of electric and magnetic fields. These include:

1. A hyperbolic band, representing magnetic selection, satisfying $\frac{ME}{q^2}$ = constant. Such a band specifies all combinations of the ion variables of Mass, Energy, and Charge which can pass through the defining slits of a particular system at fixed field.

2. A vertical band, representing electrostatic deflection through a selected value of $\frac{E}{q}$ = constant.

3. A straight band through the origin, which represents particles of constant velocity, V.

The kinematic constraints from different elements are imposed independently so that in a multiple element system the effects are superimposed to define a unique point in the $(\frac{M}{q}, \frac{E}{q})$ plane. This point specifies which particle species will be transmitted in the absence of gas or wall scattering.

It can be seen from Figure 11 that because masses of ^{12}C and ^{13}C are less than that of ^{14}C the ideal arrangement for minimizing background is an electrostatic or velocity filter followed by a magnetic element. $^{12}C^{3+}$ and $^{13}C^{3+}$ ions require a higher energy than $^{14}C^{3+}$ to satisfy the magnetic field constraints. After passing through the electrostatic filter, which specifies a given energy, there is no way that these background ions can gain this additional energy. In contrast, if a magnetic constraint precedes an electrostatic filter or velocity filter, a single wall scatterming can lower the ion energy sufficiently to efficiently transmit the particle through the succeeding element.

An additional feature of the present design is that by using an electrostatic quadrupole and an electrostatic deflector immediately following tandem acceleration, the operation of the mass spectrometer system is completely mass independent from the exit of the 90° inflection magnet to beyond the defining slits which follow the electrostatic deflector. Thus, the accelerator mass spectrometer system can be used for precision isotopic ratio measurements using current into a precision Faraday cup located after the final defining slits. Figure 12 shows the constancy of isotopic ratios measured for a carbon sample following the 15° electrostatic deflector.

The lens/deflector combination has a measured resolution $E/\Delta E \approx 150$. This is adequate to remove the fragmented ^{12}C and ^{13}C ions arising from the mass-14 beams $^{12}CH_2^-$ and $^{13}CH^-$ and ^{14}N from the mass-15 component $^{14}NH^-$.

During the ^{14}C detection phase of the measurement cycle, the precision Faraday cup is withdrawn and the particles which pass through the defining slits following the electrostatic analyzer are momentum analyzed by a strong focusing, 14^{o} sector magnetic spectrometer having a radius of curvature of 0.6 meters and a maximum ME/Z^2 rating of 27MeV.AMU. When the cup is withdrawn, a variety of unwanted particles pass through the defining slits. It is found that this spectrum is dominated by pairs of ^{12}C, ^{13}C peaks. Each pair of peaks arises from a specific charge state of the molecular fragments. Clearly, great care must be taken to avoid scattering into the deflector from the walls or from gas molecules. To minimize scattering, a series of baffles and anti-scatter slits are carefully distributed along this last section of the spectrometer system. With these baffles, very high rejection ratios are possible for unwanted particles. As an example, when 12 electrical nanoamperes of ^{13}C are injected through the defining slits into the final stage, the counting rate in the final detector is less than 1500/sec. Thus, this magnetic stage, alone, has a rejection capability in excess of 10^7, a number comparable to the very best low energy mass spectrometers.

Final Detector

The heavy ion detector and identifier is a gas-filled ion chamber having many features similar to that of the Rochester Heavy Ion Detector.[15] The detector includes an energy stage, two dE/dX stages with transverse collection, and a final range stage with longitudinal collection.

A schematic diagram of the detector and its associated electronics is shown in Figure 13. The active length of the detector is 500 millimeters. The entrance aperture is limited to a diameter of 5 millimeters and is covered by a gas-tight 1.5 micrometer mylar foil.

The operation of the detector during ^{14}C detection is shown in Figure 14. It can be seen that the only ions which enter the detector are ^{14}C and

^{14}N. Measurements on activated graphite indicate that for recent samples a statistical precision better than 1% can be achieved in a half-hour period, with the precision being only limited by counting statistics. We anticipate that, in the near future, precisions of 0.2% will be obtained in a 10 hour period. Also, that using a carbon sample older than 60,000 years, the measured background $^{14}C/^{12}C$ ratio will be less than 0.07% of modern.

No measurements have been made yet with the instrument for such other radioisotopes as ^{10}Be, ^{26}Al, and ^{36}Cl. It is expected, however, that the system will be capable of measuring these isotopes at sensitivities close to one part in 10^{15}. For ^{36}Cl, this is two orders of magnitude more sensitivity than is necessary for ground water aging.

REFERENCES

1. K.H. Purser, A.E. Litherland, and H.E. Gove; Nucl. Instr. and Meth. 162 (1979) 637-656.

2. K.H. Purser, A.E. Litherland, and J.C. Rucklidge; Surface Interface Anal. 1 (1979) 12-19.

3. A.E. Litherland; Ann. Rev. Nucl. Part. Sci. 30, (1980), 437-473.

4. K.H. Purser, P. Williams, A.E. Litherland, J.D. Stein, H.A. Storms, H.E. Gove, and C.M. Stevens; Nucl. Instr. & Methods (July, 1981).

5. R. Middleton; Nucl. Instr. & Methods 122, (1974), 35.

6. K. Brand; Nucl. Instr. & Methods 141, (1977) 519-520.

7. N. White (personal communication).

8. R.P. Beukens (personal communication).

9. K.H. Purser, R.B. Liebert, C.J. Russo; Radiocarbon 22, (1980), 794-806.

10. K.H. Purser, P.R. Hanley; Proc. First Conference on Radiocarbon Dating. ed. H.E. Gove (University of Rochester, NY, 1978).

11. M.R. Cleland (1959) U.S. Patent 2,875,394.

12. H. Fauska (personal communication).

13. K.H. Purser, H.E. Gove, T.S. Lund, and H.R.McK. Hyder; Nucl. Instr. & Meth. 122, (1974) 159-177.

14. Enge, H.A. et al,; Nucl. Instr. & Methods 97, (1971), 449.

15. Shapira, D. et al.; Nucl. Instr. & Methods 129, (1975), 123-130.

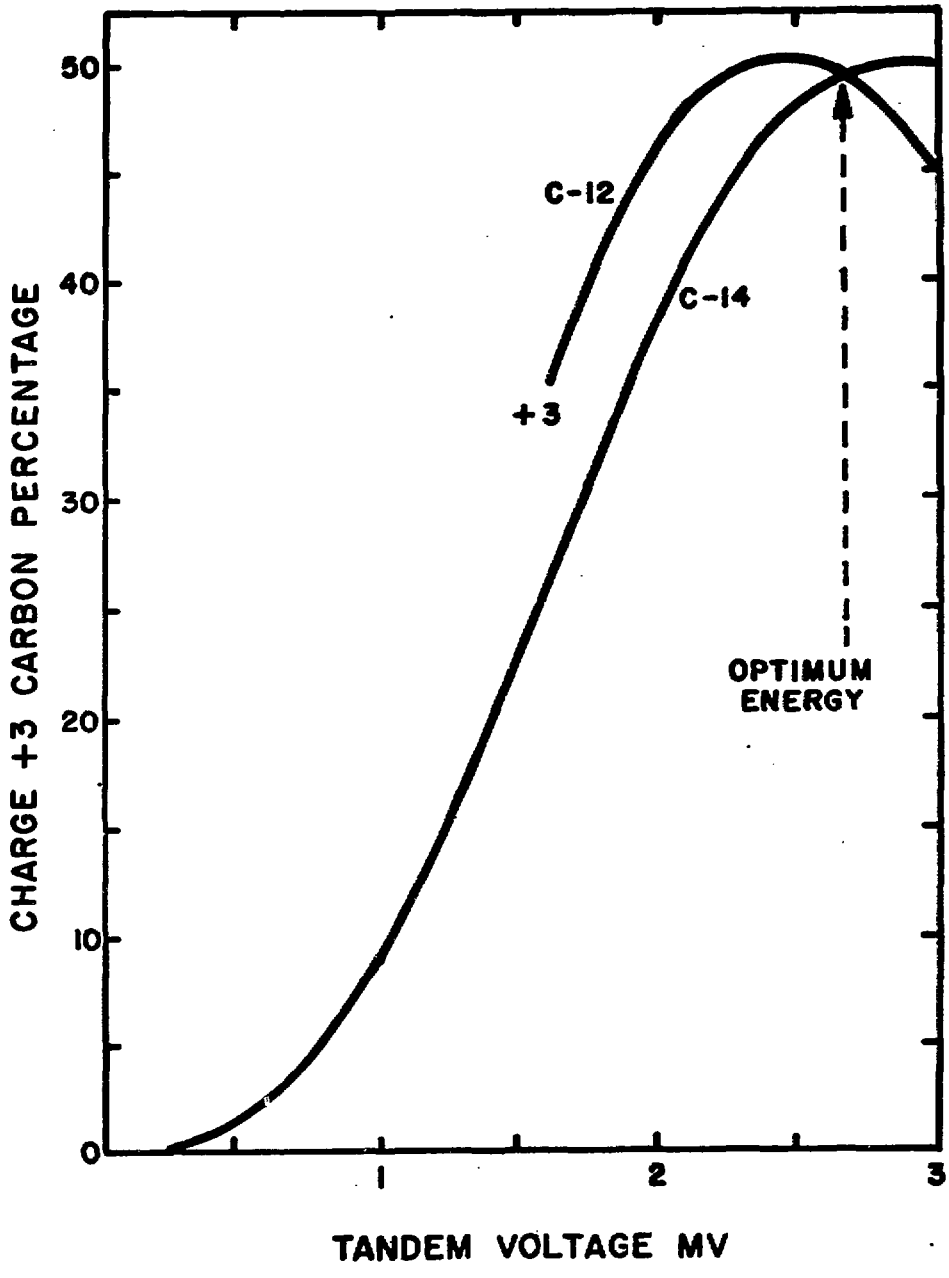

Figure 1 - Charge Exchange Efficiency as a Function of Energy

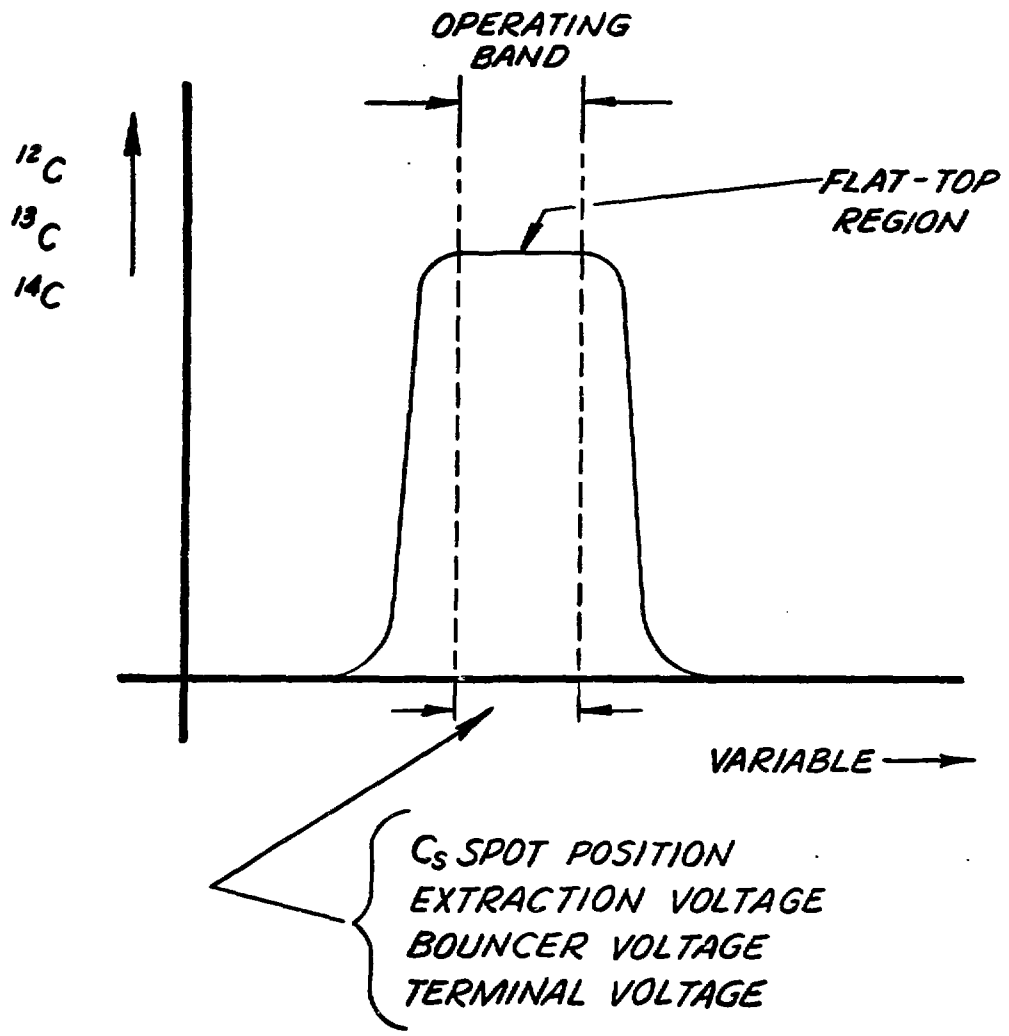

Figure 2 - The Concept of Flat-topping

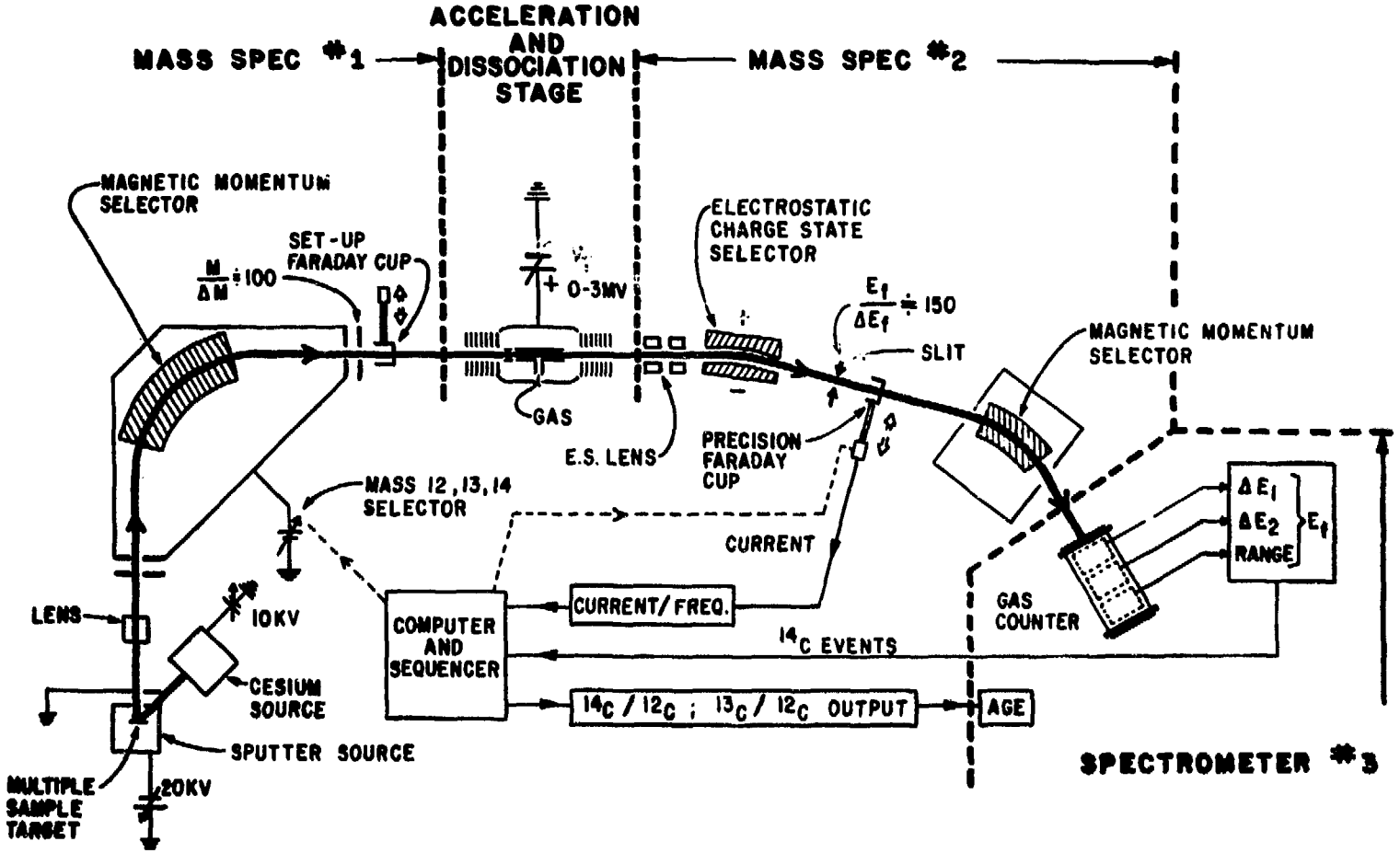

ULTRASENSITIVE SPECTROMETER SYSTEM

Figure 3

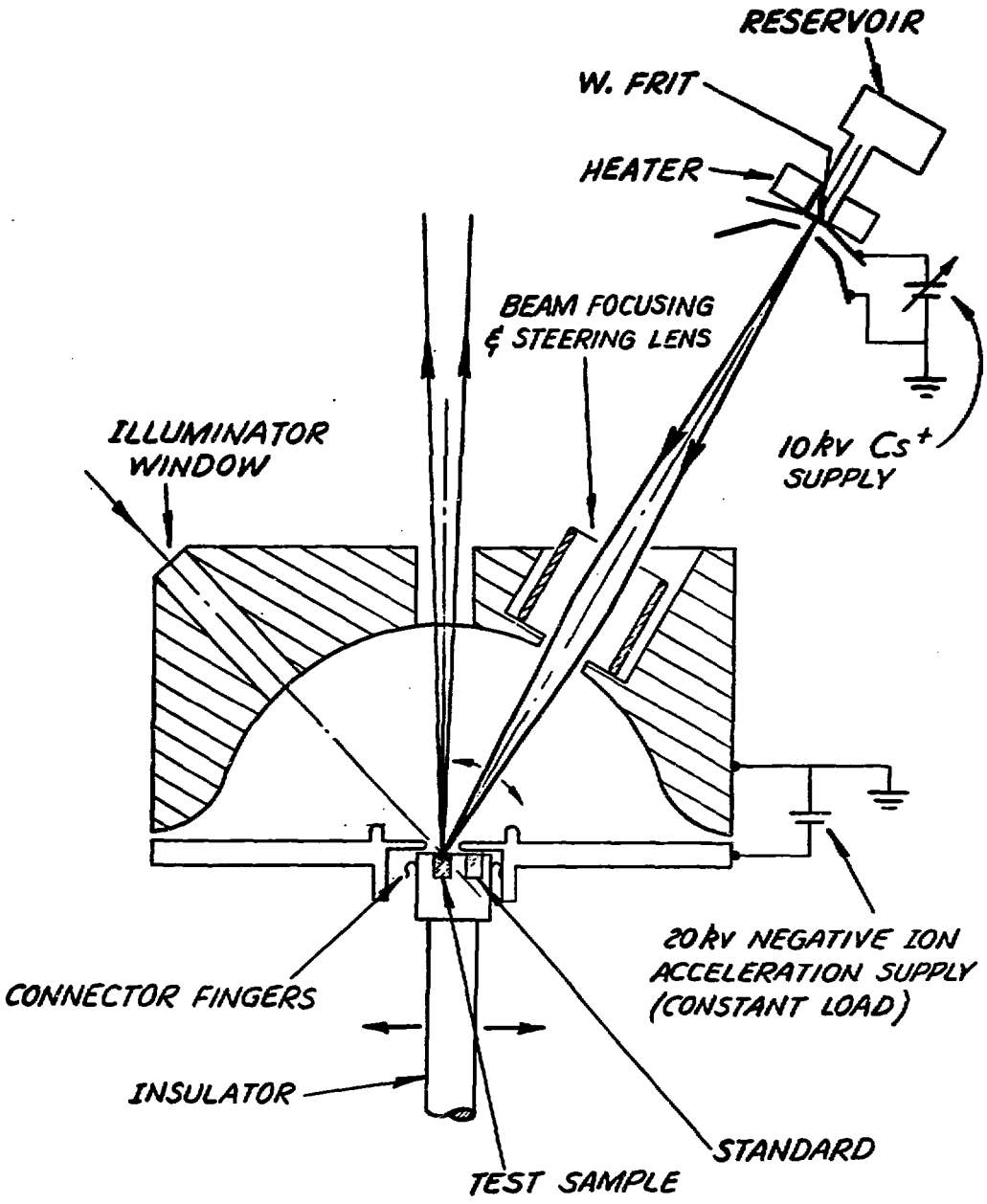

Figure 4 - The New SIMS Ion Source

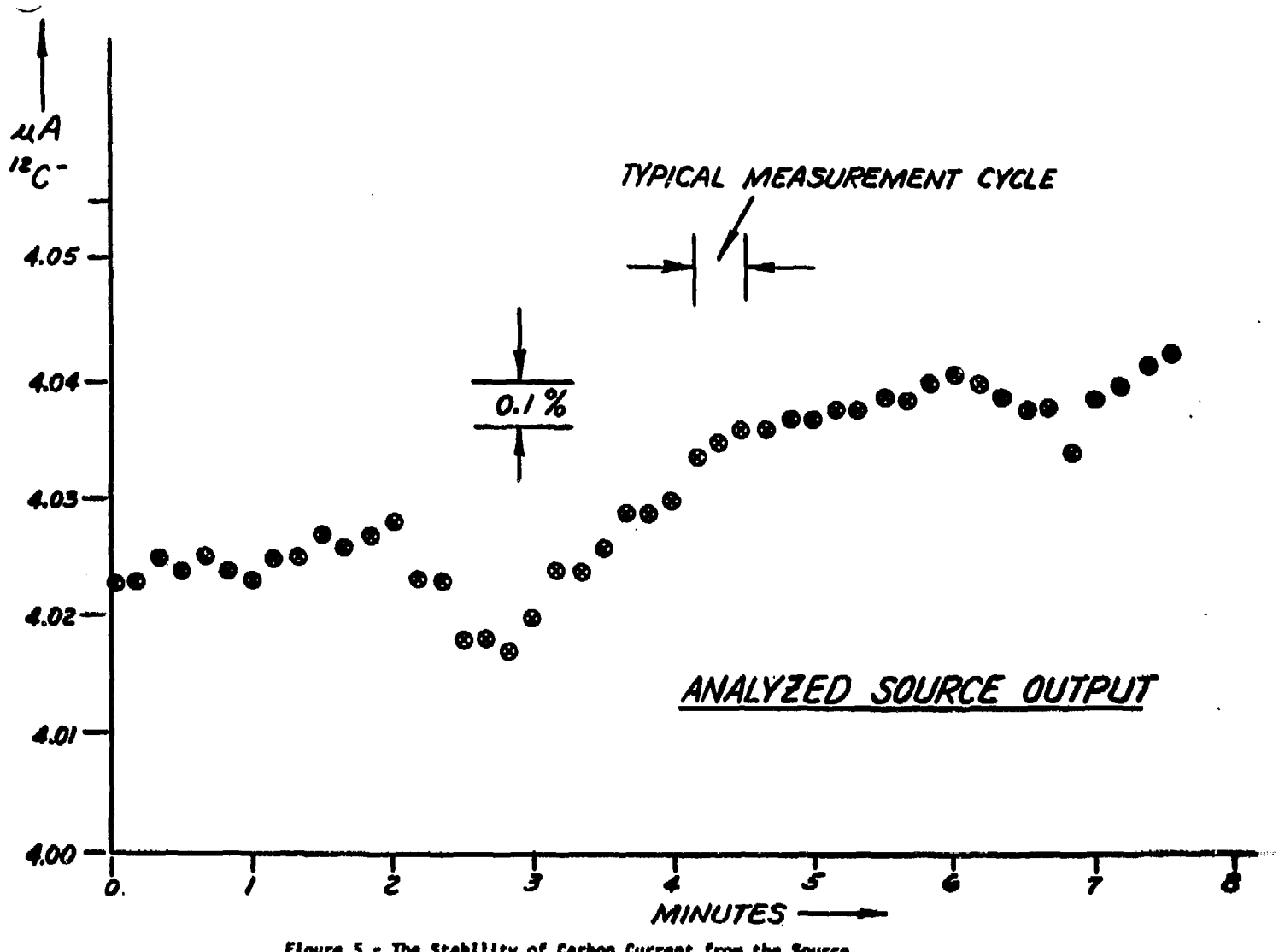

Figure 5 - The Stability of Carbon Current from the Source

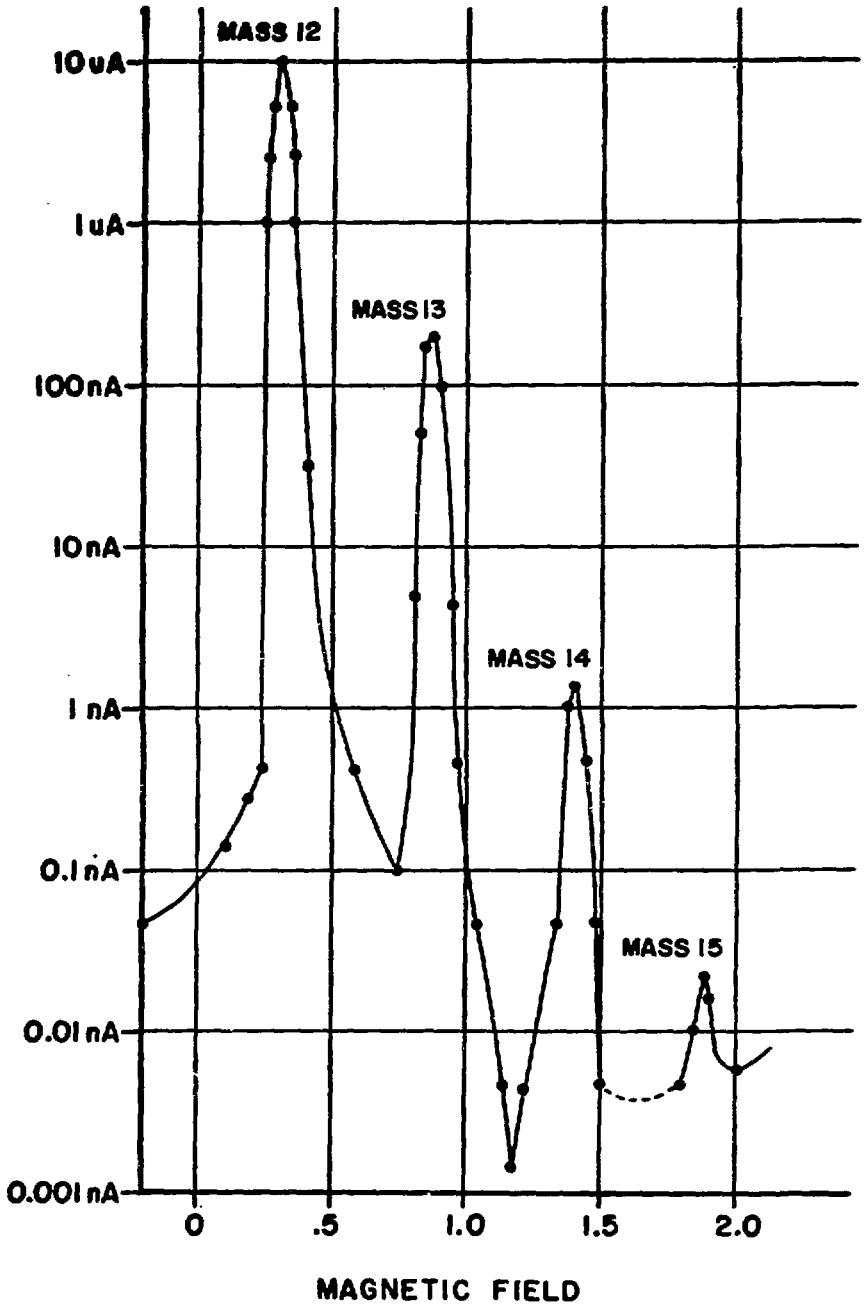

Figure 6 - The Mass Spectrum of Carbon After the First Mass Analyzer

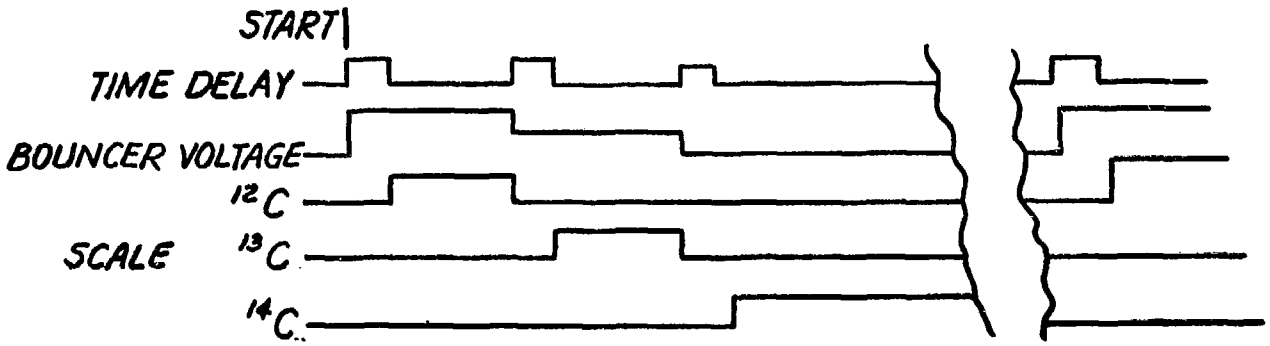

Figure 7 - Time Sequencing of Mass Injection

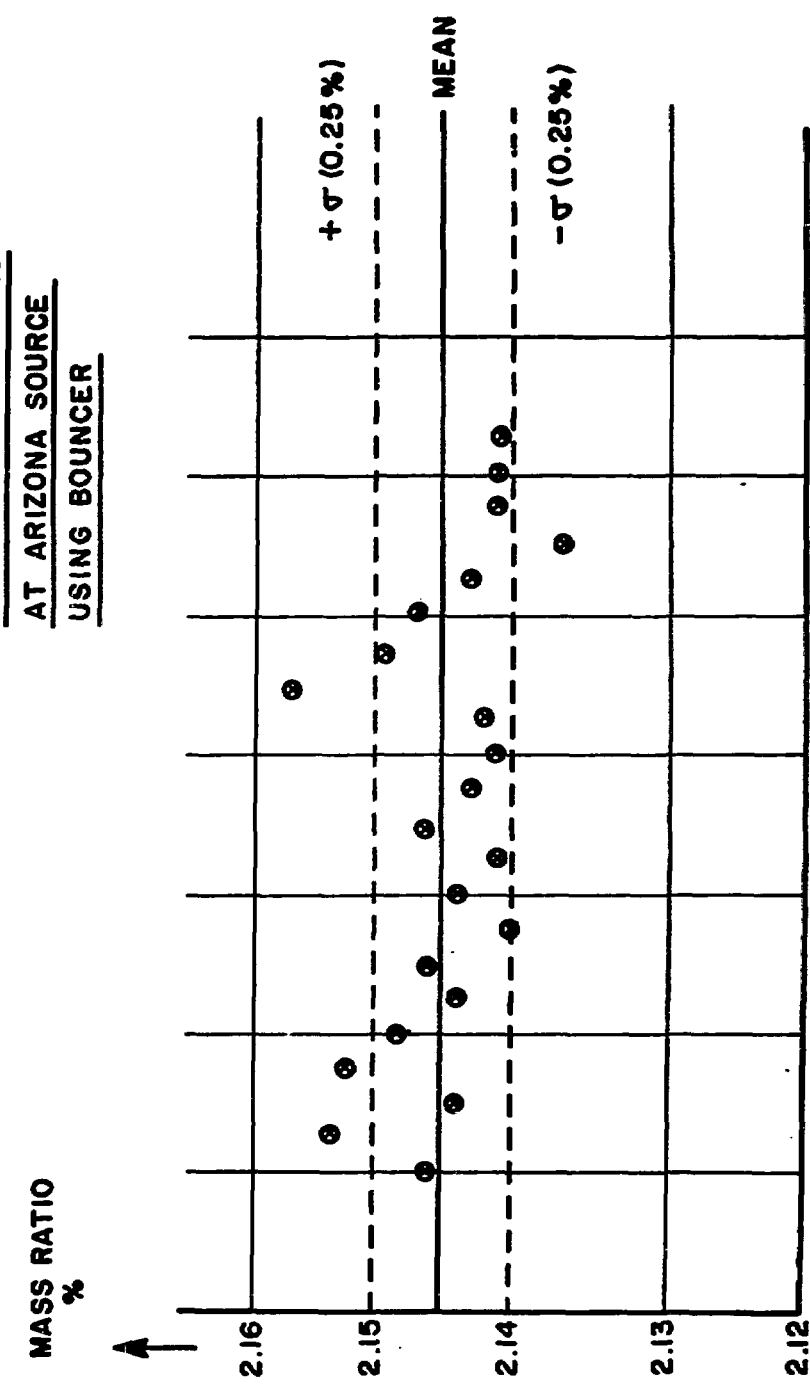

Figure 8 - A Typical Series of Current Ratio Measurements After the First Mass Analyzer

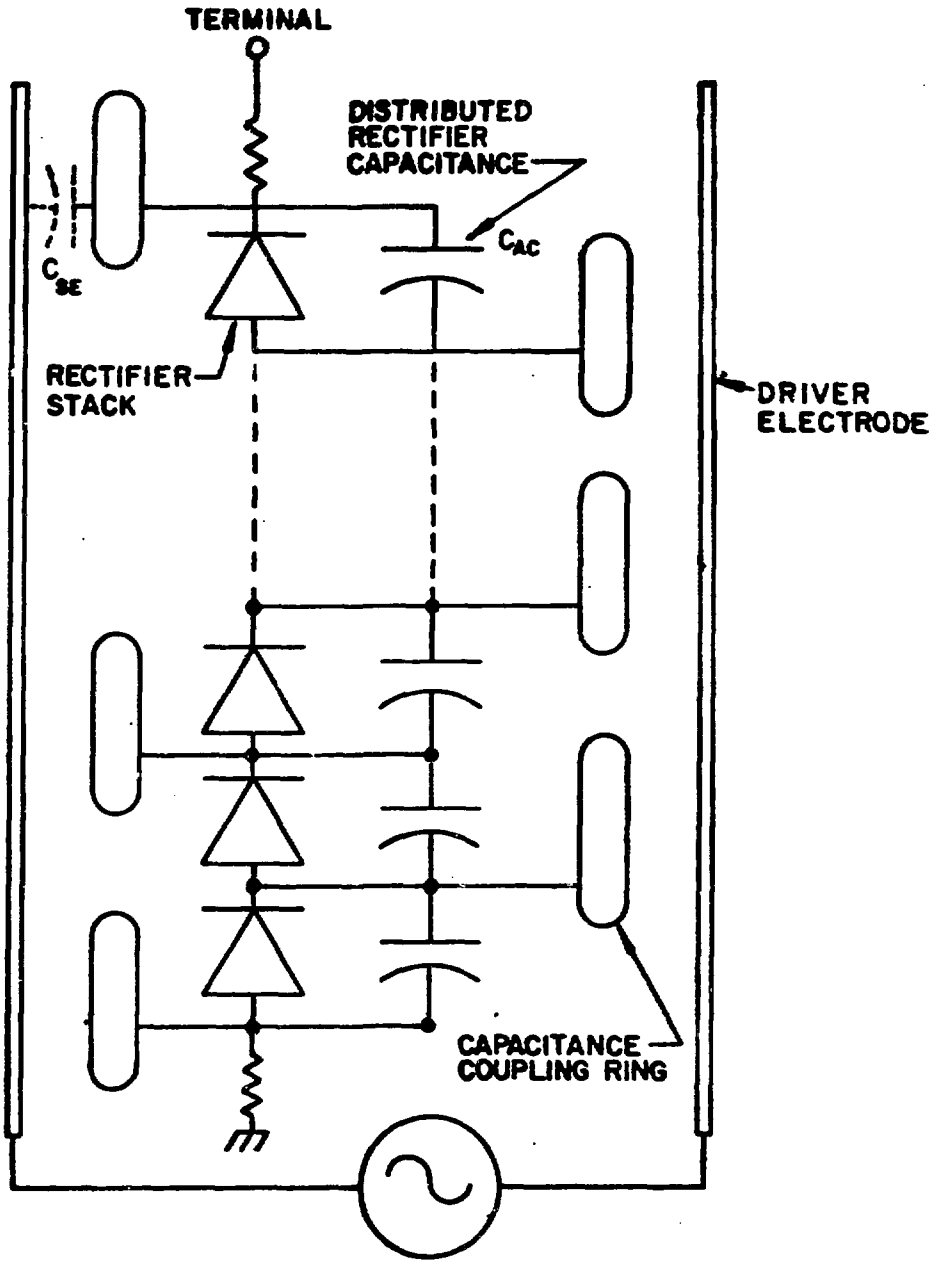

PARALLEL FED VOLTAGE MULTIPLIER

Figure 9

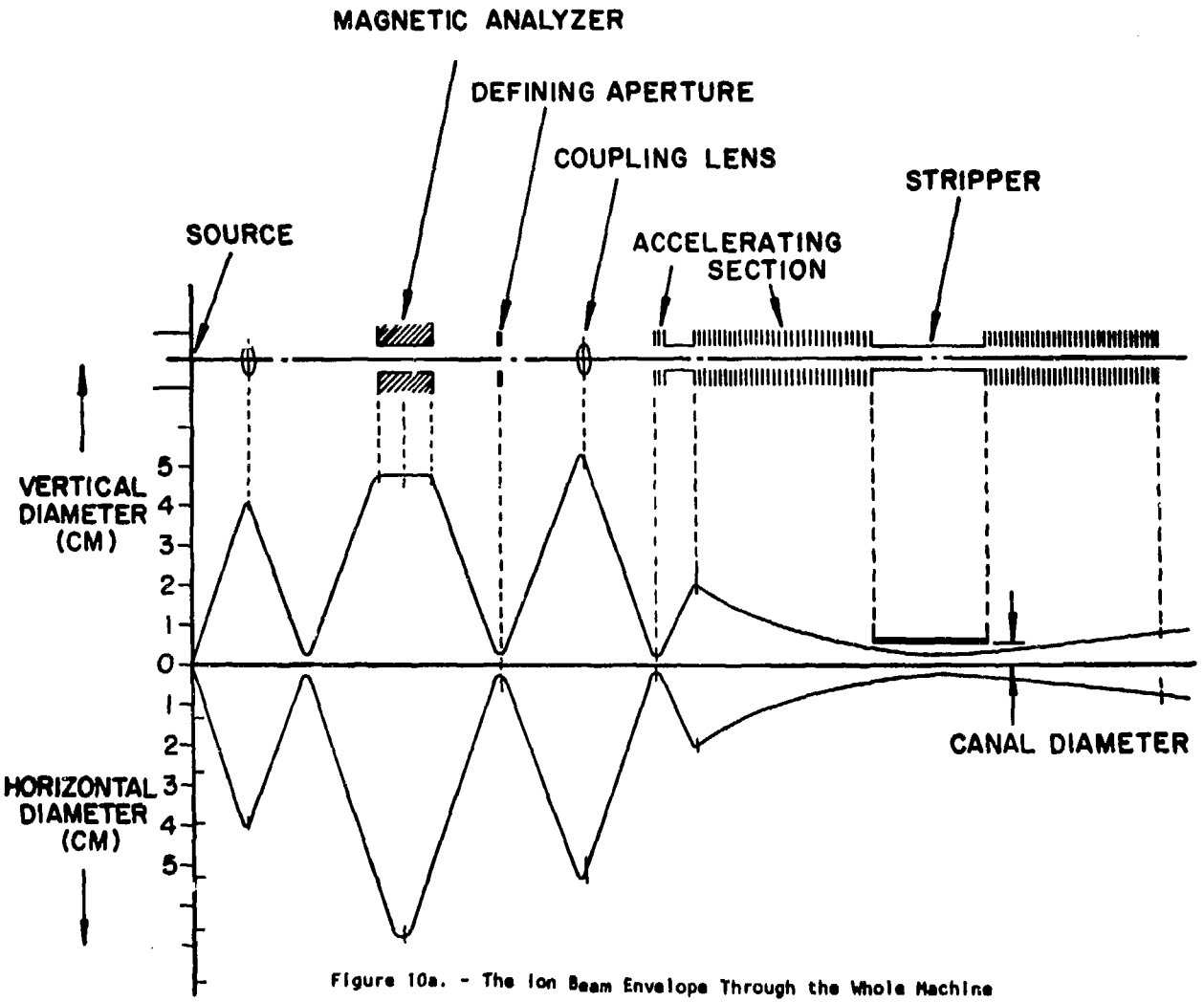

Figure 10a. - The Ion Beam Envelope Through the Whole Machine

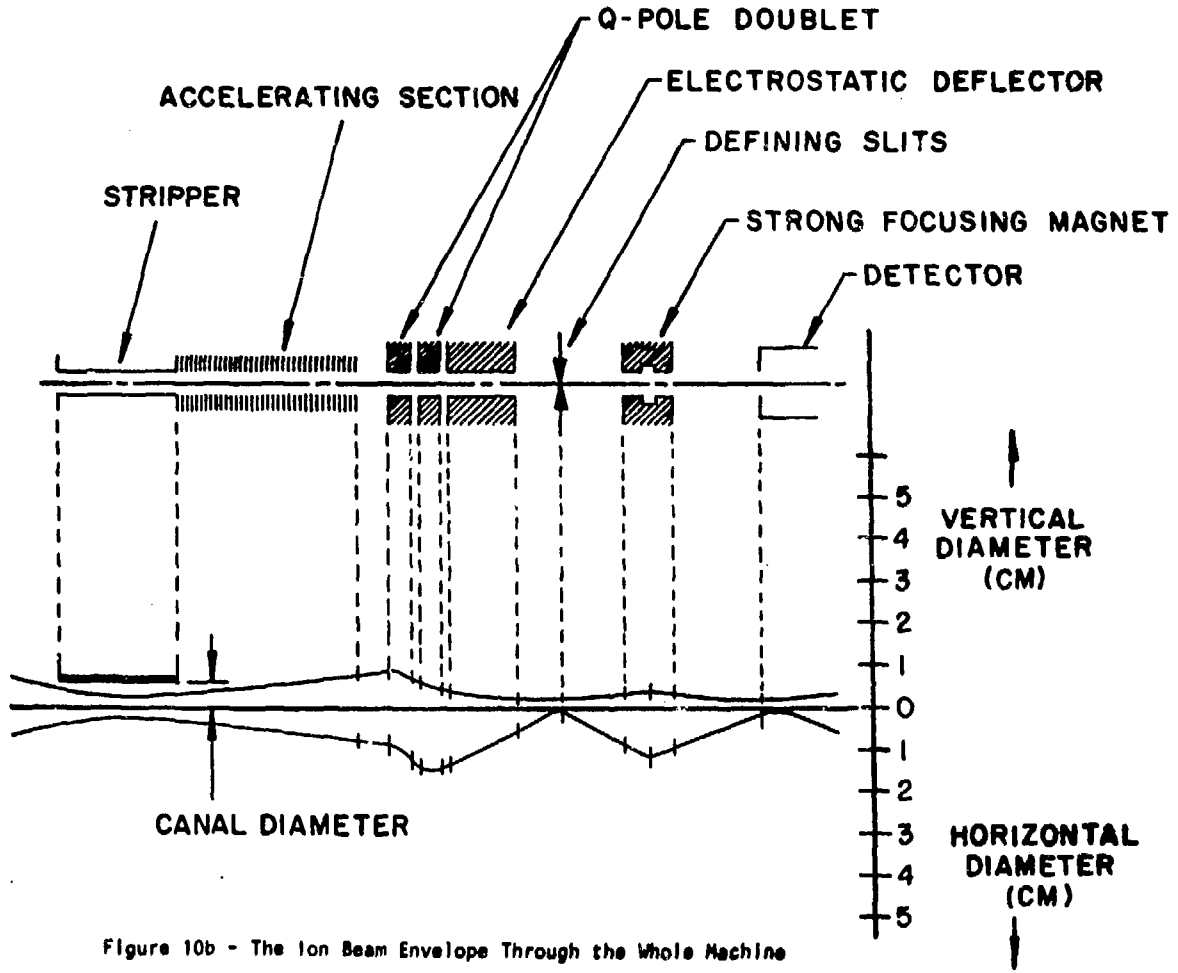

Figure 10b - The Ion Beam Envelope Through the Whole Machine

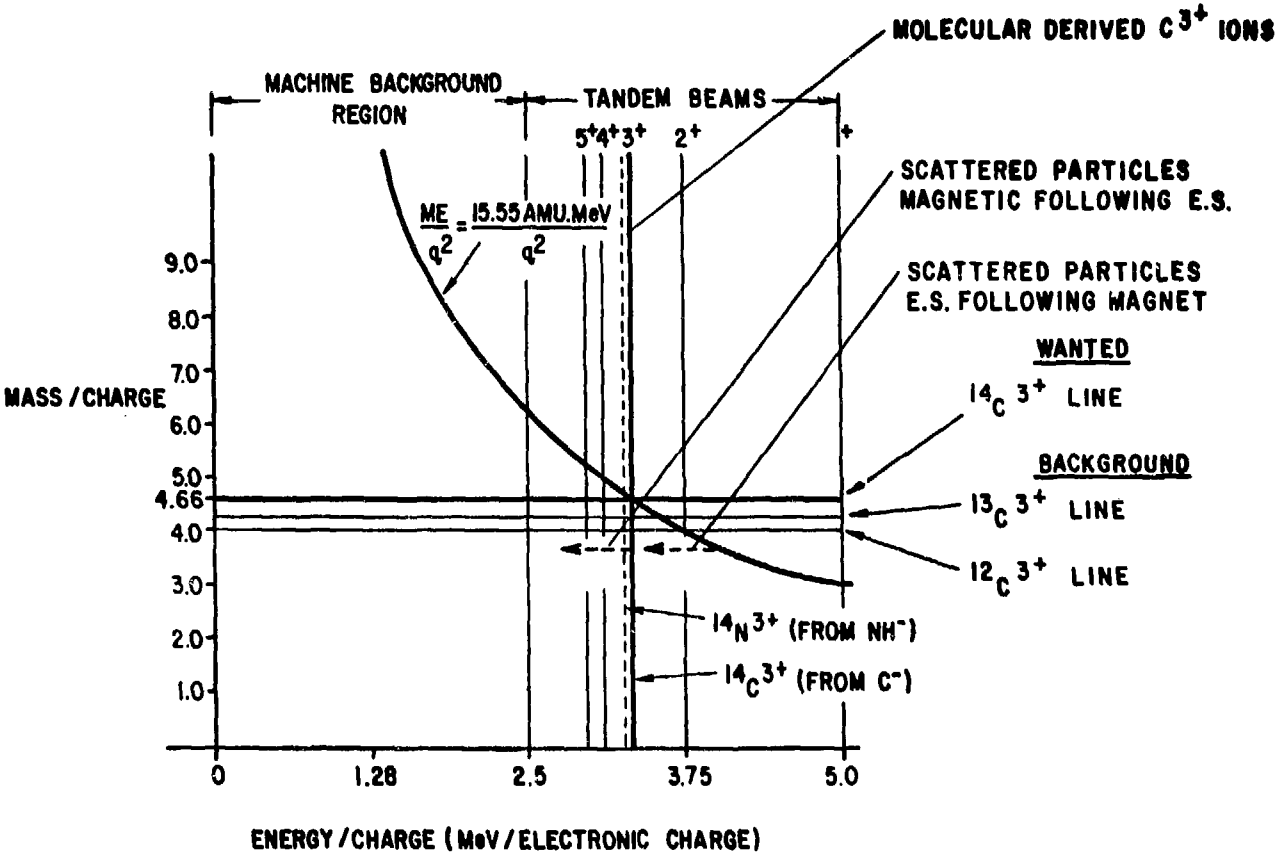

COMPARISON BETWEEN ES / MAGNET AND MAGNET / E.S. DEFLECTOR SEQUENCE

Figure 11 - The High Energy Mass Spectrometer Constraints

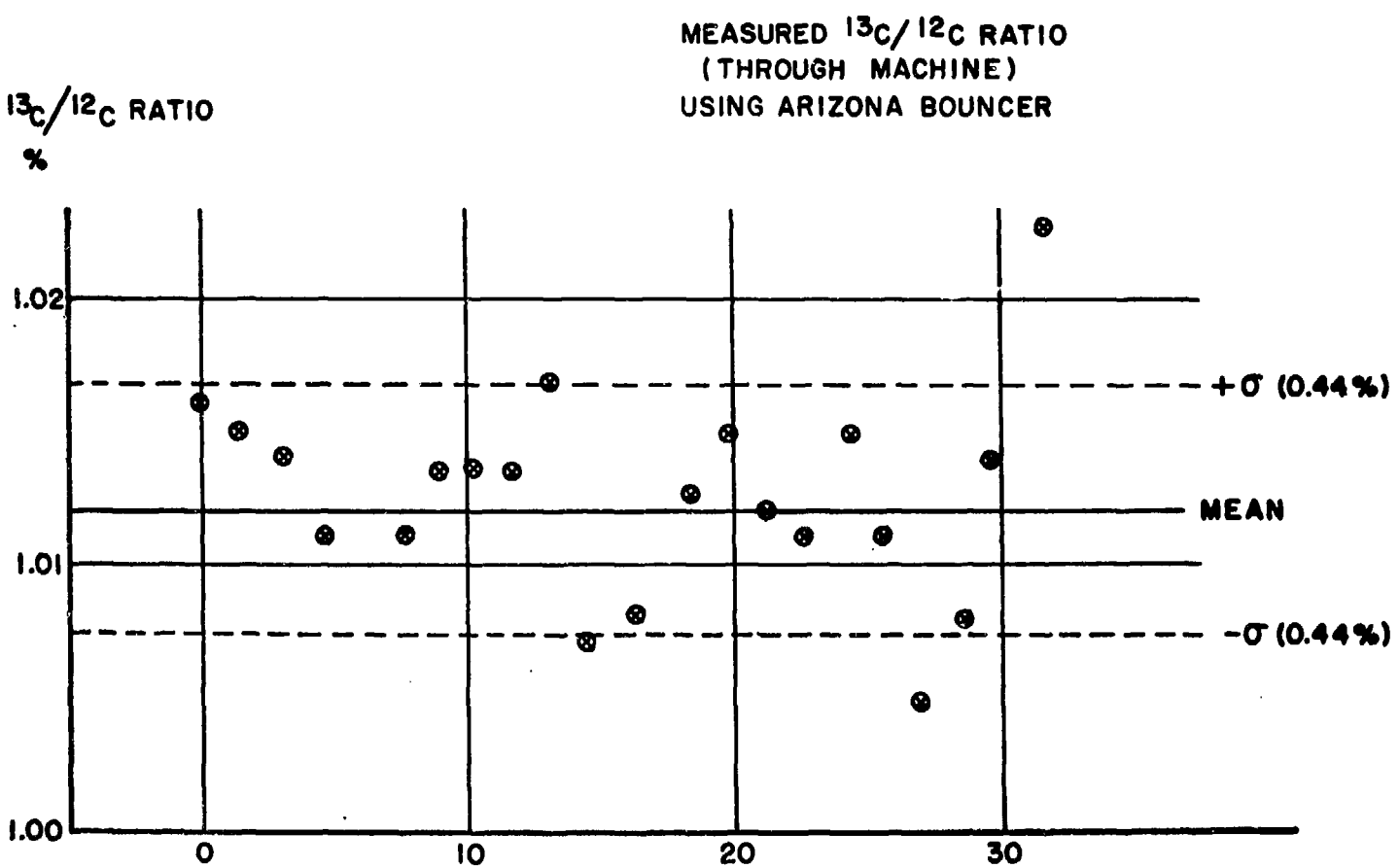

Figure 12 - The Consistency of Isotopic Ratio Measurements Following the 15° Electrostatic Deflector

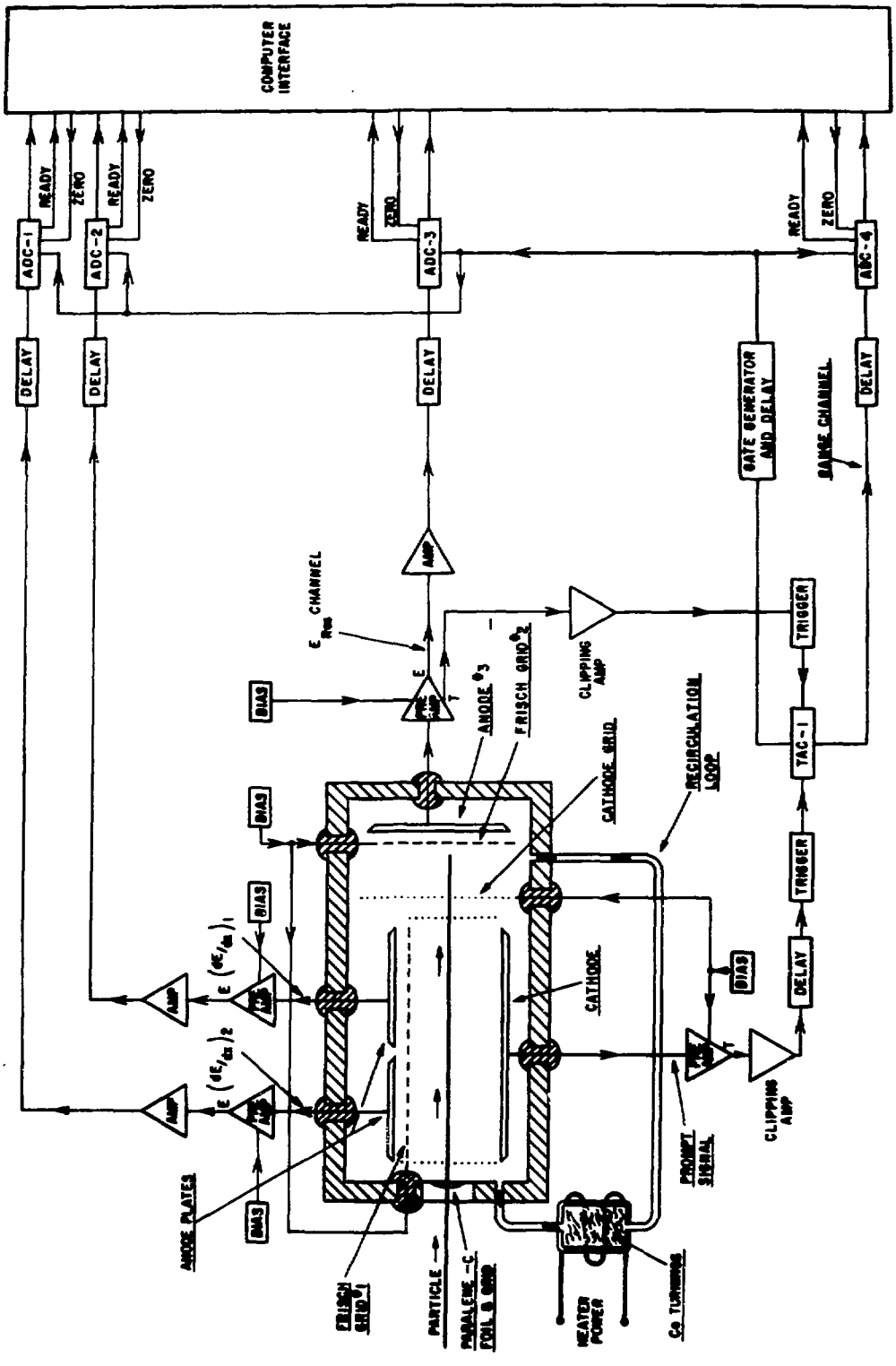

Figure 13 - A Schematic Diagram of the Detector

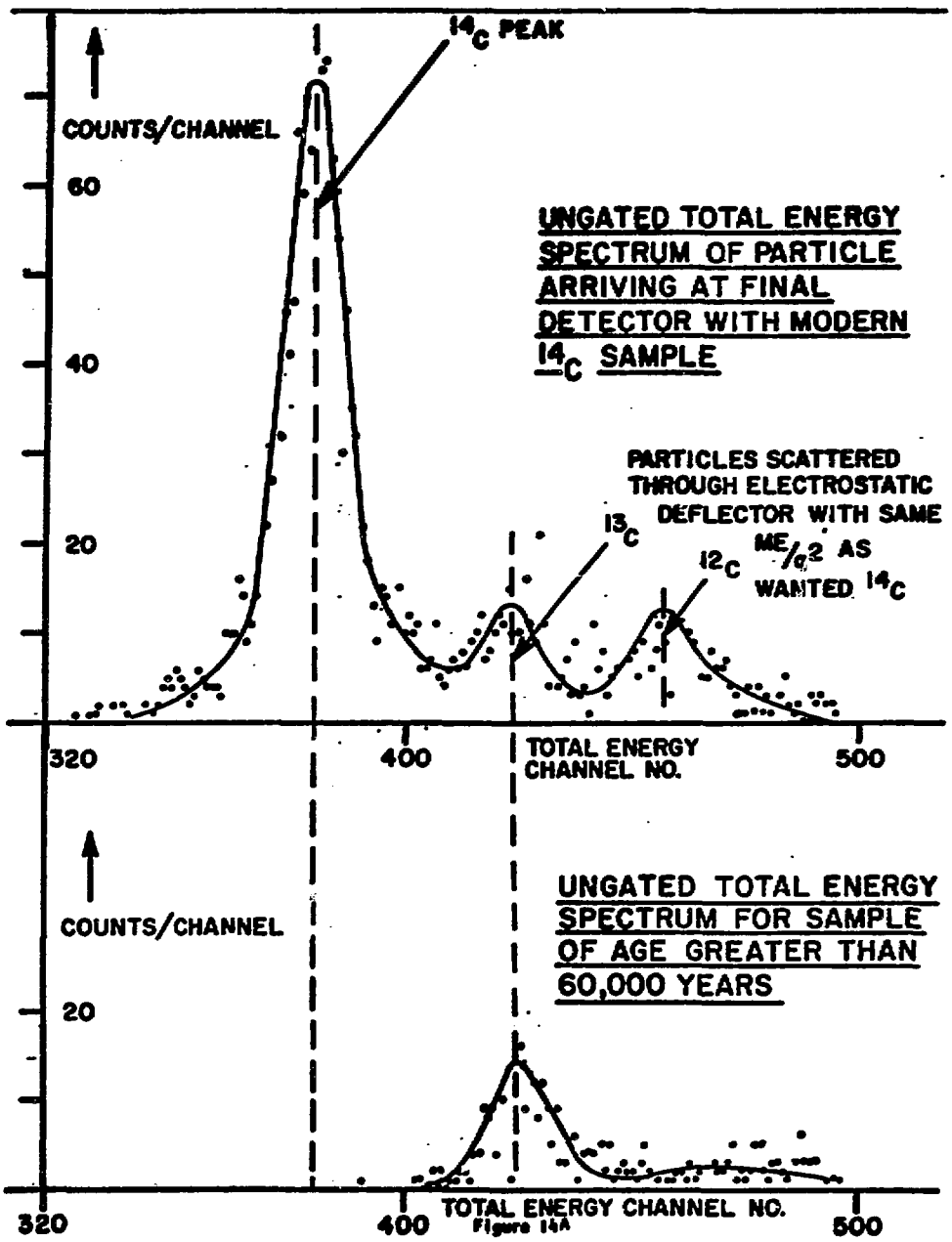
^{14}C PEAK
COUNTS/CHANNEL
60
40
20
UNGATED TOTAL ENERGY SPECTRUM OF PARTICLE ARRIVING AT FINAL DETECTOR WITH MODERN ^{14}C SAMPLE
PARTICLES SCATTERED THROUGH ELECTROSTATIC DEFLECTOR WITH SAME ME/q2 AS WANTED ^{14}C
^{13}C
^{12}C
320
400
TOTAL ENERGY CHANNEL NO.
500
COUNTS/CHANNEL
20
UNGATED TOTAL ENERGY SPECTRUM FOR SAMPLE OF AGE GREATER THAN 60,000 YEARS
320
400
TOTAL ENERGY CHANNEL NO.
500
Figure 14A

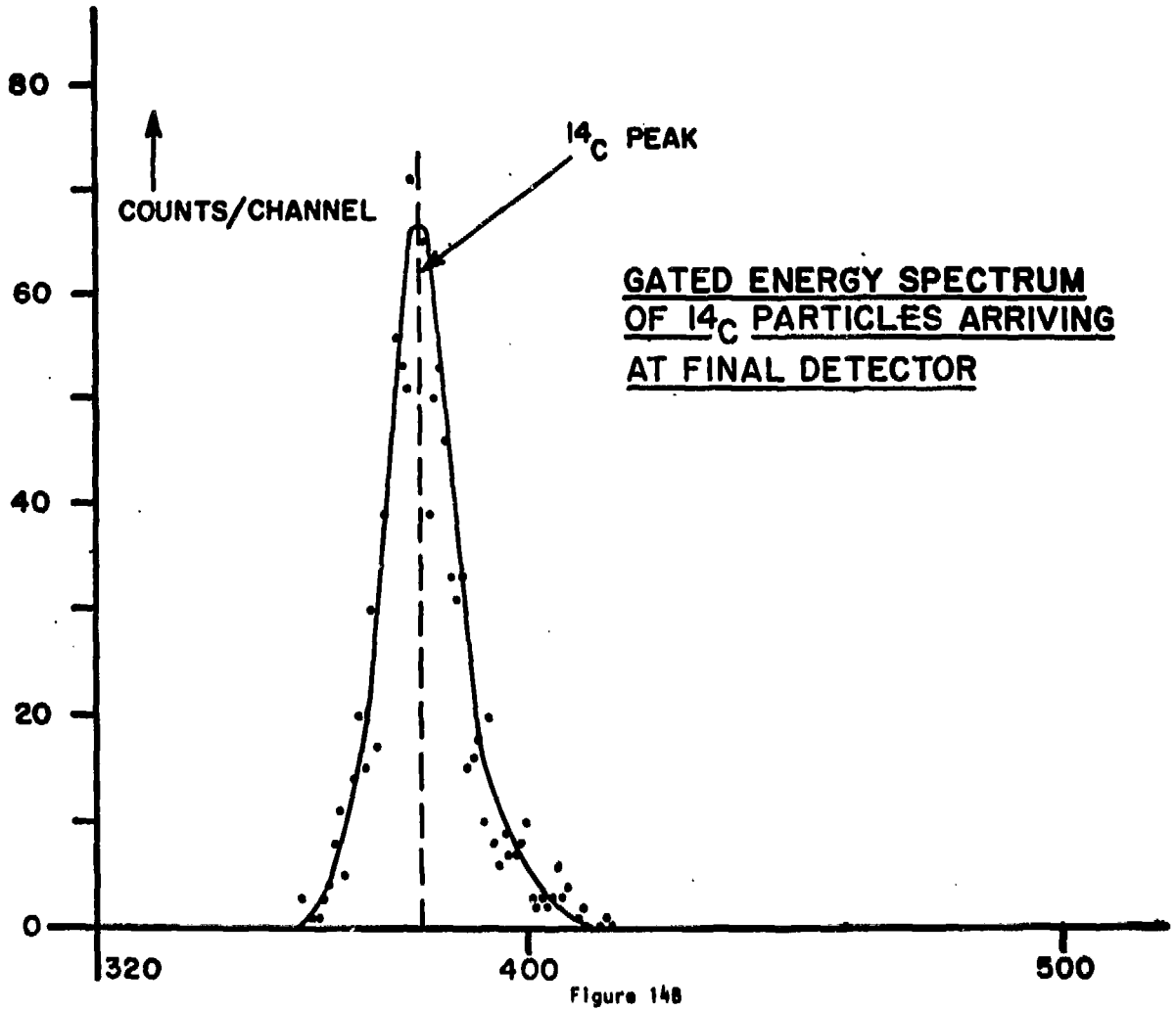
80
60
40
20
0
COUNTS/CHANNEL
^{14}C PEAK
GATED ENERGY SPECTRUM
OF ^{14}C PARTICLES ARRIVING
AT FINAL DETECTOR
320
400
500

Figure 148

THE ISOTRACE LABORATORY AT THE UNIVERSITY OF TORONTO

Roelf P. Beukens

University of Toronto, Toronto (Ont) Canada

BRIEF HISTORY OF ISOTRACE

The possibility of exploiting the instability of the nitrogen ion to count ^{14}C at natural levels was realized in the early 1960's following unsuccessful attempts to accelerate nitrogen ions with tandem accelerators. In 1973 the negative ion sputter source was developed into a sufficiently high intensity C^- ions source with low carbon consumption and, compared with the previous radiofrequency ion sources, a very low memory effect. The possibility of radiocarbon dating by atom counting and exploiting the negative nitrogen ion stability was subsequently discussed in February 1974 in Physics and Archaeology lectures at the University of Toronto.

During 1976 a nuclear physics group consisting of A.E.Litherland and R.P.Beukens started to look for a suitable tandem accelerator and sputter ion source to rigorously test the instability of the N^- ion and to detect ^{14}C at natural levels by atom counting.

At roughly the same time a proposal by K.H.Purser, T.A.Tombrello and G.Wasserburg was submitted to the NSF for an ion microprobe, using a tandem accelerator as a device for removing molecular interferences with high efficiency.

The Rochester-Toronto-General Ionex group was formed in April 1977 which led to the first observation and quantitative measurement of ^{14}C at natural levels in May 1977 [1].

The significance of this discovery for archaeology as well as for ion microprobe work caused the Physics and Archaeology group to combine its efforts in August 1978 with a group in Geology, led by D.W.Strangway, which had been studying the possibility of acquiring a secondary ion mass spectrometer for geological and material science

studies. The ISOTope and Rare Atom Counting Equipment (ISOTRACE) facility was effectively launced in April 1979 at the approval of the Natural Sciences and Engineering Research Council of Canada for the purchase of a General Ionex TANDETRON mass spectrometer. In 1980 the funds to develop the facility for the various applications were obtained from the Department of Supply and Services with the Ministry of Energy, Mines and Resources, the Canadian Geological Survey and Environment Canada as sponsors. A steering committee coordinates this development while a projects evaluation and allocation committee 2), consisting of experts from outside the ISOTRACE group, was put in place in late 1980.

INTRODUCTION

The people currently part of the ISOTRACE group are:

PHYSICS	GEOLOGY	ARCHAEOLOGY
C.E.Aardsma	N.M.Evensen	U.Franklin
R.P.Beukens	M.Gorton	W.Irving
K.H.Chang	J.C.Rucklidge	D.Markovich
E.Hallin	D.W.Strangway	C.Young
W.E.Kieser	G.C.Wilson	
L.R.Kilius		GEOPHYSICS
H.W.Lee		
A.E.Litherland		R.Farquhar

The special interest of these disciplines and the different interests of the people within these disciplines require the detection of many different stable as well as radioactive isotopes, for example:

ARCHAEOLOGY

^{14}C of slag, pottery, linen fragments, bone etc.

$^{26}Al/^{10}Be$ dating of Paleo-Archaeological samples.

HYDROLOGY

^{36}Cl groundwater dating

^{129}I groundwater tracer analysis

PHYSICS

Cross section measurements: Thermal neutron capture on ^{9}Be

$^{7}Li + {}^{7}Li = {}^{14}C + \gamma$

$^{11}B + \alpha = {}^{14}C + p$

Halflife measurements: Spontaneous fission of ^{232}Th into ^{14}C

Proton halflife from ^{98}Tc abundance

Detection of solar neutrinos: $^{7}Li + \nu = {}^{7}Be + e^{-} - 0.86$ MeV

$^{205}Tl + \nu = {}^{205m}Pb + e^{-} - 43$ keV

Search for non-integral charged quarks

Search for super heavy elements

GEOLOGICAL MICROPROBE ANALYSIS

Trace elements analysis

Isotope ratio measurements of light elements

Age determination of minerals: ^{10}Be, K/Ar, Rb/Sr, $^{207}Pb/^{206}Pb$

A number of these applications have been discussed at this conference in detail: 14C dating (R.P.Beukens), Non-integral charged quarks (K.H.Chang), Super heavy elements (L.R.Kilius), Terrestrial (J.Rucklidge) and extra-terrestrial (G.Wilson) trace analysis.

Figure 1 gives a plot of the elements of interest and the expected abundances. The detection and analysis of all these isotopes is well outside the capabilities of a standard 3 MV TANDETRON and a number of extensions and improvements to the system are under construction or have been planned. Figure 2 gives the projected floor plan of the complete facility, build around a standard 3 MV TANDETRON. In the remainder of this article the extensions and improvements will be discussed.

ION MILLIPROBE OPTION

In addition to the standard 3 MV TANDETRON, General Ionex will deliver the so called ion milliprobe option. This includes, in addition to a high energy magnet capable of analysing 18 MeV Cl^{+5} ions, a sputter ion source with a guaranteed caesium spotsize of 200 microns, a mechanism for moving the sample around by 1 cm in the X and Y directions, and an optical microscope to inspect the sample. An extra stable power supply will be provided for the inflection magnet with a mass resolution of 400.

HYDRODYNAMIC CAESIUM FIELD EMISSION SOURCE

From Oxford Applied Research (U.K.) a hydrodynamic field emission source has been purchased for applications in a ion micro probe source with a caesium beam spot of several microns and an intensity of 20 nA. This caesium source, after the addition of appropriate beam optics and scanning fields can be bolted on the source delivered with the TANDETRON.

HIGH CURRENT Al^- SOURCE

For Al/Be dating a high current (5-30 uA), efficient source for Al^- is required as the abundance of ^{26}Al is expected to be three orders of magnitude less than that for ^{10}Be. Caesium sputter negative ion sources produce less than 1 uA of Al^- with low efficiency. A LaB_6 surface ionization source, presently under construction, will provide a 1 mA primary I^- beam. A conservative estimate would indicate that this primary beam should be capable of producing a secondary Al^+ of at least 100 uA from the samples of interest. This Al^+ beam is subsequently charge exchanged to Al^- in a Na charge exchange canal with an efficiency of 10 - 15 % [3].

OPTIMIZED GAS IONIZATION DETECTOR

For particle identification a E-dE/dX gas ionization detector has been used so far by the Toronto-Rochester-General Ionex at high energies. For the detection of isotopes up to ^{36}Cl at the much lower energies, expected with the 3 MV TANDETRON, an optimized detector is being designed. The dead spaces and losses in the window will be minimized as much as possible. The operating pressure is envisioned in the region of a few torr while the gas pressure inside the detector will be accurately controlled by a MKS-254 flow controller while maintaining an accurate mixture of up to three counting gasses.

HIGH RESOLUTION TIME OF FLIGHT MASS SPECTROMETER

As gas ionization detectors cannot be used for particle identification for isotopes heavier than ^{36}Cl, a different identification technique has to be used. In the past at Rochester we have successfully employed a time of flight detector for the detection of ^{129}I, Pt and Ir isotopes. A high resolution (dM/M=2000) mass spectrometer is currently being designed for use on the ISOTRACE facility. The total energy and the flight time, determined in a time of flight mass spectrometer which is isochronous for small energy, angle and displacement variations, will provide the resolution necessary to distinguish between the heavy isotopes and the interferences from molecules such as their hydrides.

ALL ELECTRIC BROAD BAND MASS SPECTROMETER

The addition of an all electric injection system to the time of flight mass spectrometer produces in effect a broad band mass spectrometer as no mass selection is taking place and all species will be detected in the TOF detector. This is ofcourse of great importance for ion microprobe analysis where all isotopes of a single element or all elements can be analysed simultaneously.

HIGH SPEED DATA ACQUISITION AND ACCELERATOR CONTROL SYSTEM

A data acquisition and accelerator control system has been designed in cooperation with and is being built by INTEREX Computing Systems (Toronto) (Figure 3). It is based on two high speed (20 MHz) CS-90 processors with each 64kB of 16-bit memory. The two processors emulate the standard PDP-11/45 instruction set. The data acquisition processor analyses the incoming data in real time using specially designed microprogrammed instructions at data rates of up to 100,000 particles/sec from 4 ADC's (400,000 events/sec). The 11-bit, 5 usec per conversion, ADC's, preamplifiers and amplifiers are under computer control. To minimize any limiting by dead time multi-level analog and digital buffering is used. The control processor has, in addition to a special TANDETRON control interface, multiple busses (UNIBUS, CAMAC, IEEE-488, RS-232) for future extension and addition to the system. A 1024x1024 pixel display system will provide online display of the analysed data.

REFERENCES

1) K.H.Purser et al; Revue de Physique Appliquée Tome 12 (1977) 1487

2) Proposals should be submitted to:
ISOTRACE Evaluation and Allocation Committee
Prof. D. Shaw; Dean, Dept. of Geology
Mc Master University
Hamilton (Ont) Canada

3) J.Heinemeier and P.Hvelplund; Nucl.Instr.Methods Vol.148 (1978) 425

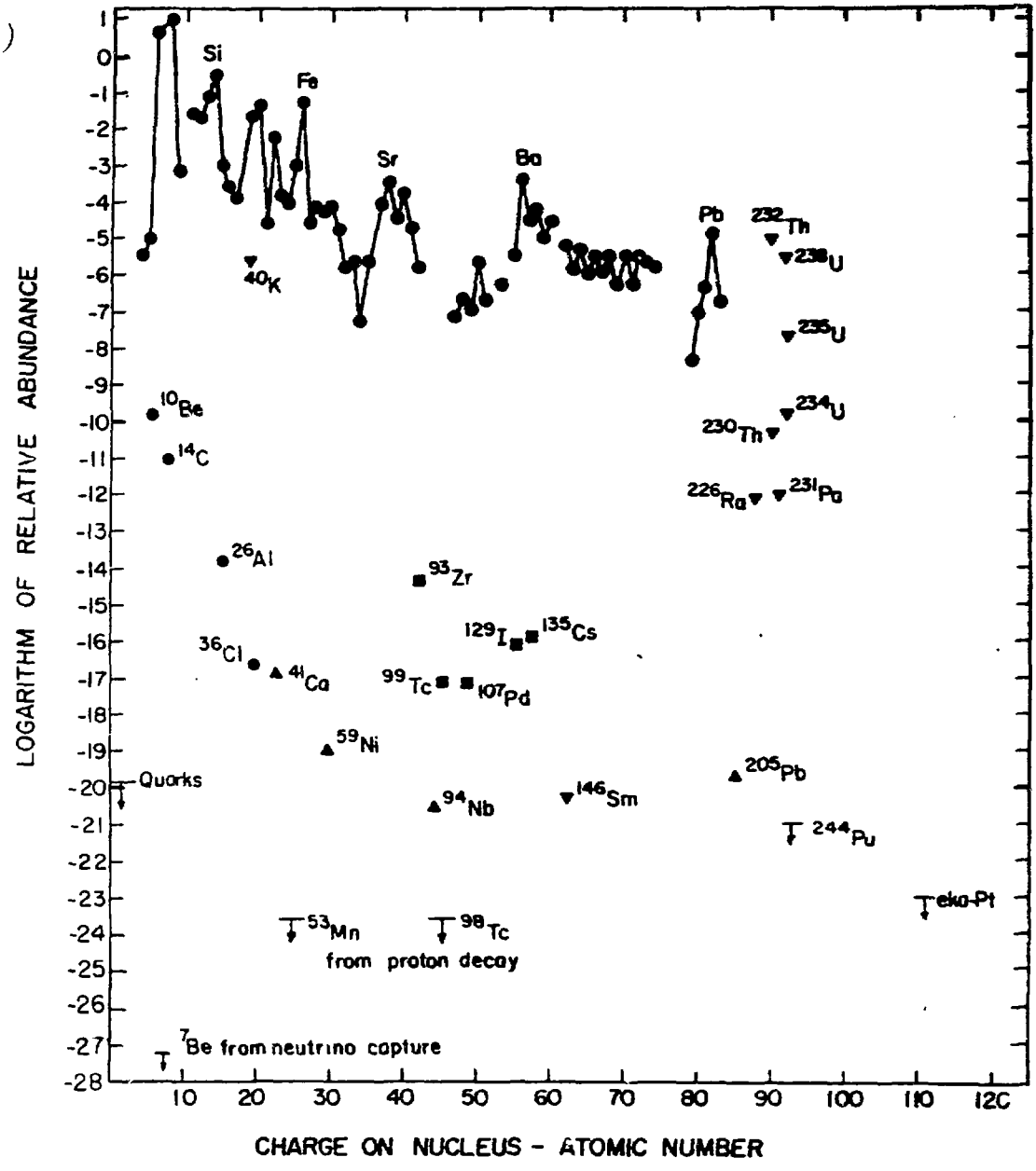

Figure 1. Relative abundance of isotopes of interest to the ISOTRACE group.

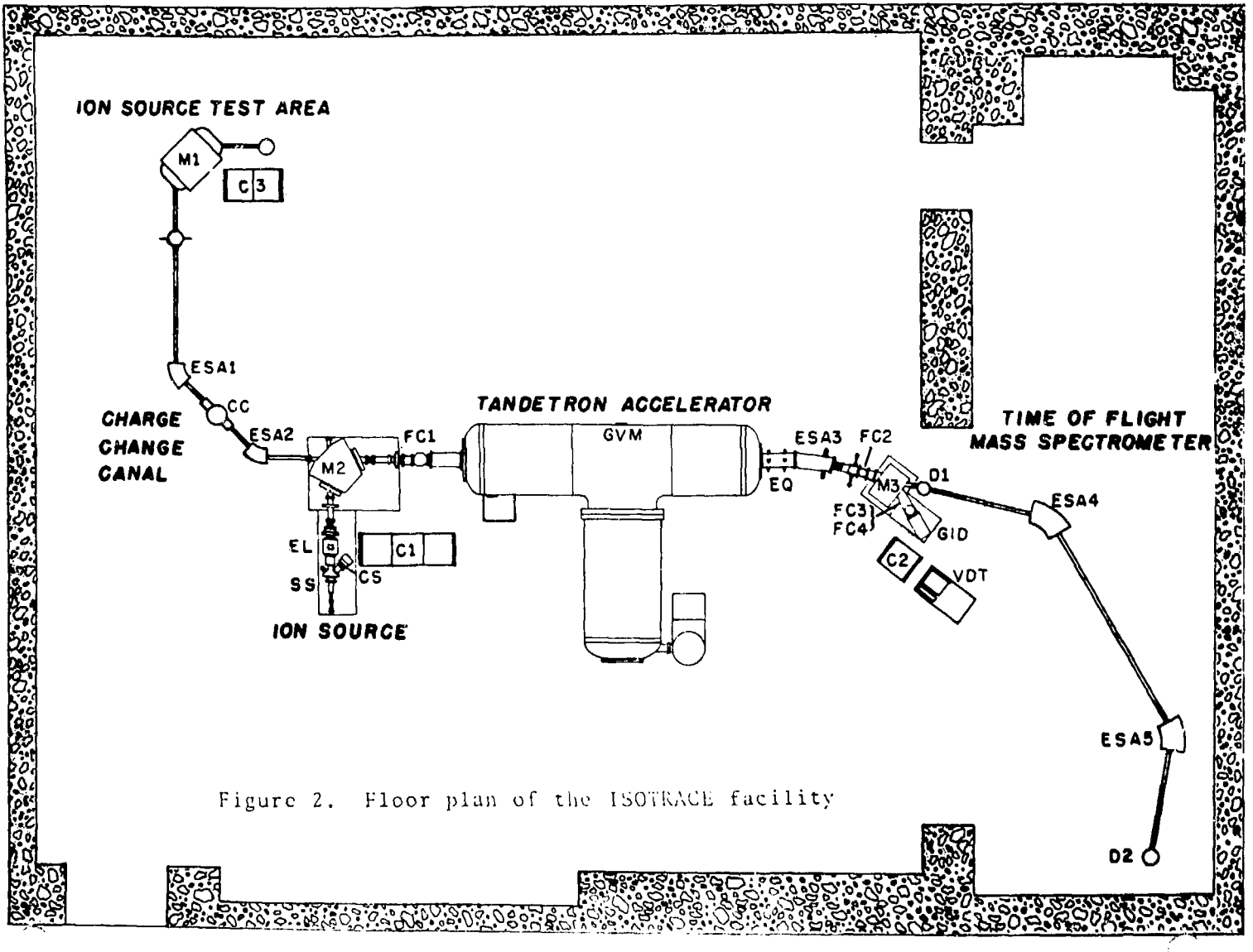

Figure 2. Floor plan of the ISOTRACE facility

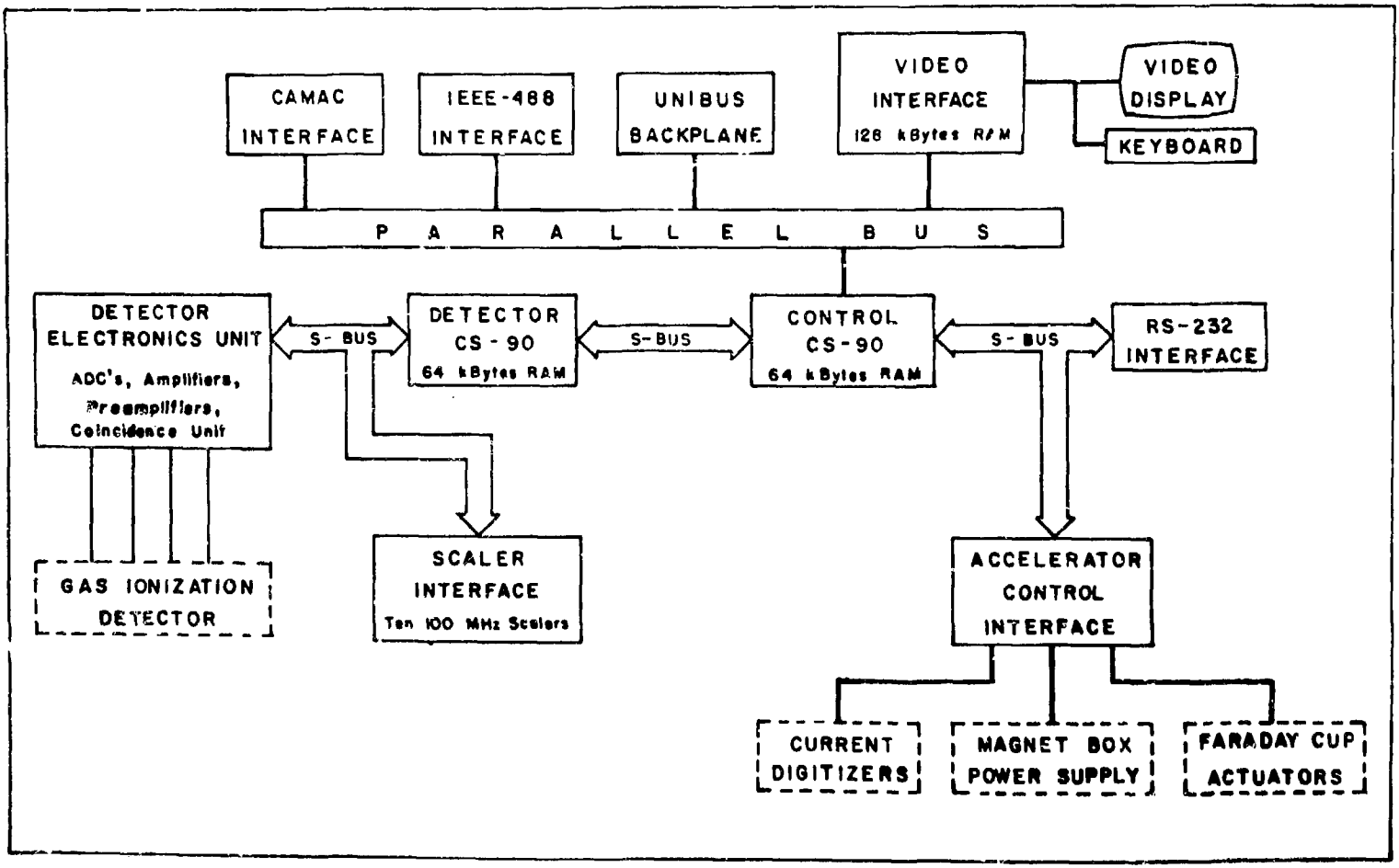

Figure 3. Block diagram of the INTEREX data acquisition and accelerator control system

THE RADIOCARBON FACILITY AT THE RESEARCH LABORATORY FOR ARCHAEOLOGY IN OXFORD - A REVIEW

N.R. White, R.E.M. Hedges, J.O. Wand and E.T. Hall
Oxford University Research Laboratory for Archaeology
and the History of Art, 6 Keble Road, Oxford, OX1 3QJ, England

The Oxford accelerator mass spectrometry facility is primarily intended for radiocarbon work. It has been designed and built within the department, except for the 3 MV tandem, which is being purchased from General Ionex and is still awaited. This sytem has been described many times before, so this paper will not give a comprehensive description of the facility, but only cover in detail areas of recent progress, or areas where our approach differs from other labs.

Fig. 1 shows the layout of the Oxford facility. Two types of caesium sputter source are used. A 90 degree magnet with a mass resolving power of 100 injects the isotopes sequentially into the accelerator; the pulsing technique is described below. Injection is at 20 - 30 MV. In the terminal of the accelerator both gas and foil strippers will be fitted, giving us flexibility and the ability to keep the pressure low should terminal pumping be unavailable. On the high energy side of the accelerator an electrostatic quadrupole doublet produces a line focus as object for an analysing magnet with a resolving power of 1000. Following this magnet, ^{12}C and ^{13}C are measured on separate Faraday cups, while the mass 14 beam is drifted through a magnetic quadrupole doublet and Wien Filter before entering the gas-filled detector, which makes two energy loss measurements and one residual energy measurement.

We have a successful technique for preparing samples for a UHV version of the reflected beam sputter ion source. This is shown schematically in fig. 2. After combustion of the sample to CO_2 it is reacted with hot lithium to form lithium carbide. Water is added to evolve acetylene, from which a graphite target is produced by pyrolysis. A tantalum wire, about 0.5 mm in diameter, is electrically heated to 2000 degrees in a pressure of about 20 to 50 torr of acetylene, and a layer of pyrolytic graphite builds up on the surface. This deposit is well attached, and the good thermal contact is believed to be an important factor in achieving high ion currents. This procedure can be successfully used for quantities of 1 - 5 milligrams. The yield is

typically 50% The process fractionates at a mean of about -14‰ for ^{14}C w.r.t. ^{12}C, and since deposition is occurring from a closed reservoir, the isotopic composition of the deposit must be structured. This has strong implications for the method of standard preparation, which should clearly be as similar as possible.

We mount 20 such wires around the circumference of an aluminium wheel by crimping them into a shallow groove, as shown in fig. 3. These wheels are then mounted in the ion source so that the caesium beam passes the edge of the wheel, to be reflected back onto the wire target by the biased negative ion extraction electrode (*fig.* 4). These targets give reproducibly large currents and high efficiencies. From a 1 mm dia wire target, 80 uA of $^{12}C^-$ are obtained with 30 keV Cs+. Smaller wires give smaller currents; 30 - 40 μA is easily obtained routinely. Conversion to negative ions is at least 10% efficient (1), for the part of the target exposed to the beam.

We have developed a technique for switching between isotopes under optically identical conditions at up to 80 Hz, with switching times of 20 uS. The vacuum chamber in the injection magnet is insulated from ground by Teflon sheets, together with lengths of beam line extending to the waists on either side. By changing the potential on this chamber, the energy of the beam at this point is altered, changing its magnetic rigidity. If a 30 keV mass 14 beam is deflected through 90 degrees with zero potential on the box, it is necessary to apply +5 kV to switch to mass 12. We have developed a hybrid electronic switch circuit using semiconductors and electron tubes which can switch the vacuum chamber between ground potential and two reservoir capacitors connected to E.H.T. supplies. This can switch the 3 nF load of the magnet vacuum chamber between 0 and 5 kV in 20μS, as shown in fig. 5. The circuit diagram is given in fig. 6. The individual switches are operated by opto-couplers.

To complement the fast pulsing of the beams we need to make fast Faraday cup measurements, and this is achieved by means of virtual earth sample-and-hold charge integrators, whose charge injection is kept to an unmeasurably low level by using photo-FETs as the gates. A fast energy correction signal for correction of the terminal energy is provided from slits mounted within the ^{12}C high energy Faraday cup. This is shown schematically in fig. 7. It can be seen that a small potential is developed across the 1M resistors due to

the current striking each slit, and this potential is measured by means of a FET op-amp. Since no charge flows through these leads beyond that drawn by the gate capacity the Faraday cup is essentially intact, and the total current measurement is not upset in any degree by the position measurement.

Quasi-continuous monitoring of the isotopic fractionation and on-line correction of the ^{14}C count mean that any alterations in system parameters are readily detected and identified. The algorithms used are discussed in a separate paper.

We estimate that the overall efficiency of the process of detecting ^{14}C present in the carbon at the beginning of the target preparation process will be about 1%; the theoretical maximum with observed efficiencies of the various processes is about 4%. This means that to date a sample of carbon about 20,000 years old to an accuracy to one standard deviation of $\pm$ 200 years would require only a few tens of micrograms of carbon; this is an accuracy of $\pm$ 1% in the date. For more recent samples a similar quantity would give only a slight improvement in the absolute error in years, which of course represents a greater fraction of the age. Current estimates of accuracy (still only guesses) are that errors of $\pm$ 40 years should be attainable without too much difficulty.

This small sample size makes it possible to do extensive chemical pre-treatment of samples to isolate where possible organic substances known to be specific to the material being dated. As an example, we give the technique developed at Oxford for dating bone samples.

Of the carbon in bone, about one quarter is contained in the inorganic calcium phosphate/carbonate matrix, and is prone to leaching and exchange. Of the organic fraction, almost all is contained in the collagen, the bone protein whose fibrils form the underlying structure of the bone. This collagen is composed of amino acids (fig. 8), of which one acid, hydroxy-proline, strictly an imino acid, constitutes about 10%. Hydroxyproline is specific to bone and a few similar materials, and dating of the carbon in this material should guarantee immunity from contamination after burial, and should even discriminate against in-situ ^{14}C production by neutrons. The inorganic matrix can be dissolved away in dilute HCl, and hydrolysis in 6N HCl will then produce a solution of separated amino acids. The hydroxy-proline can then be separated in analytical quantities by High Performance Liquid Chromatography, HPLC. Reaction with HNO_2, followed by HCl, converts

all the amino acids to alcohols, while leaving the imino acids unchanged. It is then possible to separate sufficient hydroxyproline by HPLC to yield 1 - 2 mg of carbon for dating.

Kjeldahl analysis for nitrogen generally gives a good indication of the amount of collagen in a bone sample, and 1 gram of bone (samples up to 50,000 years old have been tested so far) has been shown to usually yield sufficient hydroxyproline for dating.

Reference:

1. R.E.M. Hedges, J.O. Wand, N.R. White, Nucl. Inst. & Meth. 173 (1980), 409.

LIST OF FIGURES

Ion beam configuration for ^{14}C accelerator

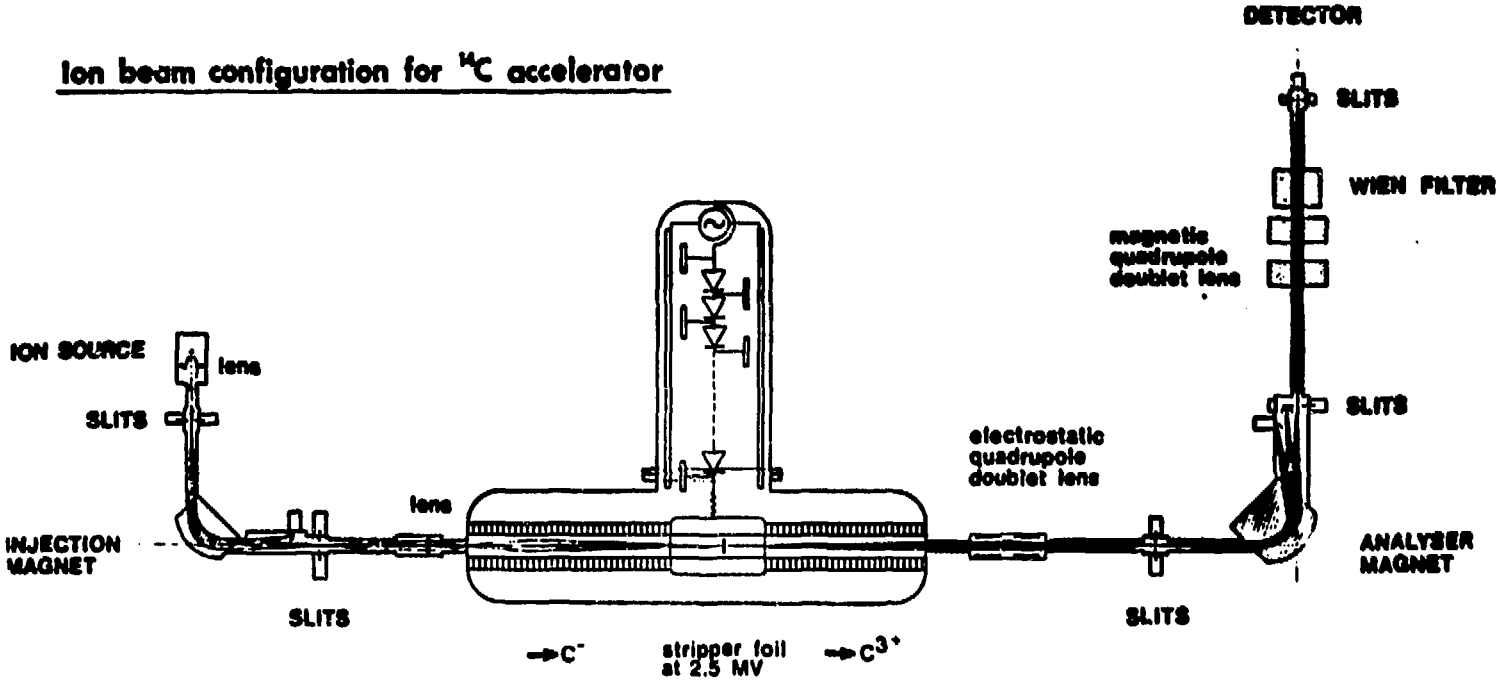

FIGURE 1

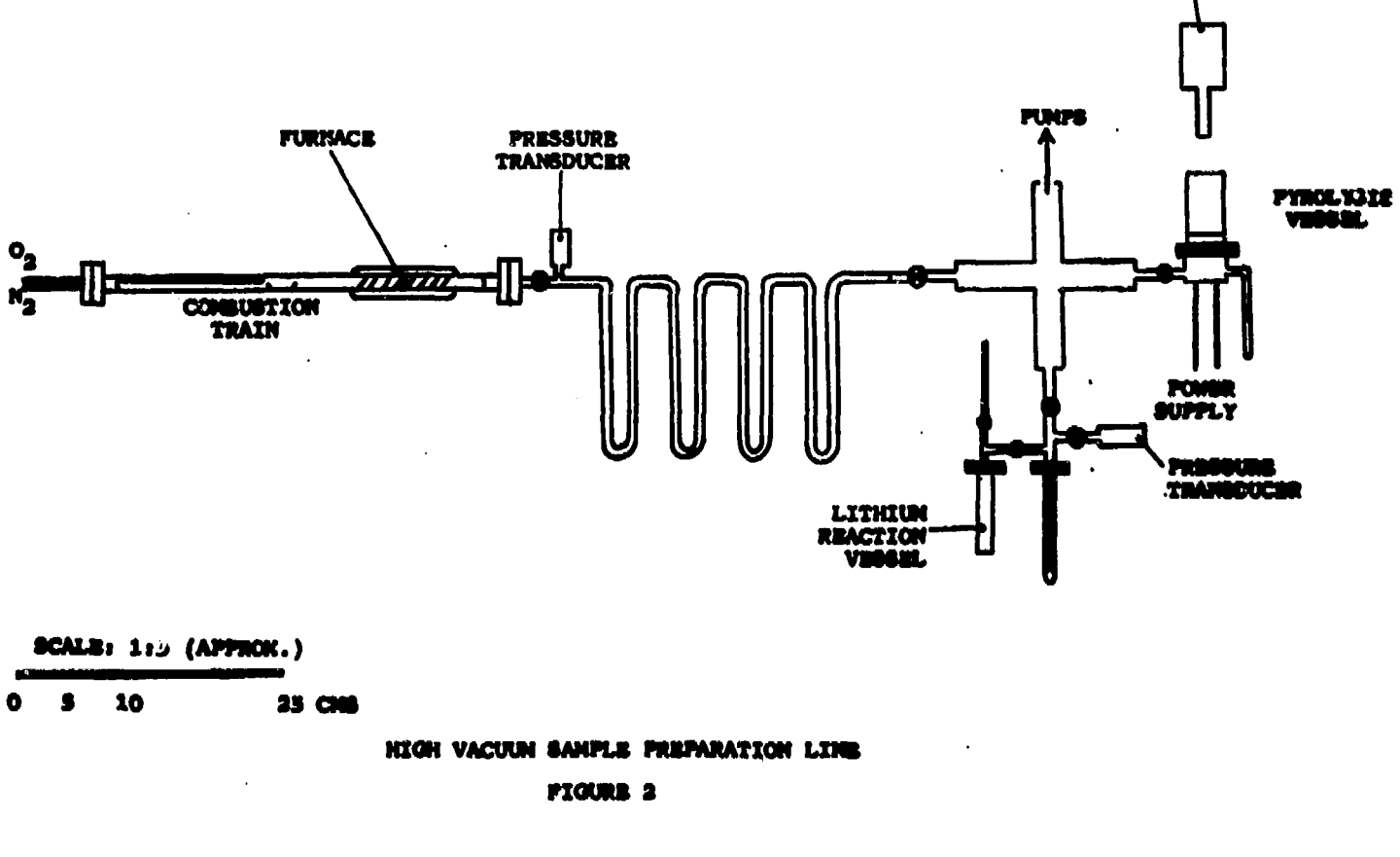

HIGH VACUUM SAMPLE PREPARATION LINE

FIGURE 2

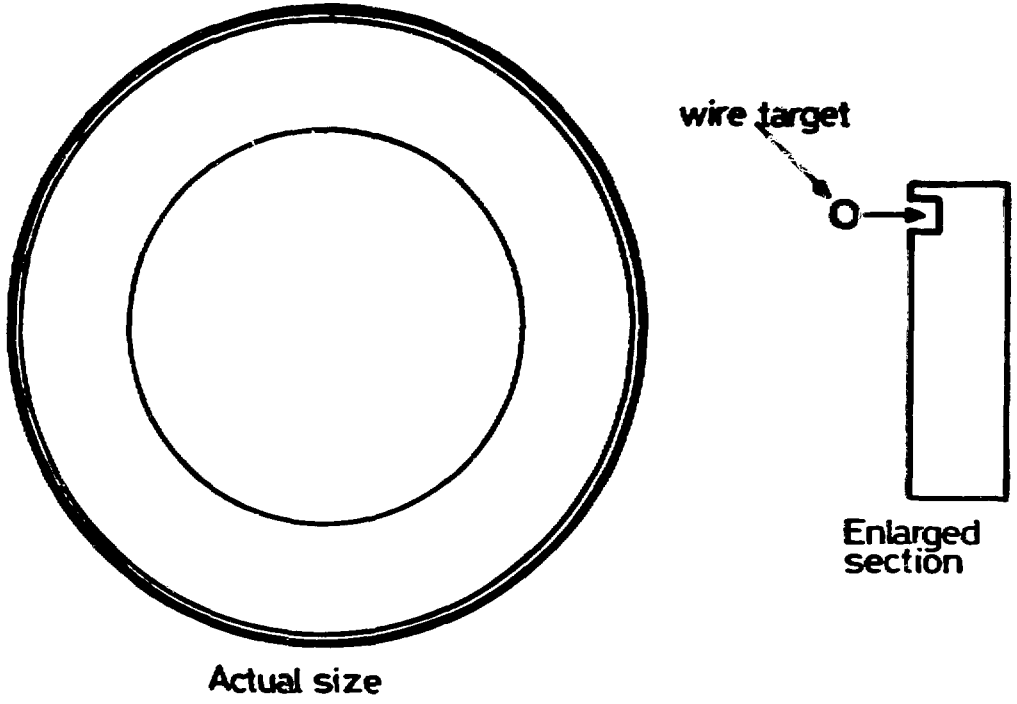

Fig. 3. The sample wheel used in the modified reflected beam source for dating work. 20 graphite coated tantalum wire sputter targets are crimped into the groove around the periphery. The wheel is made of bending grade aluminium.

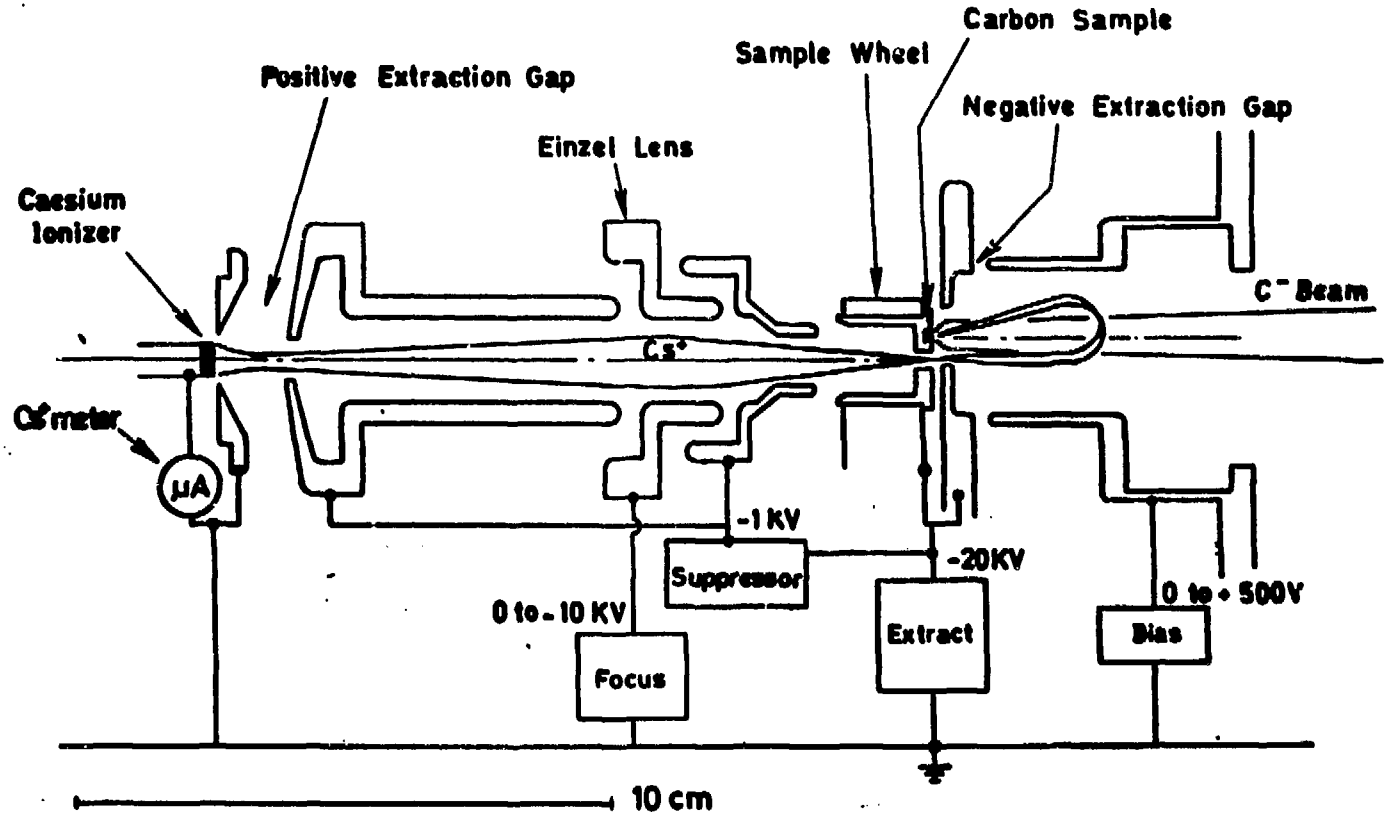

Arrangement of reflected beam sputter source

FIGURE 4

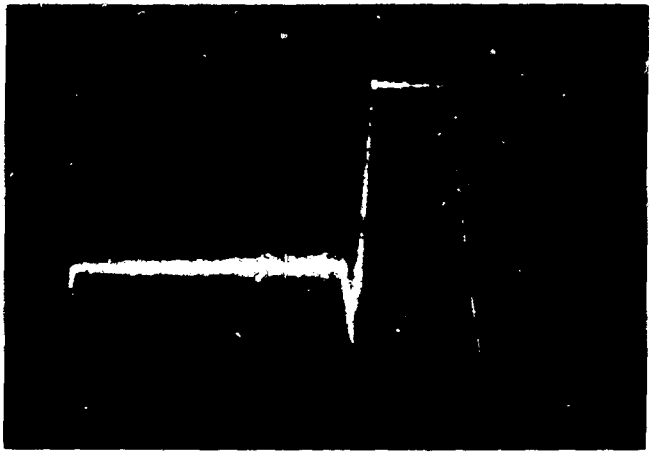

Fig. 5. Oscillogram of the pulsed voltage on the injection magnet chamber, using the circuit of fig. 6.
Calibrations: time axis: 50 uS per cm.
y axis: 1 kV per cm.

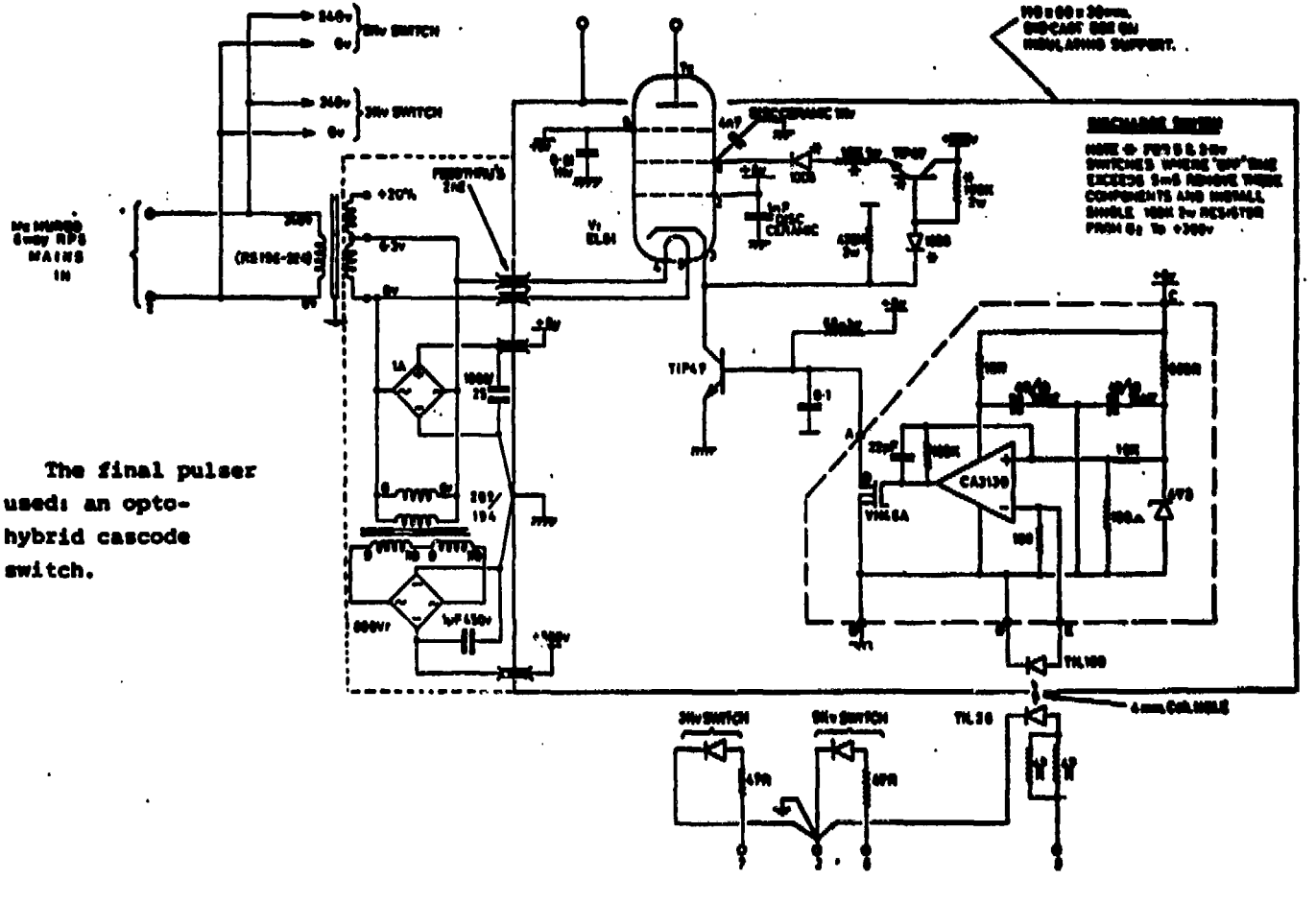

Fig. 6. The final pulser circuit used: an opto-coupled hybrid cascode current switch.

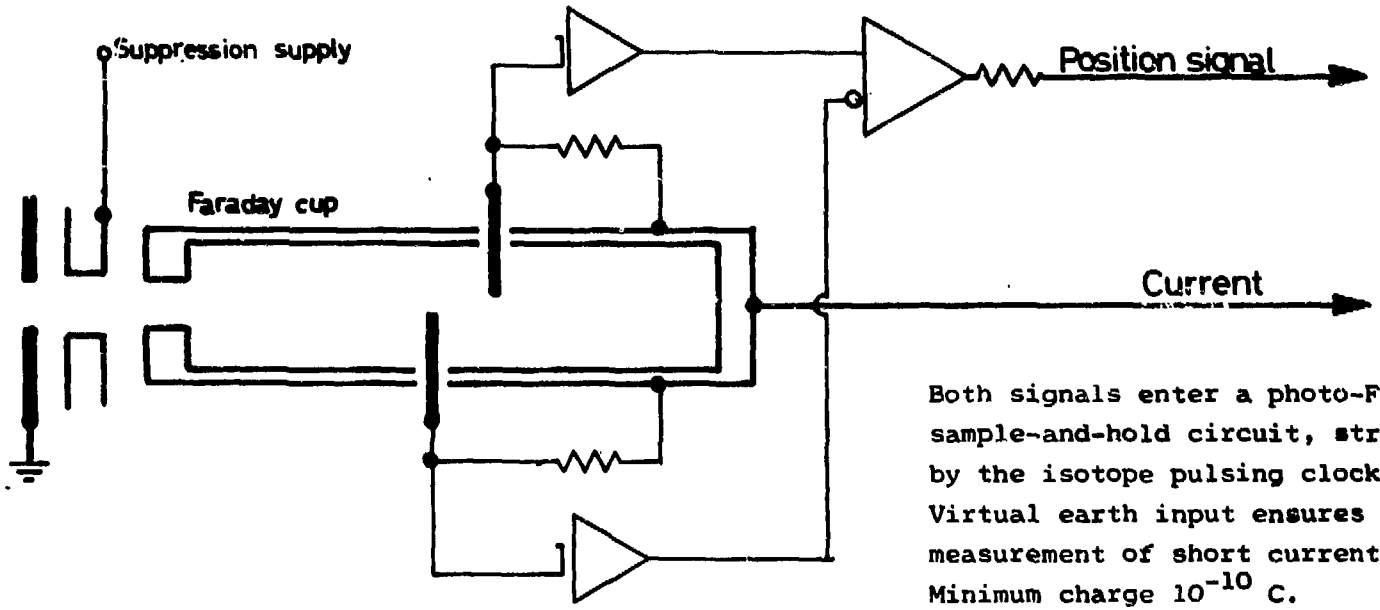

Both signals enter a photo-FET sample-and-hold circuit, strobed by the isotope pulsing clock. Virtual earth input ensures accurate measurement of short current pulses. Minimum charge 10^{-10} C.

FIGURE 7

The amino acid composition of cortical ox bone collagen (moles %)

Alanine	10.9
Glycine	33.7
Valine	2.0
Leucine	2.5
Isoleucine	1.1
Proline	12.3
Phenylalanine	1.2
Tyrosine	1.3
Serine	0.4
Threonine	3.4
Methionine	0.5
Arginine	4.9
Histidine	0.6
Lysine	2.6
Aspartic acid	5.0
Glutamic acid	7.6
Hydroxyproline	10.1
Hydroxylysine	0.6
	100.2
Total N	18.1%

From Piez and Likins (1960) in 'Calcification in Biological Systems' (R.F. Sognnes ed.) p. 411

Figure 8.

The N.S.F.-Arizona Dedicated Facility

D. J. Donahue, University of Arizona, Tucson

The N.S.F.-Arizona facility is sponsored by the National Science Foundation under its Regional Instrumentation Facilities program, and is a joint program of the Departments of Physics and Geosciences at the University of Arizona. Table 1 lists the personnel closely associated with the program.

Table 1

P. E. Damon A. Long A. T. J. Jull	Department of Geosciences
D. J. Donahue T. H. Zabel	Department of Physics
H. Bentley	Department of Hydrology & Water Resources

The primary instrument in the laboratory will be a "3 MV" tandetron and associated ion source, analyzers and detector constructed by General Ionex Corporation. We have been waiting for a year for the instrument, and have spent some of the time developing sample-preparation techniques. We have built a system for preparing CO_2 from samples, for converting CO_2 to either carbon or acetylene, and for cracking acetylene. In addition, we have done a fair amount of work on preparation of charcoal from wood and cellulose, and for making ion-source targets from charcoal. A simple method has been developed for melting iron powder-charcoal mixtures.

Approximately one half of the time on the instrument will be allocated to users outside the Departments of Physics and Geosciences. We have been in correspondence with potential users, and to illustrate some of our immediate plans, several potential experiments are described briefly.

1) Record of cosmic-ray fluctuations contained in tree rings and other geophysical reservoirs.

The University of Arizona has one of the world's preeminent Tree-Ring Laboratories and in that laboratory Dr. C. W. Ferguson and his colleagues have established a continuous chronology from the present back almost 9000 years. Dr. Damon and his coworkers have, for many years, been working to measure the ^{14}C content of these tree rings with the aim of

a) establishing a direct calibration with which ^{14}C content of an unknown sample can be related to the age of that sample; and

b) studying the fluctuation of production rates of ^{14}C over the period of the chronology, and understanding the terrestrial and solar phenomena which cause the fluctuations.

It is one of our primary aims to determine to what extent the accelerator measurements of $^{14}C/12_C$ ratios can contribute to this store of knowledge; particularly at early times at the boundary of the chronology. In the process, we will be doing many experiments to understand how the instrument works, and to determine the reliability of results obtained from it.

In addition to precise measurements on dated tree rings, the accelerator may be an important aid in extending the tree-ring

chronology - because approximate ages of old wood can be quickly determined from small samples delivered to the laboratory from the field. It is possible that such results could be made available to the dendrochronologists while they are still in the field. Such prompt information would be of great value in their search for wood with which to extend the chronology.

2) The Department of Hydrology and Water Resources at Arizona is actively involved in the use of ^{36}Cl to measure ground-water age, and to trace its movements. Harold Bentley has done some experimentation at Rochester, and we are working with him to develop techniques and procedures for performing ^{36}Cl measurements on the Arizona machine.

3) Lloyd Currie, at the National Bureau of Standards, is engaged in a program which uses ^{14}C as an atmospheric tracer. He painfully collects milligram samples of atmospheric carbon, in various forms, and determines their ^{14}C content by counting in miniature proportional counters. The results give important information on sources of air pollution and on atmospheric carbon inventories. The use of an accelerator in connection with the atmospheric carbon problem provides a striking example of the power of the technique. Dr. Currie counts his milligram samples for about 1 week, and gets results with statistical uncertainties of about ten percent. With the same samples he would expect to achieve statistical precisions of one percent in less than one hour with the accelerator.

4) We are working with Professors Sibley of the University of Georgia and Rowlett of the University of Missouri to establish a chronology for a series of Coptic textiles which spans a time period

from AD 300 to 1100.

5) We have a request from Professor Richard Ford of the University of Michigan concerning the origin of agriculture in North America. He has, for example, corn samples, which have contextual radiocarbon dates between 7000 and 8000 B.C. However, this age has been questioned by some ethnobotanists. A ^{14}C date might resolve the issue.

As long as I am talking about things we plan to do, I could probably continue indefinitely. The problems I have mentioned are just a few from a reasonably fat folder of inquiries and requests, concerning not only ^{14}C but ^{10}Be and ^{36}Cl as well. We have established a local committee to establish priorities when such action becomes necessary.

THE RESEARCH PROJECT AT NAGOYA UNIVERSITY

Michiaki Furukawa, Nobuyuki Nakai and Eizo Nakano
Radioisotope Center, Nagoya University
Chikusa, Nagoya 464, Japan

We will have a "dedicated facility" from General Ionex Corporation at the Radioisotope Center of Nagoya University in 1981 FY. The building to install the machine was already completed in March 1981. We have held meetings of potential users of the facility and various research proposals have been presented by the participants from many departments of the university.

The present research project at Nagoya is mainly devoted to the development of radiocarbon dating by the accelerator mass spectrometry, in which most of the users are interested. There are many archeological and geological samples in Japan which have too little carbon compounds for analysis by conventional radioactivity measurements. Concentrations of ^{14}C in these samples can be determined by the new technique. Some of the proposals connected with radiocarbon measurements are shown below.

1. Dating of old pottery samples There are many interesting samples in Japan which have very old ages (sometimes older than 10,000 years B.P.). Some archeologists, however, still doubt applicability of radiocarbon dating to these samples. To examine causes of possible discrepancy between "Radiocarbon age" and "archeological age", we need systematic investigations of many important samples.

2. Dating of lake sediments A big research group has been very active in the studies of Lake Biwa, the biggest lake in Japan. Sediment cores from the lake are also useful to study past variations in climate and the associated ecological changes. Carbon contents of the cores are usually so low that the dating is difficult with conventional methods.

3. Movement of active faults Radiocarbon measurements are helpful to determine rates of displacement of active faults in recent years. This type of research has close connection to problems in earthquake prediction.

4. Soil formation from volcanic ash Soil of volcanic origin is widely distributed in Japan, and it usually takes long time for the volcanic ash to be fertile soil. Radiocarbon dating is also applicable to obtain informations on the formation rate of fertile soil.

5. Radiocarbon in tree rings The ^{14}C concentrations measured by the atom counting is now less accurate than those by the radioactivity measurement. The future improvement, however, can be expected and thus annual radiocarbon fluctuations will be studied accurately. This type of informations is very important in the studies of cosmic ray intensity variations as well as many problems in the fields of geophysics.

Tritium is another nuclide to be measured by this technique, since the tracer studies are very active in biological sciences and the future plans of plasma researches in this university will possibly include handling of a relatively large amount of tritium. The measurement of low concentrations (less than 10 T.U.) may be difficult, but the small size of the sample needed for analysis is potentially an advantage over the conventional methods.

^{10}Be is one of the most interesting nuclides which can be measured by the present facility. The ratio of ^{7}Be to ^{10}Be in ground-level air or in wet precipitation is useful to obtain informations on atmospheric residence times. The most reliable sedimentation rate of deep-sea sediments can be obtained from the ^{10}Be measurement. Japanese antarctic researches have been very active for more than 20 years, and we hope we can have good ice core samples. ^{10}Be concentrations in the samples are useful to know the cosmic ray intensity variations within several million years.

We are beginning preliminary studies on the handling of samples for radiocarbon dating, and we hope we shall be able to perform accurate radiocarbon measurements. Also we are examining the feasibility of tritium measurement with the machine which has a sputter ion source.

Participants in the

Symposium on Accelerator Mass Spectrometry

May 11-13, 1981

Argonne National Laboratory

Building 203 Auditorium

Irshad Ahmad
CHM - 200
Argonne National Laboratory
9700 South Cass Avenue
Argonne, Illinois 60439
312/972-3667

Louis W. Alvarez
Lawrence Berkeley Laboratory
University of California
Berkeley, California 94720
415/486-4400

Gordon C. Ball
Chalk River Nuclear Laboratory
Chalk River, Ontario
CANADA KOJ 1JO
613/584-3311 Ext. 2424

Harold Bentley
Department of Hydrology
University of Arizona
Tucson, Arizona 85721
602/626-5729

Roelf P. Beukens
Physics Department
University of Toronto
Toronto, Ontario
CANADA M5S 1A7
416/978-4628

Louis M. Bianchi
DPHN-BE Bt 30
CEN SACLAY
B.P. 2
91190 Gif-sur-Yvette
FRANCE
---6/908-4551

Peter J. Billquist
PHY - 203
Argonne National Laboratory
9700 South Cass Avenue
Argonne, Illinois 60439
312/972-4115

Lowell M. Bollinger
PHY - 203
Argonne National Laboratory
9700 South Cass Avenue
Argonne, Illinois 60439
312/972-4897

Ivan G. Brissaud
Institut de Physique Nucleaire Bt 109
B.P. 1
91406 Orsay
FRANCE
941-7915 or 941-7185

Kai H. Chang
Physics Department
University of Toronto
Toronto, Ontario
CANADA M5S 1A7
416/978-4860

Sing Hooi Chew
Nuclear Physics Laboratory
Oxford University
Keble Road
Oxford OX1 3BE
UNITED KINGDOM

0865-59911 Ext. 260

Cary N. Davids
PHY - 203
Argonne National Laboratory
9700 South Cass Avenue
Argonne, Illinois 60439

312/972-4062

Patric K. Den Hartog
PHY - 203
Argonne National Laboratory
9700 South Cass Avenue
Argonne, Illinois 60439

312/972-4115

D. J. Donahue
Physics Department
University of Arizona
Tucson, Arizona 85721

602/626-2480

Segal E. Drummond
Chemistry Department
Oak Ridge National Laboratory
P.O. Box X
Oak Ridge, Tennessee 37830

FTS: 615/576-4600

David Elmore
Nuclear Structure Research Laboratory
University of Rochester
Rochester, New York 14627

716/275-4946

Alexander J. Elwyn
PHY - 203
Argonne National Laboratory
9700 South Cass Avenue
Argonne, Illinois 60493

312/972-4055

Hartmut J. Ernst
PHY - 203
Argonne National Laboratory
9700 South Cass Avenue
Argonne, Illinois 60439

312/972-8802

George W. Farwell
Physics Department FM-15
University of Washington
Seattle, Washington 98195

206/543-4080

Bradley W. Filippone
PHY - 203
Argonne National Laboratory
9700 South Cass Avenue
Argonne, Illinois 60439

312/972-4051

William S. Freeman
PHY - 203
Argonne National Laboratory
9700 South Cass Avenue
Argonne, Illinois 60439

312/972-4042

Michiaki Furukawa
Chemistry Department
Faculty of Science
Nagoya University
Chikusa-ku
Nagoya 464
JAPAN

501/575-4601 Ext. 32

Harry E. Gove
Department of Physics
University of Rochester
271 East River Road
Rochester, New York 14627

706/275-4943

Adrianus M. Hoogenboom
Physics and Astronomy Department
State University of Utrecht
Princetonplein 5,
Utrecht 3508 TA
NETHERLANDS

030-531650

Lawrence R. Greenwood
CEN - 205
Argonne National Laboratory
9700 South Cass Avenue
Argonne, Illinois 60439

312/972-4351

Thomas J. Humanic
PHY - 203
Argonne National Laboratory
9700 South Cass Avenue
Argonne, Illinois 60439

312/972-8802

Pieter M. Grootas
Quaternary Isotope Laboratory AJ-20
University of Washington
Seattle, Washington 98195

206/543-6327

Ian D. Hutcheon
Enrico Fermi Institute
University of Chicago
5640 Ellis Avenue
Chicago, Illinois 60637

312/753-8164

Walter F. Henning
PHY - 203
Argonne National Laboratory
9700 South Cass Avenue
Argonne, Illinois 60439

312/972-4058

A. J. Timothy Jull
Physics Department
University of Arizona
Tucson, Arizona 85721

602/626-3076

Robert L. Hershberger
Physics & Astronomy Department
177 Chem-Phys Building
University of Kentucky
Lexington, Kentucky 40383

606/258-5845 or -4661

Thomas Kaiser
Geology Department
Mail Code 170-25
California Institute of Technology
Pasadena, California 91125

213/356-6139

Robert E. Holland
PHY - 203
Argonne National Laboratory
9700 South Cass Avenue
Argonne, Illinois 60439

312/972-4061

Teng-Lek Khoo
PHY - 203
Argonne National Laboratory
9700 South Cass Avenue
Argonne, Illinois 60439

312/972-4034

William E. Kieser
Physics Department
University of Toronto
Toronto, Ontario
CANADA M5S 1A7

416/978-4860

Linas R. Kilius
Physics Department
University of Toronto
Toronto, Ontario
CANADA M5S 1A7

416/978-2258

James D. King
Physics Department
University of Toronto
Toronto, Ontario
CANADA M5S 1A7

416/978-2959 or 416/284-3124

Jeffrey Klein
Physics Department
University of Pennsylvania
209 S. 33rd Street
Philadelphia, Pennsylvania 19104

215/243-8832

Koichi Kobayashi
Department of Physics
Faculty of Science
Kyushu University
Hakozaki
Fukuoka 812
JAPAN

092/641-1101 Ext. 4488

Seth Krishnaswami
Geology Department
Yale University
P.O. Box 6666
New Haven, Connecticut 06511

203/436-0372

Theodore H. Kruse
Physics Department
Serin Physics Laboratory
Rutgers University
Piscataway, New Jersey 08854

201/932-2527

Peter W. Kubik
Physik Department E17
Technische Universitat Munchen
D8046 Garching
WEST GERMANY

089/3209-2560

Walter Kutschera
PHY - 203
Argonne National Laboratory
9700 South Cass Avenue
Argonne, Illinois 60439

312/972-4026

Samuel M. Levenson
PHY - 203
Argonne National Laboratory
9700 South Cass Avenue
Argonne, Illinois 60439

312/972-4051

Albert E. Litherland
Physics Department
University of Toronto
Toronto, Ontario
CANADA M5S 1A7

416/978-3785

Austin Long
Geosciences Department
Unviersity of Arizona
Tucson, Arizona 85721

602/626-1715

Keith W. Marlow
Radiation Survivability and
Detection Branch
Naval Research Laboratory 6610
Washington, D. C. 20375
202/767-5692

Lee T. Myers
Radiation Survivability and
Detection Branch
Naval Research Laboratory 6614
Washington, D. C. 20375
202/766-5692

Ronald L. Martin
ARF - 360
Argonne National Laboratory
9700 South Cass Avenue
Argonne, Illinois 60439
312/972-6526

Bogna Myslek-Laurikainen
Institute of Nuclear Research
Department of Physics
05-400 Swierk near Otwock
POLAND
21 4197

Roy Middleton
Physics Department
University of Pennsylvania
209 S. 33rd Street
Philadelphia, Pennsylvania 19104
215/243-8832

Kumihiko Nishiizumi
Chemistry Department B017
University of California/San Diego
La Jolla, California 92093
714/452-2909

Marc C. Monaghan
Geology & Geophysics
Yale University
P.O. Box 6666
New Haven, Connecticut 06511
203/436-0372

Gregory A. Norton
Sales Department
National Electrostatics Corporation
P.O. Box 310
Graber Road
Middleton, Wisconsin 53562
608/831-7600 Ext. 30

Robert K. Moniot
Physics Department
Rutgers University
Piscataway, New Jersey 08854
201/932-2402

Richard C. Pardo
PHY - 203
Argonne National Laboratory
9700 South Cass Avenue
Argonne, Illinois 60439
312/972-4048

Richard A. Muller
Lawrence Berkeley Laboratory 50/232
University of California
Berkeley, California 94720
415/486-5235

Peter D. Parker
Physics Department
Yale University
New Haven, Connecticut 06520
203/436-2320

Michael Paul
Racah Institue of Physics
Hebrew University of Jerusalem
Jerusalem 91904
ISRAEL

Israel-02-58-4795

Goran Possnert
Tandem Accelerator Laboratory
Box 533
S-75121 Uppsala
SWEDEN

018-100-470/14

Kenneth H. Purser
General Ionex Corporation
19 Graf Road
Newburyport, Massachusetts 01950

617/462-7147

Grant M. Raisbeck
Laboratoire Rene Bernas
Batiment 108
91406 Orsay
FRANCE

941/5264

William S. Rodney
Physics Division, Room 341
National Science Foundation
1800 G Street, N.W.
Washington, D. C. 20550

202-357-7992

Meyer Rubin
National Center 971
U. S. Geological Survey
Reston, Virginia 22092

703/860-6114

J. C. Rucklidge
Geology Department
University of Toronto
Toronto, Ontario
CANADA M5S 1A7

416/978-2258

John P. Schiffer
PHY - 203
Argonne National Laboratory
9700 South Cass Avenue
Argonne, Illinois 60439

312/972-4066

Fred H. Schmidt
Physics Department
Nuclear Physics Laboratory GL-10
University of Washington
Seattle, Washington 98195

206/543-4080

Robert K. Smither
CEN - 205
Argonne National Laboratory
9700 South Cass Avenue
Argonne, Illinois 60439

312/972-4351

John R. Southon
Archaeology Department
Simon Fraser University
Tandem Laboratory, GSB 105
Physics Department
McMaster University
Hamilton, Ontario L8S 4K1
CANADA

416/525-9140 Ext. 4046

Martin Suter
Laboratorium fur Kernphysik
Eidg. Technische Hochschule (ETH)
ETH-Honggerberg
CH-8093 Zurich
SWITZERLAND

Hongqing Tang
Physics Department
University of Pennsylvania
209 S. 33rd Street
Philadelphia, Pennsylvania 19104
215/243-8832

Pieter P. Tans
Lawrence Berkeley Laboratory
University of California
Berkeley, California 94720
416/486-5235

Anthony Taylor
MSD - 212
Argonne National Laboratory
9700 South Cass Avenue
Argonne, Illinois 60439
312/972-5109 or -5005

James H. Thomas
Whitney Nuclear Science Laboratory
Yale University
Box 6666
New Haven, Connecticut 06520
203/436-2320

Allen B. Tucker
San Jose State University
Physics Department
Stanford University
Stanford, California 94305
415/497-4563

Klaas van der Borg
Fysisch Laboratorium
State University of Utrecht
P.O. Box 80.000
3508 TA Utrecht
THE NETHERLANDS
030-532-492

John S. Vogel
Archaeology Department
Simon Fraser University
Tandem Accelerator Laboratory
McMaster University
Hamilton, Ontario L8S 4K1
CANADA
416/525-9140 Ext 4046

Martin Wahlen
Empire State Plaza
New York State Department of Health
Albany, New York 12201
518/474-5719

Gerald J. Wasserburg
Geological & Planetary Science 170-25
California Institute of Technology
Pasadena, California 91125
213/356-6139

James J. Welch
Lawrence Berkeley Laboratory, Bldg. 88
University of California, Berkeley
Berkeley, California 94720
415/486-5088

Nicholas R. White
Research Laboratory for Archaeology
Oxford University
6 Keble Road
Oxford (X1 3RH
UNITED KINGDOM
0865-513-296

Michael C. I. Wiescher
Van de Graaff Accelerator Laboratory
Ohio State University
1302 Kinnear Road
Columbus, Ohio 43212
614/422-4775

Peter Williams
Materials Research Laboratory
University of Illinois
Urbana, Illinois 61801

217/333-0386

Graham C. Wilson
Geology/Physics Department
University of Toronto
Toronto, Ontario
CANADA M5S 1A7

416/978-2258

Kurt Wolfsberg
CNC 7 Department
Mail Stop 514
Los Alamos National Laboratory
Los Alamos, New Mexico 87545

FTS: 843-4464

Francoise Yiou
Laboratoire Rene Bernas
Batiment 108
91406 Orsay
FRANCE

941-5264

Jan L. Yntema
PHY - 203
Argonne National Laboratory
9700 South Cass Avenue
Argonne, Illinois 60439

312/972-4024

AUTHOR INDEX

Distribution for ANL/PHY-81-1

Internal:

Participants (22)
W. Kutschera (73)
K. M. Pemble (5)
M. Peshkin
ANL Patent Department
ANL Libraries (2)
TIS Files (3)

External:

Participants (64)
DOE-TIC (27)
Manager, Chicago Operations Office, DOE
Chief, Office of Patent Counsel, DOE-CH
President, Argonne Universities Association
K. W. Allen, Nuclear Physics Lab, U. Oxford, England
H. R. Andrews, Chalk River Nuclear Lab, Ontario, Canada
J. R. Arnold, Chemistry Department, U. California, San Diego, La Jolla, CA
R. Balzer, Laboratorium fur Kernphysik, ETH, Zurich, Switzerland
J. Beer, Physikalisches Institut, Universitat Bern, Bern, Switzerland
J. R. J. Bennett, Rutherford and Appleton Labs, Oxon, England
B. Berthier, D.Ph.N/BE, CEN Saclay, Gif-sur-Yvette, France
P. Blasi, Laboratori Nazionali di Legnaro, Padova, Italy
G. Bonani, Laboratorium fur Kernphysik, ETH, Zurich, Switzerland
A. Breskin, Nuclear Physics Department, Weizmann Institute of Science, Rehovot, Israel
R. M. Brown, Chalk River Nuclear Lab, Ontario, Canada
N. Burn, Chalk River Nuclear Lab, Ontario, Canada
R. Chechik, Nuclear Physics Department, Weizmann Institute of Science, Rehovot, Israel
K. Cochran, Geology and Geophysics Department, Yale University, New Haven, CT
W. G. Davies, Chalk River Nuclear Lab, Ontario, Canada
S. N. Davis, Hydrology Department, U. Arizona, Tucson, AZ
G. Delibrias, C.F.R., Laboratoire mixte CNRS-CEA, Gif-sur-Yvette, France
J. McG. Dobbs, General Ionex Corporation, Newburyport, MA
H. C. Felsher, Office Under Secretary Defense, Pentagon, Washington, D.C.
D. S. Flynn, Physics and Astronomy Department, U. Kentucky, Lexington, KY
J. C. Fontes, Geology and Hydrology Lab, U. Paris, South, Orsay, France
M. Fruneau, Institut des Sciences Nucleaires, Grenoble, France
F. Gabbard, Physics and Astronomy Department, U. Kentucky, Lexington, KY
E. F. Garman, Nuclear Physics Lab, U. Oxford, England
J. M. Garnier, Geology and Hydrology Lab, U. Paris, South, Orsay, France
J. Gerber, Nuclear Physics Department, Weizmann Institute of Science, Rehovot, Israel
M. B. Goldberg, Nucl. Physics Dept., Weizmann Institute of Science, Rehovot, Israel
T. J. L. Greenway, Nucl. Physics Lab, U. Oxford, England
J. Guillot, Serv. Physique Nucl. et Neutronique, Cen. d'Etudes, Bruyeres-le-Chatel, France
E. T. Hall, Oxford U. Research Lab for Archaeology and History of Art, England
G. Hall, Chemistry Department, Rutgers U, New Brunswick, NJ
E. L. Hallin, Physics Dept, U. Toronto, Canada
E. M. Hedges, Oxford U. Research Lab for Archaeology & History of Art, England
. Heinemeier, Institute of Physics, U. Aarhus, Denmark
G. Herzog, Chemistry Department, Rutgers U., New Brunswick, NJ
G. J. Homer, Rutherford and Appleton Labs, Oxon, England
Y. Imahori, Chalk River Nuclear Lab, Ontario, Canada

R. Kaim, Nuclear Physics Department, Weizmann Institute of Science, Rehovot, Israel
J. Kalifa, Institut de Physique Nucleaire, Orsay, France
H. Kamitsubo, Institute of Physical & Chemical Research, Saitama, Japan
A. Kaufman, Isotope Research Department, Weizmann Institute of Science, Rehovot, Israel
K. Kobayashi, Kyushu U., Fukuoka, Japan
Y. Koechlin, C.F.R., Lab. mixte CNRS-CEA, Gif-sur-Yvette, France
G. Korschinek, Technical U., Munich, W. Germany
R. Korteling, Simon Fraser U., Burnaby, B.C., Canada
T. L. Ku, U. Southern California, Los Angeles, CA
D. Lal, Physical Research Lab, Ahmedabad, India
H. Laurent, Institut de Physique Nucleaire, Orsay, France
S. W. Leavitt, Physics Department, U. Arizona, Tucson, AZ
H. W. Lee, Physics Department, U. Toronto, Ontario, Canada
J. D. Lewin, Rutherford and Appleton Labs, Oxon, England
M. Lieuvin, Institut des Sciences Nucleaires, Grenoble, France
J. M. Loiseaux, Insitut des Sciences Nucleaires, Grenoble, France
A. Mangini, Geology and Geophysics Department, Yale U, New Haven, CT
T. S. Mast, Lawrence Berkeley Lab, Berkeley, CA
G. McCallum, Institute for Nuclear Sciences, Lower Hutt, New Zealand
T. Milazzo, Chemistry Department, Rutgers U., New Brunswick, NJ
J. C. D. Milton, Chalk River Nuclear Lab, Ontario, Canada
H. Morinaga, Technical U., Munich, W. Germany
N. Nakai, Radioisotope Center, Nagoya U., Nagoya, Japan
E. Nakano, Radioisotope Center, Nagoya U., Nagoya, Japan
D. E. Nelson, Simon Fraser University, Burnaby, B.C., Canada
E. Nolte, Technical U., Munich, W. Germany
I. Nowikow, McMaster U., Hamilton, Ontario, Canada
H. Oeschger, Physikalisches Institut, U. Bern, Bern, Switzerland
I. Olsson, Institute of Physics, U. Uppsala, Sweden
A. Peghaire, CSNSM-Orsay, France
S. Plattard, Serv. Phys. Nucl. et Neutron, Centre d'Etudes Bruyeres-le-Chatel, France
H. Polach, Australian National U., Canberra, Australia
R. Post, General Ionex Corporation, Newburyport, MA
M. S. Pravikoff, Technical U., Munich, W. Germany
C. J. Radnell, Lab Isotope Geochemistry, U. Arizona, Tucson, AZ
S. Raman, Physics Division, Oak Ridge National Laboratory, Oak Ridge, TN
J. C. Ravel, Institut des Sciences Nucleaires, Grenoble, France
J. L. Reyss, U. Southern California, Los Angeles, CA
R. Ricci, Laboratori Nazionali di Legnaro, Padova, Italy
Rockwell International, Electronic Systems Group, Anaheim, CA
M. Sakai, Institute for Nuclear Study, U. Tokyo, Tokyo, Japan
W. Savin, Physics Department, New Jersey Institute of Technology, Newark, NJ
R. J. Schneider, General Ionex Corporation, Newburyport, MA
P. Sharma, Physical Research Laboratory, Ahmedabad, India
C. Signorini, Laboratori Nazionali di Legnaro, Padova, Italy
P. F. Smith, Rutherford and Appleton Labs, Oxon, England
W. A. Smith, Rutherford and Appleton Labs, Oxon, England
B. Stauffer, Physikalisches Institut, Universitat Bern, Bern, Switzerland
W. E. Stephens, Physics Department, U. Pennsylvania, Philadelphia, PA
E. J. Stephenson, Indiana U. Cyclotron Facility, Bloomington, IN
Ch. Stoller, Laboratorium fur Kernphysik, ETH, Zurich, Switzerland
M. Stuiver, Quaternary Isotope Lab, U. Washington, Seattle, WA
I. Thorson, Simon Fraser U., Burnaby, B.C., Canada
I. Török, Institute of Nuclear Research, Debrecen, Hungary
T. Turekian, Geology and Geophysics Department, Yale U., New Haven, CT
J. Uzureau, Serv. Phys. Nucl. et Neutron., Centre d'Etudes, Bruyeres-le-Chatel, France

J. S. Vogel, Simon Fraser U., Burnaby, B.C., Canada
H. E. Walford, Rutherford and Appleton Labs, Oxon, England
J. O. Wand, Oxford U. Research Lab for Archaeology & History of Art, England
W. Wölfli, Laboratorium fur Kernphysik, ETH, Zurich, Switzerland
C. Zaidins, Physics Department, Colorado U., Boulder, CO
N. Zwang, Nuclear Physics Dept., Weizmann Institute of Science, Rehovot, Israel